

# Physics of Alfvén waves and energetic particles in burning plasmas

Liu Chen\*

*Institute for Fusion Theory and Simulation,  
Zhejiang University, Hangzhou,  
310027 P.R. China  
Department of Physics and Astronomy,  
University of California,  
Irvine CA 92697-4575,  
U.S.A.*

Fulvio Zonca

*Associazione Euratom-ENEA sulla Fusione,  
C.P. 65 – I-00044 Frascati, Rome,  
Italy  
Institute for Fusion Theory and Simulation,  
Zhejiang University, Hangzhou,  
310027 P.R. China*

(Dated: December 10, 2013)

Dynamics of shear Alfvén waves and energetic particles are crucial to the performance of burning fusion plasmas. This article reviews linear as well as nonlinear physics of shear Alfvén waves and their self-consistent interaction with energetic particles in tokamak fusion devices. More specifically, the review on the linear physics deals with wave spectral properties and collective excitations by energetic particles via wave-particle resonances. The nonlinear physics deals with nonlinear wave-wave interactions as well as nonlinear wave-energetic particle interactions. Both linear as well as nonlinear physics demonstrate the qualitatively important roles played by realistic equilibrium nonuniformities, magnetic field geometries, and the specific radial mode structures in determining the instability evolution, saturation, and, ultimately, energetic-particle transports. These topics are presented within a single unified theoretical framework, where experimental observations and numerical simulation results are referred to elucidate concepts and physics processes. Such a unified approach also allows drawing analogies between magnetic fusion energy and neighboring fields of physics research; such as fluid turbulence, condensed matter, nonlinear dynamics and complexity, fractional kinetics, and accelerator physics.

PACS numbers: 52.35.-g, 52.35.Bj, 52.35.Mw, 52.55.Pi, 52.55.Tn, 52.35.Sb;  
52.35.-g Waves, oscillations, and instabilities in plasmas and intense beams  
52.35.Bj Magnetohydrodynamic waves (e.g., Alfvén waves)  
52.35.Mw Nonlinear phenomena: waves, wave propagation, and other interactions (including parametric effects, mode coupling, ponderomotive effects, etc.)  
52.55.Pi Fusion products effects (e.g., alpha-particles, etc.), fast particle effects  
52.55.Tn Ideal and resistive MHD modes; kinetic modes  
52.35.Sb Solitons; BGK modes

---

\* Electronic address: liuchen@uci.edu

## CONTENTS

|   |     |
|---|-----|
| I. Introduction   | 2   |
| A. Historical review  | 3   |
| B. Scope of the present review  | 5   |
| II. Basic equations and concepts  | 6   |
| A. Gyrokinetic ordering of physical quantities  | 7   |
| B. Theoretical model and formal governing equations   | 8   |
| C. Ordering estimates of vorticity equation and physical time scales                                  | 10  |
| D. Reduced equations for low- $\beta$ drift Alfvén waves  | 11  |
| E. Drift Alfvén waves excited by energetic particles in low- $\beta$ fusion plasmas                   | 13  |
| F. Remarks on drift Alfvén wave equations adopted in numerical simulations                            | 15  |
| III. Linear Alfvén wave physics in one-dimensional nonuniform plasmas                                 | 15  |
| A. Shear Alfvén Waves: continuous spectrum and Global Alfvén Eigenmodes                               | 16  |
| B. Kinetic Alfvén Waves   | 19  |
| IV. Linear Alfvén wave physics and wave-particle interactions in two-dimensional toroidal plasmas     | 21  |
| A. The general fishbone-like dispersion relation  | 24  |
| B. Shear Alfvén waves and instabilities in toroidal magnetized plasmas                                | 27  |
| 1. The fishbone mode  | 30  |
| 2. The low frequency shear Alfvén wave spectrum   | 33  |
| 3. Toroidal Alfvén Eigenmodes   | 38  |
| 4. Energetic Particle Modes   | 42  |
| C. Experimental verification of linear Alfvén Eigenmodes and stability predictions in burning plasmas | 44  |
| V. Nonlinear Alfvén wave behaviors and self-consistent interactions with energetic particles          | 49  |
| A. General theoretical approach   | 50  |
| B. Nonlinear shear Alfvén waves in uniform plasmas  | 52  |
| 1. Effects of finite ion compressibility  | 54  |
| 2. Parametric decays of Kinetic Alfvén Waves  | 56  |
| 3. Nonlinear excitation of convective cells by Kinetic Alfvén Waves                                   | 59  |
| C. Nonlinear mode-coupling of shear Alfvén waves in toroidal plasmas                                  | 61  |
| 1. Toroidal Alfvén Eigenmode frequency cascading via nonlinear ion Landau damping                     | 62  |
| 2. Nonlinear excitation of zonal structures by Toroidal Alfvén Eigenmodes                             | 63  |
| 3. Toroidal Alfvén Eigenmode saturation via nonlinear modification of local continuum                 | 65  |
| 4. Alfvén Eigenmodes in the presence of a finite-size magnetic island                                 | 67  |
| D. Nonlinear wave-particle dynamics   | 68  |
| 1. The physics of the collisionless nonlinear beam-plasma system                                      | 70  |
| 2. The nonlinear beam-plasma system with sources and collisions                                       | 73  |
| 3. The bump-on-tail problem as paradigm for Alfvén Eigenmodes near marginal stability                 | 78  |
| 4. Numerical simulations of perturbative excitation of Alfvén Eigenmodes                              | 81  |
| 5. Nonlinear dynamics of Alfvénic fluctuations in nonuniform toroidal plasmas                         | 82  |
| 6. Nonlinear dynamics of Energetic Particle Modes and avalanches                                      | 93  |
| 7. The fishbone burst cycle   | 101 |
| E. Further remarks on general theoretical issues and broader implications                             | 107 |
| VI. Energetic particle transport in fusion plasmas  | 109 |
| A. Supra-thermal test particle transport  | 109 |
| B. Self-consistent non-perturbative energetic particle transport                                      | 110 |
| C. Transport of energetic particles by microscopic turbulence   | 111 |
| VII. Concluding remarks and outlooks  | 112 |
| A. Energetic particle transport in the presence of many modes   | 113 |
| B. Complex behaviors in burning plasmas   | 114 |
| Acknowledgments   | 116 |
| References  | 116 |

## I. INTRODUCTION

Since the mid 20th century, mankind has pursued magnetic fusion energy (MFE) research, which has reached a crucial stage with the construction of the International Thermonuclear Experimental Reactor (ITER) (Aymar *et al.*,

1997; Tamabechi *et al.*, 1991). The purpose of ITER is investigating the physics of burning plasmas, where deuterium-tritium (D-T) fusion reactions



produce  $\alpha$ -particles and neutrons. In ideal conditions for a fusion reactor,  $\alpha$ -particles thermalize (slow down) due to Coulomb collisions with the thermal plasma and sustain the fusion process by supplying the power input required to keep the plasma in “ignition” condition. Thus,  $\alpha$ -particles need to have sufficiently good confinement.

In toroidally symmetric magnetic fusion experimental devices (tokamaks); *e.g.*, ITER, the geometry of the confining equilibrium magnetic field  $\mathbf{B}_0$  is conceived to ensure properly confined charged particle orbits, including fusion  $\alpha$ -particles. While transport due to classical collisional processes is sufficiently small, the concern is transports via collective fluctuations driven unstable by  $\alpha$ -particles via wave-particle resonances. Such collective instabilities may be toroidal-symmetry breaking and, thus, could destroy the generalized toroidal motion of fusion  $\alpha$ 's; leading to enhanced  $\alpha$ -particle loss. Such “anomalous” enhanced loss is, of course, detrimental to the success of MFE research.

In order to achieve wave-particle resonances, the  $\alpha$ -particle characteristic dynamical frequencies need to match the wave frequencies of the collective instabilities. As, typically,  $\alpha$ -particle velocity-space distribution function is isotropic and, after slowing down due to Coulomb collisions, decreases with energy; *i.e.*, velocity-space gradient is stabilizing, no collective fluctuations around the cyclotron frequency (or “gyrofrequency”) will be excited. That is, the relevant instability drive is due to the finite real-space gradients of the distribution function (*i.e.*, the expansion free energy). The dynamical frequencies are, thus, associated with the guiding-center motion; *i.e.*, transit, bounce, and precessional frequencies in, *e.g.*, a tokamak device. The corresponding wave frequencies then fall inside the magnetohydrodynamic (MHD) regime (Alfvén, 1942, 1950); which are  $\mathcal{O}(10^{-2})$  smaller than  $\Omega_i$ , the ion gyrofrequency, for typical tokamak parameters. As to the three finite-frequency MHD modes, the most relevant one is the nearly incompressible, anisotropic shear Alfvén wave (SAW); with dispersion relation  $\omega = k_{\parallel}v_A$ . Here,  $k_{\parallel} = \mathbf{k} \cdot \mathbf{B}_0/B_0$  is the parallel wave vector and  $v_A = B_0/\sqrt{4\pi\rho_0}$  is the Alfvén speed, with  $\rho_0$  the plasma mass density. The compressional/fast Alfvén wave with  $\omega_f \simeq kv_A$  tends to have frequencies at least  $\mathcal{O}(10)$  higher than those of SAW and, generally, are more difficult to excite. The slow sound wave with  $\omega_s \simeq k_{\parallel}c_s$  ( $c_s$  is the sound speed), meanwhile, is also typically stable due to significant ion Landau damping with  $T_e \sim T_i$ ; where  $T_e$  and  $T_i$  are, respectively, thermal electron and ion temperatures. The above discussions are obviously applicable to energetic/fast (relative to the thermal background plasma) charged particles produced by auxiliary heating sources; such as radio-frequency waves and/or neutral beam injection. Collective excitations of SAW instabilities by energetic/fast particles (EPs) and the ensuing nonlinear consequences on EP confinement as well as, on longer time scales, the confinement and stability of thermal background plasmas are, thus, crucial issues for both present-day MFE devices and future burning-plasma experiments.

## A. Historical review

Energetic particles in burning plasmas of fusion interest consist, as mentioned above, of electrically charged fusion products as well as supra-thermal ions and electrons, generated by external power sources that are used for heating and current drive or, more generally, for tailoring and controlling equilibrium plasma profiles. The possible detrimental roles of SAWs on EP confinement in burning plasmas was brought to researchers’ attention in the MFE physics community since the pioneering works by Kolesnichenko and Oraevskij (Kolesnichenko and Oraevskij, 1967), Belikov *et al.* (Belikov *et al.*, 1968, 1969), Rosenbluth and Rutherford (Rosenbluth and Rutherford, 1975), and by Mikhailovskii (Mikhailovskii, 1975a,b). As the characteristic frequencies of EP motions in fusion devices are of the same order of those typical of SAWs, and the SAW group velocity, meanwhile, is parallel to the ambient magnetic field, resonant wave-particle interactions, thus, may, on the one hand, directly excite a variety of SAWs and, on the other hand, yield an efficient transport channel for EPs.

In the 80s, increasing theoretical attention was devoted to the analysis of the effects of fusion  $\alpha$ 's in burning plasmas; *e.g.*, in the works by (Kolesnichenko, 1980) and (Tsang *et al.*, 1981). However, the problem of SAWs interactions with EPs and of related transport processes became an issue of immediate practical interest, and not just a concern to be eventually considered in reactor relevant burning plasmas, at the time of the first observation of the fishbone mode instability in the PDX tokamak (McGuire *et al.*, 1983); causing dramatic global losses of EPs due to a secular transport process (White *et al.*, 1983). This instability has been theoretically explained as resonant excitation of an internal kink mode and its self-consistent non-linear interplay with the EP non-uniform source (Chen *et al.*, 1984). After fishbone observation and theoretical interpretation, MHD modes have been considered on the same footing as SAWs concerning their possible effect on EPs confinement in fusion devices. Essential physics ingredients in these analyses were recognized to be non-uniform equilibrium profiles of EP sources as well as of SAW continuous spectrum (Chen,

1988, 1994; Chen *et al.*, 1984; Cheng *et al.*, 1985), the corresponding continuum damping by phase mixing (Grad, 1969), and specific equilibrium geometries of magnetized plasmas confined in toroidal devices, yielding frequency gaps in the SAW continuum (D’Ippolito and Goedbloed, 1980; Kieras and Tataronis, 1982; Pogutse and Yurchenko, 1978).

An important theoretical result was that discrete Alfvén Eigenmodes (AEs), such as Toroidal Alfvén Eigenmodes (TAEs), can exist essentially free of continuum damping in the frequency gaps of the SAW continuous spectrum (Cheng *et al.*, 1985). Experimental observations of TAEs (Heidbrink *et al.*, 1991; Wong *et al.*, 1991) and of lower frequency AEs dubbed Beta induced Alfvén Eigenmodes (BAEs) (Heidbrink *et al.*, 1993), and, most importantly, the evidence that these modes may have significant impact on EP transport were the findings that finally have brought significant and continuing attention of the MFE research community to the physics of Alfvén waves and EPs in burning plasmas. In fact, only a small fraction of fusion  $\alpha$ ’s or EP losses can be tolerated in ITER without significantly degrading the fusion yield or damaging the plasma facing components (Fasoli *et al.*, 2007; ITER Physics Expert Group on Energetic Particles, Heating and Current Drive, ITER Physics Basis Editors, 1999).

Another important theoretical prediction was the existence of energetic particle continuum modes (EPM) (Chen, 1994); *i.e.*, non-normal modes of the SAW continuous spectrum, which emerge as discrete fluctuations at the frequency that maximizes wave-EP power exchange above the threshold condition set by EP drive exceeding continuum damping. In this respect, fishbones could be considered one special case and the first example of EPM. In the presence of EPM and/or fishbones, the low critical level of tolerable EP losses in a fusion device can become more severe. In fact, being non-normal modes, both fishbones and EPs maintain maximum wave-EP power exchange and ensuing EP transports through their nonlinear evolution by phase locking with resonant particles via frequency sweeping (Briguglio *et al.*, 2007, 1998; Vlad *et al.*, 2004, 2013; Zonca *et al.*, 2005). In turn, phase locking is responsible for the secular transport process first introduced by (White *et al.*, 1983) to explain fishbone induced EP losses. Intuitively, secular losses of EPs are characterized by a different energy spectrum than EP diffusive losses and tend to be more critical, since resonant EPs are typically lost before significant thermalization (Chen *et al.*, 1988; White *et al.*, 1983). The self-consistent non-linear interplay of EP spatial distributions with the EPM radial mode structures plays a crucial role in all these processes. Experimental observations of EPs and corresponding EP transports have been reported (Gorelenkov *et al.*, 2000; Gorelenkov and Heidbrink, 2002) right after their theoretical prediction. Meanwhile, first spectacular observations of these phenomena, dubbed abrupt large amplitude events (ALE) (Shinohara *et al.*, 2001), were reported in the JT-60U tokamak (Shinohara *et al.*, 2004) and are among the clearest experimental evidences of strong EP redistributions so far together with observations of EP losses/redistributions in the DIII-D (Duong *et al.*, 1993; Heidbrink and Sadler, 1994; Strait *et al.*, 1993) and NSTX tokamaks (Fredrickson *et al.*, 2009; Podestà *et al.*, 2011, 2009).

Since the early evidences of AEs (Heidbrink *et al.*, 1993, 1991; Wong *et al.*, 1991) and EPs (Gorelenkov *et al.*, 2000; Gorelenkov and Heidbrink, 2002) in tokamak plasmas, a whole “zoology” of modes have been observed (Heidbrink, 2002), with a classification following the qualitative features of experimental measurements. All these fluctuations can be actually understood and explained within the theoretical framework based on one single general fishbone-like dispersion relation (GFLDR), first introduced for the description of the fishbone mode (Chen *et al.*, 1984), and later on derived for different branches of SAW fluctuations, demonstrating its general validity (Chen, 2008; Chen and Zonca, 2007a; Zonca *et al.*, 2007a; Zonca and Chen, 2006, 2007). The usefulness of the GFLDR theoretical framework stands in its capability of providing a simple description of the underlying physics and extracting the distinctive features of the different AE/EPM branches that have been observed experimentally or in numerical simulations. Furthermore, the GFLDR also naturally introduces the spatiotemporal scales of the process involved, thereby explaining the connection between MHD fluctuations, SAWs and drift wave turbulence (DWT). The historical review of various experimental observations of AE/EPM and their theoretical interpretations is further articulated in Secs. III and IV. Successful and positive feedbacks between theory and experiment in this area were made possible by the development of impressive diagnostic techniques as well as numerical simulation capabilities (cf. Sec. IV.C), accompanied by detailed physics understanding. Meanwhile, one element of enrichment was brought by the fruitful exchanges between MFE tokamak and stellarator expert communities (Kolesnichenko *et al.*, 2011; Toi *et al.*, 2011).

Of the two “routes” to nonlinear dynamics of EP-driven SAW instabilities (Chen and Zonca, 2013); *i.e.*, nonlinear wave-wave and wave-EP interactions (cf. Sec. V), the former one was historically addressed first in the classic work by Hannes Alfvén, demonstrating the existence of the pure “Alfvénic state”, where SAW can exist in uniform, incompressible MHD plasmas independently of their amplitude due to the cancellation of Reynolds and Maxwell stresses and the incompressible plasma motion produced by SAW (Alfvén, 1942, 1950; Walén, 1944). However, in MFE research, nonlinear SAW-EP interactions have attracted most of the interest until very recently because of the important role of EP transports in burning plasmas.

Within the first “route”, it is illuminating to explore the various nonlinear wave-wave dynamics in terms of the mechanisms that yield to breaking of the “Alfvénic state” (Chen and Zonca, 2013). The effect of plasma compressibility

in the macroscopic MHD limit was investigated by (Sagdeev and Galeev, 1969), demonstrating the decay instability of a SAW into an ion sound wave (ISW) and a back-scattered SAW. Later, plasma compressibility effects were explored by (Hasegawa and Chen, 1976) for micro-scale fluctuations with wavelengths of the order of the thermal ion Larmor radius. This analysis not only generalized former results about parametric decay instability of SAW into a back-scattered SAW and an ISW, but demonstrated important consequences on plasma transport due to the different features of scattered SAW fluctuation spectra at short wavelengths. These processes are discussed in Sec. V.B, while Sec. V.C analyzes examples of processes breaking the “Alfvénic state” in toroidal geometry and responsible of cross-scale couplings between MHD fluctuations, SAWs and DWT; *i.e.*, of direct relevance to MFE and addressed in the first theoretical analyses of wave-wave interactions among Alfvénic fluctuations in fusion plasmas (Hahm and Chen, 1995; Spong *et al.*, 1994; Zonca *et al.*, 1995), recently reviewed by (Chen and Zonca, 2013).

Within the second “route” to nonlinear dynamics of EP-driven SAW instabilities (cf. Sec. V.D), the first nonlinear analysis of “thermonuclear Alfvén instability” was reported by (Belikov *et al.*, 1974), using the quasilinear description of a weakly turbulent plasma (Drummond and Pines, 1962; Vedenov *et al.*, 1961a). This case shows the important influence on MFE research of original works on nonlinear wave-particle dynamics in one-dimensional (1D) systems, investigated by pioneers in the early 60s; *e.g.*, (O’Neil and Malmberg, 1968), adopting the paradigmatic case of the interaction of a supra-thermal electron beam with a plasma in a strong axial magnetic field. This simple system provides the framework in which various processes were investigated and understood, such as mode dispersion relations, Landau damping in a finite amplitude wave (Mazitov, 1965; O’Neil, 1965), and nonlinear behaviors due to wave-particle interactions [*e.g.*, (O’Neil *et al.*, 1971)]. The interest for the beam-plasma system has been revived in the 90s, when it was proposed as paradigm for interpreting experimental observation of AEs excitation by EPs and related non-linear dynamics processes near marginal stability (Berk *et al.*, 1996b, 1997b, 1992a; Breizman *et al.*, 1997, 1993), based on their one-to-one correspondence with the evolution of the “bump-on-tail” instability (Langmuir wave) in a 1D plasma (Berk and Breizman, 1990a,b,c). This “bump-on-tail” paradigm has clear advantages of using a simple 1D system for complex dynamics studies and has been extensively applied for comparisons of theoretical model predictions with experimental observations, recently reviewed by (Breizman and Sharapov, 2011). There are however limitations of the extent to which it can be used for interpreting burning plasma behaviors in toroidal systems. The nonlinear dynamics due to the self-consistent interplay of fluctuations evolution and EP transports leads typically to secular EP losses due to EPs/fishbones and phase locking of fluctuations with resonant particles via frequency sweeping. Theoretical analyses of these processes require an alternative “fishbone” paradigm (Chen and Zonca, 2013), proposed by (White *et al.*, 1983) for explaining fishbone induced EP losses and further developed in the analyses of nonlinear EPM dynamics and ensuing EP transports (Briguglio *et al.*, 1998; Vlad *et al.*, 2004; Zonca *et al.*, 2000, 2005), where magnetic field geometry and plasma nonuniformities play major roles. Ultimately, it is possible to demonstrate the unification of these two paradigms for nonlinear wave-EP interactions (Chen and Zonca, 2013) (cf. Sec. V.D), based on the solution of the Dyson equation for the EP distribution function (Al’tshul’ and Karpman, 1965, 1966).

Due to the intrinsic difficulty of self-consistent nonlinear description of SAW interactions with EPs and of their fluctuation spectra, EP transports in burning plasmas have been typically addressed by test-particle methods (Hsu and Sigmar, 1992; Sigmar *et al.*, 1992); *i.e.*, assuming a given fluctuation spectrum and removing the possible feedback of EP redistributions on the fluctuations themselves (cf. Sec. VI). As AE fluctuations are local in nature and have generally small intensity [cf., *e.g.*, (Heidbrink, 2008)], EP redistributions by AEs are expected to be typically small, unless stochastization threshold of EP motions in phase-space is reached in the presence of many modes. Realistic predictions of test particle transport in ITER are, however, still not available. In fact, not only the threshold for stochastic EP transport is very sensitive to details of the underlying physics and adopted model (White *et al.*, 2010a,b), but predicting EP redistributions and losses requires necessarily realistic sources, geometries and boundary conditions. Such thorough and detailed calculation of AE spectra in ITER with comprehensive global gyrokinetic and/or extended hybrid MHD-gyrokinetic codes (cf. Sec. II) will be likely available in the near future. Meanwhile, the progress in computational capabilities and understanding of essential physics ingredients will soon allow first principle based numerical simulations of self-consistent EP transports in fusion plasmas; *i.e.*, including the secular losses due to EPM/fishbones, which cannot be described by test-particle methods.

## B. Scope of the present review

The first and thorough experimental review of SAW and EP physics in burning plasmas is given by (Heidbrink and Sadler, 1994). This work was followed by that by (Wong, 1999), which is focused on experiments in the Tokamak Fusion Test Reactor (TFTR) (Grove and Meade, 1985) but still provides a general overview of MFE research in this area. A dedicated review of  $\alpha$ -particle physics experiments in TFTR is given by (Zweben *et al.*, 2000), while high

performance D-T experiments in the Joint European Torus (JET) (Gibson and the JET Team, 1998) were stable to SAW excited by fusion  $\alpha$ 's (Sharapov *et al.*, 1999) (cf. Sec. IV). Meanwhile, a joint activity of the international MFE community has produced the first review of the physics of SAW and EPs in ITER plasmas in (ITER Physics Expert Group on Energetic Particles, Heating and Current Drive, ITER Physics Basis Editors, 1999), which was updated later on (Fasoli *et al.*, 2007).

Basic theoretical reviews can be found in (Mahajan, 1995), analyzing the general linear properties of the SAW fluctuation spectrum; and in (Chen and Zonca, 1995), with a discussion of the complications and twists of SAW physics in realistic toroidal geometries. A general overview of both linear and nonlinear SAW and EP physics is given by (Vlad *et al.*, 1999), along with a discussion of numerical simulation results using the hybrid MHD-gyrokinetic model (Park *et al.*, 1992). The work by (Pinches *et al.*, 2004a) mainly focuses on aspects of the interplay between advancements in nonlinear theory, also reviewed by (Breizman, 2006), and comparisons with experimental data. Other brief overviews are available, with emphasis on the self-consistent interaction of nonlinear SAW dynamics with EP transport and complex behaviors in burning plasmas (Chen and Zonca, 2007a; Zonca *et al.*, 2006).

Key issues for burning plasmas are summarized by (Heidbrink, 2002) and a general review of basic physics of Alfvénic fluctuations and EPs in toroidal plasmas is given by (Heidbrink, 2008). An updated view of experimental results since (Heidbrink, 2002; Wong, 1999) and of the further progress in nonlinear theory comparison with experimental data is presented by (Breizman and Sharapov, 2011). For stellarators, a recent experimental review can be found in (Toi *et al.*, 2011), while theoretical aspects are reviewed by (Kolesnichenko *et al.*, 2011), both with emphasis on the “affinity and difference between energetic-ion-driven instabilities in 2D and 3D toroidal systems”.

The scope of the present review is to provide a comprehensive analysis of physics processes involved with SAW and EP behaviors in burning plasmas within a unified and self-contained theoretical framework. As prevalent Alfvénic fluctuations are in the MHD frequency range ( $|\omega| \ll \Omega_i$ ), basic equations are derived from the nonlinear gyrokinetic equation (Frieman and Chen, 1982) (cf. Sec. II). Meanwhile, the general fishbone like dispersion relation (GFLDR) (cf. Sec. IV.A) provides the foundation of the unified theoretical framework used throughout this work and makes it possible to identify and isolate the physics processes underlying SAW dynamics and EP physics, recognizing their characteristic spatial and temporal scales.

Experimental observations and numerical simulation results are important elements of existing literatures in this area, and are referred to in this work as means for elucidating concepts that are introduced theoretically. Thus, the present review offers different levels of reading that are merged and integrated into the same narrative to address the different aspects that may be of interest to theoreticians, modelers and/or experimentalists. At the same time, the GFLDR theoretical framework manifests its usefulness by suggesting the interpretation of experimental observations and numerical simulation results on the basis of the underlying physics, while various models and computation techniques with different levels of approximation can be used to validate and verify theoretical predictions.

The application of the GFLDR theoretical framework to nonlinear SAW and EP dynamics (cf. Sec. V) allows separating wave-wave and wave-EP nonlinear interactions based on the respective spatiotemporal scales, and unifying the “bump-on-tail” and “fishbone” paradigms for nonlinear SAW-EP interactions based on the solution of the Dyson equation for the EP distribution function (Al'tshul' and Karpman, 1965, 1966). It also naturally yields to the formulation of a general nonlinear Schrödinger equation with integro-differential nonlinear terms (cf. Sec. V.A), which can be used to draw analogies between this area of MFE and neighboring fields of physics research; such as fluid turbulence, condensed matter, nonlinear dynamics and complexity, fractional kinetics, and accelerator physics (cf. Secs. V.D and V.E). This unified approach also elucidates the crucial role of EPs as mediators of cross scale coupling and long time scale behaviors in burning plasmas (Zonca, 2008; Zonca *et al.*, 2013a; Zonca and Chen, 2008a).

In spite of the broad range of topics discussed by this review, it is far from being complete. A summary of relevant issues left out of this work is given in Sec. VII, along with elements for reflections on some of the major research topics in the MFE field for the next decade or so, in the perspective of ITER operations.

## II. BASIC EQUATIONS AND CONCEPTS

In this section, we consider a magnetized plasma in general geometry and briefly review the dynamic equations for the description of low-frequency electromagnetic fluctuations, produced by the self-consistent charged-particle motion in the fluctuating fields. The low-frequency ordering in magnetized plasmas is referred, as usual, to oscillation frequencies that are much smaller than the ion cyclotron frequency  $\Omega_i$ , where  $\Omega = eB_0/(mc)$ , with the subscript  $i$  denoting ions,  $B_0$  denotes the strength of the local equilibrium magnetic field,  $e$  stands for the generic particle electric charge and  $m$  for its mass. Similarly, in all what follows, subscript  $e$  refers to electrons and, when needed, subscript  $E$  denotes energetic or fast (supra-thermal) particles, which may be ions and/or electrons.

A self-consistent description of low-frequency electromagnetic fluctuations is based on the derivation of gyrokinetic Maxwell equations (Antonsen and Lane, 1980; Catto *et al.*, 1981; Frieman and Chen, 1982)<sup>1</sup>, expressed in terms of moments of the gyrocenter Vlasov (Boltzmann) distribution. Within this approach, one can systematically decouple (Rutherford and Frieman, 1968; Taylor and Hastie, 1968) the the nearly periodic particle gyromotion (Kruskal, 1962; Northrop, 1963) from the fluctuation dynamics. This is achieved in two steps (Brizard, 1989; Dubin *et al.*, 1983; Hahm, 1988; Hahm *et al.*, 1988), based on asymptotic decoupling of the fast gyromotion time scale from a set of Hamilton equations by Lie-transform methods (Brizard, 1990; Littlejohn, 1982; Qin and Tang, 2004). First, the guiding-center Hamilton equations are derived eliminating the gyroangle dependence associated with the gyromotion of charged particles about equilibrium magnetic field lines. Second, the new gyrocenter Hamilton equations are obtained eliminating the gyroangle dependence in the perturbed guiding-center equations due to the presence of electromagnetic fluctuations. In this way (Brizard and Hahm, 2007), it is possible to construct the gyrocenter magnetic moment as adiabatic invariant corresponding to the fast and nearly periodic particle gyromotion in the gyrocenter gyroangle, which is an ignorable periodic coordinate, while the guiding-center magnetic moment adiabatic invariance is modified by the introduction of low-frequency electromagnetic fluctuations (Taylor, 1967).

In the following, within the theoretical framework of nonlinear gyrokinetic theory (Frieman and Chen, 1982), we discuss the dynamic equations governing the low-frequency response of a quasineutral, finite- $\beta$ , magnetized plasma, with  $\beta = 8\pi P/B_0^2$  defined as the ratio between kinetic and magnetic energy densities. We describe the low-frequency plasma oscillations in terms of three fluctuating scalar fields, having chosen to work in the Coulomb gauge: the scalar potential perturbation  $\delta\phi$ ; the parallel (to  $\mathbf{b} = \mathbf{B}_0/B_0$ ) magnetic field perturbation  $\delta B_{\parallel}$ ; and the parallel (to  $\mathbf{b}$ ) vector potential fluctuation  $\delta A_{\parallel}$ .

### A. Gyrokinetic ordering of physical quantities

The ordering of spatiotemporal scales and fluctuation strength is the usual one in gyrokinetic theory. The background plasma is described by means of the small parameter  $\epsilon_B \equiv \rho_i/L_B$ , with  $\rho_i$  denoting the ion Larmor radius and

$$|\rho_i \nabla \ln B_0| \sim \epsilon_B \quad \text{and} \quad \left| \frac{1}{\Omega_i} \frac{\partial}{\partial t} \ln B_0 \right| \sim \epsilon_B^3 . \quad (2.1)$$

A similar ordering is introduced for the background Vlasov (Boltzmann) distribution function  $f_0$

$$|\rho_i \nabla \ln f_0| \sim \epsilon_F \quad \text{and} \quad \left| \frac{1}{\Omega_i} \frac{\partial}{\partial t} \ln f_0 \right| \sim \epsilon_F^3 . \quad (2.2)$$

The usefulness of having separate orderings, based on  $\epsilon_B$  and  $\epsilon_F$ , is the possibility of introducing  $\epsilon_B/\epsilon_F$  as an auxiliary ordering parameter for exploiting the inverse aspect-ratio expansion in  $a/R_0 \sim \epsilon_B/\epsilon_F$  to simplify theoretical description of toroidal magnetized plasmas, with  $a$  and  $R_0$  the torus minor and major radii, respectively. The time-scale ordering of Eqs. (2.1) and (2.2) is consistent with the transport time-scale ordering (Hinton and Hazeltine, 1976), as noted in (Frieman and Chen, 1982).

Spatial and temporal scales in the fluctuation fields ( $\delta\phi, \delta A_{\parallel}, \delta B_{\parallel}$ ) and distribution function ( $\delta f$ ) are described in terms of the ordering parameters ( $\epsilon_{\perp}, \epsilon_{\omega}$ )

$$|\mathbf{k}_{\perp} \rho_i| \sim \epsilon_{\perp} \sim 1 \quad \text{and} \quad \left| \frac{\omega}{\Omega_i} \right| \sim \epsilon_{\omega} \ll 1 , \quad (2.3)$$

with  $\mathbf{k}$  and  $\omega$  the wave vector and angular frequency, and the subscript  $\perp$  indicating the component perpendicular to  $\mathbf{b}$ . The ordering for  $k_{\parallel}$  is obtained from the condition that strong wave-particle interactions may be described within the gyrokinetic ordering, *i.e.*, denoting by  $v_{ti}$  the ion characteristic (thermal) speed

$$\omega \sim k_{\parallel} v_{ti} \quad \text{and} \quad \left| \frac{k_{\parallel}}{\mathbf{k}_{\perp}} \right| \sim \frac{\epsilon_{\omega}}{\epsilon_{\perp}} . \quad (2.4)$$

---

<sup>1</sup> See (Brizard and Hahm, 2007) for a recent and comprehensive review.

We note that the ordering of Eqs. (2.3) and (2.4) may be applied to either thermal ions, as usual, or to supra-thermal (energetic) particles, yielding to a broad range of frequency and wavelength spectra of fluctuations that can be described within the present theoretical framework (cf. Secs. II.B, II.D and II.E as well as Sec. IV.B).

When investigating fluctuations of the Alfvén branch, the  $|k_{\parallel}/k_{\perp}|$  ratio reflects the frequency ratio of shear Alfvén to compressional Alfvén waves. In most of this work (see Sec. II.D and II.E), we will assume that these frequency scales are well separated; for this is the condition under which Alfvénic instabilities are most easily excited by both thermal and supra-thermal particles in fusion plasmas. Meanwhile, when considering compressional Alfvén waves (CAWs), the frequency ordering reads  $\omega/\Omega_i \sim |k_{\perp}|v_A/\Omega_i \sim |k_{\perp}\rho_i|/\beta^{1/2}$ , with  $v_A = B_0/\sqrt{4\pi\rho_{m0}}$  the Alfvén speed and  $\rho_{m0}$  the plasma mass density, so that the oscillation frequency can no longer be considered small compared with  $\Omega_i$  for typical conditions in fusion plasmas. In this case, a high-frequency gyrokinetic description of linear plasma dynamics may still be derived (Chen and Tsai, 1983; Lashmore-Davies and Dendy, 1989; Qin *et al.*, 2000, 1999a; Tsai *et al.*, 1984), but its discussion is outside the scope of the present review. Note that, while the ordering  $|k_{\parallel}/k_{\perp}| \simeq \epsilon_{\omega}/\epsilon_{\perp} \ll 1$  is consistent with gyrokinetic ordering, it is, in general, not necessary (Brizard and Hahm, 2007; Qin *et al.*, 1998, 1999b).

The relative fluctuation levels are estimated by the ordering parameter

$$\left| \frac{\delta f}{f_0} \right| \sim \left| \frac{\delta \mathbf{B}_{\perp}}{B_0} \right| \sim \left| \frac{\delta \dot{\mathbf{X}}_{\perp}}{v_{ti}} \right| \sim \epsilon_{\delta} \ll 1, \quad (2.5)$$

with  $\delta \dot{\mathbf{X}}_{\perp}$  the perturbed gyrocenter velocity (cf. Eq. (2.25) below)

$$\left| \delta \dot{\mathbf{X}}_{\perp} \right| \sim \left| \frac{c\delta \mathbf{E}_{\perp}}{B_0} \right| \sim \left| v_{\parallel} \frac{\delta \mathbf{B}_{\perp}}{B_0} \right| \sim \left| \epsilon_{\perp} \frac{e}{T_i} \delta \phi \right| v_{ti} \sim \left| \epsilon_{\perp} \frac{e}{T_i} \frac{v_{\parallel}}{c} \delta A_{\parallel} \right| v_{ti} \quad (2.6)$$

and  $T_i$  stands for the ion characteristic (thermal) energy. Finally, again, in most of this work it is assumed that SAW and CAW frequencies are well separated ( $|k_{\parallel}/k_{\perp}| \ll 1$ ), so that the compressional component of the magnetic field fluctuation satisfies approximately the perpendicular pressure balance (Chen and Hasegawa, 1991)

$$\nabla_{\perp} (B_0 \delta B_{\parallel} + 4\pi \delta P_{\perp}) \simeq 0. \quad (2.7)$$

Thus, the compressional component of the magnetic field fluctuation<sup>2</sup>  $\delta B_{\parallel}$  is ordered as

$$\left| \frac{\delta B_{\parallel}}{B_0} \right| \sim \beta \epsilon_{\delta} \ll 1 \quad \Rightarrow \quad \left| \mu \frac{\nabla_{\perp} \delta B_{\parallel}}{\Omega_i} \right| \sim \beta \epsilon_{\delta} v_{ti} \quad (2.8)$$

which apply in general for both low- and high- $\beta$  magnetized plasmas. Here,  $\mu = v_{\perp}^2/(2B_0)$  is the magnetic moment.

In the next subsection, we summarize the dynamic equations governing the low-frequency response of a quasineutral, finite- $\beta$ , magnetized plasma, which apply for arbitrary  $\beta$ ; *i.e.*, both in space (Chen and Hasegawa, 1991), for  $\beta \sim 1$ , and laboratory plasmas (Hahm *et al.*, 1988), for  $\beta \ll 1$ . The simplified equations for  $\beta \ll 1$ , more readily adopted for the description of the drift-Alfvén wave (DAW) dynamics in tokamak plasmas of fusion interest, which are the main focus of the present review, will be discussed in Sec. II.D. Finally, the further limiting case of the governing equations, which may be generally adopted for investigating DAW excitation by energetic particles (EPs) in burning plasmas is given in Sec. II.E.

## B. Theoretical model and formal governing equations

Due to the gyrokinetic wavelength ordering, discussed in Sec. II.A,  $k^2 \lambda_D^2 \sim \lambda_D^2/\rho_i^2 \sim \Omega_i^2/\omega_{pi}^2 \ll 1$ , with  $\lambda_D$  the Debye length and  $\omega_{pi}$  the ion plasma frequency, Poisson's equation becomes approximately the quasineutrality condition

$$\sum e \langle \delta f \rangle_v = 0, \quad (2.9)$$

where  $\sum$  implicitly indicates summation on all particle species and  $\langle \dots \rangle_v$  denotes integration in velocity space.

---

<sup>2</sup> This denomination is due to the fact that  $\delta B_{\parallel}$  modifies the magnetic energy density at order  $\epsilon_{\delta}$ .

The equation for  $\delta B_{\parallel}$  is readily obtained from the perpendicular component of the low-frequency Ampère's law (without displacement current, since  $|\mathbf{k}|^2 c^2 \gg |\omega|^2$ )

$$\nabla_{\perp} \delta B_{\parallel} = \boldsymbol{\kappa} \delta B_{\parallel} + \nabla_{\parallel} \delta \mathbf{B}_{\perp} + (\nabla \mathbf{b}) \cdot \delta \mathbf{B}_{\perp} + \frac{4\pi}{c} \sum e \langle \mathbf{b} \times \mathbf{v}_{\perp} \delta f \rangle_v . \quad (2.10)$$

Here,  $\nabla_{\parallel} \equiv \mathbf{b} \cdot \nabla$ ,  $\nabla_{\perp} \equiv \nabla - \mathbf{b} \nabla_{\parallel}$ ,  $\boldsymbol{\kappa} \equiv \mathbf{b} \cdot \nabla \mathbf{b}$  is the equilibrium magnetic field curvature and the perpendicular magnetic field fluctuation can be expressed as

$$\delta \mathbf{B}_{\perp} = \nabla_{\perp} \delta A_{\parallel} \times \mathbf{b} + (\mathbf{b} \times \boldsymbol{\kappa}) \delta A_{\parallel} + \mathbf{b} \times \nabla_{\parallel} \delta \mathbf{A}_{\perp} + (\mathbf{b} \times \nabla \mathbf{b}) \cdot \delta \mathbf{A}_{\perp} . \quad (2.11)$$

Last, the equation for  $\delta A_{\parallel}$  can be written in terms of the vorticity equation

$$\nabla \cdot \delta \mathbf{j} = \mathbf{B}_0 \cdot \nabla \left( \frac{\delta j_{\parallel}}{B_0} \right) + \nabla \cdot \delta \mathbf{j}_{\perp} = 0 . \quad (2.12)$$

Here, the fluctuating parallel current density is expressed in terms of  $\delta A_{\parallel}$  via the parallel component of the low-frequency Ampère's law

$$\begin{aligned} \delta j_{\parallel} = \frac{c}{4\pi} \mathbf{b} \cdot \nabla \times (\nabla \times \delta \mathbf{A}) &= \frac{c}{4\pi} \left\{ [-\nabla^2 + \kappa^2 + (\nabla \mathbf{b}) : (\nabla \mathbf{b})] \delta A_{\parallel} + (\nabla \times \mathbf{b})_{\parallel} \delta B_{\parallel} \right. \\ &\quad \left. + (\nabla \mathbf{b}) : (\nabla \delta \mathbf{A}_{\perp}) + \nabla \cdot [(\nabla \mathbf{b}) \cdot \delta \mathbf{A}_{\perp}] + (\boldsymbol{\kappa} \cdot \nabla \mathbf{b}) \cdot \delta \mathbf{A}_{\perp} + (\mathbf{b} \cdot \nabla \delta \mathbf{A}_{\perp}) \cdot \boldsymbol{\kappa} \right\} , \end{aligned} \quad (2.13)$$

while the fluctuating perpendicular current is obtained from the perpendicular component of the force balance

$$\frac{\partial}{\partial t} \delta (\varrho_m \mathbf{u}) = -\nabla \cdot \delta \mathcal{P} + \delta \left( \frac{\mathbf{j} \times \mathbf{B}}{c} \right) . \quad (2.14)$$

Here, as usual, we have introduced the fluctuating plasma mass density and flow

$$\delta \varrho_m = \sum m \langle \delta f \rangle_v \quad \text{and} \quad \delta (\varrho_m \mathbf{u}) = \sum m \langle \mathbf{v} \delta f \rangle_v , \quad (2.15)$$

as well as the perturbed stress tensor  $\delta \mathcal{P}$

$$\delta \mathcal{P} = \sum m \langle \mathbf{v} \mathbf{v} \delta f \rangle_v . \quad (2.16)$$

Equation (2.14) is readily solved for  $\delta \mathbf{j}_{\perp}$  and yields

$$\left( 1 + \frac{\delta B_{\parallel}}{B_0} \right) \delta \mathbf{j}_{\perp} = \frac{c}{B_0} \mathbf{b} \times \left[ \frac{\partial}{\partial t} \delta (\varrho_m \mathbf{u}) + \nabla \cdot \delta \mathcal{P} \right] - \mathbf{j}_{\perp 0} \frac{\delta B_{\parallel}}{B_0} + (j_{\parallel 0} + \delta j_{\parallel}) \frac{\delta \mathbf{B}_{\perp}}{B_0} . \quad (2.17)$$

Substituting back into Eq. (2.12), one obtains the general form of the vorticity equation

$$\begin{aligned} B_0 \left( \mathbf{b} + \frac{\delta \mathbf{B}_{\perp}}{B_0} \right) \cdot \nabla \left( \frac{\delta j_{\parallel}}{B_0} \right) &+ \delta \mathbf{B}_{\perp} \cdot \nabla \left( \frac{j_{\parallel 0}}{B_0} \right) + \delta B_{\parallel} \nabla_{\parallel} \left( \frac{\delta j_{\parallel}}{B_0} + \frac{j_{\parallel 0}}{B_0} \right) \\ &- (j_0 + \delta j) \cdot \nabla \left( \frac{\delta B_{\parallel}}{B_0} \right) + \nabla \cdot \left[ \frac{c}{B_0} \mathbf{b} \times \left( \frac{\partial}{\partial t} \delta (\varrho_m \mathbf{u}) + \nabla \cdot \delta \mathcal{P} \right) \right] = 0 . \end{aligned} \quad (2.18)$$

Equations (2.9), (2.10) and (2.18) form the closed set of dynamic equations formally governing the low-frequency response of a quasineutral, finite- $\beta$ , magnetized plasma, once the perturbed particle distribution function  $\delta f$  is given and the perpendicular magnetic field fluctuation is obtained by Eq. (2.11). Meanwhile, Eqs. (2.13) and (2.17) are considered as definitions for  $\delta j_{\parallel}$  and  $\delta \mathbf{j}_{\perp}$ , and Eqs. (2.15) and (2.16) are used for  $\delta (\varrho_m \mathbf{u})$  and  $\delta \mathcal{P}$ . In fact, given  $\delta A_{\parallel}$  and  $\delta B_{\parallel} = \mathbf{b} \cdot \nabla \times \delta \mathbf{A}$ , and noting the Coulomb gauge  $\nabla \cdot \delta \mathbf{A} = 0$ ,  $\delta \mathbf{A}_{\perp}$  is uniquely determined. By construction, Eqs. (2.9), (2.10) and (2.18), for wavelengths that are much longer than the Debye length, are completely equivalent to the gyrokinetic Maxwell equations (Brizard and Hahm, 2007), once the perturbed particle fluid moments are expressed in terms of the perturbed gyrocenter fluid moments (Brizard, 1992). These equations are also equivalent to the formulation adopted in most literatures, once the parallel Ampère's law is employed in the vorticity equation, Eq. (2.18).

### C. Ordering estimates of vorticity equation and physical time scales

Unlike most treatments available in the literature, the present theoretical framework does not assume any particular ordering of the perpendicular wavelength with respect to characteristic equilibrium spatial scales: this is the reason why Eqs. (2.10), (2.11) and (2.13) maintain terms that depend on equilibrium geometry, which may be important when treating long wavelength modes (Brizard and Hahm, 2007; Qin *et al.*, 1998, 1999b). However, while the nonlinear formal kinetic equations governing collisionless plasmas in the drift kinetic limit (vanishing Larmor radius) are given by (Kulsrud, 1983), expressions of the perturbed particle fluid moments in terms of the perturbed gyrocenter fluid moments (Brizard, 1992), valid for general low-frequency electromagnetic fluctuations and at arbitrary wavelengths are still not available at present. Thus, the formulation of Eqs. (2.9), (2.10) and (2.18) remains of little use for practical applications<sup>3</sup>. Nonetheless, it allows a detailed discussion of the relative importance of various contributions and, ultimately, the derivation of a set of reduced nonlinear equations, which will be used in the present work.

The first term in the vorticity equation, Eq. (2.18), represents the linear magnetic field line bending, which we denote to be  $\mathcal{O}(1)$ . The second one is its nonlinear extension, related with the perpendicular Maxwell stress, ordered as  $\sim \epsilon_{\perp} \epsilon_{\delta} / \epsilon_{\omega}$  within the gyrokinetic ordering introduced in Sec. II.A. The third term, representing the kink drive, is of order  $\sim \epsilon_F / \epsilon_{\perp}$ . Meanwhile, the fourth to seventh terms containing magnetic field compressions are, respectively, of order  $\beta \epsilon_{\delta}$ ,  $\beta \epsilon_B / \epsilon_{\perp}$ ,  $\beta^2 \epsilon_F / \epsilon_B$  and  $\beta^2 \epsilon_{\perp} \epsilon_{\delta} / \epsilon_{\omega}$ . The last two terms in Eq. (2.18) represent the plasma inertia response and the stress tensor contribution, which includes the usual Reynolds stress as well as the divergence of the nonlinear diamagnetic current. The linear plasma inertia response is of order  $\sim \omega^2 / k_{\parallel}^2 v_A^2$ , whereas its nonlinear contribution is an order  $\sim \epsilon_{\delta} / \epsilon_{\perp}$  higher. The stress tensor linear contribution is of the same order as the inertia term, while the nonlinear pressure stress tensor response is  $\sim (\epsilon_{\delta} \epsilon_{\perp} / \epsilon_{\omega}) (\omega^2 / k_{\parallel}^2 v_A^2)$ ; the same as the Maxwell stress.

From these estimates of the relative importance of various contributions in Eq. (2.18), we note that while the perpendicular Maxwell stress and the pressure stress tensor contribution are of the same order,  $\sim \epsilon_{\perp} \epsilon_{\delta} / \epsilon_{\omega}$ , the inertia (polarization) nonlinearity is of order  $\sim \epsilon_{\delta} / \epsilon_{\perp}$ . Therefore, we can anticipate that, for  $\epsilon_{\perp}^2 \sim \epsilon_{\omega}$ , there will be a transition between nonlinear dynamics dominated by the polarization response (Sagdeev and Galeev, 1969), where nonlinear MHD description is reasonably applicable, to a regime where dominant nonlinear interactions are due to the pressure stress tensor and Maxwell stress, which is the typical condition of gyrokinetic plasma behaviors (Hasegawa and Chen, 1975, 1976). This change in nonlinear dynamic behavior, first pointed out by (Hasegawa and Chen, 1976) for kinetic Alfvén waves (KAWs), will be further discussed in Sec. V.B and has important consequence on the spectral features of Alfvén waves and related transport processes (Chen and Zonca, 2011).

Applying the same orderings to other terms in Eq. (2.18), it can be also concluded that, in tokamaks of current interest, where  $\beta \lesssim \mathcal{O}(\epsilon_B / \epsilon_F) \sim \mathcal{O}(10^{-1})$ , the linear terms containing magnetic field compressions,  $\propto \delta B_{\parallel}$ , are  $\sim \beta \epsilon_B / \epsilon_{\perp}$  and  $\sim \beta^2 \epsilon_F / \epsilon_{\omega} \sim \beta^2 \epsilon_F / \epsilon_B \lesssim \beta$  and, hence, generally negligible. However, more careful considerations are needed concerning the nonlinear behaviors. For  $\epsilon_{\omega} > \epsilon_{\perp}^2$ , the polarization nonlinearity overwhelms the Maxwell stress and the pressure stress tensor nonlinearity and the nonlinear magnetic field compression contribution is negligible provided that

$$\mathcal{O}(\epsilon_{\delta} / \epsilon_{\perp}) \gg \mathcal{O}(\beta \epsilon_{\delta}; \beta^2 \epsilon_{\perp} \epsilon_{\delta} / \epsilon_{\omega}) \quad \Rightarrow \quad \mathcal{O}(\epsilon_{\perp}^{-1}) > \mathcal{O}(\epsilon_{\omega}^{1/2} / \epsilon_{\perp}) > \mathcal{O}(1) > \beta \quad ,$$

which is readily satisfied for laboratory plasmas of fusion interest. In the opposite limit,  $\epsilon_{\omega} < \epsilon_{\perp}^2$ , Maxwell stress and pressure stress tensor are also typically larger than the nonlinear magnetic field compression contribution, since

$$\mathcal{O}(\epsilon_{\perp} \epsilon_{\delta} / \epsilon_{\omega}) \gg \mathcal{O}(\beta \epsilon_{\delta}; \beta^2 \epsilon_{\perp} \epsilon_{\delta} / \epsilon_{\omega}) \quad .$$

However, for long wavelength incompressible shear Alfvén waves (SAW) in uniform plasmas, satisfying  $\omega^2 = k_{\parallel}^2 v_A^2$ , Reynolds and Maxwell stresses cancel exactly, yielding the well known properties of the *Alfvénic state* (Alfvén, 1942, 1950; Elsasser, 1956; Hasegawa and Sato, 1989; Walén, 1944), discussed in Sec. V.B. Although a realistic system can only approach the *Alfvénic state*, it is in this case important to make sure that residual effects of non exact cancellations of Reynolds and Maxwell stresses remain more significant than the  $\delta B_{\parallel}$  nonlinear term.

Since it is possible to formally write  $\omega = \omega_0 + i\partial_t$ , with  $\omega_0$  the typical (linear) mode frequency, significance of the nonlinear terms also depends on the relative time scales of the phenomena they produce in the dynamic evolution of the system. Ignoring the nonlinear magnetic field compression contribution for  $\epsilon_{\omega} < \epsilon_{\perp}^2$ , thus, sets a minimum

---

<sup>3</sup> Obviously, the perturbed particle fluid moments may be computed directly from the particle distribution function, reconstructing it numerically from the gyrocenter distribution function (Brizard and Hahm, 2007).

constraint on both the linear ( $\gamma_L$ ) and nonlinear ( $\tau_{NL}^{-1}$ ) rates; *i.e.*,

$$|\gamma_L/\omega_0| \sim |\omega_0\tau_{NL}|^{-1} \gg \mathcal{O}(\beta\epsilon_\delta; \beta^2\epsilon_\perp\epsilon_\delta/\epsilon_\omega) .$$

One, thus, needs to keep these self-consistency requirements in mind when making numerical simulations or theoretical analyses either close to marginal stability condition and/or examining long time-scale behaviors. In fact, nonlinear Alfvén wave behaviors and self-consistent interactions with EPs in toroidal plasmas of magnetic fusion interest (see Sec. V) are characterized by  $\tau_{NL} \sim \gamma_L^{-1} \sim \epsilon_B\epsilon_F^{-1}\beta^{-1}\omega^{-1} \ll \epsilon_B^{-1}\epsilon_\omega^{-1}\Omega^{-1}$ . For typical low- $\beta$  toroidal plasmas [ $\beta \lesssim \mathcal{O}(\epsilon_B/\epsilon_F) \sim \mathcal{O}(10^{-1})$ ], which are the main focus of this work, magnetic field compression terms in Eq. (2.18) typically affect the mode dynamics on time scales that are longer than  $\tau_{NL}$ . Thus, they can be consistently neglected in the present analysis. However, these terms may become important when considering longer time scale behaviors, *e.g.*,  $\tau_{NL} \sim \epsilon_\omega^{-1}\omega^{-1}$ , where  $\beta^2 \ll \epsilon_\omega/\epsilon_\perp$  may not be so well satisfied in tight aspect ratio tokamaks (Cox and MAST Team, 1999; Ono *et al.*, 2000). These self-consistency requirements on linear and nonlinear rates must also be obeyed when looking at mode nonlinear dynamics to explore the global variations of plasma equilibrium on the transport time scale [see Eqs. (2.1) and (2.2)]. Although this is an important issue at the forefront of magnetic fusion research, it is outside the scope of the present review.

In the next subsection, the reduced nonlinear gyrokinetic form of governing equations are derived specifically for low- $\beta$  plasmas, which may be readily adopted for the description of the DAW dynamics (Chen *et al.*, 1978; Frieman and Chen, 1982; Hahm *et al.*, 1988; Hasegawa and Chen, 1976; Mikhailovskii and Rudakov, 1963; Scott, 1997; Tang and Luhmann Jr., 1976; Tang *et al.*, 1980) in tokamak plasmas.

#### D. Reduced equations for low- $\beta$ drift Alfvén waves

Since all the works under the present review are limited to time scales

$$|\omega_0\tau_{NL}|^{-1} \sim |\gamma_L/\omega_0| \gg \epsilon_\omega ,$$

we may, as noted in the preceding subsection, self-consistently neglect the magnetic compression  $\delta B_\parallel$  terms and, following (Chen *et al.*, 2001), derive the nonlinear gyrokinetic vorticity equation by taking the moments of the nonlinear gyrokinetic equation of (Frieman and Chen, 1982). Note that this is equivalent to describing the gyrocenter Hamiltonian up to  $\sim \epsilon_\delta$  linear terms. For longer time scales, we need to include  $\sim \epsilon_\delta^2$  terms to ensure the exact conservation of the gyrokinetic energy (Brizard and Hahm, 2007).

It can be readily shown that the particle distribution function  $f$  can be written as:

$$f = e^{-\rho \cdot \nabla} \left[ \bar{F} - \frac{e}{m} \left( \frac{\partial \bar{F}}{\partial \mathcal{E}} + \frac{1}{B_0} \frac{\partial \bar{F}}{\partial \mu} \right) \langle \delta L_g \rangle \right] + \frac{e}{m} \left[ \frac{\partial \bar{F}}{\partial \mathcal{E}} \delta \phi + \frac{1}{B_0} \frac{\partial \bar{F}}{\partial \mu} \delta L \right] , \quad (2.19)$$

where  $\bar{F}$  is the gyrocenter distribution function (Brizard and Hahm, 2007),  $e^{-\rho \cdot \nabla}$  is the transformation from guiding-center to particle coordinates,  $\rho \equiv \Omega^{-1} \mathbf{b} \times \mathbf{v}$ ,  $\langle \dots \rangle$  denotes gyrophase averaging,  $\mathcal{E} = v^2/2$  is the energy per unit mass,  $\mu$  is the magnetic moment adiabatic invariant  $\mu = v_\perp^2/(2B_0) + \dots$  and,

$$\delta L_g = \delta \phi_g - \frac{v_\parallel}{c} \delta A_{\parallel g} = e^{\rho \cdot \nabla} \delta L = e^{\rho \cdot \nabla} \left( \delta \phi - \frac{v_\parallel}{c} \delta A_\parallel \right) . \quad (2.20)$$

In Eq. (2.19), all terms that are not acted upon by  $e^{-\rho \cdot \nabla}$  are the adiabatic response of the particle distribution function, the other terms obviously representing the non-adiabatic response of the guiding-center distribution (Antonsen and Lane, 1980; Brizard and Hahm, 2007; Catto *et al.*, 1981; Frieman and Chen, 1982). Up to order  $\mathcal{O}(\epsilon_\delta)$ , one can further reduce Eq. (2.19) to the following decomposition for the fluctuating particle distribution function (Frieman and Chen, 1982)

$$\delta f = e^{-\rho \cdot \nabla} \left[ \delta g - \frac{e}{m} \frac{1}{B_0} \frac{\partial \bar{F}_0}{\partial \mu} \langle \delta L_g \rangle \right] + \frac{e}{m} \left[ \frac{\partial \bar{F}_0}{\partial \mathcal{E}} \delta \phi + \frac{1}{B_0} \frac{\partial \bar{F}_0}{\partial \mu} \delta L \right] , \quad (2.21)$$

where the fluctuating gyrocenter distribution function  $\delta \bar{F}$  (Brizard and Hahm, 2007) is related to the non-adiabatic response  $\delta g$  (Frieman and Chen, 1982) as

$$\delta \bar{F} = \delta g + \frac{e}{m} \frac{\partial \bar{F}_0}{\partial \mathcal{E}} \langle \delta L_g \rangle , \quad (2.22)$$

and  $\delta g$  obeys the following nonlinear gyrokinetic equation

$$\left( \frac{\partial}{\partial t} + v_{\parallel} \nabla_{\parallel} + \mathbf{v}_d \cdot \nabla_{\perp} \right) \delta g = - \left( \frac{e}{m} \frac{\partial}{\partial t} \langle \delta L_g \rangle \frac{\partial \bar{F}_0}{\partial \mathcal{E}} + \frac{c}{B_0} \mathbf{b} \times \nabla \langle \delta L_g \rangle \cdot \nabla \bar{F}_0 \right) - \frac{c}{B_0} \mathbf{b} \times \nabla \langle \delta L_g \rangle \cdot \nabla \delta g . \quad (2.23)$$

Here, the magnetic drift velocity  $\mathbf{v}_d$  is

$$\mathbf{v}_d = \frac{\mathbf{b}}{\Omega} \times \left( \mu \nabla B_0 + \kappa v_{\parallel}^2 \right) \simeq \frac{(\mu B_0 + v_{\parallel}^2)}{\Omega} \mathbf{b} \times \boldsymbol{\kappa} , \quad (2.24)$$

where  $\nabla B_0 \simeq \boldsymbol{\kappa} B_0$  in the low- $\beta$  limit and is consistent with well-known cancellations in the linear vorticity equation, arising from the perpendicular pressure balance, Eq. (2.7), and plasma equilibrium condition (Hasegawa and Sato, 1989). In the long wavelength limit, Eq. (2.23) has to be slightly modified to account for the perturbed gyrocenter motion at  $\mathcal{O}(\epsilon_{\delta})$  being given by (Brizard and Hahm, 2007)

$$\delta \dot{\mathbf{X}}_{\perp} = \frac{c}{B_0} \mathbf{b} \times \nabla \langle \delta L_g \rangle + \frac{v_{\parallel}}{B_0} \boldsymbol{\kappa} \langle \delta A_{\parallel g} \rangle = \frac{c}{B_0} \mathbf{b} \times \nabla \langle \delta \phi_g \rangle + v_{\parallel} \frac{\langle \delta \mathbf{B}_{\perp g} \rangle}{B_0} , \quad (2.25)$$

with  $\langle \delta \mathbf{B}_{\perp g} \rangle = \nabla \times \mathbf{b} \langle \delta A_{\parallel g} \rangle$ . As shown by (Qin *et al.*, 1998, 1999b), this distinction in the long wavelength limit is important for the linear response only, for the nonlinear  $\mathbf{E} \times \mathbf{B}$  convection and nonlinear line bending are small at  $\epsilon_{\perp}^2 < \epsilon_{\omega}$  (see Sec. II.B).

The following nonlinear gyrokinetic vorticity equation (Chen *et al.*, 2001) can then be derived from Eq. (2.23) acted upon by  $\sum e e^{-\rho \cdot \nabla}$  and integrated in velocity space;

$$\begin{aligned} & B_0 \left( \nabla_{\parallel} + \frac{\delta \mathbf{B}_{\perp}}{B_0} \cdot \nabla \right) \left( \frac{\delta j_{\parallel}}{B_0} \right) - \nabla \cdot \sum \left\langle \frac{e^2 2\mu}{m \Omega^2} \left( B_0 \frac{\partial \bar{F}_0}{\partial \mathcal{E}} + \frac{\partial \bar{F}_0}{\partial \mu} \right) \left( \frac{J_0^2 - 1}{\lambda^2} \right) \right\rangle_v \nabla_{\perp} \frac{\partial}{\partial t} \delta \phi \\ & - \sum e c \mathbf{b} \times \nabla \left\langle \frac{2\mu}{\Omega^2} \bar{F}_0 \left( \frac{J_0^2 - 1}{\lambda^2} \right) \right\rangle_v \cdot \nabla \nabla_{\perp}^2 \delta \phi + \frac{c}{B_0} \mathbf{b} \times \boldsymbol{\kappa} \cdot \nabla \sum \left\langle m \left( \mu B_0 + v_{\parallel}^2 \right) J_0 \delta g \right\rangle_v \\ & + \delta \mathbf{B}_{\perp} \cdot \nabla \left( \frac{j_{\parallel 0}}{B_0} \right) + \sum e \left\langle J_0 \left[ \frac{c}{B_0} \mathbf{b} \times \nabla (J_0 \delta \phi) \cdot \nabla \delta g \right] - \frac{c}{B_0} \mathbf{b} \times \nabla \delta \phi \cdot \nabla (J_0 \delta g) \right\rangle_v \\ & + \frac{c}{B_0} \mathbf{b} \times \nabla \delta \phi \cdot \nabla \left[ \nabla \cdot \sum \left\langle \frac{e^2 2\mu}{m \Omega^2} \frac{\partial \bar{F}_0}{\partial \mu} \left( \frac{1 - J_0^2}{\lambda^2} \right) \right\rangle_v \nabla_{\perp} \delta \phi \right] = 0 . \end{aligned} \quad (2.26)$$

Here,  $J_0$  is the Bessel function of argument  $\lambda$  and  $\lambda^2 = 2\mu B_0 k_{\perp}^2 / \Omega^2$ . Nonlinear plasma behaviors enter implicitly, in the pressure curvature coupling with  $\delta g$ , and explicitly, through the perpendicular Maxwell stress (nonlinear line bending) and the next to last term on the left hand side, which can be shown to be connected with nonlinear diamagnetic response and gyrokinetic generalization of the Reynolds stress. Note that Eq. (2.26) is pertinent to the short wavelength regime ( $\epsilon_{\perp}^2 > \epsilon_{\omega}$ ), consistent with the gyrokinetic ordering discussed in Sec. II.A. In the  $\epsilon_{\perp}^2 \lesssim \epsilon_{\omega}$  long-wavelength limit, it is necessary to include an additional term on the left hand side of Eq. (2.26), due to the nonlinear polarization response; *i.e.*,

$$- \frac{c^2}{4\pi} \nabla \cdot \left( \frac{\delta \rho_m}{\rho_{m0} v_A^2} \nabla_{\perp} \frac{\partial}{\partial t} \delta \phi \right) . \quad (2.27)$$

Meanwhile, the quasineutrality condition Eq. (2.9) can be rewritten as

$$\sum \left\langle \frac{e^2}{m} \frac{\partial \bar{F}_0}{\partial \mathcal{E}} \right\rangle_v \delta \phi + \nabla \cdot \sum \left\langle \frac{e^2 2\mu}{m \Omega^2} \frac{\partial \bar{F}_0}{\partial \mu} \left( \frac{J_0^2 - 1}{\lambda^2} \right) \right\rangle_v \nabla_{\perp} \delta \phi + \sum \langle e J_0(\lambda) \delta g \rangle_v = 0 . \quad (2.28)$$

The presence of  $J_0$  and of velocity space integrals involving  $\delta g$  in Eq. (2.26) as well as in the quasineutrality condition, Eq. (2.28), shows that these governing gyrokinetic equations for DAWs are integro-differential equations. Given that  $\delta \mathbf{B}_{\perp} = [\nabla \times (\mathbf{b} \delta A_{\parallel})]_{\perp}$  and  $\delta B_{\parallel} = (\nabla \times \mathbf{b})_{\parallel} \delta A_{\parallel}$ <sup>4</sup>, these equations are closed by the nonlinear gyrokinetic equation, Eq. (2.23), along with Eq. (2.25), and by the reduced form of the parallel Ampère's law, Eq. (2.13),

$$\delta j_{\parallel} = \frac{c}{4\pi} \mathbf{b} \cdot \nabla \times (\nabla \times \delta \mathbf{A}) = \frac{c}{4\pi} \left[ -\nabla^2 + \kappa^2 + (\nabla \mathbf{b}) : (\nabla \mathbf{b}) + (\nabla \times \mathbf{b})_{\parallel}^2 \right] \delta A_{\parallel} . \quad (2.29)$$

<sup>4</sup> Note that  $\delta B_{\parallel}$  obviously includes a further contribution due to  $\delta \mathbf{A}_{\perp}$ , which ensures that Eq. (2.7) is fulfilled; this contribution is assumed to be accounted for implicitly, when using the expression of magnetic drifts given by Eq. (2.24), as discussed by (Chen and Hasegawa, 1991).

Equations (2.26) to (2.29) are the *governing gyrokinetic equations* for low- $\beta$  DAWs, adopted throughout this work to investigate their nonlinear dynamics on time scales  $\gamma_L \tau_{NL} \sim 1$ .

Equations (2.26) to (2.29) need to be supplemented by equations governing *zonal structures*, *i.e.* for fluctuations that have  $k_{\parallel} \equiv 0$  identically in the whole plasma<sup>5</sup> and play crucial roles in regulating the DAW dynamics, as shown in Sec. V. First, we note that Eqs. (2.26) and (2.28) are not independent for  $\delta\phi_z$  (Chen *et al.*, 2001), with the subscript  $z$  standing for *zonal*. While Eq. (2.26) governs the evolution of  $\delta\phi_z$ ,  $\delta A_{\parallel z}$  is governed by Eq. (2.29), with the *zonal current*  $\delta j_{\parallel z}$  computed from the solution of Eq. (2.23). Assuming, consistently throughout this review, that  $\delta j_{\parallel}$  is carried by electrons and that  $k_{\perp}^2 \delta_e^2 \sim \epsilon_{\perp}^2 \delta_e^2 / \rho_i^2 \ll 1$ , with  $\delta_e = c/\omega_{pe}$  the collisionless skin depth and  $\omega_{pe}$  the electron plasma frequency, Eq. (2.29) for the *zonal current* becomes essentially  $\delta j_{\parallel ze} \simeq 0$ , which reads

$$\frac{\partial}{\partial t} \delta A_{\parallel z} = \left( \frac{c}{B_0} \mathbf{b} \times \nabla \delta A_{\parallel} \cdot \nabla \delta \psi \right)_z, \quad (2.30)$$

after a straightforward calculation of  $\delta f_{ze}$  from Eq. (2.23), with  $\delta\psi$  defined by

$$\mathbf{b} \cdot \nabla \delta \psi \equiv -\frac{1}{c} \frac{\partial}{\partial t} \delta A_{\parallel}, \quad (2.31)$$

for given  $\delta A_{\parallel}$  with  $k_{\parallel} \neq 0$ . Note that Eq. (2.30) can also be readily derived from massless electron force balance along  $\mathbf{B}_0$ . When considering DAWs excited by EPs, Eq. (2.26) can be further reduced, and this is done in the next subsection.

### E. Drift Alfvén waves excited by energetic particles in low- $\beta$ fusion plasmas

In burning plasmas of fusion interest, EPs are characterized by an energy density, which is comparable to that of the thermal plasma, so that  $\beta_E \sim \beta$ . However, due to the significantly higher energy  $T_{0i}/T_{0E} = \mathcal{O}(10^{-2})$ , the EP density is typically low,  $n_{0E}/n_{0i} \sim T_{0i}/T_{0E}$ . Thus, it is generally possible to consider reactor relevant plasmas consisting of two components (Chen *et al.*, 1984): a core or thermal plasma component, essentially providing an isotropic Maxwellian background made of electrons ( $e$ ) and ions ( $i$ ), and an energetic component ( $E$ ), which is often anisotropic and non-Maxwellian.

A detailed discussion of the general wavelength and frequency orderings for the case of DAWs resonantly excited by EPs in space-plasmas was given by (Chen and Hasegawa, 1991) and later specialized by (Zonca and Chen, 2006) to low- $\beta$  laboratory plasmas, where

$$n_{0E}/n_{0i} \sim T_{0i}/T_{0E} = \mathcal{O}(10^{-2}) \lesssim \beta_i \sim \beta_E \lesssim \mathcal{O}(10^{-1}). \quad (2.32)$$

Meanwhile, most unstable EP driven modes are characterized by  $|k_{\theta} \rho_E| \lesssim 1$  (Berk *et al.*, 1992b; Chen, 1994; Fu and Cheng, 1992; Tsai and Chen, 1993), where  $\rho_E$  is the EP Larmor radius. More precisely, in this inequality  $\rho_E$  represents the characteristic EP magnetic drift orbit width, corresponding to the relevant wave-particle resonance and typically larger than the EP Larmor radius. Finally, thermal electrons typically have  $v_{te} \gg v_A$ , corresponding to  $\beta \gg m_e/m_i$ , and, hence, can be approximated as a massless fluid. These orderings, in addition to the general gyrokinetic orderings of Sec. II.A and the low- $\beta$  assumption used in Sec. II.D, allow us to further simplify Eqs. (2.26) and (2.28), while maintaining an accurate description of nonlinear dynamics of SAW excited by EPs in burning plasmas.

From Eq. (2.23), the thermal electron response as a massless fluid is readily obtained as

$$\left( \mathbf{b} + \frac{\delta \mathbf{B}_{\perp}}{B_0} \right) \cdot \nabla \delta g_e = - \left( \frac{e}{m_e c} \frac{\partial \delta A_{\parallel}}{\partial t} \frac{\partial \bar{F}_{0e}}{\partial \mathcal{E}} + \frac{\delta \mathbf{B}_{\perp}}{B_0} \cdot \nabla \bar{F}_{0e} \right). \quad (2.33)$$

Here,  $e$  denotes the electron charge as positive number and the part of core electron response due to particles that populate the phase space near the trapped to circulating particle boundary has been neglected. Using Eq. (2.33) for a Maxwellian electron core and recalling Eq. (2.31), the quasineutrality condition, Eq. (2.28) acted upon by  $(\mathbf{b} + \delta \mathbf{B}_{\perp}/B_0) \cdot \nabla$ , can be cast as

$$\frac{n_{0e} e^2}{T_{0e}} \left[ \mathbf{b} \cdot \nabla (\delta \phi - \delta \psi) + \frac{\delta \mathbf{B}_{\perp}}{B_0} \cdot \nabla \delta \phi \right] = \left( \mathbf{b} + \frac{\delta \mathbf{B}_{\perp}}{B_0} \right) \cdot \nabla \sum_{\neq e} (e \langle \delta f \rangle_v + e \langle \bar{F}_0 \rangle_v), \quad (2.34)$$

<sup>5</sup> See (Diamond *et al.*, 2005) for a recent review on the physics of *zonal structures*.

where  $\sum_{\neq e}$  denotes summation on particle species except for core electrons and equilibrium charge neutrality has been used explicitly. Note that Eq. (2.34) is just the extended Ohm's law

$$\left(\mathbf{b} + \frac{\delta \mathbf{B}_\perp}{B_0}\right) \cdot \delta \mathbf{E} = - \left(\mathbf{b} + \frac{\delta \mathbf{B}_\perp}{B_0}\right) \cdot \frac{\nabla P_e}{n_{0e} e}, \quad (2.35)$$

having assumed isothermal electron response. Furthermore, the ordering of Eq. (2.32) allows ignoring the contribution of EPs to the plasma density<sup>6</sup>, while the wavelength ordering  $|k_\theta \rho_E| \lesssim 1$  indicates that  $\epsilon_\perp \ll 1$  for the core plasma component. Thus, the quasineutrality condition, Eq. (2.28) or Eq. (2.34), at the lowest order reduces to the ideal MHD approximation  $\delta E_\parallel = 0$  or  $\delta \phi = \delta \psi$ .

The gyrokinetic vorticity equation is also greatly simplified with the additional ordering introduced in this subsection and readily yields

$$\begin{aligned} B_0 \left( \nabla_\parallel + \frac{\delta \mathbf{B}_\perp}{B_0} \cdot \nabla \right) \left( \frac{\delta j_\parallel}{B_0} \right) - \frac{c^2}{4\pi} \nabla \cdot \left\{ \left[ \left( 1 + \frac{\delta \varrho_m}{\varrho_{m0}} \right) \frac{1}{v_A^2} + \frac{3\pi}{B_0^2} \left( \frac{P_{0\perp i}}{\Omega_i^2} + \frac{P_{0\perp E}}{\Omega_E^2} \right) \nabla_\perp^2 \right] \nabla_\perp \frac{\partial}{\partial t} \delta \phi \right\} \\ + \frac{c^2}{4\pi} \mathbf{b} \times \nabla \left[ \frac{4\pi}{B_0^2} \left( \frac{P_{0\perp i}}{\Omega_i} + \frac{P_{0\perp E}}{\Omega_E} \right) \right] \cdot \nabla \nabla_\perp^2 \delta \phi + \frac{c}{B_0} \mathbf{b} \times \boldsymbol{\kappa} \cdot \nabla \sum \left\langle m \left( \mu B_0 + v_\parallel^2 \right) J_0 \delta g \right\rangle_v + \delta \mathbf{B}_\perp \cdot \nabla \left( \frac{j_\parallel 0}{B_0} \right) \\ + \sum_{\neq e} \frac{ec}{2\Omega^2} \left\{ \mathbf{b} \times \nabla \left( \nabla_\perp^2 \delta \phi \right) \cdot \nabla \langle \mu \delta g \rangle_v - \mathbf{b} \times \nabla \delta \phi \cdot \nabla \langle \mu \nabla_\perp^2 \delta g \rangle_v - \nabla_\perp^2 \left[ \mathbf{b} \times \nabla \delta \phi \cdot \nabla \langle \mu \delta g \rangle_v \right] \right\} = 0. \quad (2.36) \end{aligned}$$

Here, we have used the definition  $P_{0\perp} = \langle m \mu B_0 \bar{F}_0 \rangle_v$  and have adopted the long wavelength limit for both thermal and energetic ions. In this way, note that energetic ions<sup>7</sup>, even though they do not contribute to plasma inertia due to Eq. (2.32), contribute to both finite Larmor radius correction to the plasma inertia (KAW) (Briguglio *et al.*, 1998) (see Sec. IV.B.3) as well as to the diamagnetic response (Lauber *et al.*, 2012; Wang *et al.*, 2011) (see Sec. IV.B.2), for these terms depend explicitly on perpendicular pressure. Note, also, that we have omitted the long wavelength formal expansions of pressure gradient curvature coupling and nonlinear stress tensor for simplicity of notation and clarity of physics presentation.

In the case of highly energetic ions, the supra-thermal particle density is usually very low and  $\beta_E < \beta_i$ ; thus, their contribution to KAW and diamagnetic terms can be formally neglected in Eq. (2.36), which further reduces to

$$\begin{aligned} B_0 \left( \nabla_\parallel + \frac{\delta \mathbf{B}_\perp}{B_0} \cdot \nabla \right) \left( \frac{\delta j_\parallel}{B_0} \right) - \frac{c^2}{4\pi} \nabla \cdot \left\{ \left[ \left( 1 + \frac{\delta \varrho_m}{\varrho_{m0}} \right) \frac{1}{v_A^2} + \frac{3\pi}{B_0^2} \left( \frac{P_{0\perp i}}{\Omega_i^2} \right) \nabla_\perp^2 \right] \nabla_\perp \frac{\partial}{\partial t} \delta \phi \right\} \\ + \frac{c^2}{4\pi} \mathbf{b} \times \nabla \left[ \frac{4\pi}{B_0^2} \left( \frac{P_{0\perp i}}{\Omega_i} \right) \right] \cdot \nabla \nabla_\perp^2 \delta \phi + \frac{c}{B_0} \mathbf{b} \times \boldsymbol{\kappa} \cdot \nabla \sum \left\langle m \left( \mu B_0 + v_\parallel^2 \right) J_0 \delta g \right\rangle_v + \delta \mathbf{B}_\perp \cdot \nabla \left( \frac{j_\parallel 0}{B_0} \right) \\ + \sum_{\neq e} \frac{ec}{2\Omega^2} \left\{ \mathbf{b} \times \nabla \left( \nabla_\perp^2 \delta \phi \right) \cdot \nabla \langle \mu \delta g \rangle_v - \mathbf{b} \times \nabla \delta \phi \cdot \nabla \langle \mu \nabla_\perp^2 \delta g \rangle_v - \nabla_\perp^2 \left[ \mathbf{b} \times \nabla \delta \phi \cdot \nabla \langle \mu \delta g \rangle_v \right] \right\} = 0. \quad (2.37) \end{aligned}$$

Here, the nonlinear term is due to thermal ions only. It is also worthwhile noting that  $\beta_E < \beta_i$  is expected in reactor relevant plasma conditions, where  $\beta_E \sim (\tau_{sd}/\tau_E)\beta_i$  and the energetic ion (collisional) slowing down time on thermal electrons,  $\tau_{sd}$ , is short compared to the thermal energy confinement time  $\tau_E$ . In the drift kinetic limit (vanishing Larmor radius), assuming  $J_0 = 1$  in the pressure gradient curvature coupling term, Eq. (2.37) correctly describes both small and large magnetic drift orbit limit for supra-thermal ions, reproducing their nearly adiabatic response to short wavelength modes (Zonca and Chen, 2006). Since magnetic drift orbits of highly supra-thermal particles are typically much larger than their Larmor radius, considering the drift-kinetic limit and the possibility of large magnetic drift orbit energetic ions can be done in a physically consistent fashion and adequately renders both resonant as well as non-resonant supra-thermal particle dynamics (Zonca and Chen, 2006). This is crucial for the validity of many of the hybrid MHD-gyrokinetic descriptions of SAW excitations by energetic ions (Briguglio *et al.*, 1995, 1998; Park *et al.*, 1999, 1992; Todo and Sato, 1998; Todo *et al.*, 1995), which have provided the first successful numerical simulation approach to this problem.

In the linear limit, Eq. (2.37) coincides with the gyrokinetic vorticity equation discussed by (Qin *et al.*, 1998, 1999b) and, dropping KAW and diamagnetic terms as well, with the reduced form of the linear kinetic-MHD model by (Brizard, 1994).

<sup>6</sup> In doing so, some attention must be paid for applications to present day experiments, where supra-thermal particles may not be as energetic and low-density as estimated in Eq. (2.32).

<sup>7</sup> Supra-thermal electrons, if present, give a negligible contribution to KAW and diamagnetic terms.

## F. Remarks on drift Alfvén wave equations adopted in numerical simulations

In the limit, as discussed in Sec. II.B, that one may self-consistently neglect the  $\delta B_{\parallel}$  magnetic compression terms, a complete gyrokinetic description can then be obtained in terms of  $(\delta\phi, \delta A_{\parallel})$  by means of Eqs. (2.9) and (2.29) with

$$\delta j_{\parallel} = \sum e \langle v_{\parallel} \delta f \rangle_v ; \quad (2.38)$$

*i.e.*, the quasineutrality condition, and the parallel Ampère's law. This approach has been adopted as basis for recent developments of nonlinear gyrokinetic codes, which are able to address the physics of Alfvén waves and EPs in burning plasmas (Bass and Waltz, 2010; Bottino *et al.*, 2011; Chen and Parker, 2001, 2007; Deng *et al.*, 2012a; Görler *et al.*, 2011; Holod *et al.*, 2009), and whose simulation results can then be compared with hybrid kinetic-MHD (Briguglio *et al.*, 1995, 1998; Park *et al.*, 1999, 1992; Todo, 2006; Todo and Sato, 1998; Todo *et al.*, 1995, 2005; Wang *et al.*, 2011) and gyrofluid codes (Kendl *et al.*, 2010; Spong *et al.*, 1992, 1994).

In the long wavelength limit (cf. Sec. II.E), Eqs. (2.26) to (2.29) reduce to Eqs. (2.34) to (2.37) and recover reduced MHD as a well-known limiting case of nonlinear gyrokinetic theory (Brizard, 1992; Hahm *et al.*, 1988) and, with the inclusion of supra-thermal particles, they yield the hybrid MHD-gyrokinetic description of SAW excitations by energetic ions (Briguglio *et al.*, 1995, 1998; Park *et al.*, 1999, 1992; Todo and Sato, 1998; Todo *et al.*, 1995). Equations (2.34) to (2.37) in the long wavelength limit also describe kinetic interactions of low-frequency DAWs with thermal plasma (Wang *et al.*, 2011), which also play crucial roles in linear as well as nonlinear physics of toroidal plasmas (cf. Secs. IV.B.2 and V.C).

On longer time scales  $\sim \epsilon_B^{-1} \epsilon_{\omega}^{-1} \Omega^{-1} \sim \epsilon_{\omega}^{-2} \Omega^{-1}$ ,  $\delta B_{\parallel}$  may still be explicitly solved for via perpendicular pressure balance Eq. (2.7) and nonlinear magnetic field compression effects can be neglected, provided that the self-consistency requirements on linear and nonlinear rates are satisfied. However, Eq. (2.23) is not sufficiently accurate on these time scales and the gyrokinetic Lagrangian field theory (Brizard, 2000; Sugama, 2000) is needed for a self-consistent description of nonlinear gyrokinetic equation and  $(\delta\phi, \delta A_{\parallel}, \delta B_{\parallel})$  field equations, yielding exact conservation laws. The corresponding form of gyrofluid equations with finite-gyroradius electromagnetic nonlinearities and exact conservation properties has been given by (Scott, 2010).

Within the same theoretical framework, the fluid equation approach, discussed in Sec. II.B can be equivalently adopted, based on the continuity equation and the force balance equation, Eq. (2.14), where the stress tensor is computed from the particle distribution function, obtained by solution of the nonlinear gyrokinetic equation, as specified by Eq. (2.16). The fluctuating current, meanwhile, is obtained from  $\delta \mathbf{j} = (c/4\pi) \nabla \times \delta \mathbf{B}$  and  $\delta \mathbf{E}$  from a suitable form of kinetic Ohm's law, *e.g.*, derived from Eq. (2.34) (Vlad *et al.*, 2011; Wang *et al.*, 2010a).

Finally, we note that many linear codes exist, which can investigate the stability properties of DAWs in burning plasmas. It is beyond the scope of the present work to give a comprehensive survey of them. Relevant linear simulation results will be discussed in the corresponding parts of Secs. IV.B and IV.C. Here, as noted in Sec. II.E, we merely remind that the linearized Eqs. (2.34) to (2.37) in the long wavelength limit reproduce the model equations discussed by (Qin *et al.*, 1998, 1999b) and used for numerical simulation of Alfvénic modes excited by fast ions (Lauber *et al.*, 2009, 2007, 2005).

## III. LINEAR ALFVÉN WAVE PHYSICS IN ONE-DIMENSIONAL NONUNIFORM PLASMAS

Shear Alfvén waves (SAWs) are anisotropic electromagnetic waves existing in magnetized plasmas, which have parallel wavelengths,  $\lambda_{\parallel} \sim L_{\parallel}$ , comparable to the system size along the equilibrium magnetic field,  $\mathbf{B}_0$ . They can, however, have a wide range in the perpendicular wavelengths  $\lambda_{\perp}$ ,  $\rho_i < \lambda_{\perp} < L_{\perp}$ , with  $\rho_i$  the ion Larmor radius and  $L_{\perp}$  the system size perpendicular to  $\mathbf{B}_0$ . The SAW frequency is  $\omega \simeq k_{\parallel} v_A \sim \mathcal{O}(v_A/L_{\parallel})$  much less than the ion cyclotron frequency  $\Omega_i$ , with  $v_A = B_0/\sqrt{4\pi\varrho_{m0}}$  the Alfvén speed. Here, notations are those introduced in Sec. II.

SAW dynamics is, hence, of low frequency and macroscopic scales and, therefore, may cause significant perturbations in the bulk of the plasma. Furthermore, SAW dynamics is nearly incompressible, whereas compressional Alfvén (CAW) and slow sound waves tend to be stabilized by finite magnetic and/or plasma compression as well as finite ion Landau damping. These are the primary reasons why shear Alfvén waves play many important roles in laboratory and space plasmas. Some examples are (1) heating of laboratory (Chen and Hasegawa, 1974a; Grossman and Tataronis, 1973; Hasegawa and Chen, 1974; Tataronis, 1975) and solar corona plasmas (Ionson, 1982); (2) resonant interactions with energetic ions produced during high-power neutral beam and/or radio-frequency laboratory heating experiments or with alpha particles produced in D-T fusion plasmas (Belikov *et al.*, 1968, 1969; Chen, 1988; Fu and Van Dam, 1989a,b; Kolesnichenko, 1980; Kolesnichenko and Oraevskij, 1967; Mikhailovskii, 1975a,b; Rosenbluth and Rutherford, 1975;

Tsang *et al.*, 1981), which is the main subject of this review work; (3) cross-field transport in magnetospheric plasmas; *e.g.*, the dayside magnetopause (Hasegawa and Mima, 1978); and (4) acceleration of electrons along the auroral field lines (Hasegawa, 1976).

One of the unique and most important properties of SAW is that its group velocity  $\mathbf{v}_g$  is directed along  $\mathbf{B}_0$ ; *i.e.*,  $\mathbf{v}_g \simeq \mathbf{v}_A$ . In nonuniform plasmas with spatially varying  $v_A$  this property can then lead to singular oscillations at the local SAW frequency, for the wave energy is “confined” to the local field line. As the local SAW frequency varies continuously, we then have oscillations which constitute the so-called shear Alfvén continuous spectrum or SAW continuum (Grad, 1969). The existence of SAW continuum then suggests that at the layer where the frequency of the applied radio-frequency source matches the local SAW frequency, the wave equation has a singular point; leading to resonant wave absorption and the Alfvén wave heating scheme (Chen and Hasegawa, 1974a,b; Grossman and Tataronis, 1973; Hasegawa and Chen, 1974). That the wave solution becomes singular is, of course, due to the inadequacy of ideal MHD approximation. Including microscopic kinetic effects, such as finite ion Larmor radii, removes the singular behaviors by allowing small but finite  $\mathbf{v}_g$  across  $\mathbf{B}_0$ . That is, we have the linear mode conversion of resonant SAW to the kinetic Alfvén wave (KAW) (Hasegawa and Chen, 1975, 1976).

These fundamental concepts and processes of SAW in nonuniform plasmas are reviewed in this section, using the simplified description of a 1D plasma equilibrium. We also discuss the existence of Global Alfvén Eigenmodes (GAE) (Appert *et al.*, 1982; Goedbloed, 1984; Mahajan *et al.*, 1983; Ross *et al.*, 1982) as global modes in a cylindrical plasma.

### A. Shear Alfvén Waves: continuous spectrum and Global Alfvén Eigenmodes

We consider the simple configuration of a 1D plasma slab confined in straight magnetic field (Chen and Hasegawa, 1974a; Goedbloed, 1984). The equilibrium quantities (plasma density, pressure and magnetic field) are assumed to vary only along the  $x$  direction ( $\varrho_0 = \varrho_0(x)$ ,  $P_0 = P_0(x)$ ,  $\mathbf{B}_0 = \mathbf{B}_0(x)$ ) and the equilibrium magnetic field is assumed to have a shear component,

$$\mathbf{B}_0(x) = B_{0y}(x)\mathbf{e}_y + B_{0z}(x)\mathbf{e}_z. \quad (3.1)$$

Introducing the standard notation for the displacement vector  $\delta\mathbf{u} \equiv \partial_t\delta\xi$ , the force balance equation Eq. (2.14) can be written as

$$\varrho_{m0}\frac{\partial^2}{\partial t^2}\delta\xi = -\nabla\left(\delta P + \frac{B_0\delta B_{\parallel}}{4\pi}\right) + \frac{1}{4\pi}(\mathbf{B}_0 \cdot \nabla)^2\delta\xi - \frac{1}{4\pi}\mathbf{B}_0(\mathbf{B}_0 \cdot \nabla)(\nabla \cdot \delta\xi). \quad (3.2)$$

Using unit vectors ( $\mathbf{e}_x, \mathbf{e}_{\perp}, \mathbf{b}$ ), with  $\mathbf{e}_{\perp} \equiv \mathbf{b} \times \mathbf{e}_x$ , and standard Fourier plane wave representation,  $\delta\xi_{\parallel}$  can be solved in terms of  $\delta\xi_x$  and  $\delta\xi_{\perp}$ . Equation (3.2) then yields

$$\delta\xi_{\perp}(x) = \frac{i\bar{\alpha}k_{\perp}}{\bar{\alpha}k_{\perp}^2 - D_A} \frac{d\delta\xi_x}{dx}, \quad (3.3)$$

$$\frac{d}{dx}\left(\frac{B_0^2 D_A \bar{\alpha}}{\bar{\alpha}k_{\perp}^2 - D_A} \frac{d\delta\xi_x}{dx}\right) - B_0^2 D_A \delta\xi_x = 0, \quad (3.4)$$

where  $D_A \equiv (\omega^2/v_A^2) - k_{\parallel}^2$ ,  $k_{\parallel} = (k_y B_{0y} + k_z B_{0z})/B_0$ ,  $k_{\perp} = (k_y B_{0z} - k_z B_{0y})/B_0$ , and

$$\bar{\alpha}(x) \equiv 1 + \frac{\Gamma\beta\omega^2}{2\omega^2 - \Gamma\beta k_{\parallel}^2 v_A^2}, \quad (3.5)$$

where  $\Gamma$  stands for the ratio of specific heats. Equation (3.4) describes SAWs coupled with fast and slow magnetoacoustic waves by equilibrium nonuniformities. It has to be noted that the differential equation, Eq. (3.4) is singular at the points where  $B_0^2 D_A \bar{\alpha} = 0$ , which correspond to the appearance of two continuous spectra defined by

$$\omega^2 = \omega_A^2(x) \equiv k_{\parallel}^2(x)v_A^2(x), \quad (3.6)$$

and

$$\omega^2 = \omega_S^2(x) \equiv \frac{v_S^2(x)k_{\parallel}^2(x)}{1 + v_S^2(x)/v_A^2(x)}, \quad (3.7)$$

with  $v_S^2(x) = \Gamma P_0(x)/\rho_{m0}(x)$  representing the sound speed.

To further gain some insights into properties of SAWs and the continuous spectrum, we further assume that while the equilibrium plasma density varies along  $x$ ,  $\rho_0 = \rho_0(x)$ , the equilibrium magnetic field has no shear and is uniform;  $\mathbf{B}_0 = B_0 \mathbf{e}_z$ , with the plasma being confined by two perfectly conducting plates at  $z = 0$  and  $z = L$  (Chen and Zonca, 1995). Moreover, let us adopt the slow sound wave approximation [ $\Gamma\beta \rightarrow 0$ , or  $\bar{\alpha} \rightarrow 1$  in Eq. (3.4)] to reduce Eq. (3.4) to the description of the coupled SAWs and CAWs. This approach is the same as that adopted by (Chen, 1990) for the theoretical description of ultra-low frequency magnetic pulsations in the Earth's magnetosphere. Note that in this limit it is sufficient to consider the perpendicular components of the force balance equation, Eq. (3.2), which does not depend on the parallel component of the displacement  $\delta\xi_{\parallel}$ ,

$$D_A \delta\xi_{\perp} = \nabla_{\perp} \left( \frac{\delta B_{\parallel}}{B_0} \right), \quad (3.8)$$

with the parallel component of the perturbed magnetic field given by  $\delta B_{\parallel}/B_0 = -\nabla \cdot \delta\xi_{\perp}$ . Meanwhile,  $\nabla_{\perp} = \mathbf{e}_y i k_y + \mathbf{e}_x (\partial/\partial x)$  and the local shear Alfvén operator  $D_A$  is now expressed as  $D_A \equiv \omega^2/v_A^2 + \partial_z^2$ . Following (Chen and Zonca, 1995), all perturbed fields  $f$  are assumed to be decomposed in the complete orthonormal set of shear Alfvén eigenfunctions  $\psi_{A\ell}(z|x) = (2/Lv_A^2)^{1/2} \sin k_{\ell} z$ , with  $k_{\ell} = \ell\pi/L$  and  $\omega_{A\ell}^2(x) = k_{\ell}^2 v_A^2(x)$  defining the local SAW continuous spectrum frequency; *i.e.*,

$$f(\mathbf{r}, t) = e^{-i(\omega t - k_y y)} \sum_{\ell=1}^{\infty} \hat{f}_{\ell}(x_0, x_1) \psi_{A\ell}(z|x_1). \quad (3.9)$$

Note that in Eq. (3.9), the existence of continuous frequency spectra, with a corresponding singular eigenfunction behavior, has been explicitly taken into account by introducing “fast”  $x_0$  (singular) and “slow”  $x_1$  (equilibrium) radial variables. The existence of two spatial scales ( $x_0$  and  $x_1$ ) can be used to solve Eq. (3.8) via asymptotic expansions of the fluctuating fields  $\hat{f}_{\ell} = \hat{f}_{\ell}^{(0)} + \hat{f}_{\ell}^{(1)} + \dots$ , where  $|\hat{f}_{\ell}^{(1)}/\hat{f}_{\ell}^{(0)}| \approx |\partial_{x_1}/\partial_{x_0}|$  etc. With the definition of Eq. (3.9) applied to  $\delta\xi_x$ , and considering that  $|D_A| \ll k_y^2$  (*i.e.*,  $k_{\parallel}^2 \ll k_y^2$ ) for a typical SAW, Eq. (3.8) becomes, at the lowest order,

$$\left[ \frac{\partial}{\partial x_0} \epsilon_{A\ell} \frac{\partial}{\partial x_0} - k_y^2 \epsilon_{A\ell} \right] \delta\hat{\xi}_{x\ell}^{(0)} = 0, \quad (3.10)$$

where  $\epsilon_{A\ell} = \omega^2 - \omega_{A\ell}^2(x)$ . Equation (3.10) has solutions which become singular at the radial positions  $x_{R\ell}$  where the “local dispersion relation”,  $\epsilon_{A\ell} = 0$  [ $\omega^2 = \omega_{A\ell}^2(x_{R\ell})$ ], is satisfied; *i.e.*, at those positions where the SAW continuous spectrum is resonantly excited. A natural definition of the “fast” (singular) variable is  $x_0 \equiv x - x_{R\ell}$ , since  $\epsilon_{A\ell} = \epsilon'_{A\ell}(x_1)x_0$ . In this way, it is readily shown that eq. (3.10) has solutions of the form

$$\delta\hat{\xi}_{x\ell}^{(0)} = \frac{C_{\ell}(x_1)}{\epsilon'_{A\ell}(x_1)} \ln(x_0). \quad (3.11)$$

Meanwhile, Eq. (3.8) can be used to demonstrate that, at the lowest order,  $\nabla \cdot \delta\hat{\xi}_{\perp\ell}^{(0)} = 0$ , from which

$$\delta\hat{\xi}_{y\ell}^{(0)} = \frac{i}{k_y} \partial_{x_0} \delta\hat{\xi}_{x\ell}^{(0)} = \frac{i C_{\ell}(x_1)}{k_y \epsilon'_{A\ell}(x_1)} \frac{1}{x_0}. \quad (3.12)$$

Using Eq. (3.12) along with the  $y$ -component of Eq. (3.8), it is possible to show that  $\delta B_{\parallel}$  is given by

$$\delta B_{\parallel} = e^{-i(\omega t - k_y y)} \sum_{\ell=1}^{\infty} \delta\hat{b}_{\parallel\ell}(x_1) \psi_{A\ell}(z|x_1), \quad (3.13)$$

where  $\delta\hat{b}_{\parallel\ell}$  are functions of the “slow” (equilibrium) radial variable  $x_1$  only; *i.e.*,

$$\frac{\delta\hat{b}_{\parallel\ell}(x_1)}{B_0} = \frac{\epsilon'_{A\ell}(x_1)x_0}{i k_y v_A^2(x_1)} \delta\hat{\xi}_{y\ell}^{(0)} = \frac{C_{\ell}(x_1)}{k_y^2 v_A^2(x_1)}. \quad (3.14)$$

In a non-uniform plasma, Eqs. (3.11), (3.12) and (3.14) show that SAWs and CAWs are coupled together and give origin to singular solutions corresponding to the “local” SAW oscillations with continuous spectrum  $\omega^2 = \omega_{A\ell}^2(x)$ . In fact, SAW group is directed along the magnetic field lines ( $z$ -direction in the present case), whereas the CAW

generally carries energy across the field itself. Thus, the latter one “piles up” wave energy at the radial location where the SAW spectrum is resonantly excited, explaining the origin of “local singular oscillations” (Chen and Zonca, 1995).

Resonant excitation allows us to introduce the concept of SAW resonant absorption (Chen and Hasegawa, 1974a,b). In fact, a finite amount of wave energy can be absorbed at the resonant layer,  $x_{R\ell}$  and the time-averaged energy absorption rate,  $d\langle W \rangle/dt$ , is given by the Poynting energy flux into the infinitely narrow layer at  $x_{R\ell}$

$$\frac{d\langle W \rangle}{dt} = \frac{L_y k_y^2}{8} \sum_{\ell=1}^{\infty} \frac{|\omega_{\mathcal{A}\ell}(x_{R\ell})|}{|\epsilon'_{\mathcal{A}\ell}(x_{R\ell})|} \left| \delta \hat{b}_{\parallel\ell}(x_{R\ell}) \right|^2 = \frac{L_y L}{8k_y^2} B_0^2 \sum_{\ell=1}^{\infty} |\omega'_{\mathcal{A}\ell}(x_{R\ell})| \ell^2 \left| \Delta \delta \hat{\xi}_{x\ell}^{(0)} \right|^2 / (L^3 v_A^2). \quad (3.15)$$

Here,  $\Delta \delta \hat{\xi}_{x\ell}^{(0)}$  is the jump of  $\delta \hat{\xi}_{x\ell}^{(0)}$  across the singular layer [cf. Eq. (3.11)]

$$\Delta \delta \hat{\xi}_{x\ell}^{(0)} = -i\pi \operatorname{sgn} \left( \frac{\omega}{\epsilon'_{\mathcal{A}\ell}(x_{R\ell})} \right) \frac{C_{\ell}(x_{R\ell})}{\epsilon'_{\mathcal{A}\ell}(x_{R\ell})}.$$

Thus, Eq. (3.15) demonstrates resonant energy absorption at a rate  $\propto \omega'_{\mathcal{A}\ell}$ . In turn, the resonant energy absorption of a given initial perturbation takes place on time scales  $\approx (\omega'_{\mathcal{A}\ell} \Delta x)^{-1}$ , with  $\Delta x$  the perturbation “radial” extent<sup>8</sup>.

The existence of the resonant energy absorption mechanism becomes evident also when one analyzes the time asymptotic response of the system to initial perturbations. In fact, as  $\omega_{\mathcal{A}\ell} t \rightarrow \infty$ , one essentially has  $|\partial_x| \gg |k_y|$  and, thus, the relevant equation that describes the time asymptotic response is [cf. Eq. (3.10)]:

$$\partial_x [\partial_t^2 + \omega_{\mathcal{A}\ell}^2(x)] \partial_x \delta \hat{\xi}_{x\ell}(x, t) = 0. \quad (3.16)$$

Equation (3.16) can be straightforwardly integrated once and it yields

$$\partial_x \delta \hat{\xi}_{x\ell}(x, t) = \hat{C}_{\ell}(x) e^{\pm i\omega_{\mathcal{A}\ell}(x)t}, \quad (3.17)$$

where  $\hat{C}_{\ell}(x)$  depends on equilibrium non-uniformities. Now, note that  $\partial_x \cong \pm i\omega'_{\mathcal{A}\ell}(x)t$  as  $\omega_{\mathcal{A}\ell} t \rightarrow \infty$  and, thus,

$$\delta \hat{\xi}_{x\ell}(x, t) = \mp i \frac{\hat{C}_{\ell}(x)}{\omega'_{\mathcal{A}\ell}(x)t} e^{\pm i\omega_{\mathcal{A}\ell}(x)t}. \quad (3.18)$$

Meanwhile, noting Eq. (3.12), one readily derives

$$\delta \hat{\xi}_{y\ell}(x, t) = (i/k_y) \hat{C}_{\ell}(x) e^{\pm i\omega_{\mathcal{A}\ell}(x)t}. \quad (3.19)$$

Equations (3.17) and (3.19) give us further insight in the dynamics associated with the resonant excitation of the SAW continuum and resonant wave absorption: the  $\delta \hat{\xi}_{x\ell}$  component exhibits the characteristic  $(1/t)$  decay via phase mixing of the continuous spectrum (Barston, 1964; Grad, 1969; Sedláček, 1971), whereas  $\delta \hat{\xi}_{y\ell}$  shows undamped oscillations at frequencies corresponding to the SAW continuum.

These theoretical discussions on SAW continuous spectrum and phase mixing are nicely demonstrated by the satellite observations of magnetic field fluctuations in the Earth’s magnetosphere (Engebretson *et al.*, 1987). Figure 1 shows a color frequency-time spectrogram of AMPTE CCE magnetic field data for the interval 02 : 30 to 17 : 30 March 6, 1987. The satellite orbit was radially outward from about  $4R_E$  (Earth radius) and reached its apogee at  $9.1R_E$  around 10 : 00 UT. Power at frequencies from 0 to 80 mHz in each of the three orthogonal components is color coded according to the color bar shown at the right side of the figure. From top to bottom the components are  $B_R$ , radially outward from the center of the Earth;  $B_E$ , magnetically eastward; and  $B_N$  points approximately along local magnetic field lines. Thus,  $B_R$ ,  $B_E$  and  $B_N$  correspond to, respectively,  $\delta B_x(\delta \hat{\xi}_x)$ ,  $\delta B_y(\delta \hat{\xi}_y)$ ,  $\delta B_{\parallel}$ . In Fig. 1, the center ( $B_E$ ) panel clearly shows the continuous spectra of the various SAW harmonics along the field line. Meanwhile, there are no such clear spectral structures in  $B_R$ , due to  $\propto 1/t$  phase mixing, Eq. (3.17), as well as in  $B_N$ , as the compressional MHD waves are associated with solar-wind perturbations at the magnetospheric boundary (Chen and Hasegawa, 1974a,b). The same behaviors, including the  $\propto 1/t$  amplitude decay, have also been demonstrated by ideal MHD initial value numerical simulations of Alfvén wave dynamics in a cylindrical plasma (Vlad *et al.*, 1999).

In addition to the local oscillations of the SAW continuum, a Global Alfvén Eigenmode (GAE) (Appert *et al.*, 1982; Goedbloed, 1984; Mahajan *et al.*, 1983; Ross *et al.*, 1982) may also exist in a 1D nonuniform plasma. Such global

---

<sup>8</sup> Here, “radial” stands for the direction of nonuniformity, which is generally identified as the gradient of the equilibrium magnetic flux.

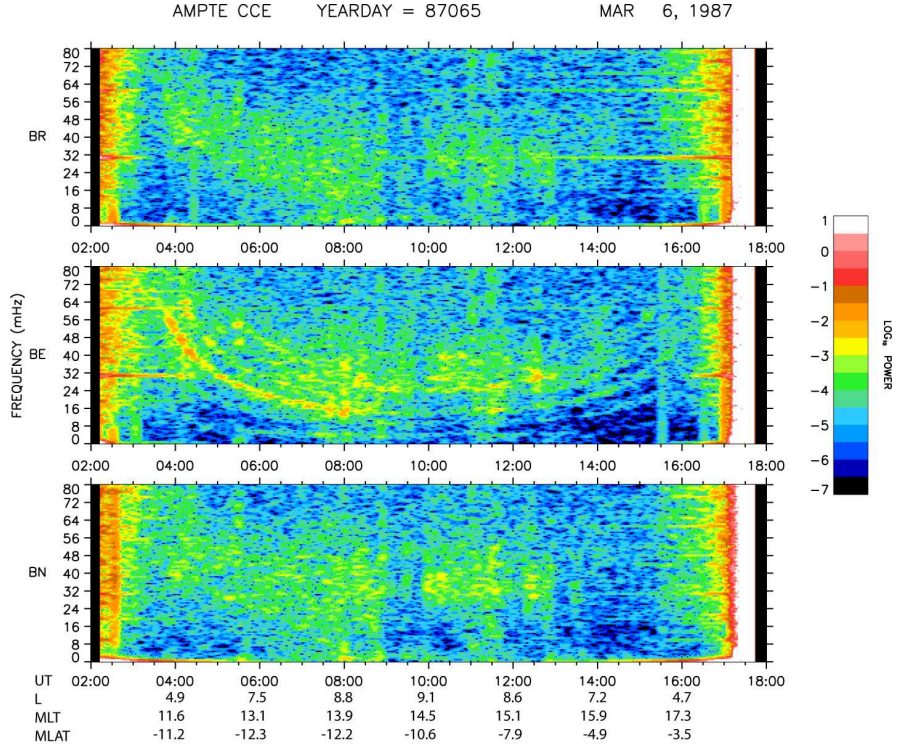


FIG. 1 Three-component dynamic power spectrum of magnetic field data from AMPTE CCE satellite for a full orbit from 02 : 30 to 17 : 30 UT March 6, 1987 (Engebretson, 2011). The geomagnetic  $B_R$ ,  $B_E$ , and  $B_N$  coordinate system used is described in the text. The colored panel represents  $\Delta B$ , the difference in field magnitude between the observed total field and the value determined from the International Geomagnetic Reference Field (IGRF) 1980 model. Apogee is at the center of the figure. Original data were published and discussed in (Engebretson *et al.*, 1987).

modes, if destabilized by energetic particles, could affect charged particle confinement over a large region of the plasma. Equation (3.15) demonstrates that, in order to minimize damping due to coupling with the SAW continuum, global mode structures are preferentially excited near regions where the resonant energy absorption rate  $\propto \omega'_{Al}$  vanishes; *i.e.*, near an extremum of the SAW continuous spectrum (cf. Sec. IV for further discussions). Detailed analyses of the mode structures, frequencies, and stability properties can be found in (Appert *et al.*, 1982; Goedbloed, 1984; Mahajan, 1995; Mahajan *et al.*, 1983; Ross *et al.*, 1982).

Global Alfvén Eigenmodes are generally considered to be benign in tokamak plasmas, because, in a two-dimensional (2D) equilibrium, toroidicity acts as a stabilizing effect (Cheng *et al.*, 1988; Fu *et al.*, 1989; Li *et al.*, 1987; Weiland *et al.*, 1987). In fact, different poloidal harmonics are coupled together and GAEs are very easily damped due to their coupling with the SAW continuous spectrum.

## B. Kinetic Alfvén Waves

Equations (3.18) and (3.19) suggest that the radial wave-vector is

$$|k_x| \cong |\omega'_{Al}(x)t|$$

and, thus,  $|k_x| \rightarrow \infty$  as  $t \rightarrow \infty$ ; *i.e.*, the wave function becomes singular in the asymptotic time limit, in agreement with eq. (3.11). The wave function singularity that emerges in the asymptotic time limit is a clear indication of the break down of the ideal MHD model, which fails when very short scale perturbations are excited. Typically, the most relevant new (with respect to the ideal MHD model) dynamics that appear on short scales are associated with charge separation, *i.e.*, with the finite parallel electric field fluctuations ( $\delta E_{\parallel}$ ) due to, *e.g.*, finite ion Larmor radius ( $\rho_i$ ), small but finite electron inertia and finite plasma resistivity. In the presence of finite  $\delta E_{\parallel}$ , additional effects due to wave-particle interactions appear, which yield collisionless wave dissipation (Landau damping). Incorporating such “kinetic” effects essentially allows finite energy propagation across the resonant surfaces  $x = x_{R\ell}$ . Thus, wave energy

will no longer “pile up” at these radial locations and, as a consequence, all wave-function singularities are removed on short scales.

A dedicated monograph on the Kinetic Alfvén Wave (KAW) is given by the recent book by (Wu, 2012). Here, we limit our discussion to the case in which  $m_e/m_i \ll \beta_e \ll 1$  (with  $\beta_e$  being the ratio between the electron kinetic and magnetic pressures), *i.e.*, the electron thermal speed is much larger than the Alfvén velocity. Furthermore, for the sake of simplicity, we also assume  $(k_x^2 + k_y^2)\rho_i^2 \equiv k_\perp^2\rho_i^2 \ll 1$ . It is then possible to show that Eq. (3.10) becomes (Chen and Zonca, 1995; Hasegawa and Chen, 1975, 1976)

$$[\omega^2 \nabla_\perp^2 \rho_K^2 \nabla_\perp^2 + \nabla_\perp \cdot \epsilon_{A\ell} \nabla_\perp] \delta \hat{\xi}_{x\ell} = 0, \quad (3.20)$$

where

$$\rho_K^2 = \left[ \frac{3}{4} (1 - i\delta_i) + \frac{T_e}{T_i} (1 - i\delta_e) \right] \rho_i^2 - i \frac{c^2 \eta}{4\pi\omega}. \quad (3.21)$$

Here,  $\delta_i$  and  $\delta_e$  indicate, respectively, ion and electron Landau damping contributions, whereas the term proportional to  $\eta$  is due to finite plasma resistivity. Equation (3.20) is readily derived from the linearized Eqs. (2.34) to (2.37), dropping magnetic curvature and diamagnetic terms in the vorticity equation, and adding resistive dissipation in the parallel Ohm’s law (cf. Sec. IV.B for more detailed derivations).

In Eq. (3.20), the singularity at  $\epsilon_{A\ell} = 0$  is clearly removed by the term including the 4th order derivative, which is also proportional to  $\rho_K^2 \ll 1$ , indicating the formation of a “boundary layer” around the SAW resonant surface. In fact, Eq. (3.20) describes the mode-conversion of a long wavelength MHD mode (the SAW) to a short wavelength kinetic mode: the KAW (Hasegawa and Chen, 1975, 1976). The rate at which KAWs are excited is exactly that of Eq. (3.15). Thus, the resonant energy absorption rate of SAW may be interpreted as a power transfer to short wavelength modes, which, eventually, may be absorbed by the background plasma. Note, however, that resonant absorption of the MHD wave and KAW dissipation are mutually independent processes. Indeed, Eq. (3.15) itself is independent on the details of the dissipation mechanism<sup>9</sup>.

The WKB local dispersion relation of KAW’s is

$$\omega^2 = (1 + k_\perp^2 \rho_K^2) \omega_{A\ell}^2. \quad (3.22)$$

Equation (3.22) indicates that KAW’s are propagating for  $\epsilon_{A\ell} > 0$  and become cut-off for  $\epsilon_{A\ell} < 0$ . Assuming that  $\omega_{A\ell}(x) \simeq \omega_{A\ell}(x_{R\ell})(1 + \kappa\zeta)$  near the resonance absorption layer, with  $\zeta = x - x_{R\ell}$  and  $\kappa = (d/dx_{R\ell}) \ln \omega_{A\ell}(x_{R\ell}) > 0$ , Eq. (3.20) becomes (Hasegawa and Chen, 1976)

$$\left( \rho_K^2 \frac{d^2}{d\zeta^2} + \kappa\zeta \right) \delta \hat{\xi}_{x\ell} = \delta \hat{\xi}_{x\ell 0}. \quad (3.23)$$

General solutions of Eq. (3.23) are written in terms of Airy functions and have the following form away from the SAW resonant absorption (mode conversion) layer

$$\delta \hat{\xi}_{x\ell} = \frac{\delta \hat{\xi}_{x\ell 0}}{\kappa\zeta} \quad \zeta < 0, \quad (3.24)$$

$$\delta \hat{\xi}_{x\ell} = \frac{\delta \hat{\xi}_{x\ell 0}}{\kappa\zeta} - \frac{\pi^{1/2} \delta \hat{\xi}_{x\ell 0}}{(\kappa\rho_K)^{2/3}} \left( \frac{\rho_K^{2/3}}{\kappa^{1/3}\zeta} \right)^{1/4} \exp \left\{ i \left[ \frac{2}{3} \left( \frac{\kappa^{1/3}\zeta}{\rho_K^{2/3}} \right)^{3/2} + \frac{\pi}{4} \right] \right\} \quad \zeta > 0. \quad (3.25)$$

Equation (3.24) represents the behavior of the long wavelength SAW, while Eq. (3.25) shows both long wavelength SAW and short wavelength KAW after mode conversion at  $\zeta = 0$  ( $x = x_{R\ell}$ ).

That KAW possesses finite  $\delta E_\parallel$  not only modifies the linear wave properties but also, perhaps more significantly, the nonlinear particle and wave dynamics. More specifically,  $\delta E_\parallel$  may lead to phase space transports; *i.e.*, heating, acceleration and cross-field transports (Chen, 1999; Hasegawa and Chen, 1976). In addition, KAW could break the so called nonlinear pure “Alfvénic state” (Alfvén, 1942, 1950; Elsasser, 1956; Hasegawa and Sato, 1989; Walén, 1944) (cf. Sec. V.B) and leads to enhanced rates of nonlinear mode-coupling effects; such as parametric decay

---

<sup>9</sup> The linear effects of nonlocal absorption of KAW are discussed in Sec. IV.C, while some of the nonlinear consequence of this interesting phenomenon are briefly presented in Sec. VII.

instabilities (DuBois and Goldman, 1965, 1967; Kaw and Dawson, 1969; Nishikawa, 1967) (cf. Sec. V.B) as well as generation of convective cells or zonal structures (Hasegawa *et al.*, 1979) (cf. Secs. V.B and V.C).

In the presence of non-ideal terms, as, *e.g.*, resistivity or finite Larmor radius effects, other discrete, closely spaced (in frequency), localized (in radius) kinetic GAE modes (KGAEs) also exist in addition to GAEs (Mahajan, 1995) (cf. Sec. III.A). These modes “replace” the Alfvén continuous spectrum, due to the trapping of KAW as a bound state in the radial region where the mode frequency exceeds the local SAW continuum frequency. That non-ideal effects discretize the SAW continuum is a general result that will be further discussed in Sec. IV.B. Meanwhile, observing the coarse nature of the SAW continuous spectrum depends on the spatiotemporal scales of the processes involved, which may either be the experimental measurements of the system response or the intrinsic space and time scales of the (often nonlinear) dynamics.

#### IV. LINEAR ALFVÉN WAVE PHYSICS AND WAVE-PARTICLE INTERACTIONS IN TWO-DIMENSIONAL TOROIDAL PLASMAS

In Sec. III, shear Alfvén waves (SAWs) were introduced as anisotropic electromagnetic waves in magnetized plasmas, satisfying the dispersion relation

$$\omega^2 = k_{\parallel}^2 v_A^2 = \omega_A^2, \quad (4.1)$$

with  $k_{\parallel}$  the parallel (to  $\mathbf{B}_0$ ) wave vector. In non-uniform plasmas, gradients across magnetic surfaces cause the SAW frequency to become dependent on the spatial location. Thus, the SAW frequency spectrum becomes a continuum, characterized by phase mixing and singular absorption, in exact analogy with collisionless dissipation in Vlasov plasmas, as emphasized by Grad (Grad, 1969) (cf. Sec. III).

In higher dimensionality systems, such as nearly two-dimensional (2D) or three-dimensional (3D) toroidal devices, the main additional complication is due to the modulations of  $v_A$  along  $\mathbf{B}_0$ . This causes the loss of translational symmetry for SAWs traveling along  $\mathbf{B}_0$  and sampling regions of periodically varying  $v_A$ . Similarly to electron wave packets traveling in a one-dimensional periodic lattice of period  $L$  [cf., *e.g.*, (Kittel, 1971)], SAWs in toroidal systems are characterized by gaps in their continuous spectrum, corresponding to the formation of standing waves at the Bragg reflection condition; *i.e.*,

$$2L = \ell\lambda, \quad \lambda \equiv \frac{2\pi}{k}, \quad \ell \in \mathbb{N}, \quad (4.2)$$

In toroidal systems,  $L = 2\pi L_0$  corresponds to the connection length; *i.e.*, the length of a magnetic field line connecting two distinct points on the same magnetic surface where the SAW frequency (or another equilibrium physical quantity of interest) is the same. Thus, Eq. (4.2) becomes

$$k_{\parallel} = \frac{\ell}{2L_0}, \quad \omega^2 = \frac{\ell^2 v_A^2}{4L_0^2}, \quad \ell \in \mathbb{N}, \quad (4.3)$$

with  $v_A$  being a “typical” value of the Alfvén speed on the reference magnetic surface.

In the study of Alfvén wave propagation in tokamak plasmas, the existence of gaps in the continuous spectrum, due to the toroidal geometry, was discussed by (D’Ippolito and Goedbloed, 1980; Kieras and Tataronis, 1982; Pogutse and Yurchenko, 1978). In this case, given that  $L_0 \simeq qR_0$  for circular plasmas with large aspect-ratio  $R_0/a$  [see Sec. II, remark following Eq. (2.2)],  $R_0/a$  being the plasma major/minor radius and  $q$  the safety factor (representing the pitch of equilibrium magnetic field lines winding on a given flux surface), the dominant frequency gap occurs at  $v_A/(2qR_0)$  and is due to the finite curvature of the system (Kieras and Tataronis, 1982). Other gaps also generally exist at  $\omega = \ell v_A/(2qR_0)$ , due to either non-circularity of the magnetic flux surfaces ( $\ell = 2, 3, \dots$ ) (Betti and Freidberg, 1991), to anisotropic trapped energetic ion population ( $\ell = 1, 2, 3, \dots$ ) (Van Dam and Rosenbluth, 1998) or to finite- $\beta$  (mainly  $\ell = 2$ , with  $\beta$  the ratio between kinetic and magnetic pressures) (Zheng and Chen, 1998a,b). A low-frequency gap, corresponding to  $\ell = 0$ , also exists because of finite plasma compressibility (Chu *et al.*, 1992, 1993; Turnbull *et al.*, 1993) at  $\omega \simeq \beta_i^{1/2} v_A/R_0 \ll v_A/R_0$ .

In order to nullify or minimize continuum damping, discrete shear Alfvén eigenmodes (AEs) must be localized in the SAW continuum frequency gaps and/or around radial positions where  $(d/dr)\omega_A(r) = 0$  (cf. Sec. III). The degeneracy of AE mode frequency with the continuous spectrum is removed by equilibrium non-uniformities, which make it possible for these fluctuations to exist as discrete modes. Continuing further the analogy with the one-dimensional periodic lattice case [cf., *e.g.*, (Kittel, 1971)], discrete AE can be localized in the continuum frequency gaps because

of MHD and/or kinetic effects due to both thermal and/or supra-thermal particles, which play the role of “defects” (Chen and Zonca, 2007a; Zonca *et al.*, 2006). The particular role of supra-thermal particles in the resonant excitation of SAWs was noted already by (Belikov *et al.*, 1968, 1969; Kolesnichenko and Oraevskij, 1967; Mikhailovskii, 1975a,b; Mikhailovskii and Shuchman, 1976; Rosenbluth and Rutherford, 1975; Tsang *et al.*, 1981), along with the possible detrimental effects of collective SAW fluctuations as well as of lower frequency MHD modes (Chen *et al.*, 1984; Coppi and Porcelli, 1986; McGuire *et al.*, 1983; White *et al.*, 1983) on supra-thermal particle confinement (see Sec. I.A). In toroidal geometry, the wave-particle resonance conditions are different for circulating particles (which move along  $\mathbf{B}_0$  without changing sign of  $v_{\parallel}$ ) and those that are trapped between magnetic mirror points. For the circulating particles, the resonance condition is

$$\omega - \overline{k_{\parallel} v_{\parallel}} - \ell \omega_t - n \bar{\omega}_d = 0, \quad \ell \in \mathbb{Z}, \quad (4.4)$$

with  $\overline{(\dots)}$  indicating orbit averaging (see Sec. IV.B),  $\omega_t \sim v_{\parallel}/(qR_0)$  the particle transit frequency around the torus,  $n$  the toroidal mode number, and  $\bar{\omega}_d$  the toroidal precession frequency, which is typically negligible for circulating particles. Meanwhile, Eq. (4.4), for trapped particles, becomes

$$\omega - n \bar{\omega}_d - \ell \omega_b = 0, \quad \ell \in \mathbb{Z}, \quad (4.5)$$

with  $\omega_b$  the bounce frequency between magnetic mirror points. These resonant conditions are functions of the invariants of particle motions (see Sec. IV.B for details) and bear the information of plasma equilibrium geometry and nonuniformities. Another crucial effect associated with plasma equilibrium geometry and nonuniformities is the wave particle energy exchange mainly due to  $\mathbf{v}_d \cdot \delta \mathbf{E}_{\perp}$ , since  $\delta E_{\parallel} \simeq 0$  and  $\delta B_{\parallel} \simeq 0$  in highly conducting, high temperature  $\beta \ll 1$  fusion plasmas (see Sec. II.E). This means that both resonant and non-resonant supra-thermal particle responses enter via magnetic drifts in most conditions of practical interest (Zonca and Chen, 2006).

Discrete AEs existing in the various frequency gaps have, accordingly, been given different names. The first example is the Toroidal AE (TAE) (Cheng *et al.*, 1985) for  $\omega \simeq v_A/(2qR_0)$ . This is a particularly important case, for it was the first demonstration of the existence of AEs in toroidal plasmas, thereby fixing a paradigm for subsequent AE investigations. Other examples are the Ellipticity induced AE (EAE) (Betti and Freidberg, 1991, 1992) for  $\omega \simeq v_A/(qR_0)$  and Non-circular triangularity (or other shaping effects) induced AE (NAE) (Betti and Freidberg, 1991, 1992) for  $\omega \simeq \ell v_A/(2qR_0)$  and  $\ell \geq 3$ , as shown by Eq. (4.3). The low frequency SAW continuum frequency gap at  $\omega \simeq \beta_i^{1/2}(7/4 + T_e/T_i)^{1/2}v_A/R_0$  (Kotschenreuther, 1986; Mikhailovskii, 1973; Zonca *et al.*, 1996) deserves a special note since, in this case, the mode frequency can be comparable with thermal (core) ion diamagnetic ( $\omega_{*pi}$ ) and/or transit ( $\omega_{ti}$ ) frequencies; *i.e.*,  $|\omega| \sim \omega_{*pi} \sim \omega_{ti}$ . We could generally refer to this frequency gap as the Kinetic Thermal Ion (KTI) gap (Chen and Zonca, 2007a). In fact, the ideal MHD accumulation point,  $\omega = 0$  at  $k_{\parallel} = 0$  from Eq. (4.3), is shifted by either the ion diamagnetic drift, as in the Kinetic Ballooning Mode (KBM) case (Biglari and Chen, 1991), or by parallel and perpendicular ion compressibility, as for the Beta induced AE (BAE) (Heidbrink *et al.*, 1993; Turnbull *et al.*, 1993), or, more generally, by the combined effects of finite ion temperature gradient ( $\nabla T_i$ ) and wave-particle resonances with thermal (core) ions, as for the Alfvén Ion Temperature Gradient driven mode (AITG) (Zonca *et al.*, 1999). For the AITG, the shear Alfvén continuum accumulation point could be shifted to the complex  $\omega$  plane (Kotschenreuther, 1986; Mikhailovskii, 1973; Zonca *et al.*, 1996) and, thus, become unstable for modes with sufficiently short wavelength ( $\lambda_{\perp} \gtrsim \rho_i$ , the ion Larmor radius). The mode localization condition inside the frequency gap [cf. the discussion above, following Eq. (4.3)] then leads to the excitation of unstable discrete AITG even in the absence of supra-thermal particle drive (Nazikian *et al.*, 2006; Zonca *et al.*, 1999, 1996, 1998). In this case, they are sometimes referred to as beta-induced temperature gradient eigenmodes (Mikhailovskii and Sharapov, 1999a,b). The predominance of either ion diamagnetic drift (KBM) or parallel and perpendicular ion compressibility (BAE) in the KTI frequency gap depends on both wave number and plasma equilibrium nonuniformity: AITG are typically excited when both effects are of the same order (Zonca *et al.*, 1999, 1996). Thus, two bands of low-frequency Alfvénic activities are generally expected, with varying frequency-dependent geodesic curvature coupling to the ion-acoustic wave (Zonca *et al.*, 2010), of which - in the long wavelength limit - the lower one refers to the ion diamagnetic frequency, consistent with some recent numerical simulation results and experimental observations (Curran *et al.*, 2012; Lauber *et al.*, 2012). Another low-frequency fluctuation branch also exists, characterized by strong coupling of the SAW to the ion-acoustic wave and dubbed Beta induced Alfvén Acoustic Eigenmode (BAAE) (Gorelenkov *et al.*, 2007a,b, 2009), which, however, is generally affected by strong Landau damping, unless  $T_e/T_i \gg 1$  (Zonca *et al.*, 2010).

Consistently with the fact that removal of the frequency degeneracy of AE with the SAW continuum depends on equilibrium non-uniformities, various local plasma profiles can produce variants of the AE mentioned above. In the case of TAE with low magnetic shear values,  $|s| = |(r/q)(dq/dr)| \ll 1$  typical of the plasma near the magnetic

axis, they have been dubbed core-localized TAE (Berk *et al.*, 1995c; Fu, 1995) or also tornado modes (Kramer *et al.*, 2004b) when they are excited within the  $q = 1$  magnetic flux surface. Global AE (GAE) (Appert *et al.*, 1982; Mahajan *et al.*, 1983; Ross *et al.*, 1982) may also exist (cf. Sec. III.A), although they tend to be more strongly damped due to coupling with the continuous spectrum (Cheng *et al.*, 1988; Fu *et al.*, 1989; Li *et al.*, 1987; Weiland *et al.*, 1987), and are localized in both frequency and radial position near an extremum of the SAW continuous spectrum,  $(d/dr)\omega_A(r) = 0$ . A special case of  $(d/dr)\omega_A(r) = 0$  is given by tokamak plasma equilibria with hollow- $q$  profiles, characterized by negative magnetic shear,  $s < 0$ , inside the the minimum- $q$  surface. For these equilibria, a frequency gap is formed in the local SAW continuous spectrum, where AE can be excited (Berk *et al.*, 2001) yielding the so called Alfvén Cascades (AC) (Sharapov *et al.*, 2001) or Reversed Shear AE (RSAE) (Kimura *et al.*, 1998; Takechi *et al.*, 2002). These modes have frequencies that are typically less than that of TAEs, although there are experimental observations of RSAE near the SAW continuum extrema connected with the EAE/NAE gaps (Kramer and Fu, 2006; Kramer *et al.*, 2008).

In addition, a variety of kinetic counterparts of the corresponding ideal AE also exists, in analogy to the existence of KAW as counterpart of SAWs, discussed in Sec. III.B. Typical examples are Kinetic TAE (KTAE) that are obtained when, *e.g.* finite resistivity (Cheng *et al.*, 1985) or finite Larmor radius (FLR) effects are accounted for, as in (Berk *et al.*, 1993; Candy and Rosenbluth, 1993, 1994; Mett and Mahajan, 1992a,b). Similarly, one could show that Kinetic BAE (KBAE) also exist (Wang *et al.*, 2011, 2010b; Zonca *et al.*, 1999, 1998) as the granularity of the Alfvén continuum becomes evident when the plasma response is probed on sufficiently short spatial scales and sufficiently long temporal scales (Chen and Zonca, 1995; Zonca and Chen, 1996). The most practically important consequence of KAW in toroidal plasmas is their excitation by mode conversion (Hasegawa and Chen, 1975, 1976), mostly via FLR effects, due to the radial singular structures of SAWs at the resonance with the continuous spectrum (cf. Sec. III.B). For KAW are not generally absorbed locally nearby the mode conversion layer in high temperature fusion plasmas (Jaun *et al.*, 1998, 2000; Kolesnichenko *et al.*, 2005). Thus, mode structures and stability properties of SAWs are truly kinetic and global in nature, and it becomes crucial to properly account for all these physics in realistic comparisons with experimental observations and in stability predictions in reactor relevant conditions.

A final important class of Alfvénic fluctuations in 2D nonuniform systems is given by Energetic Particle Modes (EPM) (Chen, 1994), which are born at marginal stability as non-normal modes of the SAW continuous spectrum and are resonantly excited at the characteristic frequency of the supra-thermal particle motions, Eqs. (4.4) and (4.5). The excitation condition of EPM is independent of the existence of AE inside the frequency gaps, but it requires that the mode drive is sufficiently strong to overcome continuum damping. Being essentially connected with a condition on the beam energy density, EPM can manifest themselves in a variety of different forms, the best known and first observed of which is the fishbone mode (McGuire *et al.*, 1983); *i.e.*, an internal kink oscillation with toroidal mode number  $n = 1$ , which is resonantly excited (typically) by the toroidal precession resonance with magnetically trapped supra-thermal ions (Chen *et al.*, 1984). As for AE, the fishbone “gap-mode” also exists, for weaker supra-thermal beam power density, in the low frequency KTI gap, dominated by diamagnetic effects (Coppi and Porcelli, 1986).

As all instabilities that tap the expansion free-energy from energetic particle (EP) spatial gradients, AE and EPM have both linear growth as well as transport rates (Chen, 1999) proportional to the mode number; thus, short wavelengths tend to be favored. On the other hand, due to the orbit-averaging effect in wave-particle interactions, the typical lower bound for  $\lambda_\perp$  is set by the characteristic EP orbit width,  $\rho_E$ , which, in toroidal devices such as tokamaks, is determined by magnetic drifts and is generally larger than Larmor radius (Berk *et al.*, 1992b; Chen, 1994; Fu and Cheng, 1992; Tsai and Chen, 1993). For this reason, modes with  $\lambda_\perp \gtrsim \rho_E$  are expected to play a dominant role for both resonant excitations of collective Alfvén instabilities as well as for producing fluctuation enhanced fast ion transport. This condition corresponds to  $n_{max}q \lesssim (r/\rho_E)$  for the maximum toroidal mode number of linearly excited Alfvénic modes. Generally, AE in the same gap have nearly degenerate frequency for the various toroidal mode numbers, as in the case of TAE (Cheng *et al.*, 1985). Moreover, each  $n$ th mode has  $\sim O(nqr/R_0)$  different possible realizations (radial eigenstates) of AE localized at different radial locations. Thus, *e.g.*, within the TAE gap we may expect  $\sim O(n^2qr/R_0)$  AE, forming a “dense population of eigenmodes (lighthouses) with unique (equilibrium-dependent) frequencies and locations” (Chen and Zonca, 2007a). In Secs. VI and VII, the significant implications of this fact on the non-linear AE physics are discussed.

In the next subsections, we discuss how all this AE Zoology (Heidbrink, 2002) and Alfvénic fluctuations can be described by one single dispersion relation written in a general “fishbone-like” form, which can be adopted for linear stability studies as well as for systematic extensions of our analyses to the nonlinear regime (cf. Sec. IV.A). In fact, the general “fishbone-like” dispersion relation can be derived by asymptotic matching the regular (ideal MHD) mode structure with the generally known form of the SAW field in the singular (inertial/kinetic) region near the SAW resonance. In the asymptotic matching procedure, no assumptions are made concerning the linearization of the plasma response. Thus, the theoretical framework of Sec. IV.A can also be adopted for nonlinear analyses,

as specifically discussed in Sec. V. We then discuss different linear applications of practical interest of the general fishbone-like dispersion relation (cf. Sec. IV.B) and we briefly summarize experimental verification of linear AE and stability predictions in burning plasmas (cf. Sec. IV.C). Readers that are more interested in applications may directly proceed to Sec. IV.B.

### A. The general fishbone-like dispersion relation

We assume that the equilibrium  $\mathbf{B}_0$  can be expressed in the usual form

$$\mathbf{B}_0 = F(\psi)\nabla\varphi + \nabla\varphi \times \nabla\psi , \quad (4.6)$$

where  $\varphi$  is the physical toroidal angle, identifying the symmetry of the system at equilibrium, and  $\psi$  is the poloidal magnetic flux function. Moreover, we use a straight magnetic field line toroidal coordinate system  $(r, \theta, \zeta)$ , where  $r$  is a radial-like coordinate depending only on the magnetic flux function  $\psi$ <sup>10</sup>, while  $\theta$  and  $\zeta$  are periodic angle-like variables, the latter being the ignorable (symmetry) coordinate of the plasma equilibrium. More precisely,  $\zeta$  is the general toroidal angle defined by

$$\frac{\mathbf{B}_0 \cdot \nabla\zeta}{\mathbf{B}_0 \cdot \nabla\theta} = q(r) , \quad (4.7)$$

where  $q(r)$  is the safety factor profile and  $\theta$  is chosen such that the Jacobian  $\mathcal{J} = (\nabla\psi \times \nabla\theta \cdot \nabla\zeta)^{-1}$  satisfies the condition of  $\mathcal{J}B_0^2$  being a flux function; *i.e.*, the Boozer coordinates (Boozer, 1981, 1982). In these  $(r, \theta, \zeta)$  coordinates, a scalar function  $f(r, \theta, \zeta)$ , describing a generic fluctuating field, can be decomposed as Fourier series

$$f(r, \theta, \zeta) = \sum_{n \in \mathbb{Z}} e^{in\zeta} F_n(r, \theta) = \sum_{m, n \in \mathbb{Z}} e^{in\zeta - im\theta} f_{m, n}(r) , \quad (4.8)$$

where the toroidal Fourier components  $F_n(r, \theta)$  are independent in the linear limit, while the poloidal Fourier components  $f_{m, n}(r)$  are not, due to the equilibrium geometry. Note that, for simplicity, time dependences are assumed implicit. In Clebsch coordinates  $(r, \theta, \xi)$  (Beer *et al.*, 1995; Cowley *et al.*, 1991; Dewar and Glasser, 1983; Roberts and Taylor, 1965; Scott, 1998), with  $\xi = \zeta - q(r)\theta$  (Kruskal and Kulsrud, 1958) and  $\mathbf{B}_0 = \nabla\xi \times \nabla\psi$ , Eq. (4.8) becomes

$$f(r, \theta, \xi) = \sum_{n \in \mathbb{Z}} e^{in\xi} f_n(r, \theta) = \sum_{m, n \in \mathbb{Z}} e^{in\xi} e^{i(nq-m)\theta} f_{m, n}(r) . \quad (4.9)$$

The derivation of a general fishbone-like dispersion relation (GFLDR) is based on the construction of a nonlinear functional form from Eqs. (2.26) and (2.28) (Chen and Hasegawa, 1991). A similar variational approach is proposed by (Edery *et al.*, 1992). The final result, as briefly noted in Sec. IV.B.1 and discussed in detail by (Chen and Hasegawa, 1991) and (Edery *et al.*, 1992), can be put in close connection with various forms of the MHD energy principle (Antonsen *et al.*, 1981; Antonsen and Lee, 1982; Bernstein *et al.*, 1958; Kruskal and Oberman, 1958; Porcelli and Rosenbluth, 1998; Rosenbluth and Rostoker, 1959; Taylor and Hastie, 1965; Van Dam *et al.*, 1982), due to the fact that, in the long wavelength limit, Eqs. (2.26) to (2.29) can be cast as Eqs. (2.34) to (2.37); *i.e.* they recover reduced MHD as a limiting case of nonlinear gyrokinetic equations (Brizard, 1992; Hahm *et al.*, 1988) and their linearized form reduces to the kinetic MHD equations discussed by (Qin *et al.*, 1998, 1999b) and (Brizard, 1994). In the present case, however, no linearization assumptions are made; so that the GFLDR can be the starting point for systematic extensions to the nonlinear regime (see Secs. V.A, V.C and V.D).

The construction of the GFLDR assumes that fluctuations are characterized by two radial scales, due to the existence of the SAW continuous spectrum (cf. Sec. III). These properties are used in the following to further reduce the nonlinear functional that can be constructed from Eq. (2.37) in the form

$$\delta\mathcal{L}(\delta\phi, \delta\psi) = \frac{1}{2} \int_V \left[ \left( \frac{\partial}{\partial t} \right)^{-1} \delta\psi^\dagger \right] \times [\text{LHS Eq. (2.37)}] dr , \quad (4.10)$$

---

<sup>10</sup> One possible choice is, *e.g.*,  $r/a = (\psi - \psi_0)^{1/2} / (\psi_a - \psi_0)^{1/2}$ , with  $\psi_0$  the value of  $\psi$  on the magnetic axis and  $\psi_a$  its value at the plasma minor radius  $r = a$ .

where  $\partial_t^{-1}$  is the formal notation for the inverse of  $\partial_t$ ,  $\delta\psi^\dagger$  is the adjoint of  $\delta\psi$  with the definition adopted by (Gerjuoy *et al.*, 1983), the integral is extended over the plasma volume and LHS stands for left hand side. This functional form is variational, when the LHS of Eq. (2.37) is linearized, due to the symmetry properties of the operators involved and coincides with the quadratic form derived by (Chen and Hasegawa, 1991). When nonlinear terms are included, however, it is generally not variational, although  $\delta\mathcal{L}(\delta\phi, \delta\psi) = 0$  by definition, when the functional is computed for the actual solution of Eqs. (2.34) and (2.37). Because of the existence of the SAW continuous spectrum, the volume integral of Eq. (4.10) can be divided into two radial regions. One corresponds to fluctuating fields with smooth regular behaviors and the  $\mathbf{k}_\perp$  spectrum is weakly anisotropic. The other corresponds to fluctuations with sharp varying radial structures and  $k_\perp \simeq k_r$ . Due to the fact that  $\delta\psi = \delta\phi$  in the regular regions, they are referred as ideal MHD regions as well; as opposed to the singular (inertial/kinetic) layers, where the difference between  $\delta\phi$  and  $\delta\psi$  may become significant. As a result, the contribution from regular regions to the integral in Eq. (4.10),  $\delta W$ , is readily separated from that due to singular layers,  $-\delta I$ , yielding  $\delta\mathcal{L} = \delta W - \delta I$  with the following definitions (Zonca and Chen, 2013)

$$\begin{aligned} \delta W = & \lim_{\vartheta_1 \rightarrow \infty} (2\pi)^3 \int_0^a dr \frac{d\psi/dr}{2} \int_{-\vartheta_1}^{\vartheta_1} \mathcal{J} d\vartheta \sum_{n, \ell \in \mathbb{Z}} e^{-2\pi i n q \ell} \left\{ \mathcal{P}_{B-n}(r, \vartheta) [\delta \mathbf{B}^\dagger] \cdot \mathcal{P}_{Bn}(r, \vartheta + 2\pi\ell) \left[ \frac{\delta \mathbf{B}}{4\pi} \right] \right. \\ & + \mathcal{P}_{B-n}(r, \vartheta) [\partial_t^{-1} \delta \phi^\dagger] \mathcal{P}_{Bn}(r, \vartheta + 2\pi\ell) \left[ -\frac{c^2}{4\pi} \nabla \cdot \left( \frac{1}{v_A^2} \nabla_\perp \frac{\partial}{\partial t} \delta \phi \right) + \frac{c^2}{4\pi} \mathbf{b} \times \nabla \left[ \frac{4\pi}{B_0^2} \left( \frac{P_{0\perp i}}{\Omega_i} \right) \right] \cdot \nabla \nabla_\perp^2 \delta \phi \right. \\ & \left. \left. + \frac{c}{B_0} \mathbf{b} \times \boldsymbol{\kappa} \cdot \nabla \sum \left\langle m \left( \mu B_0 + v_\parallel^2 \right) J_0 \delta g \right\rangle_v + \delta \mathbf{B}_\perp \cdot \nabla \left( \frac{j_{\parallel 0}}{B_0} \right) \right] \right\} , \end{aligned} \quad (4.11)$$

$$\delta I = (2\pi)^3 \int_0^a dr \frac{d\psi/dr}{2} \sum_{n, \ell \in \mathbb{Z}} e^{-2\pi i n q \ell} \left[ \frac{c^2 k_\vartheta^2}{4\pi \mathcal{J} B_0^2} \left( \partial_t^{-1} \delta \hat{\Psi}_{-n}^\dagger(\vartheta) \right) \partial_\vartheta \left( \partial_t^{-1} \delta \hat{\Psi}_n(\vartheta + 2\pi\ell) \right) \right]_{\vartheta \rightarrow 0^-}^{\vartheta \rightarrow 0^+} . \quad (4.12)$$

Here, we have adopted the mode structure decomposition approach discussed by (Lu *et al.*, 2012; Zonca *et al.*, 2004a), which, for short wavelength modes, reduces to the well known ‘‘ballooning representation’’ (Connor *et al.*, 1978, 1979; Coppi, 1977; Dewar *et al.*, 1981, 1982; Glasser, 1977; Hazeltine *et al.*, 1981; Lee and Van Dam, 1977; Pegoraro and Schep, 1978) and a generic fluctuating field  $f(r, \theta, \zeta)$ , decomposed as in Eqs. (4.8) and (4.9), can be written as

$$\begin{aligned} f(r, \theta, \zeta) &= \sum_{m, n \in \mathbb{Z}} e^{in\zeta - im\theta} \int e^{i(m-nq)\vartheta} \hat{f}_n(r, \vartheta) d\vartheta \\ &= \sum_{m, n \in \mathbb{Z}} e^{in\zeta - im\theta} \int e^{i(m-nq)\vartheta} \mathcal{P}_{Bn}(r, \vartheta) [f] d\vartheta . \end{aligned} \quad (4.13)$$

Equation (4.13) introduces and defines the projection operator  $\mathcal{P}_{Bn}(r, \vartheta) : f(r, \theta, \zeta) \mapsto \hat{f}_n(r, \vartheta)$  and its properties allow to interpret  $\vartheta$  as an extended poloidal angle. In fact, multiplication by a periodic function  $p(\theta)$  in  $(r, \theta)$  space corresponds to multiplication by a periodic function  $p(\vartheta)$  in  $(r, \vartheta)$  space and, in Clebsch coordinates,  $\mathbf{b} \cdot \nabla = (\mathcal{J}B_0)^{-1} \partial_\theta \mapsto (\mathcal{J}B_0)^{-1} \partial_\vartheta$ . Finally,

$$\nabla_\perp \mapsto \nabla r \left( -inq' \vartheta + \frac{\partial}{\partial r} \right) + in \nabla \zeta + \nabla \theta \left( \frac{\partial}{\partial \vartheta} - inq \right) - \frac{\mathbf{b}}{\mathcal{J}B_0} \frac{\partial}{\partial \vartheta} , \quad (4.14)$$

$q'$  denoting the radial derivative of  $q(r)$ , defined by Eq. (4.7), with respect to  $r$ .

Formally nonlinear terms due to core plasma dynamics (cf. Secs. II.D and II.E) may be dropped in the expression of  $\delta W$  (Zonca and Chen, 2013). For the same reason, finite thermal ion Larmor radius terms are dropped and  $\delta\phi = \delta\psi$  is explicitly imposed in Eq. (4.11). Inertia and diamagnetic terms; *i.e.*, the second line of Eq. (4.11), are negligible in the low-frequency MHD limit but, more generally, they provide a finite contribution (Biglari *et al.*, 1992; Chen, 1988, 1994; Cheng *et al.*, 1985, 1988; Tsai and Chen, 1993). As in ideal MHD, most important destabilization effects come from the last two terms, the ‘‘ballooning-interchange’’ and the ‘‘kink’’ drive, respectively (Freidberg, 1987; Furth *et al.*, 1965; Greene and Johnson, 1968). Note that the expression of  $\delta W$  is still nonlinear due to the implicit nonlinear response included in the ‘‘ballooning-interchange’’ contribution, which also maintains finite ion Larmor radius effects of EPs (Zonca and Chen, 2013). Meanwhile, the expression of  $\delta I$  adopts the notation

$$\delta \hat{\Psi}_n \equiv \hat{\kappa}_\perp \delta \hat{\psi}_n \quad \text{and} \quad k_\vartheta^2 \hat{\kappa}_\perp^2 \equiv -\nabla_\perp^2 , \quad (4.15)$$

with  $k_\vartheta \equiv -nq/r$  and  $\nabla_\perp$  given by Eq. (4.14), and contains the jump across  $\vartheta = 0$  of the quantity in square parentheses, which is obtained from the solution of Eq. (2.37) for  $\hat{\kappa}_\perp^2 = k_\perp^2/k_\vartheta^2 \simeq s^2\vartheta^2|\nabla r|^2 \gg 1$ . In other words, Eq. (4.12) contains the information on the sharp varying structures of SAW fluctuation associated with the continuous spectrum. These include finite thermal ion Larmor radius effects and formally nonlinear terms due to core plasma dynamics. They are implicitly accounted for by the solution of Eq. (2.37) for  $\hat{\kappa}_\perp^2 = k_\perp^2/k_\vartheta^2 \simeq s^2\vartheta^2|\nabla r|^2 \gg 1$ , which can also take into account finite EP responses that are non-vanishing for sufficiently long wavelength modes (cf. Secs. IV.B.2 and IV.B.3).

Adopting the normalization for  $\delta W$  in Eq. (4.11) as in the fishbone theory (Chen *et al.*, 1984), it is possible to rewrite (Zonca and Chen, 2013)

$$\delta W = \frac{2\pi^2 c^2}{|\omega|^2} \sum_{n \in \mathbb{Z}} \left. \frac{|k_\vartheta|(d\psi/dr)}{|s|^2 \mathcal{J} B_0^2} \right|_{r=r_0, \vartheta=0} \left( \delta \hat{\Psi}_{-n0+}^\dagger \delta \hat{\Psi}_{n0+} \right) \delta \hat{W}_n . \quad (4.16)$$

where magnetic shear is defined as

$$s = s(r) = r q'(r)/q(r) . \quad (4.17)$$

Similarly, Eq. (4.12) can be cast as

$$\delta I = \frac{2\pi^2 c^2}{|\omega|^2} \sum_{n \in \mathbb{Z}} \left. \frac{|k_\vartheta|(d\psi/dr)}{|s|^2 \mathcal{J} B_0^2} \right|_{r=r_0, \vartheta=0} \left( \delta \hat{\Psi}_{-n0+}^\dagger \delta \hat{\Psi}_{n0+} \right) i |s| \Lambda_n , \quad (4.18)$$

with the summation on all singular layer contributions left implicit and

$$i \Lambda_n \equiv \frac{1}{2} \left( \delta \hat{\Psi}_{-n0+}^\dagger \delta \hat{\Psi}_{n0+} \right)^{-1} \left[ \delta \hat{\Psi}_{-n}^\dagger(\vartheta) \partial_\vartheta \delta \hat{\Psi}_n(\vartheta) \right]_{\vartheta \rightarrow 0^-}^{\vartheta \rightarrow 0^+} , \quad (4.19)$$

which can be obtained from the solution of the linearized Eq. (2.37) for  $\hat{\kappa}_\perp^2 = k_\perp^2/k_\vartheta^2 \simeq s^2\vartheta^2|\nabla r|^2 \gg 1$  with outgoing wave boundary conditions, corresponding to causality constraints (Zonca and Chen, 2013).

The general fishbone like dispersion relation (GFLDR) is derived from  $\delta \mathcal{L} = \delta W - \delta I = 0$  combining Eqs. (4.16) and (4.18), and , for a single- $n$  toroidal mode, is given by

$$i |s| \Lambda_n = \delta \hat{W}_{nf} + \delta \hat{W}_{nk} . \quad (4.20)$$

The generalized inertia term  $\Lambda_n(\omega)$  accounts for the thermal ion response and can be extended to include supra-thermal particle effects for long wavelength modes (cf. Sec. II.E), as well as, for shorter wavelength modes, finite thermal ion Larmor radius effects. Meanwhile,  $\Lambda_n$  can also be modified to include stress tensor, Maxwell stress and polarization nonlinearity, by including the corresponding terms from Eq. (2.37) (see Sec V.C). The important feature of Eq. (4.20) is that, in all these cases, the expression of  $\Lambda_n$  is obtained by Eq. (4.19). The right hand side of Eq. (4.20) also distinguishes between “fluid” ( $\delta \hat{W}_{nf}$ ) and “kinetic” ( $\delta \hat{W}_{nk}$ ) contributions to the potential energy  $\delta \hat{W}_n$  (Chen *et al.*, 1984). The expression of  $\delta \hat{W}_{nf}$  is obtained from Eq. (4.16) using the “fluid” limit for the gyrokinetic particle response  $\delta g$  in Eq. (4.11), while  $\delta \hat{W}_{nk}$  accounts for the remaining “kinetic” particle response (cf. Sec. IV.B.1). In the low-frequency limit,  $\delta \hat{W}_{nf}$  is independent of frequency and reduces to the well-known MHD limiting forms, as discussed above. Meanwhile,  $\delta \hat{W}_{nk}(\omega)$  is always a function of the mode frequency  $\omega$ , as it reflects resonant as well as non-resonant wave-particle interactions. Same as the inertia term, the potential energy  $\delta \hat{W}_n$  accounts for both linear and nonlinear responses due to the presence of  $\delta g$  in Eq. (4.11). Dispersion relations in a form similar to Eq. (4.20) have been derived in many works on the effect of supra-thermal particles on low frequency MHD modes by precession resonance (Biglari and Chen, 1986a; Chen *et al.*, 1984; Coppi and Porcelli, 1986; Rewoldt and Tang, 1984; Spong *et al.*, 1985; Weiland and Chen, 1985; White *et al.*, 1985, 1990). Meanwhile, the generality of Eq. (4.20) and its applicability to low-frequency MHD modes (Chen *et al.*, 1984; Liljeström and Weiland, 1992), as well as to KBM (Biglari and Chen, 1991; Tsai and Chen, 1993) and higher frequency Alfvénic fluctuations (Biglari *et al.*, 1992; Chen, 1988; Chen *et al.*, 1989), was formulated by (Chen, 1994; Zonca *et al.*, 1996) and formalized in (Chen and Zonca, 2007a; Zonca *et al.*, 2007a; Zonca and Chen, 2006, 2007; Zonca *et al.*, 1999).

The GFLDR generally demonstrates the existence of two types of modes (Zonca and Chen, 2006): a discrete gap mode, or AE, for  $\text{Re} \Lambda_n^2 < 0$ ; and an EPM (Chen, 1994) for  $\text{Re} \Lambda_n^2 > 0$ . The combined effect of  $\delta \hat{W}_{nf}$  and  $\delta \hat{W}_{nk}$  determines the existence conditions of AEs, and various effects in  $\delta \hat{W}_{nf}$  and  $\delta \hat{W}_{nk}$  can lead to AE localization in various gaps, *i.e.*, to different species of AE [the AE Zoology (Heidbrink, 2002)], as described in (Chen and Zonca,

2007a). Clearly, the transition between AE and EPM is generally continuous with varying plasma parameters and a net distinction of one type of mode from the other is possible only when the distance of the mode frequency from the SAW accumulation point ( $\Lambda_n = 0$ ) is larger than the mode linear growth rate,  $\gamma_L$ , or the characteristic inverse nonlinear time,  $\tau_{NL}^{-1}$  (cf. Sec. II.C).

In the low-frequency limit ( $|\Lambda_n^2| \ll 1$ ), when the AE frequency is above the SAW continuum accumulation point  $\omega_\ell$ , the causality constraint for AE existence inside the SAW frequency gap is (Chen and Zonca, 2007a; Zonca and Chen, 2013)

$$\delta\hat{W}_{nf} + \mathbb{R}e\delta\hat{W}_{nk} > 0 . \quad (4.21)$$

Similarly, when the AE frequency is below the SAW continuum accumulation point  $\omega_u$ , the AE existence condition becomes

$$\delta\hat{W}_{nf} + \mathbb{R}e\delta\hat{W}_{nk} < 0 . \quad (4.22)$$

For EPM, meanwhile, the  $i\Lambda_n$  term in Eq. (4.20) represents continuum damping and the threshold in supra-thermal particle drive for effective mode excitation. In fact, near marginal stability,

$$\begin{aligned} \delta\hat{W}_{nf} + \mathbb{R}e\delta\hat{W}_{nk} = 0 , & \Rightarrow \text{determines } \omega_0 , \\ \frac{\gamma_L}{\omega_0} = \frac{|s|^{-1}\mathbb{I}m\delta\hat{W}_{kn} - \Lambda_n}{(-\omega_0|s|^{-1}\partial\mathbb{R}e\delta\hat{W}_n/\partial\omega_0)} , & \Rightarrow \text{determines } \gamma_L , \end{aligned} \quad (4.23)$$

showing the importance of resonant and non-resonant EP responses in EPM excitations (cf. Sec. IV.B.4).

Equation (4.20) explicitly shows the important role played by magnetic shear, defined in Eq. (4.17). When magnetic shear vanishes at one isolated singular layer ( $s = 0$  at  $r = r_0$ ), it is possible to construct the (local) extension of Eq. (4.20) that, in the low-frequency limit, becomes (Zonca *et al.*, 2007a)

$$iS \left( \Lambda_n^2 - k_{\parallel n0}^2 L_0^2 \right)^{1/2} \left[ \frac{1}{n} k_{\parallel n0} L_0 - \frac{i}{n} \left( \Lambda_n^2 - k_{\parallel n0}^2 L_0^2 \right)^{1/2} \right]^{1/2} = \delta\hat{W}_{nf} + \delta\hat{W}_{nk} , \quad (4.24)$$

where

$$S^2 = r_0^2 q''(r_0)/q(r_0)^2 \quad (4.25)$$

generalizes the notion of magnetic shear for  $s = 0$ , having assumed a minimum- $q$  surface at  $r_0$ . In the ideal MHD limit, Eq. (4.24) was derived first by (Hastie *et al.*, 1987b) for stability analyses of ideal and resistive internal kink modes in toroidal geometry.

Equations (4.20) and (4.24) are global by construction and can be used for computing the (generally nonlinear) mode dispersion relation. The fact that Eqs. (4.20) and (4.24) follow from a variational principle, at least in the linear limit, allows evaluating  $\delta\hat{W}_{nf}$  and  $\delta\hat{W}_{nk}$  by trial function method, thus, even with realistic mode structures obtained numerically. Meanwhile,  $\Lambda_n$  can generally be computed by solving an ordinary (nonlinear) differential equation with outgoing wave boundary conditions, Eq. (2.37) [or Eq. (2.26) in the same limit, accounting for full finite Larmor radius effects (Connor *et al.*, 1983)] for  $\hat{\kappa}_\perp^2 = k_\perp^2/k_y^2 \simeq s^2\vartheta^2|\nabla r|^2 \gg 1$ , which can be done analytically in many cases of practical interest, or numerically. Furthermore, the same approach allows accounting for finite magnetic drift orbit widths and thermal plasma plus supra-thermal particle kinetic compression effects in the long wavelength limit (Biglari and Chen, 1986b, 1991; Chen and Hasegawa, 1991; Cheng, 1982a,b; Kotschenreuther, 1986; Romanelli and Chen, 1991; Tang *et al.*, 1980). Theoretical analyses of nonlinear dynamics that are addressed by the GFLDR are discussed in Sec. V. In the rest of this section, we focus on analyses and applications of the linearized GFLDR.

## B. Shear Alfvén waves and instabilities in toroidal magnetized plasmas

The general fishbone like dispersion relation (GFLDR), Eq. (4.20), can be adopted for analyses of low mode number MHD modes (cf. Sec. IV.B.1) as well as shorter wavelength Alfvénic modes with radially localized mode structures. In this latter case, the mode structure decomposition of Eq. (4.13) reduces to the “ballooning representation” (cf. Sec. IV.A)

$$\begin{aligned} f(r, \theta, \zeta) &= \sum_{m,n \in \mathbb{Z}} A_n(r) e^{in\zeta - im\theta} \int e^{i(m-nq)\vartheta} \hat{f}_{0n}(r, \vartheta) d\vartheta \\ &= \sum_{m,n \in \mathbb{Z}} A_n(r) e^{in\zeta - im\theta} \int e^{i(m-nq)\vartheta} \mathcal{P}_{Bn}(r, \vartheta) [f_{0n}] d\vartheta , \end{aligned} \quad (4.26)$$

where  $\mathcal{P}_{B_n}(r, \vartheta) : f_{0n}(r; nq - m) \mapsto \hat{f}_{0n}(r, \vartheta)$  and the functions  $f_{0n}(r; nq - m)$  are nearly invariant under radial translations by multiples of  $(nq')^{-1}$ , while the radial envelope functions  $A_n(r)$  have characteristic spatial dependences on meso-scales, intermediate between the perpendicular wavelength and the equilibrium scale-length (Zonca, 1993a; Zonca and Chen, 1993). Because of the spatial scale separation between  $f_{0n}(r; nq - m)$ ,  $A_n(r)$  and equilibrium nonuniformities, it is possible to use the eikonal Ansatz

$$A_n(r) \sim \exp i \int nq' \theta_k(r) dr , \quad (4.27)$$

in theoretical analyses of short wavelength ballooning modes (Dewar *et al.*, 1981, 1982). Thus, Eq. (4.14) becomes

$$\nabla_{\perp} \mapsto ik_{\vartheta} \nabla r (s\vartheta - s\theta_k) + in \nabla \zeta + ik_{\vartheta} r \nabla \theta \quad (4.28)$$

and Eq. (2.37) can be rewritten as

$$\begin{aligned} & \left( \frac{\partial^2}{\partial \vartheta^2} - \frac{\partial_{\vartheta}^2 \hat{\kappa}_{\perp}}{\hat{\kappa}_{\perp}} \right) \delta \hat{\Psi}_n - \frac{\mathcal{J}^2 B_0^2}{v_A^2} \frac{\partial}{\partial t} \left[ \frac{\partial}{\partial t} + i\omega_{*pi} - \frac{3}{4} k_{\vartheta}^2 \rho_i^2 \hat{\kappa}_{\perp}^2 \left( \frac{\partial}{\partial t} + i\omega_{*pi} + i\omega_{*Ti} \right) \right] \delta \hat{\Phi}_n \\ & - \frac{4\pi \mathcal{J}^2 B_0}{ck_{\vartheta}^2 \hat{\kappa}_{\perp}} \mathbf{b} \times \boldsymbol{\kappa} \cdot \nabla \sum \left\langle m \left( \mu B_0 + v_{\parallel}^2 \right) J_0 \frac{\partial}{\partial t} \delta \hat{g}_n \right\rangle_v + [\text{NL TERMS}] = 0 . \end{aligned} \quad (4.29)$$

Here, we have introduced the notation  $\delta \hat{\Phi}_n \equiv \hat{\kappa}_{\perp} \delta \hat{\phi}_n$ , as in Eq. (4.15), and  $\omega_{*pi} = \omega_{*ni} + \omega_{*Ti}$ , with

$$\begin{aligned} \omega_{*ni} &= \left( \frac{T_0 c}{en_0 B_0} \right)_i (\mathbf{b} \times \nabla n_{0i}) \cdot \mathbf{k}_{\perp} , \\ \omega_{*Ti} &= \left( \frac{c}{eB_0} \right)_i (\mathbf{b} \times \nabla T_{0i}) \cdot \mathbf{k}_{\perp} , \end{aligned} \quad (4.30)$$

and  $\mathbf{k}_{\perp} = -i \nabla_{\perp}$ . Furthermore, we have omitted the kink drive, for it scales as  $n^{-1}$  (cf. Sec. II.C), and the nonlinear terms, since they are analyzed specifically in Sec. V.C. Equations (4.16) and (4.18), meanwhile, become

$$\delta W = \frac{2\pi^2 c^2}{|\omega|^2} \sum_{n \in \mathbb{Z}} \int_0^a dr \frac{|k_{\vartheta}|^2 (d\psi/dr)}{\mathcal{J} B_0^2} \Big|_{\vartheta=0} (\delta \hat{\Psi}_{-n0+}^{\dagger} \delta \hat{\Psi}_{n0+}) \delta \bar{W}_n , \quad (4.31)$$

$$\delta I = \frac{2\pi^2 c^2}{|\omega|^2} \sum_{n \in \mathbb{Z}} \int_0^a dr \frac{|k_{\vartheta}|^2 (d\psi/dr)}{\mathcal{J} B_0^2} \Big|_{\vartheta=0} (\delta \hat{\Psi}_{-n0+}^{\dagger} \delta \hat{\Psi}_{n0+}) i \Lambda_n , \quad (4.32)$$

with the ‘‘ballooning’’  $\delta \bar{W}_n$  expressed as, noting that  $\delta \hat{\Psi}_{-n0+}^{\dagger} \delta \hat{\Psi}_{n0+} = \delta \hat{\Phi}_{-n0+}^{\dagger} \delta \hat{\Phi}_{n0+}$ ,

$$\begin{aligned} \delta \bar{W}_n &= \delta \bar{W}_{nf} + \delta \bar{W}_{nk} = \left( \delta \hat{\Phi}_{-n0+}^{\dagger} \delta \hat{\Phi}_{n0+} \right)^{-1} \frac{1}{2} \int_{-\infty}^{\infty} \left[ \left( \frac{\partial}{\partial \vartheta} \delta \hat{\Phi}_{-n} \right)^{\dagger} \left( \frac{\partial}{\partial \vartheta} \delta \hat{\Phi}_n \right) \right. \\ & \quad + \frac{\partial_{\vartheta}^2 \hat{\kappa}_{\perp}}{\hat{\kappa}_{\perp}} \delta \hat{\Phi}_{-n}^{\dagger} \delta \hat{\Phi}_n + \delta \hat{\Phi}_{-n}^{\dagger} \frac{\mathcal{J}^2 B_0^2}{v_A^2} \frac{\partial}{\partial t} \left( \frac{\partial}{\partial t} + i\omega_{*pi} \right) \delta \hat{\Phi}_n \\ & \quad \left. + \delta \hat{\Phi}_{-n}^{\dagger} \frac{4\pi \mathcal{J}^2 B_0}{ck_{\vartheta}^2 \hat{\kappa}_{\perp}} \mathbf{b} \times \boldsymbol{\kappa} \cdot \nabla \sum \left\langle m \left( \mu B_0 + v_{\parallel}^2 \right) J_0 \frac{\partial}{\partial t} \delta \hat{g}_n \right\rangle_v \right] d\vartheta . \end{aligned} \quad (4.33)$$

Here,  $\Lambda_n$ ,  $\delta \bar{W}_n$  and other physical quantities are dependent on  $r$ , due to the global equilibrium profile variations. For very localized modes, whose radial envelope variation  $A_n(r)$  on meso-scales can be ignored, a direct comparison of Eqs. (4.16) and (4.31) yields  $\delta \hat{W}_n = |s| \delta \bar{W}_n$  and the GFLDR becomes a local dispersion relation.

In the more general case, where global plasma nonuniformities play important roles, the GFLDR, Eq. (4.20), can be cast as

$$\left[ i\Lambda_n - (\delta \bar{W}_f + \delta \bar{W}_k)_n \right] A_n(r) = D_n(r, \theta_k, \omega) A_n(r) = 0 , \quad (4.34)$$

with  $D_n(r, \theta_k, \omega)$  playing the role of a local dispersion function. This equation can be generally solved as initial value problem, using the fact that  $\omega = \omega_0 + i\partial_t$ , with  $\omega_0$  the typical (linear) mode frequency (cf. Sec. II.C). In fact, we can describe the spatiotemporal evolution of SAW wave packets in toroidal plasmas expanding the solutions of Eq. (4.34) about the characteristics

$$D_n(r, \theta_{k0}(r), \omega_0) = 0 . \quad (4.35)$$

Then, letting  $A_n(r) = \exp(-i\omega_0 t)A_{n0}(r, t)$ , with  $\partial_t A_{n0}(r, t) \sim \gamma_L A_{n0}(r, t) \sim \tau_{NL}^{-1} A_{n0}(r, t)$  (cf. Sec. II.C and V.A), the spatial-temporal evolution equation for  $A_{n0}(r, t)$  is

$$\begin{aligned} & \frac{\partial D_n}{\partial \omega_0} \left( i \frac{\partial}{\partial t} \right) A_{n0} + \frac{\partial D_n}{\partial \theta_{k0}} \left( -\frac{i}{nq'} \frac{\partial}{\partial r} - \theta_{k0} \right) A_{n0} \\ & + \frac{1}{2} \frac{\partial^2 D_n}{\partial \theta_{k0}^2} \left[ \left( -\frac{i}{nq'} \frac{\partial}{\partial r} - \theta_{k0} \right)^2 A_{n0} - \frac{i}{nq'} \frac{\partial \theta_{k0}}{\partial r} A_{n0} \right] = S_n(r, t) . \end{aligned} \quad (4.36)$$

The  $S_n(r, t)$  on the right hand side can represent either a source term [*e.g.*, (Lu *et al.*, 2012)] or nonlinear interactions (cf. Sec. V.A). The solution of Eq. (4.36) as initial value problem identifies important time scales, such as the inverse linear growth time,  $\gamma_L^{-1}$ , and the formation time of the global eigenmode structure,  $\tau_A$ , which is of the order of the wave packet bounce time between WKB turning points (Zonca *et al.*, 2004a). It can be readily shown that the global mode dispersion relation is (Zonca, 1993a,b; Zonca and Chen, 1993)

$$\Phi_0(\omega_0) = \oint nq' \theta_{k0} dr - k\pi = \ell\pi , \quad \ell \in \mathbb{N} . \quad (4.37)$$

Here,  $k = 0$  or  $k = 1$ , respectively, for  $k = 1$  for librations or rotations of  $\theta_{k0}$ -characteristics of Eq. (4.35).

Plasma equilibrium geometry and nonuniformities are also crucial to the wave-particle resonance conditions in toroidal systems. Wave-particle resonance occurs when the wave phase is constant in the reference frame moving with the particle. Meanwhile, the charged particle motion in the equilibrium  $\mathbf{B}_0$  field, characterized by the streaming along the magnetic field lines with varying  $v_{\parallel}$  plus a periodic excursion across  $\mathbf{B}_0$ , given by Eq. (2.24), causes the ‘‘particle’’ coordinates  $(r, \theta, \zeta)$  or  $(r, \theta, \xi)$  to vary in a complicated fashion. The resonance condition becomes transparent when the mode structure is projected along the particle motion in the equilibrium  $\mathbf{B}_0$ , characterized by constant actions and one time-like parameter  $\tau$ , tracing the particle position along its trajectory. This mode structure decomposition is naturally given in action angle coordinates, which are given by  $(cm^2\mu/e, \alpha)$ , with  $\mu = v_{\perp}^2/(2B_0) + \dots$  the magnetic moment (see Sec. II) and  $\alpha$  the gyrophase;  $(P_{\varphi}, \varphi)$ , with the canonical toroidal angular momentum  $P_{\varphi}$  at the leading order given by

$$P_{\phi} = \frac{e}{c} \left( F(\psi) \frac{v_{\parallel}}{\Omega} - \psi \right) ; \quad (4.38)$$

and by  $(J, \theta_c)$ , with  $J$  the ‘‘second invariant’’ and  $\theta_c$  the respective conjugate canonical angle<sup>11</sup>

$$J = m \oint v_{\parallel} dl , \quad \theta_c = \omega_b \int_0^{\theta} d\theta' / \dot{\theta}' . \quad (4.39)$$

Here,  $dl$  is the arc-length along the particle orbit and we have introduced the unified notation of  $\omega_b(\mu, J, P_{\phi})$ ,

$$\omega_b(\mu, J, P_{\phi}) = \frac{2\pi}{\oint d\theta / \dot{\theta}} , \quad (4.40)$$

for bounce and transit frequency of trapped and circulating particles, respectively. Different notations will be used only when needed. Meanwhile, from Eq. (4.39), it is readily noted that  $\theta_c = \omega_b \tau$ , with  $\tau$  the time-like parameter mentioned above. For a particle with given constants of motion, the ‘‘particle’’ coordinates  $(r, \theta, \zeta)$  or  $(r, \theta, \xi)$  are parameterized as (Zonca *et al.*, 2013b)

$$r = \bar{r} + \tilde{\rho}(\theta_c) , \quad (4.41)$$

$$\theta = \tilde{\Theta}_c(\theta_c) , \quad (4.42)$$

$$\zeta = \bar{\omega}_d \tau + \tilde{q}\theta + \tilde{\Xi}(\theta_c) , \quad (4.43)$$

for magnetically trapped particles; while, for circulating particles, Eq. (4.42) is substituted by

$$\theta = \theta_c + \tilde{\Theta}_c(\theta_c) . \quad (4.44)$$

---

<sup>11</sup> A recent review of coordinates systems and their connection with the description of the guiding center particle motion (see Sec. II) is given by (Cary and Brizard, 2009).

Here,  $\bar{r}$ ,  $\tilde{\rho}(\theta_c)$ ,  $\tilde{\Theta}_c(\theta_c)$ ,  $\tilde{\Xi}(\theta_c)$ , and

$$\bar{q} \equiv \oint q d\theta / \oint d\theta \quad (4.45)$$

are also functions of  $(\mu, J, P_\phi)$ , which can be computed from the particle equations of motion in the equilibrium  $\mathbf{B}_0$ . Furthermore,  $\tilde{\cdot}$  denotes a generic harmonic function in  $\theta_c$  with zero average, while the toroidal precessional frequency  $\bar{\omega}_d$  is

$$\bar{\omega}_d(\mu, J, P_\phi) = \frac{\omega_b}{2\pi} \oint (\dot{\xi} + \theta \dot{q}) \frac{d\theta}{\theta} . \quad (4.46)$$

Thus, the Fourier decompositions of Eqs. (4.8) and (4.9) become

$$f(r, \theta, \zeta) = \sum_{m, n \in \mathbb{Z}} e^{in\zeta - im\theta} f_{m, n}(r) = \sum_{m, n, \ell \in \mathbb{Z}} e^{i(n\bar{\omega}_d + \ell\omega_b)\tau} \mathcal{P}_{m, n, \ell} \circ f_{m, n} , \quad (4.47)$$

where the projection operators  $\mathcal{P}_{m, n, \ell}$  are defined as

$$\mathcal{P}_{m, n, \ell} \circ f_{m, n} = \frac{\lambda_{m, n}}{2\pi} \oint \exp \left\{ in\tilde{\Xi}(\theta_c) + i[n\bar{q}(\bar{r}) - m]\tilde{\Theta}_c(\theta_c) \right\} f_{m, n}(\bar{r} + \tilde{\rho}(\theta_c)) e^{-i\ell\theta_c} d\theta_c , \quad (4.48)$$

$\ell \in \mathbb{Z}$  stands for the ‘‘bounce harmonic’’, and  $\lambda_{m, n} = 1$  for trapped particles while, for circulating particles,

$$\lambda_{m, n} = \exp [i(n\bar{q}(\bar{r}) - m)\omega_b\tau] . \quad (4.49)$$

Note that this mode structure decomposition corresponds to a lifting of  $f(r, \theta, \zeta)$  to the particle phase-space. Mutatis-mutandis, the same lifting applies in the mapping space,  $\mathcal{P}_{Bn}(r, \vartheta) : f(r, \theta, \zeta) \mapsto \hat{f}_n(r, \vartheta) = A_n(r)\hat{f}_{0n}(r, \vartheta)$ , once the representations of Eqs. (4.13) or (4.26) are adopted. The integral nature of the projection operators  $\mathcal{P}_{m, n, \ell}$  and of the action of Bessel functions (cf. Sec. II.D) shows the integro-differential character of governing equations for drift Alfvén waves (DAWs) in toroidal plasmas and emphasizes the crucial roles played by plasma equilibrium geometry and nonuniformities. Assuming a monochromatic wave,  $f(r, \theta, \zeta) \propto \exp(-i\omega t)$ , the resonance condition is readily derived from Eq. (4.47) and yields

$$\omega = \omega(\mu, J, P_\phi) = n\bar{\omega}_d + \ell\omega_b \quad (4.50)$$

for magnetically trapped particles; while, for circulating particles,

$$\omega = \omega(\mu, J, P_\phi) = n\bar{\omega}_d + \ell\omega_b + (n\bar{q}(\bar{r}) - m)\omega_b , \quad (4.51)$$

where the toroidal precessional frequency  $\bar{\omega}_d$  is typically negligible for circulating particles, except for particles that are close to the trapped-to-circulating boundary in the action space.

## 1. The fishbone mode

The observation of ‘‘fishbone’’ oscillations in the PDX tokamak (McGuire *et al.*, 1983) was the first and still remains one of the most striking evidence of resonant excitations of MHD and Alfvénic modes by EPs, with clear evidence of secular loss of supra-thermal particles (White *et al.*, 1983) (cf. Sec. V.D.7) and consequent drop in the fusion reactivity, made evident by a corresponding drop in the neutron signal (McGuire *et al.*, 1983). The theoretical interpretation of experimental observation is given by (Chen *et al.*, 1984), where the general fishbone like dispersion relation (GFLDR) in the form of Eq. (4.20) was given for the first time. In this case, an internal kink mode with  $n = 1$  is resonantly excited by precession resonance with trapped supra-thermal particles<sup>12</sup>; *i.e.*, by the resonance of Eq. (4.50) with  $n = 1$  and  $\ell = 0$ , and the mode dispersion relation reads (Chen *et al.*, 1984; Coppi and Porcelli, 1986)

$$i|s| \left[ \frac{\omega(\omega - \omega_{*pi})}{\omega_A^2} (1 + \Delta) \right]^{1/2} \Big|_{r=r_s} = \delta\hat{W}_f + \delta\hat{W}_k , \quad (4.52)$$

<sup>12</sup> Fishbone oscillations driven by transit resonance were observed shortly afterwards (Heidbrink *et al.*, 1986) and later explained theoretically (Betti and Freidberg, 1993).

where  $\omega_{*pi}$  is defined in Eq. (4.30),  $\omega_A = v_A/(qR_0)$ ,  $r_s$  is the radius of the  $q(r_s) = 1$  magnetic surface and  $\Delta \propto q^2$  is the enhancement of plasma inertia due to geodesic curvature (Glasser *et al.*, 1975; Graves *et al.*, 2000). The general derivation of  $\Lambda_n^2 = \omega(\omega - \omega_{*pi})(1 + \Delta)/\omega_A^2$  will be discussed in Sec. IV.B.2. Meanwhile, the expression of  $\delta\hat{W}_f$ , in its simplest form, is given by (Bussac *et al.*, 1975)

$$\delta\hat{W}_f = 3\pi\Delta q_0 (13/144 - \beta_{ps}^2) (r_s^2/R_0^2) \quad , \quad (4.53)$$

with  $\beta_{ps} = -(R_0/r_s^2)^2 \int_0^{r_s} r^2 (d\beta/dr) dr$  and  $\Delta q_0 = 1 - q(r=0)$ . The fluid term,  $\delta\hat{W}_f$ , includes the contribution of the EP adiabatic and convective responses, which have been separated from the kinetic particle response by letting

$$\delta g \equiv \delta K + i \frac{e}{m} Q \bar{F}_0 \partial_t^{-1} \langle \delta \psi_g \rangle \quad (4.54)$$

in Eqs. (2.21) and (2.22), with  $Q \bar{F}_0$  defined as

$$i Q \bar{F}_0 = - \frac{\partial \bar{F}_0}{\partial \mathcal{E}} \frac{\partial}{\partial t} + \frac{\mathbf{b} \times \nabla \bar{F}_0}{\Omega} \cdot \nabla \quad . \quad (4.55)$$

The linearized gyrokinetic equation, Eq. (2.23), assuming  $\epsilon_B/\epsilon_F \ll 1$  (cf. Sec. II.A), can be cast as

$$\left( \frac{\partial}{\partial t} + v_{\parallel} \nabla_{\parallel} + \mathbf{v}_d \cdot \nabla_{\perp} \right) \delta K = i \frac{e}{m} [Q \bar{F}_0 \langle \delta \phi_g - \delta \psi_g \rangle - \mathbf{v}_d \cdot \nabla_{\perp} Q \bar{F}_0 \partial_t^{-1} \langle \delta \psi_g \rangle] \quad . \quad (4.56)$$

Note that working with  $\delta K$  is particularly convenient in linear analyses, since  $\delta K \rightarrow 0$  in the fluid ion ( $\omega \gg \bar{\omega}_d, \omega_b$ ) and massless electron ( $\omega_b \gg \omega, \bar{\omega}_d$ ) limits. When considering short wavelength modes,  $\epsilon_F/\epsilon_{\perp} \ll 1$ , operators

$$\mathbf{v}_d \cdot \nabla_{\perp} \equiv i \omega_d \quad (4.57)$$

and  $Q \bar{F}_0$  in Eq. (4.56) are commuting. Neglecting finite orbit width effects, assuming  $\delta \phi = \delta \psi = \delta \phi_0(r) \exp(-i\omega t + i\zeta - i\theta)$  and using Eqs. (4.42) to (4.47), it is possible to obtain

$$\delta K = \frac{e}{m} \frac{Q \bar{F}_0}{\omega} \frac{\overline{e^{iq(r)\theta} \omega_d e^{-i\theta}}}{\bar{\omega}_d - \omega} \delta \phi_0(r) e^{i(\zeta - q(r)\theta - \omega t)} \quad , \quad (4.58)$$

$\overline{(\dots)} = (\oint d\theta/\dot{\theta})^{-1} \oint (\dots) d\theta/\dot{\theta}$  denoting bounce-averaging along the particle orbit in the equilibrium  $\mathbf{B}_0$ . Meanwhile, for a high aspect-ratio circular tokamak equilibrium,  $\delta\hat{W}_k$  is given by (Chen *et al.*, 1984)

$$\delta\hat{W}_k = 4 \frac{\pi^2}{B_0^2} m \Omega^2 \frac{R_0}{r_s^2} \int_0^{r_s} \frac{r^3}{q} dr \int \mathcal{E} d\mathcal{E} d\lambda \sum_{v_{\parallel}/|v_{\parallel}| = \pm 1} \frac{\overline{e^{i\theta} \omega_d e^{-iq(r)\theta}}}{\bar{\omega}_d - \omega} \frac{\hat{\tau}_b Q \bar{F}_0}{\bar{\omega}_d - \omega} \quad , \quad (4.59)$$

where  $\lambda = \mu B_0/\mathcal{E}$ ,  $\hat{\tau}_b = \pi/\omega_b$  for trapped particles and  $Q \bar{F}_0$  is computed on the mode structure  $\sim \exp(-i\omega t + i\zeta - i\theta)$ . It is worthwhile recalling (Chen *et al.*, 1984) that Eq. (4.52), with  $\delta\hat{W}_k$  given in Eq. (4.59), reproduces the well-known forms of kinetic MHD energy principles in the collisionless (Kruskal and Oberman, 1958; Rosenbluth and Rostoker, 1959) and low-frequency limit (Antonsen *et al.*, 1981; Antonsen and Lee, 1982; Van Dam *et al.*, 1982). Furthermore, Eq. (4.59) can be extended to include the bounce-averaged response of circulating particles, for which  $\hat{\tau}_b = \tau_b = 2\pi/\omega_b$ , provided that the  $\ell = 0$  resonance condition of Eq. (4.51) is taken into account, as emphasized by (Merle *et al.*, 2012).

As mentioned in the introduction of Sec. IV, Eq. (4.52) admits two branches as solution: an EPM branch, the precessional fishbone (Chen *et al.*, 1984), and a gap mode branch, the diamagnetic fishbone (Coppi *et al.*, 1988b; Coppi and Porcelli, 1986). The former branch satisfies Eq. (4.23), noting that  $\delta\hat{W}_f$  is independent of  $\omega$  in this case (see also Sec. IV.B.2); while for the latter branch, given Eq. (4.22) causality constraints, Eq. (4.52) reads

$$-|s| \left[ \frac{\omega(\omega_{*pi} - \omega)}{\omega_A^2} (1 + \Delta) \right]^{1/2} \Bigg|_{r=r_s} = \delta\hat{W}_f + \delta\hat{W}_k \quad . \quad (4.60)$$

Since the early observation of fishbones (McGuire *et al.*, 1983) and their consequence on plasma fusion performance (McGuire *et al.*, 1983; White *et al.*, 1983), the internal kink/fishbone problem has been one of the most widely studied in the magnetic fusion literature. Further interest in the kink/fishbone stability was triggered by the observation in the Joint European Torus (JET) (JET Joint Undertaking, 1991; Rebut *et al.*, 1985; Rebut and Kenn,

1987) of sawtooth activity stabilization in plasma discharges with additional heating (Campbell *et al.*, 1988). This was explained with the strong stabilizing effect of a supra-thermal trapped particle population on the internal kink mode (Coppi *et al.*, 1988a; White *et al.*, 1988) and confirmed by later works. The stabilization of the internal kink mode by EPs, in the limit  $\omega_{*pi} \rightarrow 0$ , was noted first by (White *et al.*, 1985); later, it became evident that there is a regime free of both kink and fishbone modes (Coppi *et al.*, 1990; Porcelli, 1991a; White *et al.*, 1989, 1990), with important consequence on tokamak operations (cf. Sec. IV.C for further details).

As anticipated in Sec. IV.A, various extensions of Eq. (4.52) are possible, either in the description of the generalized inertia term  $\Lambda_n$ , defined in Eq. (4.19), or in the calculation of  $\delta\hat{W}_f$  and  $\delta\hat{W}_k$ . For  $\Lambda_n$ , effects due to resistivity (Coppi *et al.*, 1976a,b), diamagnetic drift (Ara *et al.*, 1978; Bussac *et al.*, 1976), ion viscosity (Porcelli, 1987) and finite electron inertia (Porcelli, 1991b; Wesson, 1990), as well as finite Larmor radius (Pegoraro *et al.*, 1989, 1991) and Hall terms (Zakharov and Rogers, 1992) have been included. A reasonably accurate although not very recent theoretical review can be found in (Migliuolo, 1993)<sup>13</sup>. For  $\delta\hat{W}_f$  and  $\delta\hat{W}_k$ , it is worthwhile mentioning the stabilization effect due to perpendicular compressibility, first noted by (Kruskal and Kulsrud, 1958; Rosenbluth and Rostoker, 1959; Rutherford *et al.*, 1978) and explicitly computed by (Fogaccia and Romanelli, 1995; Hastie and Hender, 1988; Kuvshinov and Mikhailovskii, 1987; Porcelli *et al.*, 1996; Wu *et al.*, 1994).

Among the various applications of Eq. (4.52), one that has recently attracted significant theoretical as well as experimental interest is the study of the so-called “electron fishbone” (e-fishbone), where the internal kink mode is resonantly excited by energetic electrons accelerated by auxiliary heating and/or current drive systems. Experimental observations of e-fishbones were first reported in DIII-D (Luxon, 2002) in conjunction with Electron Cyclotron Resonance Heating (ECRH) on the high magnetic field side (Wong *et al.*, 2000), followed by further evidence in plasmas with both ECRH and/or Lower Hybrid Heating (LHH) and current drive (LHCD) (cf. Sec. IV.C). E-fishbones are of particular interest, for the perpendicular (bounce-averaged) trapped supra-thermal electron transport closely resembles that of alpha particles produced by fusion reactions in reactor relevant plasma conditions (Zonca *et al.*, 2007a,b), which are both characterized by small magnetic drift orbit widths normalized to the macroscopic system size, unlike supra-thermal ions in present day experiments (Pizzuto *et al.*, 2010; Zonca, 2008; Zonca and Chen, 2008a). Equations (4.52) and (4.60) are readily usable for the investigation of precessional (EPM) and diamagnetic (gap mode) e-fishbone branches in monotonic  $q$  profile plasma equilibria. However, due to the important role of LHH and LHCD in some experimental conditions yielding e-fishbones (Maget *et al.*, 2006; Romanelli *et al.*, 2002; Smeulders *et al.*, 2002), the relevant fishbone dispersion relation for a hollow  $q$  profile, with the minimum value of  $q(r_s) \simeq 1$  at  $r = r_s$ , is obtained from Eq. (4.24) with  $n = 1$  and  $k_{\parallel 0} L_0 = \Delta q_s = q(r_s) - 1$ . Meanwhile, the analogue of Eq. (4.60) for the gap mode branch with  $s = 0$  (Hastie *et al.*, 1987b; Zonca *et al.*, 2007a) is

$$-S(\Delta q_s^2 - \Lambda^2)^{3/4} \left[ 1 + \Delta q_s / \sqrt{\Delta q_s^2 - \Lambda^2} \right]^{1/2} = \delta\hat{W}_f + \delta\hat{W}_k, \quad (4.61)$$

with  $\Lambda^2 \simeq \omega(\omega - \omega_{*pi})(1 + \Delta)/\omega_A^2$  as noted above (cf. also Sec. IV.B.2).

It is worthwhile commenting on the  $\Delta \propto q^2$  enhancement of plasma inertia due to geodesic curvature in Eq.(4.52). In the “banana regime” (Hinton and Hazeltine, 1976) and for circular, high aspect-ratio, tokamak plasma equilibria, the correct form was first pointed out in (Graves *et al.*, 2000)

$$\Delta = \left( 1.6(R_0/r_s)^{1/2} + 0.5 \right) q^2, \quad (4.62)$$

where the  $1.6(R_0/r_s)^{1/2}q^2$  factor comes from trapped and barely circulating particles; the  $0.5q^2$  term, meanwhile, is due to well circulating particles, *i.e.*, those particles for which the  $v_{\parallel}$  modulation along the periodic transit orbit is of order  $r_s/R_0$ . It differs from the well known  $2q^2$  factor (Glasser *et al.*, 1975) due to the intrinsic limitation of the ideal MHD model in assuming an isotropic pressure response (Zonca *et al.*, 2007a). Kinetic “bulk ion inertia enhancement” for low frequency (“banana regime”) MHD modes was analyzed by (Belikov *et al.*, 1992; Mikhailovskii and Suramlishvili, 1979; Mikhailovskii and Tsypin, 1983), where estimates were given for both inertia enhancement as well as ion Landau damping. A more systematic analytic approach was given in Refs. (Graves *et al.*, 2000) and (Bondeson and Chu, 1996). Here, it is worthwhile noting that the inertia enhancement factor is identical to the zonal flow (ZF) polarizability (Hinton and Rosenbluth, 1999; Rosenbluth and Hinton, 1998). This is due to the fact that, at long wavelengths, Eq. (2.37) predicts that SAW compressibility due to geodesic curvature coupling at  $k_{\parallel} = 0$  is identical to the corresponding dynamics of electrostatic waves with  $k_{\zeta} = k_{\theta} = 0$ , provided that diamagnetic effects are neglected and  $\bar{\omega}_{di} \ll |\omega| \ll \omega_{bi}$  (Zonca *et al.*, 2007a).

<sup>13</sup> See also (Biglari and Chen, 1986a; Pegoraro and Schep, 1986; Shi and Sui, 1997).

Parallel and perpendicular plasma compressions are also relevant for the accurate evaluation of the enhancement of plasma inertia when  $|\omega| \gtrsim \omega_{bi}$ . The importance of accounting for thermal ion transit resonance in the study of resistive MHD modes was proposed by (Romanelli and Chen, 1991), while its effect on the SAW continuous spectrum was given by (Kotschenreuther, 1986; Mikhailowskii, 1973). Using the expression of  $\Lambda^2$  computed for  $\omega_{bi} \ll |\omega| \ll \omega_A$  (cf. Sec. IV.B.2), it was demonstrated that, for  $|\omega| \gg \omega_{ti}$ , a high frequency kink/fishbone can be excited (Zonca, 2003; Zonca *et al.*, 2007a,b), satisfying the same dispersion relation, Eq. (4.20), but with

$$\Lambda^2 = \frac{\omega^2}{\omega_A^2} - \frac{\omega_{BAE}^2}{\omega_A^2} \left[ 1 + \frac{\omega_{BAE}^2 (46/49) + (32/49)(T_e/T_i) + (8/49)(T_e/T_i)^2}{q^2 \omega^2 (1 + (4/7)(T_e/T_i))^2} \right]. \quad (4.63)$$

Here  $\omega_{BAE} = q\omega_{ti}(7/4 + T_e/T_i)^{1/2}$  is the fluid limit expression of the BAE frequency and  $\omega_{ti} = (2T_i/m_i)^{1/2}/(qR_0)$ . While the high frequency EPM/fishbone branch is explicitly solved for by Eq. (4.23), the corresponding fishbone/gap mode is obtained for  $\delta\dot{W}_f + \mathbb{R}e\delta\dot{W}_k < 0$ , as specified in Eq. (4.22). High frequency fishbones have been observed in JET (Nabais *et al.*, 2005) and fluctuations with similar features, consistent with Eqs. (4.20) and (4.63), were observed for the first time during D-T experiments in TFTR (Bell *et al.*, 1995; Grove and Meade, 1985), as recently reported (Fredrickson, 2011). JET observations are consistent with theoretical predictions (Zonca *et al.*, 2007b, 2009). Meanwhile, high frequency fishbones have been investigated numerically, showing the crucial importance of properly accounting for accurate mode structures (Kolesnichenko *et al.*, 2010a).

The GFLDR theoretical framework, in summary, suggests that kink/fishbone stability may be strongly affected by kinetic effects: while potential energy is modified by supra-thermal particles as well as thermal electrons and ions, the generalized inertia is mostly affected by thermal ions, although supra-thermal ions may contribute significantly as well (see Secs. IV.B.2 and IV.B.3 for more details). This can be noted from Eqs. (4.52), (4.60) and (4.61), when using the expression of  $\Lambda^2$  obtained from Eq. (4.19) including supra-thermal ion response in the long wavelength limit.

## 2. The low frequency shear Alfvén wave spectrum

Early investigations of the low frequency SAW/DAW spectrum in toroidal geometries were focused on kinetic descriptions of wave-particle interactions with the thermal plasma component (Kotschenreuther, 1986; Mikhailowskii, 1973). Theoretical studies of collisionless kinetic ballooning modes (KBM) (Cheng, 1982a,b; Tang *et al.*, 1980) in particular attracted significant attention, with emphasis on the possibility of exciting short wavelength modes by EPs (Biglari and Chen, 1986a,b, 1991; Chen, 1994; Chen and Hasegawa, 1991; Rewoldt, 1988; Spong *et al.*, 1988; Tsai and Chen, 1993; Weiland and Chen, 1985). The experimental observation of BAEs (Heidbrink *et al.*, 1993; Turnbull *et al.*, 1993), excited by EPs in the low-frequency SAW continuous spectrum gap due to finite thermal plasma compressibility (Chu *et al.*, 1992, 1993; Turnbull *et al.*, 1993), has revived the interest in this frequency range because of the impact of these fluctuations on EP confinement (cf. Sec. IV.C).

All these modes existing near the low-frequency KTI gap are well described within the theoretical framework of the GFLDR. The generalized inertia term, Eq. (4.19), can be computed from the solution of the  $\hat{\kappa}_\perp^2 = k_\perp^2/k_\theta^2 \simeq s^2\vartheta^2|\nabla r|^2 \gg 1$  limit of the linearized Eq. (4.29), along with the same limit of the quasineutrality condition, the linearized Eq. (2.28), which reads (Zonca *et al.*, 1999, 1996, 1998)

$$\left(1 + \frac{1}{\tau}\right) (\delta\hat{\Phi}_n - \delta\hat{\Psi}_n) + \left(1 - \frac{\omega_{*pi}}{\omega}\right) k_\theta^2 \rho_i^2 \hat{\kappa}_\perp^2 \delta\hat{\Psi}_n = \frac{T_i}{n_0 e} \hat{\kappa}_\perp \left\langle \left(1 - k_\theta^2 \frac{\mu B_0}{2\Omega^2} \hat{\kappa}_\perp^2\right) \delta\hat{K}_{in} \right\rangle_v. \quad (4.64)$$

Here, we have expressed the non-adiabatic thermal ion response  $\delta\hat{g}_n$  in terms of  $\delta\hat{K}_n$ , according to Eq. (4.54), and adopted the small thermal ion Larmor radius ordering of Sec. II.E, consistent with Eq. (4.29). Furthermore, one single species of core-plasma ions with unit electric charge  $e$  has been assumed,  $n_0$  is the equilibrium core plasma density,  $\tau = T_e/T_i$  and EPs are neglected in the inertial layer, assuming that EP orbits are larger than the layer width and/or that their density is much smaller than that of the core plasma component. Taking the  $s^2\vartheta^2|\nabla r|^2 \gg 1$  limits of Eqs. (4.29) and (4.64), and noting that only trapped thermal and supra-thermal electrons enter via their bounce-average responses, one could then demonstrate that thermal ions dominate the kinetic layer response and the expression of  $\Lambda_n$  (cf. Sec. IV.A) (Chavdarovski and Zonca, 2009).

As noted in Sec. IV.A, the GFLDR can be computed numerically and/or analytically with various levels of approximation. Here, we discuss analytic derivations using the so called  $(s, \alpha)$  model equilibrium (Connor *et al.*, 1978) for the local description of a high aspect ratio tokamak (cf. Sec. II.A) with shifted circular magnetic surfaces. The

magnetic shear  $s$  is defined in Eq. (4.17),  $\alpha$  is the dimensionless ‘‘ballooning’’ pressure gradient parameter

$$\alpha = -R_0 q^2 \frac{d\beta}{dr} , \quad (4.65)$$

and  $\beta$  is defined in Sec. II. In this case, Boozer coordinates (Boozer, 1981, 1982) are easily constructed [cf., *e.g.*, (Fu, 1995)], with  $\mathcal{J} = qR_0(B_0/B^2)$  and, from Eq. (4.28)<sup>14</sup>

$$\hat{\kappa}_\perp^2 = [s(\vartheta - \theta_k) - \alpha \sin \vartheta]^2 (1 + 2\Delta' \cos \vartheta) - 2s(\vartheta - \theta_k)\Delta' \sin \vartheta + 1 - 2(r/R_0 + \Delta') \cos \vartheta , \quad (4.66)$$

where  $\Delta'$  is the radial derivative of the Shafranov shift and, consistent with the high aspect ratio tokamak ordering,  $|\Delta'| \sim r/R_0 \ll 1$ . The linearized vorticity equation, Eq. (4.29), can then be rewritten at the leading order as

$$\begin{aligned} & \left( \frac{\partial^2}{\partial \vartheta^2} + \Delta' \cos \vartheta \right) \delta \hat{\Psi}_n + \frac{\omega}{\omega_A^2} [1 + 4(r/R_0) \cos \vartheta] \left[ \omega - \omega_{*pi} - \frac{3}{4} k_\vartheta^2 \rho_i^2 \hat{\kappa}_\perp^2 (\omega - \omega_{*pi} - \omega_{*Ti}) \right] \delta \hat{\Phi}_n \\ & + \frac{4\pi R_0 q^2}{B_0} \frac{g(\vartheta, \theta_k) \omega}{ck_\vartheta \hat{\kappa}_\perp} \left[ \left\langle m_i (\mu B_0 + v_\parallel^2) \left( 1 - k_\vartheta^2 \frac{\mu B_0}{2\Omega_i^2} \hat{\kappa}_\perp^2 \right) \delta \hat{K}_{in} \right\rangle_v + \left\langle m_E (\mu B_0 + v_\parallel^2) J_0 \delta \hat{g}_{En} \right\rangle_v \right] \\ & + \left[ \frac{\alpha \cos \vartheta}{\hat{\kappa}_\perp^2} - \frac{(s - \alpha \cos \vartheta)^2}{\hat{\kappa}_\perp^4} + \frac{(\alpha_c - \alpha)g(\vartheta, \theta_k)}{\hat{\kappa}_\perp^2} \right] \delta \hat{\Psi}_n = 0 , \end{aligned} \quad (4.67)$$

where  $g(\vartheta, \theta_k) = [s(\vartheta - \theta_k) - \alpha \sin \vartheta] \sin \vartheta + \cos \vartheta$ , having expressed  $\delta \hat{g}_n$  in terms of  $\delta \hat{K}_n$  for the core plasma components and neglected kinetic thermal electron effects,  $\propto \delta \hat{K}_{en}$ , for  $|\omega| \gg |n\bar{\omega}_{dne}|$  (Chavdarovski and Zonca, 2009). Here,  $\omega_A = v_A/(qR_0)$ ,  $\alpha_c$  refers to the core plasma components only, while  $\alpha$  includes EPs as well. In the long wavelength limit,  $k_\vartheta^2 \rho_i^2 \rightarrow 0$ , and without kinetic thermal ion compression terms,  $\propto \delta \hat{K}_{in}$ , Eq. (4.67) reduces to the form used in analyses of KBM resonant excitations by EPs (Biglari and Chen, 1991; Chen, 1994; Tsai and Chen, 1993).

The generalized inertia term  $\Lambda_n$  can be computed from Eqs. (4.64) and (4.67) for  $k_\vartheta^2 \rho_i^2 \rightarrow 0$ ,  $|\delta \hat{g}_{En}| \rightarrow 0$  and  $s^2 \vartheta^2 \rightarrow \infty$ . Here, we follow (Zonca *et al.*, 1996) and consider finite mode number (Lauber *et al.*, 2009; Zonca *et al.*, 2009) in order to be able to use Eq. (4.20) also for moderate (poloidal, toroidal) mode numbers  $(m, n)$ . We also consider mode structures that may have a kinetic singular (inertial) layer located away from a mode rational surface, so that  $k_\parallel qR_0 = (nq - m)$  is generally non vanishing but still  $|k_\parallel qR_0| \ll 1$ . This allows us to derive  $\Lambda_n$  expressions that apply for  $s = 0$  as well and can be used in Eq. (4.24). Equation (4.67) shows that mode structures can be written as asymptotic series in the expansion parameter  $|\omega/\omega_A| \ll 1$ ; *i.e.*,  $\delta \hat{\Phi}_n = \delta \hat{\Phi}_n^{(0)} + \delta \hat{\Phi}_n^{(1)} + \dots$  and similarly for  $\delta \hat{\Psi}_n$ . Here,  $\delta \hat{\Phi}_n^{(0)} = \delta \hat{\Psi}_n^{(0)} = \delta \hat{\Psi}_n^{(0)}(\vartheta_1)$ ,  $\delta \hat{\Psi}_n^{(1)} = 0$ ,  $\delta \hat{\Phi}_n^{(1)} = \delta \hat{\Phi}_n^{(1)}(\vartheta_0, \vartheta_1)$ ,  $\vartheta_0 \sim 1$ , and  $\vartheta_1 \sim |\omega_A/\omega| \gg 1$ . Carrying out the expansion systematically (Zonca *et al.*, 1996), Eq. (4.67) yields, at the second order,

$$\begin{aligned} & \frac{\partial^2}{\partial \vartheta_1^2} \delta \hat{\Psi}_n^{(0)} + \Lambda_n^2 \delta \hat{\Psi}_n^{(0)} = 0 , \\ & \Lambda_n^2 = \frac{\omega(\omega - \omega_{*pi})}{\omega_A^2} + \left[ \delta \hat{\Psi}_n^{(0)} \right]^{-1} \int_0^{2\pi} \frac{2R_0 q^2}{B_0} \frac{g(\vartheta, \theta_k) \omega}{ck_\vartheta \hat{\kappa}_\perp} \left\langle m_i (\mu B_0 + v_\parallel^2) \delta \hat{K}_{in}^{(1)} \right\rangle_v \Big|_{|s\vartheta_1| \rightarrow \infty} d\vartheta_0 . \end{aligned} \quad (4.68)$$

Here,  $\delta \hat{K}_{in}^{(1)}$  is given by Eq. (4.56) and can be calculated explicitly in the limits of well circulating as well as deeply trapped ions (Chavdarovski and Zonca, 2009).

For well circulating ion,  $v_\parallel \simeq \text{constant}$ , we find (Lauber *et al.*, 2009; Zonca *et al.*, 2010, 2009)

$$\begin{aligned} \Lambda_n^2 = & \frac{\omega^2}{\omega_A^2} \left( 1 - \frac{\omega_{*pi}}{\omega} \right) + q^2 \frac{\omega_{ti}^2}{2\omega_A^2} \left[ \left( 1 - \frac{\omega_{*ni}}{\omega} \right) \left( (\omega/\omega_{ti}^{(+)})F(\omega/\omega_{ti}^{(+)}) + (\omega/\omega_{ti}^{(-)})F(\omega/\omega_{ti}^{(-)}) \right) \right. \\ & - \frac{\omega_{*Ti}}{\omega} \left( (\omega/\omega_{ti}^{(+)})G(\omega/\omega_{ti}^{(+)}) + (\omega/\omega_{ti}^{(-)})G(\omega/\omega_{ti}^{(-)}) \right) \\ & \left. - \left( (\omega/\omega_{ti}^{(+)})N_m(\omega/\omega_{ti}^{(+)}) \frac{N_{m-1}(\omega/\omega_{ti}^{(+)})}{D_{m-1}(\omega/\omega_{ti}^{(+)})} + (\omega/\omega_{ti}^{(-)})N_m(\omega/\omega_{ti}^{(-)}) \frac{N_{m+1}(\omega/\omega_{ti}^{(-)})}{D_{m+1}(\omega/\omega_{ti}^{(-)})} \right) \right] , \end{aligned} \quad (4.69)$$

where  $\omega_{ti} = (2T_i/m_i)^{1/2}/(qR_0)$ ,  $\omega_{ti}^{(\pm)}/\omega_{ti} = 1 \pm (nq - m)$  and the functions  $F(x)$  and  $G(x)$  are defined as

$$\begin{aligned} F(x) &= x(x^2 + 3/2) + (x^4 + x^2 + 1/2)Z(x) , \\ G(x) &= x(x^4 + x^2 + 2) + (x^6 + x^4/2 + x^2 + 3/4)Z(x) , \end{aligned} \quad (4.70)$$

<sup>14</sup> With a more accurate (higher order) expansion,  $\alpha$  in Eq. (4.66) is replaced by  $\alpha + 2(r/R_0) - (3 - 2s)\Delta'$  (Fu *et al.*, 2005).

and contain the plasma dispersion function  $Z(x) = \pi^{-1/2} \int_{-\infty}^{\infty} e^{-y^2}/(y-x)dy$ . Meanwhile, the functions  $N_m(x)$  and  $D_m(x)$ , to be computed at the poloidal mode number  $m$ , are also polynomials containing the  $Z(x)$  function

$$\begin{aligned} N_m(x) &= \left(1 - \frac{\omega_{*ni}}{\omega}\right) [x + (1/2 + x^2) Z(x)] - \frac{\omega_{*Ti}}{\omega} [x(1/2 + x^2) + (1/4 + x^4) Z(x)] , \\ D_m(x) &= \left(\frac{1}{x}\right) \left(1 + \frac{1}{\tau}\right) + \left(1 - \frac{\omega_{*ni}}{\omega}\right) Z(x) - \frac{\omega_{*Ti}}{\omega} [x + (x^2 - 1/2) Z(x)] . \end{aligned} \quad (4.71)$$

With the typical long wavelength ordering  $|k_{\vartheta}\rho_i| \sim |\omega^2/\omega_A^2|$  (Zonca *et al.*, 1999), we have  $\delta\hat{\Phi}_n^{(1)} \sim |\omega/\omega_A|\delta\hat{\Phi}_n^{(0)}$ ; *i.e.*, mode structures with typical SAW/DAW polarization that characterize most unstable fluctuation structures in the KTI frequency range from KMB to BAE modes (Chen and Zonca, 2007a). However, for  $D_{m\mp 1}(\omega/\omega_{ti}^{(\pm)}) \sim |\omega/\omega_A| \ll 1$ , we have  $\delta\hat{\Phi}_n^{(1)} \sim \delta\hat{\Phi}_n^{(0)}$  and mode structures have a mixed Alfvénic and acoustic polarization, which is that of BAAE (Gorelenkov *et al.*, 2007a,b, 2009). When this happens,  $D_{m\mp 1}(\omega/\omega_{ti}^{(\pm)}) \simeq 0$  gives the lowest order mode dispersion relation, and BAAE is essentially a strongly damped drift wave (DW) (Zonca *et al.*, 2010). In fact, both SAW/DAW and BAAE branches are characterized by a predominantly sinusoidal (*a.c.*) parallel electric field perturbation. However,  $\delta E_{\parallel}$  is an important component of the BAAE mode structure, while it is a perturbation for long wavelength SAW/DAW mode structures. Furthermore, typical BAAE frequencies are lower than those of SAW/DAW, so that wave-particle interactions with thermal ions are stronger. As a result, Landau damping is generally much stronger for BAAE than for SAW/DAW, unless sound wave frequency and  $\omega_{ti}$  are well separate; *i.e.*,  $T_e \gg T_i$ , or for sufficiently short wavelengths that DW is near its instability threshold (Zonca *et al.*, 2010).

It is also worthwhile reminding that, for sufficiently low frequencies comparable to the thermal ion bounce frequency,  $\omega_{bi}$ , kinetic responses of magnetically trapped core plasma ions must be accounted for (Chavdarovski and Zonca, 2009; Lauber *et al.*, 2009), especially when realistic comparisons with experimental observations are made (Curran *et al.*, 2012; Lauber *et al.*, 2009, 2012) (cf. Sec. IV.C). In this case, Eq. (4.68) can either be evaluated numerically or Eq. (4.69) can be extended to account for magnetically deeply trapped thermal ions. The resulting  $\Lambda_n^2$  expression (Chavdarovski and Zonca, 2009) smoothly connects to  $\Lambda_n^2 = \omega(\omega - \omega_{*pi})(1 + \Delta)/\omega_A^2$  for  $\bar{\omega}_{di} \ll |\omega| \ll \omega_{bi}$ , with  $\Delta$  given by Eq. (4.62); and, for  $|\omega| \gg \omega_{bi}$ , reduces to the high mode number limit of Eq. (4.69), which reads (Zonca *et al.*, 1996)

$$\Lambda_n^2 = \frac{\omega^2}{\omega_A^2} \left(1 - \frac{\omega_{*pi}}{\omega}\right) + q^2 \frac{\omega\omega_{ti}}{\omega_A^2} \left[ \left(1 - \frac{\omega_{*ni}}{\omega}\right) F(\omega/\omega_{ti}) - \frac{\omega_{*Ti}}{\omega} G(\omega/\omega_{ti}) - \frac{N_m^2(\omega/\omega_{ti})}{D_m(\omega/\omega_{ti})} \right] ; \quad (4.72)$$

and, in the  $|\omega| \gg \omega_{ti}$  limit, yields Eq. (4.63). Setting  $\Lambda_n^2 = 0$ , Eq. (4.63) demonstrates that BAE accumulation point frequency in the long wavelength limit is degenerate with the frequency of the Geodesic Acoustic Mode (GAM) (Winsor *et al.*, 1968), as noted in (Chen and Zonca, 2007a; Zonca *et al.*, 2006) and later by (Smolyakov *et al.*, 2008; Zonca and Chen, 2008b). The coupling of SAW/DAW, GAM and acoustic branches has also been addressed in the investigation of drift sound waves in the W7-AS stellarator (Kolesnichenko *et al.*, 2009).

Fluctuations of SAW/DAW and BAAE branches are described by the same GFLDR, Eq. (4.34) (Zonca *et al.*, 2010). Expressions for  $\delta\bar{W}_f$  and  $\delta\bar{W}_k$  can be obtained from Eq. (4.33), and, for the  $(s, \alpha)$  model equilibrium (Connor *et al.*, 1978), can be rewritten as (Chen, 1994; Tsai and Chen, 1993)

$$\begin{aligned} \delta\bar{W}_{nf} &= \left(\delta\hat{\Phi}_{-n0+}^{\dagger} \delta\hat{\Phi}_{n0+}^{(0)}\right)^{-1} \frac{1}{2} \int_{-\infty}^{\infty} \left[ \left(\frac{\partial}{\partial\vartheta} \delta\hat{\Phi}_{-n}^{(0)}\right)^{\dagger} \left(\frac{\partial}{\partial\vartheta} \delta\hat{\Phi}_n^{(0)}\right) \right. \\ &\quad \left. + \delta\hat{\Phi}_{-n}^{(0)\dagger} \left( \frac{(s - \alpha \cos\vartheta)^2}{\hat{\kappa}_{\perp}^4} - \frac{\alpha \cos\vartheta}{\hat{\kappa}_{\perp}^2} + \frac{\hat{\alpha}_E g(\vartheta, \theta_k)}{\hat{\kappa}_{\perp}^2} \right) \delta\hat{\Phi}_n^{(0)} \right] d\vartheta , \end{aligned} \quad (4.73)$$

$$\delta\bar{W}_{nk} = \left(\delta\hat{\Phi}_{-n0+}^{\dagger} \delta\hat{\Phi}_{n0+}^{(0)}\right)^{-1} \left(-\frac{1}{2}\right) \int_{-\infty}^{\infty} \delta\hat{\Phi}_{-n}^{(0)\dagger} \left[ \frac{4\pi R_0 q^2}{B_0} \frac{g(\vartheta, \theta_k) \omega}{ck_{\vartheta} \hat{\kappa}_{\perp}} \left\langle m_E (\mu B_0 + v_{\parallel}^2) J_0 \delta\hat{K}_{En} \right\rangle_v \right] d\vartheta . \quad (4.74)$$

Here,  $\hat{\alpha}_E$  is defined as

$$\hat{\alpha}_E = - \left(\delta\hat{\Phi}_n^{(0)}\right)^{-1} \frac{4\pi}{B_0^2} R_0 q^2 \left\langle m_E (\mu B_0 + v_{\parallel}^2) \frac{\partial \bar{F}_{0E}}{\partial r} (1 - J_0^2) \right\rangle_v \delta\hat{\Phi}_n^{(0)} ; \quad (4.75)$$

and we have used the representation of Eq. (4.54) for expressing  $\delta\hat{g}_{En}$  as a function  $\delta\hat{K}_{En}$ . Equation (4.73) can be easily evaluated using  $\delta\hat{\Phi}_n^{(0)} = 1$  as trial function and neglecting  $\propto \hat{\alpha}_E$  contributions. Meanwhile, Eq. (4.74) can also be computed analytically, by direct substitution of approximate solutions of Eq. (4.56) obtained for either well circulating [ $v_{\parallel} \simeq \text{const}$ ] or deeply trapped EPs [ $v_{\parallel} \simeq qR_0\omega_b\theta_b \cos\omega_b t$ ; with  $\omega_b = (r/R_0)^{1/2} \mathcal{E}^{1/2}/(qR_0)$  and  $\theta_b$  the

magnetic bounce angle]. Denoting by the superscript “ $u$ ” (untrapped) circulating particles and by the subscript “ $t$ ” magnetically trapped particles, one can let  $\delta\bar{W}_{nk} = \delta\bar{W}_{nk}^u + \delta\bar{W}_{nk}^t$  and obtain

$$\delta\bar{W}_{nk}^u = \frac{\pi^2}{2|s|} \frac{e^2}{mc^2} q^2 R_0^2 \left\langle \frac{(\Omega_d^2/k_\vartheta^2) Q\bar{F}_0}{\Delta_d(1+\Delta_d^2)^{3/2}} \left[ \frac{\omega}{\omega_{tr}^2 - \omega^2} \right] \right\rangle_v \Big|_E, \quad (4.76)$$

$$\delta\bar{W}_{nk}^t = \frac{\pi^2}{|s|} \frac{e^2}{mc^2} q R_0 B_0 \sum_{v_\parallel/|v_\parallel|=\pm 1} \int d\mathcal{E} \int d\mu \left( \frac{\Omega_d}{k_\vartheta} \right)^2 \tau_b Q\bar{F}_0 \times \left[ \left( 1 - \frac{\Delta_{b0}}{(1+\Delta_{b0}^2)^{1/2}} \right) \frac{1}{n\bar{\omega}_{dn} - \omega} + \frac{\theta_b^2/4}{\Delta_b(1+\Delta_b^2)^{3/2}} \frac{\omega - n\bar{\omega}_{dn}}{\omega_b^2 - (\omega - n\bar{\omega}_{dn})^2} \right] \Big|_E. \quad (4.77)$$

Here,  $\omega_{tr} = v_\parallel/(qR_0)$ ,  $\tau_b = 2\pi/\omega_b$ ,  $n\bar{\omega}_{dn} = \Omega_d = -(\mu B_0 + v_\parallel^2)k_\vartheta/(\Omega R_0)$  [cf. Eq. (4.57)], and a Padé approximation has been adopted for Bessel functions accounting for both finite Larmor radius and finite magnetic drift orbit width by means of the quantities  $\Delta_d^2 = (k_\vartheta^2/4)(\rho_L^2 + \rho_d^2/2)$ ,  $\Delta_{b0}^2 = (k_\vartheta^2/2)(\rho_L^2 + \rho_b^2)$ ,  $\Delta_b^2 = (k_\vartheta^2/4)(\rho_L^2 + \rho_b^2/2)$ , with  $\rho_L^2 = 2\mu B_0/\Omega^2$ ,  $k_\vartheta^2 \rho_d^2 = \Omega_d^2/\omega_{tr}^2$  and  $k_\vartheta^2 \rho_b^2 = \theta_b^2 \Omega_d^2/\omega_b^2$  (Chen, 1994; Tsai and Chen, 1993). Furthermore, only the dominant transit and bounce resonances have been considered for the sake of simplicity. Equations (4.76) and (4.77) demonstrate that the typical lower bound of  $\lambda_\perp$  for SAW/DAW excited by EPs is set by the characteristic EP (magnetic drift) orbit width  $\rho_E$ ,  $\lambda_\perp \gtrsim \rho_E$  (Berk *et al.*, 1992b; Chen, 1994; Fu and Cheng, 1992; Tsai and Chen, 1993) (cf. also Sec. IV.B.3).

For increasing mode numbers, Eqs. (4.34), (4.72), (4.73), and (4.76)-(4.77) demonstrate that SAW/DAW undergo a gradual transition from a prevalent EP drive, for  $\lambda_\perp \gtrsim \rho_E$ , to a prevalent core plasma drive, for  $\rho_i \ll \lambda_\perp < \rho_E$ . This is readily noted from the large argument expansion in the plasma dispersion functions of Eq. (4.72), whose real part reproduces Eq. (4.63) and, accounting for resonant wave-particle interactions with thermal ions, yields

$$\Lambda_n^2 = \frac{\omega^2}{\omega_A^2} - \frac{\omega_{BAE}^2}{\omega_A^2} \left[ 1 + \frac{\omega_{BAE}^2}{q^2 \omega^2} \frac{(46/49) + (32/49)(T_e/T_i) + (8/49)(T_e/T_i)^2}{(1 + (4/7)(T_e/T_i))^2} \right] + i\sqrt{\pi} q^2 e^{-\omega^2/\omega_{ti}^2} \frac{\omega^2}{\omega_A^2} \left( \frac{\omega_{ti}}{\omega} - \frac{\omega_{*Ti}}{\omega_{ti}} \right) \left( \frac{\omega^2}{\omega_{ti}^2} + \frac{T_e}{T_i} \right)^2. \quad (4.78)$$

This shows that the SAW accumulation point at  $\Lambda_n^2 = 0$  acquires a positive imaginary part for  $\omega_{*Ti} > \omega_{ti}^2/\text{Re}\omega$ , which corresponds to the excitation of an Alfvén Ion Temperature Gradient (AITG) (Zonca *et al.*, 1999) driven mode when the causality constraint  $\delta\bar{W}_f + \text{Re}\delta\bar{W}_k < 0$  is satisfied. Numerical analyses of AITG stability are reported, *e.g.*, by (Dong *et al.*, 1999; Falchetto *et al.*, 2003; Ganesh *et al.*, 2004; Snyder and Hammett, 2001; Zhao and Chen, 2002). Thus, there exists a broad range of mode numbers in the same frequency range [ $|\omega| \lesssim \mathcal{O}(10^{-1})\omega_A$ ], predicted theoretically (Zonca *et al.*, 1999, 1996, 1998) and observed experimentally (Nazikian *et al.*, 2006) (cf. Sec. IV.C), where both core and energetic plasma component act as free energy source with possible important consequence for cross-scale coupling and nonlinear dynamics in burning plasmas (cf. also Secs. V.A and VII.B).

For further shorter wavelengths, thermal ion finite Larmor radius and magnetic drift orbit width become important in Eqs. (4.64) and (4.67), and yield the discretization of the SAW continuous spectrum (cf. Sec. III and IV.B.3). Equation (4.68) can then be generalized to (Zonca *et al.*, 1998)

$$\frac{\partial^2}{\partial \vartheta_1^2} \delta\hat{\Psi}_n^{(0)} + \Lambda_n^2(\omega) \delta\hat{\Psi}_n^{(0)} - \vartheta_1^2 Q_n^2(\omega) \delta\hat{\Psi}_n^{(0)} = 0, \quad (4.79)$$

$$Q_n^2(\omega) = s^2 k_\vartheta^2 \rho_i^2 \frac{\omega^2}{\omega_A^2} \left[ \frac{3}{4} \left( 1 - \frac{\omega_{*pi}}{\omega} - \frac{\omega_{*Ti}}{\omega} \right) + q^2 \frac{\omega_{ti}}{\omega} S_n(\omega) + \frac{(\Lambda_n \omega_A / \omega)^4}{1/\tau + (\omega_{*ni}/\omega)} \right], \quad (4.80)$$

where the frequency dependent function  $S_n(\omega)$  accounts for finite magnetic drift orbit width

$$S_n(\omega) = \frac{q^2}{2} \left( \frac{\omega_{ti}}{\omega} \right)^2 \left[ \left( 1 - \frac{\omega_{*ni}}{\omega} \right) \left( L - 2L_{1/2} - \frac{2N}{D} (H - 2H_{1/2}) + \frac{N^2}{D^2} (F - 2F_{1/2}) \right) - \frac{\omega_{*Ti}}{\omega} \left( M - 2M_{1/2} - \frac{2N}{D} (I - 2I_{1/2}) + \frac{N^2}{D^2} (G - 2G_{1/2}) \right) \right] + \frac{q^2}{D_{1/2}} \left( \frac{\omega_{ti}}{\omega} \right)^2 \left[ \left( 1 - \frac{\omega_{*ni}}{\omega} \right) (F_{1/2} - F) - \frac{\omega_{*Ti}}{\omega} (G_{1/2} - G) - \frac{N}{D} (N_{1/2} - N) \right]^2 + \left( 1 - \frac{\omega_{*ni}}{\omega} \right) \left( T - \frac{2N}{D} V + \frac{N^2}{D^2} Z \right) - \frac{\omega_{*Ti}}{\omega} \left( U - \frac{2N}{D} W + \frac{N^2}{D^2} (V - Z/2) \right). \quad (4.81)$$

Here, the functions  $N, D, F, G$  are those defined in Eqs. (4.70) and (4.71), with subscripts  $m \simeq nq$  dropped from  $N, D$  for simplicity. Meanwhile  $V, W, H, I$  and  $T, U, L, M$  functions are defined as

$$\begin{aligned}
V(x) &= x + (x^2 + 1) Z(x) , \\
W(x) &= x^3 + 2x + (x^4 + (3/2)x^2 + 3/2) Z(x) , \\
H(x) &= x^5 + 2x^3 + 3x + (x^6 + (3/2)x^4 + (3/2)x^2 + 3/4) Z(x) , \\
I(x) &= x^7 + (3/2)x^5 + (7/2)x^3 + (27/4)x + (x^8 + x^6 + (9/4)x^4 + 3x^2 + 15/8) Z(x) . \\
T(x) &= x^3 + (5/2)x + (x^4 + 2x^2 + (3/2)) Z(x) , \\
U(x) &= x^5 + 3x^3 + (13/2)x + (x^6 + (5/2)x^4 + (9/2)x^2 + (15/4)) Z(x) , \\
L(x) &= x^7 + (5/2)x^5 + (19/4)x^3 + (63/8)x + (x^8 + 2x^6 + 3x^4 + 3x^2 + 3/2) Z(x) , \\
M(x) &= x^9 + 2x^7 + (11/2)x^5 + (25/2)x^3 + (201/8)x + (x^{10} + (3/2)x^8 + 4x^6 + (15/2)x^4 + 9x^2 + 21/4) Z(x) .
\end{aligned} \tag{4.82}$$

In Eq. (4.81), functions without subscript are computed at  $\omega/\omega_{ti}$ , while functions with subscript 1/2 are computed at  $\omega/2\omega_{ti}$  and account for wave-particle interactions at the first sideband resonance  $2\omega_{ti}$ . Noting that, for  $|\omega| \gg \omega_{ti}$ ,  $Q_n^2/(s^2\vartheta_1^2k_g^2) \simeq Q_n^2/k_\perp^2 \rightarrow \rho_K^2(\omega^2/\omega_A^2)$ , as defined in Eq. (3.21), Eq. (4.79) is the generalization of Eq. (3.20) to toroidal geometry, provided that small but finite Landau damping is maintained for thermal particles and finite resistivity is added in the parallel Ohm's law. Thus, Eq. (4.79) describes low frequency  $[|\omega| \lesssim \mathcal{O}(10^{-1})\omega_A]$  KAW in tokamak plasmas. Note, however, that the expression of  $Q_n$ , Eq. (4.80), does not include magnetically trapped particle effects.

Equation (4.79) can be readily solved, noting Eq. (4.19), to derive the following GFLDR extended to short wavelengths (Zonca *et al.*, 1998)

$$-2Q_n^{1/2} \frac{\Gamma(3/4 - \Lambda_n^2/4Q_n)}{\Gamma(1/4 - \Lambda_n^2/4Q_n)} = \delta\bar{W}_{nf} + \delta\bar{W}_{nk} , \tag{4.83}$$

where we have introduced the Euler  $\Gamma$ -function. For  $|\Lambda_n^2/4Q_n| \gg 1$ , the left hand side of Eq. (4.83) reduces to  $i\Lambda_n$ ; *i.e.*, Eq. (4.34) is recovered. This property shows that the discrete structures (“granularity”) of the SAW continuous spectrum depend on the spatial scales ( $|Q_n| \sim k_\perp \rho_i$ ) as well as the time scales ( $|\Lambda_n| \lesssim |\omega/\omega_A|$ ) on which the spectrum is “observed” (Zonca and Chen, 1996, 2008b). For sufficiently long spatial and temporal scales the discretized SAW spectrum behaves nonetheless as a “true” continuum (*cf.* also Sec. IV.B.3). Thus, Eq. (4.83) describes a variety of kinetic SAW/DAW fluctuations, including, *e.g.*, BAE and KBAE (Wang *et al.*, 2010b). Equation (4.83) has also been derived and analyzed extensively by (Nguyen *et al.*, 2008), to be then adopted in modeling of BAE observations in Tore Supra (Nguyen *et al.*, 2009) (*cf.* Sec. IV.C).

In the case of  $s = 0$  at a minimum- $q$  surface, the GFLDR form is that of Eq. (4.24), which describes RSAE (Kimura *et al.*, 1998; Takechi *et al.*, 2002) or AC (Berk *et al.*, 2001; Sharapov *et al.*, 2001). As the parallel wave vector at  $s = 0$ ,  $k_{\parallel n0}$ , is generally finite, the RSAE/AC frequency is typically larger than that of BAEs. Thus,  $\Lambda_n^2$  expression of Eq. (4.78) can be used in Eq. (4.24); which can be further simplified as (Zonca *et al.*, 2002; Zonca and Chen, 2006)

$$iS \left( \Lambda_n^2 - k_{\parallel n0}^2 q^2 R_0^2 \right)^{1/2} (k_{\parallel n0} q R_0 / n)^{1/2} = \delta\hat{W}_{nf} + \delta\hat{W}_{nk} . \tag{4.84}$$

Here, we have assumed  $\Lambda_n^2 \simeq k_{\parallel n0}^2 q^2 R_0^2$  and  $L_0 \simeq qR_0$  for modes characterized by small frequency shift with respect to the SAW accumulation point. Using  $n > 0$  as reference, it is readily noted that the optimal conditions for exciting RSAE/AC at the minimum- $q$  surface are  $-1/2 < nq_0 - m < 0$  and  $1/2 < nq_0 - m + 1 < 1$ . In fact, when this is verified, the  $(n, m)$  SAW continuum has a maximum at  $s = 0$  below the corresponding minimum of the  $(n, m-1)$  SAW continuum (Sharapov *et al.*, 2001). Therefore, the continuum damping due to non-local coupling of mode structures with the SAW continuous spectrum is minimized (Zonca *et al.*, 2002) and a wide frequency gap is formed between the local maximum of the  $(n, m)$  and the local minimum of the  $(n, m-1)$  SAW continua (Berk *et al.*, 2001). The low frequency RSAE/AC branch of AEs can, thus, exist marginally above the local (maximum) accumulation point of the  $(n, m)$  SAW continuum, provided that Eq. (4.21) is satisfied. For this reason, RSAEs/ACs have characteristic features that are similar to those of GAEs (*cf.* Sec. III). Equation (4.21) can be fulfilled either by compressibility effects of very energetic fast ions with large orbits (Berk *et al.*, 2001), yielding  $\Re\delta\hat{W}_{nk} > 0$  (Zonca *et al.*, 2002), or by thermal plasma (toroidal) geometry (Breizman *et al.*, 2003) and density gradient (Konovalov *et al.*, 2004) effects. In general, in the absence of EPs, Eq. (4.21) for weak/vanishing magnetic shear requires local macroscopic plasma stability; *i.e.*, it reduces to the Mercier stability criterion (Mercier, 1960). This result was shown explicitly by (Fu and Berk, 2006), investigating the compressibility effects on RSAE/AC in the “ideal region”, while the thermal plasma compression

effect on RSAE/AC in the “inertial layer”, *i.e.*, the  $\propto \omega_{BAE}^2$  term in Eq. (4.78), was pointed out by (Breizman *et al.*, 2005). Equation (4.21) provides only a necessary but not sufficient criterion for RSAE/AC excitation, as mode drive is generally due to resonant EPs,  $\text{Im}\delta\hat{W}_{nk} > 0$ , which, in present day experiments, are typically not the same as EPs predominantly contributing to compressibility  $\text{Re}\delta\hat{W}_{nk} > 0$  (Zonca *et al.*, 2002; Zonca and Chen, 2006). The experimental feature of RSAE/AC to typically chirp upward in frequency is readily understood, as the accumulation point of the  $(n, m)$  SAW continuum increases in absolute frequency for decreasing  $q_0$  due to, *e.g.*, resistive current diffusion (Berk *et al.*, 2001; Sharapov *et al.*, 2001). When the RSAE/AC frequency reaches the TAE frequency gap,  $(n, m)$  and  $(n, m - 1)$  SAW continua intersect and toroidicity effects become important (Breizman *et al.*, 2003; Zonca *et al.*, 2002). Accurate modeling of RSAE/AC mode frequencies and growth rates has been applied to experimental observations in JET to explain evidence of upward mode frequency chirping, and eventually downward, after reaching the TAE frequency gap (Abel *et al.*, 2009) (cf. Sec. IV.C). Theoretical analyses of downward chirping RSAE/AC are also given by (Gorelenkov *et al.*, 2011; Haverkort, 2012; Kramer *et al.*, 2004a; Marchenko and Reznik, 2011).

### 3. Toroidal Alfvén Eigenmodes

Toroidal Alfvén Eigenmodes (TAE) (Cheng *et al.*, 1985) are the first example of AEs in toroidal plasmas, theoretically predicted before their experimental observation (Heidbrink *et al.*, 1991; Wong *et al.*, 1991) (cf. Sec. IV.C) and widely studied as paradigm problem for their potential impact on EP confinement (cf. Secs. V and VI).

From Eq. (4.3) with  $\ell = 1$  and  $L_0 \simeq qR_0$ , one readily derives that  $k_{\parallel}^2 q^2 R_0^2 \simeq 1/4$  and  $\omega^2 \simeq \omega_A^2/4$  for TAE in circular plasmas with large aspect-ratio  $R_0/a$  [see Sec. II, remark following Eq. (2.2)]. Following the original work by (Cheng and Chance, 1986; Cheng *et al.*, 1985) and adopting the  $(s, \alpha)$  model equilibrium (Connor *et al.*, 1978) introduced in Sec. IV.B.2, Eqs. (4.64) and (4.67) are readily specialized to TAE and yield

$$\begin{aligned} \frac{\partial^2}{\partial \vartheta^2} \delta\hat{\Psi}_n + \frac{\omega^2}{\omega_A^2} (1 + 2\epsilon_0 \cos \vartheta) \delta\hat{\Psi}_n + \left[ \frac{\alpha \cos \vartheta}{\hat{\kappa}_{\perp}^2} - \frac{(s - \alpha \cos \vartheta)^2}{\hat{\kappa}_{\perp}^4} - \frac{\hat{\kappa}_{\perp}^2 \rho_K^2}{4} \right] \delta\hat{\Psi}_n \\ + \frac{4\pi R_0 q^2}{B_0} \frac{g(\vartheta, \theta_k) \omega}{ck_{\vartheta} \hat{\kappa}_{\perp}} \left[ \left\langle (\mu B_0 + v_{\parallel}^2) \left( m_i \delta\hat{K}_{in} + m_e \delta\hat{K}_{en} \right) \right\rangle_v + \left\langle m_E (\mu B_0 + v_{\parallel}^2) J_0 \delta\hat{K}_{En} \right\rangle_v \right] = 0 . \end{aligned} \quad (4.85)$$

Here, notations are those introduced in Sec. IV.B.2,  $\epsilon_0 = 2(r/R_0 + \Delta')$ , core plasma diamagnetic frequencies have been neglected compared to TAE frequency, and it is assumed that EP finite orbit widths are typically dominated by magnetic drifts. Meanwhile, the expression of  $\rho_K^2$  is given by Eq. (3.21); or Eq. (4.80) in the high frequency limit, where  $\delta_i = 0$  and (Candy and Rosenbluth, 1993, 1994)

$$\delta_e = \frac{\epsilon_0^{3/2}}{\epsilon_0^{3/2} + (\nu_e/\omega)^{3/2}} \sqrt{\frac{\nu_e}{\omega}} \left[ 1.4 + 0.25 \ln \left( 1 + \frac{\epsilon_0 \omega}{\nu_e} \right) \right]^{-3/2} , \quad (4.86)$$

with

$$\nu_e = \frac{4\pi e^4 n_e \ln \Lambda}{m_e^{1/2} (2T_e)^{3/2}} , \quad (4.87)$$

and  $\ln \Lambda$  the Coulomb logarithm. Assuming  $\delta_i = 0$  corresponds to neglecting higher order corrections to the usual Landau collisionless dissipation<sup>15</sup>, which is dominated by the  $\propto \delta\hat{K}_{in}$  term. Similarly, electron Landau damping is predominantly given by the  $\propto \delta\hat{K}_{en}$  contribution, originally dropped in Eq. (4.67) at low-frequency, while the expression of  $\delta_e$  in Eq. (4.86) describes other dissipative effects associated, *e.g.*, to collisions with trapped electrons (Mazur and Mikhailovskii, 1977; Mikhailovskii and Shuchman, 1976). Typically, the most important TAE dissipation mechanism due to electrons is the trapped electron collisional damping (Gorelenkov and Sharapov, 1992).

Consistent with the general case, Eq. (4.85) suggests the existence of two-scale structures for the solutions  $\delta\hat{\Psi}_n$ :  $\vartheta_0 \sim 1$  representing periodic variations due to toroidal geometry; and  $\vartheta_1 \sim \epsilon_0^{-1} \gg 1$  characterizing the radial “singular” structure of the SAW continuous spectrum. For  $|s\vartheta| \sim \hat{\kappa}_{\perp} \gg 1$ ,  $\delta\hat{\Psi}_n$  can generally be written as (Chen and Zonca, 1995; Zonca and Chen, 1996)

$$\delta\hat{\Psi}_n^{(\pm)} = \epsilon_P^{(\pm)} [A(\vartheta_1) \cos(\vartheta_0/2) \pm B(\vartheta_1) \sin(\vartheta_0/2)] , \quad (4.88)$$

<sup>15</sup> For lower frequencies, discussed in Sec. IV.B.2, these effects are, *e.g.*, accounted for in the  $Q^2$  expression of Eq. (4.80).

where  $(\pm)$  refers to the sign of  $\vartheta_1$  and  $\epsilon_P^{(\pm)}$  give the parity of the mode structures. Taking  $\epsilon_P^{(+)} \equiv 1$  for reference,  $\epsilon_P^{(-)} = \pm 1$  denotes even/odd mode structures, respectively. By direct substitution of Eq. (4.88) into Eq. (4.85), it is possible to derive the governing equations for  $A(\vartheta_1)$  and  $B(\vartheta_1)$

$$\begin{aligned} A'(\vartheta_1) &= (\Gamma_- - s^2 \vartheta_1^2 \rho_K^2/4) B(\vartheta_1) , \\ B'(\vartheta_1) &= -(\Gamma_+ - s^2 \vartheta_1^2 \rho_K^2/4) A(\vartheta_1) . \end{aligned} \quad (4.89)$$

Here,  $\Gamma_{\pm} = (\omega^2/\omega_A^2)(1 \pm \epsilon_0) - 1/4 - \beta_1$ , with  $\beta_1 = \beta_{1c} + \beta_{1E}$  and (Chen, 1988; Chen *et al.*, 1989; Cheng *et al.*, 1988; Fu and Van Dam, 1989a,b)

$$\beta_{1c} = \frac{\pi q^2}{B_0^2} \sum_{j=e,i} \sum_{\ell=1,3} \left\langle m_j (\mu B_0 + v_{\parallel}^2) \left( \frac{\omega Q \bar{F}_0}{\ell^2 \omega_{tr}^2/4 - \omega^2} \right)_j \right\rangle_v . \quad (4.90)$$

This term, which assumes for simplicity  $\bar{F}_0$  to be symmetric in  $v_{\parallel}$ , describes TAE wave-particle interactions of the core plasma component at the fundamental ( $v_{\parallel} = \pm v_A$ ) and first sideband ( $v_{\parallel} = \pm v_A/3$ ) transit resonances; *i.e.*, it accounts for electron and ion Landau damping (Betti and Freidberg, 1992). Note that  $\propto \beta_1$  and  $\propto \rho_K^2$  terms in Eq. (4.89) represent the generalized plasma inertia response discussed already for MHD modes (cf. Sec. IV.B.1) and low frequency SAWs (cf. Sec. IV.B.2). In the long wavelength limit, the generalized inertia further includes the EP contributions,  $\beta_{1E}$ . It is then possible to note that EP drive linearly increases with the toroidal mode number  $n$  until finite orbit width effects become important for  $|k_{\vartheta} \rho_E| \sim \hat{\kappa}_{\perp}^{-1} \sim |\Gamma_+ \Gamma_-|^{1/2} \sim \mathcal{O}(\epsilon_0)$ . This suggests that high- $n$  modes play the dominant role in fusion plasmas (Chen, 1988), although the first numerical investigations of TAE mode structures (Cheng and Chance, 1986) and stability (Berk *et al.*, 1992c; Cheng, 1990, 1991; Fu *et al.*, 1993; Fu and Van Dam, 1989a; Kar *et al.*, 1993; Poedts *et al.*, 1992; Spong *et al.*, 1992) focused on low- $n$  modes for intrinsic limitations of numerical simulation capabilities. In this long wavelength regime, it is also possible to take into account small but finite EP orbit widths, which modify the structure of Eq. (4.89) and generalize the expression of  $\rho_K^2$  in a qualitative and quantitative fashion that extends wave-EP resonances to the  $v_{\parallel} = \pm v_A/5$  transit sideband (Briguglio *et al.*, 1995; Vlad *et al.*, 1999).

Neglecting small but finite orbit width effects of both core and energetic plasma components, Eq. (4.89) yields  $A(\vartheta_1) \simeq (-\Gamma_-)^{1/2} \exp(-\Gamma|\vartheta_1|)$  and  $B(\vartheta_1) \simeq \Gamma_+^{1/2} \exp(-\Gamma|\vartheta_1|)$ , with  $\Gamma^2 \equiv -\Gamma_- \Gamma_+$ . From Eq. (4.19), it is then readily shown that  $\Re \Gamma^2 > 0$  identifies TAE [ $\Re \Gamma^2 < 0$  identifies EPM; cf. Sec. IV.B.4] and

$$i\Lambda_{nT} = (1/2)B(0)/A(0) = (1/2)(-\Gamma_+/\Gamma_-)^{1/2} . \quad (4.91)$$

Here and below, we adopt the subscript  $T$  that stands for the inclusion of finite toroidal coupling effects, which are crucial for TAE (Cheng *et al.*, 1985; Kieras and Tataronis, 1982). Noting that the dominant kinetic interactions in the long wavelength limit occur in the kinetic layer, the GFLDR Eq. (4.34) is fully determined provided that  $\delta \bar{W}_{nf}$  is obtained from Eq. (4.73), given the function  $\delta \hat{\Phi}_n = \delta \hat{\Psi}_n$ . In general,  $\delta \hat{\Psi}_n$  must be determined numerically, but, from Eq. (4.88), it can be shown that (Zonca, 1993a,b; Zonca and Chen, 1993)

$$\begin{aligned} \delta \bar{W}_{nfT} &= [1 - Z_f(s, \alpha, \theta_k)] i\Lambda_{nT} - \left( \frac{B(0)^2 - A(0)^2}{2A(0)^2} \right) G_f(s, \alpha, \theta_k) \\ &\quad - \left( \frac{B(0)^2 + A(0)^2}{2A(0)^2} \right) [H_f(s, \alpha, \theta_k) \cos \theta_k + L_f(s, \alpha, \theta_k) \sin \theta_k] , \end{aligned} \quad (4.92)$$

where  $Z_f, G_f, H_f, L_f$ , determined numerically, are periodic functions of  $\theta_k$  and of parameters defining the local plasma equilibrium; *i.e.*, in this case,  $(s, \alpha)$  (cf. Sec. IV.B.2). Note that Eq. (4.92) is frequency dependent through the mode structure,  $A(0)$  and  $B(0)$ , and the mode frequency location with respect to the SAW continuum. This is in contrast with respect to the case of low frequencies, discussed in Sec. IV.A following Eq. (4.20), where  $\delta \hat{W}_{nf}$  is independent of  $\omega$ . In special cases, it is possible to give analytic expressions of  $Z_f, G_f, H_f, L_f$  (Zonca, 1993b); *e.g.*, for  $|s|, |\alpha| < 1$ , when Eq. (4.88) gives a good trial function in the whole  $\vartheta$ -space and  $Z_f \simeq 1$ ,  $G_f \simeq |s|\pi/4$ ,  $(H_f \cos \theta_k + L_f \sin \theta_k) \simeq (|s|\pi/4)(\alpha/\alpha_{cr} - 2\kappa(s) \cos \theta_k)$ , with (Fu and Cheng, 1990; Zonca and Chen, 1992, 1993)

$$\alpha_{cr} = s^2/(1 + |s|) ; \quad \text{and} \quad \kappa(s) \simeq (1/2)(1 + 1/|s|) e^{-1/|s|} . \quad (4.93)$$

Thus, Eq. (4.92) becomes

$$\delta \bar{W}_{nfT} \simeq \frac{|s|\pi}{8} \left( 1 + 2\kappa(s) \cos \theta_k - \frac{\alpha}{\alpha_{cr}} \right) - \frac{B(0)^2}{A(0)^2} \frac{|s|\pi}{8} \left( 1 - 2\kappa(s) \cos \theta_k + \frac{\alpha}{\alpha_{cr}} \right) , \quad (4.94)$$

which implies that only the even parity TAE ( $|B(0)/A(0)| \ll 1$ ) can exist for moderate  $|s|, |\alpha| < 1$ . In general, only one parallel eigenstate of TAE is identified using simplified model equilibria, while different TAE radial eigenstates exist in the number of the effectively coupled poloidal harmonics. The parity of the parallel eigenstate is typically mixed and changes from even, near the lower SAW accumulation point of the TAE frequency gap, to odd, near the upper accumulation point. More general equilibria and/or the presence of a plasma free boundary in the TAE localization domain (Chen *et al.*, 2011a) may give rise to more simultaneous TAE parallel eigenstate branches.

The TAE GFLDR in the form of Eq. (4.34) can be used to calculate the global dispersion relation, Eq. (4.37), with the corresponding radial eigenstates and mode structures (Zonca, 1993b; Zonca and Chen, 1993). It is then possible to compute TAE damping due to non-local coupling to the SAW continuum from the radial locations where it is resonantly excited by EP. Adopting the  $(s, \alpha)$  model equilibrium, the corresponding TAE continuum damping has the general form (Rosenbluth *et al.*, 1992; Zonca and Chen, 1992)<sup>16</sup>

$$\frac{\gamma_{cd}}{|\omega|} = -\frac{|1/nq'L_A|^{3/2}}{4\sqrt{2}\epsilon_0} \left\{ \hat{\Gamma}_\ell(s, \alpha) e^{-2|nq'L_A|\epsilon_0\hat{T}(s, \alpha)} + \hat{\Gamma}_u(s, \alpha) e^{-2|nq'L_A|\epsilon_0\hat{R}(s, \alpha)} \right\}. \quad (4.95)$$

Here,  $L_A^{-1} \equiv \partial_r \ln \omega_A^2$  and the functions  $\hat{\Gamma}_\ell(s, \alpha)$  and  $\hat{\Gamma}_u(s, \alpha)$  represent, respectively, the absorption rate at the lower and upper SAW continuum. Meanwhile,  $\hat{T}(s, \alpha)$  and  $\hat{R}(s, \alpha)$  are the ‘‘tunneling’’ factors that describe the TAE wave cut-off while propagating towards the lower and upper SAW continua. All these functions have been calculated numerically for arbitrary values of  $(s, \alpha)$  (Zonca, 1993b; Zonca and Chen, 1993). For  $|s|, |\alpha| < 1$  these functions have explicit analytical expressions from which it is possible to note that, as  $\alpha \rightarrow \alpha_{cr}(1 - 2\kappa(s))$ , the TAE mode merges into the lower SAW continuum accumulation point (Chen, 1988; Chen *et al.*, 1989; Fu and Cheng, 1990) and  $\gamma_{cd}/|\omega|$  from Eq. (4.95) diverges, due to the strengthened coupling of the mode with the continuous spectrum (Zonca and Chen, 1992). Asymptotic techniques have been used to calculate high- $n$  TAE spectra (Chen and Zonca, 1995; Cheng *et al.*, 1995; Gorelenkov *et al.*, 1998; Vlad *et al.*, 1995a,b; Zonca and Chen, 1996), especially when perturbative treatment of EPs as well as investigation of high mode numbers made the analysis based on modified MHD codes less accurate (Borba *et al.*, 2002; Cheng, 1992; Gorelenkov *et al.*, 2000, 1999b; Jaun *et al.*, 1998, 2000). Equation (4.37) for computing global TAE dispersion relation and mode structures has been adopted also for realistic ITER equilibria (Briguglio *et al.*, 2000). However, with present day computer capabilities, the most efficient way of computing TAE spectra is via direct numerical simulations (cf. Sec. IV.C). Nonetheless, the asymptotic solution of Eq. (4.36) as initial value problem (Lu *et al.*, 2012) may allow investigating kinetic physics that are not readily available in existing numerical codes or providing a useful benchmark for codes. At the same time, benchmarking numerical results against GFLDR predictions with different models of generalized inertia may help assessing the need of kinetic models in numerical simulation codes (Zonca, 2008; Zonca *et al.*, 2010; Zonca and Chen, 2008a,c).

For  $|k_\vartheta \rho_E| \gtrsim \mathcal{O}(\epsilon_0)$ , EP dynamics becomes ignorable in the kinetic layer (cf. Secs. IV.A and IV.B.2) and, thus,  $\beta_{1E}$  can be dropped in the expression of  $\beta_1$ , Eq. (4.90). Wave-EP interactions become gradually more affected and eventually dominated by  $\delta\bar{W}_k$ ; first, they become independent of the mode number, while they eventually decrease and vanish due to finite orbit width for  $|k_\vartheta \rho_E| \gtrsim 1$  (Berk *et al.*, 1992b; Chen, 1994; Fu and Cheng, 1992; Tsai and Chen, 1993). Thus, most unstable mode numbers are expected for  $\mathcal{O}(\epsilon_0) \lesssim |k_\vartheta \rho_E| \lesssim 1$ . Similar to Eq. (4.92), it is possible to demonstrate that the general form of  $\delta\bar{W}_{nkT}$  is (Zonca and Chen, 1996)

$$\begin{aligned} \delta\bar{W}_{nkT} = & 4i\Lambda_{nT} \left\{ G_f(s, \alpha, \theta_k) (\delta\bar{W}_{nkT}^u + \delta\bar{W}_{nkT}^t) + [H_f(s, \alpha, \theta_k) \cos \theta_k + L_f(s, \alpha, \theta_k) \sin \theta_k] \delta\bar{W}_{nkT}^t \right\} \\ & + Z_f(s, \alpha, \theta_k) \left[ \delta\bar{W}_{nkT}^t - \left( \frac{B(0)^2 - A(0)^2}{2A(0)^2} \right) \delta\bar{W}_{nkT}^u \right], \end{aligned} \quad (4.96)$$

where, for the sake of simplicity, the EP  $\bar{F}_0$  has been assumed symmetric in  $v_\parallel$ . For  $|s|, |\alpha| < 1$ , Eq. (4.96) becomes

$$\delta\bar{W}_{nkT} = \delta\bar{W}_{nkT}^t + \frac{1}{2} \delta\bar{W}_{nkT}^u \left( 1 - \frac{B(0)^2}{A(0)^2} \right) \equiv \delta\bar{W}_{nkT}^t + \delta T_{nk}^u \left( 1 - \frac{B(0)^2}{A(0)^2} \right). \quad (4.97)$$

Here,  $\delta\bar{W}_{nkT}^t$  is due to trapped particles (Biglari *et al.*, 1992; Chen, 1994), and its expression is the same as that given by Eq. (4.77). Meanwhile, for untrapped EPs one has  $\delta\bar{W}_{nkT}^u \equiv 2\delta T_{nk}^u$  and (Chen, 1994)

$$\delta T_{nk}^u = \frac{\pi^2}{8|s|} \frac{e^2}{mc^2} q^2 R_0^2 \sum_{\ell=1,3} \left\langle \frac{(\Omega_d^2/k_\vartheta^2) Q \bar{F}_0}{\Delta_d(1 + \Delta_d^2)^{3/2}} \left[ \frac{\omega}{\ell^2 \omega_{tr}^2/4 - \omega^2} \right] \right\rangle_v \Big|_E. \quad (4.98)$$

<sup>16</sup> The numerical calculation of TAE continuum damping for low mode numbers is given by (Berk *et al.*, 1992c).

Similar to Eq. (4.94), Eq. (4.97) shows that the even parity TAE ( $|B(0)/A(0)| \ll 1$ ) is preferentially excited for  $|s|, |\alpha| < 1$  and it obeys the GFLDR (Chen, 1994)

$$i\Lambda_{nT} \equiv \frac{1}{2} \frac{B(0)}{A(0)} = \frac{1}{2} \sqrt{-\frac{\Gamma_+}{\Gamma_-}} = \frac{|s|\pi}{8} \left( 1 + 2\kappa(s) \cos \theta_k - \frac{\alpha}{\alpha_{cr}} \right) + \delta \bar{W}_{nkT}^t + \delta T_{nk}^u ; \quad (4.99)$$

while the typically suppressed odd parity TAE ( $|B(0)/A(0)| \gg 1$ ) dispersion relation is

$$\frac{1}{2} \frac{A(0)}{B(0)} = \frac{1}{2} \sqrt{-\frac{\Gamma_-}{\Gamma_+}} = - \left[ \frac{|s|\pi}{8} \left( 1 - 2\kappa(s) \cos \theta_k + \frac{\alpha}{\alpha_{cr}} \right) + \delta T_{nk}^u \right] . \quad (4.100)$$

For further increasing mode numbers, or when TAE radial mode structures become more singular due to the proximity with the SAW continuum,  $\propto \rho_K^2$  terms in Eq. (4.89) become important. That system of equations, in fact, can be regarded in an approximate sense as the Schrödinger equation for a particle with energy  $E_{\text{eff}} = \Gamma_+ \Gamma_-$  that moves in a potential well  $V_{\text{eff}} \simeq (\Gamma_+ + \Gamma_-) s^2 \vartheta_1^2 \rho_K^2 / 4 - s^4 \vartheta_1^4 \rho_K^4 / 16$ . Thus, for modes that are not bounded at sufficiently small  $|\vartheta_1|$  ( $\Gamma_+ \Gamma_- < 0$ , corresponding to TAE), the  $V_{\text{eff}}$  asymptotic structure is always an anti-well that yields “radiative” damping (Berk *et al.*, 1993; Candy and Rosenbluth, 1993, 1994; Mett and Mahajan, 1992a,b). These modes are KTAE and describe the discretization of the SAW continuum near the TAE gap. Due to the  $\propto (\Gamma_+ + \Gamma_-) s^2 \vartheta_1^2 \rho_K^2 / 4$  contribution in  $V_{\text{eff}}$ , lower and upper KTAE branches are not symmetric. While the lower KTAE is strongly damped ( $\Gamma_+ + \Gamma_- < 0$ ), the upper KTAE ( $\Gamma_+ + \Gamma_- > 0$ ) may be significantly bounded by the local well structure at  $s^2 \vartheta_1^2 \rho_K^2 / 4 < (\Gamma_+ + \Gamma_-)$  and be affected by radiative damping only via tunneling to higher  $\vartheta_1^2$ . The asymptotic analysis of TAE and KTAE radiative damping is reviewed by (Zonca and Chen, 1996). Here, for brevity we present the extension of the GFLDR to short wavelength KTAE near lower and upper SAW continuum accumulation points (Chen and Zonca, 1995). Considering first the lower accumulation point,  $|\Gamma_+| \ll \epsilon_0$  and  $\Gamma_- \simeq -2\epsilon_0 \omega^2 / \omega_A^2$ . In this limit, Eq. (4.89) can be readily solved for  $A(\vartheta_1)$  and  $B(\vartheta_1)$ , and yields

$$\frac{A(0)}{B(0)} = \frac{\exp(-i\pi/4) \Gamma(1/4 + a_\ell/2)}{(2\Delta_K)^{1/4} \Gamma(3/4 + a_\ell/2)}, \quad \text{and} \quad a_\ell = -\frac{i\Gamma_+}{|s|\rho_K / \sqrt{2\epsilon_0 \omega^2 / \omega_A^2}}, \quad (4.101)$$

with  $\Delta_K = (1/4) s^2 \rho_K^2 / (\epsilon_0 \omega^2 / \omega_A^2)^3$ . When substituted into Eqs. (4.99) and (4.100), Eqs. (4.101) describe, respectively, even and odd KTAE branches near the lower SAW continuum accumulation point. Thus,

$$a_\ell = -(2k + 1/2) \text{ (even)} ; \quad \text{and} \quad a_\ell = -(2k + 3/2) \text{ (odd)} ; \quad (4.102)$$

describe the lowest-order dispersion relation of the lower KTAE branch with  $k \in \mathbb{N}^+$ . Similarly, near the upper SAW continuum accumulation point, it is possible to show that

$$\frac{A(0)}{B(0)} = (2\Delta_K)^{1/4} \frac{\Gamma(3/4 + a_u/2)}{\Gamma(1/4 + a_u/2)}, \quad \text{and} \quad a_u = -\frac{\Gamma_-}{|s|\rho_K / \sqrt{2\epsilon_0 \omega^2 / \omega_A^2}} ; \quad (4.103)$$

which admit the lowest-order solutions

$$a_u = -(2k + 3/2) \text{ (even)} ; \quad \text{and} \quad a_u = -(2k + 1/2) \text{ (odd)} . \quad (4.104)$$

In analogy with Eq. (4.83) and following discussions, Eqs. (4.101) and (4.103) show that KTAE are discrete structures (“granularity”) of the SAW continuum. This is shown in Fig. 2, reporting numerical solutions of two neighbor roots of Eqs. (4.99) and (4.100) with  $A(0)/B(0)$  given by Eq. (4.103); *i.e.*, two KTAE modes (crosses and open squares). These roots are compared with the only one (open circles) obtained from the same equations with  $\Delta_K = 0$ , representing an Energetic Particle Mode (EPM) (Chen, 1994) (cf. Sec. IV.B.4). For all three modes, growth rates, represented by  $\text{Im}(\Gamma_+ \omega_A^2 / \epsilon_0 \omega^2)$  in the left frame, and real frequencies, given by  $\text{Re}(\Gamma_+ \omega_A^2 / \epsilon_0 \omega^2)$  in the right frame, are shown vs. the EP  $\alpha_E$ , defined as in Eq. (4.65). It is evident that normalized mode frequency and growth rates of KTAEs are weakly modified [ $\sim \mathcal{O}(10^{-1})$ ] by EPs below the EPM destabilization threshold at  $\alpha_E \simeq 0.18$ . Above that threshold, one of the two KTAE (crosses) behaves as and becomes the EPM. This shows that, when one of the KTAE responds more strongly (normalized mode frequency and/or growth rate change  $\simeq 0.5$ ) and its growth rate becomes larger than the characteristic frequency separation of the KTAE spectrum [in normalized units  $\sim \mathcal{O}(10^{-1})$ ], it “feels” the presence of the other KTAEs (the discretized SAW continuum) as a “true” continuous spectrum (cf. Sec. IV.B.2).

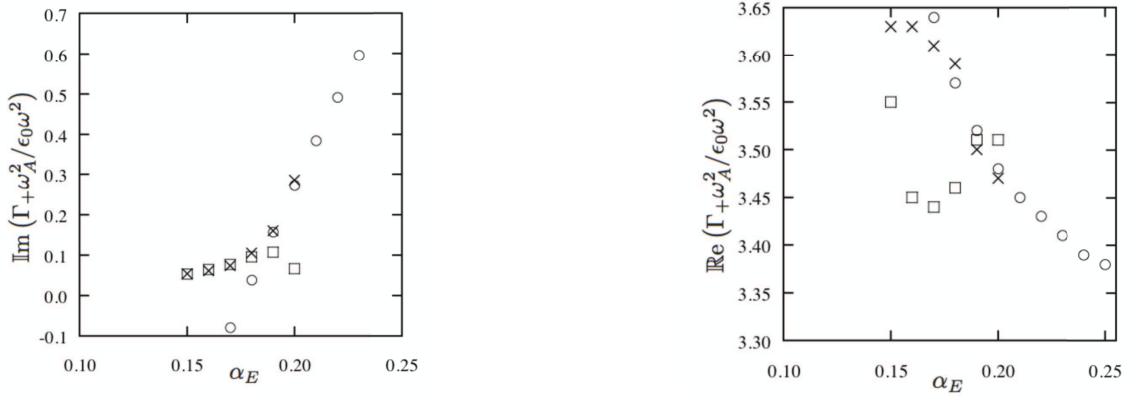


FIG. 2 Evidence of merging of one KTAE into an EPM above the EPM destabilization threshold when the spatiotemporal properties of the mode make the discretized SAW spectrum behave as a “true” continuum [from the original Fig. 3 (a)-(b) in Ref. (Zonca and Chen, 1996)].

#### 4. Energetic Particle Modes

Energetic Particle continuum Modes (EPMs) (Chen, 1994) are excited when the mode drive is sufficiently strong to overcome continuum damping, as shown by the general fishbone like dispersion relation (GFLDR), yielding the threshold condition, Eq. (4.23). The relevance of EPMs stems from their nature of being born as unstable discrete modes out of the SAW continuous spectrum at the optimal frequency for maximizing wave-particle power exchange. For this reason, above the linear EPM excitation threshold, there is a transition from local to meso-scale particle redistributions, as noted by (Briguglio *et al.*, 1998) and discussed in Secs. V.D.5.b and V.D.6. The non-perturbative nature of EPMs is reflected by the sensitivity of mode frequency and growth rates to EP sources. Thus, linear EPM dispersive properties suggest that fast frequency chirping is to be expected for these modes during their nonlinear evolution, as noted by (Gorelenkov *et al.*, 2000; Zonca and Chen, 2000) (cf. Sec. IV.C).

The excitation of EPMs is generally independent of the existence of frequency gaps in the SAW continuum, although Eq. (4.23) shows that EPM threshold is lower near an accumulation point. For this reason, sometimes EPM have been given specific names; such as Resonant TAE (RTAE) modes (Cheng *et al.*, 1995) for EPM near the TAE frequency gap. In some special conditions, EPM has also been used as acronym for indicating fluctuations observed experimentally and requiring non-perturbative EP responses for AEs to exist inside frequency gaps; *e.g.*, RSAE/AC (Berk *et al.*, 2001; Zonca *et al.*, 2002) excited by highly supra-thermal ion tails due to ion cyclotron resonance heating. Given the GFLDR theoretical framework, this use is not justified and is reported here for the sake of completeness.

After the first theoretical work on EPMs (Chen, 1994), numerical analyses of EPM stability were not numerous (Briguglio *et al.*, 2000; Cheng *et al.*, 1995; Gorelenkov *et al.*, 2000, 1998; Santoro and Chen, 1996; Zonca and Chen, 1996, 2000) until the first hybrid MHD-gyrokinetic simulation (cf. Sec. II.F) demonstrated the potential severe impact of these modes on EP confinement (Briguglio *et al.*, 1998), consistent with experimental observations. Ever since, significant efforts have been devoted in comparing numerical simulation results with experimental observations of EPMs (Briguglio *et al.*, 2007; Todo, 2006; Todo *et al.*, 2005) (cf. Sec. IV.C for more details).

A case that is particularly simple and still retains all the necessary physics ingredients to elucidate linear dispersive properties and radial structures of EPM is that of precessional resonance with magnetically trapped EPs without finite orbit width effects. This case will be also used in our discussions of the nonlinear wave-EP interactions (cf. Sec. V.D.6). Using Eq. (4.54) for separating the fast particle convective response, which is included via  $\delta\bar{W}_{nf}$  in the GFLDR dispersion relation, Eq. (4.34), Eq. (4.56) is readily solved for the EP bounce averaged response. In the case of plasma equilibria with shifted circular magnetic surfaces and assuming that particles are deeply trapped (cf. Sec. IV.B.2),  $\mathcal{J}B_0 \simeq qR_0$ ,  $n\bar{\omega}_{dn} = -k_\vartheta \mathcal{E} / (R_0 \Omega_E)$ ,  $\Omega_E$  is the fast particle cyclotron frequency computed at the magnetic axis,  $\tau_b = 2\pi q R_0 (R_0/r)^{1/2} \mathcal{E}^{-1/2}$  and, consistent with Eq. (4.77),

$$\delta\bar{W}_{nk} = \int \mathcal{E} d\mathcal{E} d\lambda \sum_{v_{\parallel}/|v_{\parallel}|=\pm} \frac{\pi^2 q R_0}{c^2 k_\vartheta^2 |s|} \frac{e^2}{m} \sum \left( \frac{\tau_b n^2 \bar{\omega}_{dn}^2 Q_{\mathbf{k},\omega} \bar{F}_0}{n\bar{\omega}_{dn} - \omega} \right). \quad (4.105)$$

Consider now one single supra-thermal particle species with an isotropic slowing down distribution function, characterized by injection energy  $E_F$  much larger than the critical energy  $E_c$  (Stix, 1972), so that for  $E_F/m_E > \mathcal{E} > E_c/m_E$

the fast particle energy is predominantly transferred to thermal electrons by collisional friction as it occurs for  $\alpha$ -particles in fusion plasmas; *i.e.*,

$$\bar{F}_0 = \frac{3P_{0E}}{4\pi E_F} \frac{H(E_F/m_E - \mathcal{E})}{(2\mathcal{E})^{3/2} + (2E_c/m_E)^{3/2}}, \quad (4.106)$$

where  $H$  denotes the Heaviside step function and the normalization condition is chosen such that the EP energy density is  $(3/2)P_{0E}$  for  $E_F \gg E_c$ . Substituting Eq. (4.106) back into Eq. (4.105) and defining  $\alpha_E$  as in Eq. (4.65) with  $\beta_E = 8\pi P_{0E}/B_0^2$ , we readily obtain<sup>17</sup>

$$\delta\bar{W}_{nk} = \frac{3\pi(r/R_0)^{1/2}\alpha_E}{8\sqrt{2}|s|} \left[ 1 + \frac{\omega}{n\bar{\omega}_{dnF}} \ln \left( \frac{n\bar{\omega}_{dnF}}{\omega} - 1 \right) + i\pi \frac{\omega}{n\bar{\omega}_{dnF}} \right], \quad (4.107)$$

with  $\bar{\omega}_{dnF} = \bar{\omega}_{dn}(\mathcal{E} = E_F/m_E)$  and having noted that  $|\omega_{*E}| \gg |\omega|$  for Alfvénic fluctuations resonantly excited by EPs. Thus, EP induced wave-particle power exchange is mainly via gradients in the radial profiles of the EP component. This result is readily applied to investigate the linear EPM excitation by deeply trapped EPs near the TAE gap, where, for moderate values of  $(s, \alpha)$ , Eq. (4.94) yields

$$\delta\bar{W}_{nfT} = \frac{|s|\pi}{8} \left( 1 + 2\kappa(s) - \frac{\alpha}{\alpha_{cr}} \right) + \frac{|s|\pi}{8} \kappa(s) \frac{1}{k_\theta^2 s^2} \frac{\partial^2}{\partial r^2}, \quad (4.108)$$

where we have assumed  $|B(0)/A(0)| \ll 1$  and  $\cos\theta_k \simeq 1 - \theta_k^2/2 = 1 + (1/2)(sk_\theta)^{-2}\partial_r^2$  for localized modes. The EP radial profile effect on EPM mode structures can be analyzed by assuming that their equilibrium pressure gradient is peaked at  $r = r_0$ , *i.e.*, (Zonca and Chen, 2000)

$$\alpha_E = \alpha_{E0} \exp \left( -\frac{(r-r_0)^2}{L_{pE}^2} \right) \simeq \alpha_{E0} \left( 1 - \frac{x^2/s^2}{k_\theta^2 L_{pE}^2} \right), \quad (4.109)$$

with  $x = |s|k_\theta(r-r_0)$  and other equilibrium quantities are considered constant for localized modes. Thus, dropping the subscript  $n$  and letting  $\bar{\omega}_{dF} \equiv n\bar{\omega}_{dnF}$ , Eq. (4.99) finally becomes

$$\begin{aligned} i\Lambda_T A &= \frac{|s|\pi}{8} \left( 1 + 2\kappa(s) - \frac{\alpha}{\alpha_{cr}} \right) A + \frac{|s|\pi}{8} \kappa(s) \frac{\partial^2 A}{\partial x^2} \\ &+ \frac{3\pi(r/R_0)^{1/2}}{8\sqrt{2}|s|} \alpha_{E0} \left( 1 - \frac{x^2/s^2}{k_\theta^2 L_{pE}^2} \right) \left\{ 1 + \frac{\omega}{\bar{\omega}_{dF}} \left[ \ln \left( \frac{\bar{\omega}_{dF}}{\omega} - 1 \right) + i\pi \right] \right\} A, \end{aligned} \quad (4.110)$$

with  $\Lambda_T = (1/2)(\Gamma_+/\Gamma_-)^{1/2} \simeq (2\epsilon_0)^{-1/2} [(1-\epsilon_0)/4 - \omega^2/\omega_A^2]^{1/2} \text{sgn}(\Re\omega)$  for modes with frequencies near the lower TAE gap accumulation point, which are favored for moderate values of  $(s, \alpha)$  (Cheng *et al.*, 1985). Equation (4.110) is readily solved for unstable localized modes, the fastest growing one being the ground state solution  $A(x, t) = A_0(x)e^{-i\omega t}$ , with  $\omega = \omega_0 + i\gamma_L$ ,  $A_0(x) = \bar{A}_0 \exp(-x^2/2\Delta^2)$ , and

$$\Delta^{-4} = \frac{3(r/R_0)^{1/2}}{\sqrt{2}\kappa(s)s^4 k_\theta^2 L_{pE}^2} \alpha_{E0} \left\{ 1 + \frac{\omega_0}{\bar{\omega}_{dF}} \left[ \ln \left( \frac{\bar{\omega}_{dF}}{\omega_0} - 1 \right) + i\pi \right] \right\}, \quad (4.111)$$

$$\frac{|s|\pi}{8} \left[ 1 + (2 - \Re(\Delta^{-2})) \kappa(s) - \frac{\alpha}{\alpha_{cr}} \right] + \frac{3\pi(r/R_0)^{1/2}}{8\sqrt{2}|s|} \alpha_{E0} \left[ 1 + \frac{\omega_0}{\bar{\omega}_{dF}} \ln \left( \frac{\bar{\omega}_{dF}}{\omega_0} - 1 \right) \right] = 0, \quad (4.112)$$

$$\frac{\gamma_L}{\omega_0} = \left[ \frac{\omega_0/\bar{\omega}_{dF}}{1 - \omega_0/\bar{\omega}_{dF}} - \frac{\omega_0}{\bar{\omega}_{dF}} \ln \left( \frac{\bar{\omega}_{dF}}{\omega_0} - 1 \right) \right]^{-1} \left[ \pi \frac{\omega_0}{\bar{\omega}_{dF}} - \left( \frac{3\pi(r/R_0)^{1/2}}{8\sqrt{2}|s|} \alpha_{E0} \right)^{-1} \left( \Lambda_T(\omega_0) + \frac{|s|\pi}{8} \kappa(s) \Im(\Delta^{-2}) \right) \right]. \quad (4.113)$$

<sup>17</sup> Note the formal difference between this expression and the linearized form of  $\delta\bar{W}_{nk}$  of (Zonca *et al.*, 2005), where  $\alpha_E$  is defined to include finite orbit width effects that, in the small orbit limit, give the additional  $(2|s|)^{-1}$  factor shown here explicitly (cf. Sec. IV.B.3).

Equations (4.111) to (4.113) summarize all the characteristic features of EPs, namely, their radial localization is determined by the EP source via wave-particle resonant drive. Equation (4.111) also shows that the most unstable EPM wave packet is excited on meso-scales  $\propto (L_{pE}/|k_{\parallel}|)^{1/2}$ . Furthermore, the real EPM frequency is determined by Eq. (4.112) and is controlled by the EP characteristic frequency, in this case  $\bar{\omega}_{dF}$ , while the mode growth rate near excitation threshold is given by Eq. (4.113), where the threshold condition is clearly set by the competition between fast particle drive and continuum damping. The crucial role of these EPM properties in the nonlinear evolutions of these fluctuations is discussed in Sec. V.D.6.

As final remark to Sec. IV.B, we note that the GFLDR is based on the existence of two characteristic radial scales of DAW fluctuations; which is generally applicable to low frequency MHD and SAWs excited by supra-thermal particles in burning plasmas. It is, however, not applicable to AEs, dubbed  $\alpha$ TAE (Hu and Chen, 2004), existing in the high- $\beta$  ideal ballooning mode “second stability region” (Coppi *et al.*, 1980), where  $\alpha \gtrsim 1$  and  $\alpha$  is the normalized pressure gradient of Eq. (4.65). More specifically,  $\alpha$ TAEs have regular mode structures with exponentially small coupling to the continuum, and, hence, GFLDR becomes inapplicable. These modes have clear connection with the higher order collisionless ballooning modes discussed by (Hirose *et al.*, 1994), whose stability boundaries were predicted by (Chen *et al.*, 1987), and investigated by (Dong *et al.*, 2004). Similarly to other AEs,  $\alpha$ TAE can also be destabilized by a EP population (Hu and Chen, 2005). The dispersion relation of these modes and their mode structures have been studied in detail in recent numerical simulation works (Bierwage *et al.*, 2010a,b), where a quadratic form similar to Eq. (4.20) is derived and  $\Lambda_n$  can be interpreted as the rate of energy leaking to smaller scales. There, it is demonstrated that, including thermal plasma kinetic effects,  $\alpha$ TAE can be viewed as modified Alfvénic ITG in the second stability region; *i.e.*, the modes first addressed by (Hirose *et al.*, 1994) and then by (Dong *et al.*, 2004). Meanwhile, in the presence of EP drive,  $\alpha$ TAE acquire their true nature of AEs destabilized by a sparse supra-thermal particle population. The relevance of  $\alpha$ TAE or other type of drift-Alfvén ballooning modes, exhibiting similar periodic stability patterns (Chen *et al.*, 1987), to present day toroidal devices is limited, for they require reaching  $\alpha \gtrsim 1$ . It may, however, be relevant to the concept for DEMO (DEMONstration Power Plant); should it pursue high- $\beta$  plasma operations.

### C. Experimental verification of linear Alfvén Eigenmodes and stability predictions in burning plasmas

The many experimental observations of AE and EPM are well documented and discussing them in detail is beyond the scope of the present work. Here, we illustrate only some of the successful and positive feedbacks between theory and experiment in this area; made possible by the development of impressive diagnostic techniques as well as numerical simulation capabilities, accompanied by detailed physics understanding. Along this path, one element of enrichment was brought by the fruitful exchanges between tokamak and stellarator expert communities. To the readers, who are especially interested in these aspects, we recommend two recent and excellent reviews on the “Affinity and difference between energetic-ion-driven instabilities in 2D and 3D toroidal systems” by (Kolesnichenko *et al.*, 2011), with a more theoretical approach, and on the “Energetic-ion-driven global instabilities in stellarator/helical plasmas and comparison with tokamak plasmas” by (Toi *et al.*, 2011), with a broader view on experimental issues.

The internal kink/fishbone problem has been widely studied in the magnetic fusion research due to its potential significant implications on fusion performance (Heidbrink and Sadler, 1994; McGuire *et al.*, 1983; White *et al.*, 1983). The fishbone mode is most frequently excited with  $n = 1$  toroidal mode number, although higher mode numbers are also observed, consistently with theoretical predictions (Biglari and Chen, 1986b, 1991; Chen, 1994; Cheng, 1982a,b; Rewoldt, 1988; Spong *et al.*, 1988; Tang *et al.*, 1980; Tsai and Chen, 1993; Weiland and Chen, 1985) and continuously connecting with the KBM branch (Biglari and Chen, 1991; Tsai and Chen, 1993). An extensive review of experimental fishbone observation can be found in (Heidbrink and Sadler, 1994) and we refer readers to that for further details. More recently, with increasing plasma performance, other types of kink/fishbone oscillations have been measured. In particular, in high- $\beta$  plasmas typical of spherical tori, the usual kink/fishbone branch may be stabilized by the reversal of the direction of the toroidal particle precession drift, as shown theoretically by (Hastie *et al.*, 1987a; Kolesnichenko *et al.*, 1999) and observed experimentally in NSTX (Fredrickson *et al.*, 2003) and START (Gryaznevich and Sharapov, 2004). However, other precession-bounce resonances with  $\ell \neq 1$  in Eq. (4.50) may effectively drive kink/fishbone modes at higher frequencies, as demonstrated by (Fredrickson *et al.*, 2003). Furthermore, “off-axis” fishbones have also been observed in plasmas with non-monotonic  $q$  profiles (Heidbrink *et al.*, 2011; Huysmans *et al.*, 1999; Matsunaga *et al.*, 2009, 2010; Okabayashi *et al.*, 2009, 2011), whose radial structure peaks near the  $q = 2$  rather than inside the  $q = 1$  surface. Although it was suggested that these modes may have an internal kink nature (Huysmans *et al.*, 1999), and fishbone modes with a double kink structure are theoretically predicted in plasmas with non-monotonic  $q$  profiles (Helander *et al.*, 1997), recent experimental evidence (Heidbrink *et al.*, 2011; Okabayashi *et al.*, 2011) suggests that these modes are external kinks, resonantly excited by supra-thermal particles. In this sense, these modes are

the EPM counterpart of the resistive wall mode (RWM) (Pfirsch and Tasso, 1971), whose stability is expected to be strongly influenced by plasma rotation, due to the ideal MHD coupling with sound wave (Betti, 1995; Bondeson and Ward, 1994) and Alfvén waves (Gregoratto *et al.*, 2001; Zheng *et al.*, 2005), or due to resistive layer (Finn, 1995; Gimblett and Hastie, 2000) and viscous boundary layer damping (Fitzpatrick and Aydemir, 1996). However, even stronger effects are expected when kinetic resonance interactions are accounted for with thermal ions, at the bounce or transit frequencies (Bondeson and Chu, 1996; Liu *et al.*, 2004), or with either trapped thermal ions or electrons at the precession frequency (Hu and Betti, 2004). All these physics must be taken into account realistically in numerical simulations [see *e.g.* (Berkery *et al.*, 2010; Liu *et al.*, 2009)], to be compared with experimental observations. Recent reviews of the physics of internal kink (sawtooth) stabilization (Chapman *et al.*, 2007; Graves *et al.*, 2010) and analyses of high- $\beta$  regimes for DEMO (Chapman *et al.*, 2011) confirm the necessity of thorough kinetic models for the description of the plasma operation control in burning plasmas.

E-fishbones have been widely investigated, since their first observation in DIII-D with ECRH (Wong *et al.*, 2000). In that case, barely trapped supra-thermal electrons, characterized by  $\bar{\omega}_{de}$  reversal, could destabilize a mode propagating in the ion diamagnetic direction in the presence of an inverted spatial gradient of the supra-thermal tail, consistent with Eq. (4.52). Observations of e-fishbones with ECRH only (Ding *et al.*, 2002) and LHH/LHCD only (Romanelli *et al.*, 2002; Smeulders *et al.*, 2002) have been also reported in HL-1M and FTU, respectively. More recently, electron fishbones have been observed in Tore Supra (Macor *et al.*, 2009; Maget *et al.*, 2006), due to resonant excitation of a double-kink mode by supra-thermal electrons generated with LH power injection, and in HL-2A (Chen *et al.*, 2009), in plasma discharges with off-axis ECRH. Similar but higher frequency modes were observed in Compass-D (Valovič *et al.*, 2000) during ECRH and LH power injection, with chirping frequency comparable with that of TAE (Cheng *et al.*, 1985),  $\omega \lesssim \omega_{TAE}$ . Due to the combined effect of ECRH and LH/LHCD in plasmas yielding e-fishbones, particular care is needed for the treatment of trapped and circulating supra-thermal particles responses<sup>18</sup> and for the modeling of the supra-thermal electron distribution function, as emphasized in the work by (Merle *et al.*, 2012). E-fishbone properties have been characterized by very detailed analyses of experimental results in HL-2A (Chen *et al.*, 2010a, 2009), FTU and Tore Supra (Guimarães-Filho *et al.*, 2012, 2011), based on the use of the GFLDR as interpretative framework, and confirmed by hybrid MHD-gyrokinetic numerical simulations (Vlad *et al.*, 2011, 2012, 2013).

The first observations of AEs were in the TAE frequency range, reported independently in TFTR (Wong *et al.*, 1991) and DIII-D (Heidbrink *et al.*, 1991). Major efforts were devoted to this area of research in the early 90's, also in connection with the first D-T experiments in laboratory plasmas in JET (JET Team, 1992) and TFTR (Bell *et al.*, 1995). The first review of experimental observations of Alfvénic and MHD modes destabilized by supra-thermal particle is given by (Heidbrink and Sadler, 1994). The different varieties of AE associated with various equilibrium geometry and nonuniformity became evident already with D-T experimental results in TFTR observing a core localized TAE, readily explained with by theoretical studies (Berk *et al.*, 1995c; Breizman and Sharapov, 1995; Candy *et al.*, 1996; Fu, 1995). Alfvénic modes in TFTR D-T plasmas received considerable theoretical attention not only for linear stability analyses, *e.g.*, (Candy and Rosenbluth, 1995; Fu *et al.*, 1996a), but also for understanding their nonlinear saturation and predicting observed fluctuation levels (Gorelenkov *et al.*, 1999a) (cf. Sec. V.D.4). An extended review of alpha particle physics experiments in TFTR is given by (Zweben *et al.*, 2000). The high performance D-T experiments in JET (Gibson and the JET Team, 1998) were instead stable with respect to resonant excitations of fusion alpha particle driven instabilities, as explained by (Sharapov *et al.*, 1999). The reason for this stems from the difference of typical operation regimes in present day experiments with respect to those expected in burning plasmas (cf. Sec. VII for more details). In particular, the relatively large fusion alpha particle orbit widths in today's machines causes their response to be nearly adiabatic (cf. Sec. II.E), and, thereby, suppress resonant wave-particle interactions.

An overview of early TAE experimental observations in JET is given by (Fasoli *et al.*, 1995b); and (Fu *et al.*, 1996b; Kramer *et al.*, 1998; Saigusa *et al.*, 1995) provide a similar summary of TAE observations in JT-60U. Short reviews of AE experimental studies in single devices are given also by (Heidbrink, 1995) for DIII-D, by (McClements *et al.*, 1999) for START, by (Snipes *et al.*, 2000) for Alcator C-Mod, by (Gryaznevich and Sharapov, 2004) for MAST and by (Gorelenkov *et al.*, 2004) for NSTX. Meanwhile, (Wong, 1999) provided the most comprehensive overview of AE observations till the end of the nineties, including a detailed analysis of TFTR results in this area. Further detailed behaviors of AE as predicted by theory were verified; *e.g.*, by (Kramer *et al.*, 1999), reporting on noncircular triangularity and ellipticity-induced AE observed in JT-60U, and by (Fredrickson *et al.*, 2000), giving evidence of modes at frequencies near the second Alfvén gap in TFTR. The stabilizing effect of finite supra-thermal ion orbit widths, compared with the mode wavelength, was discussed by (Gorelenkov *et al.*, 1999b) for TFTR plasmas, while

<sup>18</sup> Neglecting finite  $\omega_b$  effects in Eq. (4.51) implies considering barely circulating supra-thermal electrons and/or  $q \simeq 1$  (Wang *et al.*, 2007; Zonca *et al.*, 2007a,b) (cf. also Sec. IV.B.1).

similar analyses in stellarators were given by (Kolesnichenko *et al.*, 2006) for the specific case of the W7-AS device. Meanwhile, energetic ion driven MHD instabilities observed in the heliotron/torsatron devices Compact Helical System and Large Helical Device were reviewed by (Toi *et al.*, 2000, 2004). It is also interesting to note that, consistent with Eqs. (4.2) and (4.3), the spectral gap in the SAW continuous spectrum was investigated in the LAPD linear device, using a periodic array of magnetic mirrors (Zhang *et al.*, 2008b). Key issues for burning plasmas related with Alfvén wave physics are summarized by (Heidbrink, 2002), where an update of the experimental observations reviewed by (Wong, 1999) can also be found. Meanwhile, the most recent review of experimental results by (Breizman and Sharapov, 2011) has a slant toward reporting progress in nonlinear theory comparison with experimental data. A general overview of basic physics of Alfvénic fluctuations and EPs in toroidal plasmas was given by (Heidbrink, 2008).

Reproducing very accurate experimental measurements of TAE damping rates, originally obtained for  $n = 1$  modes (Fasoli *et al.*, 1995a,b) has been challenging for numerical simulation codes. Numerically calculated AE damping rates using non-perturbative kinetic models agreed qualitatively with experiments (Jaun *et al.*, 1998, 2000), but precise comparisons with measured damping rates were found to depend on plasma edge boundary conditions and kinetic effects (Fu *et al.*, 2005; Lauber *et al.*, 2005). This suggests that future developments in numerical stability analyses of burning plasmas in realistic conditions will need to incorporate accurate models of the Scrape Off Layer (SOL) and of the mode structure outside the last closed magnetic surface (Chen *et al.*, 2011a) in divertor configurations. Another critical aspect is the accurate modeling of the mode conversion of long wavelength MHD-like modes to shorter-wavelength KAW (Hasegawa and Chen, 1976). Differences in the wave propagation properties may be the explanation of different predictions on the AE kinetic damping rates in the plasma interior (Borba *et al.*, 2002; Fu *et al.*, 2005; Lauber *et al.*, 2005; Testa *et al.*, 2003). Significant improvement in the comparison between numerically computed and experimentally measured values of TAE damping rates with  $n \geq 2$  (Snipes *et al.*, 2005, 2004; Testa *et al.*, 2010) has been reported as a result of a benchmarking effort (Borba *et al.*, 2010), carried out within the International Tokamak Physics Activity (ITPA) Topical Group on Energetic Particles. Within the same ITPA Topical Group, it is also worthwhile mentioning another successful benchmarking activity of gyrokinetic, kinetic MHD and gyrofluid codes for the linear calculation of fast particle driven TAE dynamics (Könies *et al.*, 2012).

The general feature of AE in toroidal plasmas to be slightly shifted from the SAW accumulation point; *i.e.*, to closely track the frequency of the continuous spectrum at the SAW resonance, makes it possible to infer local plasma parameters by “MHD spectroscopy” (Goedbloed *et al.*, 1993; Holties *et al.*, 1997a,b), which measures the AE frequency. MHD spectroscopy has been particularly adopted as analysis technique in connection with experimental observation of AC/RSAE fluctuations (Kimura *et al.*, 1998; Nazikian *et al.*, 2003; Sharapov *et al.*, 2002; Snipes *et al.*, 2005; Takechi *et al.*, 2002). In addition to the generic information on the Alfvén speed and the plasma rotation by Doppler shift, the observation of TAE and AC/RSAE may yield information on the  $q$  profile, which is especially useful when the time evolution of the minimum- $q$  can be reconstructed (Fasoli *et al.*, 2002; Sharapov *et al.*, 2001), for it helped developing plasma operation scenarios with internal transport barriers (Joffrin *et al.*, 2003; Pinches *et al.*, 2004a; Sharapov *et al.*, 2004). Theoretical predictions of mode frequencies and linear stability of AC/RSAE in JET have also been successfully compared with experimental observations (Abel *et al.*, 2009). In those studies, furthermore, it has been shown that when the frequency sweeping of AC is downward, in contrast to the usual slow upward chirping of these modes, the magnetic shear configuration is typically weakly reversed. Discussions of experimental evidence of downward chirping AC/RSAE are also given by (Heidbrink *et al.*, 2013; Sandquist *et al.*, 2007). MHD spectroscopy has been proposed as (thermal ion) temperature diagnostics as well (Breizman *et al.*, 2005; Gorelenkov *et al.*, 2006), using the temperature ratio dependence of the BAE accumulation point (cf. Sec. IV.B.2). However, other interesting applications exist, which allow extracting from MHD spectroscopy information on the nonlinear dynamic evolution of AE (Breizman and Sharapov, 2011; Fasoli *et al.*, 2002; Pinches *et al.*, 2004b) (see Sec. V.D.3 for more details).

One important progress in comparisons between experimental observations and theoretical prediction has been driven in the recent years by the development of internal measurements of AE mode structures. DIII-D is the first to demonstrate that AE may be excited in the plasma core by both supra-thermal particles as well as thermal ions with a wide range of mode numbers (Nazikian *et al.*, 2006), consistent with the theoretical framework of Sec. IV.B.2. Other examples are the use of reflectometry and Phase Contrast Imaging (PCI) techniques (Edlund *et al.*, 2009; Hacquin *et al.*, 2007; Van Zeeland *et al.*, 2006a), providing good comparisons of 2D MHD mode structure calculations with experimental measurements (Edlund *et al.*, 2009); and of Electron Cyclotron Emission (ECE) imaging (Van Zeeland *et al.*, 2006b), yielding a visualization of actual 2D AE structures from experimental measurements (Classen *et al.*, 2011; Tobias *et al.*, 2011). ECE imaging results of RSAE mode structures are found to be influenced by the energetic ion radial profile, as expected from theory and in agreement with gyrofluid (cf. Fig. 3) and gyrokinetic simulation results (Spong *et al.*, 2012; Tobias *et al.*, 2011). Qualitatively similar results of 2D RSAE mode structures, modified by the energetic ion radial profiles, have been obtained by gyrokinetic (Deng *et al.*, 2010) and hybrid MHD gyrokinetic simulations (Deng *et al.*, 2012b; Wang *et al.*, 2011, 2010b). In general, however, such good agreement

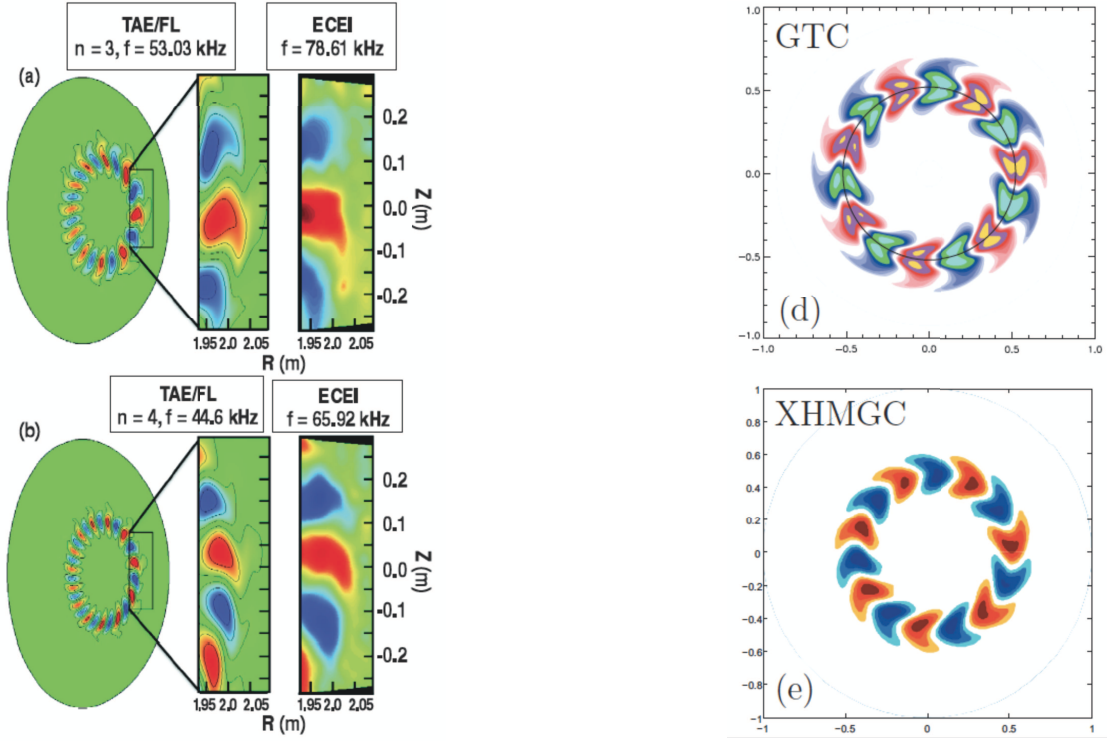


FIG. 3 Left frame [from the original Fig. 4 (a)-(b) in Ref. (Tobias *et al.*, 2011)]: Comparisons of  $n = 3$  and  $n = 4$  2D RSAE mode structures, modified by the EP profile, as measured from ECE imaging (left) and as obtained from gyrofluid simulations (right) with the TAE/FL code (Spong *et al.*, 1992, 1994). Right frame [from the original Fig. 5 (d)-(e) in Ref. (Deng *et al.*, 2010)]:  $n = 4$  2D RSAE contour plots from gyrokinetic (Deng *et al.*, 2010) [with GTC code (Lin *et al.*, 1998)] and hybrid MHD gyrokinetic simulations (Wang *et al.*, 2010b) [with the eXtended version (Wang *et al.*, 2011) of the HMGC code (Briguglio *et al.*, 1995)], showing the same effect of EP radial profiles on the mode structure (Deng *et al.*, 2012b).

between internal measurements of AE mode structures and numerical calculations are not always found. This is the case, for example, of “TAE Avalanches” (Fredrickson *et al.*, 2009), where the discrepancies between mode structures reconstructed from reflectometry and numerical simulation results are attributed to nonlinear processes (Podestà *et al.*, 2009). Furthermore, fluctuations typically have a larger experimental growth rate than that computed from linear stability calculations, and are accompanied by rapid frequency chirping (Podestà *et al.*, 2011). These observations suggest that supra-thermal particle transport and nonlinear Alfvén wave dynamics are profoundly interlinked, and that frequency chirping is an important nonlinear process, whose characteristic rate provides information on the underlying physics (cf. Secs. V.D.5 and VI.B). The observation of frequency chirping modes was readily recognized to be important (Gryaznevich and Sharapov, 2004; Heidbrink, 1995; Kramer *et al.*, 1999; McClements *et al.*, 1999; Takechi *et al.*, 1999; Wong, 1999) and their existence is strictly connected with EPM observations in many experimental devices (Bernabei *et al.*, 1999, 2001; Gorelenkov *et al.*, 2000; Gorelenkov and Heidbrink, 2002; Wong, 1999). In fact, frequency chirping is typically classified as slow, when it reflects plasma equilibrium profile changes, or fast, when it involves local modification of the EP velocity distribution function by nonlinear dynamics (Berk and Breizman, 1995), or rapid EP radial redistribution and the consequent nonlinear modification of the wave dispersive properties (Gorelenkov *et al.*, 2000; Zonca and Chen, 2000). In this latter case, the EP effect on the mode is non-perturbative, and both mode frequency and radial structures are modified by EP redistributions with important consequences on nonlinear dynamics (cf. Secs. V.D.5 to V.D.7).

The low-frequency Alfvén wave spectrum in the KTI frequency gap also attracted significant interest since the first observations of BAE modes (Heidbrink *et al.*, 1993; Turnbull *et al.*, 1993). A very detailed stability analysis of BAE modes observed in Tore Supra (Sabot *et al.*, 2006; Udintsev *et al.*, 2006) and of the experimental conditions that are necessary for effective mode excitation is given by (Nguyen *et al.*, 2009) on the basis of the GFLDR theoretical framework (cf. Sec. IV.B.2). The GFLDR was also adopted for explaining the frequency of BAE modes in FTU (Annibaldi *et al.*, 2007), where they are excited in the presence of a large magnetic island (Buratti *et al.*, 2005) (cf. Sec. V.C.4), as observed also in TEXTOR (Zimmermann *et al.*, 2005) and HL-2A (Chen *et al.*, 2011b). Significant interest was also attracted by observations of BAAE (Gorelenkov *et al.*, 2007a,b) in JET and NSTX at frequencies below the BAE

accumulation point of the SAW continuum (cf. Sec. IV.B.2), by the more recent evidence of “Sierpes modes” in ASDEX Upgrade (García-Muñoz *et al.*, 2008), interpreted as BAE excited by energetic ions generated by Ion Cyclotron Resonance Heating (ICRH) (Lauber and Günter, 2008), and also by measurements of ICRH driven BAE in Tore Supra (Sabot *et al.*, 2009). For accurate interpretation of these observations, as shown in Sec. IV.B.2, it is necessary to use kinetic theories for the proper treatment of thermal plasma compression effects, including wave-particle interactions with circulating as well as trapped thermal plasma particles (Chavdarovski and Zonca, 2009; Curran *et al.*, 2012; Lauber *et al.*, 2009, 2012; Zonca *et al.*, 2010). Some improvement in the modeling of experimental observations has been reported with simplified extensions and/or renormalization of fluid theories (Gorelenkov *et al.*, 2009). Recent detailed gyrokinetic simulations and comparisons with experimental observations in ASDEX Upgrade (Curran *et al.*, 2012; Lauber *et al.*, 2012), however, have confirmed that accurate description of kinetic interactions are needed for capturing the physics of AE and EPM at frequencies near the KTI gap. These results also confirm that two bands of low-frequency Alfvénic activities are generally expected, with predominance of either ion diamagnetic drift (KBM) or parallel and perpendicular ion compressibility (BAE) and with varying frequency-dependent geodesic curvature coupling to the ion-acoustic wave (cf. Sec. IV.B.2). Meanwhile, the BAAE branch, which, at the lowest order, is the usual (sideband) electrostatic drift wave (Zonca *et al.*, 2010), requires  $T_e/T_i \gg 1$  for minimizing Landau damping and being observable in actual experimental conditions, as those described by (Melnikov *et al.*, 2011) in TJ-II. More recently, the observation of BAE modes driven by supra-thermal electrons (e-BAE) due to ECRH near the KTI frequency gap in HL-2A (Chen *et al.*, 2011b, 2010b) has renewed the interest on the particular role that investigating fast-electron driven DAWs may have in understanding burning plasma physics. In fact, observations of fast electron driven AE have been made even in the TAE frequency range during the current rise phase in Alcator C-Mod (Snipes *et al.*, 2008). Observations of e-BAE in HL-2A can also be understood within the GFLDR theoretical framework.

Numerical simulation codes for the analysis of AE and EPM stability have been traditionally gyrofluid codes (Spong *et al.*, 1992, 1994), extended/kinetic MHD codes (Borba *et al.*, 2002; Cheng, 1992; Gorelenkov *et al.*, 1999b; Liu *et al.*, 2008; Mikhailovskii *et al.*, 1997; Pinches *et al.*, 1998; Zheng *et al.*, 2010) and hybrid MHD gyrokinetic codes (Briguglio *et al.*, 1995, 1998; Park *et al.*, 1999, 1992; Todo, 2006; Todo and Sato, 1998; Todo *et al.*, 1995, 2005; Wang *et al.*, 2011). In the recent years, there has been a significant effort to develop increasingly more accurate models for the description of DAWs, some of them with fully nonlinear simulation capability (cf. Sec. II.F). The main concern is the ability to handle the increasingly more demanding/sophisticated physics necessary for analyzing DAW stability properties in conditions of practical interest (cf. Sec. IV.B). Gyrokinetic numerical simulations of linear AE stability properties are becoming routine in the recent years (Chen *et al.*, 2010c; Lang *et al.*, 2009; Mishchenko *et al.*, 2009; Nishimura, 2009), and significant benchmarking efforts between various code predictions have been carried out (Deng *et al.*, 2010; Könies *et al.*, 2012; Zhang *et al.*, 2010a).

For ITER plasmas (Aymar *et al.*, 1997; Tamabechi *et al.*, 1991), preliminary stability analyses of Alfvénic modes were reported by (Cheng, 1991), adopting an extended MHD stability model (Cheng, 1992). The physics of Alfvén waves and EPs in ITER plasmas was first reviewed as a joint activity of the international fusion community in (ITER Physics Expert Group on Energetic Particles, Heating and Current Drive, ITER Physics Basis Editors, 1999), which was updated more recently by a similar collaborative effort (Fasoli *et al.*, 2007). Dedicated numerical studies of MHD and Alfvénic mode activities remain, however, scarce. The most recent kinetic stability analysis of the internal kink mode in ITER is given by (Hu *et al.*, 2006) and effects of  $\alpha$  particles on the RWM stability in ITER have been investigated by (Liu, 2010). Meanwhile, numerical investigations of AE and EPM stability in burning plasmas such as ITER, have shown that the most unstable (least stable) mode numbers are in the medium to high- $n$  range, *i.e.*,  $n_{max} \simeq \mathcal{O}(10)$  (Gorelenkov *et al.*, 2003; Vlad *et al.*, 2006), as expected from theory (cf. Secs. IV.B.2 and IV.B.3). In realistic geometries, stability analyses of the ITER “positive shear” reference scenario with perturbative EP dynamics demonstrate that AE are marginally stable in the presence of fusion- $\alpha$ ’s only, while instability is to be expected when supra-thermal particle tails due to 1 MeV Negative Neutral Beam Injection (NNBI) are accounted for (Gorelenkov *et al.*, 2003). Meanwhile, AE and EPM stability studies with self-consistent EP physics in model circular geometry show that, in the presence of fusion- $\alpha$ ’s only, ITER is marginally unstable for AE in all the three reference scenarios; *i.e.*, “positive shear” (SC2), “reversed shear” (SC4) and “hybrid scenario” (SCH) (Vlad *et al.*, 2006). The slight discrepancy between (Gorelenkov *et al.*, 2003) and (Vlad *et al.*, 2006) is likely due to the different equilibrium representation (shaped vs. circular), the treatment of fast ion dynamics (perturbative vs. self-consistent) and the profile differences in the reference scenarios. However, the fair agreement between existing results of Refs. (Gorelenkov *et al.*, 2003) and (Vlad *et al.*, 2006) suggests that the fundamental physics of collective mode excitations by EPs is well at hand. Simulations results also show that AE close to the plasma center are more easily excited by precession and precession-bounce resonances with trapped fusion- $\alpha$ ’s (Vlad *et al.*, 2006), due to the fact that the maximum drive due to NNBI is located more radially outward (at about mid radius of the plasma cross section). Similarly, AE structures mostly weighted in the outer plasma column are preferentially excited by NNBI via transit resonance (Gorelenkov

*et al.*, 2003, 2005). This fact explains why, due to orbit averaging effects, mode numbers of AE localized in the plasma core tend to be smaller. Generally, among the “improved confinement regimes”, AE stability in ITER is most critical for the “reversed shear” (SC4) scenario (Gorelenkov *et al.*, 2005; Vlad *et al.*, 2006), while the “hybrid scenario” (SCH) is more stable (Vlad *et al.*, 2006). However, assuming fusion- $\alpha$ ’s only, the threshold for  $n \simeq \mathcal{O}(10)$  EPM excitation in the ITER SCH scenario is reached by artificially raising the on axis  $\beta_\alpha$  by  $\approx 1.6$  at fixed profiles (Vlad *et al.*, 2006). Above this threshold, EP transports are characterized by convective processes of significant magnitude (cf. Secs. V.D.6 and VI.B). More recently, gyrokinetic simulations of TAE modes in ITER (Chen *et al.*, 2010c) have essentially confirmed prior findings (Gorelenkov *et al.*, 2003, 2005; Vlad *et al.*, 2006) and predict that most unstable mode numbers are expected for  $n_{max} \simeq \mathcal{O}(10)$ , with the dominant damping mechanism due to ion Landau damping.

The rapid increase of numerical simulation capabilities and the emergence of a unified theoretical framework for understanding and analyzing the excitation of DAWs by EPs suggest that realistic burning plasma stability analyses will be possible in the near future. Furthermore, all numerical simulation activities of Alfvénic modes in ITER are not only aiming toward stability analyses. In fact, significant efforts are also going on, *e.g.*, for providing technical support to the development of optimized diagnostic systems, such as those discussed by (Ambrosino *et al.*, 2012).

## V. NONLINEAR ALFVÉN WAVE BEHAVIORS AND SELF-CONSISTENT INTERACTIONS WITH ENERGETIC PARTICLES

The ordering estimates of vorticity equation in Sec. II.C introduce two different nonlinear dynamic regimes in the long wavelength limit. For  $\epsilon_\omega > \epsilon_\perp^2$ , nonlinear wave-wave interactions are determined by the polarization (inertia) nonlinearity and the MHD plasma description is reasonably accurate. Meanwhile, for  $\epsilon_\omega < \epsilon_\perp^2$ , Maxwell stress and pressure stress tensor nonlinearity become dominant and kinetic theory becomes necessary at increasingly shorter wavelengths. Thus, the nonlinear dynamics of Alfvén waves crucially depends on the existence of the so-called “Alfvénic state” (Alfvén, 1942, 1950; Elsasser, 1956; Hasegawa and Sato, 1989; Walén, 1944), where Reynolds and Maxwell stress cancel exactly and large amplitude shear Alfvén wave (SAW) can be supported. Consequently, physics processes that are responsible for breaking the Alfvénic state are of great importance for the nonlinear evolution of the SAW spectrum.

As anticipated in Sec. IV, the theoretical framework of the generalized fishbone like dispersion relation (GFLDR) provides a useful starting point for our analyses of nonlinear physics of Alfvén waves and energetic particles (EPs) in burning plasmas. Section V.A discusses the general theoretical approach adopted here, which is formulated as a Schrödinger equation with integro-differential nonlinear terms. That equation is then used in later sections to investigate nonlinear processes affecting drift Alfvén wave (DAW) behaviors.

Many of these issues can be analyzed and illuminated in uniform plasmas and are presented in Sec. V.B, where the finite ion compressibility effect (polarization nonlinearity) is analyzed in the long wavelength limit, showing that it yields the decay of a SAW into another SAW and an ion sound wave (Sagdeev and Galeev, 1969) (cf. Sec. V.B.1). However, for sufficiently short wavelength there is a transition to nonlinear behaviors dominated by Reynolds and Maxwell stresses, which requires accounting for wavelengths comparable with the ion Larmor radius (Hasegawa and Chen, 1975, 1976). In this case, kinetic Alfvén waves (KAWs) break the ideal Alfvénic state and the three wave SAW decay is taken over by the three wave KAW decay (Hasegawa and Chen, 1976). Such a transition has important consequences on plasma transport, since SAW decay preserves the anisotropy of the initial  $\mathbf{k}_\perp$  spectrum, while KAW decay tends to make it isotropic (cf. Sec. V.B.2). These findings, thus, demonstrate that, in general, it may be necessary to adopt the kinetic description in the study of Alfvén wave turbulence. The breaking of the Alfvénic state by KAWs also affects the nonlinear excitation of convective cells, as shown in Sec. V.B.3. Convective cells are the uniform plasma counterpart of zonal flows and fields in toroidal systems. Studying convective cells, thus, provides useful insights to understanding the more complex nonlinear interplay between Alfvén waves and zonal structures (ZS; cf. Sec. II.D), which will be further discussed later in this section and in Sec. VII within a broader physics framework.

In Sec. V.C, we show how geometry of the plasma equilibrium and spatial nonuniformities affect, both qualitatively and quantitatively, the nonlinear processes discussed above. The tokamak counterpart of the SAW decay process in a uniform plasma is Toroidal Alfvén Eigenmode (TAE) frequency cascading via nonlinear Landau damping (Hahn and Chen, 1995), discussed in Sec. V.C.1. At shorter wavelengths, as in the KAW decay, polarization nonlinearity is expected to become subdominant with respect to Maxwell stress and pressure stress tensor nonlinear terms, which thus determine the cross section of TAE frequency cascading. This analysis, however, remains to be carried out. In Sec. V.C.2, we also discuss the generation of ZS by finite amplitude TAE (Chen and Zonca, 2012; Spong *et al.*, 1994; Todo *et al.*, 2010) as toroidal geometry analogue of the generation of convective cells by KAW, considered in Sec. V.B.3. These various processes may by themselves yield to TAE or AE saturation levels that possibly explain some

experimental observations. More generally, however, saturation levels ( $|\delta B_r/B_0| \sim 10^{-3}$ ) expected for the individual nonlinear interactions, are larger than observed values ( $|\delta B_r/B_0| \lesssim 5 \times 10^{-4}$ ) [see, *e.g.*, (Heidbrink *et al.*, 2008)]. It is nonetheless important to identify and keep these processes into account, especially in conditions where a number of weak nonlinear interactions may be simultaneously active and ultimately determine the AE fluctuation amplitude. In addition to their importance in regulating turbulence intensity and, thereby, plasma transport, coherent nonlinear interaction of AE and ZS may generally influence fine structures of the AE frequency spectrum (cf. Sec. V.C.2), as it is the case of modulation interactions due to wave-particle nonlinear dynamics (Fasoli *et al.*, 1998) (cf. Sec. V.D.3 and some related discussions in Sec. V.D.6). Finally, to further illustrate the effects of equilibrium geometry and plasma nonuniformity in breaking the Alfvén state, we analyze the AE nonlinear interplay with the SAW continuous spectrum in nonuniform systems, which may either yield enhanced continuum damping (Chen *et al.*, 1998; Vlad *et al.*, 1992; Zonca *et al.*, 1995) (cf. Sec. V.C.3) or nonlinear instability, as in the case with finite amplitude MHD activity (Biancalani *et al.*, 2010a,b, 2011) (cf. Sec. V.C.4).

The nonlinear wave-particle interaction of AE and energetic particle modes (EPMs) with a population of EPs is discussed in Sec. V.D. We start from the analysis of the nonlinear dynamics of a nearly monochromatic energetic electron beam in a 1D plasma (O’Neil and Winfrey, 1972; O’Neil *et al.*, 1971), given in Sec. V.D.1, for this is the classical problem on which mode dispersion relation (Drummond and Pines, 1962; Ichimaru, 1962; O’Neil and Malmberg, 1968; Singhaus, 1964; Vedenov *et al.*, 1961b,c) and nonlinear behaviors in a beam-plasma system were formulated and understood for the first time. These processes include Landau damping in a finite amplitude wave (Mazitov, 1965; O’Neil, 1965) and nonlinear wave-particle interactions (Al’tshul’ and Karpman, 1965, 1966; Drummond and Pines, 1962; O’Neil and Winfrey, 1972; O’Neil *et al.*, 1971; Shapiro, 1963a,b; Vedenov *et al.*, 1961b,c), such as wave-particle trapping, which is the dominant saturation mechanism due to the flattening of the EP distribution function in the resonant region by phase space mixing. The 1D beam-plasma problem is also important for understanding aspects of the nonlinear interaction of AE with EPs. In fact, there are currently two paradigms for discussing these physics (Chen and Zonca, 2007a; Zonca *et al.*, 2006). One is the “bump-on-tail” paradigm, which is based on wave trapping, including effects of source and dissipation<sup>19</sup>, that occurs due to wave-particle “resonance detuning”. This paradigm has been extensively developed by Berk, Breizman and coworkers (Berk and Breizman, 1990a,b,c), and applied to explain experimental observations [cf. (Breizman and Sharapov, 2011) for a recent review]. The other paradigm may be dubbed as the “fishbone” paradigm (Chen and Zonca, 2013); in which, due to frequency chirping, there is little resonance detuning and the wave-particle phase is locked (Chen *et al.*, 1984; White *et al.*, 1983). On the other hand, the duration of wave-particle interaction is limited due to the finite radial localization of the mode structures; *i.e.*, “radial decoupling” (Briguglio *et al.*, 1998; Chen *et al.*, 1984; Zonca *et al.*, 2005).

The nonlinear physics of the “bump-on-tail” paradigm are analyzed in Sec. V.D.2, stemming from the original works by (Berk and Breizman, 1990a,b,c). Its applications to AE experimental observations are discussed in Sec. V.D.3, which also addresses its underlying assumptions and its consequent validity limits. Some of these limitations can be overcome by approximate numerical simulation models, based on perturbative treatment of EPs, which are presented in Sec. V.D.4. The “bump-on-tail” paradigm applies sufficiently close to marginal stability, when fluctuation induced radial particle excursions are smaller than the mode radial wavelength. For sufficiently strong external power inputs and, therefore, EP power density sources, nonlinear EP excursions explore regions of radially varying mode structures and, thus, a transition typical of nonuniform plasmas is expected in the AE nonlinear dynamics (Zonca *et al.*, 2005), while EP redistributions occur on meso-scales as discussed in Sec. V.D.5. The general theoretical framework, formulated in Sec. V.D.5, allows describing the transition from uniform to nonuniform plasma behaviors, illuminated by recent numerical simulation results (Briguglio *et al.*, 2013; Wang *et al.*, 2012; Zhang *et al.*, 2012). Effects of such a transition become more important as drive strength increases, and are most apparent for EPMs (cf. Sec. V.D.6) and fishbones (cf. Sec. V.D.7), which are characterized by the nonperturbative interplay of nonlinear mode dynamics and EP transport processes.

Further remarks and discussions related with the general theoretical formulation of Sec. V.A are presented in Sec. V.E, where possible interesting connections to other fields of physics research are also discussed.

## A. General theoretical approach

Here, we further elaborate the GFLDR theoretical framework and derive a general form of governing equations for addressing nonlinear physics of Alfvén waves and EPs in burning plasmas. Equation (4.36) describes the spatiotem-

<sup>19</sup> Source and dissipation account for the generation of the EP population by external heating and/or current drive systems in toroidal plasmas of fusion interest as well as for the relaxation of their distribution function via Coulomb collisions (Berk and Breizman, 1990a).

poral evolution of DAW wave packets in toroidal plasmas due to the influence of external sources and/or nonlinear dynamics. From Eq. (4.34), it is readily recognized that a useful formal interpretation of the left hand side is obtained isolating linear terms in the local dispersion function  $D_n(r, \theta_{k0}(r), \omega_0)$ , while nonlinear and external source terms are collected on the right hand side. Thus,

$$S_n(r, t) = -D_n^{NL} + S_n^{ext}(r, t) = (\delta\bar{W}_f^{NL} + \delta\bar{W}_k^{NL})_n - i\Lambda_n^{NL} + S_n^{ext}(r, t) , \quad (5.1)$$

where  $S_n^{ext}(r, t)$  explicitly denotes external sources, the superscript  $NL$  stands for nonlinear and the definition of the various terms follows straightforwardly from Eqs. (4.16) and (4.18) and Eqs. (4.31) and (4.32). In general,  $S_n(r, t)$  can be written symbolically, in terms of amplitude expansion, as (Chen *et al.*, 2005; Zonca *et al.*, 2006)

$$S_n(r, t) - S_n^{ext}(r, t) = (C_{n,0} + C_{0,n}) \circ A_{n0}(r, t) A_{z0}(r, t) + \sum_{\substack{n', n'' \neq n \\ n' + n'' = n}} C_{n', n''} \circ A_{n'0}(r, t) A_{n''0}(r, t) , \quad (5.2)$$

where  $C_{n', n''}$  are generally integro-differential operators, which imply non-local interactions in the  $n$  toroidal mode number-space, and  $A_{z0}$  and  $A_{n0}$  are, respectively, the the slowly varying envelope functions introduced in Eq. (4.36); *i.e.*, the zonal and  $n \neq 0$  components. Here, we have included nonlinear dynamics that modify the  $n = 0$  ‘‘zonal’’ particle distribution function  $\delta\bar{F}_z$ , given by Eq. (2.22) (Zonca *et al.*, 2000). Therefore,  $A_{z0}$  not only represents the amplitude of ZS, but it also symbolically indicates the nonlinear distortion of the equilibrium particle distribution function. This distortion effect enters Eq. (5.1) through velocity space integrals, implying that  $A_{z0}$ , when accounting for interactions with  $\delta\bar{F}_z$ , is by itself a nonlinear function of  $A_{n0}$  and that the dependence is quadratic,  $A_{z0} \propto |A_{n0}|^2$ . As will be explained in Sec. V.D.5.c, we refer to these contributions as phase-space ZS (Zonca *et al.*, 2013a,b). Thus, the source term in Eq. (5.1) is intended to contain a cubic nonlinearity with respect to the envelope function,  $A_{n0}(r, t)$ . The remaining terms in Eq. (5.2) account for three wave interactions and, in general, non-local spectral transfers. Combining all the various terms, Eq. (4.36) can be cast in the form of a nonlinear Schrödinger equation with integro-differential terms

$$\begin{aligned} & \frac{\partial D_n}{\partial \omega_0} \left( i \frac{\partial}{\partial t} \right) A_{n0}(r, t) + \frac{\partial D_n}{\partial \theta_{k0}} \left( -\frac{i}{nq'} \frac{\partial}{\partial r} - \theta_{k0} \right) A_{n0}(r, t) + \frac{1}{2} \frac{\partial^2 D_n}{\partial \theta_{k0}^2} \left[ \left( -\frac{i}{nq'} \frac{\partial}{\partial r} - \theta_{k0} \right)^2 - \frac{i}{nq'} \frac{\partial \theta_{k0}}{\partial r} \right] A_{n0}(r, t) \\ & = S_n^{ext}(r, t) + (C_{n,0} + C_{0,n}) \circ A_{n0}(r, t) A_{z0}(r, t) + \sum_{\substack{n', n'' \neq n \\ n' + n'' = n}} C_{n', n''} \circ A_{n'0}(r, t) A_{n''0}(r, t) , \end{aligned} \quad (5.3)$$

which can be used for analyzing all various nonlinear dynamics introduced above and discussed later in this section. In fact, Eq. (5.3) describes both short wavelength modes, for which Eq. (4.36) was derived, as well as global long wavelength modes with one isolated singular layer. The argument yielding Eq. (5.3) from Eqs. (4.34) and (4.36) can be straightforwardly repeated for the GFLDR in the form of Eq. (4.20). As a result, one obtains Eq. (5.3) again, provided that  $\theta_{k0} = \partial/\partial r = 0$  is assumed; *i.e.*, considering  $A_{n0}$  as the slowly varying amplitude of the  $n$  mode at the singular layer (cf. Sec. V.D.7). The same also applies for the vanishing magnetic shear case, described by Eq. (4.24). Thus, we may consider Eq. (5.3) as the general form of governing equations for addressing nonlinear physics of Alfvén waves and EPs in burning plasmas. Expressions of the nonlinear-coupling operators,  $C_{n', n''}$ , depend on the specific nonlinear interactions under consideration, and some examples will be discussed in the remainder of this section.

Equation (5.3) allows us to readily recognize the various spatiotemporal scales for the nonlinear dynamic evolution of DAWs. In addition to the inverse linear growth rate,  $\gamma_L^{-1}$ , and the formation time of the global eigenmode structure  $\tau_A$  (Zonca *et al.*, 2004a) (cf. Sec. IV.B), in fact, one can identify nonlinear processes and corresponding time scale separating ideal region response from singular layer dynamics, as suggested by Eq. (5.1). Recalling from Sec. II.C that the characteristic nonlinear time scale of DAWs considered in this work is  $\tau_{NL} \sim \gamma_L^{-1}$ , different behaviors are expected for  $\tau_A < \tau_{NL} \sim \gamma_L^{-1}$ , typical of AE, and for  $\tau_A \sim \tau_{NL} \sim \gamma_L^{-1}$ , which generally applies for EPM.

Equation (5.3) is also a useful starting point for constructing reduced nonlinear dynamic models with various levels of approximation to be used in connection with numerical simulations for understanding selected aspects of the processes under investigation. Following the concluding remarks of Sec. IV.B.1, different terms entering Eq. (5.3) can be evaluated either analytically or with simplified numerical descriptions; helping, thus, building models with reliable predictive capabilities. Three wave couplings modify the nonlinear dynamics via the processes discussed in Secs. V.B and V.C, which are the dominant nonlinear dynamics of the DAW spectrum caused by the core plasma component (cf. Sec. II.E) and affecting directly fluctuation induced transports of the thermal plasma. Meanwhile, when dealing with a spectrum of low-amplitude fluctuations,  $|\delta\mathbf{B}_\perp/B_0| \sim 10^{-4}$ , characterized by  $|\gamma_L/\omega_0| \sim |\omega_0\tau_{NL}|^{-1} \ll 1$  as in the case

of DAWs excited by EPs in fusion plasmas (cf. Sec. II.E), transport processes are dominated by wave-particle resonant interactions (White *et al.*, 1983, 2010a,b). Furthermore, the shortest (most relevant) nonlinear time scale processes are those describing the evolution of phase-space ZS [cf. Eq. (5.174) and Sec. V.D.5]. In this case, the field equations for Alfvénic fluctuations are Eq. (5.3) without the last term on the right hand side; and Eqs. (2.26) and (2.30) for the  $\delta\phi_z$  and  $\delta A_{\parallel z}$ , respectively. Nonlinear wave-wave couplings and wave-particle interactions in the dynamic evolution of DAW fluctuations excited by EPs are historically considered separately, for the sake of simplicity and clarity of the analysis. However, noting that the existence of the SAW continuous spectrum could lead to the excitation of short-wavelength modes via resonant mode conversion of longer scale-length mode excited by the EP component, EPs could, then, act as mediators of cross-scale couplings (Zonca, 2008; Zonca and Chen, 2008a)<sup>20</sup> and play a unique role in determining complex behaviors in burning plasmas (cf. also Secs. V.E and VII.B). Thus, a comprehensive understanding on the nonlinear physics of DAW instabilities excited by EPs would require a self-consistent treatment of both nonlinear wave-wave and wave-particle interactions and is beyond the scope of this review. In the following subsections, we will mainly focus on nonlinear dynamics of single- $n$  modes<sup>21</sup>, and separate the analysis of wave-wave and wave-particle nonlinear interactions in order to delineate more clearly the underlying physics mechanisms.

## B. Nonlinear shear Alfvén waves in uniform plasmas

In order to provide insights to nonlinear wave-wave interactions among SAWs in tokamak plasmas, let us first explore such interactions in the simple limit of an infinite, uniform plasma with  $\mathbf{B}_0 = B_0 \hat{z}$ . Within the generally valid approximation of quasi-neutrality condition and  $m_i \gg m_e$ , we have the following one-fluid equation of motion

$$\varrho_m(\partial_t + \mathbf{u} \cdot \nabla) \mathbf{u} = -\nabla \cdot \mathbf{P} + \mathbf{j} \times \mathbf{B}/c, \quad (5.4)$$

where  $\varrho_m = \sum_j n_j m_j \simeq n_i m_i$  and  $\mathbf{u} \simeq \mathbf{u}_i$ . Equation (5.4) is readily obtained from Eq. (2.14) decomposing the stress tensor as pressure and Reynolds stress, as usual; *i.e.*, defining  $\mathcal{P} \equiv \mathbf{P} + \varrho_m \mathbf{u} \mathbf{u}$ . Letting  $\mathbf{u} = \mathbf{u}_0 + \delta \mathbf{u}$ , etc., and noting  $\mathbf{u}_0 = \mathbf{j}_0 = 0$ , Eq. (5.4) becomes,

$$(\varrho_{m0} + \delta \varrho_{m0})(\partial_t + \delta \mathbf{u} \cdot \nabla) \delta \mathbf{u} = -\nabla \cdot \delta \mathbf{P} + \delta \mathbf{j} \times \mathbf{B}/c. \quad (5.5)$$

We further assume that shear and compressional Alfvén wave frequencies are well separated ( $|\nabla_{\perp}| \gg |\nabla_{\parallel}|$ ) and  $\beta \ll 1$ . Thus, Eqs. (2.7) and (2.8) apply and only dynamics of SAW and slow sound waves are kept. If we now further make the crucial assumption that all the interacting waves are SAWs, which are nearly incompressible, we then have  $\nabla \cdot \delta \mathbf{u} \simeq 0$  and  $\delta \varrho_m \simeq 0$ ,  $\delta \mathbf{P} \simeq 0$ . Then, Eq. (5.5) becomes, approximately,

$$\varrho_{m0} \partial_t \delta \mathbf{u} = \mathbf{F}_p^{(2)} + \delta \mathbf{j} \times \mathbf{B}_0/c, \quad (5.6)$$

where the nonlinear ponderomotive force  $\mathbf{F}_p^{(2)}$  is defined as

$$\mathbf{F}_p^{(2)} = \delta \mathbf{j} \times \delta \mathbf{B}/c - \varrho_{m0} \delta \mathbf{u} \cdot \nabla \delta \mathbf{u} = -\nabla(\delta B)^2/(8\pi) - \mathbf{M} \mathbf{x} - \mathbf{R} \mathbf{e};$$

and

$$\begin{aligned} \mathbf{M} \mathbf{x} &= -(\delta \mathbf{B} \cdot \nabla) \delta \mathbf{B}/(4\pi) \simeq -(\delta \mathbf{B}_{\perp} \cdot \nabla) \delta \mathbf{B}_{\perp}/(4\pi), \\ \mathbf{R} \mathbf{e} &= \varrho_{m0} (\delta \mathbf{u} \cdot \nabla) \delta \mathbf{u} \simeq \varrho_{m0} (\delta \mathbf{u} \cdot \nabla) \delta \mathbf{u}_{\perp}, \end{aligned} \quad (5.7)$$

are, respectively, the divergence of Maxwell and Reynolds stresses. The approximations are justified since  $\beta \ll 1$  and  $|\nabla_{\perp}| \gg |\nabla_{\parallel}|$ ; both  $\delta B_{\parallel}$  and  $\delta u_{\parallel}$  are, hence, suppressed here. Equation (5.6) may be regarded as the basic equation for SAW interactions subject to the above constrains.

Equation (5.6) gives  $\delta \mathbf{j}_{\perp}$  as

$$\delta \mathbf{j}_{\perp} = \delta \mathbf{j}_{\perp}^{(1)} + \delta \mathbf{j}_{\perp}^{(2)}, \quad (5.8)$$

<sup>20</sup> This aspect has been recently explored in great detail by (Qiu *et al.*, 2012) in connection with the analysis of radial structures of EP driven geodesic acoustic modes (Berk *et al.*, 2006; Fu, 2008).

<sup>21</sup> Note that, in toroidal geometry, this corresponds anyhow to many coupled poloidal Fourier harmonics in Eq. (4.26) and, due to nonlinear interactions, to the coupling of different radial states (not necessarily eigenstates) of the same toroidal mode  $n$ .

where  $\delta \mathbf{j}_\perp^{(1)} = (c/B_0) \mathbf{b} \times \rho_{m0} \partial_t \delta \mathbf{u}_\perp$  is the well-known linear polarization current,  $\mathbf{b} \equiv \mathbf{B}_0/B_0$ , and  $\delta \mathbf{j}_\perp^{(2)}$  is the nonlinear current

$$\delta \mathbf{j}_\perp^{(2)} = -(c/B_0) \mathbf{b} \times \mathbf{F}_p^{(2)}. \quad (5.9)$$

For SAW dynamics, the quasi-neutrality condition  $\nabla \cdot \delta \mathbf{j} = 0$ , Eq. (2.12), along with the parallel Ampere's law, Eq. (2.13),  $\nabla^2 \delta A_\parallel \simeq \nabla_\perp^2 \delta A_\parallel = -(4\pi/c) \delta j_\parallel$ , yields the following vorticity equation

$$(\mathbf{b} \cdot \nabla) (-c/4\pi) \nabla_\perp^2 \delta A_\parallel + \nabla_\perp \cdot \delta \mathbf{j}_\perp = 0, \quad (5.10)$$

where we have adopted the potential representation of the fields; i.e.,  $\delta \mathbf{B} = \nabla \times \delta \mathbf{A}$ ,  $\delta \mathbf{E} = -(\nabla \delta \phi + \partial_t \delta \mathbf{A}/c)$  and  $\delta \mathbf{A} \simeq \delta A_\parallel \mathbf{b}$ . Thus, we have  $\delta \mathbf{E}_\perp \simeq -\nabla_\perp \delta \phi$  and  $\delta E_\parallel = -\mathbf{b} \cdot \nabla \delta \phi - \partial_t \delta A_\parallel/c$ . Equation (5.10) is the  $k_\perp \rho_i \ll 1$ ,  $\beta \ll 1$  limit of Eq. (2.26) and, adopting the flux function  $\delta \psi$  defined in Eq. (2.31), it can be written as

$$(c^2/4\pi) (\mathbf{b} \cdot \nabla)^2 \nabla_\perp^2 \delta \psi + \partial_t (\nabla_\perp \cdot \delta \mathbf{j}_\perp) = 0. \quad (5.11)$$

We now make the final MHD approximations,

$$\delta \mathbf{u}_\perp \simeq (c/B_0) \delta \mathbf{E}_\perp \times \mathbf{b} = (c/B_0) \mathbf{b} \times \nabla_\perp \delta \phi, \quad (5.12)$$

and

$$\delta E_\parallel = -\mathbf{b} \cdot \nabla (\delta \phi - \delta \psi) \simeq 0. \quad (5.13)$$

Equation (5.11) then becomes

$$c^2 [(\mathbf{b} \cdot \nabla)^2 - v_A^{-2} \partial_t^2] \nabla_\perp^2 \delta \phi + 4\pi \partial_t [\nabla \cdot \delta \mathbf{j}_\perp^{(2)}] = 0, \quad (5.14)$$

and

$$\nabla \cdot \delta \mathbf{j}_\perp^{(2)} = -(c/B_0) \mathbf{b} \cdot \nabla \times (\mathbf{R}e + \mathbf{M}x). \quad (5.15)$$

Equation (5.15) has the interesting properties that  $\nabla_\perp \cdot \delta \mathbf{j}_\perp^{(2)} = 0$  if  $\mathbf{R}e + \mathbf{M}x = 0$  or

$$\delta \mathbf{u}_{\perp w}/v_A = \pm \delta \mathbf{B}_{\perp w}/B_0. \quad (5.16)$$

Equation (5.16) is the Walén relation (Walén, 1944). In terms of  $\delta \phi$  and  $\delta A_\parallel$ , we have

$$\delta \phi_w/v_A = \pm \delta A_{\parallel w}/c,$$

or

$$\partial_t (\delta \phi_w/v_A) = \mp (\mathbf{b} \cdot \nabla) \delta \psi_w = \mp (\mathbf{b} \cdot \nabla) \delta \phi_w. \quad (5.17)$$

Equation (5.17) thus demonstrates that given the Walén relation, Eq. (5.16),

$$[(\mathbf{b} \cdot \nabla)^2 - v_A^{-2} \partial_t^2] \delta \phi_w = 0, \quad (5.18)$$

and Eq. (5.14) is self-consistently satisfied regardless of the magnitude of  $\delta \phi_w$  and  $\delta A_w$  or  $\delta \mathbf{u}_{\perp w}$  and  $\delta \mathbf{B}_{\perp w}$ . This is the celebrated Alfvénic state (Alfvén, 1942, 1950; Elsasser, 1956; Hasegawa and Sato, 1989; Walén, 1944). That is, a purely co-propagating  $[\partial_t + (\mathbf{b} \cdot \nabla)] \delta \phi_{w+} = 0$  or counter-propagating  $[\partial_t - (\mathbf{b} \cdot \nabla)] \delta \phi_{w-} = 0$  finite-amplitude SAW is a self-consistent solution to the nonlinear SAW equation, Eq. (5.14). Nonlinear interactions thus can only occur among oppositely propagating SAWs. There exist a vast amount literatures [see, *e.g.*, (Biskamp, 1993)] investigating the consequence of such interactions within the incompressibility and ideal MHD assumptions, and we will not go into details here. Instead, the present paper will be focusing on effects relevant to fusion plasmas, which breaks the constraints leading to the existence of Alfvénic states. More specifically, motivated by wave modes such as AE as well as SAW continuum and, consequently, the KAW in realistic fusion plasma (cf. Sec. V), we shall, in the following sections, investigate nonlinear SAW dynamics including effects of finite compressibility, ion Larmor radii and geometries, which could break up the Alfvénic state.

### 1. Effects of finite ion compressibility

By relaxing the incompressibility constraints, it was first shown by (Sagdeev and Galeev, 1969) that SAW can parametrically decay into a sound wave and a back-scattered SAW. Specifically, let us consider the 3-wave interactions among the pump SAW  $\Omega_0 = (\omega_0, \mathbf{k}_0)$ , the daughter sound wave,  $\Omega_- = (\omega_s, \mathbf{k}_s)$ , and the lower-side-band SAW,  $\Omega_+ = (\omega_+, \mathbf{k}_+)$ , where  $\omega_+ = \omega_s + \omega_0$  and  $\mathbf{k}_+ = \mathbf{k}_s + \mathbf{k}_0$ . Note that, in the  $\Omega_s$  mode, the dynamics is predominantly along  $\mathbf{B}_0$ . One can then show that the dominant nonlinear effect of SAW on the  $\Omega_s$  mode enters via the parallel ponderomotive force; *i.e.*,

$$\mathbf{b} \cdot (\delta \mathbf{j}_\perp \times \delta \mathbf{B}_\perp)_s / c = -\nabla_\parallel (\delta B_\perp^2)_s / (8\pi) = -n_0 e \nabla_\parallel \delta \phi_{ps} , \quad (5.19)$$

$\delta \mathbf{B}_\perp = \sum_{\mathbf{k}} \delta \mathbf{B}_{\mathbf{k}\perp} \exp(-i\omega_{\mathbf{k}}t + i\mathbf{k} \cdot \mathbf{x})$ ,  $(\delta B_\perp^2)_s = \delta \mathbf{B}_{0\perp} \cdot \delta \mathbf{B}_{-\perp}$ , and  $\delta \phi_{ps}$  is the corresponding ponderomotive potential. That is,

$$\varrho_{m0}(-i\omega_s)\delta u_{\parallel s} = -ik_{s\parallel} (\delta P_s + \delta \mathbf{B}_{0\perp} \cdot \delta \mathbf{B}_{-\perp} / 8\pi) . \quad (5.20)$$

Applying the equation of state, we have  $\delta P_s = (\gamma_e T_e + \gamma_i T_i)\delta n_s \equiv T\delta n_s$ . Continuity equation,  $n_0 k_{s\parallel} \delta u_{\parallel s} = \omega_s \delta n_s$ , then yields

$$\omega_s^2 \epsilon_s \delta \varrho_{ms} = k_{s\parallel}^2 \delta \mathbf{B}_{0\perp} \cdot \delta \mathbf{B}_{-\perp} / (8\pi), \quad (5.21)$$

and

$$\epsilon_s = 1 - k_{s\parallel}^2 c_s^2 / \omega_s^2, \quad (5.22)$$

with  $c_s^2 \equiv T/m_i$ .

As to the  $\Omega_-$  SAW sideband, the dominant coupling effect to  $\Omega_s$  is via  $\delta \varrho_{ms}$  in the polarization current term in Eq. (5.5); *i.e.*,

$$\delta \mathbf{j}_{\perp -}^{(2)} = (c/B_0) \mathbf{b} \times [\delta \varrho_{ms} \partial_t \delta \mathbf{u}_\perp]_- = (c/B_0) \delta \varrho_{ms} (i\omega_0) \mathbf{b} \times \delta \mathbf{u}_{\perp 0}^* . \quad (5.23)$$

The vorticity equation, Eq. (5.14), for the  $\Omega_-$  mode, then becomes

$$\epsilon_{A-} k_{-\perp}^2 \delta \phi_- = (\delta \varrho_{ms} / \varrho_{m0}) (\mathbf{k}_{0\perp} \cdot \mathbf{k}_{-\perp}) \delta \phi_0^*; \quad (5.24)$$

where

$$\epsilon_{A-} = 1 - k_{-\parallel}^2 v_A^2 / \omega_-^2 ; \quad (5.25)$$

and we have adopted the field variables  $\delta \phi$ ,  $\delta A_\parallel$  or  $\delta \psi$  and noted  $\delta \phi_{0,-} \simeq \delta \psi_{0,-}$ . Equation (5.21), in terms of the potential variables, along with Eq. (5.24) then yields the following parametric dispersion relation

$$\epsilon_s \epsilon_{A-} = \frac{1}{2} k_{0\perp}^2 \rho_s^2 \cos^2 \theta_c \left( \frac{k_{-\parallel}}{k_{0\parallel}} \right) |\Phi_0|^2, \quad (5.26)$$

where  $\Phi_0 = e\delta \phi_0 / T$ ,  $\rho_s = c_s / \Omega_i$  and  $\theta_c$  is the angle between  $\mathbf{k}_{0\perp}$  and  $\mathbf{k}_{-\perp}$ . For resonant decays, we have  $\omega_s = i\gamma + \omega_{sr}$ ,  $\omega_{sr} = k_{s\parallel} c_s$ ,  $\omega_- = i\gamma + (\omega_{sr} - \omega_0)$  and  $(\omega_0 - \omega_{sr}) = |k_{-\parallel}| v_A$ , Eq. (5.26) then reduces to

$$\frac{\gamma^2}{\omega_0 \omega_{sr}} = \frac{1}{8} k_{\perp}^2 \rho_s^2 \cos^2 \theta_c \left( \frac{k_{-\parallel}}{k_{0\parallel}} \right) |\Phi_0|^2. \quad (5.27)$$

Equation (5.27) shows that instability sets in when  $k_{0\parallel} / k_{-\parallel} > 0$ . Since  $|\omega_0| \gg |\omega_s|$ , we have  $|\omega_-| \simeq \omega_0$  or  $k_{-\parallel} = k_{s\parallel} - k_{0\parallel} \simeq k_{0\parallel}$  or  $k_{s\parallel} \simeq 2k_{0\parallel}$ , and meanwhile,  $\omega_- / k_{-\parallel} \simeq -v_A$ ; *i.e.*, the parallel phase velocity of the lower-sideband SAW is opposite to that of the pump wave. Equation (5.27) also shows that the parametric instability maximizes around  $\theta_c = 0$ ; *i.e.*,  $\mathbf{k}_{-\perp}$  aligns with  $\mathbf{k}_{0\perp}$ . As will be discussed later in Sec. V.B.2, this carries a significant implication to the transport process induced by the SAW turbulence.

For fusion plasmas, we have, typically,  $T_e \lesssim T_i$  and the ion sound wave becomes a quasi mode due to significant ion Landau damping. In this case, we need to treat ions kinetically and the corresponding parametric decay process becomes a non-resonant decay via nonlinear ion Landau damping (Cohen and Dewar, 1974; Kulsrud, 1978; Sagdeev

and Galeev, 1969). From the previous one-fluid analysis on the resonant decay, one sees readily that nonlinearities enter via ion dynamics only. Thus, for the  $\Omega_s$  ion sound wave, we have  $\delta n_{se}/n_0 = e\delta\phi_s/T_e$ ; with  $\delta\phi_s$  being the self-consistent electrostatic potential, and

$$\delta n_{si}/n_0 = -e\chi_{is}(\delta\phi_s + \delta\phi_{ps}) . \quad (5.28)$$

Here,  $\delta\phi_{ps}$  is given by Eq. (5.19) and

$$\chi_{is} = (1/T_i)\langle F_{0i}k_{s\parallel}v_{\parallel}/(k_{s\parallel}v_{\parallel} - \omega_s)\rangle_v = (1/T_i)[1 + \xi_s Z(\xi_s)] , \quad (5.29)$$

$\langle \dots \rangle_v$  denotes  $\int d\mathbf{v}(\dots)$ ,  $F_{0i}$  is taken to be Maxwellian,  $Z(\xi_s)$  is the plasma dispersion function [cf., *e.g.*, (Stix, 1992)],  $\xi_s = \omega_s/(|k_{s\parallel}|v_{ti})$  and  $v_{ti} = (2T_i/m_i)^{1/2}$ . Quasi-neutrality condition then gives

$$\epsilon_{sk}\delta\phi_s = -T_e\chi_{is}\delta\phi_{ps}; \quad (5.30)$$

where

$$\epsilon_{sk} = 1 + T_e\chi_{is}. \quad (5.31)$$

Equations (5.19) and (5.30) then yield

$$\epsilon_{sk}\frac{\delta\rho_{ms}}{\rho_{m0}} = -\frac{\chi_{is}}{8\pi n_0}\delta\mathbf{B}_{0\perp} \cdot \delta\mathbf{B}_{-\perp}. \quad (5.32)$$

Note that, for  $|\omega_s| \gg |k_{s\parallel}|v_{ti}$ , Eq. (5.32) recovers the the fluid result of Eq. (5.21) with  $c_s^2 = T_e/m_i$ .

Substituting Eq. (5.32) into Eq. (5.24), with  $\Phi_0 \equiv e\delta\phi_0/T_e$ , and proceeding as in the previous one-fluid analysis, one readily derives the following parametric decay dispersion relation

$$\epsilon_{sk}\epsilon_{A-} = -\frac{1}{2}T_e\chi_{is}k_{\perp}^2\rho_s^2 \cos^2\theta_c \left(\frac{k_{-\parallel}}{k_{0\parallel}}\right) |\Phi_0|^2. \quad (5.33)$$

While  $\Omega_s$  is a quasi mode since  $|\text{Im}\epsilon_{sk}| \sim O(1)$ ,  $\Omega_-$  remains a normal mode. Thus, let  $\omega_- = \omega_{-r} + i\gamma$  and  $\omega_{-r} = \omega_{sr} - \omega_0 = |k_{-\parallel}|v_A$ ; the imaginary part of Eq. (5.33) then yields, noting  $T_e\chi_{is} = \epsilon_{sk} - 1$ ,

$$\frac{2\gamma}{\omega_0} = \frac{1}{2}k_{0\perp}^2\rho_s^2 \cos^2\theta_c \left(\frac{k_{-\parallel}}{k_{0\parallel}}\right) \cdot \frac{T_e\text{Im}\chi_{is}}{|\epsilon_{sk}|^2} |\Phi_0|^2 ; \quad (5.34)$$

where, from Eq. (5.29),

$$\text{Im}\chi_{is} = (1/T_i)\text{Im}[\xi_s Z(\xi_s)] \simeq (\pi/T_i)\omega_{sr}\langle F_{0i}\delta(k_{s\parallel}v_{\parallel} - \omega_{sr})\rangle_v. \quad (5.35)$$

Thus, the non-resonant decay maximizes around  $|\omega_{sr}| = |\omega_0 + \omega_{-r}| \approx |k_{s\parallel}|v_{ti} = |k_{0\parallel} + k_{-\parallel}|v_{ti}$ . Since  $|\omega_0| \simeq |\omega_{-r}| \gg |k_{\parallel}v_{ti}|_{0,-}$ , maximal interaction requires  $k_{0\parallel}k_{-\parallel} > 0$ ; *i.e.*,  $k_{-\parallel} \simeq k_{0\parallel}$ ,  $k_{s\parallel} \simeq 2k_{0\parallel}$ , and  $\omega_-/k_{-\parallel} \simeq -v_A$ , similar to resonant decay. Furthermore, from Eq. (5.34) and (5.35), the decay instability ( $\gamma > 0$ ) occurs when  $\omega_{sr} > 0$ ; *i.e.*,  $|\omega_{-r}| = |\omega_{sr} - \omega_0| < \omega_0$ ; that is, the parametrically excited lower sideband SAW has a real frequency lower than  $\omega_0$ ,  $|\omega_{-r}| \simeq \omega_0 - 2k_{0\parallel}v_{ti}$ , and a parallel phase velocity opposite to that of the pump wave.

We note that the current analysis has made assumptions on the relative importance of the various nonlinearities (Chen and Zonca, 2011, 2013), which are valid for

$$|k_{\perp}\rho_s|_{0,-}^2 < |\omega_0/\Omega_i| \ll 1. \quad (5.36)$$

Equation (5.36) is the same condition derived in Sec. II.C, when discussing in a very general framework the criterion for the transition between nonlinear (MHD) dynamics dominated by the polarization response to a regime where dominant nonlinear (gyrokinetic) interactions are due to the pressure stress tensor and Maxwell stress. Thus, for SAWs with  $|k_{\perp}\rho_s| > |\omega_0/\Omega_i|^{1/2} \sim \mathcal{O}(10^{-1})$  typically, we need to employ the nonlinear gyrokinetic equation, Eq. (2.23), and, as will be shown in the next section, the parametric decay precesses are significantly altered both quantitatively and qualitatively.

## 2. Parametric decays of Kinetic Alfvén Waves

We now consider three-wave interactions among  $\Omega_0$ ,  $\Omega_s$  and  $\Omega_-$ ; with  $|k_\perp \rho_i|$  formally of  $\mathcal{O}(1)$ . Here, we only sketch the derivations and refer to (Chen and Zonca, 2011) for details. Again  $\beta \ll 1$  and we adopt  $\delta\phi$  and  $\delta A_\parallel$  as the field variables. Meanwhile, following (Frieman and Chen, 1982), we can adopt the nonlinear gyrokinetic theoretical framework of Sec. II.D. Thus, assuming that both electrons and ions have  $\bar{F}_0 = F_M \equiv n_0 F_0$ , with  $F_0$  taken to be Maxwellian, Eq. (2.21) for the perturbed particle distribution function,  $\delta f$ , yields

$$\delta f = -(e/T) F_M \delta\phi + \exp(-\boldsymbol{\rho} \cdot \nabla) \delta g \quad , \quad (5.37)$$

while Eq. (2.23) for  $\delta g$  becomes

$$(\partial_t + v_\parallel \mathbf{b} \cdot \nabla + \langle \delta \mathbf{u}_{Eg} \rangle \cdot \nabla) \delta g = (e/T) F_M \partial_t \langle \delta L_g \rangle \quad . \quad (5.38)$$

Here, all notations are those of Sec. II (in particular of Sec. II.D) and, recalling that  $\langle A \rangle$  denotes gyroaveraging of  $A$ , we introduced the notation  $\langle \delta \mathbf{u}_{Eg} \rangle = (c/B_0) \mathbf{b} \times \nabla \langle \delta L_g \rangle$ . In terms of Fourier modes, Eq. (5.38) can be expressed as

$$i(k_\parallel v_\parallel - \omega_k) \delta g_k - (c/B_0) \Lambda_{k'}^{k''} [\langle \delta L_g \rangle_{k'} \delta g_{k''} - \langle \delta L_g \rangle_{k''} \delta g_{k'}] = -i\omega_k (e/T) F_M \langle \delta L_g \rangle_k \quad , \quad (5.39)$$

where  $\Lambda_{k'}^{k''} \equiv \mathbf{b} \cdot (\mathbf{k}'_\perp \times \mathbf{k}''_\perp)$ . Meanwhile, the quasineutrality condition, Eq. (2.28), becomes

$$(1 + T_i/T_e) \delta\phi_k = T_i/(n_0 e) \langle J_k \delta g_{ki} - \delta g_{ke} \rangle_{\mathbf{v}} \quad , \quad (5.40)$$

where  $e$  stands for the (positive) electron charge, and the vorticity equation, Eq. (2.26), can be written as

$$\begin{aligned} ik_\parallel \delta j_{\parallel k} - i \frac{c^2}{4\pi} \frac{\omega_k k_\perp^2}{v_A^2 b_k} (1 - \Gamma_k) \delta\phi_k &= -\Lambda_{k'}^{k''} \left( \delta A_{\parallel k'} \frac{\delta j_{\parallel k''}}{B_0} - \delta A_{\parallel k''} \frac{\delta j_{\parallel k'}}{B_0} \right) \\ &+ \frac{ec}{B_0} \Lambda_{k'}^{k''} \langle [(J_k J_{k'} - J_{k''}) \delta L_{k'} \delta g_{k''i} - (J_k J_{k''} - J_{k'}) \delta L_{k''} \delta g_{k'i}] \rangle_{\mathbf{v}} \quad , \end{aligned} \quad (5.41)$$

with  $\delta j_{\parallel k} = (c/4\pi) k_\perp^2 \delta A_{\parallel k}$ . Here,  $\langle \delta L_g \rangle_k = J_k (\delta\phi - v_\parallel \delta A_\parallel / c)_k \equiv J_k \delta L_k$ ,  $J_k = J_0(k_\perp \rho)$  and  $\mathbf{k} = \mathbf{k}' + \mathbf{k}''$ . Furthermore,  $b_k = k_\perp^2 \rho_i^2 = k_\perp^2 (T_i/m_i)/\Omega_i^2$ ,  $\Gamma_k = \langle J_k^2 F_{0i} \rangle_{\mathbf{v}} = I_0(b_k) \exp(-b_k)$ ,  $I_0$  is the modified Bessel function and  $|k_\perp \rho_e| \ll 1$  was assumed. On the right hand side of Eq. (5.41), the first term represents the usual Maxwell stress, whereas the second term reduces to the well-known Reynolds stress for  $k_\perp \rho_i \ll 1$ . Noting the ordering  $|k_\parallel v_{te}| \gg |\omega_k| \gg |k_\parallel v_{ti}|$ , introduced in Sec. III.B, with  $v_{te}$  and  $v_{ti}$  denoting the electron and ion thermal velocities, and defining  $\delta\psi_k = (\omega \delta A_\parallel / ck_\parallel)_k$ , consistent with Eq. (2.31), we can readily recover the following linear KAW results (Hasegawa and Chen, 1975, 1976):

$$\delta\psi_k \simeq [1 + \tau(1 - \Gamma_k)] \delta\phi_k \equiv \sigma_k \delta\phi_k \quad , \quad (5.42)$$

where  $\tau = T_e/T_i$ , and the KAW linear dispersion relation (cf. Sec. III.B)

$$\omega^2 / (k_\parallel^2 v_A^2) \simeq \sigma_k b_k / (1 - \Gamma_k) \quad . \quad (5.43)$$

As to the excitation of ion sound wave,  $\Omega_s$ , by the two KAWs,  $\Omega_0$  and  $\Omega_-$ , we note that, due to the frequency ordering discussed in Sec. V.B.1,  $\Omega_s$  is predominantly an electrostatic mode. Equation (5.39) can then be used to calculate linear and nonlinear responses of  $\delta g_s$  for both electrons and ions (Chen and Zonca, 2011). Substituting these results into the quasi-neutrality condition, Eq. (5.40), we then obtain

$$\epsilon_{sK} \delta\phi_s = -i(c/B_0 \omega_-) \Lambda_0^s \beta_1 \delta\phi_- \delta\phi_0 \quad , \quad (5.44)$$

where

$$\epsilon_{sK} = 1 + \tau + \tau \Gamma_s \xi_s Z(\xi_s) \quad , \quad (5.45)$$

$$\beta_1 = \tau F_1 (1 + \xi_s Z(\xi_s)) + \sigma_- \sigma_0 \quad , \quad (5.46)$$

$\epsilon_{sK}$  is the short wavelength extension of  $\epsilon_{sk}$  introduced in Eq. (5.31),  $F_1 = \langle J_s J_0 J_- F_{0i} \rangle_{\mathbf{v}}$  and we have applied the corresponding linear KAW wave properties, noting that  $\Omega_0$  and  $\Omega_-$  are normal modes.

Since the ion sound mode,  $\Omega_s$ , could be a heavily damped quasi mode (cf. Sec. V.B.1), we need to include both linear as well as nonlinear responses of  $\delta g_s$  in its coupling to  $\Omega_-$  via  $\Omega_0$ . The corresponding quasi-neutrality condition, Eq. (5.40), then becomes

$$\delta\psi_- = [\sigma_- + \sigma_-^{(2)}] \delta\phi_- + D_1 \delta\phi_s \delta\phi_0^* \quad , \quad (5.47)$$

where  $\sigma_-$  is defined in Eq. (5.42),

$$\sigma_-^{(2)} = \left( \frac{c}{B_0 \omega_-} \Lambda_0^s \right)^2 \left[ \tau (1 + \xi_s Z(\xi_s)) \langle J_0^2 J_-^2 \rangle_i - \frac{k_{\parallel 0}}{k_{\parallel -}} \sigma_0^2 \sigma_- \right] |\delta \phi_0|^2 \quad (5.48)$$

and

$$D_1 = -i(c/B_0 \omega_-) \Lambda_0^s \tau (1 + \xi_s Z(\xi_s)) F_1 \quad (5.49)$$

Proceeding in the same way, we may compute the vorticity equation, Eq. (5.41), for the KAW sideband. In this case, it is worthwhile noting that the Maxwell stress does not contribute to the nonlinear dynamics, for  $\Omega_s$  is a predominantly electrostatic mode. Thus, the parametric decay is mediated by the generalized Reynolds' stress in Eq. (5.41). Applying the results of  $\delta g_s$  derived earlier, we can readily obtain

$$\begin{aligned} k_{\perp -}^2 \left[ \left( 1 - \Gamma_- + \alpha_-^{(2)} \right) b_-^{-1} \delta \phi_- \right. \\ \left. - \left( k_{\parallel}^2 v_A^2 / \omega^2 \right)_- \delta \psi_- \right] = (D_2 / \rho_s^2) \delta \phi_s \delta \phi_0^* , \end{aligned} \quad (5.50)$$

where  $\rho_s^2 = \tau \rho_i^2$  and  $\alpha_-^{(2)}$  and  $D_2$  are due to the nonlinear ion response

$$\alpha_-^{(2)} = (c/B_0 \omega_-)^2 \Lambda_0^{s2} (1 + \xi_s Z(\xi_s)) \left[ \langle J_0^2 J_-^2 F_{0i} \rangle_v - F_1 \right] |\delta \phi_0|^2 \quad , \quad (5.51)$$

$$D_2 = i(c/B_0 \omega_-) \Lambda_0^s \tau \left[ (1 + \xi_s Z(\xi_s)) F_1 - \xi_s Z(\xi_s) \Gamma_s - \Gamma_0 \right] \quad (5.52)$$

Combining Eqs. (5.47) and (5.50), we then obtain the following equation for the  $\Omega_-$  KAW modified by the nonlinear coupling between  $\Omega_s$  and  $\Omega_0$  modes;

$$b_{s-} \left( \epsilon_{AK-} + \epsilon_{AK-}^{(2)} \right) \delta \phi_- = i(c/B_0 \omega_-) \Lambda_0^s \beta_2 \delta \phi_s \delta \phi_0^* \quad , \quad (5.53)$$

where  $b_{s-} = \tau b_-$ ,

$$\epsilon_{AK-} = \left[ (1 - \Gamma_-) / b_- - \left( k_{\parallel}^2 v_A^2 / \omega^2 \right)_- \sigma_- \right] \quad (5.54)$$

is the short wavelength extension of Eq. (5.25),

$$\epsilon_{AK-}^{(2)} = \left[ \alpha_-^{(2)} / b_- - \left( k_{\parallel}^2 v_A^2 / \omega^2 \right)_- \sigma_-^{(2)} \right] \quad , \quad (5.55)$$

and

$$\begin{aligned} \beta_2 &= \left( \frac{F_1}{\Gamma_s} \right) (\epsilon_{sK} - \sigma_s) \left[ 1 - \left( \frac{k_{\parallel}^2 v_A^2}{\omega^2} \right)_- b_{s-} \right] - \epsilon_{sK} + \sigma_0 \\ &= [(\epsilon_{sK} - \sigma_s) F_1 / \Gamma_s + \sigma_- (\sigma_0 - \sigma_s)] / \sigma_- \\ &= \beta_1 / \sigma_- - \epsilon_{sK} \quad . \end{aligned} \quad (5.56)$$

Combining Eqs. (5.44) and (5.53), the resultant parametric instability dispersion relation becomes

$$\epsilon_{sK} \left( \epsilon_{AK-} + \Delta_{A-}^{(2)} + \chi_{A-}^{(2)} \right) = C_k |\Phi_0|^2 \quad , \quad (5.57)$$

where  $\Phi_0 = e \delta \phi_0 / T_e$ ,  $C_k = (\lambda H)^2$ ,

$$\begin{aligned} \Delta_{A-}^{(2)} &= [(\sigma_s / \Gamma_s) (F_1^2 / \Gamma_s - G) + (\sigma_- - 2F_1 / \Gamma_s \\ &\quad - \sigma_0 k_{\parallel 0} / k_{\parallel -}) \sigma_0 \sigma_- + \sigma_0^2 \sigma_-^2 k_{\parallel 0} / k_{\parallel -}] \lambda^2 |\Phi_0|^2 \quad , \end{aligned} \quad (5.58)$$

$$\chi_{A-}^{(2)} = \epsilon_{sK} (\lambda^2 / \Gamma_s) G |\Phi_0|^2 \quad , \quad (5.59)$$

$$\lambda^2 = (\Omega_i / \omega_0)^2 \rho_s^4 \Lambda_0^{s2} / (\sigma_- b_{s-}) \quad , \quad (5.60)$$

$$G = \langle J_0^2 J_-^2 F_{0i} \rangle_v - F_1^2 / \Gamma_s \quad , \quad (5.61)$$

and

$$H = (\sigma_0\sigma_- - F_1\sigma_s/\Gamma_s) . \quad (5.62)$$

Note also that, in Eq. (5.61),  $G \geq 0$  from Schwartz inequality. On the left hand side of Eq. (5.57), the  $\propto \Delta_{A-}^{(2)}$  term describes nonlinear frequency shift only, while the contribution  $\propto \chi_{A-}^{(2)}$  accounts for processes involving resonant wave-particle interactions due to low-frequency nonlinear thermal ion response to  $\Omega_0$  and  $\Omega_-$  KAW modes. Therefore, this process involves spectral transfer of fluctuation energy towards the low-frequency region and is generally referred to as nonlinear ion Compton scattering (Sagdeev and Galeev, 1969). Meanwhile, the non-resonant scatterings of  $\Omega_0$  off the fluctuations due to the  $\Omega_s$  mode are described by the right hand side, which, thus, accounts for shielded-ion scatterings. Ignoring nonlinear frequency shift and keeping terms relevant to the stability analysis, the resultant parametric dispersion relation becomes

$$\epsilon_{sK} \left( \epsilon_{AK-} + \chi_{A-}^{(2)} \right) = C_k |\Phi_0|^2 . \quad (5.63)$$

The nonlinear ion Compton scatterings term  $\propto \chi_{A-}^{(2)}$  in Eq. (5.63), as will be discussed below, is absent in the previous drift-kinetic analysis (Hasegawa and Chen, 1975, 1976). This can be understood, since  $|G| \sim \mathcal{O}(k_{\perp}^4 \rho_i^4)$  for  $|k_{\perp} \rho_i| \ll 1$  and the drift-kinetic analysis formally keeps only  $\mathcal{O}(k_{\perp}^2 \rho_i^2)$  terms. Meanwhile, for  $|k_{\perp} \rho_i| \ll 1$ ,  $H \simeq \tau(b_0 + b_- + \tau b_0 b_- - b_s)$  and the drift-kinetic results are nicely recovered.

For  $T_e \gtrsim 5T_i$ , both  $\Omega_s$  and  $\Omega_-$  are weakly damped normal modes, and Eq. (5.63) yields the following resonant-decay dispersion relation

$$(\gamma + \gamma_{dA-})(\gamma + \gamma_{ds}) = (\lambda H |\Phi_0|)^2 \left[ -\frac{\partial \epsilon_{sKr}}{\partial \omega_{sr}} \frac{\partial \epsilon_{AK-r}}{\partial \omega_{A-r}} \right]^{-1} , \quad (5.64)$$

where  $\gamma$  is the parametric growth rate,  $\gamma_{dA-}$  and  $\gamma_{ds}$  are, respectively, the linear damping rates of the KAW sideband and ion sound waves, and  $\omega_{A-r}$  and  $\omega_{sr}$  are, meanwhile, the corresponding normal mode frequencies; *i.e.*,  $\epsilon_{AK-r}(\omega_{A-r}) = 0$  and  $\epsilon_{sKr}(\omega_{sr}) = 0$ ,  $-\partial \epsilon_{AK-r} / \partial \omega_{A-r} \simeq 2(1 - \Gamma_-) / (\omega_{0r} b_-)$  and  $\partial \epsilon_{sKr} / \partial \omega_{sr} \simeq 2\sigma_s / \omega_{sr}$ . Note that, similar to Sec. V.B.1 analysis for SAW, KAW parametric decay instability requires  $\omega_{0r} \omega_s > 0$ , *i.e.*  $-\omega_{0r} < \omega_{A-r} < 0$ , having chosen  $\omega_{0r} > 0$  without loss of generality.

For  $T_e \sim T_i$ ,  $\Omega_s$  becomes a quasi mode; while  $\Omega_- \simeq -\Omega_A \equiv -(\omega_A, \mathbf{k}_A)$  remains a KAW normal mode. The growth rate of the parametric decay instability is then given by

$$\begin{aligned} (\gamma + \gamma_{dA-}) \left( -\frac{\partial \epsilon_{AK-r}}{\partial \omega_{A-r}} \right) &= \text{Im} \left[ \chi_{A-}^{(2)} - \frac{C_k}{\epsilon_{sK}} |\Phi_0|^2 \right] \\ &= |\lambda \Phi_0|^2 [G/\Gamma_s + H^2/|\epsilon_{sK}|^2] \text{Im} \epsilon_{sK} , \end{aligned} \quad (5.65)$$

where, again,  $G \geq 0$ ,

$$\text{Im} \epsilon_{sK} = \tau \Gamma_s \text{Im} [\xi_s Z_s(\xi_s)] , \quad (5.66)$$

and  $\xi_s = (\omega_0 - \omega_{Ar}) / |k_{\parallel 0} - k_{\parallel A}| v_{ti}$ . In Eq. (5.65), the  $G$  and  $H^2$  terms correspond, respectively, to the nonlinear ion Compton and shielded-ion scatterings. Note that for  $|k_{\perp} \rho_i| \sim \mathcal{O}(1)$ ,  $G \sim H^2 \sim |\epsilon_{sK}|$ , the two scattering processes are additive and have comparable magnitudes. Same as in previous studies (Hasegawa and Chen, 1976; Sagdeev and Galeev, 1969), Eq. (5.66) indicates that the scattering is maximized when  $k_{\parallel 0} k_{\parallel A} < 0$ ; *i.e.*, backscattered KAW daughter wave (since  $\omega_{0r} \omega_{Ar} > 0$ ), and  $\gamma > 0$  requires  $\xi_s > 0$ ; *i.e.*,  $\omega_0 > \omega_{Ar}$ , or the parametric decay process leads to cascading in KAW frequencies. Note also that, while for  $|k_{\perp} \rho_i| \ll 1$   $\gamma$  increases with  $|k_{\perp}|$ , it decreases as  $|k_{\perp} \rho_i|^{-1}$  for  $|k_{\perp} \rho_i| \gg 1$ ; and, thus, the decay processes tend to maximize around  $|k_{\perp} \rho_i| \sim \mathcal{O}(1)$ .

It is illuminating to compare the present gyrokinetic with the MHD results, derived in Sec. V.B.1. In fact, if in Eq. (5.63)

$$C_k = (\Omega_i / \omega_0)^2 (\tau b_0 / \sigma_-) H^2 \sin^2 \theta_c \quad (5.67)$$

is replaced by

$$C_I = [\tau b_0 / (\gamma_e + \gamma_i T_i / T_e)] \cos^2 \theta_c , \quad (5.68)$$

one readily recovers Eq. (5.26) in the MHD limit. For  $k_{\perp} \rho_i \sim \mathcal{O}(1)$ ,  $H \sim \mathcal{O}(1)$  and  $|C_k| / |C_I| \sim \mathcal{O}(\Omega_i^2 / \omega_0^2) \gg 1$ . In fact, for  $|k_{\perp} \rho_i| < 1$ ,  $\sigma_- \simeq 1$ ,  $H \sim k_{\perp}^2 \rho_i^2 \tau$  and  $|C_k| / |C_I| \sim (\Omega_i / \omega_0)^2 (k_{\perp} \rho_i)^4$ ; that is, consistent with general discussions

of Sec. II.C on relative roles of various nonlinear interactions and with arguments leading toward Eq. (5.36), the kinetic process dominates for  $k_{\perp}^2 \rho_i^2 > |\omega_0/\Omega_i| \sim 10^{-2}$ , typically. Thus, while the ideal MHD theory holds for  $k_{\perp}^2 \rho_i^2 \ll 1$  in the linear physics description, it breaks down much earlier in nonlinear physics applications. Furthermore,  $C_k$  and  $C_I$  peak, respectively, at  $\theta_c = \pi/2$  and  $\theta_c = 0$ . Thus, while the ideal MHD results predict KAWs are excited with  $\mathbf{k}_{\perp}$  parallel to the pump  $\mathbf{k}_{0\perp}$ , the kinetic excitation process shows that  $\mathbf{k}_{\perp}$  is predominantly perpendicular to  $\mathbf{k}_{0\perp}$ . This difference has significant qualitative implications to plasma transport induced by KAWs. More specifically, let the pump KAW be excited via resonant mode conversion and, thus,  $\mathbf{k}_{0\perp} \simeq k_{0r} \mathbf{r}$ , with  $\mathbf{r}$  being unit vector in the radial direction. Ideal MHD theory would predict the KAW spectrum peaks along  $k_r$  with little  $k_{\theta}$  components in the  $\mathbf{b} \times \mathbf{r}$  direction and, hence, little radial transports. On the other hand, the kinetic theory would predict KAW spectrum with significant  $k_{\theta}$  components and, hence, significant radial plasma transports.

These findings, based on fundamental nonlinear dynamics properties, question the applicability of MHD based theories for realistic comparisons with experimental measurements and observations of Alfvénic fluctuation spectra and related transports even more severely than those stemming from accurate linear physics descriptions, *e.g.*, the original theoretical analyses of kinetic ballooning modes (KBM) in laboratory (Tang *et al.*, 1980) and space plasmas (Cheng and Lui, 1998).

### 3. Nonlinear excitation of convective cells by Kinetic Alfvén Waves

Zonal structures such as zonal flows are known to play crucial roles in dynamically regulating plasma transport in tokamak plasmas. The analogues in uniform plasma are the convective cells, which have been extensively studied in the 1970's (Chu *et al.*, 1978; Lin *et al.*, 1978; Okuda and Dawson, 1973; Taylor and McNamara, 1971) in the context of cross-field transport (Shukla *et al.*, 1984), especially with regard to potential applications to space plasmas. In particular, it is worthwhile mentioning the extensive studies of convective cells excitation by kinetic Alfvén waves (KAW) in the context of generation of turbulence flows in the upper ionosphere (Sagdeev *et al.*, 1978a,b).

As can be anticipated from previous discussions on the Alfvénic state, since the shear Alfvén waves (SAW) participating in the nonlinear generation of zonal structures are co-propagating along  $\mathbf{B}_0$ , nontrivial finite nonlinear couplings have long been known to rely on deviations from the ideal MHD approximations. Nonetheless, previous theoretical analyses often rely on two limiting assumptions: (i) neglecting the finite ion Larmor radius (FLR) corrections to the Reynolds stress; (ii) decoupling between the electrostatic (ESCC, described by  $\delta\phi_z$  only) and the magnetostatic (MSCC, described by  $\delta A_{\parallel z}$  only) convective cells. Both assumptions, as will be shown, could lead to erroneous conclusions on the spontaneous excitation of convective cells by KAW<sup>22</sup>. The details of the analysis are complicated and, in the following, we simply demonstrate that one needs to employ the nonlinear gyrokinetic equation in order to properly account for the the finite non-ideal effects.

Let  $\Omega_0 = (\omega_0, \mathbf{k}_0)$  be the pump KAW,  $\Omega_z = (\omega_z, \mathbf{k}_z)$  be the zonal mode, and  $\Omega_+ = (\omega_+, \mathbf{k}_+)$  and  $\Omega_- = (\omega_-, \mathbf{k}_-)$  be the, respectively, upper and lower sideband KAW. Here, we note that  $|\omega_z| \simeq 0$ ,  $\mathbf{k}_z \cdot \mathbf{b} = 0$ , and  $\omega_{\pm} = \omega_z \pm \omega_0$ ,  $\mathbf{k}_{\pm} = \mathbf{k}_z \pm \mathbf{k}_0$ . We also assume  $\mathbf{k}_z \perp \mathbf{k}_{0\perp}$ , which maximizes the nonlinear coupling. Let us first consider how the zonal mode is generated by the KAWs. The vorticity equation, Eq. (5.10), for the  $\Omega_z$  mode is given by

$$\nabla_{\perp} \cdot \delta \mathbf{j}_{z\perp} = 0,$$

or

$$-i\omega_z \frac{c^2}{B_0^2} \varrho_{m0} k_z^2 \delta\phi_z = -\langle \nabla_{\perp} \cdot \delta \mathbf{j}_{\perp}^{(2)} \rangle_z; \quad (5.69)$$

where, in terms of Fourier modes  $\delta\phi_k$  and  $\delta\psi_k \equiv (k_{\parallel} c/\omega_k) \delta A_{\parallel k}$ , Eq. (5.15) becomes (Chen and Zonca, 2013)

$$\begin{aligned} \langle \nabla \cdot \delta \mathbf{j}_{\perp}^{(2)} \rangle_z = & -\frac{1}{2} \left( \frac{c}{B_0} \right)^3 \varrho_{m0} \sum_{\mathbf{k}' + \mathbf{k}'' = \mathbf{k}_z} \Lambda_{k'}^{k''} (k_{\perp}'^2 - k_{\perp}''^2) \\ & \cdot \left[ G_{k'} G_{k''} \delta\phi_{k'} \delta\phi_{k''} - \left( \frac{k_{\parallel}' v_A}{\omega_{k'}} \right) \left( \frac{k_{\parallel}'' v_A}{\omega_{k''}} \right) \delta\psi_{k'} \delta\psi_{k''} \right]; \end{aligned} \quad (5.70)$$

<sup>22</sup> See, *e.g.*, the recent analysis and summary of previous literatures on this topic given by (Zhao *et al.*, 2011).

$\Lambda_{k'}^{k''} = (\mathbf{k}'_{\perp} \times \mathbf{k}''_{\perp}) \cdot \mathbf{b}$  was defined in Sec. V.B.2 and in the Reynolds stress, Eq. (5.7), we have let

$$\delta \mathbf{u}_{\perp k} = i \frac{c}{B_0} (\mathbf{b} \times \mathbf{k}_{\perp}) G_k \delta \phi_k, \quad (5.71)$$

with  $G_k$  accounting for the ion FLR effects (Chen and Zonca, 2013). In the small  $b_k$  limit,  $G_{k'} G_{k''} \simeq 1 - (3/4)(b_{k'} + b_{k''}) - b_z$ , having used the notations of Sec. V.B.2. Equation (5.70) provides the following illuminating perspectives in the long-wavelength ( $|k_{\perp} \rho_i|, |k_{\perp} \rho_s| \rightarrow 0^+$ ) limit. First, we have  $G_k \rightarrow 1$ , and the  $\delta E_{\parallel k} \rightarrow 0$  for KAW, such that  $\delta \phi_k = \delta \psi_k$ . Meanwhile,  $|\omega_k| \rightarrow |k_{\parallel} v_A|$ . The same limiting behaviors apply for KAW pump and sideband modes. Now with  $k''_{\parallel} = k_{z\parallel} - k'_{\parallel}$ ,  $k_{z\parallel} = 0$ ,  $\omega_{k''} = \omega_z - \omega_{k'}$  and  $|\omega_z| \ll |\omega_k|$ , we have  $\mathbf{k}''_{\parallel} = -\mathbf{k}'_{\parallel}$  and  $\omega_{k''} \simeq -\omega_{k'}$ ; and thus,  $\langle \nabla \cdot \delta \mathbf{j}_{\perp}^{(2)} \rangle_z \rightarrow 0$  in this limit. This, in fact, can be expected since, in the  $|k_{\perp} \rho_i| \rightarrow 0$  limit,  $\mathbf{k}'$  and  $\mathbf{k}''$  modes reduce to co-propagating ideal MHD SAWs; which do not interact nonlinearly.

It is, therefore, clear that in order to nonlinearly generate  $\delta \phi_z$  in uniform plasmas, one needs to introduce finite  $|k_{\perp} \rho_i|$  effects, which, in turn, induce finite  $\langle \nabla \cdot \delta \mathbf{j}_{\perp} \rangle_z$  by modifying the various terms mentioned above. Previous theoretical analyses have been focusing on effects of the finite  $\delta E_{\parallel}$  as well as deviations from the ideal MHD SAW dispersion relation; while ignoring the  $k_{\perp} \rho_i$  corrections to the  $G_k$  term. Since these finite corrections are of the same order of magnitude as those correction terms kept perviously (except in the unrealistic  $T_e \gg T_i$  limit), the corresponding results, as shown below, are often erroneous.

To properly take into account FLR corrections to the Reynolds stress, one needs to employ the nonlinear gyrokinetic equation. Noting that, for the KAWs, we have  $v_e \gg |\omega_k/k_{\parallel}| \gg v_i$  and  $|\delta \psi_k| \sim |\delta \phi_k|$ ; the gyrokinetic vorticity equation, Eq. (5.41), for the scalar potential  $\delta \phi_z$  then becomes, in the  $b_k \ll 1$  limit and after some algebra,

$$\begin{aligned} -i\omega_z b_z \delta \phi_z &= \frac{c}{2B_0} \rho_i^2 \sum_{\mathbf{k}' + \mathbf{k}'' = \mathbf{k}_z} \Lambda_{k'}^{k''} (k_{\perp}''^2 - k_{\perp}'^2) \\ &\cdot \left\{ \delta \phi_{k'} \delta \phi_{k''} \left[ 1 - \frac{3}{4}(b_{k'} + b_{k''}) - b_z \right] - \left( \frac{k'_{\parallel} v_A}{\omega_{k'}} \right) \left( \frac{k''_{\parallel} v_A}{\omega_{k''}} \right) \delta \psi_{k'} \delta \psi_{k''} \right\}, \end{aligned} \quad (5.72)$$

where the  $b_k$  terms inside the angle bracket may be regarded as the ion FLR corrections to Reynolds stress, as mentioned above. Meanwhile, the equation governing the vector potential,  $\delta A_{z\parallel}$ , can readily be derived from Eq. (2.30) and is given by

$$\delta A_{z\parallel} = (i/2) \sum_{\mathbf{k}' + \mathbf{k}'' = \mathbf{k}_z} \Lambda_{k'}^{k''} (\delta A_{k'} \delta A_{k''} / k'_{\parallel} B_0). \quad (5.73)$$

For the KAW sidebands,  $\Omega_+$  and  $\Omega_-$ , we have, from the quasi-neutrality condition, Eq. (5.40), noting  $|\omega/k_{\parallel}| \ll v_e$  and, again,  $b_k \ll 1$ ,

$$(1 + \tau b_k) \delta \phi_k - \delta \psi_k = -i(c/B_0) \Lambda_{k_z}^{k''} (\delta \phi_{k''} / \omega_k) (\delta \phi_z - \delta \psi_z), \quad (5.74)$$

where  $\mathbf{k} = \mathbf{k}_{\pm}$ ,  $\mathbf{k}'' = \pm \mathbf{k}_0$ ,  $\mathbf{k} = \mathbf{k}'' + \mathbf{k}_z$ , and  $\delta \psi_z \equiv (\omega_0 \delta A_{z\parallel} / ck_0)$ . The corresponding gyrokinetic vorticity equation, from Eq. (5.41), can be shown to become

$$k_{\perp}^2 [(1 - 3b_k/4) \delta \phi_k - (k_{\parallel}^2 v_A^2 / \omega_k^2) \delta \psi_k] = i(c/B_0) \Lambda_{k_z}^{k''} \cdot (k_{\perp}''^2 - k_{\perp}'^2) \delta \phi_{k''} (\delta \phi_z - \delta \psi_z). \quad (5.75)$$

Combing Eqs. (5.74) and (5.75) then yields

$$\epsilon_{AK} \delta \phi_k = i(c/B_0) \Lambda_{k_z}^{k''} [2b_0 / \omega_k (b_0 + b_z)] \delta \phi_{k''} (\delta \phi_z - \delta \psi_z), \quad (5.76)$$

where, consistent with Eq. (5.54),

$$\epsilon_{AK} = 1 - (3/4)b_k - (k_{\parallel}^2 v_A^2 / \omega_k^2) (1 + \tau b_k) \quad (5.77)$$

is the KAW linear dielectric constant in the  $b_k \ll 1$  limit. Meanwhile, substituting Eqs. (5.74) and (5.75) into Eq. (5.72) and neglecting higher-order nonlinearities, Eq. (5.72) reduces to

$$-i k_z^2 \omega_z \delta \phi_z = -(c/B_0) \Lambda_{k_z}^{k''} \delta \phi_{k'} \delta \phi_{k''} (k_{\perp}''^2 - k_{\perp}'^2) [(\tau + 3/4)(b_0 + b_z)]. \quad (5.78)$$

Equations (5.73), (5.76) and (5.78) are the desired set of equations for  $\Omega_+$ ,  $\Omega_-$  and  $\Omega_z$  coupled via  $\Omega_0$ .

To analyze the modulational stability properties of  $\Omega_z$ , we first note that  $\Omega_0$  is a normal KAW mode and, thus,  $\epsilon_{A0} = 0$ . Letting  $\Omega_z = i\gamma_z$ , we then have

$$\epsilon_{A\pm} \simeq \pm(2/\omega_0)(i\gamma_z \mp \Delta), \quad (5.79)$$

where  $\Delta \simeq (\omega_0/2)(\tau + 3/4)b_z$  is the frequency mismatch between  $\omega_0$  and the normal mode frequency of  $\Omega_+$  and  $\Omega_-$ . Substituting Eq. (5.76) along with Eq. (5.79) into Eq. (5.78) and noting that, on the right hand side of Eq. (5.78),  $\mathbf{k}' = \mathbf{k}_-$  and  $\mathbf{k}'' = \mathbf{k}_0$  as well as  $\mathbf{k}' = \mathbf{k}_+$  and  $\mathbf{k}'' = -\mathbf{k}_0$ , we have

$$\delta\phi_z = -\alpha_\phi(\delta\phi_z - \delta\psi_z)/(\gamma_z^2 + \Delta^2), \quad (5.80)$$

where

$$\alpha_\phi = \left| \frac{ck_z k_{0\perp} \delta\phi_0}{B_0} \right|^2 \frac{2b_0[(\tau + 3/4)(b_0 + b_z) + b_z]}{b_0 + b_z}. \quad (5.81)$$

Similarly, Eq. (5.73) reduces to

$$\delta\psi_z = -\alpha_\psi(\delta\phi_z - \delta\psi_z)/(\gamma_z^2 + \Delta^2), \quad (5.82)$$

where

$$\alpha_\psi = \left| \frac{ck_z k_{0\perp} \delta\phi_0}{B_0} \right|^2 \frac{b_0 b_z (\tau + 3/4)}{b_0 + b_z}. \quad (5.83)$$

Equations (5.80) and (5.83) then yields the following dispersion relation for the modulational excitation of the  $\Omega_z$  zonal mode

$$1 = -(\alpha_\phi - \alpha_\psi)/(\gamma_z^2 + \Delta^2). \quad (5.84)$$

Note that  $\alpha_\phi - \alpha_\psi > 0$ . Hence,  $\gamma_z^2 = -\omega_z^2 < 0$  and, KAW can not spontaneously excite convective cells or zonal structures in the  $b_k \ll 1$  limit; regardless of the  $\tau = T_e/T_i$  value (Chen and Zonca, 2013), consistent with some of the recent results by (Zhao *et al.*, 2011) and in contrast with the analysis of (Mikhailovskii *et al.*, 2007; Onishchenko *et al.*, 2004; Pokhotelov *et al.*, 2004).

Equations (5.80) and (5.82) are, respectively, the generating equations for ESCC and MSCC. Thus, it is readily noted that they are excited by KAW simultaneously, as  $|\delta\psi_z/\delta\phi_z| = \mathcal{O}(1)$ . Artificially assuming that  $\delta\psi_z$  is suppressed yields the incorrect ESCC dispersion relation, Eq. (5.84) with  $\alpha_\psi = 0$ , but still the correct qualitative conclusion that ESCC are not spontaneously excited by KAW in the long wavelength limit. However, the analogous assumption that  $\delta\phi_z$  is suppressed delivers the erroneous MSCC dispersion relation, Eq. (5.84) with  $\alpha_\phi = 0$ , as well as erroneous claim that MSCC can be spontaneously excited by KAW for  $b_k \ll 1$  [cf., *e.g.*, the recent discussions given by (Zhao *et al.*, 2011)].

### C. Nonlinear mode-coupling of shear Alfvén waves in toroidal plasmas

In this section, we illustrate how equilibrium geometry and plasma nonuniformity can contribute to breaking the Alfvénic state (cf. Sec. V). As counterpart of the process by which a “pump” shear Alfvén wave (SAW) can excite a lower frequency “daughter” SAW via nonlinear Landau damping in a uniform plasma (cf. Sec. V.B.1), Sec. V.C.1 discusses Toroidal Alfvén Eigenmode (TAE) frequency cascading (Hahm and Chen, 1995). Similarly, Sec. V.C.2 addresses the generation of zonal structures by finite amplitude TAE (Chen and Zonca, 2012; Spong *et al.*, 1994; Todo *et al.*, 2010) as toroidal geometry analogue of the generation of convective cells by KAW, considered in Sec. V.B.3. Particular emphasis is given on the importance of spontaneous vs. forced generation of zonal structures (Chen and Zonca, 2012), given their potentially important self-regulatory roles on Alfvénic oscillations and, more broadly speaking, on drift Alfvén turbulence.

As geometry effects importantly affect the SAW continuous spectrum (cf. Sec. IV), Sec. V.C.3 discusses the AE nonlinear interplay with the SAW continuum and describes the mechanism by which this may yield enhanced continuum damping (Chen *et al.*, 1998; Vlad *et al.*, 1992; Zonca *et al.*, 1995). Finite amplitude MHD activity can also yield to deformation of the SAW continuum (Biancalani *et al.*, 2010a,b, 2011), as illustrated in Sec. V.C.4. In this case, however, due to a quasi-static helical deformation of the axisymmetric tokamak equilibrium, this effect may be destabilizing for beta induced AEs (BAEs) (Biancalani *et al.*, 2010a,b, 2011; Marchenko and Reznik, 2009). Within the general theoretical framework of Sec. V.A, Secs. V.C.3 and V.C.4 may be viewed as examples of how the renormalization of the general plasma inertia response, represented by the  $\propto \Lambda_n^{NL}$  term in Eq. (5.1), can be computed.

### 1. Toroidal Alfvén Eigenmode frequency cascading via nonlinear ion Landau damping

First, we recall that, in uniform plasmas (Sec. V.B), a pump SAW can parametrically excite a daughter SAW with a lower frequency and opposite parallel phase velocity via nonlinear ion Landau damping. (Hahm and Chen, 1995) applied this frequency cascading mechanism to the nonlinear saturation of TAE with high- $n$  toroidal mode numbers. Noting that, due to realistic equilibrium profile variations, there, in general, exists  $O(nq_a)$  TAEs with the same toroidal mode number  $n$ . Here,  $q_a$  is the safety factor at the outmost flux surface. Thus, for  $|nq_a| \gg 1/\epsilon = R_0/r$ , many TAEs with different mode frequencies may exist within the frequency gaps.

Following (Hahm and Chen, 1995) or, equivalently, the uniform plasma analysis (Sec. V.B), let the  $\mathbf{k}'$  be the pump wave,  $\mathbf{k}$  be the decay wave, and  $\mathbf{k}'' = \mathbf{k} - \mathbf{k}'$  be the sound wave, and applying the parametric decay dispersion relation, Eq. (5.34), to the wave intensity  $I_k = |\overline{\nabla_{\perp} \phi_k}|^2$ , where  $\overline{(\dots)}$  denotes appropriate averaging of  $(\dots)$  over the radial TAE mode structure, we can readily obtain the following wave-kinetic equation

$$\frac{\partial}{\partial t} I_k = \gamma_L(\mathbf{k}) I_k - \sum_{\mathbf{k}'} M_{k,k'} I_{k'} I_k, \quad (5.85)$$

where

$$M_{k,k'} = \frac{\omega'}{2} \frac{\text{Im} \chi_{is} m_i}{|\epsilon_{sk}|^2 B_0^2} \equiv \omega' V_s, \quad (5.86)$$

$\chi_{is}$  and  $\epsilon_{sk}$  are defined by, respectively, Eqs. (5.29) and (5.31), with  $\omega_{sr} = \omega - \omega'$  and  $k_{s\parallel} = k_{\parallel} - k'_{\parallel}$ , and we have summed over all the  $\mathbf{k}'$  pump modes. Now  $M_{k,k'}$  has a maximum frequency interaction width  $|\omega - \omega'| \simeq |2k'_{\parallel} v_{ti}| \sim v_{ti}/qR_0$  and, thus, if the adjacent TAE's frequency difference,  $|\Delta\omega| \sim |v_A/(nq^2 R_0)|$ , is smaller than  $v_{ti}/(qR_0)$  or  $\beta_i^{1/2} \gg |1/(nq)|$ , we can replace the sum over  $\mathbf{k}'$  by an integral over  $\omega'$ ; that is, Eq. (5.85) becomes approximately

$$\frac{\partial}{\partial t} I(\omega) = \gamma_L(\omega) I(\omega) - I(\omega) \int_{\omega}^{\omega_M} d\omega' I(\omega') \omega' V_s(\omega - \omega'). \quad (5.87)$$

Here,  $\omega_M \simeq \omega_u$ , the upper TAE gap accumulation point frequency, corresponds to the highest frequency of linearly unstable TAEs. Noting that  $I(\omega)$  has a frequency width typically of the order of the frequency gap,  $\sim \epsilon v_A/(qR_0)$ , and  $V_s(\omega'' = \omega - \omega')$  being an odd function in  $\omega''$  with an interacting width  $\sim v_{ti}/(qR_0)$ , we can perform an expansion about  $\omega' = \omega + \omega' - \omega$ , assuming  $\epsilon v_A/(qR_0) > v_{ti}/(qR_0)$  or  $\epsilon > \beta_i^{1/2}$ , and render Eq. (5.87) into the following differential equation

$$\frac{\partial}{\partial t} I(\omega) = \gamma_L(\omega) I(\omega) + I(\omega) U_1(\omega) \frac{\partial}{\partial \omega} I(\omega), \quad (5.88)$$

where (Hahm and Chen, 1995)

$$\begin{aligned} U_1(\omega) &= \int_{\omega_M - \omega}^{\omega - \omega_1} (\omega - \omega') V_s(\omega - \omega') d\omega' \simeq \int_{-\infty}^{\infty} \omega'' V_s(\omega'') d\omega'' \\ &= \frac{\pi}{2} [(1 + \tau) B_0 q R_0]^{-2} \equiv \overline{U}_1. \end{aligned} \quad (5.89)$$

Here, the standard notation  $\tau \equiv T_e/T_i$  was used and  $\omega_1 \approx \omega_{\ell}$ , the lower TAE gap accumulation point frequency, corresponds to the low-frequency end of  $I(\omega)$ . Note that  $\gamma_L(\omega_1) < 0$  and,  $I(\omega_1) \simeq 0$ . At saturation,  $\partial I/\partial t = 0$ ; Eq. (5.88) then yields

$$I(\omega) \simeq (1/\omega) \int_{\omega}^{\omega_M} [\gamma_L(\omega')/\overline{U}_1] d\omega'. \quad (5.90)$$

Here, noting that the spectral transfer of the wave energy is toward the lower frequency, we have let  $I(\omega) \approx 0$  at the highest frequency end,  $\omega_M$ ; i.e.,  $I(\omega)$  tends to peak away from  $\omega_M$ . The corresponding overall magnetic fluctuation level, recalling that for SAWs  $|\delta B_r/B_0| \simeq |ck_{\theta} \delta\phi/B_0 v_A|$ , is then given by

$$\left| \frac{\delta B_r}{B_0} \right|^2 \simeq \left( \frac{k_{\theta}}{k_r} \right)^2 (1 + \tau)^2 \frac{2/\pi}{\omega_A^2} \int_{\omega_1}^{\omega_M} \gamma_L(\omega) \ln \left( \frac{\omega}{\omega_1} \right), \quad (5.91)$$

where  $\omega_A = v_A/(qR_0)$ . Expanding  $\omega = \omega_1 + (\omega - \omega_1)$ , Eq. (5.91) gives the following rough estimate

$$\left| \frac{\delta B_r}{B_0} \right|^2 \sim \frac{1}{2\pi} (1 + \tau)^2 \left( \frac{\bar{\gamma}_L}{\omega_A} \right) \epsilon^2 \epsilon_{\text{eff}}^2, \quad (5.92)$$

with  $\epsilon_{\text{eff}} = 1 - \omega_1/\omega_M$ ,  $\bar{\gamma}_L$  a typical value of  $\gamma_L(\omega)$  and having noted  $|k_\theta/k_r| \sim \epsilon$ . Quantitatively, with the estimate  $|\bar{\gamma}_L/\omega_A| \lesssim O(10^{-2})$ ,  $\epsilon_{\text{eff}} \sim \epsilon \sim 10^{-1}$ , and  $\tau \lesssim 1$ , Eq. (5.92) yields a saturation amplitude at  $|\delta B_r/B_0| \lesssim 10^{-3}$ .

## 2. Nonlinear excitation of zonal structures by Toroidal Alfvén Eigenmodes

Zonal flows or, more generally, zonal structures are known to play important self-regulatory roles in the dynamics of microscopic drift-wave type turbulences. Since zonal structures are predominantly only radially varying, the self regulation is achieved via spontaneous excitations of modulational instabilities, and, consequently, the damping of the driving instabilities via scatterings to the short-radial wavelength stable domain (Chen *et al.*, 2000). However, while zonal electric fields and corresponding zonal flows are widely measured in experiments with properties that are consistent with the general theoretical framework (Diamond *et al.*, 2005), zonal magnetic fields and currents, predicted theoretically (Chen *et al.*, 2001; Diamond *et al.*, 2005; Gruzinov *et al.*, 2002; Guzdar *et al.*, 2001b), have been only recently observed in experiments in the compact helical system (CHS) (Fujisawa *et al.*, 2007).

As TAE plays crucial roles in the SAW instabilities in burning fusion plasmas, it is, thus, important to understand and assess the possible roles of zonal structures on the nonlinear dynamics of TAE. First numerical analyses of this problem were reported by (Spong *et al.*, 1994). More recently, numerical simulation results by (Todo *et al.*, 2010) showed that zonal structures may be forced-driven by finite amplitude TAE, while the importance of spontaneous vs. forced generation of zonal structures has been emphasized by (Chen and Zonca, 2012) (cf. Sec.V).

We shall follow the theoretical approach of (Chen *et al.*, 2000) as well as (Chen *et al.*, 2001); which is also adopted in Sec. V.B for our treatment of convective cells generated by kinetic Alfvén waves (KAWS) in uniform plasmas. Thus, adopting the field variables,  $\delta\phi$  and  $\delta A_{\parallel}$ , we shall consider the nonlinear couplings among the pump TAE,  $\Omega_0$ , the upper and lower sideband TAEs,  $\Omega_+$  and  $\Omega_-$ , and the zonal mode  $\Omega_z$ . We then have, for example,  $\delta\phi = \delta\phi_A + \delta\phi_z$  and  $\delta\phi_A = \delta\phi_0 + \delta\phi_+ + \delta\phi_-$ .

Assuming  $|k_{\perp}\rho_i|^2 \sim |k_z\rho_s|^2 < \epsilon = r_0/R_0 < 1$ , we can then adopt the ideal MHD approximation and obtain, from the vorticity equation of the  $\Omega_z$  mode, Eq. (5.72),

$$-i\omega_z\chi_{iz}\delta\phi_z = -\frac{c}{B_0}k_zk_{\theta}k_z^2\rho_i^2 \left\langle \left( 1 - \frac{k_{0\parallel}^2 v_A^2}{\omega_0^2} \right) \right\rangle_x (A_0^*A_+ - A_0A_-); \quad (5.93)$$

where  $\chi_{iz} \simeq 1.6q^2\epsilon^{-1/2}k_z^2\rho_i^2$  corresponds to the magnetically trapped-ion enhanced polarizability (Rosenbluth and Hinton, 1998),  $k_{\parallel} = (x - j)/qR_0$ ,  $\langle \dots \rangle_x \equiv \int dx |\Phi_0|^2(\dots)$ ,  $\langle 1 \rangle_x = 1$ ,  $\Phi_0(x - j) = \delta\phi_{n0}(r; nq - m)$  describes the radial dependence of the  $m$ th poloidal harmonics, and  $A_0$  and  $A_{\pm}$  are, respectively, amplitudes of the pump and sidebands. Noting that  $|\Phi_0|^2(x)$  is localized at and even<sup>23</sup> with respect to  $|x| = 1/2$  with a width  $\Delta_x \sim O(\epsilon)$ , Eq. (5.93) becomes

$$-i\omega_z\chi_{iz}\delta\phi_z = -(c/B_0)k_zk_{\theta}k_z^2\rho_i^2(1 - \omega_A^2/4\omega_0^2)(A_0^*A_+ - A_0A_-), \quad (5.94)$$

where  $\omega_A = v_A/(qR_0)$ .  $\delta A_{z\parallel}$  or  $\delta\psi_z \equiv \omega_0\delta A_{z\parallel}/ck_{0\parallel}$ , meanwhile, is given by the weighted averaging  $\langle \dots \rangle_x$  of Eq. (5.73),

$$\delta\psi_z = i(ck_zk_{\theta}/\omega_0B_0)(A_0^*A_+ + A_0A_-). \quad (5.95)$$

Including the nonlinear correction to ideal MHD Ohm's law, the nonlinear vorticity equations for the  $\Omega_{\pm}$  sidebands can be rendered into a set of differential-difference equations (Chen and Zonca, 2012); which, after weighted averaging, yields

$$A_{\pm}\epsilon_{A\pm}b_{\pm} = -2i\frac{c}{B_0}k_{\theta}k_z\omega_0b_0 \begin{pmatrix} A_0 \\ A_0^* \end{pmatrix} (\delta\phi - \delta\psi)_z, \quad (5.96)$$

<sup>23</sup> This is strictly valid for TAEs near SAW continuum accumulation points. As shown in Sec. IV.B.3, however, TAE mode structures have generally mixed parity. Here, we strictly follow (Chen and Zonca, 2012) and, for simplicity, assume  $|\Phi_0|^2(x)$  is even, noting that the present analysis is readily generalized to mixed parity modes.

where  $b_0 = \rho_i^2 \langle |\nabla_0 \Phi_0|^2 \rangle_x$ ,  $b_+ = \rho_i^2 \langle |\nabla_+ \Phi_0|^2 \rangle = b_0 + b_z$ ,  $b_z = k_z^2 \rho_i^2$  and  $b_- = b_+$ . Meanwhile,

$$\epsilon_{A\pm} = \left( \frac{\omega_A^4}{\epsilon_0 \omega^2} \Lambda_{T0}(\omega) D_0(\omega, k_z) \right)_{\omega=\omega_{\pm}}, \quad (5.97)$$

with  $\epsilon_0 = 2(r/R_0 + \Delta')$ ,  $D_0(\omega, k_z) = -2\Gamma_- D(\omega, k_z)$  and  $D(\omega, k_z)$  the TAE dispersion function consistent with Eq. (4.34) in the notations introduced in Sec. IV.B.3. Meanwhile,  $\Lambda_{T0} = -2\Gamma_- \Lambda_T = (-\Gamma_+ \Gamma_-)^{1/2}$ , consistent with Eq. (4.91)<sup>24</sup>. Solutions of  $D_0(\omega, k_z) = 0$  are  $\omega = \pm \omega_T(k_z)$ , with the pump TAE frequency given by  $\omega_0 = \omega_T(k_z = 0)$ . In the light of the general discussions of Sec. V.A and of Eq. (5.97), Eq. (5.96) can be considered as the implicit definition of  $\propto \Lambda_n^{NL}$  term in Eq. (5.1), showing that the effect of zonal structures on TAE nonlinear dynamics results in a renormalization of the (sideband) inertia. This is more generally the case also for other types of AEs (cf. also discussions in Sec. V.D.7).

Combing Eq. (5.96) with Eqs. (5.94) and (5.95) and letting  $-i\omega_z = \gamma_z$  yield

$$\delta\phi_z = 2i \left( \frac{c}{B_0} k_\theta k_z \right)^2 \frac{b_z}{\chi_{iz}} \left( 1 - \frac{\omega_A^2}{4\omega_0^2} \right) \frac{\omega_0 b_0}{\gamma_z b_+} |A_0|^2 \left( \frac{1}{\epsilon_{A+}} - \frac{1}{\epsilon_{A-}} \right) (\delta\phi - \delta\psi)_z, \quad (5.98)$$

and

$$\delta\psi_z = 2 \left( \frac{c}{B_0} k_\theta k_z \right)^2 \frac{b_0}{b_+} |A_0|^2 \left( \frac{1}{\epsilon_{A+}} + \frac{1}{\epsilon_{A-}} \right) (\delta\phi - \delta\psi)_z. \quad (5.99)$$

Noting that  $D_0(\omega_{\pm}, k_z) = \pm(\partial D_0/\partial\omega_0)(i\gamma_z \mp \Delta_T)$ , with  $\Delta_T \equiv \omega_T(k_z) - \omega_0$ , Eqs. (5.98) and (5.99) further reduce to, in analogy with Eqs. (5.80) and (5.82),

$$\begin{aligned} \delta\phi_z &= 2 \left( \frac{c}{B_0} k_\theta k_z |A_0| \right)^2 \left( \frac{\omega_0^2}{\omega_A^2} - \frac{1}{4} \right) \left( \frac{b_z}{\chi_{iz}} \right) \frac{b_0}{b_+} \frac{\epsilon_0}{\Lambda_{T0}(\omega_0)} \frac{2\omega_0/\omega_A^2}{\partial D_0/\partial\omega_0} \frac{(\delta\phi - \delta\psi)_z}{\gamma_z^2 + \Delta_T^2} \\ &\equiv -\alpha_{\phi T} \frac{(\delta\phi - \delta\psi)_z}{\gamma_z^2 + \Delta_T^2}, \end{aligned} \quad (5.100)$$

and

$$\begin{aligned} \delta\psi_z &= -2 \left( \frac{c}{B_0} k_\theta k_z |A_0| \right)^2 \left( \frac{b_0}{b_+} \right) \left( \frac{\Delta_T}{\omega_0} \right) \frac{\epsilon_0 \omega_0^2/\omega_A^2}{\Lambda_{T0}(\omega_0)} \frac{2\omega_0/\omega_A^2}{\partial D_0/\partial\omega_0} \frac{(\delta\phi - \delta\psi)_z}{\gamma_z^2 + \Delta_T^2} \\ &\equiv -\alpha_{\psi T} \frac{(\delta\phi - \delta\psi)_z}{\gamma_z^2 + \Delta_T^2}. \end{aligned} \quad (5.101)$$

Equations (5.100) and (5.101) then yield the following desired dispersion relation

$$\gamma_z^2 = \alpha_{\psi T} - \alpha_{\phi T} - \Delta_T^2; \quad (5.102)$$

*i.e.*, instability will set in when

$$\left( \frac{c}{B_0 \omega_0} k_\theta k_z |A_0| \right)^2 \frac{b_0}{b_+} \frac{\epsilon_0 \omega_0^2/\omega_A^2}{\Lambda_{T0}(\omega_0)} \frac{4\omega_0/\omega_A^2}{\partial D_0/\partial\omega_0} \left[ \frac{\Delta_T}{\omega_0} + \frac{b_z}{\chi_{iz}} \left( 1 - \frac{\omega_A^2}{4\omega_0^2} \right) \right] > \left( \frac{\Delta_T}{\omega_0} \right)^2 \quad (5.103)$$

Note that, typically,  $|\Delta_T/\omega_0| \sim O(\epsilon_0)$  and  $|b_z(1 - 1/4\omega_0^2)/\chi_{iz}| \sim O(\epsilon_0^{3/2}/q^2)$ . Meanwhile, we typically have  $\omega_0(\partial D_0/\partial\omega_0) > 0$  (Chen and Zonca, 2012). Thus, Eq. (5.103) becomes approximately

$$\Delta_T/\omega_0 > 0, \quad (5.104)$$

and

$$\left( \frac{c}{B_0 \omega_0} k_\theta k_z |A_0| \right)^2 \frac{b_0}{b_+} \frac{\epsilon_0 \omega_0^2/\omega_A^2}{\Lambda_{T0}(\omega_0)} \frac{4\omega_0/\omega_A^2}{\partial D_0/\partial\omega_0} > \frac{\Delta_T}{\omega_0}. \quad (5.105)$$

<sup>24</sup> Here, for simplicity, we adopt the notations of (Chen and Zonca, 2012) and use  $D_0$  and  $\Lambda_{T0}$ , symmetric with respect to lower and upper continuum accumulation points, rather than  $D$  and  $\Lambda_T$ .

This inequality essentially determines the condition for the spontaneous excitation of the zonal field  $\delta\psi_z$ , given by Eq. (5.101), which dominates over the usual zonal flow  $\delta\phi_z$  because of the enhanced magnetic trapped-ion polarizability. The sign of  $\Delta_T/\omega_0$  depends on the specific equilibria and plasma parameters, and must be computed for individual cases. For the case of nearly circular plasmas with monotonic  $q$  profiles,  $\Delta_T/\omega_0 < 0$  (Zonca, 1993a; Zonca and Chen, 1993), so that Eq. (5.104) is violated. However, Eq. (5.103) can still be satisfied for mode frequencies in the upper TAE gap,  $\omega_0^2 > \omega_A^2/4$ , and small  $|\Delta_T/\omega_0|$ , with  $\delta\phi_z$  dominating over  $\delta\psi_z$ . Note that, especially when strongly driven by energetic particles (EPs), TAE modes tend to be characterized by  $\omega_0^2 < \omega_A^2/4$ . This is a plausible explanation for the numerical simulation results by (Todo *et al.*, 2010), where the zonal structure response to TAE is found to be forced driven rather than spontaneously excited (cf. also Secs. V.C.3 and V.D.4).

In order to give a quantitative estimate for the onset condition of the modulational instability, Eq. (5.103), we recall that TAE linear stability analysis (cf. Sec. IV.B.3) yields

$$\frac{\epsilon_0\omega_0^2/\omega_A^2}{\Lambda_{T0}(\omega_0)} \frac{4\omega_0/\omega_A^2}{\partial D_0/\partial\omega_0} \sim 1 .$$

Thus, considering  $b_z \lesssim k_\theta^2 \rho_i^2 \sim \epsilon_0 b_0$  and  $2qR_0 k_{\parallel 0} \simeq 1$ , the threshold condition for spontaneous excitation of the most unstable zonal mode with  $b_0 \sim \epsilon_0$  becomes

$$\left( \frac{c}{B_0\omega_0} k_\theta k_z |A_0| \right)^2 \sim \left| \frac{\Delta_T}{\omega_0} \right| \sim \epsilon_0 \frac{b_z}{k_\theta^2 \rho_i^2} \sim \frac{b_z}{\epsilon_0} , \quad \Leftrightarrow \quad \left| \frac{\delta B_r}{B_0} \right|_{\text{th}}^2 \sim \frac{\rho_i^2}{4\epsilon_0 q^2 R_0^2} . \quad (5.106)$$

For some typical tokamak parameters, this estimate yields  $|\delta B_r/B_0|_{\text{th}}^2 \sim \mathcal{O}(10^{-8})$ , suggesting that spontaneous excitation of zonal structures may be a process effectively competing with other nonlinear dynamics in determining the saturation level of TAE and other AE modes; if constraints specified below Eq. (5.105) can be satisfied.

Coherent nonlinear interactions of AE and zonal structures that, if spontaneously excited, may play important self-regulatory roles in AE nonlinear dynamics, can generally influence fine structures of the AE frequency spectrum. These features in experimental observations [cf., *e.g.*, (Fasoli *et al.*, 1998) and the recent review by (Breizman and Sharapov, 2011)], are generally interpreted as evidence of modulation interactions due to wave-particle nonlinear dynamics (cf. Sec. V.D.3). In principle, it should be possible to discriminate these different underlying physics processes on the basis, *e.g.*, of the different scaling of the frequency splitting with the ‘‘pump AE’’ amplitude, predicted by Eq. (5.102) in the modulation interactions of TAE and zonal structures<sup>25</sup>.

### 3. Toroidal Alfvén Eigenmode saturation via nonlinear modification of local continuum

Since the difference between TAE frequency and the lower or upper SAW continuum accumulation frequencies is relatively small,  $|\Delta\omega| \lesssim (\epsilon v_A/qR_0)$  with  $\epsilon \equiv r/R_0$ , an efficient nonlinear saturation mechanism is via nonlinear modification of the local SAW continuum structures, such that the frequency difference  $\Delta\omega$  vanishes, due to the corresponding nonlinear frequency shift. Within the general theoretical framework of Sec. V.A, this process is accounted for by the  $\propto \Lambda_n^{NL}$  term in Eq. (5.1). As the TAE frequency gap is due to the coupling of  $(m \pm 1, n)$  and  $(m, n)$  modes (cf. Sec. IV.B.3), the contribution to  $\Lambda_n^{NL}$  may be produced by  $(m = \pm 1, n = 0)$  components of  $\delta\mathbf{E} \times \mathbf{b}$  flow and  $\delta\mathbf{B}_\perp$  field line bending, rather than by the generation of zonal structures, discussed in Sec. V.C.2. So far, two such mechanisms have been proposed. One depends on the nonlinear modification in the magnetic surface structure (Zonca *et al.*, 1995) and the other depends on the nonlinear modification in the density structures (Chen *et al.*, 1998). Although of different underlying nature, these two processes are described by essentially the same nonlinear equations. Therefore, we will discuss in some details only the former, referring the reader to the original work for the latter.

In general, mechanisms for nonlinear modification of the local SAW continuum structures at short radial scales, mentioned above, yield mode saturation above a critical amplitude threshold because of the appearance of fine scales in the mode structure; *i.e.*, of enhanced mode damping in the presence of finite dissipation. This phenomenon may be physically interpreted as mode conversion to short scale damped oscillations, produced by the TAE modes due to the nonlinear SAW continuum distortion. Note, here, that this mechanism is different from that discussed more recently by (Todo *et al.*, 2010, 2012a,b), which is connected with power transfer to nonlinear driven oscillations, which are damped possibly through the fine structures connected with resonant excitation of higher toroidal mode number

<sup>25</sup> It is worthwhile noting that modulation interactions of Alfvénic fluctuations are expected in more strongly driven cases (Zonca *et al.*, 2000), such as for energetic particle modes, as discussed in Sec. V.D.6.

continuous spectra (cf. also Sec. V.D.4). For this last particular aspect, we show below that the local interaction with the higher toroidal mode number SAW continuum is typically smaller than the local interaction with the nonlinearly modified SAW continuum itself.

Let us consider a the local TAE structure that consists of toroidal mode number  $n$  and poloidal mode numbers  $m$  and  $m + 1$ , with given frequency  $\omega_0$ . The dominant nonlinear interactions among these Fourier harmonics yield a low frequency fluctuation with  $(m = 1, n = 0)$  and  $(2m + 1, 2n)$  driven component at  $2\omega_0$ , which are readily expressed as (Vlad *et al.*, 1992, 1995a, 1999; Zonca *et al.*, 1995):

$$\begin{aligned} \delta\phi_{1,0} &= -\frac{ck_{\theta 0}}{\omega_0 B_0} \frac{\partial}{\partial r} (\delta\phi_{m,n}^* \delta\phi_{m+1,n}) \quad , \\ \delta A_{\parallel 1,0} &= \frac{c^2 k_{\theta 0}}{\omega_0 B_0 v_A} \left( \delta\phi_{m,n}^* \frac{\partial}{\partial r} \delta\phi_{m+1,n} - \delta\phi_{m+1,n} \frac{\partial}{\partial r} \delta\phi_{m,n}^* \right) \quad ; \end{aligned} \quad (5.107)$$

$$\begin{aligned} \frac{\partial}{\partial r} \delta\phi_{2m+1,2n} &= \frac{ck_{\theta 0}}{\omega_0 B_0} \left( 2 \frac{\partial}{\partial r} \delta\phi_{m,n} \frac{\partial}{\partial r} \delta\phi_{m+1,n} - \right. \\ &\quad \left. \delta\phi_{m,n} \frac{\partial^2}{\partial r^2} \delta\phi_{m+1,n} - \delta\phi_{m+1,n} \frac{\partial^2}{\partial r^2} \delta\phi_{m,n} \right) \quad , \\ \delta A_{\parallel 2m+1,2n} &= -\frac{c^2 k_{\theta 0}}{\omega_0 B_0 v_A} \left( \delta\phi_{m+1,n} \frac{\partial}{\partial r} \delta\phi_{m,n} - \delta\phi_{m,n} \frac{\partial}{\partial r} \delta\phi_{m+1,n} \right) \quad . \end{aligned} \quad (5.108)$$

These equations are readily derived from Eqs. (2.35) and (2.37), neglecting thermal ion compressions and EP contribution in the narrow radial layer where the coupling of two neighboring poloidal Fourier harmonics yields the formation of the TAE frequency gap in the SAW continuum (cf. Sec. IV.B.3). Furthermore, we have assumed  $|n| \gg 1$  for simplicity and defined  $k_{\theta 0} = -m/r_0$ , with  $r_0$  the radial position of the considered local TAE frequency gap. In particular, in Eq. (5.107), we have also neglected the effect of thermal ion Landau damping, considering a very narrow TAE spectrum centered at  $\omega_0$ . The effect of ion Landau damping may become important for a broader TAE frequency spectrum, *e.g.*, taking into account different radial states of the same  $n$  (cf. Sec. IV); and can be readily included in the present analysis following the derivations of Sec. V.B. It is also worthwhile noting that, due to toroidal geometry,  $(2m, 2n)$  and  $(2m + 2, 2n)$  Fourier modes are nonlinearly driven at  $2\omega_0$  in addition to the  $(2m + 1, 2n)$  harmonic given by Eq. (5.108). These modes, may locally interact with the SAW continuum, since the frequency gap at  $\simeq v_A/(qR_0)$  is very narrow for toroidal equilibria with circular flux surfaces (Zheng and Chen, 1998a,b). In this case, the effect of the local coupling of the  $2n$  nonlinear mode to the SAW continuum can be quite significant and can importantly contribute to the saturation of the ‘‘pump’’ TAE mode (Todo *et al.*, 2012b). More generally, however, the  $(2m, 2n)$  and  $(2m + 2, 2n)$  Fourier modes at  $2\omega_0$  do not locally interact with the SAW continuum, due to the prevailing effect of magnetic flux surface ellipticity in determining the frequency gap in the SAW continuum at  $\simeq v_A/(qR_0)$  (Betti and Freidberg, 1991). Therefore, in the typical case of elongated plasmas, the effect of  $(2m, 2n)$  and  $(2m + 2, 2n)$  Fourier modes results into a nonlinear frequency shift that is  $\mathcal{O}(\epsilon)$  smaller than that due to the  $(2m + 1, 2n)$  harmonic given in Eq. (5.108), which is the reason why this effect was originally neglected in (Vlad *et al.*, 1992, 1995a; Zonca *et al.*, 1995).

Adopting the general notation of Eq. (4.26) for the fluctuating fields structure, it is convenient to introduce the definitions

$$\begin{aligned} U &= 8\sqrt{2}mqs \left( \frac{R_0}{r_0} \right) \left( \frac{\beta b_s}{\epsilon_0^3} \right)^{1/2} \frac{e}{T_e + T_i} \delta\phi_{0n}(r; nq - m) \quad , \\ V &= 8\sqrt{2}mqs \left( \frac{R_0}{r_0} \right) \left( \frac{\beta b_s}{\epsilon_0^3} \right)^{1/2} \frac{e}{T_e + T_i} \delta\phi_{0n}(r; nq - m - 1) \quad , \end{aligned} \quad (5.109)$$

where  $b_s = k_{\theta 0}^2(T_e + T_i)/(m_i\Omega_i^2)$  and other symbols are consistent with the definitions of Sec. IV.B.3. Meanwhile, the dimensionless time can be defined as  $\tau \equiv \epsilon_0 v_{At}/(4qR_0)$ , so that the corresponding dimensionless frequency is normalized to the half width of the TAE frequency gap; whereas the corresponding normalization of the radial coordinate is  $x \equiv (4/\epsilon_0)(nq - m - 1/2)$ . The effect of the low frequency fluctuation with  $(m = 1, n = 0)$  and  $(2m + 1, 2n)$  driven component at  $2\omega_0$  back onto the ‘‘pump’’ TAE mode is readily obtained by direct substitution of Eqs. (5.107) and (5.108) into the coupled vorticity equations for  $(m, n)$  and  $(m + 1, n)$  modes near  $r_0$  (cf. Sec. IV.B.3). In terms of the just introduced variables and fields, the final governing equations are

$$\begin{aligned} (i\partial_\tau - x) \partial_x U + \partial_x V - \partial_x^2 |V|^2 \partial_x U &= \bar{A} \quad , \\ (i\partial_\tau + x) \partial_x V + \partial_x U - \partial_x^2 |U|^2 \partial_x V &= -\bar{A} \quad . \end{aligned} \quad (5.110)$$

Here,  $\bar{A}$  and  $\bar{B}$  (used below) are defined as

$$\begin{pmatrix} \bar{A} \\ \bar{B} \end{pmatrix} = \frac{8}{\sqrt{\pi}} m q \left( \frac{R_0}{r_0} \right) \left( \frac{\beta b_s}{\epsilon_0^3} \right)^{1/2} \frac{e}{T_e + T_i} \begin{pmatrix} A(0) \\ B(0) \end{pmatrix}, \quad (5.111)$$

$A(0) \equiv A(\theta = 0)$  and  $B(0) \equiv B(\theta = 0)$ , given the canonical representation of the TAE fluctuation field as  $\delta\hat{\Phi}_n = A(\theta) \cos(\theta/2) + B(\theta) \sin(\theta/2)$  [cf. Eq. (4.29), as well as Sec. IV.B.3]. The local TAE dispersion relation in the form of the GFLDR (cf. Secs. IV and V) is readily obtained from the solutions of Eq. (5.110) with the matching condition

$$\int_{-\infty}^{\infty} \partial_x U dx = - \int_{-\infty}^{\infty} \partial_x V dx = -\pi \bar{B}. \quad (5.112)$$

Since the ratio  $\bar{B}/\bar{A}$  depends only on  $\delta\hat{W}_f$  in the absence of EPs (cf. Sec. IV.B.3), Eq. (5.112) describes the nonlinear frequency shift with respect to  $\omega_0$ , produced by the finite TAE amplitude via the generation of the nonlinear fluctuations of Eqs. (5.107) and (5.108). It is readily verified that, above a certain critical  $\bar{A} = \bar{A}_c(\delta\hat{W}_f)$ , the solutions of Eq. (5.110) start producing fine radial structures due to enhanced interaction with the local continuous spectrum. The critical fluctuation level for this to occur can be estimated as

$$\left( \frac{\delta B_r}{B_0} \right)_c \sim \frac{1}{8|s|mq} \frac{r_0}{R_0} \epsilon_0^{3/2} |U| \sim \frac{1}{4|s|mq} \left( \frac{r_0}{R_0} \right)^{5/2} \bar{A}_c(\delta\hat{W}_f) \lesssim 10^{-3} \bar{A}_c(\delta\hat{W}_f). \quad (5.113)$$

As  $\bar{A}_c(\delta\hat{W}_f) \ll 1$  for some choice of plasma equilibrium profiles, (nonlinear) enhanced continuum damping may effectively yield mode saturation.

Again, we note that the local SAW continuum may also be modified via nonlinear density changes (Chen *et al.*, 1998). The corresponding critical fluctuation level for enhanced continuum damping is given by

$$\left( \frac{\delta B_r}{B_0} \right)_c \sim (\beta \epsilon_0^3)^{1/2} \bar{\mathcal{A}}_c(\delta\hat{W}_f) \lesssim 10^{-2} \bar{\mathcal{A}}_c(\delta\hat{W}_f). \quad (5.114)$$

As for  $\bar{A}_c(\delta\hat{W}_f)$  in Eq. (5.113),  $\bar{\mathcal{A}}_c(\delta\hat{W}_f)$  may become very small in Eq. (5.114). However, the critical amplitude in Eq. (5.114) is typically larger than that in Eq. (5.113). That is, the dominant mechanism for nonlinearly enhanced continuum damping is expected to be due to the nonlinear modification in the magnetic surface structure and plasma flow.

#### 4. Alfvén Eigenmodes in the presence of a finite-size magnetic island

Theoretical analyses of Alfvénic fluctuations in the presence of a finite-size magnetic island were originally motivated by the experimental observation of BAEs in FTU (Annibaldi *et al.*, 2007), where they are excited without EP drive but in the presence of a sufficiently large magnetic island (Buratti *et al.*, 2005), as also reported in TEXTOR (Zimmermann *et al.*, 2005) and HL-2A (Chen *et al.*, 2011b) (cf. Sec. IV.C).

Theoretically, the low-frequency magnetic island can be considered as cause of non-axisymmetric distortion of the tokamak equilibrium, whose detailed analytical studies are given by (Biancalani *et al.*, 2010a,b, 2011). This situation has evident analogies with the formation of frequency gaps in the SAW continuous spectrum in helical devices [cf., *e.g.*, (Kolesnichenko *et al.*, 2011; Toi *et al.*, 2011)]. Here, we will remark on a case of particular interest, when the toroidal periodicity of the singular perturbations representing the SAW continuum is the same as that of the magnetic island, assumed to have  $(m_0, n_0)$  poloidal/toroidal mode numbers. In this case, the SAW continuous spectrum is qualitatively modified as in Fig. 4, where dashed blue and red lines represent, respectively, the SAW continuous spectrum and BAE mode frequency,  $\omega_{BAE0}$ , in the reference axisymmetric tokamak equilibrium without magnetic island. Meanwhile, solid blue and red lines show, respectively, how SAW continuum and BAE frequency,  $\omega_{BAE}$ , are modified by the magnetic island, with  $r_{sx1}$  and  $r_{sx2}$  denoting the inner and outer separatrix radii, and  $r_0$  the island O-point position, where the axisymmetric tokamak equilibrium has safety factor  $q_0 = m_0/n_0$ . The BAE frequency upshift due to the finite size magnetic island can be written as

$$\omega_{BAE} = \omega_{BAE0} \left[ 1 + \frac{n_0^2 s^2 q_0^2}{4} \frac{W_{isl}^2}{r_0^2} \frac{\omega_A^2}{\omega_{BAE-CAP}^2} \right]^{1/2}, \quad (5.115)$$

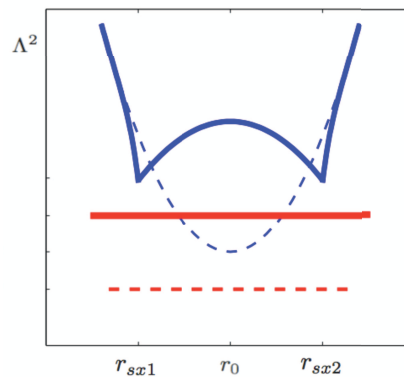


FIG. 4 Qualitative modification of the SAW continuum with the same toroidal mode number of a finite size magnetic island,  $r_{sx1}$  and  $r_{sx2}$  denoting the inner and outer separatrix radii, and  $r_0$  the island O-point position [from original Fig. 5 of (Biancalani *et al.*, 2011)].

where  $W_{isl}$  stands for the magnetic island (half) width,  $\omega_{BAE-CAP}$  denotes the BAE continuum accumulation point frequency defined as  $\Lambda^2(\omega_{BAE-CAP}) = 0$  and  $\omega_A = v_A/(q_0 R_0)$ , using the notations of Sec. IV.B.2. Equation (5.115) has been successfully tested against FTU experimental observations for sufficiently small magnetic island width (Tucillo *et al.*, 2011).

The actual physics determining the minimum threshold in magnetic island size above which BAE modes are excited is not fully clarified. Two possible mechanisms have been proposed so far: (i) the core plasma profiles, modified inside the finite size magnetic island, along with the modified SAW continuum structures, may alter the stability properties of BAE modes and eventually excite them even in the absence of EPs (Biancalani *et al.*, 2011); (ii) the island-induced modification of the thermal ion equilibrium distribution function (Smolyakov *et al.*, 2007) may be sufficient to yield a change in sign of ion Landau damping and cause mode excitation (Marchenko and Reznik, 2009).

#### D. Nonlinear wave-particle dynamics

As anticipated in the introduction to Sec. V, there are currently two paradigms for discussing nonlinear interactions of Alfvénic fluctuations with supra-thermal particles in fusion plasmas (Chen and Zonca, 2013): the “bump-on-tail” and the “fishbone” paradigms. It is possible to adopt the former one, with obvious advantages for complex dynamics studies, provided that the system is sufficiently close to marginal stability. In particular, the nonlinear modification of resonant EP orbits must be small compared with the characteristic fluctuation wavelength (Berk and Breizman, 1990b,c). Thus, this model can account only for local EP transports in the presence of an isolated resonance; *i.e.*, unless the threshold is exceeded for the onset of stochasticity in the particle phase-space due to resonance overlap (cf. Secs. VI.A and VII.A). The essential physics of the bump-on-tail paradigm are the same as those originally introduced in the analysis of the temporal evolution of a small cold electron beam interacting with a plasma in a 1D system (Al’tshul’ and Karpman, 1965, 1966; Mazitov, 1965; O’Neil, 1965; O’Neil *et al.*, 1971); and are discussed in Sec. V.D.1. There, we also give the self-consistent nonlinear solution for the low frequency beam distribution function in the presence of a periodic fluctuation, as derived by (Al’tshul’ and Karpman, 1965, 1966). In fact, this is the solution of the Dyson equation for a 1D uniform plasma, which is the starting point for its extension to nonuniform systems (Zonca *et al.*, 2005) and provides the theoretical basis for the construction of the fishbone paradigm later on. The dynamics of the nonlinear beam-plasma system with sources and collisions are analyzed in Sec. V.D.2, based on the original works by (Berk and Breizman, 1990a,b,c). These include steady-state and bursting behaviors (periodic and chaotic) (Berk *et al.*, 1996b, 1992a; Breizman *et al.*, 1997, 1993), formation of hole/clump pairs in the resonant particle phase space (Berk *et al.*, 1999, 1997b; Breizman *et al.*, 1997); and the existence of subcritical states (Berk *et al.*, 1999). Applications of the 1D bump-on-tail paradigm to AE experimental observations are discussed in Sec. V.D.3, with notable examples being fine structures (frequency splitting) of AE spectral lines (Fasoli *et al.*, 1998) as well as AE adiabatic frequency chirping (Gryaznevich and Sharapov, 2006; Pinches *et al.*, 2004a; Vann *et al.*, 2005). Section V.D.3 also addresses the assumptions underlying the 1D bump-on-tail paradigm and analyzes its validity limits. In particular, the requirement that frequency chirping be an adiabatic process and that EP dynamics be perturbative are not intrinsic to the model and can be actually overcome by numerical solution of

the fully nonlinear beam-plasma system (Vann *et al.*, 2007). What is left out of this paradigm model by definition are equilibrium geometry and plasma nonuniformity effects, which importantly modify AE linear (cf. Sec. IV) and nonlinear behaviors when EP excursions are of the order of the fluctuation wavelength, and may significantly affect the threshold for the onset of stochastic EP transport in the presence of many modes [cf. also Secs. VI.A and VII.A].

One possible approximate method for analyzing finite AE mode width effects is based on perturbative treatment of EPs and prescribed AE structures, which ultimately yields AE nonlinear dynamics in terms of time evolution of wave amplitudes and phases (Chen and White, 1997). Numerical simulation results using this approach are presented in Sec. V.D.4. In burning fusion plasmas, however, EP effects are generally non-perturbative and modify the plasma dielectric response as well as the fluctuation structure and frequency. These behaviors are related with equilibrium geometry and plasma nonuniformity effects via EP resonance conditions, Eqs. (4.50) and (4.51), which depend on EP constants of motion; and via finite mode structures, set by plasma profiles and affecting wave-EP interactions. Unless EP response is perturbative, the nonlinear mode dynamics becomes non-adiabatic when nonlinear EP excursions are of the order of the fluctuation wavelength, since the plasma dielectric response undergoes an  $\mathcal{O}(1)$  change in one characteristic nonlinear time  $\tau_{NL} \sim \gamma_L^{-1}$ . These issues are analyzed in Sec. V.D.5. First, with a comparison of the finite wave-particle interaction length<sup>26</sup> with the fluctuation wavelength (Zonca *et al.*, 2005), yielding an estimate of  $|\gamma_L/\omega|$  for the transition from local redistributions to meso-scales EP transports and the corresponding shift from the bump-on-tail to the fishbone paradigm. Then, these physics are demonstrated from the perspective of numerical simulation results, which clarify the underlying nonlinear dynamics (Briguglio, 2012; Briguglio and Wang, 2013; Briguglio *et al.*, 1998; Wang *et al.*, 2012; Zhang *et al.*, 2012). At last, Sec. V.D.5 derives the general equations for the nonlinear dynamics of phase-space ZS within the theoretical framework of Sec. V.A, yielding the generalization of the Dyson equation introduced in Sec. V.D.1 (Al'tshul' and Karpman, 1965, 1966) to nonuniform plasmas with the addition of sources and collisions. This result is then used to demonstrate the unification of bump-on-tail and fishbone paradigms.

In nonuniform plasmas, with the mode frequency set by the nonlinear dispersion relation, the nonlinear mode evolution is dominated by resonant EPs whose phase is locked with the wave, since these maximize wave-EP power exchange while, at the same time, are most efficiently displaced by the mode (Chen, 1999). Depending on the wave dispersive properties, the mode can nonlinearly modify its structure to further enhance the wave-EP power exchange by tapping the stronger free energy source (steeper spatial gradient regions) due to phase-locked resonant EPs. Different modes, with their own dispersion relation, respond differently to the non-adiabatic nonlinear change of the EP distribution function. This is demonstrated in Sec. V.D.5 by comparing numerical simulation results for nonlinear dynamics of beta induced AE (BAE) (Wang *et al.*, 2012; Zhang *et al.*, 2012) and radially localized energetic particle mode (EPM) (Briguglio, 2012). When the mode can readily respond by readapting its frequency and/or mode structure to the modified EP distribution, resonant EP radial motion is secular as long as wave-particle phase locking is maintained, as theoretically predicted (White *et al.*, 1983) and observed experimentally (Duong *et al.*, 1993; Heidbrink, 2008). This process, dubbed as “mode-particle pumping” in the original work by (White *et al.*, 1983), where it was introduced to explain EP losses due to fishbones in PDX (McGuire *et al.*, 1983), describes nonlinear dynamics of radially extended EPM (cf. Sec. V.D.6) and fishbones (cf. Sec. V.D.7), and is accompanied by fast non-adiabatic frequency chirping,  $|\dot{\omega}| \gtrsim \omega_B^2$  with  $\omega_B$  the wave-particle trapping frequency for fixed  $\omega$ , that suppresses wave-particle trapping as shown in Sec. V.D.5. The ability to adapt and “follow” phase locked EPs is characteristic of EPMs, of which fishbones are the first and one well-known example (Chen and Zonca, 2007a), and it is borne in the mode dispersion relation. Section V.D.6, furthermore, discusses the radial modulation effects of the self-consistent interplay of AE/EPM mode structures and EP transport, which are the analogue of the modulation interaction of AE with ZS, discussed in Sec. V.C.2, extended to generally include wave-particle resonance effects in the case of phase-space ZS. In general, modulation interactions of AE/EPM with (phase-space) ZS can influence fine features of the AE/EPM frequency spectra, of different nature from those connected with the modulation interaction due to wave-particle nonlinear dynamics (Fasoli *et al.*, 1998), discussed in Sec. V.D.3.

More generally, the study of convectively amplified EPM wavepackets as soliton-like solutions of a complex nonlinear Schrödinger equation introduces interesting analogies with research fields other than plasma physics (cf. Sec. V.D.6). These include possible formulations of fractional derivative extensions of the nonlinear Schrödinger equation as well as Fokker-Planck equation, based on a first-principle physics model derived from general equations governing the nonlinear evolution of a nonuniform plasma system with wave-particle resonant interactions that are responsible of nonlocal spatiotemporal behaviors. Further discussions of general implications of the theoretical framework introduced in Sec. V.A are given in Sec. V.E.

---

<sup>26</sup> The wave-particle interaction length is defined as the distance one resonant particle can travel before losing the phase coherence with the wave itself. By analogy, it is possible to define the wave-particle interaction time.

## 1. The physics of the collisionless nonlinear beam-plasma system

The temporal evolution of a small cold electron beam interacting with a plasma in a 1D system was described by (O'Neil *et al.*, 1971). The spatial growth of the most unstable beam mode was considered by (O'Neil and Winfrey, 1972) and is more closely related with interpretation of experimental observations. However, for the scope of the present review, it does not introduce any significant difference. Thus, it will not be further mentioned. The treatment by (O'Neil *et al.*, 1971) was a significant step forward, since the numerical problem could be put in terms of simple scaled quantities, yielding a general solution. Following the linear analysis of (O'Neil and Malmberg, 1968), let us consider a uniform 1D beam-plasma systems, where electrons have density  $n$  and are Maxwellian, with a thermal speed  $v_T$  significantly lower than the electron beam drifting speed  $v_D$ , such that the collisionless dissipation due to thermal electron Landau damping is negligible. Beam electrons, of density  $n_B \ll n$ , have a Lorentzian distribution with velocity spread  $v_B$ , while thermal ions are considered as a fixed neutralizing background.

The most unstable wave is a beam mode, which is nearly degenerate with the Langmuir wave; *i.e.*,  $\omega = \omega_0 + \delta\omega$  and  $k = k_0 + \delta k$ , with  $\omega_0 = \omega_p$  and  $k_0 = \omega_p/v_D$ . More precisely, introducing  $x = (\delta k/k_0)(2n/n_B)^{1/3}$ ,  $y = (\delta\omega/\omega_0)(2n/n_B)^{1/3}$ ,  $s = (v_B/v_D)(2n/n_B)^{1/3}$  (O'Neil and Malmberg, 1968), the most unstable mode for  $s = 0$  has  $x = 0$ ,  $y = -(1/2) + i\sqrt{3}/2$  and group velocity  $\partial\omega/\partial k = (2/3)v_D$ . The half-width  $\Delta k$  of the linear growth rate spectrum is given by  $\Delta k = (3/2)k_0(n_B/2n)^{1/3}$ . For  $(n_B/2n)^{1/3} \ll 1$ , beam electrons are moving locally over a single wave with relative velocity  $\Delta v \sim (n_B/n)^{1/3}v_D$ . When the wave grows to an amplitude such  $\phi \sim m\Delta v^2/e \sim (n_B/n)^{2/3}mv_D^2/e$ , the wave saturates and starts oscillating (O'Neil *et al.*, 1971). Meanwhile, the nonlinear evolution takes place in two stages (Shapiro, 1963a,b): first, the beam-plasma interaction heats the beam, as the nonlinear  $\Delta v \gtrsim v_B$ ; second, the beam distribution is modified (flattened by phase mixing; cf. later) in velocity space by nonlinear interactions.

Following (O'Neil *et al.*, 1971), we consider  $\delta\phi = \delta\phi_0(t)\exp(ik_0x) + c.c.$ ,  $x = z - v_D t$  and  $\omega_0 = \omega_p$ . A general direct solution of the Poisson's equation can be obtained assuming that, in one wavelength  $2\pi/k_0$ , the beam spatial charge is made of  $i = 1, 2, 3, \dots, M$  charge sheets located at  $x_j$  with charge  $(-2\pi en_B)/(Mk_0)$ . Thus, recalling that the plasma can be treated as a linear dielectric medium and that the wave is nearly monochromatic; and introducing the normalized quantities  $\xi_j(\tau) = k_0 x_j(t)$ ,  $\tau = \omega_0 t (n_B/2n)^{1/3}$  and  $\Phi(\tau) = -(2n/n_B)^{2/3} e \delta\phi_0(t) / (mv_D^2)$ ,

$$\dot{\Phi}(\tau) = \frac{-i}{M} \sum_{j=1}^M \exp[-i\xi_j(\tau)] \quad , \quad (5.116)$$

$$\ddot{\xi}_j(\tau) = -i\Phi(\tau) \exp[i\xi_j(\tau)] + c.c. \quad , \quad (5.117)$$

are, respectively, the evolution equation for  $\Phi(\tau) = \Phi(0) \exp(-i \int_0^\tau y(\tau') d\tau')$ , with  $y$  the normalized frequency variable introduced above, and the equation of motion for the electron beam charge sheets. It is readily verified that Eqs. (5.116) and (5.117) recover the linear dispersion relation  $y^3 = 1$ , for the most unstable beam mode in the cold beam case (O'Neil *et al.*, 1971). They describe the early nonlinear evolution of the most unstable beam-plasma wave, under the single mode assumption. Numerical solution shows that, when waves grow exponentially out of the thermal noise, the fastest growing mode eventually dominates the dynamics and grows until electrons are trapped and begin sloshing back and forth in the wave. Then, the wave stops growing and begins oscillating about a mean value due to energy exchange between electrons and the wave itself. This process is similar to the oscillatory behaviors observed with an externally launched large amplitude wave (Mazitov, 1965; O'Neil, 1965). Equations (5.116) and (5.117), describing the nonlinear interaction of a supra-thermal electron beam with one single wave, can be seen as dynamical system and formally obtained in the framework of Hamiltonian system theory (Antoni *et al.*, 1998; Mynick and Kaufman, 1978; Tennyson *et al.*, 1994). An interesting aspect of this description is that it results in a self-consistent Hamiltonian formulation, which is formally equivalent to that of the free-electron laser dynamics (Antoniazzi *et al.*, 2008). Furthermore, using the same formulation, it has been recently shown (Carlevaro *et al.*, 2013) that the supra-thermal electron distribution function in the quasi-stationary states (intermediate out-of-equilibrium states) produced by the nonlinear evolution of the beam-plasma system are accurately predicted by the maximum entropy principle proposed by Lynden-Bell (Antoni *et al.*, 1998; Lynden-Bell, 1967).

Conservation laws can be derived by manipulation of Eqs. (5.116) and (5.117). Using vanishing initial conditions, momentum and energy conservations are obtained, respectively, as (O'Neil *et al.*, 1971)

$$|\Phi(\tau)|^2 + \frac{1}{M} \sum_{j=1}^M \dot{\xi}_j(\tau) = 0 \quad , \quad (5.118)$$

$$\Re y |\Phi(\tau)|^2 + \frac{1}{4M} \sum_{j=1}^M \dot{\xi}_j^2(\tau) = 0 \quad , \quad (5.119)$$

yielding  $\Re y(\tau) = (1/4) \sum_j \dot{\xi}_j^2(\tau) / \sum_j \dot{\xi}_j(\tau)$ . Noting that  $\Im y(\tau) = (1/2)(d/d\tau)|\Phi(\tau)|^2/|\Phi(\tau)|^2$  by definition, the nonlinear frequency oscillation is always downward, as shown by Eq. (5.119); and it occurs with a frequency which is twice that of  $|\Phi(\tau)|$  oscillations and maximum negative excursions corresponding to the minima of fluctuation intensity (O’Neil *et al.*, 1971). The excursions of both  $\Re y(\tau)$  and  $\Im y(\tau)$  are  $\mathcal{O}(1)$ , as can be estimated from the optimal ordering  $\dot{\omega} \sim k_0 \dot{v} \sim \omega_B^2$ .

An important nonlinear phenomenon connected with wave-particle trapping is the so-called spatial bunching (O’Neil *et al.*, 1971). This is due to the fact that most important contribution to kinetic energy and charge density comes from particles near the bottom of the instantaneous trapping well of the wave and that “small oscillations” tend to be bunched in  $\xi$  after one quarter of the trapping period. Therefore, the nonlinear distortion of the particle distribution function can also drive higher order fluctuation harmonics, in addition to usual wave-wave couplings that, however, are explicitly smaller by  $(n_B/2n)^{1/3}$  with respect to the most unstable mode  $\Phi(\tau)$ .

On long time scales, the wave cannot be considered monochromatic any longer and the (total) energy dependence of the particle trapping period causes the particle distribution function inside the separatrix to smooth out the increasingly finer structures by phase mixing. This is the coarse-grain distribution function (Sagdeev and Galeev, 1969) and, when it is asymptotically formed on long time scales, the mode amplitude reaches a steady state (Mazitov, 1965; O’Neil, 1965)<sup>27</sup>. Considering  $E_z = E_{z0} \sin \xi$  in the wave moving frame, particle motion is described by

$$\dot{\xi}^2 = (4\omega_B^2/\kappa^2) [1 - \kappa^2 \sin^2(\xi/2)] \quad , \quad (5.120)$$

where  $\omega_B^2 = |ekE_{z0}/m|$  is the trapping frequency of deeply trapped particles,  $\kappa^2 = 2eE_{z0}/(kW + eE_{z0})$  and  $W$  is the total energy. This is the equation of a nonlinear pendulum, with  $\kappa^2 < 1$  describing rotations,  $\kappa^2 > 1$  denoting oscillations or librations and  $\kappa^2 = 1$  defining the separatrix. Defining  $\Delta W = (\partial W/\partial v)\Delta v = \text{const}$ , the coarse-grain distribution function is given by (O’Neil, 1965; Sagdeev and Galeev, 1969):

$$[f] = \frac{\oint F_0(v)\Delta v d\xi}{\oint \Delta v d\xi} \simeq F_0(\omega_0/k_0) + \frac{\partial F_0(\omega_0/k_0)}{\partial v} \frac{\oint d\xi/k_0}{\oint d\xi/\dot{\xi}} \quad , \quad (5.121)$$

where  $[f] = (2\pi)^{-1} \oint f d\xi$ . For  $\kappa^2 > 1$ , *i.e.*, for trapped particles, it is readily noted that  $[f] = F_0(\omega_0/k_0)$ . Thus, the time asymptotic coarse-grain distribution function takes up the constant value corresponding to the equilibrium particle distribution at resonance. Meanwhile, for circulating particles,  $\kappa^2 < 1$ ,

$$[f] = F_0(\omega_0/k_0) + \frac{\partial F_0(\omega_0/k_0)}{\partial v} \frac{\pi\omega_B/k_0}{\kappa\mathbb{K}(\kappa)} \quad , \quad (5.122)$$

with  $\mathbb{K}(\kappa)$  the complete elliptic integral of the first kind. It is readily noted that the coarse-grain distribution is continuous at the separatrix  $\kappa^2 = 1$  but has discontinuous derivatives. The flattened coarse-grain particle distribution function in the resonance region explains why the nonlinear oscillations eventually fade away due to phase mixing. This is exactly the same time asymptotic state reached when a large amplitude plasma wave is externally driven, at a fluctuation level corresponding to  $\omega_B \gg \gamma_L$ , *i.e.*, the Landau damping due to resonant wave particle interactions (Mazitov, 1965; O’Neil, 1965). The main difference between the nonlinear dynamic evolution of a large amplitude wave and the beam-plasma system is in the relative value of fluctuation amplitude oscillations: in the former case, amplitude is characterized by small oscillations about an essentially constant value; whereas in the latter case, amplitude is fluctuating by an  $\mathcal{O}(1)$  quantity about the mean value, as the system evolves from the initial exponential growth, with  $\omega_B \ll \gamma_L$ , to the saturation phase, with  $\omega_B \sim \gamma_L$  (O’Neil and Winfrey, 1972; O’Neil *et al.*, 1971; Onishchenko *et al.*, 1970a,b; Shapiro and Shevchenko, 1971a,b). The absence of an evident expansion parameter makes numerical approach necessary. After resonant electrons get trapped and begin sloshing back and forth in the wave,  $\mathcal{O}(1)$  amplitude oscillations at  $\omega_B$  and harmonics progressively decrease and eventually fade away, due to phase mixing, with the wave amplitude reaching a constant level at  $\omega_B \simeq 3\gamma_L$  (Levin *et al.*, 1972a,b).

A different approach to the beam-plasma problem was given by (Al’tshul’ and Karpman, 1965, 1966), based on the general solution of the nonlinear Poisson equation

$$E_{kz} = -\frac{4\pi}{k} i\delta\hat{\rho}_k = \frac{4\pi}{k} ie \int dv \delta f_k \quad , \quad (5.123)$$

<sup>27</sup> It is worthwhile noting the difference between this time asymptotic equilibrium state, characterized by the coarse-grain distribution function (Sagdeev and Galeev, 1969), and the quasi-stationary states, which have been recently discussed (Carlevaro *et al.*, 2013) in the context of the Lynden-Bell approach (Lynden-Bell, 1967).

with  $\delta f_k$  obtained from the Vlasov equation

$$(\partial_t + ik_u)\delta f_k = -\frac{e}{m} \sum_q i(k-q)\delta\phi_{k-q} \frac{\partial}{\partial v} f_q , \quad (5.124)$$

solved for assuming a monochromatic wave. This assumption, as shown by (O'Neil, 1965; O'Neil *et al.*, 1971), is valid in the early nonlinear saturation phase. The approach of (Al'tshul' and Karpman, 1965, 1966) is relevant for the issues dealt with in Secs. V.D.2 to V.D.7. Furthermore, it touches important aspects of the theory of nonlinear oscillations in collisionless plasmas. Thus, we briefly summarize their main results hereafter. Recalling that the thermal plasma is a linear dielectric medium and  $\omega = \omega_0 + i\partial_t$  for a nearly monochromatic wave, Eq. (5.123) can be cast as

$$\frac{2}{\omega_p} \frac{\partial}{\partial t} \delta\phi_{k_0} = \frac{4\pi}{k_0^2} i e \int dv \delta f_{Ek_0} , \quad (5.125)$$

where the subscript  $E$  stands for energetic beam electrons (cf. Sec. II.E) and is dropped in the following for simplicity of notation. Introducing the standard definition

$$\delta f_k(t) = \int_{-\infty}^{+\infty} e^{-i\omega t} \delta \hat{f}_k(\omega) d\omega , \quad \text{and} \quad \delta \hat{f}_k(\omega) = \frac{1}{2\pi} \int_0^{+\infty} e^{i\omega t} \delta f_k(t) dt \quad (5.126)$$

for the Laplace transform, the solution of Eq. (5.124) for  $k = 0$  is readily obtained as

$$\hat{f}_0(\omega) = \frac{i}{2\pi\omega} F_0 + \frac{e}{m} \frac{k_0}{\omega} \int_{-\infty}^{+\infty} \left[ \delta \hat{\phi}_{k_0}(\omega') \frac{\partial}{\partial u} \delta \hat{f}_{-k_0}(\omega - \omega') - \delta \hat{\phi}_{-k_0}(\omega') \frac{\partial}{\partial u} \delta \hat{f}_{k_0}(\omega - \omega') \right] d\omega' . \quad (5.127)$$

Meanwhile, assuming vanishing initial conditions for  $\delta f_{k_0}$ ,

$$\delta \hat{f}_{k_0}(\omega) = \frac{e}{m} \frac{k_0}{\omega - k_0 u} \int \delta \hat{\phi}_{k_0}(\omega') \frac{\partial}{\partial u} \hat{f}_0(\omega - \omega') d\omega' . \quad (5.128)$$

By direct substitution of Eq. (5.128) back into Eqs. (5.125) and (5.127), one readily obtains, respectively,

$$\frac{2}{\omega_p} \frac{\partial}{\partial t} \delta\phi_{k_0} = \frac{\omega_p^2}{nk_0} i \int dv \iint_{-\infty}^{+\infty} e^{-i\omega t} \frac{\delta \hat{\phi}_{k_0}(\omega')}{\omega - k_0 u} \frac{\partial}{\partial u} \hat{f}_0(\omega - \omega') d\omega d\omega' , \quad (5.129)$$

$$\begin{aligned} \hat{f}_0(\omega) = & \frac{i}{2\pi\omega} F_0 - \frac{e^2}{m^2} \frac{k_0^2}{\omega} \iint_{-\infty}^{+\infty} \left[ \delta \hat{\phi}_{k_0}(\omega') \delta \hat{\phi}_{-k_0}(\omega'') \frac{\partial}{\partial u} \left( \frac{1}{\omega - \omega' + k_0 u} \frac{\partial}{\partial u} \hat{f}_0(\omega - \omega' - \omega'') \right) \right. \\ & \left. + \delta \hat{\phi}_{-k_0}(\omega') \delta \hat{\phi}_{k_0}(\omega'') \frac{\partial}{\partial u} \left( \frac{1}{\omega - \omega' - k_0 u} \frac{\partial}{\partial u} \hat{f}_0(\omega - \omega' - \omega'') \right) \right] d\omega' d\omega'' . \end{aligned} \quad (5.130)$$

This last equation is the analogue of the Dyson's equation [cf., *e.g.*, (Kaku, 1993)] in quantum field theory, as noted by (Al'tshul' and Karpman, 1965, 1966), and is valid for arbitrary distortion of the initial distribution function  $F_0(v)$ . The physics processes described by Eqs. (5.129) and (5.130) are schematically depicted in Fig. 5. When Eq. (5.130) is solved by formal expansion in the field amplitudes, the lowest order solution is  $\hat{f}_0(\omega) = iF_0/(2\pi\omega)$ . Assuming that

$$\delta \hat{\phi}_{k_0}(\omega) = \frac{i}{2\pi} \frac{\delta\phi_{k_0}}{\omega - \omega_{k_0}} , \quad (5.131)$$

with  $\delta\phi_{k_0}$  being the  $k_0$  field with frequency  $\omega_{k_0}$  in the linear approximation, the subsequent steps in the iterative expansion for the solution of the ‘‘Dyson’’ equation, Eq. (5.130), will have a second order pole at  $\omega = 0$ , corresponding to a secular term  $\propto t$  in the  $t$ -representation and to the second order diagram in Fig. 5 (middle panel), and so on. Similarly, in the solution of Eq. (5.129), a second order pole at  $\omega = \omega_{k_0}$  in the nonlinear expression on the right hand side corresponds to a secular term  $\propto t \exp(-i\omega_{k_0} t)$ , and so on. Even accounting for a complex frequency  $\omega_{k_0}$ , would replace the secular terms  $\propto t^\ell$  with terms  $\propto (\text{Re}\omega_{k_0}/\text{Im}\omega_{k_0})^\ell \gg 1$  (Al'tshul' and Karpman, 1965, 1966; Montgomery, 1963). For this reason, it is crucial to take into account all terms in the Dyson series, as shown in Fig. 5 (right panel, bottom frame). In general, Eqs. (5.129) and (5.130) can be written for a generic fluctuation spectrum of waves with  $|\text{Im}\omega_{k_0}/\text{Re}\omega_{k_0}| \ll 1$  under the assumption that the evolution of the fluctuating fields is dominated by the nonlinear modification of  $\hat{f}_0(\omega)$ , given by Eq. (5.130), rather than by the generation of nonlinear harmonics in the fields and the distribution function. For the case of many waves with overlapping resonances, (Al'tshul' and Karpman, 1965, 1966)

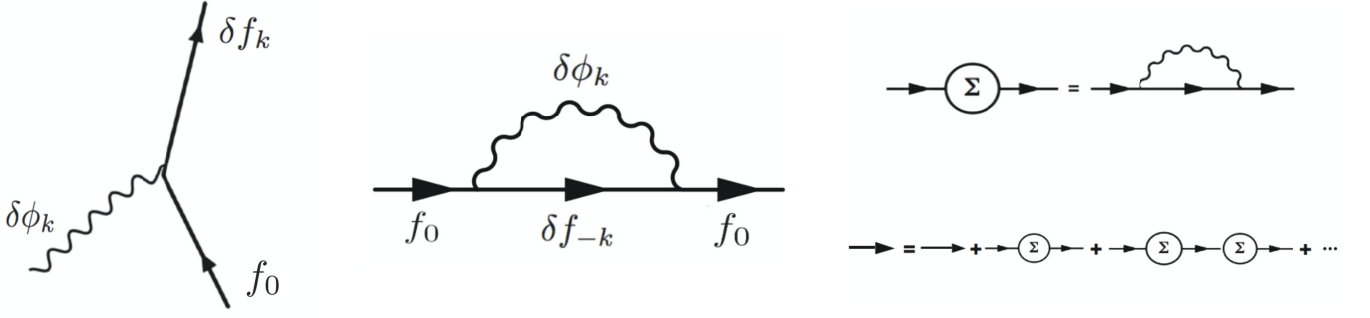


FIG. 5 Left panel: Diagram showing the generation of the distribution  $\delta f_k$  due to the interaction of  $f_0$  with the field  $\delta\phi_k$ , corresponding to the solution of Eq. (5.128). Middle panel: Nonlinear distortion of  $f_0$  due to emission and absorption of the field  $\delta\phi_k$ . Right panel: The diagram of the process is defined in the top frame, while the solution of the “Dyson” equation, Eq. (5.130), corresponds to the summation of all terms in the Dyson series (bottom) (Al’tshul’ and Karpman, 1965, 1966).

have demonstrated that Eqs. (5.129) and (5.130) reduce to the well-known quasilinear theory of a weakly turbulent plasma (Drummond and Pines, 1962; Vedenov *et al.*, 1961a). In this sense, they can be referred to as generalized quasilinear equations (Galeev *et al.*, 1965). Meanwhile, in the case of a nearly monochromatic wave with constant amplitude in time, Eq. (5.131), (Al’tshul’ and Karpman, 1965, 1966) have shown that Eq. (5.130) admits a solution which oscillates around the coarse-grain distribution in the resonant region, with a frequency spectrum given by the wave particle trapping frequency  $\omega_B$  and harmonics. More specifically,

$$F_0(u, t) = F_0(0) + \frac{\alpha}{k_0} \sum_{\ell=0}^{\infty} \frac{\beta_{\ell}}{(2\ell+1)} \frac{d}{du} \psi_{\ell} \left( \frac{k_0 u}{\alpha} \right) \left[ 1 - \cos \left( \sqrt{2\ell+1} \alpha t \right) \right], \quad (5.132)$$

with the notation  $\alpha^2 \equiv \sqrt{2} |ek_0 E_{k_0}/m| = \sqrt{2} \omega_B^2$ ,  $x = k_0 u/\alpha$ ,  $\psi_{\ell}(x) \equiv (2^{\ell} \ell! \pi^{1/2})^{-1/2} e^{-x^2/2} H_{\ell}(x)$  with  $H_{\ell}(x)$  the Hermite polynomials, and  $\beta_{\ell} \equiv \int_{-\infty}^{\infty} (dF_0(0)/dx) \psi_{\ell}(x) dx$ . Note that Eq. (5.132) describes the oscillations of particles that are trapped in the wave, which, however, do not decay in time as expected in consequence of phase mixing. Thus, the approach based on Eqs. (5.130) does not describe the relaxation to the coarse grain particle distribution function (Sagdeev and Galeev, 1969). Unlike in (Mazitov, 1965; O’Neil, 1965) for the case of the nonlinear oscillations of a large amplitude wave, which asymptotically decay in time, this solution continues oscillating as  $t \rightarrow \infty$ . It was pointed out by (O’Neil, 1965) that the reason for this stands in the assumption of negligible harmonic generation at  $k = \ell k_0 (\ell \geq 2)$  in both  $\delta\phi_k$  and  $\delta f_k$ , which breaks down on long time scales; as discussed earlier in this subsection.

## 2. The nonlinear beam-plasma system with sources and collisions

In a series of papers in 1990s, (Berk and Breizman, 1990a,b,c) reconsidered the nonlinear beam-plasma problem (cf. Sec. V.D.1) including the additional physics of sources and dissipations, and applied it to the description of nonlinear dynamics of AEs near marginal stability. In this case (Berk and Breizman, 1990a), the coarse-grain distribution function, Eq. (5.121), maintains a residual slope (Zakharov and Karpman, 1962, 1963) inside the separatrix including the phase-space of resonant trapped particles, so that a steady state can be reached when the residual nonlinear drive balances the background dissipation. The possibility of extending this analysis to the case of electrostatic waves in a plasma slab with a sheared equilibrium magnetic field  $\mathbf{B}_0$ , destabilized by an energetic particle beam with a spatial gradient transverse to  $\mathbf{B}_0$ , is discussed by (Berk and Breizman, 1990b). Meanwhile, (Berk and Breizman, 1990c) further extend the same approach to AEs destabilized by nonuniform EP sources. In general, fundamental assumptions of these analyses are: (i) one single low amplitude wave, such that linear mode structures can be assumed to drop out of the problem<sup>28</sup>; (ii) finite background dissipation that does not depend on the finite amplitude wave; (iii) wave dispersiveness set by the background plasma and independent of the EP dynamics.

<sup>28</sup> When the Hamiltonian is accidentally degenerate, *i.e.*, the resonance condition is verified for particular values of the action coordinates, the maximum excursion of the action about the resonance scales as the square root of the perturbation strength [cf., *e.g.*, (Lichtenberg and Lieberman, 1983, 2010)]

a. *Steady-state saturation of the collisional beam-plasma system.*

The saturation level of fluctuations at steady state is reached when background dissipation balances wave drive reduced by nonlinear interactions (cf. Sec. V.D.1)

$$\frac{d}{dt}T = \frac{nm}{2} \int dv v^2 \frac{\partial}{\partial t} [f] \simeq \frac{nm \omega_0^2}{2 k_0^2} \int dv \frac{\partial}{\partial t} [f] = -2\gamma_d \mathcal{W} , \quad (5.133)$$

where the left hand side is the rate of particle kinetic energy increase due to resonant wave-particle interactions and the right hand side is the wave power dissipation by background damping.

With a simple source term  $Q(v)$  and particle annihilation at a rate  $\nu(v)$ , the Vlasov equation is

$$\partial_t f + v \partial_x f + \dot{v} \partial_v f = -\nu(v) f + Q(v) . \quad (5.134)$$

For  $\nu \ll \omega_B$ , the lowest order time asymptotic  $[f]$  is still given by the coarse-grain distribution function, Eqs. (5.121) and (5.122), which is readily obtained with  $F_0(v) = Q(v)/\nu(v)$ . At next order in  $\nu/\omega_B$ , the small but finite residual slope within the wave particle trapping region,  $\kappa > 1$  with the notations of Eq. (5.120), yielding a residual drive with respect to the linear expression  $(dT/dt)_L$ , is given by (Berk and Breizman, 1990a)

$$(dT/dt) = 1.9 (\nu/\omega_B) (dT/dt)_L . \quad (5.135)$$

Thus, noting  $(dT/dt)_L = -2\gamma_L \mathcal{W}$ , Eqs. (5.133) and (5.135) readily yield the saturation level  $\omega_B \simeq 1.9(\nu/\gamma_d)\gamma_L$ .

In order to emulate a beam slowing down, (Berk and Breizman, 1990a) also consider the case of a source at fixed velocity  $v_0$  and particle drag

$$\partial_t f + v \partial_x f + \dot{v} \partial_v f = -\nu(v) f + Q_0 \delta(v - v_0) + a \partial_v f . \quad (5.136)$$

Denoting the Heaviside step function as  $H$ , the corresponding equilibrium steady state solution is  $F_0 = (Q_0/a) \times \exp[(\nu/a)(v - v_0)] H(v_0 - v)$ , which, again, yields the lowest order time asymptotic  $[f]$  in terms of the coarse-grain distribution function by Eqs. (5.121) and (5.122). For  $\omega_B^2 > ka$ , *i.e.*, for a sufficiently large perturbation, the rate at which particles cross a separatrix width in velocity space because of drag is  $\nu_{\text{eff}} = ka\omega_B^{-1} \sim \nu(\omega/\omega_B)$ . Thus,  $\omega_B > \nu_{\text{eff}} \gg \nu$  and, for adiabatically growing wave amplitude, trapping regions cannot be filled by drag, so that the distribution function eventually vanishes because of particle annihilation. In this scenario, a discontinuity is expected in the particle distribution function near the separatrix and the residual nonlinear drive is enhanced

$$(dT/dt) = (16/\pi^2) (\nu_{\text{eff}}^2/\nu^2) (\nu/\omega_B) (dT/dt)_L . \quad (5.137)$$

Using this expression, the steady state saturation level can be computed as for Eqs. (5.133) and (5.135) above.

In a more realistic description with sources and sinks, the Vlasov equation is (Berk and Breizman, 1990b)

$$d_t f = \nu_d \partial_\lambda (1 - \lambda^2) \partial_\lambda f + (\nu/v^2) \partial_v [(v^3 + v_c^3) f] + (4\pi v_0^2)^{-2} Q \delta(v - v_0) , \quad (5.138)$$

where the term  $\propto \nu_d$  on the right hand side accounts for pitch angle scattering, with  $\lambda = \mathbf{v} \cdot \mathbf{B}_0 / (vB_0)$ . Depending on the relative ordering of  $\nu$  and  $\nu_d$ , three different regimes can be identified: (i)  $\nu_d(\omega^2/\omega_B^2) \ll \nu$ , where particles slow down completely, without appreciable pitch angle scattering; (ii)  $\nu_d(\omega/\omega_B) \ll \nu < \nu_d(\omega^2/\omega_B^2)$ , particles slow down one separatrix width without appreciable diffusion; (iii)  $\nu \ll \nu_d(\omega/\omega_B)$ , particles are pitch angle scattered before they slow down one separatrix width. The regime to be expected in fusion plasmas is (iii), for which the residual nonlinear drive, given  $\nu_{\text{eff}} = \nu_d(\omega^2/\omega_B^2) \ll \omega_B$ , is given by<sup>29</sup>

$$(dT/dt) \sim (\nu_{\text{eff}}/\omega_B) (dT/dt)_L , \quad (5.139)$$

which, with help of Eq. (5.133), yields the respective saturation level.

---

<sup>29</sup> Detailed discussions of the various collisional regimes and corresponding saturation levels are given by (Berk and Breizman, 1990b).

*b. Collisional beam-plasma system with periodic and chaotic pulsations.*

Steady state solutions with constant amplitude are not the only possibility for nonlinear dynamics of the beam-plasma system. Different scenarios are possible depending on the relative ordering of  $\gamma_L$ ,  $\nu_{\text{eff}} \sim \nu_d(\omega^2/\omega_B^2)$  and  $\gamma_d$  (Berk *et al.*, 1992a; Breizman *et al.*, 1993). In Sec. V.D.1, it is shown that a finite amplitude wave modifies the particle distribution in a region of width  $\Delta v \sim \omega_B/k_0$  near an isolated resonance, eventually yielding to flattening of the (coarse-grain) distribution function by phase mixing. Meanwhile, the distribution function is reconstructed at a rate  $\nu_{\text{eff}}$ , while energy is dissipated at a rate  $\gamma_d$ . Thus, for  $\gamma_d < \nu_{\text{eff}}$ , the predicted steady state level trapping frequency is larger than the linear drive  $\omega_B \sim \gamma_L \nu_{\text{eff}}/\gamma_d$  and steady state solutions can be sustained (cf. Sec. V.D.2.a). Conversely, for  $\gamma_d > \nu_{\text{eff}}$ , the background distribution is not effectively reconstructed and, after saturation at  $\omega_B \sim \gamma_L$  (cf. Sec. V.D.1), the mode amplitude decays at rate  $\gamma_d$ , so that fluctuation bursting must be expected. The typical interval between bursts scales as  $\sim 1/\nu_{\text{eff}}$ , while the transition between steady state and bursting behaviors takes place when  $\omega_B \sim \gamma_L$  and  $\nu_{\text{eff}} = \nu_{\text{eff}0} = \nu_d \omega^2/\gamma_L^2 \simeq \gamma_d$  (Berk *et al.*, 1992a; Breizman *et al.*, 1993). Numerical particle-in-cell (PIC) simulations of a single Langmuir wave excited by an inverted (positive) gradient  $F_0(v) = Q(v)/\nu(v)$  confirm analytical predictions about bursting vs. steady-state saturation for the bump-on-tail problem (Berk *et al.*, 1995b).

Changing the externally imposed dissipation or, equivalently, changing  $\gamma \equiv \gamma_L - \gamma_d$  for fixed  $\gamma_L$ , changes the qualitative features of numerical solutions of the Vlasov-Poisson system obtained for a monochromatic wave (Berk *et al.*, 1996b). In particular,  $\omega_B = \alpha(\gamma_L - \gamma_d)$  at the maximum oscillation amplitude, with  $\alpha$  varying from  $\alpha = 3.2$  to  $\alpha = 2.9$  when  $\gamma_d/\gamma_L$  is varied from  $\gamma_d/\gamma_L = 0$  to  $\gamma_d/\gamma_L = 0.6$ . More importantly, however, when  $\gamma$  is reduced to a sufficiently low level, the amplitude of the system oscillates rather than decay at a rate  $\sim \gamma_d$  after reaching the peak amplitude at  $\omega_B \sim \gamma$ . To investigate this phenomenology near marginal stability, the Poisson's equation, Eq. (5.123), can be replaced by (Berk *et al.*, 1996b)

$$\partial_t E_{kz} = 4\pi e \int dv v \delta f_k - \gamma_d E_{kz} \quad , \quad (5.140)$$

in order to introduce an imposed extrinsic damping. Again, treating the plasma as a linear dielectric medium and using  $\omega = \omega_0 + i\partial_t$  for a nearly monochromatic wave, Eq. (5.140) becomes

$$\frac{2}{\omega_p} \frac{\partial}{\partial t} \delta \phi_{k_0} = \frac{4\pi}{k_0^2} i e \int dv \delta f_{E_{k_0}} - \frac{2\gamma_d}{\omega_p} \delta \phi_{k_0} \quad ; \quad (5.141)$$

*i.e.*, Eq. (5.125) adding an ad hoc background dissipation. Meanwhile, the Vlasov equation, Eq. (5.124), is modified to account for source/sink and collision terms on the right hand side, in the form of one of the models discussed above, *e.g.*, as in Eq. (5.134). Introducing  $E = E_0(t) \cos \xi$ , with  $\xi = k_0 z - \omega_0 t = k_0 x$  and  $\omega_0 = \omega_p$  (cf. Sec. V.D.1), and dropping subscripts  $k_0$  and  $E$  in Eq. (5.141) for the sake of simplicity, the solution of Eq. (5.134) can be cast as

$$f = f_0 + \sum_{n=1}^{\infty} \delta f_n e^{in\xi} + c.c. \quad , \quad (5.142)$$

$$\partial_t f_0 + \nu f_0 = Q(v) - \omega_B^2(t) \partial_u \mathbb{R}e \delta f_1 \quad , \quad (5.143)$$

$$\partial_t \delta f_1 + iu \delta f_1 + \nu \delta f_1 = -(1/2) \omega_B^2(t) \partial_u (f_0 + \delta f_2) \quad , \quad (5.144)$$

and so on. Here,  $\omega_B^2(t) = ek_0 E_0(t)/m$  and  $u = k_0 v - \omega_0$ , while Eq. (5.141) becomes

$$\frac{d}{dt} \omega_B^2 = -\frac{\omega_p^2}{n_0} \frac{\omega_0}{k_0} \int_{-\infty}^{\infty} \mathbb{R}e \delta f_1 du - \gamma_d \omega_B^2 \quad . \quad (5.145)$$

For monochromatic fluctuations (dropping  $\delta f_2$ ), Eqs. (5.143) to (5.145) are the  $t$ -representation of Eqs. (5.128) to (5.131), with the addition of finite  $\nu$ ,  $Q$  and  $\gamma_d$ . Near marginal stability,  $f_0 = F_0 + \delta f_0$ , with  $F_0 = Q(v)/\nu(v)$ , and the problem can be solved iteratively, with a perturbative asymptotic expansion based on the ordering  $\gamma \equiv \gamma_L - \gamma_d \sim \nu \sim |u| \ll \gamma_L$  and expansion parameter  $\omega_B^2/\nu^2 \sim \omega_B^2/u^2 \sim \omega_B^2/\gamma^2 \sim (\gamma/\gamma_L)^{1/2}$ , which applies for  $\omega_B t \ll 1$  (Berk *et al.*, 1996b). The iterative solution corresponds to writing

$$\begin{aligned} \delta f_0 &= - \int_0^t e^{-\nu(t-t_1)} \omega_B^2(t_1) \partial_u \mathbb{R}e (\delta f_{1L} + \dots) dt_1 \quad , \\ \delta f_1 &= -(1/2) \int_0^t e^{-(\nu+iu)(t-t_1)} \omega_B^2(t_1) \partial_u f_0 dt_1 \quad , \end{aligned} \quad (5.146)$$

where  $\delta f_{1L}$  is the linearized form of  $\delta f_1$ , obtained for  $f_0 \rightarrow F_0 = Q(v)/\nu(v)$ . Introducing  $\tau = (\gamma_L - \gamma_d)t$ ,  $\hat{\nu} = \nu/(\gamma_L - \gamma_d)$  and  $A(\tau) = (\omega_B^2/\gamma^2)\gamma_L^{1/2}/\gamma^{1/2}$ , the validity limits of the asymptotic analysis impose  $\tau \ll (\gamma/\gamma_L)^{-1/4}$  (from  $\omega_B t \ll 1$ ) and  $A \sim \hat{\nu} \sim 1$ . Meanwhile, the iterative solution of Eqs. (5.145) and (5.146) yields

$$\frac{d}{d\tau}A = A - \frac{1}{2} \int_0^{\tau/2} z^2 A(\tau - z) dz \int_0^{\tau-2z} A(\tau - z - x) A(\tau - 2z - x) e^{-\hat{\nu}(2z+x)} dx . \quad (5.147)$$

Here, the occurrence of the secular term  $\propto z^2$  in the normalized time variable is a consequence of the truncation of the Dyson series in the iterative expansion (cf. Fig. 5), as discussed below Eq. (5.131). Equation (5.147) admits a fixed point solution  $A_0 = 2\sqrt{2}\hat{\nu}^2$ , which is stable for  $\hat{\nu} > \hat{\nu}_{cr} \simeq 4.38$ . For  $\hat{\nu} < \hat{\nu}_{cr}$  the solution  $A(\tau)$  first oscillates and, for further decreasing  $\hat{\nu}$ , it loses the periodic behavior, entering a chaotic regime (Breizman *et al.*, 1997). Meanwhile, for sufficiently low values of  $\hat{\nu}$  the system exhibits a finite time singularity, which is unphysical and consequence of the truncation of the Dyson series.

The work of (Berk *et al.*, 1996b) was generalized by (Breizman *et al.*, 1997) [cf. also (Berk *et al.*, 1997a)] to the generic case of weakly unstable modes excited by resonant wave-particle interactions, for which

$$\frac{d}{d\tau}A = A - e^{i\phi} \int_0^{\tau/2} z^2 A(\tau - z) dz \int_0^{\tau-2z} A(\tau - z - x) A^*(\tau - 2z - x) e^{-\hat{\nu}(2z+x)} dx . \quad (5.148)$$

Here, the factor  $e^{i\phi}$  depends on the linear physics of the underlying mode. (Breizman *et al.*, 1997) also investigated the effect of replacing the source/collisional term  $-\nu(f - F_0)$  and  $F_0 = Q(v)/\nu(v)$  with a diffusive-like collision operator  $\nu_{\text{eff}}^3(\partial^2/\partial\Omega^2)(f - F_0)$ , with  $\Omega = \dot{\xi} = \partial H/\partial I$  and  $(I, \xi)$  the action-angle coordinates of the relevant wave-particle resonance. Thus,  $\exp[-\hat{\nu}(2z+x)]$  in Eq. (5.148) is replaced by  $\exp[-\hat{\nu}^3 z^2(2z/3+x)]$  with  $\hat{\nu} = \nu_{\text{eff}}/\gamma$ , yielding

$$\frac{d}{d\tau}A = A - e^{i\phi} \int_0^{\tau/2} z^2 A(\tau - z) dz \int_0^{\tau-2z} A(\tau - z - x) A^*(\tau - 2z - x) e^{-\hat{\nu}^3 z^2(2z/3+x)} dx . \quad (5.149)$$

Similar to Eq. (5.147), Eqs. (5.148) and (5.149) also admit a fixed point for  $\hat{\nu} > \hat{\nu}_{cr}$ . At  $\hat{\nu} = \hat{\nu}_{cr}$  a first bifurcation occurs and  $A(\tau)$  has a solution in the form of a limit cycle, which then goes through subsequent period doubling bifurcations for further decreasing  $\hat{\nu}$  and eventually becomes chaotic (Breizman *et al.*, 1997; Fasoli *et al.*, 1998; Heeter *et al.*, 2000). In the case of Eq. (5.149),  $\hat{\nu}_{cr} \simeq 2.05$  for  $|\phi| \ll 1$  (Breizman *et al.*, 1997).

Systematic numerical investigations of the Vlasov-Poisson system were carried out (Lesur *et al.*, 2009; Vann *et al.*, 2005, 2003) in order to characterize the fully nonlinear solutions of Eq. (5.140) and of the Vlasov equation for monochromatic waves with different source/sink and collisionality models. In particular, (Lesur *et al.*, 2009) and, more recently, (Lesur and Idomura, 2012) adopt a model collision term in the form of Eq. (5.134) and carefully discuss the validity limits of aforementioned analytical works, comparing fully nonlinear solutions with analytic ones where appropriate. It is shown that there are conditions where the thermal plasma does not respond as a linear dielectric medium, *e.g.*, when the resonance involves a finite amount of thermal electrons. The bifurcation diagram in the  $(\gamma_d, \nu)$  parameter space, similar to that discussed by (Vann *et al.*, 2003), confirms that, at fixed  $\gamma_d$  and for decreasing values of  $\nu$ , numerical solutions are damped, converge to a steady state (cf. Sec. V.D.2.a), are periodic, or chaotic, or characterized by frequency sweeping phase space structures. This latter behavior is discussed in Sec. V.D.2.c and corresponds to the parameter regime, where the analytic solutions of Eqs. (5.147) to (5.149) exhibit finite time singularity. Furthermore, (Lesur *et al.*, 2009) demonstrate the existence of subcritical states, consistent with former numerical results (Berk *et al.*, 1999) that nonlinear excitation of phase space structures is possible if fluctuation is initialized at sufficiently large amplitude,  $\omega_B^2 \sim (\nu + \gamma)^{5/2}(\gamma_L)^{-1/2}$  (Berk *et al.*, 1999). Metastable kinetic modes are also investigated by (Nguyen *et al.*, 2010b), where it is shown that purely nonlinear steady-state regimes are found by numerical simulations, when the nonlinear reduction of the resonant damping rate due to thermal plasma is larger than the corresponding reduction of the EP drive. Such processes may be relevant for BAE nonlinear dynamics (cf. Sec. IV.B.2), for which purely nonlinear steady-state regimes could exist for typical tokamak equilibrium conditions (Nguyen *et al.*, 2010a). Nonlinear instabilities of phase-space structures in both marginally unstable and linearly stable (subcritical) regimes have been recently discussed by (Lesur and Diamond, 2013).

### c. Nonlinear dynamics of phase-space holes and clumps.

For sufficiently small  $\hat{\nu}$ , Eqs. (5.148) and (5.149) exhibit the same finite time singularity of Eq. (5.147) due to the unphysical truncation of the Dyson series (cf. Fig. 5). This fourth dynamic regime of Eqs. (5.147) to (5.149), in addition to steady-state (cf. Sec. V.D.2.a), periodic and chaotic regimes (cf. Sec. V.D.2.b) (Breizman *et al.*, 1997),

was investigated by numerical solution of the Poisson's equation, Eq. (5.141), and the Vlasov equation with a variety of source/sink and collision models (Berk *et al.*, 1999, 1997a,b; Breizman *et al.*, 1997). In particular, it was shown that numerical solutions are characterized by the formation of pairs of phase space holes (Berk *et al.*, 1970; Berman *et al.*, 1983; Dupree, 1982; Tetreault, 1983) and clumps (Berman *et al.*, 1983; Dupree, 1970, 1972, 1982; Tetreault, 1983). After formation, holes and clumps move away from the original resonance in velocity space, corresponding to energy extraction from the particle distribution function and to respectively upward (hole) and downward (clump) frequency sweeping phase space structures, which can be viewed as Bernstein-Greene-Kruskal (BGK) modes (Bernstein *et al.*, 1957). Since the work by (Breizman *et al.*, 1997), the steady-state, periodic and chaotic regimes of the solution of the Vlasov-Poisson system are referred to as “soft” nonlinear behaviors, to discriminate them from the “hard” nonlinear regime, where hole/clump structures are formed. The definition of a “hard” nonlinear regime for describing the finite time singularity of the solutions of Eqs. (5.147) to (5.149) is more properly justified by noting that, for fixed  $\nu_{\text{eff}}$ , sufficiently low  $\hat{\nu}$  can be achieved for sufficiently strong net drive  $\gamma = \gamma_L - \gamma_d$ . In the work by (Berk *et al.*, 1999), it was noted that this “hard” regime is not observed for  $\gamma_d/\gamma_L \lesssim 0.4$ . On the other hand, (Lesur *et al.*, 2009) show that frequency chirping is observed in numerical simulations for  $\gamma_d/\gamma_L$  as low as  $\gamma_d/\gamma_L = 0.2$ .

Recently, (Lilley *et al.*, 2009) re-considered Eqs. (5.143) to (5.145) with a model collision term in the form

$$d_t f = (\nu^3 k_0^{-2} \partial_v^2 + \alpha^2 k_0^{-1} \partial_v - \beta) (f - F_0) \quad , \quad (5.150)$$

where  $F_0$  is the equilibrium distribution function and  $\nu$ ,  $\alpha$  and  $\beta$  control, respectively, velocity space diffusion, dynamical friction and particle annihilation rate. Equations. (5.147) to (5.149) are then generalized to

$$\frac{d}{d\tau} A = A - \frac{1}{2} \int_0^{\tau/2} z^2 A(\tau - z) dz \int_0^{\tau-2z} A(\tau - z - x) A^*(\tau - 2z - x) e^{-\hat{\nu}^3 z^2 (2z/3+x) - \hat{\beta} (2z+x) + i\hat{\alpha}^2 z(z+x)} dx \quad , \quad (5.151)$$

with  $\hat{\nu} = \nu/\gamma$ ,  $\hat{\alpha} = \alpha/\gamma$ ,  $\hat{\beta} = \beta/\gamma$  and  $\gamma = \gamma_L - \gamma_d$ . For  $\hat{\nu} = \hat{\beta} = 0$ ; *i.e.*, with dominant dynamical friction, (Lilley *et al.*, 2009) showed that Eq. (5.151) always exhibits finite time singularity, in contrast to Eqs. (5.147) to (5.149), whose evolutions exhibit both “soft” and “hard” nonlinear dynamic behaviors (cf. Sec. V.D.2.b). This result is confirmed by numerical solutions of Eqs. (5.141) [or Eq. (5.145)] and (5.150), which show frequency sweeping holes and clumps when dynamical friction is the dominant collisional process (Lilley *et al.*, 2010).

The first analytical theory of hole-clump frequency sweeping was proposed by (Berk *et al.*, 1999, 1997b), assuming that the frequency separation of holes and clumps is larger than  $\gamma_L$  and  $\omega_B$ , so that they are treated independently as isolated structures, and postulating an adiabatic evolution of mode amplitude and frequency, *i.e.*,  $|\dot{\omega}| \ll \omega_B^2$ ,  $|\dot{\omega}_B| \ll \omega_B^2$ , etc.. Defining  $\omega = \omega_0 + \delta\omega(t)$ , the angle coordinate in the wave moving frame becomes  $q = \xi - \int_0^t \delta\omega(t') dt'$  and, using the generating function  $F_2 = (p + \delta\omega(t)) \left( \xi - \int_0^t \delta\omega(t') dt' \right)$  for the corresponding canonical transformation, with  $p = \Omega - \omega_0 - \delta\omega(t)$ ,  $\xi$  defined above in this section and  $\Omega = \dot{\xi}$ , the Hamiltonian is (Berk *et al.*, 1999)

$$\mathcal{H} = p^2/2 - \delta\omega^2/2 - \omega_B^2 \cos q + q\delta\dot{\omega} \quad . \quad (5.152)$$

Meanwhile, Eq. (5.141) becomes

$$\left( \frac{d}{dt} + \gamma_d \right) A(t) = -\frac{i}{\pi^2} \frac{\gamma_L}{\partial F_0 / \partial \Omega} \int dq dp e^{-iq - i \int_0^t \delta\omega(t') dt'} f(q, p, t) \quad . \quad (5.153)$$

Since wave amplitude and frequency change slowly, there exist an adiabatic action invariant and, at lowest order, particle response is independent of the corresponding angle. Thus,  $f$  slightly deviates from the coarse-grain distribution (cf. Sec. V.D.1) and, inside the separatrix,  $f = F_0 + g$  that, at lowest order, becomes (Berk *et al.*, 1999)

$$g \simeq g_0 = F_0(\omega_0) - F_0(\omega_0 + \delta\omega) \quad . \quad (5.154)$$

Furthermore, the dynamics is adiabatic and maintains near marginal stability at every instant. Therefore, frequency sweeping, connected with the hole/clump evolution, is obtained from the condition of balancing background dissipation with power released by hole/clump motion in phase space (Berk *et al.*, 1999). By means of Eqs. (5.153) and (5.154), it is possible to show that the adiabatic evolution of hole-clump motion in the phase space becomes

$$\frac{\omega_B}{\gamma_L} = \frac{16}{3\pi^2} \quad , \quad \text{and} \quad \frac{\delta\omega}{\gamma_L} = \frac{16}{3\pi^2} \sqrt{\frac{2}{3}} (\gamma_d t)^{1/2} \quad ; \quad (5.155)$$

having assumed  $\hat{g}(x) = [F_0(\omega_0 + x) - F_0(\omega_0)] / [F_0'(\omega_0)x] \simeq 1$ . This result consistently describes the adiabatic evolution of hole/clump structures for times  $|\omega_B t| \gg 1$ , as implied by the assumption  $|\delta\omega| \gg \omega_B$ . This limit is the opposite

one with respect to the  $|\omega_B t| \ll 1$  assumption underlying Eqs. (5.147) to (5.149) and reflects the condition under which  $f$  is maintained near marginal stability during the adiabatic evolution of hole/clump structures.

The theory of adiabatic frequency chirping of hole/clump structures in phase space for the bump-on-tail problem near marginal stability was recently investigated by (Breizman, 2010), extending the water bag model of driven, continuously phase-locked coherent structures in uniform unmagnetized plasmas and of the associated BGK modes, developed by (Barth *et al.*, 2008; Khain and Friedland, 2007). The theoretical analysis of (Breizman, 2010) assumes that the background plasma can be described as a linear dielectric medium (O’Neil *et al.*, 1971) (cf. Sec. V.D.1) and solves Poisson’s equation for the BGK mode in terms of the self-similar scalar potential

$$\delta\phi_{k_0} \equiv -(1/e)U[z - s(t); t] , \quad (5.156)$$

where  $U[z - s(t); t]$  is a periodic function of  $z - s(t)$  and a slowly varying function of  $t$ . The wave phase velocity  $\propto \dot{s} = ds(t)/dt$ , with  $\dot{s}_0 = \omega_0/k_0$  at the initial time, is determined by the condition that the power released by the phase-space structure motion balances collisional dissipation due to the friction force exerted by bulk plasma electrons. The exact nonlinear solution of this problem (Breizman, 2010) shows, as expected from Eq. (5.154), that  $U[z - s(t); t]$  depends on the narrow depletion (hole) or protrusion (clump) inside the separatrix; *i.e.*, on  $F_0(\dot{s}) - F_0(\dot{s}_0)$ . Meanwhile, assuming that the motion of the hole/clump structure is adiabatic and maintained near marginal stability, the predicted time evolution of the BGK mode recovers Eq. (5.155) in the early stage, where  $\dot{s} \simeq \dot{s}_0$ ; but it can significantly depart from that at later times for significant deviations of  $\dot{s}$  from  $\dot{s}_0$ . In this respect, this model can describe long range frequency sweeping events (cf. also Sec. V.D.3), provided that the thermal plasma response remains that of a linear dielectric medium. For a more detailed description of this recent theoretical analysis, we refer the reader to the original work (Breizman, 2010) [cf. also (Breizman, 2011; Breizman and Sharapov, 2011)].

The first evidence of long range frequency sweeping was reported in numerical simulations of Eqs. (5.140) and (5.150) with  $\alpha = \nu = 0$ , aimed at investigating the nonlinear behaviors of strongly driven 1D bump-on-tail systems (Vann *et al.*, 2007), with similar values of the thermal plasma and beam densities and as well as velocity spread. In these simulations, upwards frequency sweeping holes are preferentially formed, connected with strong nonlinear distortions of both thermal and energetic particle distribution functions (cf. Sec. V.D.1). Meanwhile, only the time averaged particle distribution function is maintained near marginal stability, with a structure that is more stable than the marginal distribution function (Vann *et al.*, 2007), as it is expected for strongly nonlinear bursting behaviors, following which the particle distribution function is slowly rebuilt by external sources.

For significantly less strong drive and near mode marginal stability, numerical simulation results of Eqs. (5.141) and (5.150) confirm the existence of the long range frequency sweeping events described by (Breizman, 2010, 2011; Breizman and Sharapov, 2011), which correspond to convective particle transport in buckets, due to the adiabatic evolution of the underlying BGK modes. The frequency sweeping phase space structures, described by (Lilley *et al.*, 2010), move upwards (holes) and downwards (clumps) until the nonlinear frequency shift exceeds the frequency width of the linear unstable spectrum<sup>30</sup>, which must be much smaller than the frequency of the initial linear instability as underlying assumption of the adopted model<sup>31</sup>. Thus, holes and clumps eventually “stuck-up” and, by resonance overlap, cause a relaxation of the particle distribution function to a plateau extending throughout the linearly unstable region (Lilley *et al.*, 2010), corresponding to maximized energy extraction from fast particle phase space. This extended flattening has been recently shown to be more important near marginal stability than quasi-linear diffusion in the presence of many modes (Lilley and Breizman, 2012). Long range chirping also occurs in the collisionless limit, near marginal stability. In this case, the continuous generation of hole/clump pairs is due to the steepening of the ambient distribution function in the wake of such structures (Lilley *et al.*, 2010).

### 3. The bump-on-tail problem as paradigm for Alfvén Eigenmodes near marginal stability

A very detailed discussion of applications of the bump-on-tail paradigm to AE nonlinear dynamics is given by (Breizman and Sharapov, 2011). Thus, readers that are specifically interested in these issues are referred to this recent review paper. In this section, we only discuss the underlying physics assumptions on which such applications are based. Meanwhile, Sec. V.D.4 presents different approaches that are used to investigate AE nonlinear dynamics near marginal stability and to interpret their experimental observations; removing some of the limiting assumptions of the 1D bump-on-tail paradigm.

<sup>30</sup> Here, by frequency width of the linear unstable spectrum, we mean that which would be obtained in an infinite 1D plasma system, to avoid the discretization effect of the continuous spectrum imposed by the finite length of the system.

<sup>31</sup> Note, however, that using Eq. (5.140) and including the kinetic response of the thermal plasma component allows the investigation of nonlinear frequency shift of the order of the linear mode frequency (Vann *et al.*, 2007).

The first application of the bump-on-tail paradigm to experimental observations is the interpretation of the pitchfork splitting of TAE spectral lines in JET during Ion Cyclotron Resonance Heating (ICRH) (Fasoli *et al.*, 1998; Heeter *et al.*, 2000) as manifestation of the “soft” nonlinear regime of the bump-on-tail nonlinear dynamics (Breizman *et al.*, 1997). More precisely, (Fasoli *et al.*, 1998) used the frequency spectrum of the limit cycle solution of Eq. (5.149) at the bifurcation point; *i.e.*, with  $\hat{v} = \hat{v}_{cr} \simeq 2.05$  for  $|\phi| \ll 1$  (cf. Sec. V.D.2), and compared it with high resolution measurements of TAE frequency. This work motivated further analyses, aimed at providing information on the values of  $\gamma_L$ ,  $\gamma_d$  and  $\nu_{\text{eff}}$  from MHD spectroscopy (Fasoli *et al.*, 2002; Pinches *et al.*, 2004a,b), with the advantage of using a simple paradigm model for interpreting some features of AE experimental observations and of having information on local kinetic plasma parameters, which is otherwise difficult to obtain. In the work by (Pinches *et al.*, 2004a), it was also noted that the frequency chirping expression from Eq. (5.155) agrees with the experimentally observed chirping in experimental devices near marginal stability. Meanwhile, (Vann *et al.*, 2005) interpreted the observation of frequency chirping AEs in MAST (Gryaznevich and Sharapov, 2004; Pinches *et al.*, 2004a) as evidence of the “hard” nonlinear regime of the bump-on-tail nonlinear dynamics (Breizman *et al.*, 1997).

The different types of chirping modes observed in MAST (Gryaznevich and Sharapov, 2006; Gryaznevich *et al.*, 2008) have recently attracted significant interest in connection with the different dynamic behaviors that are predicted by the 1D bump-on-tail paradigm with different collision models and EP sources (Lilley *et al.*, 2009, 2010). In particular, special emphasis was given to numerical solutions of Eqs. (5.145) and (5.150), showing that frequency sweeping holes and clumps are the only type of nonlinear behavior when dynamical friction dominates (cf. Sec. V.D.2.c). These findings have been proposed by (Lilley *et al.*, 2009, 2010) as possible explanation of why “soft” nonlinear behaviors are expected for ICRH heated plasmas, with prevailing velocity space diffusion, whereas Neutral Beam Injection (NBI), mostly affected by dynamical friction, generally yields “hard” nonlinear regimes<sup>32</sup>.

As application of the numerical method by (Lesur *et al.*, 2009) (cf. Sec. V.D.2), and with a model collision term in the form of Eq. (5.150), (Lesur *et al.*, 2010) analyzed experimental measurements of quasi-periodic chirping TAE in JT-60U (Oyama and the JT-60 Team, 2009) and developed a fitting procedure for calculating  $\gamma_L$ ,  $\gamma_d$  and collision frequencies from the frequency spectrum provided by Mirnov coil measurements at the plasma edge. Reconstructed drive and damping rates are in qualitative and quantitative agreement with experimental findings, as are the reconstructed collision frequencies compared with values from experimental equilibrium data. Furthermore, dynamical friction and velocity-space diffusion are found to be essential to reproduce nonlinear features observed in experiments, with dynamical friction playing a crucial role in the asymmetry between hole and clump chirping (Lesur and Idomura, 2012; Lesur *et al.*, 2010), as also noted by (Lilley *et al.*, 2009, 2010). These analyses (Lesur *et al.*, 2010) clarify that TAE in JT-60U typically exist in regimes away from marginal stability and that frequency sweeping events are generally non-adiabatic. This is indeed not surprising as adiabatic nonlinear dynamics is in one-to-one correspondence with the proximity of the system to marginal stability [cf. Sec. V.D.2.c) and Eq. (5.155)].

The applicability of the bump-on-tail paradigm to AE nonlinear dynamics requires that the system be sufficiently close to marginal stability that the three fundamental assumptions listed at the beginning of Sec. V.D.2 are preserved. More precisely, the fluctuation-induced EP excursions must be small compared with the radial wavelength (Berk and Breizman, 1990b,c), which allows assuming constant mode amplitude in the radial direction as implicitly required by the formal equivalence  $r \leftrightarrow v$ . Quantitatively, how close the system must be to marginal stability in order to use the 1D bump-on-tail paradigm is discussed in Sec. V.D.5. The answer depends on the type of resonant EPs that are considered as well as on the wave dispersive properties and mode structures; *i.e.*, on the plasma nonuniformity and equilibrium geometry. For circulating resonant EPs, for which the validity limits of the bump-on-tail paradigm are less stringent, the upper bound on the drive strength is in the range  $(\gamma_L/\omega_0) \lesssim 10^{-2}$ . Meanwhile, for EPM (Chen, 1994) the bump-on-tail paradigm is never applicable, since mode structure and frequency depend on EPs and frequency dependent background damping is due to the SAW continuous spectrum (cf. Secs. IV.B.4 and V.D.6). In order to partly overcome these restrictions and with the aim of investigating long range chirping modes in MAST (Gryaznevich and Sharapov, 2006), which, in some conditions, suggest that modes may be chirping down from the TAE frequency gap into the continuous spectrum, (Ge Wang and Berk, 2012) have proposed to add a complex contribution to the otherwise fixed damping rate, which is frequency dependent and modeled to account for the coupling with the SAW continuum. While this assumption captures some aspects of frequency sweeping modes when the mode is outside the frequency gap, other issues remain open (Ge Wang and Berk, 2012), connected with the existence of “singular” mode structures in the continuous spectrum and the other general assumptions mentioned above (cf. Sec. V.D.2). These same conditions for the applicability of the 1D bump-on-tail paradigm also imply that small EP redistributions

---

<sup>32</sup> It is worthwhile mentioning that experimental observations of “hard” nonlinear behaviors in ICRH heated plasmas also exist, as in the case of high-frequency fishbones (cf. Sec. IV.B.1 and V.D.7).

are expected in the case of an isolated resonance and that the long range frequency sweeping events, described by (Breizman, 2010, 2011; Breizman and Sharapov, 2011; Lilley and Breizman, 2012; Lilley *et al.*, 2010), have no counterpart in AE or EPM nonlinear dynamics. In fact, by exchanging  $r \leftrightarrow v$ , these events would correspond to local radial perturbations in the EP distribution function propagating across  $\mathbf{B}_0$  for a distance comparable with the EP equilibrium profile scale length. Thus, the absence of mode structures and plasma nonuniformities in this model, makes improper its generalization to either AE or EPM nonlinear dynamics in toroidal plasmas (cf. Sec. V.D.5.b).

Frequency sweeping is a very important phenomenon, as recognized since early experimental observations of chirping AEs and EPMs (cf. Sec. IV.C) and the first theoretical analyses of these phenomena (Berk and Breizman, 1995), emphasizing that wave-particle energy exchange can be enhanced by resonance sweeping. In particular, (Berk and Breizman, 1995) show that this enhancement is higher for adiabatic than for non-adiabatic frequency chirping. This result is consistent with the phenomenology of autoresonance (Meerson and Friedland, 1990), discussed in Sec. V.E, where adiabatic chirping of a phase-locked resonance structure is imposed externally for optimized energy extraction from the particle phase space. When the system dynamically evolves sufficiently near marginal stability, an adiabatic evolution of hole/clump structures may be expected for nonlinear AEs. In these conditions, described in Sec. V.D.2.c, the coarse-grain particle distribution function (cf. Sec. V.D.1) in the resonance region preserves its value at the initial linear resonance and its dynamics is set by the balance between the power extraction from the particle phase space and the energy dissipation rate, determined by background damping and collisions (Breizman, 2010). However, in the case of AE and EPM nonlinear dynamics, the frequency sweeping rate is self-consistently determined by the evolution of the system, composed by particles and fluctuations. It is, thus, the maximization of the wave-particle power rather than energy exchange that determines the self-consistent mode frequency evolution. For sufficiently strong drive that radial mode structures as well as plasma nonuniformity and equilibrium geometry become important, non-adiabatic frequency sweeping via phase locking becomes the condition for maximized wave-particle power exchange (cf. Sec. V.D.5.b) and is associated with rapid EP profile redistributions (Gorelenkov *et al.*, 2000; Zonca and Chen, 2000). For EPM, furthermore, new distinctive features and non-adiabatic bursting behaviors that are discussed in Sec. V.D.6 are expected, due to the interplay between nonlinear dynamics, mode structures, and EP transports.

Deviation from adiabatic frequency sweeping for sufficiently strong drive is also expected in the solutions of the 1D bump-on-tail problem. This is observed, *e.g.*, by numerical simulations of Eqs. (5.140) and (5.150) with  $\alpha = \nu = 0$ , showing non-perturbative and fast chirping events with frequency sweeping  $\propto t$  rather than  $\propto t^{1/2}$ . These are qualitatively similar to EPM in their general phenomenological features, as they involve bursting behaviors of a strongly driven nonlinear system. Non-adiabatic processes also underly the formation of phase-space structures, such as clumps and holes. In fact, phase-space structures can be formed only if the separatrix of the initial resonance can be crossed by particles before they become trapped in the structures that are about to form and then separate; which is typically the case for  $\omega_{BT} \sim 1$ . This is the mechanism underlying, *e.g.*, the continuous generation of hole/clump pairs in the collisionless 1D bump-on-tail problem near marginal stability (Lilley *et al.*, 2010) (cf. Sec. V.D.2.c); with similarities to what occurs in the case of EPM nonlinear dynamics (Briguglio, 2012; Briguglio *et al.*, 2013; Zonca *et al.*, 2005) (cf. Sec. V.D.5.b). However, in both these examples, the absence of an intrinsic interplay between mode structures and particle transports in the 1D bump-on-tail problem remains a crucial and fundamental difference.

We now briefly remark on the case of many modes, which is less explored in depth than the single-mode case discussed above. The role of radial mode structures is more subtle in the case of the dense spectrum of AEs characterizing burning plasmas (Chen and Zonca, 2007a) (cf. Sec. IV), where resonance overlap (Chirikov, 1979) of finite size phase space islands can yield enhanced stochastic transport (Breizman *et al.*, 1993; Hsu and Sigmar, 1992; Sigmar *et al.*, 1992). The qualitative scenario of onset of stochastic transport within the 1D bump-on-tail paradigm has been recently reviewed by (Breizman, 2011; Breizman and Sharapov, 2011) and the implications of quasi-linear diffusion in the presence of many modes have been discussed by (Lilley and Breizman, 2012). Sufficiently above stochasticity threshold and for a sufficiently dense and broad AE spectrum, finite radial mode structures and, thus, plasma nonuniformities are expected to not significantly affect diffusive transport. Nonetheless, equilibrium geometry will still play important roles in setting the wave-particle decorrelation time via wave particle resonance conditions (Chen, 1999), as noted in the work by (Zhang *et al.*, 2010b) on EP turbulent transport (cf. Sec. VI.C) and as it more generally applies to turbulent transport [cf., *e.g.*, (Lin *et al.*, 2007)]. The detailed mechanisms by which a 1D uniform plasma in the presence of many modes reaches the onset condition for diffusive transport by stochastization of particle orbits in the phase-space, due to resonance overlap (Chirikov, 1979), has been addressed by (Breizman *et al.*, 1993). Onset of stochasticity is rarely global in phase space (Lichtenberg and Lieberman, 1983, 2010) and, actually, the energy release from the particle distribution function in the considered phase-space region affected by diffusive transport may induce the growth of additional fluctuations, otherwise disallowed, in adjacent phase-space domains, where local gradients are enhanced as predicted, *e.g.*, by Eqs. (5.121) and (5.122). This “domino effect” (Berk *et al.*, 1996a, 1995a) qualitatively resembles that of avalanches in sandpile systems involving self organized criticality (SOC) (Bak *et al.*, 1987); *i.e.*, of

“chain reactions” of transport events. For investigating this process applied to multiple toroidal mode number AEs, (Berk *et al.*, 1995a) introduced a “line-broadened quasi-linear burst model” for treating resonance overlap of modes with bursting behavior and applied it to characterize the nonlinear response of driven systems in weak turbulence theory (Berk *et al.*, 1996a). These studies suggest that, near the onset of stochasticity, especially in present day experiments, where the AE spectrum is discrete and characterized by moderate mode numbers, equilibrium geometry and nonuniformity of plasma profiles significantly affect nonlinear dynamics through radial mode structures and their influence on nonlinear particle orbits, whose typical size is of the order of the radial width of the single poloidal Fourier harmonics [cf. Eq. (4.13) in Sec. IV] for typical values of the linear mode growth rate (cf. Sec. V.D.5). This is supported by recent findings of test particle simulations of EP transports in DIII-D (White *et al.*, 2010a,b), which are the usually adopted method for studying EP transport in experimentally relevant conditions (cf. Sec. V.D.4) and show that the stochastic threshold depends on modeling details, as reported in Sec. VI.A. These physics may also be addressed within the theoretical framework of Eq. (5.3), as shown in Sec. V.D.5.c. Such investigations, however, belong to ongoing research activities and are beyond the scope of the present review. These issues are also further discussed in Sec. VII.A, when addressing EP transport studies in the presence of many modes.

#### 4. Numerical simulations of perturbative excitation of Alfvén Eigenmodes

For the investigation of AE nonlinear dynamics driven by EPs, simplification of the numerical treatment is possible by considering perturbative EP dynamics<sup>33</sup>. The mode structures, meanwhile, are computed from a linear stability analysis and taken to be fixed. More specifically, the EP distribution function, computed in the given AE fields taking into account sources and collisions, yields the corresponding EP currents, which are used to obtain the time evolution of wave amplitudes and phases (Chen and White, 1997). This numerical approach is very efficient and can provide an accurate description of AE nonlinear evolution with perturbative EP dynamics even in the presence of many modes, provided that the predicted nonlinear frequency shifts are consistent with the fixed radial structure of the single poloidal Fourier harmonics [cf. Eq. (4.13) in Sec. IV]<sup>34</sup>. For practical applications and comparisons of numerical simulation results of EP transport with experimental observations, however, further simplifications are often employed. In fact, test particle analyses are adopted (cf. Sec. VI.A), where not only AE mode structures are assumed from linear stability computations, but also mode amplitude and phases are given from experimental data.

Perturbative EP numerical analyses have been adopted by (Wu *et al.*, 1994) for investigating the effect of a single TAE mode in typical TFTR and ITER plasmas; and by (Wu *et al.*, 1995), where the saturation level of the bump-on-tail problem in the absence of collisions and background dissipation was found to be  $\omega_B \simeq 3.3\gamma_L$ , consistent with (Levin *et al.*, 1972a,b), while the saturation of a  $n = 3$  TAE mode in ITER was estimated to scale as  $\omega_B \simeq 4\gamma_L$ . With a similar approach, (Candy *et al.*, 1997) have developed a Lagrangian representation for AEs time evolution driven weakly by a perturbative EP population. Meanwhile, introducing collisions with the simplified model of Eq. (5.134), (Vernon Wong and Berk, 1998) verified the scaling of steady-state TAE saturation amplitude predicted by Eq. (5.135) and, for decreasing collisionality, the existence of amplitude fluctuations, whose down- and up-shifted frequency components are compatible with the  $\propto t^{1/2}$  scaling of Eq. (5.155). A more systematic theoretical framework for handling collisions was presented by (Chen and White, 1997) considering the same collision operator of Eq. (5.138), by means of which (Chen *et al.*, 1999) have verified the theoretically predicted scaling of the saturation amplitude with linear growth rate and collision rate, as derived from Eq. (5.139). This approach was used to predict the saturation levels of TAE excited by fusion alpha particles in TFTR and to successfully compare theoretical predictions with experimental observations (Gorelenkov *et al.*, 1999a). The same approach was also used by (Bergkvist and Hellsten, 2004) to show that ICRH can also have an effect similar to the pitch angle scattering term in Eq. (5.138), pointing out that both processes have a diffusive nature in velocity space, but Coulomb collisions are more effective at low energies while ICRH interactions are more effective at high energies. In plasma scenarios typical for JET, and accounting for collisions and ICRH on the same footing, (Bergkvist *et al.*, 2005) have shown that time evolution of TAE amplitude, computed with the perturbative analysis of (Chen and White, 1997; Chen *et al.*, 1999), is consistent with experimental observations and typically dominated by the effect of ICRH. For example, accounting for ICRH effects improves the comparison of the computed numerical TAE spectrum with the observed splitting of TAE spectral lines (Fasoli *et al.*, 1998; Heeter *et al.*, 2000). Furthermore, due to the fact that ICRH acts as an effective resonance broadening (Bergkvist *et al.*, 2007), ICRH is expected to be important in the onset of stochasticity in phase space and enhanced fluctuation

<sup>33</sup> This method does not apply to EPs, for which even the linear description requires a non-perturbative analysis of the EP response (Chen, 1994) (cf. Sec. IV.B.4).

<sup>34</sup> We recall, here, that the radial structure of poloidal Fourier harmonics changes with the mode frequency and tends to become singular as the accumulation point of the SAW continuous spectrum is approached.

induced transport in the case of resonance overlap in the case of many modes (cf. Secs. VI.A and VII.A). More recently, (Fu *et al.*, 2010) discussed plasma micro-turbulence as a possible mechanism to enhance EP phase space diffusion (cf. Sec VI.C). In particular, letting  $D_r$  being the EP radial diffusion coefficient, it was argued that the pitch angle scattering part of the collision operator in Eq. (5.138), near a resonance  $\Omega = \omega - k_{\parallel}v_{\parallel} = 0$ , can be rewritten as

$$\nu_d(1 - \lambda^2) (\partial_{\lambda}\Omega)^2 \partial_{\Omega}^2 f , \quad (5.157)$$

while the effect of turbulence driven radial diffusion becomes

$$D_r (\partial_r\Omega)^2 \partial_{\Omega}^2 f , \quad (5.158)$$

to be added on the right hand side. On the basis of comparisons of Eqs. (5.157) and (5.158), (Fu *et al.*, 2010) conclude that turbulence-induced radial diffusion might be more important than collisional effects in determining the saturation level of EP driven AEs near marginal stability in burning plasma experiments.

Hybrid MHD-gyrokinetic codes, which have the capability of treating non-perturbative kinetic EP responses and are based on the model equations historically developed for studying the effect of an EP population on long wavelength MHD modes (Park *et al.*, 1992) (cf. Secs. II.E and II.F), have also been adopted for the investigation of EP driven TAE nonlinear dynamics near marginal stability, showing the evidence of saturation by wave-particle trapping, as in the case of the beam-plasma system (O'Neil *et al.*, 1971) (cf. Sec. V.D.1), yielding the expected scaling  $\omega_B \sim \gamma_L$  or, equivalently,  $|\delta\mathbf{B}_{\perp}/B_0| \sim (\gamma_L/\omega_0)^2$  for the fluctuation level at saturation (Fu and Park, 1995; Park *et al.*, 1999; Todo *et al.*, 1995). Deviations from this scaling was shown to occur in hybrid MHD-gyrokinetic numerical simulations of TAEs for increasing EP drive, when the nonlinear EP radial displacement was comparable with the characteristic radial wavelength of the mode (Briguglio *et al.*, 1998) (cf. Sec. V.D.5.b). Energetic particle losses have also been observed in early hybrid MHD-gyrokinetic simulations in the presence of multiple TAEs (Todo and Sato, 1998). Fokker-Planck collision models with source terms have also been implemented in hybrid MHD-gyrokinetic simulations (Lang *et al.*, 2010; Todo *et al.*, 2001) and applied to verification of theoretical predictions (Berk *et al.*, 1999) (cf. Sec V.D.2) based on the bump-on-tail paradigm (Lang *et al.*, 2010), as well as to the investigation of recurrent TAE bursts observed in TFTR NBI heated plasmas (Todo *et al.*, 2003), for which the numerical repetition time of subsequent TAE bursts is close to experimental values. Neglecting mode-mode nonlinear couplings, the stored beam energy is found to be  $\sim 40\%$  of that expected in the absence of fluctuations, although the predicted saturation level of  $|\delta\mathbf{B}_{\perp}/B_0| \simeq 2 \times 10^{-2}$  is significantly larger than that observed experimentally,  $|\delta\mathbf{B}_{\perp}/B_0| \sim 10^{-3}$ . Meanwhile, particle phase-space mapping show that EP redistributions are due to both resonance overlap of different eigenmodes as well as stochasticization of particle orbits due to secondary and higher order resonances of a single eigenmode. The same numerical simulation has been repeated recently (Todo *et al.*, 2012a), with the inclusion of MHD mode-mode couplings, finding lower TAE saturations levels and two possible scenarios; *i.e.*, TAE steady-state saturation at  $|\delta\mathbf{B}_{\perp}/B_0| \simeq 2 \times 10^{-3}$  for low MHD dissipation coefficients and TAE bursting with peak fluctuation levels at  $|\delta\mathbf{B}_{\perp}/B_0| \simeq 5 \times 10^{-3}$  for the higher dissipation case. The lower saturation level, in this case, is attributed to the enhanced dissipation due to the nonlinearly driven modes, with both  $n = 0$  and  $n \neq 0$ . In other words, this process is essentially that of unstable modes transferring energy to nonlinear driven oscillations, which are damped and eventually dissipate energy into the short scales (Todo *et al.*, 2010, 2012a), possibly through the fine structures connected with resonant excitation of higher toroidal mode number continuous spectra (Todo *et al.*, 2012b). Thus, it is different from the enhanced nonlinear coupling with the SAW continuum or the spontaneous generation of ZS, analyzed in Secs. V.C.2 and V.C.3, which are collisionless processes and are expected to play important roles in high temperature burning plasmas.

Model Fokker-Planck collision terms in the form of Eq. (5.138) have been also implemented in gyrokinetic codes for investigating nonlinear TAE dynamics as, *e.g.*, by (Chen and Parker, 2011). There, it is shown that an  $n = 15$  TAE in ITER, found to be the most unstable mode from previous linear stability analyses of the considered reference scenario (Chen *et al.*, 2010c) (cf. Sec. IV.C), nonlinearly evolves up to a peak fluctuation amplitude, consistent with  $\omega_B \sim \gamma_L$ , and then decays to a steady state saturation level, which scales as  $\nu_d^{2/3}$ , consistent with Eq. (5.139), and is typically dominated by pitch angle scattering (Chen and Parker, 2011).

## 5. Nonlinear dynamics of Alfvénic fluctuations in nonuniform toroidal plasmas

Nonlinear wave-particle interactions are importantly modified by geometry of the plasma equilibrium and spatial nonuniformities, as in Sec. V.C it is shown to be the case for nonlinear wave-wave couplings. In this section, we first present a qualitative discussion of these modifications, showing that they occur for sufficiently strong EP drive, giving estimates of the deviation from marginal stability that is necessary for them to take place. Then, we give a

quantitative and formal description of the same phenomena, based on numerical simulation results and the general theoretical framework introduced in Sec. V.A. This allows us to ultimately derive general equations for the nonlinear dynamics of phase-space ZS and to demonstrate the unification of “bump-on-tail” and “fishbone” paradigms.

A detailed analysis of resonant wave particle interactions in 2D toroidal plasmas is given by (Zonca *et al.*, 2013a,b), using the general time scale ordering  $|\omega_0\tau_{NL}|^{-1} \sim |\gamma_L/\omega_0| \gg \epsilon_\omega \sim \mathcal{O}(\omega/\Omega_i)$ , discussed in Sec. II.D, to motivate the assumption that for every bounce/transit the effect of nonlinear dynamics is small enough that wave-particle resonances are not altered significantly or destroyed. In this way, nonlinear dynamics connected with wave-particle resonances can be understood as cumulative effects of bounce/transit-averaged processes on linear particle motions. The resonant particle response to a fluctuating field  $f(r, \theta, \zeta)$  can then be written as

$$f(r, \theta, \zeta) = \sum_{m,n,\ell} e^{i(n\bar{\omega}_d + \ell\omega_b)\tau + i\Theta_{m,n,\ell}} \mathcal{P}_{m,n,\ell} \circ f_{m,n}(\bar{r} + \Delta r) . \quad (5.159)$$

This is the nonlinear extension of Eq. (4.47); *i.e.*, a lifting of  $f(r, \theta, \zeta)$  to the particle phase-space<sup>35</sup>, which is useful for resonant particles satisfying the resonance conditions Eqs. (4.50) and (4.51). Here, the  $\mathcal{P}_{m,n,\ell} \circ f_{m,n}$  functions are defined in Eq. (4.48), while  $\Theta_{m,n,\ell}$  is the nonlinear wave-particle phase shift, defined as (Zonca *et al.*, 2013a,b)

$$\begin{aligned} \Theta_{m,n,\ell} = & n\Delta\zeta - m\Delta\theta + n \left( \frac{\partial\bar{\omega}_d}{\partial P_\phi} \int_0^\tau \delta P_\phi d\tau' + \frac{\partial\bar{\omega}_d}{\partial J} \int_0^\tau \delta J d\tau' \right) \\ & + \ell \left( \frac{\partial\omega_b}{\partial P_\phi} \int_0^\tau \delta P_\phi d\tau' + \frac{\partial\omega_b}{\partial J} \int_0^\tau \delta J d\tau' \right) - \int_0^\tau \delta\omega d\tau' \\ & + (n\bar{q}(\bar{r}) - m) \left( \frac{\partial\omega_b}{\partial P_\phi} \int_0^\tau \delta P_\phi d\tau' + \frac{\partial\omega_b}{\partial J} \int_0^\tau \delta J d\tau' \right) + n\omega_b \frac{d\bar{q}}{d\bar{r}} \int_0^\tau \delta r d\tau' , \end{aligned} \quad (5.160)$$

and accounting for “resonance detuning”.  $\Delta\zeta$  and  $\Delta\theta$  are the cumulative nonlinear shifts in  $\zeta$  and  $\theta$ , while  $\delta P_\phi$  and  $\delta J$  are the nonlinear deviations from particle constants of motions, corresponding to the radial nonlinear deviation  $\delta r = r - \bar{r}$ ; and integrations are along the unperturbed particle orbits. Meanwhile, the nonlinear frequency shift  $\delta\omega = \omega(\tau) - \omega_0$  for a nearly monochromatic wave (cf. Sec. II.C) is explicitly taken into account, leaving implicit only the time dependence of the reference linear instability. Note that the last line of Eq. (5.160) applies to circulating particles only and is the nonlinear extension of  $(-i \ln \lambda_{m,n})$ , with  $\lambda_{m,n}$  defined in Eq. (4.49). Furthermore,  $\Delta r$  in the argument of  $\mathcal{P}_{m,n,\ell} \circ f_{m,n}$  is the bounce-averaged nonlinear radial particle displacement, which describes the role of finite radial mode structures; *i.e.*, “radial decoupling”. Equation (5.159) states that nonlinear wave-particle resonant interactions must be computed with bounce averaged fields strength at the actual particle position, including the nonlinear radial displacement. It is also worthwhile noting that both resonance detuning and radial decoupling for EPs are dominated by  $\Delta r$ , due to the fact that  $|\omega_{*E}/\omega_0| \gg 1$  (Chen *et al.*, 1988).

In nonuniform plasmas, it is important to compare the characteristic scale of radial mode structures (“radial decoupling”) with the finite interaction length  $\Delta r_L$  for particles to detune from resonance (“resonance detuning”). Assuming that  $\tau_{NL} \sim \dot{\Theta}_{m,n,\ell}^{-1} \sim (3\gamma_L)^{-1}$ ,  $\Delta r_L$  is respectively derived as (Zonca *et al.*, 2013a,b)

$$3\gamma_L \sim nq'\omega\epsilon_\omega\Delta r_L ; \quad (5.161)$$

$$3\gamma_L \sim \omega\epsilon_\omega(\Delta r_L/r) , \quad (5.162)$$

for circulating and magnetically trapped EPs, noting that  $\gamma_L$  from now on is intended as net growth rate. In these expressions, the factor  $\epsilon_\omega = 1$  for fixed frequency modes, whereas  $\epsilon_\omega < 1$  for non-adiabatic frequency sweeping modes ( $\dot{\omega} \sim \omega_B^2$ , cf. Sec. V.D.5.a). For them, wave-particle resonance condition may be maintained via “phase locking”; *i.e.*,  $|\dot{\Theta}_{m,n,\ell}| \ll 1$  is preserved during nonlinear interaction, within the constraints imposed by wave dispersive properties and plasma nonuniformity. There is no adiabatic invariant connected with phase-space particle motion for “phase locked” fluctuations, which may suppress wave-particle trapping, as the effective bounce frequency is reduced by  $\sim \epsilon_\omega^{1/2}$  and EPs explore regions of varying mode structure (radial decoupling) without significant resonance detuning.

When fluctuations maintain wave-particle resonance condition via “phase locking”, the chirping rate is proportional to mode amplitude, as observed experimentally, *e.g.*, by (Heidbrink, 2008; Podestà *et al.*, 2011), and in numerical simulations of nonlinear EPM evolutions (Briguglio *et al.*, 2013, 2002, 1998; Vlad *et al.*, 2004, 1999; Zonca *et al.*, 2002) as well as nonlinear fishbone dynamics (Fu *et al.*, 2006; Vlad *et al.*, 2012, 2013). This behavior is also demonstrated

<sup>35</sup> This can be intended as the long time scale effective averaged action of  $f(r, \theta, \zeta)$  on a particle, given its constants of motion.

analytically for nonlinear EPM dynamics (Zonca *et al.*, 2005). Meanwhile, resonant particle motion is secular and corresponding transport is ballistic/convective: this particular nonlinear dynamic regime has been dubbed “mode particle pumping” in the original work (White *et al.*, 1983), where it was proposed for interpreting EP transport caused by fishbones (cf. Sec. V.D.7). Equations (5.161) and (5.162) can be concisely expressed as

$$(\Delta r_L/r) \sim 3\epsilon_{\omega}^{-1}\lambda_n^{-1}(\gamma_L/\omega) , \quad (5.163)$$

where  $\lambda_n = |nrq'|$  for circulating EPs and  $\lambda_n = 1$  for trapped EPs, respectively. This expression for  $(\Delta r_L/r)$  implies that circulating EP transport is expected to be mostly diffusive in the presence of many high- $n$  modes, typical of ITER conditions (cf. Secs. VI.A and VII.A). On the contrary, magnetically trapped EP transports may be affected by convective (ballistic) processes (cf. Sec. V.D.6) with intrinsically non-local features (Briguglio *et al.*, 2002, 1998; Vlad *et al.*, 2004, 1999); *i.e.*, characterized by meso-scales larger than  $|nrq'|^{-1}$ , with analogies to electron behaviors in gyrokinetic numerical simulations of collisionless trapped electron mode turbulence (Xiao and Lin, 2011). For moderate or low- $n$  fluctuations, more typical of present day tokamaks, the situation is less well defined and requires more articulation, as shown hereafter.<sup>36</sup>

*a. From local to meso-scale energetic particle redistributions*

Equation (5.163) should be compared with the characteristic scale of radial mode structures,  $\Delta r_d$ , which determines radial decoupling due to nonlinear wave-particle dynamics in nonuniform plasmas. From the general form of mode structures in toroidal geometry [cf., *e.g.*, Eq. (4.26) in Sec. IV.B], one can readily write

$$(\Delta r_d/r) \sim \epsilon_{\Delta}|nrq'|^{-1} , \quad (5.164)$$

where  $\epsilon_{\Delta}$  accounts for the mode frequency shift  $\delta\omega_L$  with respect to the SAW continuum accumulation point. For example,  $\epsilon_{\Delta} \sim \beta^{1/2}(\delta\omega_L/\omega)^{1/2}$  for BAE (cf. Sec. IV.B.2), while  $\epsilon_{\Delta} \sim \epsilon_0^{1/2}(\delta\omega_L/\omega)^{1/2}$  for TAE (cf. Sec. IV.B.3). As  $|\delta\omega_L| \gtrsim \gamma_L$ , Eq. (5.164) reflects the short scale radial structure of both AEs and EPs due to the removal of mode degeneracy with the continuous spectrum. Meanwhile, if  $\epsilon_{\Delta} \sim 1$  is assumed in Eq. (5.164), one obtains an estimate of the radial scale length of single poloidal harmonics connected with magnetic shear. From Eqs. (5.163) and (5.164), it is clear that “radial decoupling” becomes just as or more significant than “radial detuning” when

$$(\gamma_L/\omega) \gtrsim \lambda_n|nrq'|^{-1}\epsilon_{\omega}\epsilon_{\Delta}/3 . \quad (5.165)$$

This condition, which depends on mode dispersive properties via  $\epsilon_{\omega}\epsilon_{\Delta}$  and on the type of resonance via  $\lambda_n$ , can also be considered as criterion for estimating the validity limits of the bump-on-tail paradigm for interpretation of AE behaviors in toroidal plasmas. In addition, since significant EP radial redistributions take place on the characteristic fluctuation length scale, both the mode dispersiveness and structures may be affected, when this condition is satisfied. Equation (5.165) is most difficult for circulating EPs, for which  $\lambda_n = |nrq'|$  and the condition for “radial decoupling” to become important can be estimated as

$$(\gamma_L/\omega) \gtrsim \epsilon_{\omega}\epsilon_{\Delta}/3 \sim 3 \times 10^{-2} , \quad (5.166)$$

as an upper bound, having assumed  $\epsilon_{\omega}\epsilon_{\Delta} \lesssim 10^{-1}$ . Meanwhile, for magnetically trapped EPs, the corresponding condition is  $(\gamma_L/\omega) \gtrsim 10^{-2}$  for moderate mode numbers and  $(\gamma_L/\omega) \gtrsim 10^{-3}$  for the high- $n$  modes expected in ITER.

Once the condition of Eq. (5.165) is exceeded, the transition to a regime, where effects of mode structures become important, is initially gradual and then gives rise to novel behaviors due to interplay between mode structures and EP transport (Zonca *et al.*, 2005). This transition can also be understood in terms of EP redistributions, which, for isolated resonances, change in nature from the local character connected with the short radial scale of AEs, as upper bound, to meso-scale features  $\gtrsim |nrq'|^{-1}$ . That is, the initial gradual transition occurs when  $\epsilon_{\Delta}$  reflects the short AEs radial scale, as discussed after Eq. (5.164), and can be considered complete when  $\epsilon_{\Delta} = 1$  in Eq. (5.165). From Eq. (5.165) with  $\epsilon_{\Delta} = 1$ , this occurs for

$$(\gamma_L/\omega) \gtrsim |nrq'|^{-1}\epsilon_{\omega}/3 , \quad (5.167)$$

---

<sup>36</sup> This point, together with similar remarks made earlier about wave-wave couplings (cf. Sec. V.C) and the different nonlinear dynamic regimes expected in burning plasmas with respect to those in present day devices, may suggest that understanding nonlinear SAW and EP physics in existing experiments may be more difficult than in burning plasmas. This indeed partly applies to sufficiently short time-scale behaviors (cf. Secs. II.C and II.D). However, more generally, this point also shows the need of theory and numerical simulations for reliable extrapolations of present understanding of nonlinear SAW dynamics to burning plasmas conditions, especially when tackling new physics issues, as those of complex behaviors and spatiotemporal cross-scale couplings, discussed in Sec. VII.B.

for magnetically trapped EPs. For circulating EPs, meanwhile, the same condition is more stringent and reads

$$(\gamma_L/\omega) \gtrsim \epsilon_{\dot{\omega}}/3 . \quad (5.168)$$

This means that for magnetically trapped EPs, the transition between local to meso-scale redistributions can take place for  $(\gamma_L/\omega) \sim 10^{-2}$ . On the contrary, for circulating EPs, the same transition would occur at  $(\gamma_L/\omega) \sim 10^{-1}$  with fast non-adiabatic frequency sweeping and “phase locking” ( $\epsilon_{\dot{\omega}} < 1$ ). For moderate mode numbers, for which Eqs. (5.167) and (5.168) predict similar transition threshold from local to meso-scale EP transport, “mode particle pumping” may convectively redistribute magnetically trapped and circulating resonant EPs on a significant portion of the plasma<sup>37</sup>. For increasingly higher mode numbers, instead, typical of ITER conditions, redistribution of circulating resonant EPs, unlike that of magnetically trapped EPs (cf. Sec. V.D.5), tends to become local, so that significant (diffusive) transport may occur only above stochastic threshold in the presence of many modes (cf. Secs. VI.A and VII.A). In the light of Eqs. (5.167) and (5.168), it is also possible to conclude that, for significant fast non-adiabatic frequency sweeping and “phase locking”, particle redistributions are generally characterized by meso-scale secular processes, typical of “mode particle pumping” (White *et al.*, 1983). In other words, frequency chirping rate gives a clear measure for discriminating weak from strong EP transports (cf. Sec. VI.B). Meanwhile, the spatial range of EP redistributions is typically  $\sim |nrq'|^{-1}$  for circulating particles and may be larger for magnetically trapped ones, depending on radial mode structures; *i.e.*, radial decoupling.

In general, both threshold conditions given by Eqs. (5.167) and (5.168) can be exceeded in situations of practical interest. In fact, in weakly collisional plasmas of fusion interest, the short time scale ( $\tau_{NL}^{-1} \sim \gamma_L$ ; cf. Secs. II.C, II.D and V.A) EP power density is linearly proportional to time and injected power (cf. Sec. V.D.7). Thus, the effective strength of EP drive is directly controlled by additional power input, which may be tuned equally well to achieve plasma conditions with either AEs excited near marginal stability (cf. Secs. V.D.3 and V.D.4) or with strongly driven AE and EPM, as routinely observed in experiments with strong ICRH [*e.g.*, (Bernabei *et al.*, 1999, 2001; Nabais *et al.*, 2005; Zonca *et al.*, 2009)] and neutral NBI [*e.g.*, (Gryaznevich and Sharapov, 2004, 2006; Lesur *et al.*, 2010; Podestà *et al.*, 2011)]. It is also interesting to note that threshold conditions given by Eqs. (5.167) and (5.168) can be exceeded nonlinearly, due to the combined effect of different fluctuations. An experimental evidence of this case may be given by “TAE avalanches” in NSTX (Fredrickson *et al.*, 2009; Podestà *et al.*, 2009), where significant rapid EP losses occur in bursts of non-adiabatic frequency sweeping modes (Podestà *et al.*, 2012, 2011), which are consistent with the general features of EPs and cause up to  $\sim 30\%$  EP losses, following the activity of quasi-periodic TAE fluctuations with limited frequency chirping (Fredrickson *et al.*, 2009; Podestà *et al.*, 2009). In this case, resonance overlap may enhance the EP free energy source in the first phase of quasi-periodic TAE fluctuations (cf. Sec. V.D.5.b) and, once the EPM excitation threshold is exceeded, the dominant “TAE avalanche” is triggered (cf. Sec. VI.B).

#### b. Numerical simulation results of meso-scale energetic particle redistributions

The transition from local to meso-scale nonlinear EP redistributions was investigated numerically for the first time by (Briguglio *et al.*, 1998) for the case of TAE and EPM. In this work, linear TAE and EPM regimes were identified from the behavior of mode growth rate vs. EP energy density, revealing the EPM threshold condition as discussed in Sec. IV.B.4 and Fig. 2(a). In the same work, it was also shown that TAE to EPM transition is properly described only with a fully non-perturbative treatment of the EPs.

The work by (Briguglio *et al.*, 1998) confirms that nonlinear saturation of TAE modes occurs because of wave-particle trapping, as noted in earlier hybrid MHD-gyrokinetic simulations of TAE modes excited by EPs (Fu and Park, 1995; Todo *et al.*, 1995). However, for increasing growth rate, EP redistributions by finite amplitude TAE affect an increasingly broader radial region, which eventually becomes of the same order of the characteristic fluctuations length scale (cf. Sec. V.D.5.a). Thus, TAE saturation becomes gradually more affected by radial decoupling than by resonance detuning. This is also visible in the scaling of TAE saturation amplitude vs. the linear growth rate shown in Fig. 6(a). The overall EP density profile, however, is not appreciably affected, since only resonant EPs are subject to a significant nonlinear radial displacement. As noted by (Briguglio *et al.*, 1998), when the radial width of the wave-particle resonant region becomes comparable with the finite mode width, the saturation amplitude deviates from the simple scaling  $|\delta \mathbf{B}_{\perp}/B_0| \sim (\gamma_L/\omega)^2$  (cf. Secs. V.D.1 and V.D.4) and eventually becomes independent of the linear drive. For this case of TAE excited by EPs via transit resonance, the  $|\delta \mathbf{B}_{\perp}/B_0| \sim (\gamma_L/\omega)^2$  behavior holds

<sup>37</sup> It is also worthwhile noting that the effect of finite EP orbit widths and radial nonuniformity may also reduce the threshold condition of this criterion. In fact, the estimate of Eq. (5.161), where Eq. (5.168) is derived from, predicts, *e.g.*, that the transit resonance frequency in Eq. (4.51) is reduced to zero for a radial displacement  $\sim |nrq'|^{-1}$ , while this may be an overestimate of resonance detuning as a consequence of the equilibrium orbit averaging in the definition of  $\bar{q}$ , Eq. (4.45). These effects may be precisely computed case by case and the criterion of Eq. (5.168) may then be given more accurately. A similar argument also applies to trapped particles.

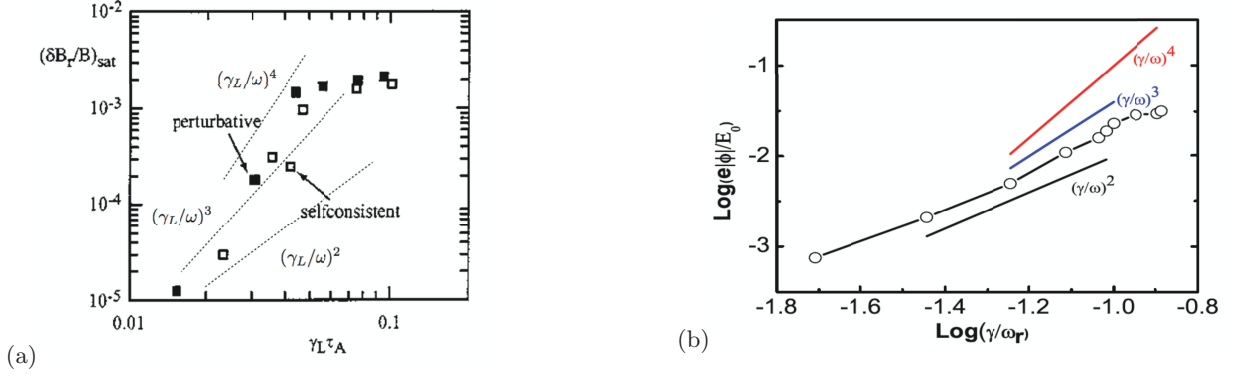


FIG. 6 Left frame (a) [from the original Fig. 9 in Ref. (Briguglio *et al.*, 1998)]: TAE saturation amplitude vs. the normalized linear growth rate, expressed in Alfvén time units,  $\tau_A = R_0/v_A$ , computed at the magnetic axis and with  $R_0$  denoting the geometric center of the circular toroidal plasma (Briguglio *et al.*, 1995). Right frame (b) [from the original Fig. 4 in Ref. (Wang *et al.*, 2012)]: BAE saturation amplitude, expressed by the peak scalar potential energy normalized with respect to the EP birth energy, whose distribution function is an isotropic slowing down, is shown vs. the normalized mode linear growth rate.

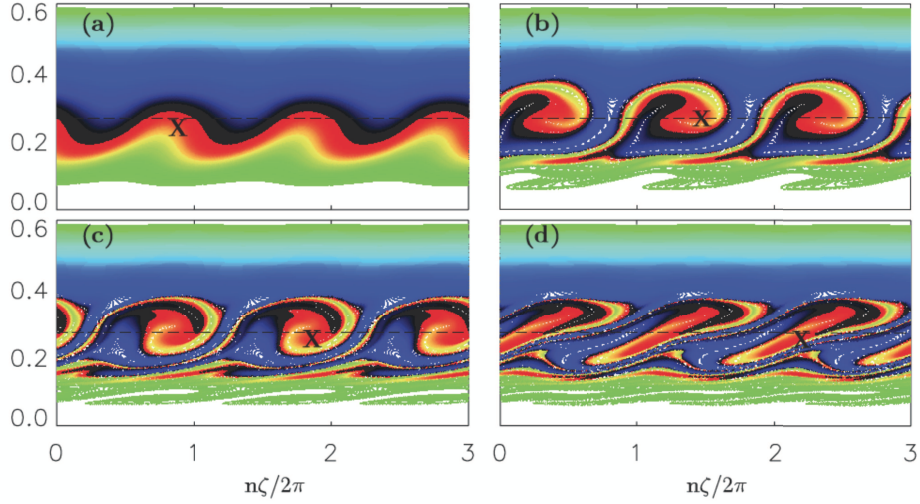


FIG. 7 [from the original Fig. 4 in Ref. (Zhang *et al.*, 2012)]: Nonlinear evolution of the EP distribution function during a BAE nonlinear burst cycle.  $P_\zeta$  is the canonical angular momentum conjugate to the angle  $\zeta$  (cf. Sec. IV.A), normalized to  $(-e\psi/c)$  (cf. Sec. IV.B) at the plasma boundary, and the particle marker color denotes the initial value of  $P_\zeta$ . Frame (a) refers to the initial (linear) unstable phase, accompanied by non-adiabatic downward frequency chirping. Frames (b) and (c) capture the early and later BAE decay phase after the mode burst maximum is reached. Frame (d) corresponds to the further growth of the mode, *i.e.*, the second BAE burst, after the minimum mode amplitude is reached.

for  $\gamma_L/\omega \lesssim 10^{-2}$ , as shown in Fig. 6(a), consistent with the criterion of Eq. (5.166). The same type of behavior has been recently observed in BAE hybrid MHD-gyrokinetic simulations and is reported in Fig. 6(b). The mechanism by which radial decoupling changes the scaling of the saturation amplitude with  $(\gamma_L/\omega_0)$  is also explained by (Wang *et al.*, 2012) in terms of a simplified analytical model, which incorporates wave-particle resonance as well as finite interaction domain due to mode localization. The observed deviation of the mode saturation amplitude from the  $\sim (\gamma_L/\omega)^2$  scaling in simulations (Briguglio, 2012; Briguglio *et al.*, 2013, 2012; Wang *et al.*, 2012; Zhang *et al.*, 2012) is, thus, indicative of the increasing importance of radial decoupling with respect to resonance detuning.

Another important aspect of the transition from local to meso-scale EP redistributions is that the system is not near marginal stability, as discussed in Secs. V.D.2 and V.D.3, and its dynamics is non-adiabatic. This is a consequence of the fact that the non-perturbative power exchange between waves and EPs undergoes an  $\mathcal{O}(1)$  variation on the characteristic time  $\tau_{NL}$  (cf. Sec V.D.5.a). These physics are clearly demonstrated in recent numerical simulations of BAE nonlinear dynamics with both gyrokinetic (Zhang *et al.*, 2012) and hybrid MHD-gyrokinetic (Wang *et al.*,

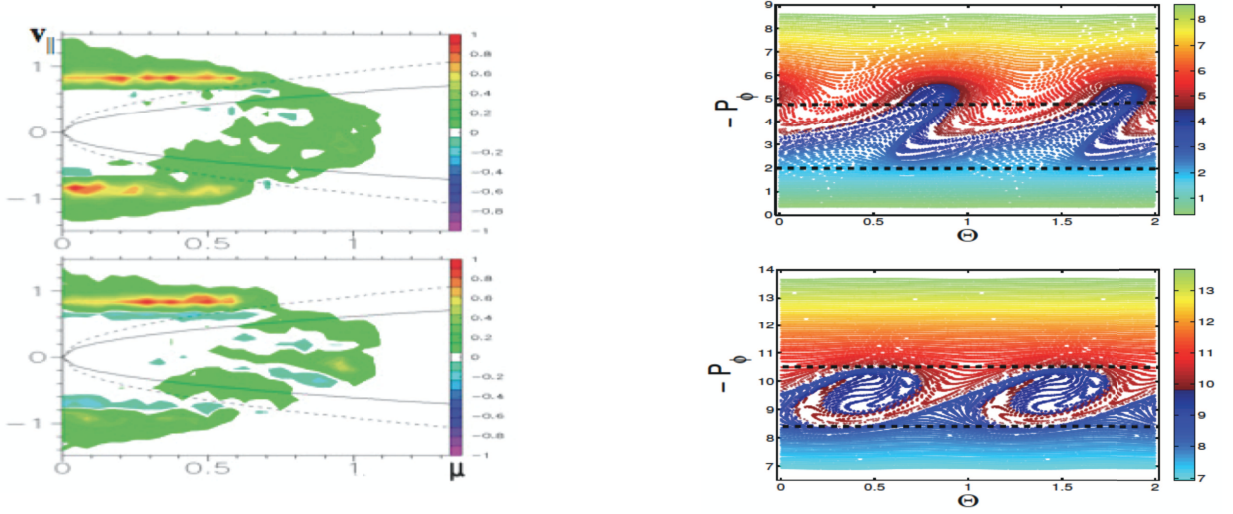


FIG. 8 Left frame [from the original Fig. 2 in Ref. (Wang *et al.*, 2012)]: BAE-EP power exchange in  $(\mu, v_{\parallel})$  space in the growing (upper panel) and saturation (lower panel) phases of the BAE burst. Velocity space variables  $\mu$  and  $v_{\parallel}$  are normalized w.r.t.  $E_0/\Omega$  and  $(E_0/m)^{1/2}$ , respectively, with  $E_0$  the maximum EP energy in the isotropic slowing down distribution function, assumed as initial condition. The positive sign in the color bar corresponds to EPs driving the wave. Solid and dashed lines are magnetically trapped to passing EP boundaries at the inner and outer limits of the mode radial half width. Right frame [from the original Fig. 3 in Ref. (Wang *et al.*, 2012)]: Kinetic Poincaré plots (Briguglio, 2012; White, 2012) of phase-space ZS near  $v_{\parallel} > 0$  (upper panel) and  $v_{\parallel} < 0$  (lower panel) resonances in  $(\Theta, -P_{\phi})$  space, normalized w.r.t.  $2\pi$  and  $a(mE_0)^{1/2}$ , respectively, with  $a$  the plasma minor radius. Marker color denotes the initial  $P_{\phi}$  value, and dashed horizontal lines indicate the radial mode half width.

2012) approaches. In the work by (Zhang *et al.*, 2012), BAE is excited predominantly by trapped EPs via precession resonance and nonlinear mode evolution is characterized by continuous bursting without EP sources or sinks and with EPs assumed to initially have an isotropic Maxwellian distribution function. These nonlinear dynamics are illustrated in Fig. 7, showing the evolution of the EP distribution function in the  $(\zeta, P_{\zeta})$  space, with  $P_{\zeta}$  the canonical angular momentum conjugate to the angle  $\zeta$  (cf. Sec. IV.A), normalized to  $(-e\psi/c)$  (cf. Sec. IV.B) at the plasma boundary, and the particle marker color denoting the initial value of  $P_{\zeta}$ . In the growth phase of the BAE mode, shown in Fig. 7(a), the frequency sweeps downward, consistently with the mode dispersion relation. Particles, which are moving outward (upward in normalized  $P_{\zeta}$ ) and drive the mode, more easily maintain the phase locking condition for magnetically trapped particles, stemming from  $\ddot{\Theta}_{m,n,\ell} \simeq 0$  and Eq. (5.160), and noting  $|\omega_{*E}/\omega| \gg 1$  (Chen, 1988):

$$\delta\dot{\omega} \simeq (n\partial_{\bar{r}}\bar{\omega}_d + \ell\partial_{\bar{r}}\bar{\omega}_b) \Delta\dot{r} . \quad (5.169)$$

Vice-versa, particles that are moving inward (downward in normalized  $P_{\zeta}$ ) and damp the mode are more easily detuned from resonance. Thus, power transfer from particles to the wave is maximized, as well as are particle nonlinear radial displacement and mode growth, which continues until mode saturates and then starts decaying due to radial decoupling, as shown in Fig. 7(b). This is visible from two clear features (Zhang *et al.*, 2012): (i) the resonance detuning of the upper phase-space structure is limited with respect to that of the lower structures; (ii) the wave amplitude decay starts before significant resonance detuning, suggesting the important role of radial decoupling, which is also evident from the particle radial displacement compared to the mode width (Zhang *et al.*, 2012). In the further evolution of the mode, after resonant particles are radially decoupled with respect to the mode peak and the mode amplitude further decreases as in Fig. 7(c), the distribution function free energy is partly recovered in Fig. 7(d), when the wave-particle phase  $\Theta$  (dropping the subscripts in  $\Theta_{m,n,\ell}$ ) completes one whole oscillation in the instantaneous fluctuation-induced potential well, producing a second BAE burst (Zhang *et al.*, 2012). Similar behaviors are observed by (Wang *et al.*, 2012), where BAE is destabilized by EPs via transit resonance and nonlinear mode dynamics is produced uniquely by wave-EP interaction, as thermal ion kinetic response is linearized. In this case, the frequency sweeps upward in the growth phase of the BAE mode, consistently with the mode dispersion relation (Wang *et al.*, 2012). Thus, the phase locking condition analogous to Eq. (5.169) for circulating EPs,

$$\delta\dot{\omega} \simeq n(d_{\bar{r}}\bar{q})\omega_t\Delta\dot{r} , \quad (5.170)$$

is more easily maintained for positive than negative parallel velocities for EPs that move outward and drive the mode, causing symmetry breaking in  $v_{\parallel}$  for the wave-particle power exchange, as shown in Fig. 8 (left). As the mode grows, frequency chirping and  $v_{\parallel}$  symmetry breaking are more evident. This is illustrated also in Fig. 8 (right), showing kinetic Poincaré plots (Briguglio, 2012; White, 2012) for  $v_{\parallel} > 0$  (upper panel) and  $v_{\parallel} < 0$  (lower panel) resonances in  $(\Theta, -P_{\phi})$  space at mode saturation, which demonstrate rapid resonance detuning for  $v_{\parallel} < 0$ , while phase locking for  $v_{\parallel} > 0$  allows particles to be most efficiently transported outward, when driving the mode.

In both these recent works on nonlinear BAE dynamics (Wang *et al.*, 2012; Zhang *et al.*, 2012), the role of EPs is non-perturbative and results in non-adiabatic frequency chirping, while dominant wave-EP resonant interactions are those satisfying phase locking as predicted by Eqs. (5.169) and (5.170). As EPs are displaced outward while driving the mode and phase-space ZS evolve in time, the mode behaves as wave packet driven at the local growth rate, adjusting its radial structure to maximize wave-particle power exchange within the limits imposed by its dispersive properties (cf. the following discussion). To further illuminate the physics of phase locking and radial decoupling, (Briguglio, 2012) has set up a dedicated numerical simulation experiment, where radial equilibrium profiles are chosen to excite a radially localized  $n = 2$  EPM near the TAE frequency gap<sup>38</sup>; and introduced novel high-resolution numerical diagnostics for the EP phase-space, based on Hamiltonian mapping techniques. In this case, radial EPM localization is controlled by the choice of weak magnetic shear, which yields an EPM with two dominant Fourier harmonics,  $(3, 2)$  and  $(4, 2)$ , near the radial position where  $q \simeq 7/4$ . Kinetic Poincaré plots, analogous to those of Fig. 8, demonstrate that mode saturation occurs by radial decoupling in a characteristic time, which is about half of the wave-particle trapping time. When this occurs, similarly to the BAE cases discussed above, the wave-particle power exchange becomes most negative (damping) at the original resonance location and, at the same time, steeper gradient regions are formed at the outer limits of the radial mode structure, as these are the positions where EPs tend to accumulate due to radial decoupling and diminishing fluctuation amplitude. This is clearly demonstrated by further kinetic Poincaré plots, where EP markers label the instantaneous wave-particle power transfer rather than the initial particle  $P_{\phi}$  (Briguglio, 2012; Briguglio and Wang, 2013). However, unlike the BAE cases above, the instantaneous strengthening of the mode drive at higher and lower frequencies, with respect to that of the original EPM, “locally forces” wave packets of the SAW continuous spectrum; and EPM mode structure and frequency tend to split. In the case of a radially extended EPM mode structure, only one of the two possible SAW continuum wave packets, stemming from the original linear unstable EPM, is effectively driven due to the radial symmetry breaking caused by global equilibrium nonuniformities; and the corresponding dynamics is that of an avalanche (Zonca *et al.*, 2005) (cf. Sec. V.D.6). Meanwhile, for radially localized EPM, the following EPM evolution shows merging of the separate EPM wave-packets, which contribute to reconstructing the unstable EP distribution at the radial position of original linear unstable EPM; while wave-packets in the strengthened drive regions farther in  $P_{\phi}$  are not effectively excited due to the increased continuum damping (Briguglio, 2012). The main difference of EPM evolution with respect to BAE nonlinear dynamics consists in the “radial singular” structures characterizing the SAW continuum, which allow SAW wave packets to readily respond to instantaneous local forcing, while broader mode structures and wave dispersiveness cause BAE to be less suited to significant mode structure changes (Wang *et al.*, 2012; Zhang *et al.*, 2012). Nonetheless, for sufficiently strong EP drive, also BAE and TAE exhibit mode structure splitting and merging as well as nonlinear oscillation of mode amplitudes accompanying EP phase locking and AE saturation by radial decoupling (Briguglio, 2012; Briguglio and Wang, 2013).

The above results for both BAE and localized EPM clearly indicate that, for non-perturbative EP drive satisfying Eqs. (5.167) and (5.168), the EP redistributions occur on meso-scales and dominant wave-particle interactions follow the phase locking condition. Meanwhile, the mode frequency dynamics is non-adiabatic,  $\dot{\omega} \sim \omega_B^2$ , as it is readily verified from Eqs. (5.169) and (5.170); and from the the estimate  $\sim \delta \dot{\mathbf{X}}_{\perp}$  (cf. Sec. II.D), with

$$\omega_B^2 \simeq \lambda_n \left| (\omega/r) \delta \dot{\mathbf{X}}_{\perp} \right| \simeq \lambda_n |(\omega/r)(nq/r)(c/B_0)\delta\phi| \quad . \quad (5.171)$$

These results, furthermore, confirm that formation and modification of phase-space ZS occur on a time scale  $\omega_B t \sim 1$ , as anticipated in Sec. V.D.3. They also suggest that the dynamic process underlying the “continuous generation” of phase-space holes and clumps in the collisionless limit of the 1D bump-on-tail problem (Lilley and Breizman, 2012; Lilley *et al.*, 2010), in the absence of sources and sinks, starts as a non-adiabatic process, similar to that discussed above for localized EPM (Briguglio, 2012; Briguglio and Wang, 2013; Zonca *et al.*, 2005), for then evolving as adiabatic (Berk *et al.*, 1999, 1997a,b; Breizman *et al.*, 1997) or non-adiabatic process [cf., *e.g.*, (Vann *et al.*, 2007)], depending on the proximity to marginal stability<sup>39</sup>.

<sup>38</sup> The case of radially extended EPMs is discussed in Sec. V.D.6.

<sup>39</sup> This remark is connected with the relevant time scales of the problem. In the case of adiabatic continuous generation of holes and clumps,

c. *Nonlinear equations for energetic particle phase-space zonal structures*

After the original work by (Bernstein *et al.*, 1957) on Bernstein-Greene-Kruskal (BGK) modes, significant attention was devoted to the investigation of dynamics of phase-space structures in uniform plasmas, generally dubbed as holes (Berk *et al.*, 1970; Berman *et al.*, 1983; Dupree, 1982; Tetreault, 1983), when the phase-space structure density is lower than that of the phase-space containing it, or clumps (Berman *et al.*, 1983; Dupree, 1970, 1972, 1982; Tetreault, 1983), if the phase-space structure density is higher than in the surrounding region (cf. Sec. V.D.2.c). These analyses have been adopted and extended in the 1D bump-on-tail paradigm for the interpretation of AE behaviors in toroidal plasmas by Berk, Breizman and coworkers since the early 1990's (cf. Secs. V.D.2 and V.D.3).

When looking at transport processes in 2D systems with two periodic angle-like coordinates, one of which defines the equilibrium symmetry, phase-space structures that are of direct interest are those obtained by averaging out dependences on angle-like variables. In terms of the Fourier decomposition and general coordinates introduced in Sec. IV.A, this means that most relevant phase-space structures are characterized by  $n = m = 0$ ; *i.e.*, they may be generally referred to as “phase-space ZS” (Zonca *et al.*, 2013a,b), as this condition is necessary and sufficient for having  $\mathbf{k} \cdot \mathbf{b} = 0$  everywhere (cf. Secs. II.D and V)<sup>40</sup>. The concept of phase-space ZS is very general and encompasses the modification of particle distribution functions as consequence of fluctuation induced transport processes and, thereby, the corresponding corrugations of equilibrium radial profiles (Zonca *et al.*, 2006, 2000, 2005) (cf. Sec. V.D.6); as well as zonal flows and fields/currents (Chen *et al.*, 2000, 2001; Gruzinov *et al.*, 2002; Guzdar *et al.*, 2001b; Hasegawa *et al.*, 1979; Lin *et al.*, 1998) (cf. Secs. V.A, V.B.3 and V.C.2). In fact, zonal flows and fields/currents may be considered as generators of nonlinear equilibria (Chen and Zonca, 2007b), which have their own “modified” particle distribution functions and dynamically evolve on characteristic “transport” time scales, which are generally of the same order of the nonlinear time scale of the underlying fluctuations, although time scale separation may apply in various circumstances as, *e.g.*, it is frequently (but not always) the case of drift-wave turbulence (shorter characteristic times) and turbulent transport (longer time scales). Thus, zonal modifications of particle distribution functions and zonal flows and fields/currents are fundamentally interconnected and should be consistently addressed on the same footing, as argued in the general discussion of Sec. V.A.

Phase-space holes and clumps are particular cases of phase-space ZS, where time scale separation applies between their long characteristic dynamic nonlinear evolution and the much shorter wave-particle trapping time. As a consequence, it is always possible to identify an adiabatic invariant as the action integral connected with the EP bounce motion in the trapping well of the wave, and the EP distribution function, at the lowest order, is independent of the corresponding conjugate angle. Furthermore, there must exist a separatrix between the inner and outer phase-space region of holes and clumps, which cannot be crossed by particles in the dynamic evolution of phase-space ZS (cf. Secs. V.D.2 and V.D.3). More generally, for increasing drive strength, phase-space ZS evolve on typical scales of wave-packet radial structures. One can identify this new condition as breaking of the action integral invariance in the instantaneous trapping well of the wave, whose separatrix can now be crossed by resonant EPs interacting with the wave-packet. Thus, the concept itself of phase-space holes and clumps becomes questionable in its generally adopted meaning, although it maintains its literal sense of a lack or excess of particles in a certain phase-space region with respect to the equilibrium particle distribution function. For these reasons, we will refer from now on only to phase-space zonal structures, bearing in mind that this terminology is equivalent to phase-space holes and clumps in the case of uniform plasmas, sufficiently near marginal stability and with adiabatic nonlinear dynamics.

In this section we analyze the self-consistent and generally non-adiabatic nonlinear evolution of Alfvénic fluctuations and resonant EP phase-space ZS, allowing the investigation of the transition from local to meso-scale EP redistributions (cf. Secs. V.D.5.a and V.D.5.b). Thus, the key novel feature, analyzed in the following, is connected with the role of plasma nonuniformity and equilibrium magnetic field geometry in the dynamics of phase-space ZS.

For low frequency fluctuations, the nonlinear equations for EP phase-space ZS are obtained from the nonlinear gyrokinetic equations (Frieman and Chen, 1982); *i.e.*, the zonal particle distribution function, from Eq. (2.21), is

$$\delta f_z = \sum_m \left\{ \mathcal{P}_{m,0,0} \circ [J_0(\lambda)\delta g]_{m,0} \right\} - \left[ J_0(\lambda) \left( \frac{e}{m} \frac{1}{B_0} \frac{\partial \bar{F}_0}{\partial \mu} \langle \delta L_g \rangle \right) \right]_{0,0} + \frac{e}{m} \left[ \frac{\partial \bar{F}_0}{\partial \mathcal{E}} \delta \phi + \frac{1}{B_0} \frac{\partial \bar{F}_0}{\partial \mu} \delta L \right]_{0,0}, \quad (5.172)$$

where notations are those introduced in Sec. II.D, and the projection operator  $\mathcal{P}_{0,0,0}$  is a particular case of  $\mathcal{P}_{m,n,\ell}$  defined in Eq. (4.48) and used in the nonlinear representation of Eq. (5.159). Meanwhile, the evolution equation for

---

the process may be seen as “secondary instability” of the coarse-grain distribution function, connected with the BGK mode. In the case of non-adiabatic formation of hole and clump pairs, there is no adiabatic invariant and resonant particles never reach the coarse-grain distribution function (Sagdeev and Galeev, 1969). This issue is also connected with the existence of quasi-stationary states (Carlevaro *et al.*, 2013) in the context of the “Lynden-Bell approach” (cf. Sec. V.D.1).

<sup>40</sup> More precisely, it is also necessary to take  $\ell = 0$  in the lifting of  $f(r, \theta, \xi)$  to the particle phase-space, defined by Eq. (5.159).

the zonal component of  $\delta g$  is obtained from Eq. (2.23)

$$\frac{\partial \delta g_z}{\partial t} = - \sum_m \mathcal{P}_{m,0,0} \circ \left( \frac{e}{m} \frac{\partial}{\partial t} \langle \delta L_g \rangle \frac{\partial \bar{F}_0}{\partial \mathcal{E}} + \frac{c}{B_0} \mathbf{b} \times \nabla \langle \delta L_g \rangle \cdot \nabla \bar{F}_0 \right)_{m,0} - \sum_m \mathcal{P}_{m,0,0} \circ \left( \frac{c}{B_0} \mathbf{b} \times \nabla \langle \delta L_g \rangle \cdot \nabla \delta g \right)_{m,0} . \quad (5.173)$$

Assuming that  $|k_{\parallel}| \ll |\mathbf{k}_{\perp}|$  (cf. Sec. II.A), Eq. (5.173) can be cast as (Zonca *et al.*, 2005)

$$\frac{\partial \delta g_z}{\partial t} = - \mathcal{P}_{0,0,0} \circ \left( \frac{e}{m} \frac{\partial}{\partial t} \langle \delta L_g \rangle_z \frac{\partial \bar{F}_0}{\partial \mathcal{E}} \right)_{0,0} + i \sum_m \mathcal{P}_{m,0,0} \circ \frac{c}{d\psi/dr} \frac{\partial}{\partial r} \sum_n n \left( \delta g_n \langle \delta L_g \rangle_{-n} \right)_{m,0} , \quad (5.174)$$

where  $\sum_n$  stands for summation on toroidal mode numbers, which have been specified as subscript of fluctuating fields where needed. In turn, the evolution equation for  $\delta g_n$  is readily written as

$$\left( \frac{\partial}{\partial t} - \frac{inc}{d\psi/dr} \langle \delta L_g \rangle_z \frac{\partial}{\partial r} + v_{\parallel} \nabla_{\parallel} + \mathbf{v}_d \cdot \nabla_{\perp} \right) \delta g_n = i \frac{e}{m} \left( Q \bar{F}_0 - \frac{n B_0}{\Omega d\psi/dr} \mathcal{P}_{0,0,0} \circ \frac{\partial \delta g_z}{\partial r} \right) \langle \delta L_g \rangle_n . \quad (5.175)$$

Here,  $Q \bar{F}_0$  is defined by Eq. (4.55), the contribution  $\propto \langle \delta L_g \rangle_z$  on the left hand side represents the Doppler-shifted mode frequency in the zonal flows and fields/currents, while the term  $\propto \partial_r \delta g_z$  on the right hand side accounts for the ‘‘quasilinear’’ modification of the equilibrium particle distribution function (cf. Secs. V.A, V.D.6 and V.D.7)

Equations (5.174) and (5.175), along with the field equations for Alfvénic fluctuations, *i.e.*, Eq. (5.3) without the last term on the right hand side; and Eqs. (2.26) and (2.30) for  $\delta \phi_z$  and  $\delta A_{\parallel z}$ , respectively, fully characterize the short time scale nonlinear evolution of DAWs and EPs. These equations are, hence, the relevant equations for the self-consistent evolution of phase-space ZS excited by EPs and related transports. Despite their general yet relatively simple form, which makes them suitable for investigating various aspects of cross-scale couplings and complex behaviors in burning plasmas (cf. also Secs. V.E and VII.B), these equations have so far been only investigated in simplified limits; either dropping the second term on the right hand side of Eq. (5.174) (Chen *et al.*, 2000, 2001; Chen and Zonca, 2007b, 2012, 2013; Guo *et al.*, 2009), *i.e.*, the contribution of wave-particle resonances; or neglecting  $\langle \delta L_g \rangle_z$  (Zonca *et al.*, 2006, 2000, 2005, 2007b), *i.e.*, the effect of zonal flows and fields/currents. The former limit has been discussed already in Sec. V.C, while the latter case will be analyzed in the following and in the remaining part of Sec. V.D.5. Thus, as anticipated in Sec. V.A, the simplified evolution equations for phase-space ZS excited by EPs and related transports, used hereafter, are the nonlinear Schrödinger [*i.e.*, Gross-Pitaevsky (Gross, 1961; Pitaevsky, 1961) or Zakharov (Zakharov, 1968)] equation, Eq. (5.3), without the last term on the right hand side, closed by Eqs. (5.174) and (5.175), rewritten as

$$\frac{\partial F_0}{\partial t} = i \mathcal{P}_{0,0,0} \circ \sum_m \mathcal{P}_{m,0,0} \circ \frac{c}{d\psi/dr} \frac{\partial}{\partial r} \sum_n n \left( \delta g_n \langle \delta L_g \rangle_{-n} \right)_{m,0} , \quad (5.176)$$

and

$$\left( \frac{\partial}{\partial t} + v_{\parallel} \nabla_{\parallel} + \mathbf{v}_d \cdot \nabla_{\perp} \right) \delta g_n = i \frac{e}{m} Q F_0 \langle \delta L_g \rangle_n . \quad (5.177)$$

Here,  $F_0 \equiv \bar{F}_0 + \mathcal{P}_{0,0,0} \circ \delta g_z$ . Furthermore, we have taken into account that, for EPs with  $|\omega_{*E}| \gg |\omega_0|$  (Chen, 1988), the right hand side of Eq. (5.175) reduces to that of Eq. (5.177), except for an higher order term. These equations may be used to investigate a number of nonlinear dynamics problems involving a generic DAW spectrum with  $|\gamma_L/\omega_0| \sim |\omega_0 \tau_{NL}|^{-1} \ll 1$ , accounting the reaction of waves on the particle distribution function.

In order to simplify the present analysis further, we restrict Eqs. (5.176) and (5.177) to precessional resonance with magnetically trapped EPs while neglecting finite orbit width effects. Then, Eq. (5.176) readily reduces to

$$\begin{aligned} \frac{\partial F_0}{\partial t} &= i \sum_n \frac{nc}{d\psi/dr} \frac{\partial}{\partial r} (\delta \bar{g}_n \delta \bar{\phi}_{-n} - \delta \bar{g}_{-n} \delta \bar{\phi}_n) \\ &= \sum_n \frac{1}{|\omega_n|^2} \frac{nc}{d\psi/dr} \frac{\partial}{\partial r} \left( \frac{nc}{d\psi/dr} \frac{\partial F_0}{\partial r} \frac{\partial}{\partial t} |\delta \bar{\phi}_n|^2 \right) \\ &\quad + i \sum_n \frac{nc}{d\psi/dr} \frac{\partial}{\partial r} (\delta \bar{K}_n \delta \bar{\phi}_{-n} - \delta \bar{K}_{-n} \delta \bar{\phi}_n) . \end{aligned} \quad (5.178)$$

Here, we have accounted for the vanishing bounce averaged velocity of magnetically trapped EPs, and used the analysis of Sec. V.D.5 to write

$$\delta\bar{g}_n = e^{in(\zeta-q\theta)} \sum_m \mathcal{P}_{m,n,0} \circ \delta g_{m,n} \quad (5.179)$$

for  $\delta\bar{g}_n$ , the bounce averaged expression of  $\delta g_n$ , while

$$\delta\bar{\phi}_n = e^{in(\zeta-q\theta)} \sum_m \mathcal{P}_{m,n,0} \circ \delta\phi_{m,n} = e^{-inq\theta} \overline{e^{inq\theta} \delta\phi_n} \quad , \quad (5.180)$$

with  $\overline{(\dots)} = \tau_b^{-1} \oint (\dots) d\theta/\dot{\theta}$  denoting magnetic drift bounce averaging (cf. Sec. IV.B.1). Furthermore, we have used the definition of  $\delta K$  given by Eq. (4.54) and the ideal MHD condition  $\delta\phi = \delta\psi$  to rewrite explicitly the right hand side of Eq. (5.178), formally separating trivially reversible from irreversible processes connected with wave-particle interactions, which dominate the nonlinear dynamics in Eq. (5.178). In fact, the contribution of reversible processes is  $\sim (\epsilon_\delta/\epsilon_B)^2 \epsilon_F/\epsilon_\perp$  with respect to the left hand side (cf. Sec. II.A) and, hence, will be neglected in the following.

Adopting the notation of Eq. (5.126) for the Fourier-Laplace transform, Eq. (5.178) is readily solved as

$$\hat{F}_0(\omega) = \frac{i}{\omega} \text{St}\hat{F}_0(\omega) + \frac{i}{\omega} \hat{S}_0(\omega) + \frac{i}{2\pi\omega} \bar{F}_0(0) + \frac{nc}{\omega(d\psi/dr)} \frac{\partial}{\partial r} \int_{-\infty}^{\infty} \left[ \delta\hat{\phi}_k(y) \delta\hat{K}_{-k}(\omega-y) - \delta\hat{\phi}_{-k}(y) \delta\hat{K}_k(\omega-y) \right] dy \quad . \quad (5.181)$$

Here, we have straightforwardly included the effect of collisions, formally denoted by  $\text{St}\hat{F}_0(\omega)$ , and of an external source term,  $\hat{S}_0(\omega)$ , while  $\bar{F}_0(0)$  denotes the initial value of  $F_0$  at  $t=0$ . Moreover, for the sake of notation clarity, we have explicitly indicated only the dependences on  $\omega$  (and  $y$ , as dummy integration frequency variable) and the summation on mode numbers has been replaced by an implicit summation on the subscript  $k$ , which, from now on, we have adopted as short notation for  $(m,n)$ . Meanwhile, by straightforward recasting of Eqs. (4.58) as Fourier-Laplace transform, we readily obtain

$$\delta\hat{K}_k(\omega) = \frac{e}{m} \int_{-\infty}^{+\infty} \frac{\hat{\omega}_{dk}}{y} \frac{Q_{k,y} \hat{F}_0(\omega-y)}{n\bar{\omega}_{dk} - \omega} \delta\hat{\phi}_k(y) dy \quad , \quad (5.182)$$

where the subscripts in  $Q_{k,y} \hat{F}_0$  denote wave number and frequency at which the operator defined by Eq. (4.55) must be evaluated; and we have introduced the definition

$$e^{-inq\theta} \overline{e^{inq\theta} \omega_d \delta\phi_n} \equiv \hat{\omega}_{dk} \delta\hat{\phi}_k \quad . \quad (5.183)$$

It is straightforward to verify that Eq. (5.182) gives back the linear limit for  $\hat{F}_0(\omega) = (2\pi\omega)^{-1} i\bar{F}_0(0)$ . By substitution of Eq. (5.182) into Eq. (5.181), one readily obtains

$$\begin{aligned} \hat{F}_0(\omega) = & \frac{i}{\omega} \text{St}\hat{F}_0(\omega) + \frac{i}{\omega} \hat{S}_0(\omega) + \frac{i}{2\pi\omega} \bar{F}_0(0) + \frac{e}{m} \frac{nc}{\omega(d\psi/dr)} \frac{\partial}{\partial r} \iint_{-\infty}^{\infty} \left[ \delta\hat{\phi}_k(y) \frac{\hat{\omega}_{d-k}}{y'} \frac{Q_{-k,y'} \hat{F}_0(\omega-y-y')}{-n\bar{\omega}_{d-k} + y - \omega} \delta\hat{\phi}_{-k}(y') \right. \\ & \left. - \delta\hat{\phi}_{-k}(y) \frac{\hat{\omega}_{dk}}{y'} \frac{Q_{k,y'} \hat{F}_0(\omega-y-y')}{n\bar{\omega}_{dk} + y - \omega} \delta\hat{\phi}_k(y') \right] dy dy' \quad . \quad (5.184) \end{aligned}$$

This equation is the analogue of Eq. (5.130); *i.e.*, the Dyson's equation [cf. *e.g.*, (Kaku, 1993)] in quantum field theory, describing the nonlinear processes schematically shown in Fig. 5, and extended to the case of nonuniform toroidal plasmas under investigation with the addition of sources and collisions. Following (Al'tshul' and Karpman, 1965, 1966), it is possible to show that, in the case of many waves with overlapping resonances, Eq. (5.184) reduces to the quasilinear theory of a weakly turbulent plasma (Drummond and Pines, 1962; Vedenov *et al.*, 1961a), as noted already in Sec. V.D.1 for Eqs. (5.129) and (5.130). Thus, Eq. (5.184) can also be considered as a quasilinear equation (Galeev *et al.*, 1965); generalized to arbitrary distortions of the particle distribution function and including effects of equilibrium geometries and plasma nonuniformity. It, thus, addresses resonance detuning and radial decoupling in wave-particle interactions on the same footing. This demonstrates *a fortiori* that the present approach may be used to explore the transition of EP transports through stochasticity threshold with all the necessary physics ingredients for a realistic comparison with experimental observations.

In Secs. V.D.6 and V.D.7, we focus on the case where the DAW spectrum is very narrow, *e.g.*, the case of a ‘‘monochromatic’’ (cf. Sec. V.D.1) or, more precisely, periodic fluctuation, whose frequency may be evolving in time,

provided that  $|\dot{\omega}_k| \ll |\gamma_{Lk}\omega_k|$ . Therefore, this case includes both adiabatic ( $|\dot{\omega}_k| \ll \omega_B^2$ ) as well as non-adiabatic ( $|\dot{\omega}_k| \lesssim \omega_B^2$ ) frequency sweeping and may well represent the nonlinear dynamic evolution of a single toroidal mode number AE or EPM<sup>41</sup>. Using the representation

$$\delta\hat{\phi}_k(\omega) = \frac{i}{2\pi} \frac{\delta\bar{\phi}_{k0}(r, \tau)}{\omega - \omega_k(\tau)}, \quad \text{and} \quad \delta\hat{\phi}_{-k}(\omega) = \frac{i}{2\pi} \frac{\delta\bar{\phi}_{-k0}(r, \tau)}{\omega + \omega_k^*(\tau)}, \quad (5.185)$$

we readily reduce Eq. (5.184) to the following form

$$\begin{aligned} \hat{F}_0(\omega) = & \frac{i}{\omega} \text{St}\hat{F}_0(\omega) + \frac{i}{\omega} \hat{S}(\omega) + \frac{i}{2\pi\omega} \bar{F}_0(0) + \frac{e}{m} \frac{nc}{\omega(d\psi/dr)} \frac{\partial}{\partial r} \left\{ \left[ \frac{Q_{k, \omega_k}^*(\tau)}{\omega_k^*(\tau)} \right. \right. \\ & \times \left. \left. \frac{\hat{F}_0(\omega - 2i\gamma(\tau))}{\omega - \omega_k(\tau) + n\bar{\omega}_{dk}} + \frac{Q_{k, \omega_k}(\tau)}{\omega_k(\tau)} \frac{\hat{F}_0(\omega - 2i\gamma(\tau))}{\omega + \omega_k^*(\tau) - n\bar{\omega}_{dk}} \right] \hat{\omega}_{dk} |\delta\bar{\phi}_{k0}(r, \tau)|^2 \right\}. \end{aligned} \quad (5.186)$$

Here, we have explicitly denoted the slow time dependence of the mode frequency as  $\omega_k(\tau)$  in order to remind the condition  $|\dot{\omega}_k| \ll |\gamma_{Lk}\omega_k|$ . Furthermore, we have kept explicit  $(r, \tau)$  dependences only in  $\delta\bar{\phi}_{0k}$ , as these are the most relevant for emphasizing the important role of radial mode structures, which may change in time along with the particle distribution function. Meanwhile,  $\gamma_k(\tau) \equiv \text{Im}(\omega_k(\tau))$ ,  $(-n)\bar{\omega}_{d-k} = -n\bar{\omega}_{dk}$ ,  $\hat{\omega}_{d-k} = -\hat{\omega}_{dk}$ ,  $Q_{-k, -\omega_k^*(\tau)} = -Q_{k, \omega_k(\tau)}^*$ , and Eq. (5.185) is the analogue of Eq. (5.131) for frequency sweeping modes.

Equations (5.184) and (5.186) are the general formulation for nonlinear DAW interactions with a EP population and, thus, and provide the unification of the ‘‘bump-on-tail’’ and ‘‘fishbone’’ paradigms (Chen and Zonca, 2013). More specifically, the correspondence to the nonlinear beam-plasma system (cf. Sec. V.D.1) can be readily established ignoring the effect of plasma nonuniformities and geometry. That is, postulating constant  $\delta\hat{\phi}_k(\omega)$  fluctuations, and, with  $|\omega_{*E}| \gg |\omega|$ , letting

$$k_0 \frac{\partial}{\partial u} \leftrightarrow -\frac{m}{e} \frac{nc}{d\psi/dr} \frac{\partial}{\partial r}, \quad (5.187)$$

and  $n\bar{\omega}_{dk} - \omega_k \simeq n\bar{\omega}_{dk0}(r - r_0)/L_{dk0} \leftrightarrow k_0 u$ , with  $L_{dk0}$  the characteristic length of variation of  $\bar{\omega}_{dk}$ <sup>42</sup>, one can draw a one on one correspondence between Eqs. (5.128) and (5.182) as well as between Eqs. (5.130) and (5.184), which become identically the same. This also holds for the reduced forms, *e.g.*, Eq. (5.186), once the monochromatic wave hypothesis is introduced by Eqs. (5.131) and (5.185), respectively. As pointed out at the beginning of Sec. V.D, this reduction of the general formulation for nonlinear DAW interactions with an EP population illuminates both the validity limits of the ‘‘bump-on-tail’’ paradigm and its applicability conditions, as well as to the qualitative and quantitative differences that are introduced by equilibrium geometry and plasma nonuniformity. These issues, analyzed already in general in Secs. V.D.5.a and V.D.5.b, are summarized by Eqs. (5.184) and (5.186) for the simplified case of precessional resonance with magnetically trapped EPs and no finite orbit width effects. Due to the invariance of  $\mu$  and  $J$  actions (cf. Sec. IV.B), this specific problem is one-dimensional and is particularly suited to discuss the transition from the ‘‘bump-on-tail’’ to the ‘‘fishbone’’ paradigm. Properties pertinent to toroidal geometries, in this case, are particle radial transport at essentially constant energy<sup>43</sup>, the energy dependence of  $\bar{\omega}_{dk}$  and  $\hat{\omega}_{dk}$  that gives a completely different weighting of the particle phase-space contributing to the resonant mode drive with respect to the uniform plasma case; and the characteristic radial displacement of magnetically trapped particles, which makes radial decoupling dominant with respect to resonance detuning at relatively low mode growth rate, as indicated by Eq. (5.165) with  $\lambda_n = 1$  and Eq. (5.167).

To be more precise, let us consider the uniform plasma limit of Eq. (5.187). Introducing a simple Krook collision operator, Eq. (5.184) then becomes

$$\begin{aligned} (-i\omega + \nu)\delta\hat{f}_0(\omega) = & i \frac{e^2 k_0^2}{m^2} \frac{\partial}{\partial u} \iint_{-\infty}^{\infty} \left[ \delta\hat{\phi}_{k_0}(y) \frac{-\partial_u \hat{F}_0(\omega - y - y')}{y - k_0 u - \omega - i\nu} \delta\hat{\phi}_{-k_0}(y') \right. \\ & \left. - \delta\hat{\phi}_{-k_0}(y) \frac{\partial_u \hat{F}_0(\omega - y - y')}{y + k_0 u - \omega - i\nu} \delta\hat{\phi}_{k_0}(y') \right] dy dy', \end{aligned} \quad (5.188)$$

<sup>41</sup> Here, we remind the reader, again, that one single toroidal mode number involves the coupling of many poloidal harmonics, due to the toroidal geometry of the plasma equilibrium.

<sup>42</sup> Note that Eq. (5.187) implies that directions of incrementing  $u$  corresponds to decreasing  $r$  and vice-versa; however,  $\bar{\omega}_{dk}$  is also a generally decreasing function of  $r$ .

<sup>43</sup> This property is an interesting combination of the conservation of particle Hamiltonian in the extended phase-space and of the condition  $|\omega_{*E}| \gg |\omega|$  (Chen, 1988) that typically applies to EPs resonantly interacting with DAWs.

when expressed for the nonlinear deviation  $\delta\hat{f}_0(\omega)$  of the particle distribution function from the equilibrium (initial) value  $F_0(0) = Q(v)/\nu(v)$  (cf. Sec. V.D.2.b). The iterative solution of Eq. (5.146) corresponds to taking  $\hat{F}_0(\omega - y - y') = i(2\pi)^{-1}F_0(0)(\omega - y - y')^{-1}$  in Eq. (5.188), *i.e.*, to considering only the first loop in the Dyson series, schematically shown in Fig 5. Moving to the  $t$ -representation, the recursive solution of Eq. (5.188) is then obtained as

$$\begin{aligned} \left(\frac{\partial}{\partial t} + \nu\right) \delta f_0 = & i \frac{e^2 k_0^2}{m^2} \frac{\partial}{\partial u} \iint_{-\infty}^{\infty} e^{-i(y+y')t} \left[ \delta\hat{\phi}_{k_0}(y) \frac{\partial_u F_0(0)}{y' + k_0 u + i\nu} \delta\hat{\phi}_{-k_0}(y') \right. \\ & \left. + \delta\hat{\phi}_{-k_0}(y) \frac{\partial_u F_0(0)}{y' - k_0 u + i\nu} \delta\hat{\phi}_{k_0}(y') \right] dy dy' , \end{aligned} \quad (5.189)$$

which is readily cast as

$$\left(\frac{\partial}{\partial t} + \nu\right) \delta f_0 = \frac{\omega_B^2(t)}{4} \frac{\partial}{\partial k_0 u} \int_0^t \left[ e^{-(\nu + ik_0 u)(t-t')} + c.c. \right] \omega_B^2(t') \frac{\partial F_0(0)}{\partial k_0 u} dt' . \quad (5.190)$$

This equation coincides with Eq. (5.146), noting that, here,  $\omega_B^4 \equiv 4(e/m)^2 k_0^4 |\delta\phi_{k_0}|^2$ , in order to preserve the same normalizations of Fourier amplitudes used in Sec. V.D.2.b.

Finally, as elucidation of Eq. (5.186) in the uniform plasma case, we follow (Al'tshul' and Karpman, 1965, 1966) and assume that the periodic fluctuation of Eq. (5.185) is weakly growing ( $\gamma_L \ll \omega_B$ ) such that Eq. (5.186), with no sources and collisions and accounting for Eq. (5.187), yields the solution of Eq. (5.132). Here, we remind that Eq. (5.132) describes the oscillations of particles that are trapped in the wave, which, however, do not decay in time as expected as consequence of phase mixing. Therefore, the scalar field  $\delta\phi_{k_0}$  oscillations are also predicted to continue indefinitely rather than to fade away, as in actual physical conditions (O'Neil, 1965), due to the fact that the processes described in Fig. 5 do not account for  $k_0$ -harmonics generation produced by spatial bunching (cf. Sec. V.D.1). This limitation is not significative for the analyses of Secs. V.D.6 and V.D.7, since phase locking makes wave-particle trapping essentially ineffective; *de facto* suppressing harmonic generation.

## 6. Nonlinear dynamics of Energetic Particle Modes and avalanches

The novel feature of EPM nonlinear dynamics with respect to that characterizing AEs is the interplay between EP transport and mode structure evolution, which is crucially influenced by the structure of the SAW continuous spectrum (Briguglio *et al.*, 1998) [cf. also (Bierwage *et al.*, 2012, 2011; Briguglio *et al.*, 2007, 2002; Vlad *et al.*, 2004, 2009, 2006, 1999)].

The first analysis of EPM nonlinear behaviors was given by (Briguglio *et al.*, 1998), reporting numerical results from hybrid MHD-gyrokinetic simulations. In that work, it is shown that, unlike in the TAE case analyzed therein (cf. Sec. V.D.5.b), EPM saturation occurs because of “macroscopic outward displacement of the energetic-ion population”, which is shown in Fig. 9 and is characterized by a convective secular process, demonstrated by the line-density  $rn(r)$  contour plot in the  $(r/a, \omega_A t)$  plane. Figure 9 also proves that MHD nonlinearities weakly affect the EPM evolution by direct comparison of two different simulations, carried out without (left) and with (right) MHD mode-mode couplings. These results are consistent with theoretical analyses showing the fundamental role played by EPs in determining EPM dispersive properties and threshold condition (Chen, 1994; Chen and Zonca, 1995; Zonca and Chen, 1996) as well as radial mode structure and spatial localization (Zonca and Chen, 1996, 2000). The overall non-perturbative effect of EPM nonlinear dynamics on the EP line-density profile is displayed in Fig. 10, while Fig. 11 shows the outward secular motion of a resonant circulating particle, typical of mode particle pumping (White *et al.*, 1983).

Most of the distinctive features of low mode number EPM are the same as those typical of fishbone modes, which are discussed in greater detail in Sec. V.D.7. However, the property to be characterized by a nonperturbative interplay of EP transport with mode structures is peculiar to EPM and is most evident, as well as relevant, for high mode numbers typical of ITER (Briguglio *et al.*, 2002; Vlad *et al.*, 2004; Zonca *et al.*, 2005), since the characteristic scale of EP profiles are longer than the typical mode width (cf. Sec. IV). In these conditions and for sufficiently strong wave-particle power exchange, EP transport occurs in avalanches, *i.e.*, as a secular loss process that is accompanied by a convectively amplified EPM wave packet (Briguglio *et al.*, 2002; Vlad *et al.*, 2004; Zonca *et al.*, 2005) and by a local gradient steepening of the EP pressure profile; followed eventually by a relaxation phase (Zonca *et al.*, 2006). This mechanism was demonstrated with hybrid MHD-gyrokinetic numerical simulation results by (Vlad *et al.*, 2004), investigating the EPM nonlinear dynamics in ITER-FEAT reversed shear scenario (cf. Sec. VI.B for more details). The simulation results are summarized in Fig. 12, where  $\beta_E$  radial profiles are shown along with  $(m, n)$  Fourier components of the EPM scalar potential fluctuations during the linear growth (left), the end of the EPM avalanche

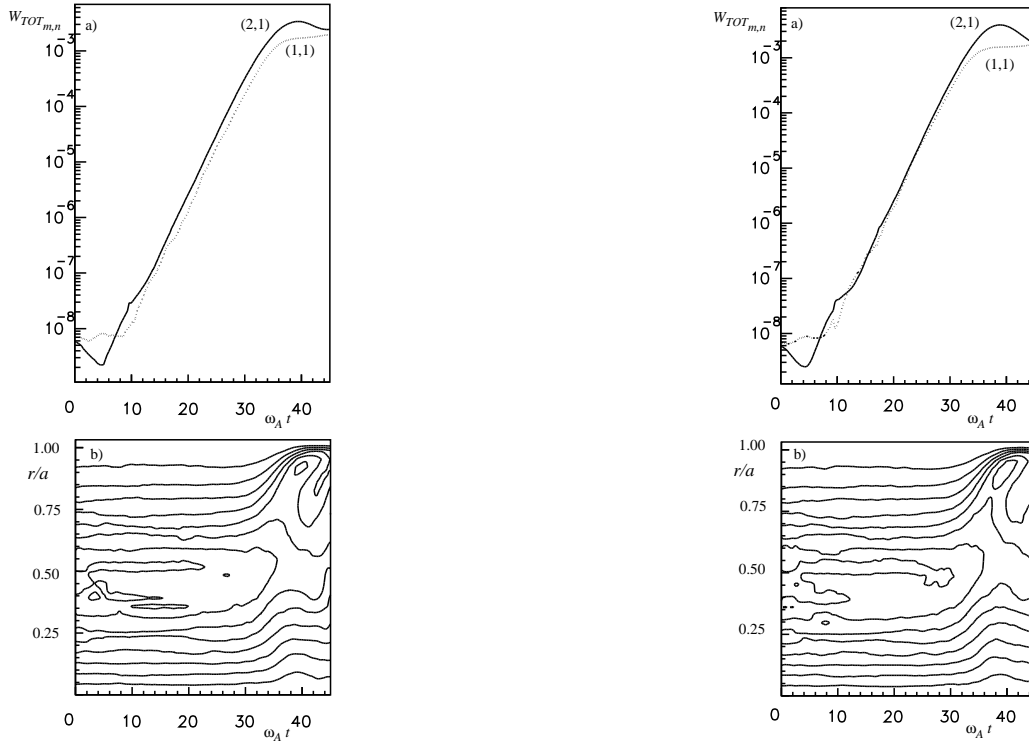


FIG. 9 The total energy of the poloidal components of the  $n = 1$  mode (a), and contour plot of the line-density  $rn(r)$  in the  $(r/a, \omega_A t)$  plane (b) for the EPM simulation by (Briguglio *et al.*, 1998). Normalized time is  $\omega_A t$ , with  $\omega_A = v_A/R_0$  computed at the magnetic axis. Left frame: without MHD nonlinearities [from the original Fig. 21 in Ref. (Briguglio *et al.*, 1998)]. Right frame: with MHD nonlinearities [from the original Fig. 19 in Ref. (Briguglio *et al.*, 1998)].

(middle), and saturation phase (right). Meanwhile, Fig. 13 gives evidence of the peak EP pressure gradient value steepening at the location where the EPM wave packet is localized (Zonca *et al.*, 2005; Zonca and Chen, 2000). Thus, an EPM avalanche consists of an unstable wave packet that is convectively amplified as it radially propagates outward, in phase with the strengthening EP free energy source (pressure gradient). This process continues as long as the EPM wave packet can be amplified by resonant wave-particle interactions and is eventually followed by mode saturation due to radial decoupling, during which EP transport becomes diffusive and the pressure gradient relaxes (Zonca *et al.*, 2006), as shown in Fig. 13. Similar results were obtained by (Briguglio *et al.*, 2002), studying EP transport in hollow current profile plasmas and showing that the minimum- $q$  magnetic surface is the natural location, where the radial

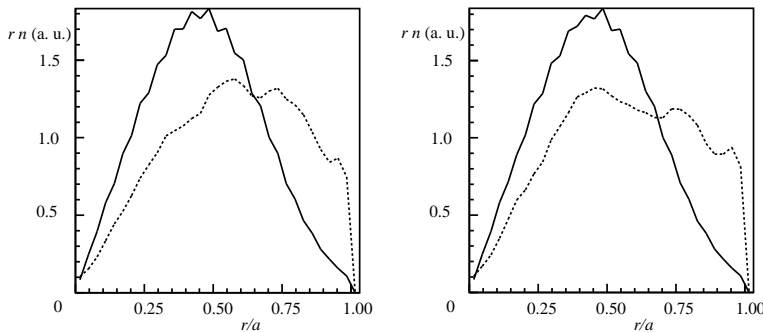


FIG. 10 The initial (solid line) and final (dashed line) line-density profile for the EPM simulation by (Briguglio *et al.*, 1998). Left frame: without MHD nonlinearities [from the original Fig. 22 in Ref. (Briguglio *et al.*, 1998)]. Right frame: with MHD nonlinearities [from the original Fig. 20 in Ref. (Briguglio *et al.*, 1998)].

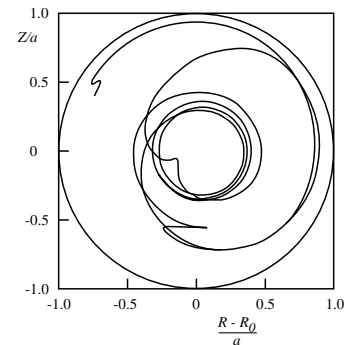


FIG. 11 Poloidal-plane projection of a typical resonant circulating EP orbit, with initial radial coordinate  $r/a = 0.4$ , showing secular radial displacement [from the original Fig. 17 in Ref. (Briguglio *et al.*, 1998)].

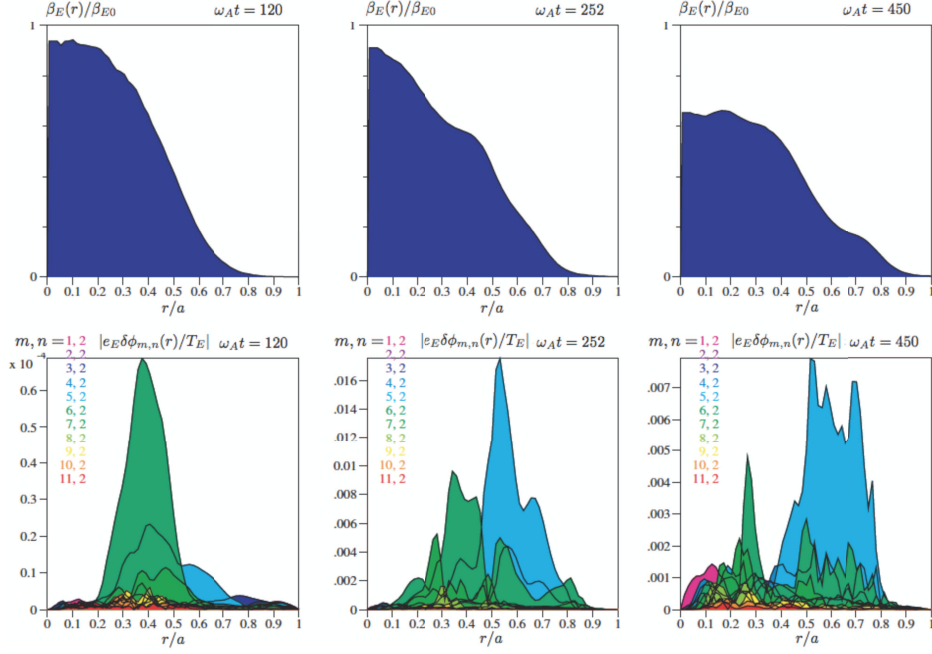


FIG. 12 Radial profiles of  $\beta_E$  and  $(m, n = 2)$  Fourier components of the EPM scalar potential fluctuations during the linear growth (left), the end of the EPM avalanche (middle), and saturation phase (right) [from the original Fig. 6 in Ref. (Vlad *et al.*, 2004)]. Time normalization is the same as in Figs. 9.

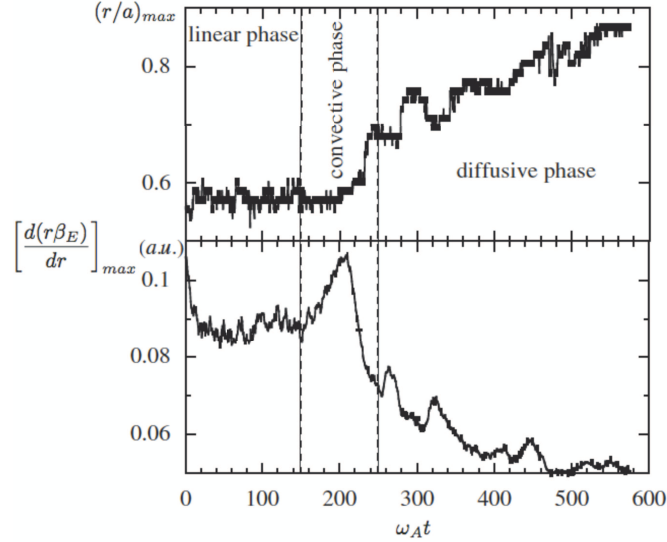


FIG. 13 Radial position  $(r/a)_{max}$  (top) and value of the maximum gradient  $[d(r\beta_E)/dr]_{max}$  vs.  $\omega_{At}$  for the EPM simulation in Fig. 12. The strong convection, characteristic of the avalanche phase, is accompanied by gradient steepening, followed by a relaxation phase, characterized by diffusive EP transport. [from the original Fig. 7 in Ref. (Vlad *et al.*, 2004)].

propagation of EPM induced EP avalanches are expected to stop.

These peculiar EPM nonlinear dynamics have been studied analytically by (Zonca *et al.*, 2005), where their distinctive features and onset conditions are put in connection with the transition from local to meso-scale EP redistributions; dubbed there as transition from weak to strong EP transports (cf. Sec. V.D.5.a). For the sake of simplicity, we analyze EPM excitation by precessional resonance of magnetically trapped EPs, neglecting finite orbit width effects, which

were kept in (Zonca *et al.*, 2005). The description of nonlinear dynamics of phase-space ZS, thus, readily follows the analysis of Sec. V.D.5.c. The theoretical framework adopted here for the non-perturbative description of the interaction of a periodic EPM fluctuation with an EP population is, therefore, that of Eq. (5.3), without the last term on the right hand side, and the Dyson equation, Eq. (5.186). We, furthermore, make the simplifying assumption that the resonant EPs are deeply trapped and the EPM is located near the TAE gap for a tokamak equilibrium with moderate  $(s, \alpha)$  values and shifted circular magnetic flux surfaces (cf. Sec. IV.B.4). We also, in order to compare analytic theory with hybrid MHD-gyrokinetic simulations of EPM avalanches, assume an initial (equilibrium) EP distribution in the form of Eq. (4.106) as well as ignore source and collision terms in Eq. (5.186). The analysis, consequently, is then reduced to computing the nonlinear contribution to  $\delta\bar{W}_{nk}$ , which, considering Eq. (4.105) together with Eq. (5.182), can be written as

$$\delta\bar{W}_{nk} = \int \mathcal{E}d\mathcal{E}d\lambda \sum_{v_{\parallel}/|v_{\parallel}|=\pm} \frac{\pi^2 q R_0}{c^2 k_{\parallel}^2 |s|} \frac{e^2}{m} \left( \frac{\tau_b n^2 \bar{\omega}_{dn}^2}{\omega(\tau)} \right) \int_{-\infty}^{+\infty} \frac{\omega + \omega(\tau)}{n\bar{\omega}_{dn} - \omega(\tau) - \omega} e^{-i\omega t} Q_{k, \omega(\tau)} \hat{F}_0(\omega) d\omega . \quad (5.191)$$

Note that, here,  $\omega(\tau) = \omega_0(\tau) + i\gamma(\tau)$  is the slowly changing frequency of the periodic EPM fluctuation (cf. Sec. V.D.5.c), allowing non-adiabatic frequency chirping processes. With the notations of Sec. V.A and the use of Eq. (5.186), the nonlinear contribution to  $\delta\bar{W}_{nk}$  can be written as

$$\begin{aligned} \delta\bar{W}_{nk}^{NL} &\simeq i \int \mathcal{E}d\mathcal{E}d\lambda \sum_{v_{\parallel}/|v_{\parallel}|=\pm} \frac{\pi^2 q R_0}{c^2 k_{\parallel}^2 |s|} \frac{e^2}{m} \left( \frac{\tau_b n^2 \bar{\omega}_{dn}^2}{\omega(\tau)} \right) k_{\parallel}^2 v_E^2 \rho_{LE}^2 \\ &\times \partial_t^{-2} \frac{\partial^2}{\partial r^2} \left[ \left( \int_{-\infty}^{+\infty} \frac{n\bar{\omega}_{dn}(\gamma - i\omega) e^{-i\omega t} Q_{k, \omega(\tau)} \hat{F}_0(\omega)}{(n\bar{\omega}_{dn} - \omega)^2 + (\gamma - i\omega)^2} d\omega \right) \left| \frac{e_E}{T_E} \delta\bar{\phi}_n(r, t) \right|^2 \right] , \end{aligned} \quad (5.192)$$

where we have, again, noted  $|\omega_{*E}| \gg |\omega|$  (cf. Secs. IV.B.4 and V.D.5.c),  $v_E^2 = T_E/m_E$ ,  $T_E = E_F/m_E$ ,  $\rho_{LE}^2 = v_E^2/\Omega_E^2$ , and  $\partial_t^{-2}$  denotes action of  $-(\omega + 2i\gamma)^{-2}$  under the integration in  $d\omega$ . Meanwhile, the fluctuation intensity in Eq. (5.192) can be rewritten as

$$\left| \frac{e_E}{T_E} \delta\bar{\phi}_n(r, t) \right|^2 = (2\pi)^2 \left| \frac{e_E}{T_E} A_n(r, t) \right|^2 \sum_{\ell, \ell'} e^{-2\pi i n q \ell'} \overline{\frac{\delta\hat{\Phi}_{-n}^{\dagger}}{\hat{k}_{\perp}} \Big|_{\vartheta=2\pi(\ell-\ell')}} \overline{\frac{\delta\hat{\Phi}_n}{\hat{k}_{\perp}} \Big|_{\vartheta=2\pi\ell}} . \quad (5.193)$$

Here, we have used the mode structure decomposition and notations of Eqs. (4.26) and (5.180). Equation (5.193) demonstrates the existence of fine radial structures of the order of or less than  $|nq'|^{-1}$ , due to nonlinear modulations via wave-particle interactions of the EP radial profiles. While such fine structures are visible in the mode of Fig. 12, they are smoothed out in the pressure profiles due to velocity space integration. These features are very general and have been recently observed in gyrokinetic numerical simulations addressing the effect of Ion Temperature Gradient turbulence driven zonal flows on nonlinear SAW dynamics excited by EPs (Bass and Waltz, 2010) (cf. Sec. VII.B). These fine structures have been demonstrated to be modulationally stable below a critical threshold amplitude of the driving modes (Zonca *et al.*, 2000). For this reason, we consider for now only the  $\ell' = 0$  component in Eq. (5.193). We will discuss later the conditions under which radial corrugations in the EP profiles are produced spontaneously (Zonca *et al.*, 2000). Thus, Eq. (5.193) can be rewritten as (cf. Sec. IV.B.4)

$$\left| \frac{e_E}{T_E} \delta\bar{\phi}_n(r, t) \right|^2 \simeq \frac{2\pi^2}{|s|} \left( \delta\hat{\Phi}_{-n0}^{\dagger} \delta\hat{\Phi}_{n0} \right) \left| \frac{e_E}{T_E} A_n(r, t) \right|^2 \equiv |\bar{A}_n(r, t)|^2 , \quad (5.194)$$

where normalizations are consistent with those of (Zonca *et al.*, 2005).

Equation (5.192) can be readily used to formally write the EPM nonlinear equation (Zonca *et al.*, 2006, 2005)

$$D_n(x, -i\partial_x, \omega_0(t) + i\partial_t) \bar{A}_{n0}(x, t) = \delta\bar{W}_{nk}^{NL} \bar{A}_{n0}(x, t) , \quad (5.195)$$

where the fast time dependence has been isolated and  $\bar{A}_n(r, t) \equiv \bar{A}_{n0}(x, t) \exp(-i \int^t \omega_0(t') dt')$ . Equation (5.195) is one example of possible applications of the GFLDR theoretical framework to nonlinear physics of SAW and EPs (cf. Sec. V.A). Equations (5.192) and (5.195) are closed by the leading order evolution equation for  $F_0(t)$ ; *i.e.*,

$$\frac{\partial}{\partial t} F_0(t) \simeq 2k_{\parallel}^2 v_E^2 \rho_{LE}^2 \left( \frac{n\bar{\omega}_{dn}}{\omega_0} \right) \frac{\partial}{\partial r} \left[ \left( \int_{-\infty}^{+\infty} \frac{(\gamma - i\omega)}{(n\bar{\omega}_{dn} - \omega)^2 + (\gamma - i\omega)^2} e^{-i\omega t} \frac{\partial \hat{F}_0(\omega)}{\partial r} d\omega \right) |\bar{A}_{n0}(r, t)|^2 \right] . \quad (5.196)$$

Note that, here, we have ignored terms  $\propto \text{St}\hat{F}_0(\omega)$  and  $\propto \hat{S}(\omega)$  in Eq. (5.186). These terms, however, can be readily included (cf. Sec. V.D.7). Furthermore, as in the case of Eq. (5.192),  $\partial_t^{-1}$  formally applied on the right hand side, when explicitly integrating Eq. (5.196), denotes the action of  $(-i\omega + 2\gamma)^{-1}$  under the integration in  $d\omega$ .

The complex features of EPM nonlinear dynamics and, more generally, of DAW resonantly excited by EPs are clearly visible from the structure of Eq. (5.196). It was already emphasized by (Al'tshul' and Karpman, 1965; Galeev *et al.*, 1965) that it can be considered as a generalized quasilinear equation, which formally reduces to quasilinear theory for a sufficiently broad wave packet. However, as noted in Secs. V.D.5.a and V.D.5.b, Eq. (5.196) also describes the phenomenon of mode particle pumping (White *et al.*, 1983) for sufficiently strong EP drive such that the role of plasma nonuniformities becomes important and “radial decoupling” competes with and becomes more important than “resonance detuning” in the nonlinear wave-particle power exchange, maximized by “phase locking” (Wang *et al.*, 2012). Furthermore, in the case of EPM, the maximization of wave-particle power-exchange implies that radial structures of  $\hat{F}_0(\omega)$  and  $|\bar{A}_{n0}|$  are varying self-consistently, while the mode frequency continuously readjusts to the resonance condition due to mode dispersive properties and radial envelope structures, discussed in Sec. IV.B.4. In turn, particles are most effectively transported outward as they amplify the mode. In Eq. (5.196), phase locking and frequency chirping ensure that the  $\propto (n\bar{\omega}_{dn} - \omega_0)^2$  at the denominator is essentially vanishing for resonant particles. Thus, it is readily recognized that the nature of Eq. (5.196) may change from parabolic to hyperbolic for “phase locked” particles that play a fundamental role in the EPM avalanche of Fig. 12, the hyperbolic nature being strictly connected with ballistic resonant particle transport.

The investigation of Eqs. (5.192), (5.195) and (5.196) is matter of ongoing research based on analytic/numerical works and comparisons with hybrid MHD-gyrokinetic simulations (Briguglio, 2012; Briguglio *et al.*, 2012; Briguglio and Wang, 2013). However, their solution in the simple limit describing the early phase of the EPM wave packet convective amplification was given by (Zonca *et al.*, 2005) and is summarized hereafter, as it helps clarifying the general concepts discussed above. In this case, the nonlinear distortion of the EP distribution function is sufficiently small that  $\hat{F}_0(\omega)$  in Eq. (5.192) takes on its equilibrium value, *i.e.*,  $\hat{F}_0(\omega) = (2\pi\omega)^{-1}i\bar{F}_0(0)$ , with  $\bar{F}_0(0)$  chosen as in Eq. (4.106) and a Gaussian EP profile, as in Eq. (4.109). The expression of  $\delta\bar{W}_{nk}^{NL}$  is then readily reduced to

$$\delta\bar{W}_{nk0}^{NL} \simeq \frac{3\pi(r/R_0)^{1/2}\alpha_E}{8\sqrt{2}|s|} i\pi \frac{\omega_0}{n\bar{\omega}_{dnF}} k_{\vartheta}^2 v_E^2 \rho_{LE}^2 \partial_t^{-2} \frac{\partial^2}{\partial r^2} |\bar{A}_{n0}|^2, \quad (5.197)$$

where we have assumed that the radial scale of  $\alpha_E$  is longer than that of  $|\bar{A}_{n0}|$  (cf. Sec. IV.B.4). In Eq. (5.197), it is crucial to note that the whole right hand side is computed at the instantaneous frequency  $\omega_0$  and at the radial location of the EPM wave packet. With  $\delta\bar{W}_{nk0}^{NL}$  replacing  $\delta\bar{W}_{nk}^{NL}$ , Eq. (5.195) recovers the nonlinear EPM envelope equation of (Zonca *et al.*, 2005), whose solution can be expressed as the convectively amplified propagating (self-similar) wave packet

$$\bar{A}_{n0}(\xi, t) = U(\xi) e^{\int^t \gamma(t') dt'} \equiv W(\xi) e^{i\varphi(\xi) + \int_0^t \gamma(t') dt'}, \quad (5.198)$$

with  $\xi$  given by

$$\xi - \xi_0 \equiv \frac{k_{n0}}{|sk_{\vartheta}|} (x - x_0) \equiv \frac{k_{n0}}{|sk_{\vartheta}|} \left( x - |sk_{\vartheta}| \int_0^t v_g(t') dt' \right), \quad (5.199)$$

$k_{n0}$  denoting the nonlinear wave vector,  $v_g$  the nonlinear group velocity and  $x = |sk_{\vartheta}|(r - r_0)$  (cf. Sec. IV.B.4). Adopting the general procedure for isolating the behavior of the wave packet soliton, one can balance the nonlinear term in Eq. (5.195), for  $\delta\bar{W}_{nk}^{NL} \rightarrow \delta\bar{W}_{nk0}^{NL}$ , with the linear dispersiveness of  $D_n$  in Eq. (4.110), which gives

$$k_{n0}^2 v_g^2 = \frac{3\pi(r/R_0)^{1/2}\alpha_E}{2\sqrt{2}\kappa(s)} \frac{\omega_0}{\bar{\omega}_{dF}} k_{\vartheta}^4 v_E^2 \rho_{LE}^2 \exp\left(2 \int_0^t \gamma(t') dt'\right), \quad (5.200)$$

in the notation of Sec. IV.B.4 ( $n\bar{\omega}_{dnF} \equiv \bar{\omega}_{dF}$ ); while  $U(\xi)$  satisfies the nonlinear equation

$$\partial_{\xi}^2 U = \lambda_0 U - 2iU|U|^2. \quad (5.201)$$

Note that Eq. (5.200) fixes the product  $k_{n0}v_g$ , but the nonlinear group velocity still remains to be determined. For the time being, we simply let

$$v_g^2 \simeq k_{\vartheta}^2 v_E^2 \rho_{LE}^2 \lambda_g^2 \exp\left(2 \int_0^t \gamma(t') dt'\right), \quad (5.202)$$

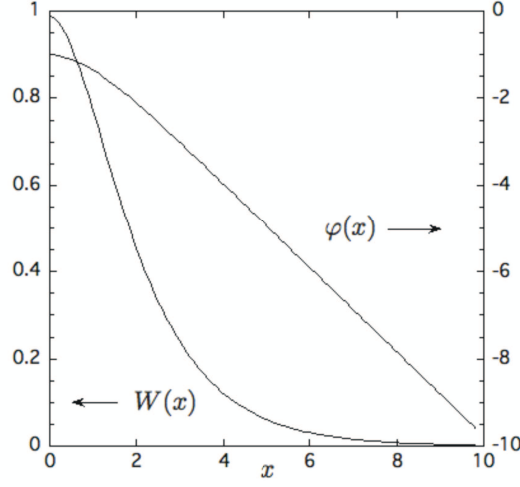


FIG. 14 The functions  $W(x)$  and  $\varphi(x)$  describing the self-similar shape  $U(x) = W(x)e^{i\varphi(x)}$  of the EPM wave packet propagation in the early phase of its nonlinear evolution (Zonca *et al.*, 2005).

where  $\lambda_g < 1$  is a coefficient, whose value is set by the maximization of the wave-particle power transfer in the “phase locking” regime, as discussed below. In this way, Eqs (5.200) and (5.202) can be rewritten as

$$k_{n0}^2 = \frac{3\pi(r/R_0)^{1/2}\alpha_E}{2\sqrt{2}\kappa(s)} \frac{\omega_0}{\bar{\omega}_{dF}} \frac{k_\vartheta^2}{\lambda_g^2} . \quad (5.203)$$

Meanwhile, the solution of Eq. (5.201) is shown in Fig. 14 for the value of  $\lambda_0 \simeq -0.47 + i1.32$ , which corresponds to the ground state of the corresponding complex nonlinear oscillator. Noting Eqs. (5.200) to (5.203), mode frequency and growth rate are then defined by the dispersion relation

$$\frac{|s|\pi}{8} \left[ 1 + 2\kappa(s) - \frac{\alpha}{\alpha_c} \right] + \frac{3\pi(r/R_0)^{1/2}}{8\sqrt{2}|s|} \alpha_{E0} \exp\left(-\frac{x_0^2/s^2}{k_\vartheta^2 L_{pE}^2}\right) \left\{ 1 + \frac{\omega_0}{\bar{\omega}_{dF}} \left[ \ln\left(\frac{\bar{\omega}_{dF}}{\omega_0} - 1\right) + \frac{\pi}{2\lambda_g^2} \text{Im}\lambda_0 \right] \right\} = 0 , \quad (5.204)$$

$$\begin{aligned} \frac{\gamma}{\omega_0} = & \left[ \frac{\omega_0/\bar{\omega}_{dF}}{1 - \omega_0/\bar{\omega}_{dF}} - \frac{\omega_0}{\bar{\omega}_{dF}} \ln\left(\frac{\bar{\omega}_{dF}}{\omega_0} - 1\right) \right]^{-1} \left[ \pi \frac{\omega_0}{\bar{\omega}_{dF}} \left( 1 + \frac{1}{2\lambda_g^2} \text{Im}\lambda_0 \right) \right. \\ & \left. - \left( \frac{3\pi(r/R_0)^{1/2}}{8\sqrt{2}|s|} \alpha_{E0} \right)^{-1} \exp\left(\frac{x_0^2/s^2}{k_\vartheta^2 L_{pE}^2}\right) \Lambda_T(\omega_0) \right] ; \end{aligned} \quad (5.205)$$

which are the nonlinear extension of Eqs. (4.112) and (4.113). The value of  $\lambda_g^2$ , by maximization of the wave-particle power transfer in the phase locking regime, is obtained from Eqs. (5.204) and (5.205); and the condition

$$\frac{d\gamma}{d\lambda_g^2} = \frac{\partial\gamma}{\partial\lambda_g^2} + \frac{\partial\gamma}{\partial\omega_0} \frac{d\omega_0}{d\lambda_g^2} = 0 . \quad (5.206)$$

This equation has a solution  $\lambda_g^2 \lesssim 1$  due to the optimal ordering in the nonlinear dispersion relation above and to the fact that  $d\gamma/d\lambda_g^2 > 0$  for  $\lambda_g^2 \rightarrow 0$ , while  $d\gamma/d\lambda_g^2 < 0$  for  $\lambda_g^2 \rightarrow \infty$ . For typical tokamak parameters, one obtains  $\lambda_g \simeq 0.5 \div 0.6$ , with a spread  $\Delta\lambda_g \simeq \Delta\lambda_g^2 \simeq \gamma^{1/2} [-d^2\gamma/(d\lambda_g^2)^2]^{-1/2} \sim 0.1$ . This is readily verified to yield phase locking of the EPM wave packet with the dominant resonant particle fraction contributing to wave-particle power exchange. In fact, the average value of  $\bar{W}$  in Fig. 14<sup>44</sup>, weighted by the wave particle power transfer  $\propto W^2$  (Briguglio, 2012; Briguglio and Wang, 2013; Vlad *et al.*, 2012, 2013), yields  $\bar{\lambda}_g = \bar{W} \simeq 0.635$ , while the deviation  $\Delta\bar{\lambda}_g = (\bar{W}^2 - \bar{W}^2)^{1/2} \simeq 0.305$ .

<sup>44</sup> More precisely,  $\bar{W} = \int d\tau W \cdot W^2 / \int d\tau W^2 = \int dx W^2 / \int dx W$ .

Therefore, resonant EPs that are co-moving with the EPM wave packet considerably slow down resonance detuning, whereas counter-moving resonant EPs go out of phase with the wave roughly twice as fast with respect to the case of a non-traveling wave-structure. These features are clearly recognizable in the numerical simulation results of Figs. 12 and 13. The residual resonance detuning that affects the nonlinear EPM evolution, *i.e.*, the parameter  $\epsilon_{\dot{\omega}}$  introduced in Eqs. (5.161) and (5.162) and measuring the reduction by  $\sim \epsilon_{\dot{\omega}}^{1/2}$  of the effective bounce frequency of trapped resonant EPs, can be estimated as  $\epsilon_{\dot{\omega}} \sim \Delta\lambda_g/\lambda_g \ll 1$  [cf. Eq. (5.202)]. An intrinsic contribution to  $\epsilon_{\dot{\omega}}$  is also due to plasma nonuniformities and finite size of the EPM wave packet. In the initial linear phase (cf. Sec. IV.B.4)

$$\epsilon_{\dot{\omega}} \sim \frac{(L_{pE}/|k_{\vartheta}|)^{1/2}}{r_0} \sim \frac{1}{(|k_{\vartheta}|L_{pE})^{1/2}}, \quad (5.207)$$

where  $r_0 \sim L_{pE}$  has been considered; while in the early nonlinear evolution

$$\epsilon_{\dot{\omega}} \sim (k_{n0}r_0)^{-1} \sim \frac{\kappa(s)^{1/2}}{\alpha_E^{1/2} (L_{pE}/R_0)^{1/4} |k_{\vartheta}|L_{pE}}. \quad (5.208)$$

Assuming, for typical tokamak parameters,  $\kappa(s) \sim \mathcal{O}(1)$ ,  $\alpha_E \sim L_{pE}/R_0$ ,  $|k_{\vartheta}|L_{pE} \sim (R_0/L_{pE})^2$  and  $\rho_{LE}/R_0 \sim (L_{pE}/R_0)^3$ , so that  $|k_{\vartheta}|\rho_{LE} \sim \mathcal{O}(1)$ , Eqs. (5.207) and (5.208) give very similar results, which are also consistent with  $\epsilon_{\dot{\omega}} \sim \Delta\lambda_g/\lambda_g$ . Thus, the criterion for the onset of EPM avalanches and for the transition from weak to strong EP transport is readily estimated by Eqs. (5.167) and (5.168), and is given by (Zonca *et al.*, 2005)<sup>45</sup>

$$\frac{\gamma_L}{|\omega_0|} \gtrsim \frac{\epsilon_{\dot{\omega}}}{3|k_{\vartheta}|L_{pE}} \sim \left| \frac{\omega_0}{\omega_{*E}} \right|^3, \quad \text{and} \quad \frac{\gamma_L}{|\omega_0|} \gtrsim \frac{\epsilon_{\dot{\omega}}}{3} \sim \left| \frac{\omega_0}{\omega_{*E}} \right|, \quad (5.209)$$

for magnetically trapped and circulating EPs, respectively.

In the initial EPM avalanche phase, characterized by phase locking and wave packet convective amplification, Eq. (5.204) yields a frequency shift  $\Delta\omega$ , relative to the “linear” (initial) mode frequency  $\omega_{0L}$ ,

$$\frac{\Delta\omega}{\omega_{0L}} \simeq (s-1) \frac{x_0}{|sk_{\vartheta}r_0|} = \frac{s-1}{r_0} \int_0^t v_g(t') dt'; \quad (5.210)$$

*i.e.*, a frequency chirping rate that is proportional to the mode amplitude, as discussed at the beginning of Sec. V.D.5. Meanwhile, Eq. (5.205) shows that the EPM wave packet can be convectively amplified, yielding the avalanching process of Fig. 12, as long as the strengthening of mode drive, due to pressure gradient steepening, compensates the reduced drive, due to equilibrium nonuniformities. Equilibrium geometry and plasma nonuniformities influence the wave packet propagation speed and characteristic width as well. Because of its form, the intensity of the convectively amplified wave packet grows as the square of the distance; reminding us, thus, of the superradiance (Dicke, 1954) operation regime of a free electron laser (FEL), where the peak power also increases as the square of the distance along the undulator (Bonifacio *et al.*, 1990, 1994; Giannessi *et al.*, 2005; Watanabe *et al.*, 2007). The EPM wave packet propagation could generally be in either radial directions. However, outward propagation is favored, as the moving wave packet can more easily maintain the phase locking condition with the larger fraction of EPs that are transported outward while driving the mode, due to the conservation of the Hamiltonian in the extended phase-space. Another important factor that may break the symmetry in the radial propagation direction is equilibrium nonuniformity, connected with both EP profiles and continuum damping. Thus, unless radial nonuniformity inhibits outward propagation, frequency chirping is predicted to be generally downward for EPM avalanche events, since characteristic EP resonant frequencies are radially decreasing for typical equilibrium radial profiles.

As a final point, we analyze the conditions under which radial corrugations in the EP profiles, briefly discussed above in connection with Eq. (5.193), are excited spontaneously (Zonca *et al.*, 2000). Adopting for upper/lower EPM sidebands due to EPM wave packet pump scattering off the corrugated EP profile the same representation introduced in Sec. V.C.2, the nonlinear dispersion relation for the EPM modulational instability can be written as

$$\left| \frac{\partial D_0}{\partial \omega_0} \right|^2 (\Delta_T^2 - (\omega_z + i\gamma_d)^2) + \frac{4i\gamma_M^2}{(\omega_z + 2i\gamma)^2} \left( (\omega_z + i\gamma_d) \frac{\partial \text{Re}D_0}{\partial \omega_0} - i\Delta_T \frac{\partial \text{Im}D_0}{\partial \omega_0} \right) + \frac{3\gamma_M^4}{(\omega_z + 2i\gamma)^4} = 0. \quad (5.211)$$

<sup>45</sup> This estimate may be obviously made more precise for a given specific problem under investigation.

Here,  $D_0$  stands for  $D_n$  of the EPM pump with frequency  $\omega_0$  and growth rate  $\gamma$ ,  $\gamma_d$  is the sideband damping and  $\Delta_T$  the frequency mismatch, while

$$\gamma_M^2 = \frac{3\pi^2(r/R_0)^{1/2}\alpha_E}{8\sqrt{2}|s|} \frac{\omega_0}{\bar{\omega}_{dF}} k_{\parallel}^2 \rho_{LE}^2 k_z^2 v_E^2 |\bar{A}_0|^2 . \quad (5.212)$$

Equation (5.211) shows common features with the dispersion relation of ZS induced by finite amplitude TAE, discussed in Sec. V.C.2. The novel element, here, is that resonant wave particle interactions typically produce modulational instability of the EP pressure profile (Vlad *et al.*, 2004; Zonca *et al.*, 2006) characterized by both finite growth rate as well as real frequency shift (Zonca *et al.*, 2000). As pointed out in Sec. V.C.2, all physical processes yielding fluctuation amplitude modulation may result in nonlinear splitting of the corresponding spectral lines. From ordering considerations, it is evident that the onset condition for the EPM induced modulational instability gives  $|\omega_z| \sim \epsilon_0 \omega_0 \sim \gamma_d \sim \gamma \sim \gamma_M/|\Delta_T/\omega_0|^{1/2}$ , with  $\Delta_T \sim \epsilon_0 \omega_0$  (cf. Sec. IV.B.3 and IV.B.4). Thus, considering the normalizations of Eq. (5.194), the threshold condition for  $|\delta B_r/B_0|$  in this case is  $\sim \epsilon_0^{1/4} \alpha_E^{-1/2}$  higher than in the case where TAE induced ZS are dominated by the zonal current; and  $\sim \epsilon_0^{1/2} q^{-1} \alpha_E^{-1/2}$  higher than when TAE induced ZS are dominated by zonal flows (cf. Sec. V.C.2) (Chen and Zonca, 2012, 2013). These results suggest that, for sufficiently strong EP drive, *i.e.*, sufficiently high  $\alpha_E$ , zonal flows and fields are expected to not significantly modify the nonlinear EPM dynamics (Zonca *et al.*, 2000). In particular, when analyzing the modulational instability of EPM driven by EP transit resonance, the criterion for neglecting the effect of zonal flows becomes  $\alpha_E \gg \epsilon_0^{3/2}/q^2$ , as the EPM drive is not reduced by the trapped particle fraction. This is consistent with the empirical scaling  $\alpha_E > \beta_e q^2$ ,  $\beta_e$  being the thermal electron plasma  $\beta$ , obtained from numerical gyrokinetic simulation results (Bass and Waltz, 2010).

It is worthwhile to make further general remarks and comments as conclusion of this analysis of EPM nonlinear dynamics. Note that Eq. (5.201) is similar to that of a nonlinear oscillator in the so-called ‘‘Sagdeev potential’’  $V = (-U^2 + U^4)/2$ , which generates the equation of motion

$$\partial_{\xi}^2 U = U - 2U^3 , \quad (5.213)$$

and gives  $U = \text{sech}(\xi)$ . This form appears in soliton-like solutions of the nonlinear Schrödinger equations; *e.g.*, the Gross-Pitaevsky equation (Gross, 1961; Pitaevsky, 1961) describing the ground state of a quantum system of identical bosons using the pseudo-potential interaction model, as well as the envelope of modulated water wave groups, as demonstrated by (Zakharov, 1968). The same form has also been more recently shown to appear, *e.g.*, in the propagation of the short optical pulse of a FEL in the superradiant regime (Bonifacio *et al.*, 1990, 1994; Giannessi *et al.*, 2005), briefly discussed above, as well as in the radial spreading of drift wave – zonal flow turbulence via soliton formation (Guo *et al.*, 2009). The complex nature of Eq. (5.201), however, is novel and connected with the unique role of wave-particle resonances, which dominate the nonlinear dynamics of EPs via resonant wave-particle power exchange. Maximization of such power exchange yields two effects: (i) the mode radial localization, similar to the analogous mechanism discussed for the linear EPM mode structure (cf. Sec. IV.B.4); and (ii) the strengthening of mode drive [ $\text{Im}\lambda_0 > 0$  in Eq. (5.205)], connected with the steepening of pressure gradient, convectively propagating with the EPM wave packet. These two effects are consistent with and clearly illustrated by the numerical simulation results of Fig. 12 (Zonca *et al.*, 2005).

More generally, Eqs. (5.192), (5.195) and (5.196) are of integro-differential nature and, thus, they describe processes characterized by nonlocality in space and time connected with wave-particle resonant interactions of Alfvénic fluctuations with EPs. This case can be appreciated from the structure of Eq. (5.192) and the operator  $\partial_t^{-2} \partial_r^2$ . Assuming that Eq. (5.195) admits a self-similar solution in the form  $\bar{A}_{n0}(\xi)$ , as in Eq. (5.198), and that the radial profile of  $\hat{F}_0(\omega)$  can be described by a stretched Gaussian distribution  $\propto \exp[-|\xi - \xi_0|^\mu]$ , with some fractional  $\mu \in (1, 2)$ ,  $\delta \bar{W}_{nk}^{NL} \bar{A}_{n0}$  can be rewritten in terms of fractional derivative operators (Zonca *et al.*, 2006),  $\propto \partial_{\xi}^{2-\mu} |\bar{A}_{n0}|^2$ , with

$$\partial_{\xi}^{2-\mu} \Psi \equiv \frac{1}{\Gamma(\mu-1)} \frac{\partial}{\partial \xi} \int_{-\infty}^{\xi} \frac{\Psi(\xi')}{(\xi - \xi')^{2-\mu}} d\xi' , \quad (5.214)$$

corresponding to the Weyl definition of fractional derivative [cf., *e.g.*, (Metzler and Klafter, 2000)]. Its appearance in the nonlinear evolution equation above, Eq. (5.195), reminds about fractional generalizations of the Ginzburg-Landau and nonlinear Schrödinger equations (Milovanov and Rasmussen, 2005; Weitzner and Zaslavsky, 2003), reviewed in (Zelenyi and Milovanov, 2004), characterized by a competition between a weak nonlinearity and space-time nonlocal properties. Indeed, equations built on fractional-derivative operators incorporate in a natural, unified way the key features of non-Gaussianity and long-range dependence that often break down the restrictive assumptions of locality

and lack of correlations underlying the conventional statistical mechanical paradigm [cf. (Metzler and Klafter, 2004) for a review of this subject]. It is worthwhile noting that, following Eq. (5.214) and (Zonca *et al.*, 2006), when the free energy source function in Eq. (5.192) is taken to be Gaussian; *i.e.*,  $\tilde{F}_0(\omega) \propto \exp[-(\xi - \xi_0)^2]$ , Eq. (5.195) can be reduced to the canonical form of the Ginzburg-Landau equation (Lifshitz and Pitaevsky, 1980), which finds many applications other than fusion plasma physics.

Fractional time derivatives can also be introduced for the description of Eq. (5.196) nonlocality in time (and correspondingly in space), which is strictly connected with ballistic resonant particle transport but, more generally, may describe a wider class of behaviors as well. Doing so naturally yields fractional Fokker-Planck equations and, thus, applications of general interest [cf., *e.g.*, the recent work by (Górska *et al.*, 2012)]; with their further extension to nonlinear problems, which is intrinsic to Eq. (5.196). This shows the very peculiar role of EPs in fusion plasmas, which introduce a completely novel class of nonlinear behaviors due to the existence of the SAW continuous spectrum, and the property of EPs to lock onto the proper resonance for maximizing wave-particle power exchange and particle transport (Chen, 2008; Chen and Zonca, 2007a; Zonca *et al.*, 2006).

## 7. The fishbone burst cycle

The observation of fishbone oscillations (McGuire *et al.*, 1983), interpreted as bursts of internal kink modes resonantly excited by EPs via precessional resonance (Chen *et al.*, 1984; Coppi and Porcelli, 1986), is undoubtedly the first key experimental evidence of the rich nonlinear dynamics involving the self-consistent interaction of EPs with MHD as well as Alfvénic fluctuations. The extremely diverse phenomenologies connected with fishbones observations are due to the correspondingly diverse experimental conditions, characterized by a variety of external power sources, generating both supra-thermal ions by ICRH/NBI and supra-thermal electrons by ECHR/LHH/LHCD, and different reference plasma scenarios and corresponding MHD equilibria and stability properties. These observations, briefly summarized in Sec. IV.C, demonstrate that nonlinear fishbone dynamics is determined by both wave-wave (MHD) nonlinearities as well as wave-particle nonlinear interactions. However, the key role played by EPs in the fishbone dynamics, described in Sec. IV.B.1, was clear from the early experimental evidence that fluctuations are locked onto the characteristic (precessional) frequency of EPs that resonantly excite them, while they are transported out preserving the resonance condition by the mode particle pumping mechanism (White *et al.*, 1983). Thus, it is intuitive that, for sufficiently strong power input, fishbone dynamics must be dominated by wave-particle nonlinear interactions.

Due to complexities intrinsic to self-consistent kinetic analyses of interactions between MHD modes and EPs, the early analyses of the fishbone burst cycle relied on simplified predator-prey models (Chen *et al.*, 1984; Coppi *et al.*, 1988b; Coppi and Porcelli, 1986); on which more detailed discussions are given later in this section. Fishbone induced EP transports studies and comparisons with experimental observations were, meanwhile, based on test-particle numerical simulations (White *et al.*, 1983) (cf. Secs. VI and VI.A). The first nonlinear numerical studies of fishbone excitation by non-perturbative wave-particle interactions with EPs are reported by (Candy *et al.*, 1999), assuming a linear MHD description and mode structure given by a rigid  $(m, n) = (1, 1)$  radial displacement (Chen *et al.*, 1984). The nonlinear EP kinetic response is computed numerically and used to calculate EP nonlinear contribution to the potential energy in a kinetic energy principle; *i.e.*, Eq. (4.52) with a simplified form of the inertia enhancement (Glasser *et al.*, 1975). In their work, (Candy *et al.*, 1999) reproduce the dynamics of a fishbone burst, with downward frequency chirping and mode saturation due to nonlinear wave-particle interactions. From dimensional analysis, they obtain the estimate  $|\delta\xi_r/r_s| \sim 1$  at mode saturation for the radial displacement  $\delta\xi_r$  with respect to  $r_s$ , the radial position of the  $q = 1$  surface; which is an upper bound for fishbone saturation and a factor  $\sim 10$  larger than the value obtained in the numerical simulation. Meanwhile, (Candy *et al.*, 1999) also estimate that MHD nonlinearity can be neglected if “through diffusive effects the plasma can cross a magnetic island in a time short compared to the time to complete a bounce inside the island” itself, concluding that in their case this condition is marginally satisfied. The relative role of MHD and EP nonlinearities can, however, be more precisely estimated on the basis of Eq. (4.20), by comparing  $\Lambda_n^{NL}$ , *i.e.*, the contribution of MHD wave-wave couplings to the generalized inertia in the singular layer region (Ödholm *et al.*, 2002), with the nonlinear contribution  $\delta\tilde{W}_{nk}^{NL}$  of EPs to the potential energy in the regular region (Zonca *et al.*, 2007a,b). In Ref. (Ödholm *et al.*, 2002), it is demonstrated that  $\Lambda_n^{NL}$  is predominantly determined by ZS (flows and currents), generated self-consistently by the dominant  $(m, n) = (1, 1)$  component of the fishbone fluctuation, since the contribution of higher resonant toroidal harmonics is typically smaller by the ratio of the singular layer width to  $r_s$ . The MHD model employed by (Ödholm *et al.*, 2002) ignores kinetic thermal ion and geometry effects and yields

$$\Lambda^{NL} \sim \frac{|\delta\xi_{r0}|^2}{\Delta^2} \Lambda \sim \frac{|\delta\xi_{r0}|^2}{r_s^2(\gamma_L/\omega_0)^2} \frac{s^2}{\Lambda}, \quad (5.215)$$

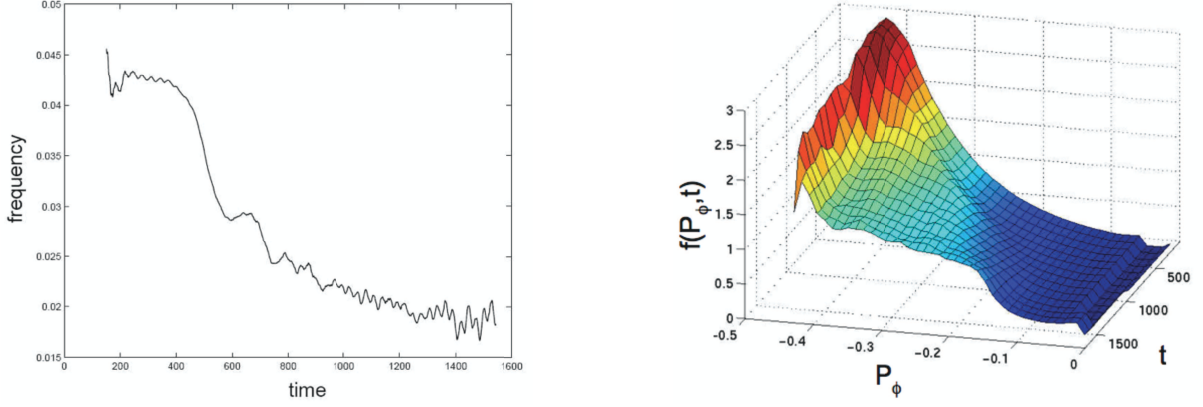


FIG. 15 Left [from the original Fig. 9 in Ref. (Fu *et al.*, 2006)]: Evolution of the fishbone frequency versus time. Frequency is expressed in units of  $\omega_{A0} = v_{A0}/R_0$  and time in units of  $\omega_{A0}^{-1}$ . Right [from the original Fig. 11 in Ref. (Fu *et al.*, 2006)]: Evolution of the resonant EP distribution function for  $v/v_{A0} = 0.8$  and  $\mu B_0/\mathcal{E} = 1$ .

where we have dropped the  $n$  subscript as  $n = 1$  in this case,  $\delta\xi_{r0}$  represents the rigid  $(m, n) = (1, 1)$  radial displacement,  $\Delta \sim r_s(\Lambda/s)(\gamma_L/\omega_0)$  is the inertial layer width,  $s$  is the magnetic shear at the  $q = 1$  surface and  $\Lambda$  can be estimated at its typical linear value. Including inertia enhancement, Eq. (5.215) still applies but a realistic estimate yields  $|\Lambda| \sim |s|$  (Zonca *et al.*, 2007b). Meanwhile, using the theoretical framework of Sec. V.D.5.c, the estimate for  $\delta\hat{W}_{nk}^{NL}$  is readily obtained as [cf. Eq. (5.226) below]

$$\delta\hat{W}_k^{NL} \sim \text{Im}\delta\hat{W}_k^L \frac{|\delta\xi_{r0}|^2}{r_s^2(\gamma_L/\omega_0)^2}, \quad (5.216)$$

where  $\text{Im}\delta\hat{W}_k^L \sim (R_0/r_s)\beta_{Er}$ , with  $\beta_{Er}$  being the  $\beta_E$  value of resonant EPs. Thus, noting Eqs. (4.20), (5.215) and (5.216), one can conclude that EP nonlinearities dominate the fishbone burst cycle for  $\beta_{Er} \gg |s|^3(r_s/R_0)|\Lambda|^{-1}$ . Meanwhile, for typical  $|\Lambda| \sim |s|$  and near marginal stability for precessional fishbones, both nonlinear effects have, in general, to be kept on the same footing. A similar argument can also be constructed for the diamagnetic fishbone (cf. Sec. IV.B.1). In this section, we focus on fishbone nonlinear dynamics well above excitation threshold, where wave-wave (MHD) nonlinearities can be neglected and the evolution of the system is dominated by the self-consistent interplay between mode frequency chirping and EP transport via the mode particle pumping mechanism (Chen *et al.*, 1984; White *et al.*, 1983). This allows us to explain the physics underlying frequency chirping and fishbone burst saturation by secular EP ejection from the region where the mode drive is localized in the linear unstable phase.

Comprehensive numerical fishbone simulations based on the hybrid MHD-gyrokinetic model equations (Park *et al.*, 1992) (cf. Sec. II) are more recent (Fu *et al.*, 2006; Vlad *et al.*, 2012, 2013). Fishbone linear stability analyses based on the same approach are reported by (Park *et al.*, 1999). Meanwhile, the first nonlinear simulation of a fishbone burst cycle is given by (Fu *et al.*, 2006), where it is shown that mode saturation and frequency chirping are connected with the secular outward motion of resonant EPs, as depicted in Fig. 15. More specifically, Fig. 15 shows both frequency variation in time and the change in the resonant EP distribution function for  $v/v_{A0} = 0.8$  and  $\mu B_0/\mathcal{E} = 1$  (cf. Sec. II.D), with  $v_{A0}$  the Alfvén speed on magnetic axis. The normalization of  $P_\phi$  is such that  $P_\phi = -0.42$  corresponds to the plasma center and  $P_\phi = 0$  to the plasma boundary. In the numerical simulations by (Fu *et al.*, 2006), MHD nonlinearities are found to reduce the mode saturation level, but not drastically, yielding to the conclusion that wave-particle nonlinear interplay is sufficient to explain the dominant features of mode saturation and frequency dynamics; consistent with comparing Eq. (5.215) and Eq. (5.216). Although (Fu *et al.*, 2006) noted the possible qualitative similarity of the mode frequency evolution in Fig. 15 with the  $\propto t^{1/2}$  frequency chirping of phase-space holes and clumps (Berk *et al.*, 1999), discussed in Sec. V.D.2.c, it can be readily recognized that the nonlinear fishbone dynamics is non-adiabatic, in the sense discussed in Secs. V.D.5 and V.D.6 above. Thus, frequency chirping and phase locking are expected to accompany the secular loss of resonant particles, while mode saturation is due to radial decoupling.

Further demonstration of the nonlinear physics underlying the fishbone burst cycle has been recently provided by hybrid MHD-gyrokinetic simulations of “electron fishbones” (e-fishbones) (Vlad *et al.*, 2012, 2013) (cf. Sec. IV.B.1). The relevance of e-fishbones is primarily related to the fact that supra-thermal electrons are characterized by relatively small orbit width compared with those of fast ions, similar to the case of alpha particles in burning plasmas. Moreover,

precessional resonance depends on energy, not mass. Thus, e-fishbones give the opportunity to study the coupling between EPs and MHD like modes in burning plasma relevant conditions even in present day machines. In particular, supra-thermal electron transport perpendicular to the equilibrium magnetic field caused by these modes can reflect some properties of fluctuation induced transport of fusion alphas due to precessional resonance (Zonca *et al.*, 2007a,b). The numerical simulation results by (Vlad *et al.*, 2012, 2013) are consistent with those by (Fu *et al.*, 2006) and demonstrate that nonlinear mode saturation is accompanied by downward frequency chirping. In addition, they illuminate and fully clarify the nonlinear dynamics of the strongly driven fishbone burst cycle by means of the phase-space numerical diagnostics introduced by (Briguglio, 2012; Briguglio and Wang, 2013) (cf. Sec. V.D.6). In this case, in order to model typical Frascati Tokamak Upgrade (FTU) operations with e-fishbones (Zonca *et al.*, 2007a), the  $q$  profile has slightly negative shear inside the minimum  $q$  surface at  $r_s/a \simeq 0.35$ , where  $q_{min}(r_s) \simeq 1.05$ , while  $q_0 \simeq 1.25$  on the magnetic axis. For this reason, the dominant  $(m, n) = (1, 1)$  component of the fishbone fluctuation is different from the usual rigid displacement inside the  $q = 1$  surface and decreases more gradually from  $r \sim r_s$  toward the plasma edge (cf. Fig. 16). In these simulations (Vlad *et al.*, 2012, 2013), supra-thermal electron are represented by an anisotropic Maxwellian (magnetically trapped particles), with a peak radial gradient located slightly inside  $r_s$ . This distribution is given as initial value and let self-consistently evolve with e-fishbone fluctuations without external sources and collisions, as in (Fu *et al.*, 2006). Meanwhile, thermal ion kinetic effects are also included (Wang *et al.*, 2011) to properly handle enhanced plasma inertia and ion Landau damping (Kolesnichenko *et al.*, 2010a; Zonca *et al.*, 2007a, 2009) (cf. Sec. IV.B.1)<sup>46</sup>. The convective resonant particle motion yielding mode saturation by radial decoupling is demonstrated by a time sequence of kinetic Poincaré plots (White, 2012), which show EPs moving outward at essentially constant wave-particle phase and the formation of a steeper gradient region that is also outward moving. At the same time, a flatter region in the EP particle distribution is formed at smaller radii, which extends further inward as more EPs are convectively pumped outward. This evidence is consistent with Fig. 15 (Fu *et al.*, 2006). Meanwhile, as resonant EPs are convected outward and their  $\bar{\omega}_d$  decreases, the mode chirps downward and readjusts its frequency by minimizing resonance detuning in order to maximize wave-particle power exchange; corresponding to maximizing mode growth and resonant EP transport at the same time, as in the case of EPM (cf. Sec. V.D.6). This is shown in Fig. 16(left), which illustrates the time evolution of  $\bar{\omega}_D$  and  $\delta\omega_D$ , defined as (Vlad *et al.*, 2012, 2013)

$$\bar{\omega}_D \equiv \frac{\sum_i P_i^{\text{lin}} \bar{\omega}_{di}}{\sum_i P_i^{\text{lin}}} , \quad \text{and} \quad \delta\omega_D \equiv \left[ \frac{\sum_i P_i^{\text{lin}} (\bar{\omega}_{di} - \bar{\omega}_D)^2}{\sum_i P_i^{\text{lin}}} \right]^{1/2} ; \quad (5.217)$$

with the summation extended on simulation particles and weighted by  $P_i^{\text{lin}}$ , the wave-particle power exchange in the linear phase. With the same definition of Eq. (5.217), it is also possible to define  $\bar{\Theta}$  and  $\delta\Theta$ , as well as the average radial position of EPs contributing to the initial (linear) drive,  $\bar{r}$ , and its corresponding spread,  $\delta r$ , which are also shown in Fig. 16(center) and Fig. 16(right), respectively. In particular, Fig. 16(center) shows that frequency chirping is due to phase locking (black line) and that, with no frequency chirping accounted for,  $\bar{\Theta}|_{\omega=\text{const}}$  (red line) would yield rapid resonance detuning. Saturation of the fishbone burst, instead, is due to radial decoupling, as illustrated in Fig. 16(right), showing the time evolution of  $\bar{r}$  (black line) and  $\bar{r} \pm \delta r$  (red lines), referred to the linear mode structure (in arbitrary units)  $|(m/r)\delta\phi_{m,n}| \propto |\delta\xi_{r m,n}|$ . Note that  $\bar{\omega}_D = \bar{\omega}_d(\bar{r})$  for resonant EPs. Due to the strong energy weighting  $\propto \bar{\omega}_d^2$  in the definition of  $\delta\hat{W}_k$  and the anisotropic Maxwellian distribution assumed as initial reference equilibrium for EPs in this case, the values of  $\delta\omega_D$  and  $\delta\Theta \sim \delta\omega_D/\omega_{A0}$  overestimate the actual frequency spread around the phase locking condition in EP phase space, which is more precisely represented by  $\sim (1/2)|\bar{\omega}_d(\bar{r} + \delta r) - \bar{\omega}_d(\bar{r} - \delta r)|$ .

We may understand the above simulation results on the nonlinear fishbone dynamics (Fu *et al.*, 2006; Vlad *et al.*, 2012, 2013) within the theoretical framework introduced in Sec. V.D.5.c. Assuming deeply trapped EPs and neglecting finite orbit widths, as in Sec. V.D.6, in order to simplify the detailed analyses, and considering a rigid plasma displacement as dominant component of the fishbone fluctuation<sup>47</sup>, from Eq. (4.59) we readily have

$$\delta\hat{W}_k = 2 \frac{\pi^2}{B_0^2} m \Omega^2 \frac{R_0}{r_s^2} \int_0^{r_s} \frac{r^3}{q} dr \int \mathcal{E} d\mathcal{E} d\lambda \sum_{v_{\parallel}/|v_{\parallel}|=\pm 1} \frac{\tau_b \bar{\omega}_d^2}{\omega(\tau)} \int_{-\infty}^{\infty} \frac{\omega + \omega(\tau)}{\bar{\omega}_d - \omega(\tau) - \omega} e^{-i\omega t} Q_{k,\omega(\tau)} \hat{F}_0(\omega) d\omega , \quad (5.218)$$

where, in analogy with Eq. (5.191),  $\omega(\tau) = \omega_0(\tau) + i\gamma(\tau)$  is the time evolving complex fishbone frequency. The

<sup>46</sup> Please, refer to (Vlad *et al.*, 2012, 2013) for further details about equilibrium profiles used in numerical simulations.

<sup>47</sup> A fully self-consistent treatment must generally allow the mode structure to evolve due to non-perturbative redistributions of EPs.

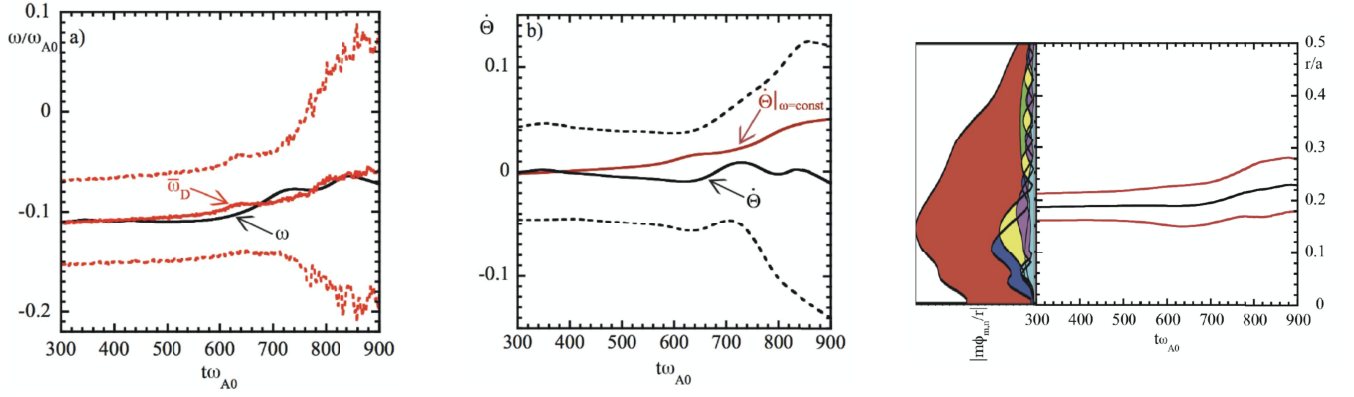


FIG. 16 [From the original Fig. 11 in Ref. (Vlad *et al.*, 2013)]: (Left) Time evolution of  $\bar{\omega}_D$  (red line) and  $\bar{\omega}_D \pm \delta\omega_D$  (dashed red lines), compared with the time evolving mode frequency from simulation results (black line). (Center) Time evolution of  $\bar{\theta}$  (black line) and  $\bar{\theta} \pm \delta\bar{\theta}$  (dashed black lines);  $\bar{\theta}|_{\omega=\text{const}}$ , obtained neglecting frequency chirping is also shown (red line). (Right) [from the original Fig. 12 in Ref. (Vlad *et al.*, 2013)]: Time evolution of  $\bar{r}$ , the average radial position of EPs contributing to the initial (linear) drive (black line), and of  $\bar{r} \pm \delta r$  (red lines). The linear mode structure is also shown by  $|(m/r)\delta\phi_{m,n}| \propto |\delta\xi_{r,m,n}|$  in abscissa, vs. the normalized radial position on the vertical axis. The harmonic in red refers to the dominant  $(m, n) = (1, 1)$  component.

evolution equation for  $F_0(t)$ , meanwhile, is also readily obtained from Eq. (5.186) and, assuming  $|\omega_{*E}| \gg |\omega(\tau)|$ ,

$$\frac{\partial}{\partial t} F_0(t) \simeq \text{St}F_0(t) + S(t) + 2 \left( \frac{\bar{\omega}_d}{\omega_0(\tau)} \right) \frac{\partial}{\partial r} \left[ \left( \int_{-\infty}^{+\infty} \frac{(\gamma - i\omega) - (\bar{\omega}_d - \omega_0)(\gamma/\omega_0)}{(\bar{\omega}_d - \omega_0)^2 + (\gamma - i\omega)^2} e^{-i\omega t} \frac{\partial \hat{F}_0(\omega)}{\partial r} |\omega_0(\tau)|^2 |\delta\xi_{r0}|^2 d\omega \right) \right]. \quad (5.219)$$

Equation (5.219) is the analogue of Eq. (5.196), having maintained explicitly external source and collision terms as well as the next order correction terms in the asymptotic expansion in  $\gamma/\omega_0$ . Note that, as in Eq. (5.196), the inverse operator  $\partial_t^{-1}$  acting on the nonlinear term on the right hand side, when integrating Eq. (5.219) in time, corresponds to  $(2\gamma - i\omega)^{-1}$  under the integration in  $d\omega$ . Furthermore, recalling the discussion following Eq. (5.196), Eq. (5.219) can be considered as a generalized quasilinear equation (Al'tshul' and Karpman, 1965; Galeev *et al.*, 1965), which also accounts for mode-particle pumping (White *et al.*, 1983) when frequency chirping and phase locking are considered. With  $\delta\hat{W}_k$  given by Eqs. (5.218) and (5.219), the GFLDR Eq. (4.20)<sup>48</sup> provides a description of the fishbone burst cycle dominated by EP nonlinearity (Zonca *et al.*, 2007b), reducing to the case investigated numerically by (Candy *et al.*, 1999) if the core plasma response is described by ideal MHD (Glasser *et al.*, 1975). Due to the global nature of the fishbone mode structures, these equations generally require a numerical solution, which is not given in the literature except that in the MHD limit considered by (Candy *et al.*, 1999). However, further analytic progress is possible if one introduces subsidiary approximations, which help elucidating the nature of saturation process and EP transport due to fishbone bursts (Zonca *et al.*, 2007b).

We may assume that the EP response  $\delta\hat{W}_k$  is predominantly provided from a localized radial region inside  $r_s$ ; consistent with numerical simulation results in Fig. 16 (Vlad *et al.*, 2012, 2013). The same assumption is also consistent with our focus on strongly driven fishbone modes, which are characterized by steep EP radial gradients inside  $r_s$ , and with the radial structure of the integrand in the expression for  $\delta\hat{W}_k$  provided by Eq. (5.218). Using the formal decomposition  $\delta\hat{W}_k \equiv \delta\hat{W}_k^L + \delta\hat{W}_k^{NL}$  as in Sec. V.D.6, it is readily verified that  $\text{Re}\delta\hat{W}_k \simeq \text{Re}\delta\hat{W}_k^L$  at the leading order of the asymptotic expansion in  $\gamma/\omega_0$ ; *i.e.*, the non-resonant EP response is formally linear. For radially localized EP response,

$$(\bar{\omega}_d - \omega(\tau) - \omega)^{-1} \simeq \tilde{\omega}_d^{-1} (\mathcal{E} - \mathcal{E}_0 - i(\gamma - i\omega)/\tilde{\omega}_d)^{-1}, \quad (5.220)$$

with  $\bar{\omega}_d \equiv \tilde{\omega}_d \mathcal{E}$  and  $\omega_0 \equiv \tilde{\omega}_d \mathcal{E}_0$ . Meanwhile, noting that  $\tau_b = 2\pi q R_0 \mathcal{E}^{-1/2} (R_0/r)^{1/2}$  for deeply trapped particles, as well as  $k_\vartheta \propto -(nq/r)$ ,  $\bar{\omega}_d^2 \propto \tilde{\omega}_d^2 \propto (nq/r)^2$  and  $|\omega_{*E}| \gg |\omega(\tau)|$  (Chen, 1988), we can write

$$\text{Re}\delta\hat{W}_k \simeq \text{Re}\delta\hat{W}_k^L = -\frac{R_0}{r_s} \int_0^{r_s} q^2 \frac{r}{r_s} \left( \frac{R_0}{r} \right)^{1/2} \frac{\partial}{\partial r} \left[ \left( \frac{r}{R_0} \right)^{1/2} \hat{\beta}_E(r; \omega_0(\tau)) \right] dr, \quad (5.221)$$

<sup>48</sup> This is equivalent to Eq. (4.52) with the inclusion of a general kinetic expression of the inertia enhancement.

where

$$\hat{\beta}_E(r; \omega_0(\tau)) = 2 \frac{\pi^2}{B_0^2} m |\Omega| \frac{r}{q^2} \int \mathcal{E} d\mathcal{E} d\lambda \sum_{v_{\parallel}/|v_{\parallel}|=\pm 1} \tau_b \bar{\omega}_d^2 \int_{-\infty}^{\infty} \frac{(\bar{\omega}_d - \omega)}{(\bar{\omega}_d - \omega)^2 + (\gamma - i\omega)^2} e^{-i\omega t} \hat{F}_0(\omega) d\omega . \quad (5.222)$$

This definition, for simplicity, assumes that modes have positive frequency when rotating in the particle diamagnetic direction; *i.e.*,  $n = 1$  for energetic ions and  $n = -1$  for energetic electrons. The expression of  $\hat{\beta}_E$  depends only on the ratio  $\omega_0/\bar{\omega}_{dF}$ , with  $\bar{\omega}_{dF}$  the characteristic EP precessional frequency that, in the case of the isotropic slowing down distribution function considered in Secs. IV.B.4 and V.D.6, is the precessional frequency at the injection energy of the EP beam. Thus, Eq. (4.20) yields

$$\delta \hat{W}_f + \Re \delta \hat{W}_k^L \simeq 0 , \quad (5.223)$$

and Eq. (5.221) shows that the fishbone frequency is set by the condition  $\omega_0/\bar{\omega}_{dF} \simeq \text{const}$ , to be computed at the position of the radial shell where the most significant EP contribution is localized. Meanwhile, we can write<sup>49</sup>

$$\begin{aligned} \text{Im} \delta \hat{W}_k &= -\frac{R_0}{r_s} \int_0^{r_s} q^2 \frac{r}{r_s} \left( \frac{R_0}{r} \right)^{1/2} \frac{\partial}{\partial r} \left[ \left( \frac{r}{R_0} \right)^{1/2} \beta_{Er}(r; \omega_0(\tau)) \right] dr \\ &= \frac{R_0}{r_s} \int_0^{r_s} \left[ -r q^2 \frac{\partial \beta_{Er}}{\partial r} - q^2 \frac{\beta_{Er}}{2} \right] \frac{dr}{r_s} , \end{aligned} \quad (5.224)$$

where the resonant EP  $\beta_E$  is defined as

$$\beta_{Er}(r; \omega_0(\tau)) = 2 \frac{\pi^2}{B_0^2} m |\Omega| \frac{r}{q^2} \int \mathcal{E} d\mathcal{E} d\lambda \sum_{v_{\parallel}/|v_{\parallel}|=\pm 1} \tau_b \bar{\omega}_d^2 \int_{-\infty}^{\infty} \frac{(\gamma - i\omega)}{(\bar{\omega}_d - \omega)^2 + (\gamma - i\omega)^2} e^{-i\omega t} \hat{F}_0(\omega) d\omega . \quad (5.225)$$

By substitution of the formal solution of Eq. (5.219) into Eq. (5.224), it is possible to obtain

$$\beta_{Er} = \partial_t^{-1} \left( \dot{\beta}_{ErS} - \nu_{ext} \beta_{Er} \right) + \partial_t^{-2} \left( \frac{R_0}{r} \right)^{1/2} \left\{ \frac{q}{r} \frac{\partial}{\partial r} \left[ \frac{r}{q} |\omega_0|^2 |\delta \xi_{r0}|^2 \frac{\partial}{\partial r} \left( \left( \frac{r}{R_0} \right)^{1/2} \beta_{Er} \right) \right] \right\} . \quad (5.226)$$

Together with Eq. (5.224), this last equation justifies the estimate for  $\delta \hat{W}_k^{NL}$  given in Eq. (5.216), which yields the optimal ordering for the saturation amplitude of the fishbone burst as  $|\delta \xi_{r0}| \sim r_s |\gamma_L / \omega_0|$ , consistent with numerical simulation results reported by (Vlad *et al.*, 2013). Here, we have also introduced the effects of sources and collisions on the resonant EP population using the definitions

$$\dot{\beta}_{ErS} \equiv 2 \frac{\pi^2}{B_0^2} m |\Omega| \frac{r}{q^2} \int \mathcal{E} d\mathcal{E} d\lambda \sum_{v_{\parallel}/|v_{\parallel}|=\pm 1} \tau_b \bar{\omega}_d^2 \frac{\gamma}{(\bar{\omega}_d - \omega)^2 + \gamma^2} S(t) , \quad (5.227)$$

$$\nu_{ext} \beta_{Er} \equiv -2 \frac{\pi^2}{B_0^2} m |\Omega| \frac{r}{q^2} \int \mathcal{E} d\mathcal{E} d\lambda \sum_{v_{\parallel}/|v_{\parallel}|=\pm 1} \tau_b \bar{\omega}_d^2 \frac{\gamma}{(\bar{\omega}_d - \omega)^2 + \gamma^2} \text{St} F_0(t) , \quad (5.228)$$

which explicitly separate these contributions as suggested by (White, 2010), to emphasize their different roles in the dynamics of fishbone burst cycle on time scales longer than  $\tau_{NL} \sim \gamma_L^{-1}$  (cf. following discussion). Finally, the system of Eqs. (5.221) to (5.228) is closed by the evolution equation for  $|\delta \xi_{r0}|$  that, using Eq. (4.20), can be written as

$$\frac{\partial}{\partial t} \ln |\delta \xi_{r0}|^2 = \frac{2(R_0/r_s)}{(-\partial \Re \delta \hat{W}_k^L / \partial \omega_0)} \left\{ - \int_0^{r_s} q^2 \frac{r}{r_s} \left( \frac{R_0}{r} \right)^{1/2} \frac{\partial}{\partial r} \left[ \left( \frac{r}{R_0} \right)^{1/2} \beta_{Er}(r; \omega_0(\tau)) \right] dr - \left( \frac{r_s}{R_0} |s| \Lambda(\omega_0) \right) \right\} . \quad (5.229)$$

Without sources and collisions, and assuming  $q \sim \text{const}$  as well as  $\omega_0/\bar{\omega}_{dF} \sim \text{const}$ , Eq. (5.226) describes the propagation of  $(r/R_0)^{1/2} \beta_{Er}$  as a function of  $(r^2 - 2r|\omega_0| |\delta \xi_{r0}|)$ ; *i.e.*, for sufficiently steep pressure gradient, the

<sup>49</sup> Note that, here, we use a slightly different definition than in (Zonca *et al.*, 2007b) in order to take into account the assumption of deeply trapped EPs.

radial shell location providing the dominant contribution to the mode drive and EP compression propagates with speed  $\dot{r} \simeq |\omega_0| |\delta \xi_{r0}|$ , which is a function of  $r$ . This is the mechanism of mode particle pumping (White *et al.*, 1983) that yields mode saturation by ejection of resonant particles from the  $r = r_s$  surface when the ejection rate  $\sim |\omega_0| |\delta \xi_{r0}| / r_s$  balances the growth rate  $\sim \gamma_L$ . Thus, as resonant EPs are convected outward and the mode growth rate decreases, the downward frequency shift can be computed by Eq. (5.210), with  $v_g = |\omega_0| |\delta \xi_{r0}|$ . This picture is consistent with numerical simulation results reported in Fig. 16 (right) (Vlad *et al.*, 2012, 2013) and is, in essence, similar to that of nonlinear EPM dynamics (cf. Sec. V.D.6) with one additional twist connected with the different underlying mode structure. In the case of EPM, the nonlinear interplay of EP transport and mode structure causes convective wave-packet amplification as a soliton structure, while resonant EPs are transported outward locked into resonance at essentially constant energy, due to the conservation of the Hamiltonian in the extended phase space and the condition  $|\omega_{*E}| \gg |\omega(\tau)|$ . The same process occurs in the fishbone case but, when particles that most efficiently provide mode drive are transported sufficiently outward that radial decoupling becomes important, they are gradually replaced by lower energy particles, which resonate at smaller  $r$  value and continue driving the mode (White, 2000). In this way, particles can be extracted from increasingly lower energies and inner regions of the plasma core (Fu *et al.*, 2006; Vlad *et al.*, 2012, 2013) (cf., *e.g.*, Fig. 15) and be pumped outward, far beyond the  $r_s$  surface and up to the plasma boundary (White *et al.*, 1983). Proceeding further in the  $\gamma/\omega_0$  asymptotic expansion, at  $\mathcal{O}(\gamma/\omega_0)$  it is found that resonant particles also determine  $\text{Re} \delta \hat{W}_k^{NL}$ , while non-resonant particles enter only at  $\mathcal{O}(\gamma^2/\omega_0^2)$  (Zonca *et al.*, 2007b). This higher order expansion can be used to determine frequency sweeping rate with a better precision than based on the simple expression  $\omega_0/\bar{\omega}_{dF} \sim \text{const}$ .

Equations (5.226) with sources and collisions and (5.229) can be used to derive reduced nonlinear models for the fishbone burst cycle. Without nonlinear term, Eq. (5.226) gives the asymptotic solution  $\beta_{Er} = \beta_{Er0} = \dot{\beta}_{ErS}/\nu_{ext}$ . For the strongly driven fishbone case, considered here, we may consider  $\beta_{Er0}$  significantly larger than the threshold condition for fishbone excitation. Thus, when the threshold condition  $\beta_{Er} = \beta_c$  is reached, we may well assume that  $\beta_{Er}$  is linearly increasing in time due to  $\dot{\beta}_{ErS}$ . Formally acting with  $\partial_t$  on Eq. (5.226), estimating  $\partial_r^2 \sim -1/r_s^2$ , and considering the remaining  $\partial_t^{-1} \sim \tau_{NL} \sim r_s/(|\omega_0| |\delta \xi_{r0}|)$ , Eqs. (5.226) and (5.229) can be modeled as

$$\begin{aligned} d\beta/d\tau &= S - A\beta_c, \\ dA/d\tau &= \gamma_0 (\beta/\beta_c - 1) A, \end{aligned} \quad (5.230)$$

where we have dropped the subscript in  $\beta_{Er}$  to introduce the same notation used by (White, 1989),  $\tau$  is a normalized time,  $A = |\delta \xi_{r0}|/r_s$  is the normalized fishbone amplitude and  $\gamma_0$  is a measure of the linear growth rate. Equations (5.230), given here in the form adopted in problem # 3 on p. 280 of the book by (White, 1989), is the same as that originally proposed by (Chen *et al.*, 1984) for the interpretation of the fishbone burst cycle<sup>50</sup>. As noted by (Chen *et al.*, 1984; White, 1989), the solution of Eqs. (5.230) is cyclic; *i.e.*, it can be generally written as  $F(A, \beta) = \text{const}$ , where  $F(A, \beta)$  has a maximum at the fixed point position  $\beta = \beta_c$ ,  $A = S/\beta_c$ . A crucial feature of Eqs. (5.230) is the linear dependence on  $A$  of the loss term in the  $\beta$  evolution equation. From Eq. (5.226), this is readily recognized to be a consequence of the  $\partial_t^{-2}$  operator acting on the nonlinear response, which is the manifestation of secular resonant EP losses by mode particle pumping (White *et al.*, 1983). This term was proposed in the original model by (Chen *et al.*, 1984) on the basis of intuitive representation of the underlying physics of the fishbone burst cycle, and indicates the fundamental difference of that approach with respect to the predator-prey model discussed by (Coppi *et al.*, 1988b; Coppi and Porcelli, 1986), which adopts a loss term  $\propto A^2$ .

In the form of Eqs. (5.230), the temporal nonlocality built in Eq. (5.226) and, more generally, in Eq. (5.219) is lost. However, it has been recently proposed, in the context of predator-prey modeling of TAE bursting behaviors, that nonlocal time behaviors may be accounted for by introducing a time delay in the wave-particle power exchange and in the phase-space island induced particle diffusion (Parker and White, 2010). When doing so, the nature of solutions of the nonlinear dynamic system may change and, *e.g.*, solutions modeling TAE nonlinear behaviors may change from stable limit point to limit cycle. Similar behaviors may be expected for the fishbone case (White, 2010). Another worthwhile remark concerns the role of the collision term  $\propto -\nu_{ext}\beta_{Er}$  in Eq. (5.226). By definition,  $\nu_{ext}$  reduces to the well-known (linear) effective collision frequency only in the weakly nonlinear case. For sufficiently strong nonlinear distortions  $\nu_{ext}$  may even change sign and, therefore, modify the nonlinear behavior of the dynamic system of Eqs. (5.230) with a formal substitution  $S \rightarrow S + \nu\beta \rightarrow \nu\beta$ , as hinted at in (Zonca *et al.*, 2007b), while the loss term may become  $\sim -A\beta$  for large fluctuations. Both the time delay (Parker and White, 2010) and the nonlinear  $\nu_{ext}$  models (Zonca *et al.*, 2007b), however, have not yet been fully explored.

<sup>50</sup> Note that (Chen *et al.*, 1984) assume that the nonlinear term in the  $\beta$  evolution equation is multiplied by the Heaviside function  $H(\beta - \beta_{\min})$ ; *i.e.*, it is considered effective only if  $\beta$  is above a minimum  $\beta_{\min}$  value, considered to be that reached as consequence of the secular expulsion of EPs from within the  $r = r_s$  magnetic surface.

Much richer physics is expected to become increasingly more relevant as plasma conditions approach marginal stability; *e.g.*, MHD nonlinearities cannot be neglected (Ödholm *et al.*, 2002). Correspondingly, more theory and simulation studies are needed to fully understand and explain the diverse experimental evidence discussed in Sec. IV.C, and more recently reported and summarized by (Guimarães-Filho *et al.*, 2012) for the specific case of electron fishbones. In general, the present understanding of wave-particle and wave-wave nonlinear effects on fishbone dynamics call for a comprehensive treatment addressing these physics on the same footing, while accounting for kinetic core plasma response in realistic toroidal geometry.

### E. Further remarks on general theoretical issues and broader implications

Equation (5.3) evidently has similarities with the wave kinetic equation

$$\frac{\partial}{\partial t}I(\mathbf{r}, \mathbf{k}, t) + \frac{\partial \omega}{\partial \mathbf{k}} \cdot \frac{\partial}{\partial \mathbf{r}}I(\mathbf{r}, \mathbf{k}, t) - \frac{\partial \omega}{\partial \mathbf{r}} \cdot \frac{\partial}{\partial \mathbf{k}}I(\mathbf{r}, \mathbf{k}, t) = 2\gamma_L(\mathbf{k})I(\mathbf{r}, \mathbf{k}, t) + [\text{NL TERMS}] , \quad (5.231)$$

where  $I(\mathbf{r}, \mathbf{k}, t)$  is proportional to the wave energy density, which has been derived in plasma physics literature in different ways: (1) from qualitative extension to weakly nonuniform system of the evolution equation of the occupation number of a mode due to nonlinear interaction with other modes (Kadomtsev, 1965; Sagdeev and Galeev, 1969; Swift, 1972); (2) by use of geometric optics in space and time varying plasmas (Bernstein and Baldwin, 1977); (3) by adopting the Weyl representation (Weyl, 1931) for electromagnetic waves (McDonald and Kaufman, 1985)<sup>51</sup>. While this formal similarity may seem striking, it is generally a consequence of the procedure used for obtaining kinetic equations for weakly-nonideal systems (Balescu, 1963; Prigogine, 1962; Van Hove, 1955). The similarity with the analyses given by (Kadomtsev, 1965; Sagdeev and Galeev, 1969; Swift, 1972), instead, is only formal, because in that case the wave kinetic equation is seen as random-phase spectral evolution equation. Furthermore, the  $\tau_{NL} \sim \gamma_L^{-1}$  ordering with  $|\gamma_L/\omega_0| \ll 1$  (cf. Sec. II.C) is crucial in the present case for coherent resonant wave particle interactions to play important roles both in the linear excitation of DAWs as well as in their nonlinear dynamic evolution. On the contrary, the phase coherence between wave and particles is rapidly lost in the case of weak turbulence theory, where the simultaneous action of many waves with relative random phases are considered (Sagdeev and Galeev, 1969), and becomes a notion of lesser importance when dealing with transport in fully developed plasma turbulence. Another difference is given by the role of equilibrium geometry and plasma nonuniformity in determining the wave packet propagation in Eq. (5.3), which is clearly not accounted for in Eq. (5.231) while it plays important roles in the DAW dynamics.

By construction, Eq. (5.3) is inapplicable to investigations of broad band plasma turbulence. However, it has been used successfully to investigate nonlinear processes in drift wave (DW) turbulence, where time scale separation may be systematically applied. Notable examples are the excitation of ZS by coherent wave-wave interactions (Chen *et al.*, 2000, 2001; Guzdar *et al.*, 2001a), turbulence spreading (Hahm *et al.*, 2004; Lin *et al.*, 2002; Lin and Hahm, 2004) due to the propagation of dispersive waves enhanced by DW-zonal flow interaction (Chen *et al.*, 2004; White *et al.*, 2005; Zonca *et al.*, 2004b); and saturation of electron temperature gradient driven turbulence due to inverse cascade via scatterings off driven low mode-number quasi-modes (Chen *et al.*, 2005; Lin *et al.*, 2005). Equation (5.3) can also be used for addressing spatiotemporal cross-scale couplings between DAWs and EP dynamics on one hand and DW turbulence and turbulent transport on the other hand (see also Sec. VII.B). In fact, due to the disparate spatiotemporal scale involved in these process, it may be conjectured that cross-scale coupling are mediated by the formation of ZS (Zonca *et al.*, 2006), which could eventually determine the long time scale behaviors of burning plasmas (Zonca, 2008; Zonca and Chen, 2008a). Furthermore, ZS may be spontaneously excited above a critical amplitude threshold of the driving fluctuation and, hence, they can be very efficient in providing a self-regulation mechanism of plasma turbulence and fluctuation induced transports (Diamond *et al.*, 2005)<sup>52</sup>. Thus, the formal separation of nonlinear interaction with ZS on the right hand side of Eq. (5.3) captures two different processes, *i.e.*, the coherent nonlinear interaction with the ZS generated by the fluctuation itself (self-interaction) and the incoherent interaction with ZS generated by other fluctuating fields, including DW turbulence. Assuming, for illustration, non-dispersive waves along with local nonlinear interactions in  $n$ -space, the form of Eq. (5.3) becomes that of a discrete Anderson nonlinear Schrödinger equation with randomness, *e.g.*, (Iomin, 2010; Krivolapov *et al.*, 2010; Pikovsky and

<sup>51</sup> For application to the analysis of scalar fields, see also (Katou, 1981).

<sup>52</sup> The importance of spontaneous excitation of ZS in collisionless burning plasmas is also analyzed in Secs. V.C.2 and V.D.6.

Shepelyansky, 2008; Shepelyansky, 1993)

$$i\hbar\frac{\partial}{\partial t}\psi_n = \hat{H}_L\psi_n + \zeta|\psi_n|^2\psi_n, \quad (5.232)$$

where  $\hat{H}_L$  is the Hamiltonian of the linear problem in the tight-binding approximation, accounting for the random transitions between nearest-neighbor states on a lattice in terms of a hopping matrix with disorder (Anderson, 1958). In Eq. (5.3), the ZS self-interaction gives the nonlinearity, while ZS incoherent coupling and the three wave interaction term act as random potential<sup>53</sup>. An important feature, which arises in the analysis of Eq. (5.232) as well as Eq. (5.3), is competition between nonlinearity and randomness. Indeed, it has been argued and discussed in the literature that, when the nonlinearity parameter  $\zeta$  is sufficiently small, the random properties play the dominant role through the dynamics, *e.g.*, (Krivolapov *et al.*, 2010; Wang and Zhang, 2009), thus sustaining the phenomena of Anderson localization, likewise to the linear localization case (Anderson, 1958). That means that the diffusion is suppressed and an initially localized wave packet will not spread to infinity. Despite this evidence, it is found that, in direct numerical simulations of one-dimensional discrete nonlinear Schrödinger lattice with disorder (Flach *et al.*, 2009; Pikovsky and Shepelyansky, 2008), the phenomena of Anderson localization are destroyed above a certain critical strength of repulsive ( $\zeta > 0$ ) nonlinearity and an unlimited subdiffusive spreading of the wave field across the lattice occurs. In the attempt to bridge the various specialized model regimes, (Milovanov and Iomin, 2012) have proposed that the loss of Anderson localization in the presence of nonlinearity is a critical phenomenon and that the delocalization occurs spontaneously above a threshold value of  $\zeta$ , similarly to the percolation transition in random lattices. Meanwhile, soliton solutions of Eq. (5.232) are typically found for attractive nonlinearity ( $\zeta < 0$ ) (Zelenyi and Milovanov, 2004). Similarities with DW turbulence spreading due to coherent DW-zonal flow interaction, again, become evident; considering that the zonal flow self-interaction term is attractive (Chen *et al.*, 2004) and, therefore, that turbulence spreading may occur via soliton structure formation (Guo *et al.*, 2009).

Furthermore, the theoretical analysis of AE nonlinear dynamics near marginal stability, presented in Sec. V.D.2, suggests a clear connection between these studies and autoresonance in driven 1D Vlasov-Poisson systems. Autoresonance (Meerson and Friedland, 1990) is the phenomenon of a nonlinear pendulum that can be driven to large amplitude, which evolves in time to instantaneously match the nonlinear pendulum frequency with that of an external drive with sufficiently slow downward frequency sweeping. This phenomenon is common in many fields of physics and “was first observed in particle accelerators, and has since been noted in atomic physics, fluid dynamics, plasmas, nonlinear waves, and planetary dynamics”, as remarked in the review of the autoresonance fundamental physics given by (Fajans and Friedland, 2001). In fusion plasmas, the idea of autoresonance and resonant particle transport in buckets was proposed by (Mynick and Pomphrey, 1994) for removing helium ash from the plasma core and other possible applications, such as burn control, profile control and diagnostic tool. The same notion has clear analogies to the idea of affecting the direct coupling of fusion alpha particle power, known as “alpha channeling” (Fisch and Rax, 1992) (*cf.* Sec. VII). Autoresonance is a process with a critical threshold in the amplitude of the external drive, which scales as  $\sim \dot{\omega}^{3/4}$  and was observed in experiments with trapped electron clouds (Fajans *et al.*, 1999). Electron phase space holes were formed and controlled in a plasma by adiabatic nonlinear phase locking (autoresonance) with a chirped frequency driving wave via Cherenkov-type resonance (Friedland *et al.*, 2006), for which a kinetic theory interpretation was given by (Khain and Friedland, 2007), based on the phase-locked evolution of dissipationless nonlinear waves; *i.e.*, BGK modes (Bernstein *et al.*, 1957). As noted by (Friedland *et al.*, 2006), one important difference emerges when BGK structures are formed by instabilities, as they are poorly controllable. As long as the effect of EP transport on the plasma dielectric response can be considered small, as in the case of the 1D beam-plasma system (*cf.* Sec. V.D.1) or when AE are sufficiently close to marginal stability (*cf.* Sec. V.D.2), the connection between autoresonance in driven 1D Vlasov-Poisson systems and the hole-clump nonlinear dynamics in the 1D beam-plasma problem with sources and sinks (Berk *et al.*, 1999, 1997b) is preserved. In the former case, the frequency sweeping is imposed by the external drive; in the latter one, chirping is set by balancing the rate of energy extraction of hole-clump dynamics in phase space with dissipation. However, when EPM induced transport significantly affects the nonlinear dynamics by changing the plasma dielectric response, resonant particle radial motion is secular as long as wave-particle phase locking is maintained and frequency chirping is nonadiabatic, as discussed in Secs. V.D.5 and V.D.6. The same remark applies to the case of fishbones (Chen *et al.*, 1984; White *et al.*, 1983) (*cf.* Sec. V.D.7). The secular EP loss, predicted theoretically (White *et al.*, 1983) and observed experimentally (Duong *et al.*, 1993), may also be considered

---

<sup>53</sup> The structure of Eq. (5.232) is obtained from Eq. (5.3) even without the three wave interaction term, since each  $A_{n0}$  has different possible radial states due to toroidicity induced poloidal mode couplings, corresponding to different radial localizations. Three wave interactions are, thus, a further twist in the physics described by Eq. (5.3).

an autoresonant effect, spontaneously driven by EP transport for sufficiently strong drive. In between these two limiting behaviors, there is a transition where the role of equilibrium geometry and plasma nonuniformity becomes increasingly more important for increasing mode drive (Briguglio *et al.*, 2013; Wang *et al.*, 2012; Zhang *et al.*, 2012). These physics, embedded in Eq. (5.3) by the integro-differential nature of nonlinear terms and, more specifically, by the renormalized solution for the EP distribution function, Eqs. (5.184) and (5.186) (Dyson equation), suggest a number of possible model nonlinear Schrödinger equations, possibly with fractional partial derivatives, to be used for the description of multi spatiotemporal scale dynamics, as discussed in Secs. V.D.6 and V.D.7.

## VI. ENERGETIC PARTICLE TRANSPORT IN FUSION PLASMAS

One fundamental issue in studies of collective mode excitation by energetic ions in burning plasmas is to assess whether or not significant degradation in the plasma performance can be expected in the presence of shear Alfvén wave (SAW) fluctuations and, if yes, what level of wall loading and damaging of plasma facing materials can be caused by energy and momentum fluxes due to collective fast ion losses. Energetic particle (EP) losses up to 70% of the entire fast particle population have both been predicted theoretically and found experimentally (Duong *et al.*, 1993; Heidbrink and Sadler, 1994; Strait *et al.*, 1993).

The standard approach to modeling EP losses due to a given spectrum of SAW fluctuations (AEs and EPs; cf. Sec. IV) is based on test-particle transport studies. These are expected to well represent the actual transport phenomena provided that transport processes themselves do not significantly modify the fluctuation spectrum. However, it cannot describe the transition to secular transport phenomena, where the interplay of nonlinear mode dynamics and transport processes themselves is intrinsically nonperturbative, as in the case of EPM avalanches, discussed in Sec. V.D.6 (cf. also Sec. VII.A). One important “exception” is the case of fishbones, for which the interplay of nonlinear mode dynamics and transport processes does not significantly modify the linear MHD mode structure<sup>54</sup>, but predominantly causes the mode frequency to rapidly chirp downward (cf. Secs. V.D.7 and VI.B). In this case test particle transport studies give good agreement between simulation results and experimental measurements of EP redistributions even assuming that the mode frequency is fixed, for the projection of the particle phase-space island (cf. Sec. V.D) along the plasma radial coordinate is comparable with the machine size, due to the weak radial dependence of the precessional frequency (White *et al.*, 1983). Thus, accounting for the observed frequency sweeping is not crucial for EPs to be pumped out of the system. In many cases of practical interest, however, test-particle transport improves accuracy in comparisons of simulation results against experimental observations when the measured frequency sweeping is accounted for [cf. *e.g.* (Fredrickson *et al.*, 2009)]. This important point was noted in the early test-particle simulations of EPs by fast frequency chirping modes (White, 2000).

### A. Supra-thermal test particle transport

Test particle loss mechanism is essentially of two types (Hsu and Sigmar, 1992; Sigmar *et al.*, 1992): (1) transient losses, which scale linearly ( $\approx \delta B_r/B$ ) with the mode amplitude, due to resonant drift motion across the orbit-loss boundaries in the EP phase space; (2) diffusive losses above a stochastic threshold, which scale as  $\approx (\delta B_r/B)^2$ , due to EP stochastic diffusion and eventually transport across the orbit-loss boundaries. Due to the large system size, mainly stochastic losses are expected to play a significant role in ITER, while the dominant loss mechanism below stochastic threshold is expected to be that of scattering of barely counter-passing particles into unconfined “fat” banana orbits (Hsu and Sigmar, 1992; Sigmar *et al.*, 1992)<sup>55</sup>. After the first work on fishbone induced EP losses (White *et al.*, 1983), numerical simulations of test particle transport have been successfully adopted for investigating alpha particle redistributions by MHD activity in TFTR (Zweben *et al.*, 1999), beam ion transport during tearing modes in the DIII-D tokamak (Carolipio *et al.*, 2002), EP confinement in the presence of stochastic magnetic fields in the MST reversed field pinch (Fiksel *et al.*, 2005) and, more recently, to model neoclassical tearing mode induced EP losses in ASDEX Upgrade (García-Muñoz *et al.*, 2007).

Supra-thermal particle transport by AEs has been addressed in many works (Appel *et al.*, 1995; Candy *et al.*, 1999; Carolipio *et al.*, 2001; Pinches *et al.*, 2006; Sigmar *et al.*, 1992; Todo *et al.*, 2003; Todo and Sato, 1998), all yielding the similar conclusion that appreciable losses (above the stochastic threshold) require mode amplitudes in the order of

<sup>54</sup> The linear fishbone mode structure may instead be importantly modified in the case of high frequency fishbones (cf. Sec. IV.B.1), as discussed by (Kolesnichenko *et al.*, 2010a).

<sup>55</sup> This same mechanism has been experimentally shown to be the dominant EP loss mechanism due to RSAE (Pace *et al.*, 2011) and EGAM (Kramer *et al.*, 2011) in some recent DIII-D experiments.

$\delta B_r/B \sim 10^{-3}$ , when single- $n$  (toroidal mode number) modes are considered. An actual quantitative estimate of the stochastic threshold in the multiple- $n$  modes case depends on the specific features of the system being considered (see following discussions), although it has been shown that the multiple-mode stochastic threshold may be greatly reduced [ $(\delta B_r/B) \lesssim 10^{-4}$ ] with respect to the single- $n$  mode case (Hsu and Sigmar, 1992; Sigmar *et al.*, 1992). The critical aspects connected with the stochastic threshold for EP transport have been discussed in a pair of recent works (White *et al.*, 2010a,b), which analyzed in detail the modification of deuterium beam distribution in DIII-D plasmas due to the interaction with AEs (TAE and RSAE). The main finding of test particle transport analyses is that observed fluctuation levels are slightly above the stochastic threshold of the system, making simulation very sensitive not only to mode amplitudes but also to other small effects: *e.g.*, omitting the scalar potential fluctuations component of the magnetic perturbations while retaining all other relevant features in the modeling “leads to beam transport more than an order of magnitude too small to explain the observed profile flattening”. Near the onset of local stochasticity in the particle phase-space (Chirikov, 1979; Lichtenberg and Lieberman, 1983, 2010), transport events due to resonance overlap of different- $n$  AEs (Berk *et al.*, 1996a, 1995a; Breizman *et al.*, 1993) (avalanches) may exhibit characteristic aspects of sandpile physics and have been observed in numerical simulations of ITER plasmas (Candy *et al.*, 1997); showing negligible  $\alpha$ -particle transport due to weakly damped core-localized modes, and of TAE mode bursting in a TFTR-like plasma during Neutral Beam Injection (NBI) (Candy *et al.*, 1999). These issues are closely connected with the crucial roles played by equilibrium geometry and plasma nonuniformity in the nonlinear EP phase space dynamics and the onset of stochasticity.

Hybrid MHD gyrokinetic simulations have also been used to analyze central flattening of the EP profile in reversed-shear DIII-D discharges, assuming an initial EP profile computed from classical NBI deposition (Vlad *et al.*, 2009). Simulation results show a good agreement of the relaxed EP profile due to fast growing  $n = 1$  and  $n = 2$  EPs with the experimental profiles measured with the FIDA diagnostics. Furthermore, in the EPM saturated phase, EPs are transformed to weak RSAE modes, which agree well with experimental measurement both in frequency and radial localization. After the initial nonlinear evolution, remarkably, multi-mode hybrid MHD gyrokinetic simulations (Vlad *et al.*, 2009) obtain results for EP redistributions consistent with those obtained by test particle transport (White *et al.*, 2010a,b). This suggests that, with an adequate modeling of the EP source, nonlinear gyrokinetic or equivalent numerical simulations (cf. Sec. II.F) have the capability of analyzing EP transport in the presence of multiple AEs, and the results may be comparable to test particle transport calculations, if particle redistributions and nonlinear mode dynamics are not strongly interlinked.

## B. Self-consistent non-perturbative energetic particle transport

When the interplay of nonlinear mode dynamics and transport processes themselves is intrinsically nonperturbative (cf. Secs. V.D and VII.A), test particle transport simulations do not necessarily reflect the physics of the processes underlying EP redistributions. The first evidence of secular EP transport by EPM is given by (Briguglio *et al.*, 1998), showing that mode saturation is due to radial particle redistribution and that, at saturation, the finite radial mode structure characteristic scale is comparable to the fluctuation induced EP displacement (cf. Sec. V.D.5).

Hybrid MHD gyrokinetic numerical simulations have confirmed the fact that rapid EP transport is expected when the system is significantly above marginal stability and that fast radial particle redistributions lead to fishbone mode saturation and downward frequency chirping (Fu *et al.*, 2006; Vlad *et al.*, 2012). Simulation results also elucidate that fluid nonlinearities do not qualitatively alter the nonlinear dynamics of the fishbone burst cycle and EP transport (Fu *et al.*, 2006).

Dramatic transport events, such as those observed in connection with fishbones and EPs, occur on time scales of a few inverse linear growth rates (generally,  $100 \div 200$  Alfvén times) and have a ballistic character (White *et al.*, 1983) that basically differentiates them from the diffusive nature of multiple- $n$  AE induced transport. Experimental observations in the JT-60U tokamak have also confirmed macroscopic and rapid EP radial redistributions in connection with the so-called abrupt large amplitude events (ALE) (Shinohara *et al.*, 2001). Numerical simulations of an  $n = 1$  EPM burst (Briguglio *et al.*, 2007) show that radial profiles of EPs, computed before and after the EPM induced particle redistributions, agree qualitatively and quantitatively with experimental measurements (Shinohara *et al.*, 2004). Good agreement is also obtained on the burst duration. The EP transport, meanwhile, also explains the saturation of the ALE burst. These simulation results have been recently confirmed by further numerical studies of ALE nonlinear dynamics, with detailed investigations of the importance of equilibrium geometry (Bierwage *et al.*, 2011) and plasma compressibility effects (Bierwage *et al.*, 2012). Hybrid MHD gyrokinetic simulations of single- $n$  modes were also used to compare linear and nonlinear dynamics of Alfvénic oscillations in ITER burning plasmas scenarios (Gorelenkov *et al.*, 2003; Vlad *et al.*, 2006).

In experimental conditions of practical interest, situations in which AE and EPM may coexist and even be interlinked by nonlinear transport processes are not infrequent. This is, *e.g.*, the case of slow upward sweeping ACs observed in JET together with repeated rapid down-sweeping modes (Pinches *et al.*, 2004a). This observation, as suggested by hybrid MHD gyrokinetic simulations of JET experimental conditions (Zonca *et al.*, 2002), may be explained in terms of early resonant excitation of a EPM within the  $q$ -minimum surface and followed later, due to nonlinear dynamic evolution of the fluctuations, by the formation of a cascade mode at the  $q$ -minimum surface. Similar coexistence of TAE and EPM are the plausible interpretation of “TAE avalanches” in NSTX (Fredrickson *et al.*, 2009; Podestà *et al.*, 2011, 2009), where the activity of quasi-periodic TAE fluctuations with limited frequency chirping is followed by the so called “TAE avalanche”. Such phenomenon causes EP losses of up to  $\sim 30\%$  over  $1ms$  and manifests itself as a larger burst amplitude with nonadiabatic frequency sweeping. Test particle transport simulations show reasonable agreement of predicted particle losses with experimental observations, whose features are consistent with the onset of stochastic diffusion discussed by (Berk *et al.*, 1996a, 1995a). On the other hand, the evidence of nonadiabatic frequency chirping suggests that resonance overlap may enhance the free energy source in the first phase of quasi-periodic TAE fluctuations with limited frequency chirping and, once the EPM excitation threshold is exceeded<sup>56</sup>, EPMs may be triggered that are characterized by nonadiabatic frequency sweeping and cause rapid and secular particle redistributions discussed in Sec. V.D.5. Further indications in support of interesting nonlinear interplay between mode structures and EP transport in the case of “TAE avalanches” (Fredrickson *et al.*, 2009) come from the experimental growth rates,  $\sim 10^{-1}(\omega_0/2\pi)$  (Podestà *et al.*, 2011), that are typically larger than those computed from linear stability analyses,  $\sim 10^{-2}(\omega_0/2\pi)$ , and from the mode structures that are not always the same as those reconstructed from reflectometry measurements (Podestà *et al.*, 2009).

The synergy between AE and MHD activity, notably sawteeth, is also connected with nonperturbative redistributions of EPs. In the case of DIII-D, *e.g.*, the use of high harmonic ICRH generates an EP population that transiently stabilizes the sawtooth instability (cf. Sec. IV.B.1) but destabilizes TAEs (Heidbrink *et al.*, 1999). In the further evolution of the plasma discharge, saturation of the central heating correlates with the onset of the TAEs, while sawtooth crash is eventually caused by the continued expansion of the  $q = 1$  surface radius. Similar observations are made in TFTR plasmas (Bernabei *et al.*, 2000, 2001), where the eventual crash of long-period sawteeth is explained in terms of the loss of the stabilizing effect of EPs that are transported outward by EPM from within the  $q = 1$  surface. An effect similar to that of EPM on sawteeth can also be induced by TAEs when, with high values of the safety factor at the  $q(r = a)$  at the plasma boundary, their mode structures are shifted deeper into the plasma core, where they can cause sufficient EP redistributions to affect sawtooth stabilization. Meanwhile, in some TFTR plasma discharges, it has been demonstrated that the loss of ICRH efficiency may be due to the combined effect of EPM and TAE, which eventually redistribute EPs in a broader region of the plasma volume and may even cause global particle losses (Bernabei *et al.*, 1999). More recent analyses of the impact of strongly driven fishbones and AEs on EP losses in JET is given by (Nabais *et al.*, 2010).

### C. Transport of energetic particles by microscopic turbulence

The problem of EP transport by microscopic turbulence was addressed in the early work by (Belikov *et al.*, 1976), discussing the energy spectrum of  $\alpha$ -particles escaping from a plasma as a result of turbulent diffusion. A later and more systematic theoretical description of the fusion  $\alpha$ -particles confinement in tokamaks was provided by (White and Mynick, 1989), demonstrating that supra-thermal particle confinement is much less deteriorated by microturbulence than that of thermal plasma, due to orbit averaging and wave-particle decorrelation effects. This picture was also confirmed by numerical simulations of test-particle transport in strong electrostatic drift wave turbulence (Manfredi and Dendy, 1996) and, more recently, by numerical simulation of turbulent transport of a slowing down distribution of supra-thermal particles with high birth energy compared to the thermal plasma energy (Angioni and Peeters, 2008; Angioni *et al.*, 2009; Zhang *et al.*, 2008a). Experimental observations confirmed these general expectations and quantitatively estimated the turbulent diffusivity of EPs to be one order of magnitude less than that of thermal ions for particle energies  $E/T_c \gtrsim 10$  (Heidbrink and Sadler, 1994; Zweben *et al.*, 2000),  $T_c$  standing for the core plasma thermal energy. Significant interest in this topic was revived more recently by experimental observations in plasmas with NBI, showing evidence of anomalies in EP transport in AUG (Günter *et al.*, 2007), JT-60U (Suzuki *et al.*,

<sup>56</sup> Note that, for sufficiently strong mode drive, of the order of the real frequency shift from the continuous spectrum accumulation point, there is no clear distinction between AE and EPM, as discussed in Sec. IV.A, and EPMs could easily exist inside the SAW frequency gap. In addition, in typical NSTX experimental conditions, equilibrium mean flow shear is strong enough to significantly alter the SAW continuous spectrum and generally cause strong coupling of TAEs with the SAW continuous spectrum and, thereby, with EPMs (Podestà, 2012).

2008) and DIII-D (Heidbrink *et al.*, 2009a,b), which might have raised concerns about the negative NBI efficiency in ITER. These observations were connected with theoretical (Vlad and Spineanu, 2005) and numerical simulation analyses (Albergante *et al.*, 2009; Angioni *et al.*, 2009; Estrada-Mila *et al.*, 2005, 2006), supporting that a significant level of EP transport could be driven by microturbulence. The nature of the discrepancy of experimental measurements from neo-classical predictions of cross-field diffusion of EPs was clarified by (Heidbrink *et al.*, 2009a,b), looking at DIII-D plasmas where EP diffusivity was dominated by Ion Temperature Gradient (ITG) driven turbulence and showing that anomalies were more pronounced at low  $E/T_c$ , where the effect of microturbulence is strongest. Numerical simulation results (Zhang *et al.*, 2010b) have demonstrated that supra-thermal particle diffusivities are consistent with theoretical predictions based on quasi-linear theory (Chen, 1999), confirming the conclusions of original theoretical and numerical works. Thus, EP transport by microturbulence in reactor relevant conditions and above the critical energy (at which plasma ions and electrons are heated at equal rates by EPs) is negligible and supra-thermal particle turbulent diffusivities have intrinsic interest mostly in connection with the explanation of present day experiments with low characteristic values of  $E/T_c$ . The potential problem of EP transport that might have been induced in ITER by magnetic fluctuations (Hauff *et al.*, 2009), as also reported in the recent review by (Breizman and Sharapov, 2011), is, therefore, resolved by these findings (Heidbrink *et al.*, 2009a,b; Zhang *et al.*, 2010b), and is further confirmed in dedicated numerical simulations of electromagnetic turbulent transport of EPs in burning plasmas (Albergante *et al.*, 2012, 2011, 2010). The main possible concern remains the increased supra-thermal particle diffusivities that may be expected in DEMO (DEMONstration Power Plant), due to the significantly larger operation temperature and consequent lower value of  $E/T_c$  (Albergante *et al.*, 2012).

A final aspect which is worthwhile mentioning is the impact of SAW oscillations on thermal plasma transport. In Sec. IV.B, the broad range of frequencies and mode numbers of drift Alfvén wave (DAW) are emphasized together with the different roles of EPs and thermal plasma acting as free energy source in the various regimes. The continuous transition between EP driven long wavelength fluctuations to thermal plasma driven DAW turbulence (Zonca and Chen, 2008c) (cf. also Sec. IV.B.2) corresponds to a similar transition in the weighting of fluctuation induced transport from mainly affecting supra-thermal particles to predominantly contributing to thermal plasma losses (Scott, 1997). There are not many detailed experimental studies of such behaviors, but some interesting evidence in this respect is given by the direct observations of the local plasma potential perturbation and turbulent particle flux in NBI plasmas of TJ-II stellarator, using Heavy Ion Beam Probe (HIBP) diagnostics. The results show that AE's contribution to the turbulent particle flux was typically found to be widely variable from a negligibly low level up to being comparable to the total turbulence flux (Melnikov *et al.*, 2010).

## VII. CONCLUDING REMARKS AND OUTLOOKS

The present work has addressed a wide range of linear and nonlinear physics problems related with shear Alfvén waves (SAWs) and energetic particles (EPs) in burning plasmas, without the intention of being comprehensive.

Among the physics issues addressed in this work, the theoretical formulation of the general fishbone like dispersion relation provides a unified framework for linear as well as nonlinear physics studies and may serve as useful interpretative tool for numerical simulation results and experimental observations. Linear stability problems essentially require the use of already available comprehensive gyrokinetic (or equivalent) codes together with careful modeling of realistic plasma equilibria and physical boundary conditions in order to allow realistic predictions of drift-Alfvén wave (DAW) stability properties in burning plasmas, such as ITER. The many benchmarking activities in progress worldwide give confidence that such predictions on linear physics will be available in the near future. As to nonlinear physics, we have shown that the governing equation has the theoretical structure of a nonlinear Schrödinger equation with integro-differential nonlinear terms. In simplified examples, this equation is shown to yield convective amplification of radially outward moving energetic particle mode (EPM) wave packets, accompanied by secular displacement of resonant EPs; as well as fishbone burst cycle, which is the first and probably best known example of EPM. Comparisons between reduced nonlinear theoretical models, numerical simulations results and experimental observations in present toroidal devices have already started providing new insights into the fundamental issues underlying these processes. Current theoretical understandings of nonlinear physics have, in particular, indicated the crucial importance of equilibrium geometry, plasma nonuniformities, and kinetic processes. Simplified descriptions, based on the analogy of the resonant excitation of SAWs by EPs with the 1D bump-on-tail problem, are capable of capturing some of the important nonlinear dynamics near marginal stability and have been extensively applied to the interpretation of experimental observations. However, by assumptions, these theories do not address the important roles of radial mode structures and plasma nonuniformities, which can change the nonlinear behaviors qualitatively and quantitatively. Nonlinear physics, therefore, would require substantially more significant efforts to reach the level of maturity for

actual and reliable predictions of Alfvénic fluctuation and related transports in reactor relevant conditions. The rapid development of impressive diagnostics systems and numerical simulation capabilities renders it feasible that one can expect rapid advance in this important area.

The intended scope of the present review has left out several important issues. For example, high frequency fluctuations ( $|\omega| \gtrsim \Omega_i$ ) have been entirely neglected, although there are evidences of fusion alpha particle driven ion cyclotron emission [see, *e.g.*, (Cauffman *et al.*, 1995)], interpreted as resonantly excited Compressional Alfvén Eigenmodes (CAE) (Belikov *et al.*, 1995; Fülöp *et al.*, 1997; Gorelenkov and Cheng, 1995a,b). In fact, the CAE phenomenology has been widely studied in NSTX (Fredrickson *et al.*, 2004), but their global implication on fast ion confinement is minor (Fredrickson *et al.*, 2002). Another important aspect, involving the interaction of EPs with waves in the high Radio Frequency (RF) range, is the so-called “alpha channeling” (Fisch and Rax, 1992); *i.e.*, “the diversion of energy from energetic alpha particles to waves” (Fisch, 2000), as “attempt at detailed control over plasma behavior”. This, of course, is a very ambitious but highly rewarding task, for it could considerably facilitate the development of an economical fusion reactor. For a recent review of the elementary processes underlying alpha channeling in tokamaks, we refer the reader to (Fisch, 2012) and to the comprehensive, but somewhat more outdated work (Fisch, 2000), which was further articulated in (Fisch, 2006, 2010). The idea of alpha-channeling is generally connected with the global character of nonlinear dynamics of DAW in fusion plasmas and related transport phenomena. The use of bucket transport in fusion plasmas for removing helium ash from the plasma core as well as burn control, profile control and diagnostic tool was proposed by (Mynick and Pomphrey, 1994) (cf. Sec. V.E). Recently, (Kolesnichenko *et al.*, 2010b,c) have pointed out that DAW may channel the energy and momentum of EPs to different spatial regions, where waves are absorbed. In this way, EP driven instabilities may not only affect the EP radial profiles, but alter thermal plasma transport as well, notably the electron heat transport across the equilibrium magnetic field and the plasma rotation profile (Kolesnichenko *et al.*, 2010b). In (Kolesnichenko *et al.*, 2010c), it is further argued that these processes are consistent with the observation of thermal electron transport by broad-band GAE in NSTX (Stutman *et al.*, 2009) and the strong thermal crashes in W7-AS, connected with the outward radial propagation of KAW (Kolesnichenko *et al.*, 2005). Furthermore, it is worthwhile mentioning that (Wong *et al.*, 2005) have shown the possibility of producing an internal transport barrier, induced by radial redistribution of EPs due to Alfvénic instabilities. Finally, this review has not addressed important issues related to the intrinsic 3D nature of all real systems, including “axisymmetric” toroidal devices. For problems, such as toroidal field ripple induced transport (Goldston and Towner, 1981; Goldston *et al.*, 1981), which arise from the breaking of axisymmetry in 2D toroidal system, we refer readers to the comprehensive ITER summaries (Fasoli *et al.*, 2007; ITER Physics Expert Group on Energetic Particles, Heating and Current Drive, ITER Physics Basis Editors, 1999). Here, we emphasize that AEs may cause global EP losses through induced ripple trapping, as discussed by (White *et al.*, 1995). For the similarities and differences between tokamaks and stellarators, the most recent and comprehensive reviews are (Kolesnichenko *et al.*, 2011; Toi *et al.*, 2011), as mentioned already.

Looking beyond, we note that there are two issues, which have received increasing attention within the fusion community. One deals with EP transport in the presence of many modes; as expected in ITER. The other deals with the investigation of burning fusion plasmas as complex systems, with many interacting degrees of freedom, where the long time scale behaviors will ultimately determine the reactor performance. These two interlinked issues are further articulated in the following two subsections, which then conclude the present review.

### A. Energetic particle transport in the presence of many modes

Collective oscillations excited by EPs in burning plasmas are characterized by a dense spectrum of modes with characteristic frequencies and spatial locations (Chen, 2008; Chen and Zonca, 2007a). One crucial issue, as noted at the beginning Sec. VI, remains the realistic prediction of global transports of EPs/fusion products and their impact on the system material walls. While quasilinear theory is suited for explaining EP transport by plasma turbulence (cf. Sec. VI), it was argued that the onset of phase-space stochasticity may be described by a “line-broadened” quasilinear model (Berk *et al.*, 1995a), accounting for a discrete spectrum of overlapping modes in the case of multiple AE (Berk *et al.*, 1996a) and which has been recently extended and applied to the analysis of beams interacting with AE in DIII-D (Ghantous *et al.*, 2012). The actual transition to stochastic behaviors in realistic systems, however, depends on the details of plasma nonuniformities and equilibrium geometries via resonance conditions and finite mode structures (cf. Sec. VI), as recently shown by (White *et al.*, 2010a,b). For this reason, the only presently viable modeling of EP losses by multiple AE are test particle transport or more sophisticated nonlinear simulations with gyrokinetic or equivalent codes (cf. Sec. II.F). Other reduced nonlinear dynamic description are possible, as discussed in Secs. V.A and V.D.5.c, which may offer a useful tool for gaining deeper insights into the underlying physics. Meanwhile, EP transport can

occur not only via phase-space stochastic diffusion, but also as rapid secular loss, as in the case of fishbones (Chen *et al.*, 1984; White *et al.*, 1983) and EPM (Briguglio *et al.*, 1998; Zonca *et al.*, 2000, 2005), for which the spectrum is nearly monochromatic, due to the more stringent excitation condition. In addition, the mode frequency is rapidly (non-adiabatically) sweeping in time due to phase locking, *de facto* preventing wave-particle trapping to occur and thereby maximizing wave-particle power exchange as well as particle transport (cf. Secs. V.D.5, V.D.6 and V.D.7).

The qualitative difference between AE and EPM non-linear dynamics and the fluctuation induced EP transports they respectively cause can be intuitively explained within the conceptual framework of (Newman *et al.*, 1996), which assumes that magnetized fusion plasmas are close to marginal stability and their dynamics are governed by self-organized criticality (SOC) (Bak *et al.*, 1987). In this context, the single transport events due to AEs (avalanches) (Berk *et al.*, 1996a, 1995a) may exhibit characteristic aspects of sandpile physics involving SOC (Dendy and Helander, 1997). Meanwhile, EPs are excited when the system is driven significantly away from marginal stability and the single transport events due to EPs are characterized by radially moving unstable fronts, which are convectively amplified via self-consistent profile steepening before the final gradient relaxation phase (cf. Sec. V.D.6). In this respect, EPM bursts and transport events have also been dubbed as avalanches (Zonca *et al.*, 2005), although the intrinsic coherent nature of nonlinear wave-particle interactions and the ballistic (secular) EP transport basically differentiates them from the diffusive phase space trajectories due to multiple AE induced transport events.

Another important difference between AE and EPM nonlinear dynamics stands in the fact that self-consistent description of DAW nonlinear behaviors requires taking into account wave dynamics and related transport on the same footing, *i.e.*, allowing for a significant change in the system response to fluctuations and vice-versa; and that, a transition from AE to EPM behavior occurs for increasing strength of the EP free energy source and of the fluctuation level. Here, it is interesting to note that similar notions apply to SOC since, to qualify as SOC, the system must possess many interacting spatial degrees of freedom, be open and coupled with the exterior, and its dynamics must be thresholded and nonlinear (Sornette, 1992). “Nonlinear”, here, implies that a feedback occurs between the various dynamical processes involved. Examples of this include feedback of the order parameter on the control parameter(s), as discussed by (Sornette, 1992), as well as a feedback of boundary dissipation on the dynamical fluctuation state of the lattice (Milovanov, 2010). By analogy with the nonlinear behaviors in fusion plasmas, and in particular with the case of fishbone nonlinear dynamics<sup>57</sup>, an ideal SOC state is destabilized above a certain critical level of external forcing and that the dynamics become dominated by bursting periodic relaxation events, for which the name of “fishbone-like instability of SOC” has been suggested (Milovanov, 2010, 2011). Equilibrium geometry and plasma nonuniformity also play crucial roles in the transition between these two behaviors (cf. Secs. V.D.3, V.D.5 and VI).

The DAW spectrum in present day experiments is significantly different from that of burning plasmas (much lower mode numbers, corresponding to much larger relative EP orbits compared with machine size). The same holds for the associated kinetic processes and cross-scale couplings yielding to complex behaviors, which will be further discussed in Sec. VII.B. Nonetheless, some aspects of complex behaviors may still be addressed in existing machines, providing precious feedbacks for theory and modeling, and, thereby, the basis for predictions and extrapolations to burning plasmas conditions. One example is the analysis of EP transport during “TAE avalanches” in NSTX, where multiple modes are excited and the resultant EP redistributions are so far not completely understood (cf. Sec. VI). Nonlinear hybrid codes (Briguglio *et al.*, 1995, 1998; Park *et al.*, 1999, 1992; Todo, 2006; Todo and Sato, 1998; Todo *et al.*, 1995, 2005; Wang *et al.*, 2011) or equivalent gyrokinetic (Bass and Waltz, 2010; Bottino *et al.*, 2011; Chen and Parker, 2001, 2007; Deng *et al.*, 2012a; Görler *et al.*, 2011; Holod *et al.*, 2009) or gyrofluid (Kendl *et al.*, 2010; Spong *et al.*, 1992, 1994) simulation tools may be needed to yield more reliable interpretations of these observations (Fredrickson *et al.*, 2009). The impressive advance of numerical simulation capabilities and of experimental diagnostics, together with continuing progress in fundamental nonlinear theory, are the fundamental ingredients that will significantly advance the physics understanding in this area.

## B. Complex behaviors in burning plasmas

A burning plasma is a complex self-organized system, where among the crucial processes to understand there are (turbulent) transport and fast ion/fusion product induced collective effects (Zonca *et al.*, 2006). Complexity and self-organization are intrinsic to the very nature of burning plasmas, where the self-sustainment of fusion reactions for efficient power production requires that stationary conditions are achieved when, in D-T plasmas, (almost) the whole

---

<sup>57</sup> Here, the feedback of boundary dissipation on the dynamical fluctuation state of the lattice plays the role of the feedback of transport processes on the nonlinear mode dynamics.

power density balance to compensate losses is provided by heating from fusion alphas. Meanwhile, fast ions in the same (MeV) energy range will be used to heat and fuel the thermal plasma, to provide rotation and to drive current, mainly by Ion Cyclotron Resonance Heating (ICRH) and Negative Neutral Beam Injection (NNBI). Together with fusion produced alphas, these fast ions are a potential free energy source for driving collective plasma oscillations, which may induce or enhance transport processes. Complexity and self-organization are consequence of the interaction of EPs with plasma instabilities and turbulence; of the strong nonlinear coupling that will take place between fusion reactivity profiles, pressure driven currents, MHD stability, transport and plasma boundary interactions, mediated by the EP population; and finally of the long time scale nonlinear (complex) behaviors that may affect the overall fusion performance and eventually pose issues for the stability and control of the fusion burn. The role of EPs is also unique as mediators of cross-scale couplings, for they can drive instabilities on the meso-scales, intermediate between the microscopic thermal ion Larmor radius and the macroscopic plasma equilibrium scale length. Energetic particle driven Alfvénic instabilities could provide a nonlinear feedback onto the system on the macro-scales via the interplay of plasma equilibrium and fusion reactivity profiles, as well as excite microscopic radial mode structures at SAW continuum resonances, which by mode conversion yield fluctuations that may propagate and be absorbed elsewhere (Kolesnichenko *et al.*, 2010b). The role of EPs as mediators of micro- to meso- to macro-scales was recently emphasized by (Qiu *et al.*, 2012). Furthermore, noting that instabilities may also be excited from micro- to meso- to macro-scales (cf. Sec. IV) has made the theoretical approach based on an extended inertial range (Goldreich and Sridhar, 1995, 1997) dubious at best for burning fusion plasmas.

These physics are unique to burning plasmas and require a conceptual shift with respect to the way phenomena are currently investigated in present day experiments. For example, EP power density profiles and characteristic wavelengths of the collective modes in reactor relevant plasmas will be different, while MeV energy ion tails introduce dominant electron heating and different weighting of the electron driven micro-turbulence. Furthermore, plasma operation scenarios will reflect different plasma edge conditions and plasma wall interactions at high density and low collisionality. For these reasons, among others, important roles will be played by predictive capabilities based on numerical simulations (Batchelor *et al.*, 2007) as well as by fundamental theories for developing simplified yet relevant models, needed for gaining insights into the basic physics processes, which determine the long time scale nonlinear dynamics of burning plasmas. Experiments have a key role in this respect and provide experimental evidences for modeling verification and validation. In the perspective of ITER (Aymar *et al.*, 1997; Tamabechi *et al.*, 1991), it is crucial to investigate these physics, exploiting positive feedbacks between experiment, numerical simulation and theory, and integrating the largest number of aspects that are important for complexity in reactor relevant plasmas. Interest in developing experimental capabilities to explore multi-scale physics is a common element of plasma physics in general; *e.g.*, in magnetic fusion (Pizzuto *et al.*, 2010) and geo-space physics (Savin *et al.*, 2011).

It has been recognized that drift wave (DW) turbulence is the channel through which turbulent transport occurs. Meanwhile, in the description of turbulent transport processes, it is crucially important to account for the radial structures that are spontaneously generated by turbulence itself and regulate turbulence intensity and turbulent transport (Diamond *et al.*, 2005). Among those structures, zonal flows (ZF) (Hasegawa *et al.*, 1979) or, more generally, zonal structures (ZS) play a major role in the nonlinear dynamics of DWs. These are toroidally and poloidally symmetric flow patterns, due to the low frequency radial electric field nonlinearly generated by DWs (Hasegawa *et al.*, 1979), which regulate turbulence intensity and turbulent transport, as demonstrated in numerical simulations (Lin *et al.*, 1998). Zonal flows are ubiquitous in plasmas and fluids, *e.g.*, in atmospheric pressure systems where Coriolis forces drive Rossby wave turbulence (Rossby, 1940), which is known to obey the same nonlinear partial differential equations as DW turbulence (Hasegawa *et al.*, 1979). As a consequence, it is often said that ZFs in burning plasmas are the counterpart of the Jupiter's stripes, which are signatures of ZFs driven by Rossby wave turbulence (Busse, 1994). Similar to ZF, other toroidally symmetric flow patterns with more complicated poloidal structures and finite frequency, the geodesic acoustic modes (GAM) (Winsor *et al.*, 1968), are known to play a role in regulating plasma turbulence (Diamond *et al.*, 2005; Itoh *et al.*, 2006). Magnetic field patterns can be generated as well (Fujisawa *et al.*, 2007), generically dubbed as zonal fields (Chen *et al.*, 2001; Gruzinov *et al.*, 2002; Guzdar *et al.*, 2001b).

Zonal flows and fields are also generated by nonlinear AE and EPM dynamics, depending on proximity to marginal stability (cf. Sec. V.C). Meanwhile, strongly driven EPM cause radial modulations in EP profiles, thus affecting the EP distribution function (cf. Secs. V.D.5 and V.D.6), which may produce similar structures in the electron temperature profile and eventually alter the free energy source driving DW turbulence and transport. In general, all these ZS can be viewed as generators of nonlinear equilibria (Chen and Zonca, 2007b), whose intrinsic time scale is that of DAWs (cf. Secs. II.B and II.D),  $\tau_{NL} \sim \gamma_L^{-1}$ , and whose evolution must be self-consistently determined with that of all other relevant nonlinearly coupled degrees of freedom. Thus, these behaviors determine the long time scale nonlinear dynamics of burning plasmas, affecting the reactor fusion performance.

Due to the very disparate spatiotemporal scales involved in the mutual interactions between collective modes and

EP dynamics with DW turbulence and turbulent transport, complex self-organized behaviors will be likely dominated by their nonlinear interplay via ZS (Zonca, 2008; Zonca and Chen, 2008a). Furthermore, the different ZS ( $\omega, \mathbf{k}$ ) spectra generated by the different degrees of freedom will have important effects on the cross-scale couplings. Thus, one relevant open issue is the determination of hierarchy of relevant non-linear time scales for cross-scale couplings in realistic conditions; such as proper equilibrium geometry, spatial nonuniformity and kinetic effects. Since all scales are involved on the same footing, no unique approach is applicable to analyze nonlinear mode dynamics (*e.g.*, local vs. non-local spectral transfers in  $\mathbf{k}$  space) and particle transports. Numerical simulations as well as experimental studies are beginning to address these issues. Multi-scale simulations of plasma turbulence have been reported, *e.g.*, by (Li *et al.*, 2009), and recent numerical simulation work has addressed the effect of zonal flows on AE nonlinear dynamics (Bass and Waltz, 2010).

In the analysis of complex burning plasma behaviors, the low-frequency SAW continuous spectrum has attracted significant attention because of the similar frequencies of DAWs, plasma turbulence and ZS (cf. Sec. IV.B.2), and because a variety of modes with different wavelengths can be driven unstable by both thermal ion temperature gradients and EPs (Nazikian *et al.*, 2006; Zonca *et al.*, 1999) in the kinetic thermal ion gap (Chen and Zonca, 2007a). Furthermore, the experimental evidence of EP driven GAM (EGAM) (Berk *et al.*, 2006; Nazikian *et al.*, 2008) has motivated even further interest (Berk and Zhou, 2010; Fu, 2008; Qiu *et al.*, 2010, 2011, 2012; Sasaki *et al.*, 2011), due to the possible effects of EGAM on plasma transport. The actual relevance of EGAM in burning plasmas is, however, not obvious, since anisotropic EP distribution functions are needed for its linear excitation (Berk *et al.*, 2006; Fu, 2008; Nazikian *et al.*, 2008).

## ACKNOWLEDGMENTS

We are grateful to many colleagues for their contributions to the writing of this review: S. Bernabei, A. J. Brizard, A. Cardinali, N. Carlevaro, W. Chen, C. Z. Cheng, D. S. Darrow, G. Dattoli, J. Decker, R. O. Dendy, W. Deng, X. T. Ding, C. di Troia, J. Q. Dong, M. J. Engebretson, A. Fasoli, G. Fogaccia, G. Y. Fu, X. Garbet, L. Giannessi, N. N. Gorelenkov, J. P. Graves, Z. O. Guimarães-Filho, Z. Guo, T. S. Hahm, P. Helander, C. Hidalgo, Ya. I. Kolesnichenko, A. Könies, M. Lesur, Y. Lin, Z. Lin, A. V. Melnikov, A. Merle, G. Montani, R. Nazikian, C. Nguyen, S. D. Pinches, B. D. Scott, K. Shinohara, P. K. Shukla, G. Sonnino, D. A. Spong, L. Stenflo, D. Testa, B. J. Tobias, Y. Todo, K. Toi, M. A. Van Zeeland, R. E. Waltz, A. Weller, H. S. Zhang, and L. J. Zheng. In particular, we are indebted to in depth discussions with A. Biancalani, A. Bierwage, S. Briguglio, I. Chavdarovski, E. D. Fredrickson, W. W. Heidbrink, Ph. Lauber, Z. X. Lu, A. V. Milovanov, M. Podestà, Z. Y. Qiu, G. Vlad, X. Wang and R. B. White. We are also grateful to A. Biancalani, S. Briguglio, W. Deng, M. J. Engebretson, G. Y. Fu, B. J. Tobias, G. Vlad, X. Wang and H. S. Zhang for granting their permission of reproducing in this review figures from their original works. This work was supported by US DoE, NSF, ITER-CN, and NSFC grants, and by Euratom Communities under the contract of Association between EURATOM/ENEA.

## REFERENCES

- Abel, I. G., B. N. Breizman, S. E. Sharapov, and JET-EFDA Contributors, 2009, *Phys. Plasmas* **16**, 102506.
- Albergante, M., A. Fasoli, J. P. Graves, S. Brunner, and W. A. Cooper, 2012, *Nucl. Fusion* **52**, 094016.
- Albergante, M., J. P. Graves, A. Fasoli, F. Jenko, and T. Dannert, 2009, *Phys. Plasmas* **16**, 112301.
- Albergante, M., J. P. Graves, A. Fasoli, M. Jucker, X. Lapillonne, and W. A. Cooper, 2011, *Plasma Phys. Control. Fusion* **53**, 054002.
- Albergante, M., J. P. Graves, A. Fasoli, and X. Lapillonne, 2010, *Nucl. Fusion* **50**, 084013.
- Alfvén, H., 1942, *Nature* **150**, 405.
- Alfvén, H., 1950, *Cosmical Electrodynamics* (Clarendon, Oxford, UK).
- Al'tshul', L. M., and V. I. Karpman, 1965, *Zh. Eksp. Teor. Fiz.* **49**, 515.
- Al'tshul', L. M., and V. I. Karpman, 1966, *Sov. Phys. JETP* **22**, 361.
- Ambrosino, G., S. Arshad, G. Vayakis, R. Albanese, V. Coccione, A. Pironti, G. Rubinacci, L. Appel, T. Hender, M. Ariola, P. Bettini, M. Brombin, R. Delogu, S. Peruzzo, L. Zabeo, C. Cianfarani, F. Crisanti, V. Fusco, P. Micozzi, G. Ramogida, O. Tudisco, G. Vlad, M. Mattei, and F. Villone, 2012, in *Proceedings of the 24th International Conference on Fusion Energy* (International Atomic Energy Agency, Vienna) pp. [http://www-naweb.iaea.org/napc/physics/FEC/FEC2012/papers/40\\_ITRP531.pdf](http://www-naweb.iaea.org/napc/physics/FEC/FEC2012/papers/40_ITRP531.pdf).
- Anderson, P. W., 1958, *Phys. Rev.* **109**, 1492.
- Angioni, C., and A. Peeters, 2008, *Phys. Plasmas* **15**, 052307.
- Angioni, C., A. G. Peeters, G. V. Pereverzev, A. Bottino, J. Candy, R. Dux, E. Fable, T. Hein, and R. E. Waltz, 2009, *Nucl. Fusion* **49**, 055013.

- Annibaldi, S. V., F. Zonca, and P. Buratti, 2007, *Plasma Phys. Control. Fusion* **49**, 475.
- Antoni, M., Y. Elskens, and D. F. Escande, 1998, *Phys. Plasmas* **5**, 841.
- Antoniazzi, A., R. S. Johal, D. Fanelli, and S. Ruffo, 2008, *Comm. Nonlin. Sci. Num. Sim.* **13**, 2.
- Antonsen, T. M., and B. Lane, 1980, *Phys. Fluids* **23**, 1205.
- Antonsen, T. M., B. Lane, and J. J. Ramos, 1981, *Phys. Fluids* **24**, 1465.
- Antonsen, T. M., and Y. C. Lee, 1982, *Phys. Fluids* **25**, 132.
- Appel, L. C., H. L. Berk, D. Borba, B. N. Breizman, T. C. Hender, G. T. A. Huysmans, W. Kerner, M. S. Pekker, S. D. Pinches, and S. E. Sharapov, 1995, *Nucl. Fusion* **35**, 1697.
- Appert, K., R. Gruber, F. Troyon, and J. Vaclavik, 1982, *Plasma Phys.* **24**, 1147.
- Ara, G., B. Basu, B. Coppi, G. Laval, M. N. Rosenbluth, and B. V. Waddell, 1978, *Ann. Phys.* **112**, 443.
- Aymar, R., V. Chuyanov, M. Huguet, R. Parker, Y. Shimamura, and the ITER Joint Central Team and Home Teams, 1997, in *Proceedings of the 16th International Conference on Fusion Energy 1996*, Vol. 1 (International Atomic Energy Agency, Vienna) p. 3.
- Bak, P., C. Tang, and K. Wiesenfeld, 1987, *Phys. Rev. Lett.* **59**, 381.
- Balescu, R., 1963, *Statistical Mechanics of Charged Particles* (Interscience, New York).
- Barston, E. M., 1964, *Ann. Phys.* **29**, 282.
- Barth, I., L. Friedland, and A. G. Shagalov, 2008, *Phys. Plasmas* **15**, 082110.
- Bass, E., and R. E. Waltz, 2010, *Phys. Plasmas* **17**, 112319.
- Batchelor, D. A., M. Beck, A. Becoulet, R. V. Budny, C. S. Chang, P. H. Diamond, J. Q. Dong, G. Y. Fu, A. Fukuyama, T. Hahm, D. E. Keyes, Y. Kishimoto, S. Klasky, L. L. Lao, K. Li, Z. Lin, B. Ludaescher, J. Manickam, N. Nakajima, T. Ozeki, N. Podhorszki, W. M. Tang, M. A. Vouk, R. E. Waltz, S. J. Wang, H. R. Wilson, X. Q. Xu, M. Yagi, and F. Zonca, 2007, *Plasma Sci. Technol.* **9**, 312.
- Beer, M. A., S. C. Cowley, and G. W. Hammett, 1995, *Phys. Plasmas* **2**, 2687.
- Belikov, V. S., Ya. I. Kolesnichenko, and V. N. Oraevskij, 1968, *Zh. Eksp. Teor. Fiz.* **5**, 2210.
- Belikov, V. S., Ya. I. Kolesnichenko, and V. N. Oraevskij, 1969, *Sov. Phys. JETP* **28**, 1172.
- Belikov, V. S., Ya. I. Kolesnichenko, and V. N. Oraevskij, 1974, *Sov. Phys. JETP* **39**, 828.
- Belikov, V. S., Ya. I. Kolesnichenko, and O. A. Silivra, 1992, *Nucl. Fusion* **32**, 1399.
- Belikov, V. S., Ya. I. Kolesnichenko, and O. A. Silivra, 1995, *Nucl. Fusion* **35**, 1603.
- Belikov, V. S., Ya. I. Kolesnichenko, and V. A. Yavorskij, 1976, *Nucl. Fusion* **16**, 783.
- Bell, M. G., K. M. McGuire, V. Arunasalam, C. W. Barnes, S. H. Batha, G. Bateman, M. A. Beer, R. E. Bell, M. Bitter, N. L. Bretz, R. V. Budny, C. E. Bush, S. R. Cauffman, Z. Chang, C.-S. Chang, C. Z. Cheng, D. S. Darrow, R. O. Dendy, W. Dorland, H. H. Duong, R. D. Durst, P. C. Efthimion, D. Ernst, H. Evenson, N. J. Fisch, R. K. Fisher, R. J. Fonck, E. D. Fredrickson, G. Y. Fu, H. P. Furth, N. N. Gorelenkov, B. Grek, L. R. Grisham, G. W. Hammett, G. R. Hanson, R. J. Hawryluk, W. W. Heidbrink, H. W. Herrmann, K. W. Hill, J. C. Hosea, H. Hsuan, M. H. Hughes, R. A. Hulse, A. C. Janos, D. L. Jassby, F. C. Jobs, D. W. Johnson, L. C. Johnson, J. Kesner, H. W. Kugel, N. T. Lam, B. Leblanc, F. M. Levinton, J. Machuzak, R. Majeski, D. K. Mansfield, E. Mazzucato, M. E. Mauel, J. M. McChesney, D. C. McCune, G. McKee, D. M. Meade, S. S. Medley, D. R. Mikkelsen, S. V. Mirnov, D. Mueller, G. A. Navratil, R. Nazikian, D. K. Owens, H. K. Park, W. Park, P. B. Parks, S. F. Paul, M. P. Petrov, C. K. Phillips, M. W. Phillips, C. S. Pitcher, A. T. Ramsey, M. H. Redi, G. Rewoldt, D. R. Roberts, J. H. Rogers, E. Ruskov, S. A. Sabbagh, M. Sasao, G. Schilling, J. F. Schivell, G. L. Schmidt, S. D. Scott, I. Semenov, S. Sesnic, C. H. Skinner, B. C. Stratton, J. D. Strachan, W. Stodiek, E. J. Synakowski, H. Takahashi, W. M. Tang, G. Taylor, J. L. Terry, M. E. Thompson, W. Tighe, S. Von Goeler, R. B. White, R. M. Wieland, J. R. Wilson, K.-L. Wong, P. Woskov, G. A. Wurden, M. Yamada, K. M. Young, M. C. Zarnstorff, and S. J. Zweben, 1995, *Nucl. Fusion* **35**, 1429.
- Bergkvist, T., and T. Hellsten, 2004, in *Theory of Fusion Plasmas*, edited by J. W. Connor, O. Sauter, and E. Sindoni (Editrice Compositori, Società Italiana di Fisica, Bologna, Italy) p. 123.
- Bergkvist, T., T. Hellsten, and K. Holmström, 2007, *Nucl. Fusion* **47**, 1131.
- Bergkvist, T., T. Hellsten, T. Johnson, and M. Laxåback, 2005, *Nucl. Fusion* **45**, 485.
- Berk, H. L., D. N. Borba, B. N. Breizman, S. D. Pinches, and S. E. Sharapov, 2001, *Phys. Rev. Lett.* **87**, 185002.
- Berk, H. L., C. J. Boswell, D. Borba, A.C.A. Figueiredo, T. Johnson, M.F.F. Nave, S. D. Pinches, S. E. Sharapov, and JET EFDA contributors, 2006, *Nucl. Fusion* **46**, S888.
- Berk, H. L., and B. N. Breizman, 1990a, *Phys. Fluids B* **2**, 2226.
- Berk, H. L., and B. N. Breizman, 1990b, *Phys. Fluids B* **2**, 2235.
- Berk, H. L., and B. N. Breizman, 1990c, *Phys. Fluids B* **2**, 2246.
- Berk, H. L., and B. N. Breizman, 1995, IFTS Technical Report, Texas Univ., DOE/ET/53088.
- Berk, H. L., B. N. Breizman, J. Candy, M. Pekker, and N. V. Petiashvili, 1999, *Phys. Plasmas* **6**, 3102.
- Berk, H. L., B. N. Breizman, J. Fitzpatrick, M. S. Pekker, H. V. Wong, and K. L. Wong, 1996a, *Phys. Plasmas* **3**, 1827.
- Berk, H. L., B. N. Breizman, J. Fitzpatrick, and H. V. Wong, 1995a, *Nucl. Fusion* **35**, 1661.
- Berk, H. L., B. N. Breizman, and M. Pekker, 1995b, *Phys. Plasmas* **2**, 3007.
- Berk, H. L., B. N. Breizman, and M. Pekker, 1996b, *Phys. Rev. Lett.* **76**, 1256.
- Berk, H. L., B. N. Breizman, and M. S. Pekker, 1997a, *Plasma Phys. Rep.* **23**, 778.
- Berk, H. L., B. N. Breizman, and N. V. Petiashvili, 1997b, *Phys. Lett. A* **234**, 213.
- Berk, H. L., B. N. Breizman, and H. Ye, 1992a, *Phys. Rev. Lett.* **68**, 3563.
- Berk, H. L., B. N. Breizman, and H. Ye, 1992b, *Phys. Lett. A* **162**, 475.
- Berk, H. L., R. R. Mett, and D. M. Lindberg, 1993, *Phys. Fluids B* **5**, 3969.

- Berk, H. L., C. W. Nielson, and K. W. Roberts, 1970, *Phys. Fluids* **13**, 980.
- Berk, H. L., J. W. Van Dam, D. Borba, J. Candy, G. T. A. Huysmans, and S. Sharapov, 1995c, *Phys. Plasmas* **2**, 3401.
- Berk, H. L., J. W. Van Dam, Z. Guo, and D. M. Lindberg, 1992c, *Phys. Fluids B* **4**, 1806.
- Berk, H. L., and T. Zhou, 2010, *Nucl. Fusion* **50**, 035007.
- Berkery, J. W., S. A. Sabbagh, H. Reimerdes, R. Betti, B. Hu, R. E. Bell, S. P. Gerhardt, J. Manickam, and M. Podestà, 2010, *Phys. Plasmas* **17**, 082504.
- Berman, R. H., D. J. Tetreault, and T. H. Dupree, 1983, *Phys. Fluids* **26**, 2437.
- Bernabei, S., M. G. Bell, R. Budny, D. Darrow, E. D. Fredrickson, N. Gorelenkov, J. C. Hosea, R. Majeski, E. Mazzucato, R. Nazikian, C. K. Phillips, J. H. Rogers, G. Schilling, R. White, J. R. Wilson, F. Zonca, and S. Zweben, 1999, *Phys. Plasmas* **6**, 1880.
- Bernabei, S., M. G. Bell, R. V. Budny, E. D. Fredrickson, N. N. Gorelenkov, J. C. Hosea, R. Majeski, E. Mazzucato, C. K. Phillips, G. Schilling, and J. R. Wilson, 2000, *Phys. Rev. Lett.* **84**, 1212.
- Bernabei, S., R. V. Budny, E. D. Fredrickson, N. N. Gorelenkov, J. C. Hosea, C. K. Phillips, R. B. White, J. R. Wilson, C. C. Petty, R. I. Pinsky, R. W. Harvey, and A. P. Smirnov, 2001, *Nucl. Fusion* **41**, 513.
- Bernstein, I. B., and D. E. Baldwin, 1977, *Phys. Fluids* **20**, 116.
- Bernstein, I. B., E. A. Frieman, M. D. Kruskal, and R. M. Kulsrud, 1958, *Proc. Roy. Soc. Ser. A* **244**, 17.
- Bernstein, I. B., J. M. Greene, and M. D. Kruskal, 1957, *Phys. Rev.* **108**, 546.
- Betti, R., 1995, *Phys. Rev. Lett.* **74**, 2949.
- Betti, R., and J. P. Freidberg, 1991, *Phys. Fluids B* **3**, 1865.
- Betti, R., and J. P. Freidberg, 1992, *Phys. Fluids B* **4**, 1465.
- Betti, R., and J. P. Freidberg, 1993, *Phys. Rev. Lett.* **70**, 3428.
- Biancalani, A., L. Chen, F. Pegoraro, and F. Zonca, 2010a, *Phys. Rev. Lett.* **105**, 095002.
- Biancalani, A., L. Chen, F. Pegoraro, and F. Zonca, 2010b, *Phys. Plasmas* **17**, 122106.
- Biancalani, A., L. Chen, F. Pegoraro, and F. Zonca, 2011, *Plasma Phys. Control. Fusion* **53**, 025009.
- Bierwage, A., N. Aiba, Y. Todo, W. Deng, M. Ishikawa, G. Matsunaga, K. Shinohara, and M. Yagi, 2012, *Plasma Fus. Res.* **7**, 2403081.
- Bierwage, A., L. Chen, and F. Zonca, 2010a, *Plasma Phys. Control. Fusion* **52**, 015004.
- Bierwage, A., L. Chen, and F. Zonca, 2010b, *Plasma Phys. Control. Fusion* **52**, 015005.
- Bierwage, A., Y. Todo, N. Aiba, K. Shinohara, M. Ishikawa, and M. Yagi, 2011, *Plasma Fus. Res.* **6**, 2403109.
- Biglari, H., and L. Chen, 1986a, *Phys. Fluids* **29**, 1760.
- Biglari, H., and L. Chen, 1986b, *Phys. Fluids* **29**, 2960.
- Biglari, H., and L. Chen, 1991, *Phys. Rev. Lett.* **67**, 3681.
- Biglari, H., F. Zonca, and L. Chen, 1992, *Phys. Fluids B* **4**, 2385.
- Biskamp, D., 1993, *Nonlinear Magnetohydrodynamics* (Cambridge University Press, Cambridge, UK).
- Bondeson, A., and M. S. Chu, 1996, *Phys. Plasmas* **3**, 3013.
- Bondeson, A., and D. J. Ward, 1994, *Phys. Rev. Lett.* **72**, 2709.
- Bonifacio, R., L. De Salvo, P. Pierini, and N. Piovela, 1990, *Nucl. Instrum. Methods Phys. Res., Sect. A* **296**, 358.
- Bonifacio, R., L. De Salvo, P. Pierini, N. Piovela, and C. Pellegrini, 1994, *Phys. Rev. Lett.* **73**, 70.
- Boozer, A. H., 1981, *Phys. Fluids* **24**, 1999.
- Boozer, A. H., 1982, *Phys. Fluids* **25**, 520.
- Borba, D., H. L. Berk, B. N. Breizman, A. Fasoli, F. Nabais, S. D. Pinches, S. E. Sharapov, D. Testa, and contributors to the EFDA-JET Work Programme, 2002, *Nucl. Fusion* **42**, 1029.
- Borba, D., A. Fasoli, N. N. Gorelenkov, S. Günter, Ph. Lauber, N. Mellet, R. Nazikian, T. Panis, S. D. Pinches, D. Spong, D. Testa, and JET-EFDA contributors, 2010, in *Proceedings of the 23rd International Conference on Fusion Energy 2010* (International Atomic Energy Agency, Vienna) pp. CD-ROM file THW/P7-08.
- Bottino, A., T. Vernay, B. Scott, S. Brunner, R. Hatzky, S. Jolliet, B. F. McMillan, T. M. Tran, and L. Villard, 2011, *Plasma Phys. Control. Fusion* **53**, 124027.
- Breizman, B. N., 2006, *AIP Conf. Proc.* **871**, 15.
- Breizman, B. N., 2010, *Nucl. Fusion* **50**, 084014.
- Breizman, B. N., 2011, *Fus. Sci. Technol.* **59**, 549.
- Breizman, B. N., H. L. Berk, M. Pekker, F. Porcelli, G. V. Stupakov, and K. L. Wong, 1997, *Phys. Plasmas* **4**, 1559.
- Breizman, B. N., H. L. Berk, M. S. Pekker, S. D. Pinches, and S. E. Sharapov, 2003, *Phys. Plasmas* **10**, 3649.
- Breizman, B. N., H. L. Berk, and H. Ye, 1993, *Phys. Fluids B* **5**, 3217.
- Breizman, B. N., M. S. Pekker, S. E. Sharapov, and JET EFDA contributors, 2005, *Phys. Plasmas* **12**, 112506.
- Breizman, B. N., and S. E. Sharapov, 1995, *Plasma Phys. Control. Fusion* **37**, 1057.
- Breizman, B. N., and S. E. Sharapov, 2011, *Plasma Phys. Control. Fusion* **53**, 054001.
- Briguglio, S., 2012, *Private Communication*.
- Briguglio, S., L. Chen, J. Q. Dong, G. Fogaccia, R. A. Santoro, G. Vlad, and F. Zonca, 2000, *Nucl. Fusion* **40**, 701.
- Briguglio, S., G. Fogaccia, G. Vlad, X. Wang, L. Chen, and F. Zonca, 2013, *Europhys. Lett.*, to be submitted.
- Briguglio, S., G. Fogaccia, G. Vlad, F. Zonca, K. Shinohara, M. Ishikawa, and M. Takechi, 2007, *Phys. Plasmas* **14**, 055904.
- Briguglio, S., G. Vlad, X. Wang, and F. Zonca, 2012, in *Report on benchmark for nonlinear code* (8th Meeting of the ITPA Energetic Particle Physics Topical Group (Held in Conjunction with the 19th meeting of the ITPA MHD Stability Topical Group), Toki, Japan, March 5 - 9).
- Briguglio, S., G. Vlad, F. Zonca, and G. Fogaccia, 2002, *Phys. Lett. A* **302**, 308.

- Briguglio, S., G. Vlad, F. Zonca, and C. Kar, 1995, *Phys. Plasmas* **2**, 3711.
- Briguglio, S., and X. Wang, 2013, *Private Communication*.
- Briguglio, S., F. Zonca, and G. Vlad, 1998, *Phys. Plasmas* **5**, 3287.
- Brizard, A., 1994, *Phys. Plasmas* **1**, 2460.
- Brizard, A. J., 1989, *J. Plasma Phys.* **41**, 541.
- Brizard, A. J., 1990, *Ph. D. Thesis* (Princeton University, Princeton, NJ).
- Brizard, A. J., 1992, *Phys. Fluids B* **4**, 1213.
- Brizard, A. J., 2000, *Phys. Plasmas* **7**, 4816.
- Brizard, A. J., and T. S. Hahm, 2007, *Rev. Mod. Phys.* **79**, 421.
- Buratti, P., P. Smeulders, F. Zonca, S. Annibaldi, M. De Benedetti, H. Kroegler, G. Regnoli, O. Tudisco, and the FTU-team, 2005, *Nucl. Fusion* **45**, 1446.
- Bussac, M. N., D. Edery, R. Pellat, and J. L. Soulé, 1976, in *Plasma Physics and Controlled Nuclear Fusion Research*, Vol. 1, Proceedings of the 6th International Conference, Berchtesgaden (IAEA, Vienna) p. 607.
- Bussac, M. N., R. Pellat, D. Edery, and J. L. Soulé, 1975, *Phys. Rev. Lett.* **35**, 1638.
- Busse, F. H., 1994, *Chaos* **4**, 123.
- Campbell, D. J., D. F. H. Start, J. A. Wesson, D. V. Bartlett, V. P. Bhatnagar, M. Bures, J. G. Cordey, G. A. Cottrell, P. A. Dupperex, A. W. Edwards, C. D. Challis, C. Gormezano, C. W. Gowers, R. S. Granetz, J. H. Hammen, T. Hellsten, J. Jacquino, E. Lazzaro, P. J. Lomas, N. Lopes Cardozo, P. Mantica, J. A. Snipes, D. Stork, P. E. Stott, P. R. Thomas, E. Thompson, K. Thomsen, and G. Tonetti, 1988, *Phys. Rev. Lett.* **60**, 2148.
- Candy, J., H. L. Berk, B. N. Breizman, and F. Porcelli, 1999, *Phys. Plasmas* **6**, 1822.
- Candy, J., D. Borba, H. L. Berk, G. T. A. Huysmans, and W. Kerner, 1997, *Phys. Plasmas* **4**, 2597.
- Candy, J., B. N. Breizman, J. W. Van Dam, and T. Ozeki, 1996, *Phys. Lett. A* **215**, 299.
- Candy, J., and M. N. Rosenbluth, 1993, *Plasma Phys. Control. Fusion* **35**, 957.
- Candy, J., and M. N. Rosenbluth, 1994, *Phys. Plasmas* **1**, 356.
- Candy, J., and M. N. Rosenbluth, 1995, *Nucl. Fusion* **35**, 1069.
- Carlevaro, N., D. Fanelli, X. Garbet, P. Ghendrih, G. Montani, and M. Pettini, 2013, submitted to *Plasma Phys. Control. Fusion*, arXiv:1309.5263v1 [physics.plasm].
- Carolipio, E. M., W. W. Heidbrink, C. Z. Cheng, M. S. Chu, G. Y. Fu, D. A. Spong, A. D. Turnbull, and R. B. White, 2001, *Phys. Plasmas* **8**, 3391.
- Carolipio, E. M., W. W. Heidbrink, C. B. Forest, and R. B. White, 2002, *Nucl. Fusion* **42**, 853.
- Cary, J. R., and A. J. Brizard, 2009, *Rev. Mod. Phys.* **81**, 693.
- Catto, P. J., W. M. Tang, and D. E. Baldwin, 1981, *Phys. Fluids* **23**, 639.
- Cauffman, S., R. Majeski, K. G. McClements, and R. O. Dendy, 1995, *Nucl. Fusion* **35**, 1597.
- Chapman, I. T., R. Kemp, and D. J. Ward, 2011, *Fus. Eng. Des.* **86**, 141.
- Chapman, I. T., S. D. Pinches, J. P. Graves, R. J. Akers, L. C. Appel, R. V. Budny, S. Coda, N. J. Conway, M. de Bock, L.-G. Eriksson, R. J. Hastie, T. C. Hender, G. T. A. Huysmans, T. Johnson, H. R. Koslowski, A. Krämer-Flecken, M. Lennholm, Y. Liang, S. Saarelma, S. E. Sharapov, I. Voitsekhovitch, the MAST and TEXTOR Teams, and JET EFDA Contributors, 2007, *Plasma Phys. Control. Fusion* **40**, B385.
- Chavdarovski, I., and F. Zonca, 2009, *Plasma Phys. Control. Fusion* **51**, 115001.
- Chen, E. Y., H. L. Berk, B. N. Breizman, and L. J. Zheng, 2011a, *Phys. Plasmas* **18**, 052503.
- Chen, L., 1988, in *Theory of Fusion Plasmas*, edited by J. Vaclavik, F. Troyon, and E. Sindoni (Association EURATOM, Bologna) p. 327.
- Chen, L., 1990, in *Physics of Space Plasmas, SPI Conference Proceedings and Reprint Series, Number 10* (Scientific Publishers, Inc., Cambridge, MA) p. 17.
- Chen, L., 1994, *Phys. Plasmas* **1**, 1519.
- Chen, L., 1999, *J. Geophys. Res.* **104**, 2421.
- Chen, L., 2008, *Plasma Phys. Control. Fusion* **50**, 124001.
- Chen, L., A. Bondeson, and M. S. Chance, 1987, *Nucl. Fusion* **27**, 1918.
- Chen, L., and A. Hasegawa, 1974a, *Phys. Fluids* **17**, 1399.
- Chen, L., and A. Hasegawa, 1974b, *J. Geophys. Res.* **79**, 1024.
- Chen, L., and A. Hasegawa, 1991, *J. Geophys. Res.* **96**, 1503.
- Chen, L., J. Y. Hsu, P. K. Kaw, and P. H. Rutherford, 1978, *Nucl. Fusion* **18**, 1371.
- Chen, L., Z. Lin, and R. B. White, 2000, *Phys. Plasmas* **7**, 3129.
- Chen, L., Z. Lin, R. B. White, and F. Zonca, 2001, *Nucl. Fusion* **41**, 747.
- Chen, L., and S. T. Tsai, 1983, *Plasma Phys.* **25**, 349.
- Chen, L., J. Vaclavik, and G. W. Hammett, 1988, *Nucl. Fusion* **28**, 389.
- Chen, L., R. B. White, G. Rewoldt, P. L. Colestock, P. H. Rutherford, M. N. Bussac, Y. P. Chen, F. J. Ke, and S. T. Tsai, 1989, in *Proceedings of the 12th International Conference on Plasma Physics and Controlled Nuclear Fusion Research, Nice (France), vol. 2* (International Atomic Energy Agency, Vienna) p. 77.
- Chen, L., R. B. White, and M. N. Rosenbluth, 1984, *Phys. Rev. Lett.* **52**, 1122.
- Chen, L., R. B. White, and F. Zonca, 2004, *Phys. Rev. Lett.* **92**, 075004.
- Chen, L., and F. Zonca, 1995, *Phys. Scr.* **T60**, 81.
- Chen, L., and F. Zonca, 2007a, *Nucl. Fusion* **47**, S727.
- Chen, L., and F. Zonca, 2007b, *Nucl. Fusion* **47**, 886.

- Chen, L., and F. Zonca, 2011, *Europhys. Lett.* **96**, 35001.
- Chen, L., and F. Zonca, 2012, *Phys. Rev. Lett.* **109**, 145002.
- Chen, L., and F. Zonca, 2013, *Phys. Plasmas* **20**, 055402.
- Chen, L., F. Zonca, and Z. Lin, 2005, *Plasma Phys. Control. Fusion* **47**, B71.
- Chen, L., F. Zonca, R. A. Santoro, and G. Hu, 1998, *Plasma Phys. Control. Fusion* **40**, 1823.
- Chen, W., X. T. Ding, Yi. Liu, Q. W. Yang, X. Q. Ji, M. Isobe, G. L. Yuan, Y. P. Zhang, Y. Zhou, X. Y. Song, Y. B. Dong, W. Li, J. Zhou, G. J. Lei, J. Y. Cao, W. Deng, X. M. Song, X. R. Duan, and HL-2A Team, 2010a, *Nucl. Fusion* **50**, 084008.
- Chen, W., X. T. Ding, Yi. Liu, Q. W. Yang, X. Q. Ji, G. L. Yuan, Y. P. Zhang, M. Isobe, Y. B. Dong, Y. Huang, J. Zhou, Y. Zhou, W. Li, B. B. Feng, X. M. Song, J. Q. Dong, Z. B. Shi, X. R. Duan, and HL-2A Team, 2011b, *Nucl. Fusion* **51**, 063010.
- Chen, W., X. T. Ding, Yi. Liu, G. L. Yuan, Y. P. Zhang, Y. B. Dong, X. Y. Song, J. Zhou, X. M. Song, W. Deng, Q. W. Yang, X. Q. Ji, X. R. Duan, Y. Liu, and the HL-2A Team, 2009, *Nucl. Fusion* **49**, 075022.
- Chen, W., X. T. Ding, Q. W. Yang, Yi. Liu, X. Q. Ji, Y. P. Zhang, J. Zhou, G. L. Yuan, H. J. Sun, W. Li, Y. Zhou, Y. Huang, J. Q. Dong, B. B. Feng, X. M. Song, Z. B. Shi, Z. T. Liu, X. Y. Song, L. C. Li, X. R. Duan, Y. Liu, and HL-2A team, 2010b, *Phys. Rev. Lett.* **105**, 185004.
- Chen, Y., and S. E. Parker, 2001, *Phys. Plasmas* **8**, 441.
- Chen, Y., and S. E. Parker, 2007, *J. Comp. Phys.* **220**, 839.
- Chen, Y., and S. E. Parker, 2011, *Phys. Plasmas* **18**, 055703.
- Chen, Y., S. E. Parker, J. Lang, and G.-Y. Fu, 2010c, *Phys. Plasmas* **17**, 102504.
- Chen, Y., and R. B. White, 1997, *Phys. Plasmas* **4**, 3591.
- Chen, Y., R. B. White, G.-Y. Fu, and R. Nazikian, 1999, *Phys. Plasmas* **6**, 226.
- Cheng, C. Z., 1982a, *Nucl. Fusion* **22**, 773.
- Cheng, C. Z., 1982b, *Phys. Fluids* **25**, 1020.
- Cheng, C. Z., 1990, *Phys. Fluids B* **2**, 1427.
- Cheng, C. Z., 1991, *Phys. Fluids B* **3**, 2463.
- Cheng, C. Z., 1992, *Phys. Rep.* **211**, 1.
- Cheng, C. Z., and M. S. Chance, 1986, *Phys. Fluids* **29**, 3695.
- Cheng, C. Z., L. Chen, and M. S. Chance, 1985, *Ann. Phys. (N.Y.)* **161**, 21.
- Cheng, C. Z., G. Y. Fu, and J. W. Van Dam, 1988, in *Theory of Fusion Plasmas*, edited by J. Vaclavik, F. Troyon, and E. Sindoni (Association EURATOM, Bologna) p. 259.
- Cheng, C. Z., N. N. Gorelenkov, and C. T. Hsu, 1995, *Nucl. Fusion* **35**, 1639.
- Cheng, C. Z., and A. T. Y. Lui, 1998, *Geophys. Res. Lett.* **25**, 4091.
- Chirikov, B. V., 1979, *Phys. Rep.* **52**, 263.
- Chu, C., M.-S. Chu, and T. Ohkawa, 1978, *Phys. Rev. Lett.* **41**, 653.
- Chu, M. S., J. M. Greene, L. L. Lao, A. D. Turnbull, and M. S. Chance, 1992, *Phys. Fluids B* **4**, 3713.
- Chu, M. S., A. D. Turnbull, J. M. Greene, L. L. Lao, M. S. Chance, H. L. Berk, B. N. Breizman, W. Q. Li, D. M. Lindberg, S. M. Mahajan, R. R. Mett, D. W. Ross, J. W. Van Dam, J. C. Wiley, H. Ye, J. Candy, and M. N. Rosenbluth, 1993, in *Plasma Physics and Controlled Nuclear Fusion Research 1992*, Vol. I CN-56/D-2-3 (International Atomic Energy Agency, Vienna) p. 855.
- Classen, I. G. J., Ph. Lauber, D. Curran, J. E. Boom, B. J. Tobias, C. W. Domier, N. C. Luhmann Jr., H. K. Park, M. García-Muñoz, B. Geiger, M. Maraschek, M. A. Van Zeeland, S. da Graça, and the ASDEX Upgrade Team, 2011, *Plasma Phys. Control. Fusion* **53**, 124018.
- Cohen, R. H., and R. L. Dewar, 1974, *J. Geophys. Res.* **79**, 4174.
- Connor, J. W., R. J. Hastie, and J. B. Taylor, 1978, *Phys. Rev. Lett.* **40**, 396.
- Connor, J. W., R. J. Hastie, and J. B. Taylor, 1979, *Proc. R. Soc. London Ser. A* **365**, 1.
- Connor, J. W., W. M. Tang, and J. B. Taylor, 1983, *Phys. Fluids* **26**, 158.
- Coppi, B., 1977, *Phys. Rev. Lett.* **39**, 939.
- Coppi, B., A. Ferreira, and J. J. Ramos, 1980, *Phys. Rev. Lett.* **44**, 990.
- Coppi, B., R. Galvao, R. Pellat, M. N. Rosenbluth, and P. H. Rutherford, 1976a, *Fiz. Plazmy* **2**, 961.
- Coppi, B., R. Galvao, R. Pellat, M. N. Rosenbluth, and P. H. Rutherford, 1976b, *Sov. J. Plasma Phys.* **2**, 533.
- Coppi, B., R. J. Hastie, S. Migliuolo, F. Pegoraro, and F. Porcelli, 1988a, *Phys. Lett. A* **132**, 267.
- Coppi, B., S. Migliuolo, F. Pegoraro, and F. Porcelli, 1990, *Phys. Fluids B* **2**, 927.
- Coppi, B., S. Migliuolo, and F. Porcelli, 1988b, *Phys. Fluids* **31**, 1630.
- Coppi, B., and F. Porcelli, 1986, *Phys. Rev. Lett.* **57**, 2272.
- Cowley, S. C., R. M. Kulsrud, and R. N. Sudan, 1991, *Phys. Fluids B* **3**, 2767.
- Cox, M., and MAST Team, 1999, *Fus. Eng. Des.* **46**, 397.
- Curran, D., Ph. Lauber, P. J. Mc Carthy, S. da Graça, V. Igochine, and the ASDEX Upgrade Team, 2012, *Plasma Phys. Control. Fusion* **54**, 055001.
- Dendy, R. O., and P. Helander, 1997, *Plasma Phys. Control. Fusion* **39**, 1947.
- Deng, W., Z. Lin, and I. Holod, 2012a, *Nucl. Fusion* **52**, 023005.
- Deng, W., Z. Lin, I. Holod, X. Wang, Y. Xiao, and W. Zhang, 2010, *Phys. Plasmas* **17**, 112504.
- Deng, W., Z. Lin, I. Holod, Z. Wang, Y. Xiao, and H. Zhang, 2012b, *Nucl. Fusion* **52**, 043006.
- Dewar, R. L., and A. H. Glasser, 1983, *Phys. Fluids* **26**, 3038.
- Dewar, R. L., J. Manickam, R. C. Grimm, and M. S. Chance, 1981, *Nucl. Fusion* **21**, 493.

- Dewar, R. L., J. Manickam, R. C. Grimm, and M. S. Chance, 1982, *Nucl. Fusion* **22**, 307.
- Diamond, P. H., S.-I. Itoh, K. Itoh, and T. S. Hahm, 2005, *Plasma Phys. Control. Fusion* **47**, R35.
- Dicke, R. H., 1954, *Phys. Rev.* **93**, 99.
- Ding, X. T., Yi. Liu, G. C. Guo, E. Y. Wang, K. L. Wong, L. W. Yan, J. Q. Dong, J. Y. Cao, Y. Zhou, J. Rao, Y. Yuan, H. Xia, Yong Liu, and the HL-1M group, 2002, *Nucl. Fusion* **42**, 491.
- D'Ippolito, D. A., and J. P. Goedbloed, 1980, *Plasma Phys.* **22**, 1091.
- Dong, J. Q., L. Chen, and F. Zonca, 1999, *Nucl. Fusion* **39**, 1041.
- Dong, J. Q., L. Chen, F. Zonca, and G. D. Jian, 2004, *Phys. Plasmas* **11**, 997.
- Drummond, W. E., and D. Pines, 1962, *Nucl. Fusion Suppl. Pt. 3*, 1049.
- Dubin, D., J. A. Krommes, C. Oberman, and W. W. Lee, 1983, *Phys. Fluids* **26**, 3524.
- DuBois, D. F., and M. V. Goldman, 1965, *Phys. Rev. Lett.* **14**, 544.
- DuBois, D. F., and M. V. Goldman, 1967, *Phys. Rev. Lett.* **19**, 1105.
- Duong, H. H., W. W. Heidbrink, E. J. Strait, T. W. Petrie, R. Lee, R. A. Moyer, and J. G. Watkins, 1993, *Nucl. Fusion* **33**, 749.
- Dupree, T. H., 1970, *Phys. Rev. Lett.* **25**, 789.
- Dupree, T. H., 1972, *Phys. Fluids* **15**, 334.
- Dupree, T. H., 1982, *Phys. Fluids* **25**, 277.
- Edey, D., X. Garbet, J. Roubin, and A. Samain, 1992, *Plasma Phys. Control. Fusion* **34**, 1089.
- Edlund, E. M., M. Porkolab, G. J. Kramer, L. Lin, Y. Lin, and S. J. Wukitch, 2009, *Phys. Rev. Lett.* **102**, 165003.
- Elsasser, W. M., 1956, *Rev. Mod. Phys.* **28**, 135.
- Engbretson, M. J., 2011, *Private Communication*.
- Engbretson, M. J., L. J. Zanetti, T. A. Potemra, W. Baumjohann, H. Lühr, and M. H. Acuna, 1987, *J. Geophys. Res.* **92**, 10053.
- Estrada-Mila, C., J. Candy, and R. E. Waltz, 2005, *Phys. Plasmas* **12**, 022305.
- Estrada-Mila, C., J. Candy, and R. E. Waltz, 2006, *Phys. Plasmas* **13**, 112303.
- Fajans, J., and L. Friedland, 2001, *Am. J. Phys.* **69**, 1096.
- Fajans, J., E. Gilson, and L. Friedland, 1999, *Phys. Rev. Lett.* **82**, 4444.
- Falchetto, G. L., J. Vaclavik, and L. Villard, 2003, *Phys. Plasmas* **10**, 1424.
- Fasoli, A., D. Borba, G. Bosia, D. J. Campbell, J. A. Dobbing, C. Gormezano, J. Jacquinet, P. Lavanchy, J. B. Lister, P. Marmillod, J.-M. Moret, A. Santagiustina, and S. Sharapov, 1995a, *Phys. Rev. Lett.* **75**, 645.
- Fasoli, A., B. N. Breizman, D. Borba, R. F. Heeter, M. S. Pekker, , and S. E. Sharapov, 1998, *Phys. Rev. Lett.* **81**, 5564.
- Fasoli, A., C. Gormenzano, H. L. Berk, B. N. Breizman, S. Briguglio, D. S. Darrow, N. N. Gorelenkov, W. W. Heidbrink, A. Jaun, S. V. Konovalov, R. Nazikian, J. Noterdaeme, S. E. Sharapov, K. Shinohara, D. Testa, K. Tobita, Y. Todo, G. Vlad, and F. Zonca, 2007, *Nucl. Fusion* **47**, S264.
- Fasoli, A., J. B. Lister, S. E. Sharapov, S. Ali-Arshad, G. Bosia, D. Borba, D. J. Campbell, N. Deliyankis, J. A. Dobbing, C. Gormezano, H. A. Holties, G. Huysmans, J. Jacquinet, A. Jaun, W. Kerner, P. Lavanchy, J. Moret, L. Porte, A. Santagiustina, and L. Villard, 1995b, *Nucl. Fusion* **35**, 1485.
- Fasoli, A., D. Testa, S. Sharapov, H. L. Berk, B. Breizman, A. Gondhalekar, R. F. Heeter, M. Mantsinen, and contributors to the EFDA-JET Workprogramme, 2002, *Plasma Phys. Control. Fusion* **33**, B159.
- Fiksel, G., B. Hudson, D. J. Den Hartog, R. M. Magee, R. O'Connell, S. C. Prager, A. D. Beklemishev, V. I. Davydenko, A. A. Ivanov, and Yu. A. Tsidulko, 2005, *Phys. Rev. Lett.* **95**, 125001.
- Finn, J., 1995, *Phys. Plasmas* **2**, 198.
- Fisch, N., 2000, *Nucl. Fusion* **40**, 1095.
- Fisch, N. J., 2006, *Phys. Rev. Lett.* **97**, 225001.
- Fisch, N. J., 2010, *J. Plasma Phys.* **76**, 627.
- Fisch, N. J., 2012, in *Internal Report PPPL-4766* (PPL, Princeton, NJ).
- Fisch, N. J., and J. M. Rax, 1992, *Phys. Rev. Lett.* **69**, 612.
- Fitzpatrick, R., and A. Y. Aydemir, 1996, *Nucl. Fusion* **36**, 11.
- Flach, S., D. O. Krimer, and Ch. Skokos, 2009, *Phys. Rev. Lett.* **102**, 024101.
- Fogaccia, G., and F. Romanelli, 1995, *Phys. Plasmas* **2**, 227.
- Fredrickson, E., R. V. Budny, D. Darrow, G. Y. Fu, J. Hosea, C. K. Phillips, J. R. Wilson, and J. W. Van Dam, 2000, *Phys. Plasmas* **7**, 4121.
- Fredrickson, E. D., 2011, *Private Communication*.
- Fredrickson, E. D., L. Chen, and R. B. White, 2003, *Nucl. Fusion* **43**, 1258.
- Fredrickson, E. D., N. A. Crocker, R. E. Bell, D. S. Darrow, N. N. Gorelenkov, G. J. Kramer, S. Kubota, F. M. Levinton, S. Liu, S. S. Medley, M. Podestà, K. Tritz, R. B. White, and H. Yuh, 2009, *Phys. Plasmas* **16**, 122505.
- Fredrickson, E. D., N. Gorelenkov, C. Z. Cheng, R. Bell, D. Darrow, D. Gates, D. Johnson, S. Kaye, B. LeBlanc, D. McCune, J. Menard, L. Roquemore, and S. Kubota, 2002, *Phys. Plasmas* **9**, 2069.
- Fredrickson, E. D., N. N. Gorelenkov, and J. Menard, 2004, *Phys. Plasmas* **11**, 3653.
- Freidberg, J. P., 1987, *Ideal Magnetohydrodynamics* (Plenum Press, New York and London).
- Friedland, L., P. Khain, and A. G. Shagalov, 2006, *Phys. Rev. Lett.* **96**, 225001.
- Frieman, E. A., and L. Chen, 1982, *Phys. Fluids* **25**, 502.
- Fu, G. Y., 1995, *Phys. Plasmas* **2**, 1029.
- Fu, G. Y., 2008, *Phys. Rev. Lett.* **101**, 185002.

- Fu, G. Y., and H. L. Berk, 2006, *Phys. Plasmas* **13**, 052502.
- Fu, G. Y., H. L. Berk, and A. Pletzer, 2005, *Phys. Plasmas* **12**, 082505.
- Fu, G. Y., C. Cheng, R. Budny, Z. Chang, D. Darrow, E. Fredrickson, E. Mazzucato, R. Nazikian, K. Wong, and S. Zweben, 1996a, *Phys. Plasmas* **3**, 4036.
- Fu, G. Y., and C. Z. Cheng, 1990, *Phys. Fluids B* **2**, 985.
- Fu, G. Y., and C. Z. Cheng, 1992, *Phys. Fluids B* **4**, 3722.
- Fu, G. Y., C. Z. Cheng, H. Kimura, T. Ozeki, and M. Saigusa, 1996b, *Nucl. Fusion* **36**, 1759.
- Fu, G. Y., C. Z. Cheng, and K. L. Wong, 1993, *Phys. Fluids B* **5**, 4040.
- Fu, G. Y., J. Lang, Y. Chen, H. L. Berk, E. Fredrickson, N. Gorelenkov, and M. Podestà, 2010, in *Proceedings of the 23rd International Conference on Fusion Energy 2010* (International Atomic Energy Agency, Vienna) pp. CD-ROM file THW/2-2Rb.
- Fu, G. Y., and W. Park, 1995, *Phys. Rev. Lett.* **74**, 1594.
- Fu, G. Y., W. Park, H. R. Strauss, J. Breslau, J. Chen, S. Jardin, and L. E. Sugiyama, 2006, *Phys. Plasmas* **13**, 052517.
- Fu, G. Y., and J. W. Van Dam, 1989a, *Phys. Fluids B* **1**, 1949.
- Fu, G. Y., and J. W. Van Dam, 1989b, *Phys. Fluids B* **1**, 2404.
- Fu, G. Y., J. W. Van Dam, M. N. Rosenbluth, D. W. Ross, Y. Z. Zhang, H. L. Berk, S. M. Mahajan, C. Z. Cheng, R. L. Miller, X. H. Wang, A. Bhattacharjee, M. E. Mauel, and B. Breizman, 1989, in *Plasma Physics and Controlled Nuclear Fusion Research 1988, Nice*, Vol. 1 (International Atomic Energy Agency, Vienna) p. 291.
- Fujisawa, A., K. Itoh, A. Shimizu, H. Nakano, S. Ohshima, H. Iguchi, K. Matsuoka, S. Okamura, T. Minami, Y. Yoshimura, K. Nagaoka, K. Ida, K. Toi, C. Takahashi, M. Kojima, S. Nishimura, M. Isobe, C. Suzuki, T. Akiyama, Y. Nagashima, S. Itoh, and P. H. Diamond, 2007, *Phys. Rev. Lett.* **98**, 165001.
- Fülöp, T., Ya. I. Kolesnichenko, M. Lisak, and D. Anderson, 1997, *Nucl. Fusion* **37**, 1281.
- Furth, H. P., J. Killeen, M. N. Rosenbluth, and B. Coppi, 1965, in *Plasma Physics and Controlled Nuclear Fusion Research 1964*, Vol. I (IAEA, Vienna) p. 103.
- Galeev, A. A., V. I. Karpman, and R. Z. Sagdeev, 1965, *Sov. Phys. Doklady* **9**, 681.
- Ganesh, R., P. Angelino, J. Vaclavik, and L. Villard, 2004, *Phys. Plasmas* **11**, 3106.
- García-Muñoz, M., H.-U. Fahrbach, S. Günter, V. Igochine, M. J. Mantsinen, M. Maraschek, P. Martin, P. Piovesan, K. Sassenberg, and H. Zohm, 2008, *Phys. Rev. Lett.* **100**, 055005.
- García-Muñoz, M., P. Martin, H.-U. Fahrbach, M. Gobbin, S. Günter, M. Maraschek, L. Marrelli, H. Zohm, and the ASDEX Upgrade Team, 2007, *Nucl. Fusion* **47**, L10.
- Gerjuoy, E., A. Rau, and L. Spruch, 1983, *Rev. Mod. Phys.* **55**, 725.
- Ge Wang, and H. L. Berk, 2012, *Nucl. Fusion* **52**, 094003.
- Ghantous, K., N. N. Gorelenkov, H. L. Berk, W. W. Heidbrink, and M. A. V. Zeeland, 2012, *Phys. Plasmas* **19**, 092511.
- Giannessi, L., P. Musumeci, and S. Spampinati, 2005, *J. Appl. Phys.* **98**, 043110.
- Gibson, A., and the JET Team, 1998, *Phys. Plasmas* **5**, 1839.
- Gimblett, C. G., and R. J. Hastie, 2000, *Phys. Plasmas* **7**, 258.
- Glasser, A. H., 1977, in *Finite Beta Theory Workshop, Varenna, 1977*, Vol. CONF-7709167 (U.S. Department of Energy, Washington, DC) p. 55.
- Glasser, A. H., J. M. Green, and J. L. Johnson, 1975, *Phys. Fluids* **18**, 875.
- Goedbloed, J. P., 1984, *Physica* **12D**, 107.
- Goedbloed, J. P., H. A. Holties, S. Poedts, G. T. A. Huysmans, and W. Kerner, 1993, *Plasma Phys. Control. Fusion* **35**, B277.
- Goldreich, P., and S. Sridhar, 1995, *Astrophys. J.* **438**, 763.
- Goldreich, P., and S. Sridhar, 1997, *Astrophys. J.* **485**, 680.
- Goldston, R. J., and H. H. J. Towner, 1981, *J. Plasma Phys.* **26**, 283.
- Goldston, R. J., R. B. White, and A. H. Boozer, 1981, *Phys. Rev. Lett.* **47**, 647.
- Gorelenkov, N. N., E. Belova, H. L. Berk, C. Z. Cheng, E. Fredrickson, W. W. Heidbrink, S. Kaye, , and G. J. Kramer, 2004, *Phys. Plasmas* **11**, 2586.
- Gorelenkov, N. N., H. L. Berk, R. Budny, C. Z. Cheng, G. Fu, W. W. Heidbrink, G. J. Kramer, D. Meade, and R. Nazikian, 2003, *Nucl. Fusion* **43**, 594.
- Gorelenkov, N. N., H. L. Berk, and R. V. Budny, 2005, *Nucl. Fusion* **45**, 226.
- Gorelenkov, N. N., H. L. Berk, N. A. Crocker, E. D. Fredrickson, S. Kaye, S. Kubota, H. Park, W. Peebles, S. A. Sabbagh, S. E. Sharapov, D. Stutmat, K. Tritz, F. M. Levinton, H. Yuh, the NSTX Team, and JET EFDA Contributors, 2007a, *Plasma Phys. Control. Fusion* **49**, B371.
- Gorelenkov, N. N., H. L. Berk, E. Fredrickson, S. E. Sharapov, and JET EFDA Contributors, 2007b, *Phys. Lett. A* **370**, 70.
- Gorelenkov, N. N., S. Bernabei, C. Z. Cheng, K. W. Hill, R. Nazikian, S. Kaye, Y. Kusama, G. J. Kramer, K. Shinohara, T. Ozeki, and M. V. Gorelenkova, 2000, *Nucl. Fusion* **40**, 1311.
- Gorelenkov, N. N., Y. Chen, R. B. White, and H. L. Berk, 1999a, *Phys. Plasmas* **6**, 629.
- Gorelenkov, N. N., and C. Z. Cheng, 1995a, *Phys. Plasmas* **2**, 1961.
- Gorelenkov, N. N., and C. Z. Cheng, 1995b, *Nucl. Fusion* **35**, 1743.
- Gorelenkov, N. N., C. Z. Cheng, and G. Y. Fu, 1999b, *Phys. Plasmas* **6**, 2802.
- Gorelenkov, N. N., C. Z. Cheng, and W. M. Tang, 1998, *Phys. Plasmas* **5**, 3389.
- Gorelenkov, N. N., and W. W. Heidbrink, 2002, *Nucl. Fusion* **42**, 150.
- Gorelenkov, N. N., G. J. Kramer, and R. Nazikian, 2006, *Plasma Phys. Control. Fusion* **48**, 1255.
- Gorelenkov, N. N., G. J. Kramer, and R. Nazikian, 2011, *Phys. Plasmas* **18**, 102503.

- Gorelenkov, N. N., and S. E. Sharapov, 1992, *Phys. Scr.* **45**, 163.
- Gorelenkov, N. N., M. A. Van Zeeland, H. L. Berk, N. A. Crocker, D. Darrow, E. Fredrickson, G. Fu, W. W. Heidbrink, J. Menard, and R. Nazikian, 2009, *Phys. Plasmas* **16**, 056107.
- Görler, T., X. Lapillonne, S. Brunner, T. Dannert, F. Jenko, F. Merz, and D. Told, 2011, *J. Comp. Phys.* **230**, 7053.
- Górska, K., K. A. Penson, D. Babusci, G. Dattoli, and G. H. E. Duchamp, 2012, *Phys. Rev. E* **85**, 031138.
- Grad, H., 1969, *Phys. Today* **32** (12), 34.
- Graves, J. P., I. T. Chapman, S. Coda, T. Johnson, M. Lennholm, B. Alper, M. de Baar, K. Crombe, L.-G. Eriksson, R. Felton, D. Howell, V. Kiptily, H. R. Koslowski, M.-L. Mayoral, I. Monakhov, I. Nunes, S. D. Pinches, and JET-EFDA Contributors, 2010, *Nucl. Fusion* **50**, 052002.
- Graves, J. P., R. J. Hastie, and K. I. Hopcraft, 2000, *Plasma Phys. Control. Fusion* **42**, 1049.
- Greene, J. M., and J. L. Johnson, 1968, *Plasma Phys.* **10**, 729.
- Gregoratto, D., A. Bondeson, M. S. Chu, and A. M. Garofalo, 2001, *Plasma Phys. Control. Fusion* **43**, 1425.
- Gross, E. P., 1961, *Nuovo Cimento* **20**, 454.
- Grossman, W., and J. Tataronis, 1973, *Z. Phys.* **261**, 217.
- Grove, D. J., and D. M. Meade, 1985, *Nucl. Fusion* **25**, 1167.
- Gruzinov, I., A. Das, P. H. Diamond, and A. Smolyakov, 2002, *Phys. Lett A* **302**, 119.
- Gryaznevich, M. P., and S. E. Sharapov, 2004, *Plasma Phys. Control. Fusion* **46**, S15.
- Gryaznevich, M. P., and S. E. Sharapov, 2006, *Nucl. Fusion* **46**, S942.
- Gryaznevich, M. P., S. E. Sharapov, M. Lilley, S. D. Pinches, A. R. Field, D. Howell, D. Keeling, R. Martin, H. Meyer, H. Smith, R. Vann, P. Denner, E. Verwichte, and the MAST Team, 2008, *Nucl. Fusion* **48**, 084003.
- Guimarães-Filho, Z. O., S. Benkadda, D. Elbeze, A. Botrugno, P. Buratti, G. Calabrò, J. Decker, N. Dubuit, X. Garbet, P. Maget, A. Merle, G. Pucella, R. Sabot, A. A. Tuccillo, and F. Zonca, 2012, *Nucl. Fusion* **52**, 094009.
- Guimarães-Filho, Z. O., D. Elbeze, R. Sabot, D. Molina, J.-L. Ségui, C. Nguyen, J. Decker, P. Maget, A. Merle, X. Garbet, N. Dubuit, and S. Benkadda, 2011, *Plasma Phys. Control. Fusion* **53**, 074012.
- Günter, S., G. Conway, S. da Graça, H. U. Fahrbach, C. Forest, M. García-Muñoz, T. Hauff, J. Hobirk, V. Igochine, F. Jenko, K. Lackner, Ph. Lauber, P. McCarthy, M. Maraschek, P. Martin, E. Poli, K. Sassenberg, E. Strumberger, G. Tardini, E. Wolfrum, H. Zohm, and ASDEX Upgrade Team, 2007, *Nucl. Fusion* **47**, 920.
- Guo, Z., L. Chen, and F. Zonca, 2009, *Phys. Rev. Lett.* **103**, 055002.
- Guzdar, P. N., R. G. Kleva, and L. Chen, 2001a, *Phys. Plasmas* **8**, 459.
- Guzdar, P. N., R. G. Kleva, A. Das, and P. K. Kaw, 2001b, *Phys. Rev. Lett.* **87**, 015001.
- Hacquín, S., S. E. Sharapov, B. Alper, C. D. Challis, A. Fonseca, E. Mazzucato, A. Meigs, L. Meneses, I. Nunes, S. D. Pinches, and the JET EFDA Contributors, 2007, *Plasma Phys. Control. Fusion* **49**, 1371.
- Hahm, T. S., 1988, *Phys. Fluids* **31**, 2670.
- Hahm, T. S., and L. Chen, 1995, *Phys. Rev. Lett.* **74**, 266.
- Hahm, T. S., P. H. Diamond, Z. Lin, K. Itoh, and S.-I. Itoh, 2004, *Plasma Phys. Control. Fusion* **46**, A323.
- Hahm, T. S., W. W. Lee, and A. J. Brizard, 1988, *Phys. Fluids* **31**, 1940.
- Hasegawa, A., 1976, *J. Geophys. Res.* **81**, 5083.
- Hasegawa, A., C. G. MacLennan, and Y. Kodama, 1979, *Phys. Fluids* **22**, 2122.
- Hasegawa, A., and K. Mima, 1978, *J. Geophys. Res.* **83**, 1117.
- Hasegawa, A., and T. Sato, 1989, *Space Plasma Physics - Stationary Processes*, Vol. 1 (Springer, New York).
- Hasegawa, H., and L. Chen, 1974, *Phys. Rev. Lett.* **32**, 454.
- Hasegawa, H., and L. Chen, 1975, *Phys. Rev. Lett.* **35**, 370.
- Hasegawa, H., and L. Chen, 1976, *Phys. Fluids* **19**, 1924.
- Hastie, R. J., Y. P. Chen, F. J. Ke, S. T. Tsai, and L. Chen, 1987a, *Chinese Phys. Lett.* **4**, 561.
- Hastie, R. J., and T. Hender, 1988, *Nucl. Fusion* **28**, 585.
- Hastie, R. J., T. C. Hender, B. A. Carreras, L. A. Charlton, and J. A. Holmes, 1987b, *Phys. Fluids* **30**, 1756.
- Hauff, T., M. J. Pueschel, T. Dannert, and F. Jenko, 2009, *Phys. Rev. Lett.* **102**, 075004.
- Haverkort, J. W., 2012, *Plasma Phys. Control. Fusion* **54**, 025005.
- Hazeltine, R. D., D. A. Hitchcock, and S. M. Mahajan, 1981, *Phys. Fluids* **24**, 180.
- Heeter, R. F., A. F. Fasoli, and S. E. Sharapov, 2000, *Phys. Rev. Lett.* **85**, 3177.
- Heidbrink, W. W., 1995, *Plasma Phys. Control. Fusion* **37**, 937.
- Heidbrink, W. W., 2002, *Phys. Plasmas* **9**, 2113.
- Heidbrink, W. W., 2008, *Phys. Plasmas* **15**, 055501.
- Heidbrink, W. W., M. E. Austin, R. K. Fisher, M. García-Muñoz, G. Matsunaga, G. R. McKee, R. A. Moyer, C. M. Muscatello, M. Okabayashi, D. C. Pace, K. Shinohara, W. M. Solomon, E. J. Strait, M. A. Van Zeeland, and Y. B. Zhu, 2011, *Plasma Phys. Control. Fusion* **53**, 085028.
- Heidbrink, W. W., M. E. Austin, D. A. Spong, B. J. Tobias, and M. A. Van Zeeland, 2013, *Phys. Plasmas* **20**, 082504.
- Heidbrink, W. W., K. Bol, D. Buchenauer, R. Fonck, G. Gammel, K. Ida, R. Kaita, S. Kaye, H. Kugel, B. LeBlanc, W. Morris, M. Okabayashi, E. Powell, S. Sesnic, and H. Takahashi, 1986, *Phys. Rev. Lett.* **57**, 835.
- Heidbrink, W. W., E. D. Fredrickson, T. K. Mau, C. C. Petty, R. I. Pinsky, M. Porkolab, and B. W. Rice, 1999, *Nucl. Fusion* **39**, 1369.
- Heidbrink, W. W., M. Murakami, J. M. Park, C. C. Petty, M. A. Van Zeeland, J. H. Yu, and G. R. McKee, 2009a, *Plasma Phys. Control. Fusion* **51**, 125001.
- Heidbrink, W. W., J. M. Park, M. Murakami, C. C. Petty, C. Holcomb, and M. A. Van Zeeland, 2009b, *Phys. Rev. Lett.* **103**,

- 175001.
- Heidbrink, W. W., and G. J. Sadler, 1994, Nucl. Fusion **34**, 535.
- Heidbrink, W. W., E. J. Strait, M. S. Chu, and A. D. Turnbull, 1993, Phys. Rev. Lett. **71**, 855.
- Heidbrink, W. W., E. J. Strait, E. Doyle, and R. Snider, 1991, Nucl. Fusion **31**, 1635.
- Heidbrink, W. W., M. A. Van Zeeland, M. E. Austin, K. H. Burrell, N. Gorelenkov, G. Kramer, Y. Luo, M. A. Makowski, G. R. McKee, C. Muscatello, R. Nazikian, E. Ruskov, W. M. Solomon, R. B. White, and Y. Zhu, 2008, Nucl. Fusion **48**, 084001.
- Helander, P., C. G. Gimblett, and a. K. G. McClements. R. J. Hastie, 1997, Phys. Plasmas **4**, 2181.
- Hinton, F. L., and R. D. Hazeltine, 1976, Rev. Mod. Phys. **48**, 239.
- Hinton, F. L., and M. N. Rosenbluth, 1999, Plasma Phys. Control. Fusion **41**, A653.
- Hirose, A., L. Zhang, and M. Elia, 1994, Phys. Rev. Lett. **72**, 3393.
- Holod, I., W. L. Zhang, Y. Xiao, and Z. Lin, 2009, Phys. Plasmas **16**, 122307.
- Holties, H. A., A. Fasoli, J. P. Goedbloed, G. T. A. Huysmans, and W. Kerner, 1997a, Phys. Plasmas **4**, 709.
- Holties, H. A., J. P. Goedbloed, G. T. A. Huysmans, and W. Kerner, 1997b, Plasma Phys. Control. Fusion **39**, 73.
- Hsu, C., and D. Sigmar, 1992, Phys. Fluids B **4**, 1492.
- Hu, B., and R. Betti, 2004, Phys. Rev. Lett. **93**, 105002.
- Hu, B., R. Betti, and J. Manickam, 2006, Phys. Plasmas **13**, 112505.
- Hu, S., and L. Chen, 2004, Phys. Plasmas **11**, 1.
- Hu, S., and L. Chen, 2005, Plasma Phys. Control. Fusion **47**, 1251.
- Huysmans, G.T.A., T. C. Hender, B. Alper, Yu. F. Baranov, D. Borba, G. D. Conway, G. A. Cottrell, C. Gormezano, P. Helander, O. J. Kwon, M. F. F. Nave, A. C. C. Sips, F. X. Söldner, E. J. Strait, W. P. Zwingmann, and JET Team, 1999, Nucl. Fusion **39**, 1489.
- Ichimaru, S., 1962, Phys. Fluids **5**, 1224.
- Iomin, A., 2010, Phys. Rev. E **81**, 017601.
- Ionson, J. A., 1982, Astrophys. J. **254**, 318.
- ITER Physics Expert Group on Energetic Particles, Heating and Current Drive, ITER Physics Basis Editors, 1999, Nucl. Fusion **39**, 2471.
- Itoh, K., S.-I. Itoh, P. H. Diamond, T. S. Hahm, A. Fujisawa, G. R. Tynan, M. Yagi, and Y. Nagashima, 2006, Phys. Plasmas **13**, 055502.
- Jaun, A., A. Fasoli, and W. W. Heidbrink, 1998, Phys. Plasmas **5**, 2952.
- Jaun, A., A. Fasoli, J. Vaclavik, and L. Villard, 2000, Nucl. Fusion **40**, 1343.
- JET Joint Undertaking, 1991, in *World Survey of Activities in Controlled Fusion Research [Nuclear Fusion special supplement 1991]* (International Atomic Energy Agency, Vienna) p. 22.
- JET Team, 1992, Nucl. Fusion **32**, 187.
- Joffrin, E., C. D. Challis, G. D. Conway, X. Garbet, A. Gude, S. Günter, N. C. Hawkes, T. C. Hender, D. F. Howell, G. T. A. Huysmans, E. Lazzaro, P. Maget, M. Marachek, A. G. Peeters, S. D. Pinches, S. E. Sharapov, and JET-EFDA contributors, 2003, Nucl. Fusion **43**, 1167.
- Kadomtsev, B. B., 1965, *Plasma Turbulence* (Academic Press, New York).
- Kaku, M., 1993, *Quantum Field Theory: A Modern Introduction* (Oxford University Press, Inc., New York).
- Kar, C., G. Vlad, and F. Romanelli, 1993, Phys. Lett. A **182**, 309.
- Katou, K., 1981, J. Phys. Soc. Jpn. **50**, 642.
- Kaw, P. K., and J. M. Dawson, 1969, Phys. Fluids **12**, 2586.
- Kendl, A., B. D. Scott, and T. T. Ribeiro, 2010, Phys. Plasmas **17**, 072302.
- Khain, P., and L. Friedland, 2007, Phys. Plasmas **14**, 082110.
- Kieras, C. E., and J. A. Tataronis, 1982, J. Plasma Phys. **28**, 395.
- Kimura, H., Y. Kusama, M. Saigusa, G. J. Kramer, K. Tobita, M. Nemoto, T. Kondoh, T. Nishitani, O. Da Costa, T. Ozeki, T. Oikawa, S. Moriyama, A. Morioka, G. Y. Fu, C. Z. Cheng, and V. I. Afanas'ev, 1998, Nucl. Fusion **38**, 1303.
- Kittel, C., 1971, *Introduction to Solid State Physics*, 4th ed. (Wiley, New York).
- Kolesnichenko, Ya. I., 1980, Nucl. Fusion **20**, 727.
- Kolesnichenko, Ya. I., V. V. Lutsenko, and V. S. Marchenko, 1999, Phys. Rev. Lett. **82**, 3260.
- Kolesnichenko, Ya. I., V. V. Lutsenko, A. Weller, H. Thomsen, Yu. V. Yakovenko, J. Geiger, and A. Werner, 2009, Europhys. Lett. **85**, 25004.
- Kolesnichenko, Ya I., V. V. Lutsenko, A. Weller, A. Werner, H. Wobig, , Yu V. Yakovenko, J. Geiger, and S. Zegenhagen, 2006, Nucl. Fusion **46**, 753.
- Kolesnichenko, Ya I., V. V. Lutsenko, A. Weller, A. Werner, H. Wobig, Yu V. Yakovenko, J. Geiger, and S. Zegenhagen, 2011, Plasma Phys. Control. Fusion **53**, 024007.
- Kolesnichenko, Ya. I., V. V. Lutsenko, and R. B. White, 2010a, Nucl. Fusion **50**, 084017.
- Kolesnichenko, Ya. I., and V. N. Oraevskij, 1967, At. Energ. **23**, 289.
- Kolesnichenko, Ya. I., Yu. V. Yakovenko, and V. V. Lutsenko, 2010b, Phys. Rev. Lett. **104**, 075001.
- Kolesnichenko, Ya. I., Yu. V. Yakovenko, V. V. Lutsenko, R. B. White, and A. Weller, 2010c, Nucl. Fusion **50**, 084017.
- Kolesnichenko, Ya I., Yu V. Yakovenko, A. Weller, A. Werner, J. Geiger, V. V. Lutsenko, and S. Zegenhagen, 2005, Phys. Rev. Lett. **94**, 165004.
- Könies, A., S. Briguglio, N. Gorelenkov, T. Fehér, M. Isaev, Ph. Lauber, A. Mishchenko, D. A. Spong, Y. Todo, W. A. Cooper, R. Hatzky, R. Kleiber, M. Borchardt, G. Vlad, and ITPA EP TG, 2012, in *Proceedings of the*

- 24th International Conference on Fusion Energy* (International Atomic Energy Agency, Vienna) pp. [http://www-naweb.iaea.org/napc/physics/FEC/FEC2012/papers/437\\_ITRP134.pdf](http://www-naweb.iaea.org/napc/physics/FEC/FEC2012/papers/437_ITRP134.pdf).
- Kononov, S. V., A. B. Mikhailovskii, M. S. Shirokov, and T. Ozeki, 2004, *Phys. Plasmas* **11**, 2303.
- Kotschenreuther, M., 1986, *Phys. Fluids* **29**, 2898.
- Kramer, G. J., C. Z. Cheng, G. Y. Fu, Y. Kusama, R. Nazikian, T. Ozeki, and K. Tobita, 1999, *Phys. Rev. Lett.* **83**, 2961.
- Kramer, G. J., and G. Y. Fu, 2006, *Plasma Phys. Control. Fusion* **48**, 1285.
- Kramer, G. J., G. Y. Fu, R. Nazikian, R. V. Budny, C. Z. Cheng, N. N. Gorelenkov, S. D. Pinches, S. E. Sharapov, K. Zastrow, and JET-EFDA Contributors, 2008, *Plasma Phys. Control. Fusion* **50**, 082001.
- Kramer, G. J., N. N. Gorelenkov, R. Nazikian, and C. Z. Cheng, 2004a, *Plasma Phys. Control. Fusion* **46**, L23.
- Kramer, G. J., M. Saigusa, T. Ozeki, Y. Kusama, H. Kimura, T. Oikawa, K. Tobita, G. Y. Fu, and C. Z. Cheng, 1998, *Phys. Rev. Lett.* **80**, 2594.
- Kramer, G. J., S. E. Sharapov, R. Nazikian, N. N. Gorelenkov, and R. V. Budny, 2004b, *Phys. Rev. Lett.* **92**, 015001.
- Kramer, J. G., G. Y. Fu, R. Nazikian, M. A. Van Zeeland, R. K. Fisher, W. W. Heidbrink, L. Chen, and D. C. Pace, 2011, *Bull. Am. Phys. Soc.* **56**, 98.
- Krivolapov, Y., S. Fishman, and A. Soffer, 2010, *New J. Phys.* **12**, 063035.
- Kruskal, M., 1962, *J. Math. Phys.* **3**, 806.
- Kruskal, M. D., and R. M. Kulsrud, 1958, *Phys. Fluids* **1**, 265.
- Kruskal, M. D., and C. R. Oberman, 1958, *Phys. Fluids* **1**, 275.
- Kulsrud, R. M., 1978, in *Important Advances in Twentieth Century Astronomy*, Anniversary volume for Bengt Stromgren (Copenhagen University Observatory, Copenhagen) pp. 317–325.
- Kulsrud, R. M., 1983, in *Basic Plasma Physics*, Vol. I, edited by A. A. Galeev and R. N. Sudan (North-Holland, Amsterdam) pp. 115–146.
- Kuvshinov, N., and A. B. Mikhailovskii, 1987, *Sov. J. Plasma Phys.* **13**, 527.
- Lang, J., Y. Chen, S. E. Parker, and G.-Y. Fu, 2009, *Phys. Plasmas* **16**, 102101.
- Lang, J. Y., G. Y. Fu, and Y. Chen, 2010, *Phys. Plasmas* **17**, 042309.
- Lashmore-Davies, C. N., and R. O. Dendy, 1989, *Phys. Fluids B* **1**, 1565.
- Lauber, Ph., M. Brüdgam, D. Curran, V. Igochine, K. Sassenberg, S. Günter, M. Maraschek, M. García-Muñoz, N. Hicks, and the ASDEX Upgrade Team, 2009, *Plasma Phys. Control. Fusion* **51**, 124009.
- Lauber, Ph., I. G. J. Classen, D. Curran, V. Igochine, B. Geiger, S. da Graça, M. García-Muñoz, M. Maraschek, P. J. McCarthy, and the ASDEX Upgrade Team, 2012, *Nucl. Fusion* **52**, 094007.
- Lauber, Ph., and S. Günter, 2008, *Nucl. Fusion* **48**, 084002.
- Lauber, Ph., S. Günter, A. Könies, and S. D. Pinches, 2007, *J. Comput. Phys.* **226/1**, 447.
- Lauber, Ph., S. Günter, and S. D. Pinches, 2005, *Phys. Plasmas* **12**, 122501.
- Lee, Y. C., and J. W. Van Dam, 1977, in *Finite Beta Theory Workshop, Varenna, 1977*, Vol. CONF-7709167 (U.S. Department of Energy, Washington, DC) p. 93.
- Lesur, M., and P. H. Diamond, 2013, *Phys. Rev. E* **87**, 031101.
- Lesur, M., and Y. Idomura, 2012, *Nucl. Fusion* **52**, 094004.
- Lesur, M., Y. Idomura, and X. Garbet, 2009, *Phys. Plasmas* **16**, 092305.
- Lesur, M., Y. Idomura, K. Shinohara, X. Garbet, and the JT-60 Team, 2010, *Phys. Plasmas* **17**, 122311.
- Levin, M. B., M. G. Lyubarskii, I. N. Onishchenko, V. D. Shapiro, and V. I. Shevchenko, 1972a, *Zh. Eksp. Teor. Fiz.* **62**, 1725.
- Levin, M. B., M. G. Lyubarskii, I. N. Onishchenko, V. D. Shapiro, and V. I. Shevchenko, 1972b, *Sov. Phys. JETP* **35**, 898.
- Li, J., Y. Kishimoto, Y. Kouduki, Z. X. Wang, and M. Janvier, 2009, *Nucl. Fusion* **49**, 095007.
- Li, Y. M., S. M. Mahajan, and D. W. Ross, 1987, *Phys. Fluids* **30**, 1466.
- Lichtenberg, A. J., and M. A. Lieberman, 1983, *Regular and Stochastic Motion* (Springer - Verlag).
- Lichtenberg, A. J., and M. A. Lieberman, 2010, *Regular and Chaotic Dynamics*, 2nd ed. (Springer - Verlag).
- Lifshitz, E. M., and L. P. Pitaevsky, 1980, *Statistical Physics. Pt. 2. Theory of Condensed Matter* (Pergamon Press, Oxford, UK).
- Liljeström, M., and J. Weiland, 1992, *Phys. Fluids B* **4**, 630.
- Lilley, M. K., and B. N. Breizman, 2012, *Nucl. Fusion* **52**, 094002.
- Lilley, M. K., B. N. Breizman, and S. E. Sharapov, 2009, *Phys. Rev. Lett.* **102**, 195003.
- Lilley, M. K., B. N. Breizman, and S. E. Sharapov, 2010, *Phys. Plasmas* **17**, 092305.
- Lin, A. T., J. M. Dawson, and H. Okuda, 1978, *Phys. Rev. Lett.* **41**, 753.
- Lin, Z., L. Chen, and F. Zonca, 2005, *Phys. Plasmas* **12**, 056125.
- Lin, Z., S. Ethier, T. S. Hahm, and W. Tang, 2002, *Phys. Rev. Lett.* **88**, 195004.
- Lin, Z., and T. S. Hahm, 2004, *Phys. Plasmas* **11**, 1099.
- Lin, Z., T. S. Hahm, W. W. Lee, W. M. Tang, and R. B. White, 1998, *Science* **281**, 1835.
- Lin, Z., I. Holod, L. Chen, P. H. Diamond, T. S. Hahm, and S. Ethier, 2007, *Phys. Rev. Lett.* **99**, 265003.
- Littlejohn, R. G., 1982, *J. Math. Phys.* **23**, 742.
- Liu, Y., 2010, *Nucl. Fusion* **50**, 095008.
- Liu, Y. Q., A. Bondeson, Y. Gribov, and A. Polevoi, 2004, *Nucl. Fusion* **44**, 232.
- Liu, Y. Q., I. T. Chapman, M. S. Chu, H. Reimerdes, F. Villone, R. Albanese, G. Ambrosino, A. M. Garofalo, C. G. Gimblett, R. J. Hastie, T. C. Hender, G. L. Jackson, R. J. La Haye, M. Okabayashi, A. Pironti, A. Portone, G. Rubinacci, and E. J. Strait, 2009, *Phys. Plasmas* **16**, 056113.
- Liu, Y. Q., M. S. Chu, I. T. Chapman, and T. C. Hender, 2008, *Phys. Plasmas* **15**, 112503.

- Lu, Z. X., F. Zonca, and A. Cardinali, 2012, *Phys. Plasmas* **19**, 042104.
- Luxon, J. L., 2002, *Nucl. Fusion* **42**, 614.
- Lynden-Bell, D., 1967, *Mon. Not. RAS* **136**, 101.
- Macor, A., M. Goniche, J. F. Artaud, J. Decker, D. Elbeze, X. Garbet, G. Giruzzi, G. T. Hoang, P. Maget, D. Mazon, D. Molina, C. Nguyen, Y. Peysson, R. Sabot, and J. L. Ségui, 2009, *Phys. Rev. Lett.* **102**, 155005.
- Maget, P., F. Imbeaux, G. Giruzzi, V. S. Udintsev, G. T. A. Huysmans, J.-L. Ségui, M. Goniche, Ph. Moreau, R. Sabot, and X. Garbet, 2006, *Nucl. Fusion* **46**, 797.
- Mahajan, S. M., 1995, *Phys. Scr.* **T60**, 160.
- Mahajan, S. M., W. Ross, and G. L. Chen, 1983, *Phys. Fluids* **26**, 2195.
- Manfredi, G., and R. O. Dendy, 1996, *Phys. Rev. Lett.* **76**, 4630.
- Marchenko, V. S., and S. N. Reznik, 2009, *Nucl. Fusion* **49**, 022002.
- Marchenko, V. S., and S. N. Reznik, 2011, *Phys. Plasmas* **18**, 040701.
- Matsunaga, G., N. Aiba, K. Shinohara, Y. Sakamoto, A. Isayama, M. Takechi, T. Suzuki, N. Oyama, N. Asakura, Y. Kamada, T. Ozeki, and JT-60 Team, 2009, *Phys. Rev. Lett.* **103**, 045001.
- Matsunaga, G., K. Shinohara, N. Aiba, Y. Sakamoto, A. Isayama, N. Asakura, T. Suzuki, M. Takechi, N. Oyama, H. Urano, and the JT-60 Team, 2010, *Nucl. Fusion* **50**, 084003.
- Mazitov, R. K., 1965, *Zh. Prikl. Mekh. Fiz.* **1**, 27.
- Mazur, V. A., and A. B. Mikhailovskii, 1977, *Nucl. Fusion* **3**, 193.
- McClements, K. G., M. P. Gryaznevich, S. E. Sharapov, R. J. Akers, L. C. Appel, G. F. Counsell, C. M. Roach, and R. Majeski, 1999, *Plasma Phys. Control. Fusion* **41**, 661.
- McDonald, S. W., and A. N. Kaufman, 1985, *Phys. Rev. A* **32**, 1708.
- McGuire, K., R. Goldston, and M. Bell et al., 1983, *Phys. Rev. Lett.* **50**, 891.
- Meerson, B., and L. Friedland, 1990, *Phys. Rev. A* **41**, 5233.
- Melnikov, A. V., L. G. Eliseev, R. Jiménez-Gómez, E. Ascasibar, C. Hidalgo, A. A. Chmyga, A. D. Komarov, A. S. Kozachok, I. A. Krasilnikov, S. M. Khrebtov, L. I. Krupnik, M. Liniers, S. E. Lysenko, V. A. Mavrin, J. L. de Pablos, M. A. Pedrosa, S. V. Perfilov, M. V. Ufimtsev, T. Ido, K. Nagaoka, S. Yamamoto, Yu. I. Tachev, A. I. Zhezhera, and A. I. Smolyakov, 2010, *Nucl. Fusion* **50**, 084023.
- Melnikov, A. V., L. G. Eliseev, M. A. Ochando, K. Nagaoka, E. Ascasibar, A. Cappa, F. Castejon, T. Estrada, C. Hidalgo, S. E. Lysenko, J. L. de Pablos, M. A. Pedrosa, S. Yamamoto, S. Ohshima, HIBP group, and TJ-II team, 2011, *Plasma Fus. Res.* **6**, 2402030.
- Mercier, C., 1960, *Nucl. Fusion* **1**, 47.
- Merle, A., J. Decker, X. Garbet, R. S. Z. Guimarães-Filho, and N. Timothée, 2012, *Phys. Plasmas* **19**, 072504.
- Mett, R. R., and S. M. Mahajan, 1992a, *Phys. Fluids B* **4**, 2885.
- Mett, R. R., and S. M. Mahajan, 1992b, in *Theory of Fusion Plasmas*, edited by J. Vaclavik, F. Troyon, and E. Sindoni (Editrice Compositori, Società Italiana di Fisica, Bologna) p. 243.
- Metzler, R., and J. Klafter, 2000, *Phys. Rep.* **339**, 1.
- Metzler, R., and J. Klafter, 2004, *J. Phys. A: Math. Gen.* **37**, R161.
- Migliuolo, S., 1993, *Nucl. Fusion* **33**, 1721.
- Mikhailovskii, A. B., 1975a, *Sov. Phys. JETP* **41**, 890.
- Mikhailovskii, A. B., 1975b, *Zh. Eksp. Teor. Fiz.* **68**, 1772.
- Mikhailovskii, A. B., G. T. A. Huysmans, S. E. Sharapov, and W. O. Kerner, 1997, *Plasma Phys. Rep.* **23**, 844.
- Mikhailovskii, A. B., E. A. Kovalishen, M. S. Shirokov, A. I. Smolyakov, V. S. Tsypin, and R. M. Galvao, 2007, *Plasma Phys. Rep.* **33**, 117.
- Mikhailovskii, A. B., and L. I. Rudakov, 1963, *Sov. Phys. JETP* **17**, 621.
- Mikhailovskii, A. B., and S. E. Sharapov, 1999a, *Plasma Phys. Rep.* **25**, 803.
- Mikhailovskii, A. B., and S. E. Sharapov, 1999b, *Plasma Phys. Rep.* **25**, 838.
- Mikhailovskii, A. B., and I. G. Shuchman, 1976, *Zh. Eksp. Teor. Fiz.* **71**, 1813.
- Mikhailovskii, A. B., and G. I. Suramlshvili, 1979, *Sov. J. Plasma Phys.* **5**, 523.
- Mikhailovskii, A. B., and V. S. Tsypin, 1983, *Sov. J. Plasma Phys.* **9**, 91.
- Mikhailovskii, A. B., 1973, *Nucl. Fusion* **13**, 259.
- Milovanov, A. V., 2010, *Europhys. Lett.* **89**, 60004.
- Milovanov, A. V., 2011, *New J. Phys.* **13**, 043034.
- Milovanov, A. V., and A. Iomin, 2012, *Europhys. Lett.* **100**, 10006.
- Milovanov, A. V., and J. J. Rasmussen, 2005, *Phys. Lett. A* **337**, 75.
- Mishchenko, A., A. Könies, and R. Hatzky, 2009, *Phys. Plasmas* **16**, 082105.
- Montgomery, D., 1963, *Phys. Fluids* **6**, 1109.
- Mynick, H. E., and A. N. Kaufman, 1978, *Phys. Fluids* **21**, 653.
- Mynick, H. E., and N. Pomphrey, 1994, *Nucl. Fusion* **34**, 1277.
- Nabais, F., D. Borba, M. García-Muñoz, T. Johnson, V. G. Kiptily, M. Reich, M. F. F. Nave, S. D. Pinches, S. E. Sharapov, and JET-EFDA contributors, 2010, *Nucl. Fusion* **50**, 115006.
- Nabais, F., D. Borba, M. Mantinen, M. F. F. Nave, S. E. Sharapov, and Joint European Torus-European Fusion Development Agreement JET-EFDA CONTRIBUTORS, 2005, *Phys. Plasmas* **12**, 12102509.
- Nazikian, R., H. L. Berk, R. V. Budny, K. H. Burrell, E. J. Doyle, R. J. Fonck, N. N. Gorelenkov, C. Holcomb, G. J. Kramer, R. J. Jayakumar, R. J. La Haye, G. R. McKee, M. A. Makowski, W. A. Peebles, T. L. Rhodes, W. M. Solomon, E. J. Strait,

- M. A. Van Zeeland, and L. Zeng, 2006, Phys. Rev. Lett. **96**, 105006.
- Nazikian, R., G. Y. Fu, M. E. Austin, H. L. Berk, R. V. Budny, N. N. Gorelenkov, W. W. Heidbrink, C. T. Holcomb, G. J. Kramer, G. R. McKee, M. A. Makowski, W. M. Solomon, M. Shafer, E. J. Strait, and M. A. Van Zeeland, 2008, Phys. Rev. Lett. **101**, 185001.
- Nazikian, R., G. J. Kramer, C. Z. Cheng, N. N. Gorelenkov, H. L. Berk, and S. E. Sharapov, 2003, Phys. Rev. Lett. **91**, 125003.
- Newman, D. E., B. A. Carreras, P. H. Diamond, and T. S. Hahm, 1996, Phys. Plasmas **3**, 1858.
- Nguyen, C., X. Garbet, V. Grandgirard, J. Decker, Z. Guimarães-Filho, M. Lesur, H. Lütjens, A. Merle, and R. Sabot, 2010a, Plasma Phys. Control. Fusion **52**, 124034.
- Nguyen, C., X. Garbet, R. Sabot, L.-G. Eriksson, M. Goniche, P. Maget, V. Basiuk, J. Decker, D. Elbèze, G. T. A. Huysmans, A. Macor, J.-L. Ségui, and M. Schneider, 2009, Plasma Phys. Control. Fusion **51**, 095002.
- Nguyen, C., X. Garbet, and A. I. Smolyakov, 2008, Phys. Plasmas **15**, 112502.
- Nguyen, C., H. Lütjens, X. Garbet, V. Grandgirard, and M. Lesur, 2010b, Phys. Rev. Lett. **105**, 205002.
- Nishikawa, K., 1967, J. Phys. Soc. Jpn. **24**, 916.
- Nishimura, Y., 2009, Phys. Plasmas **16**, 030702.
- Northrop, T. G., 1963, *Adiabatic Motion of Charged Particles* (Wiley, New York).
- Ödöblom, A., B. N. Breizman, S. E. Sharapov, T. C. Hender, and V. P. Pastukhov, 2002, Phys. Plasmas **9**, 155.
- Okabayashi, M., I. N. Bogatu, M. S. Chance, M. S. Chu, A. M. Garofalo, Y. In, G. L. Jackson, R. J. La Haye, M. J. Lanctot, J. Manickam, L. Marrelli, P. Martin, G. A. Navratil, H. R. E. J. Strait, H. Takahashi, A. S. Welander, T. Bolzonella, R. Budny, J. S. Kim, R. Hatcher, Y. Q. Liu, and T. C. Luce, 2009, Nucl. Fusion **49**, 125003.
- Okabayashi, M., G. Matsunaga, J. S. deGrassie, W. W. Heidbrink, Y. In, Y. Q. Liu, H. Reimerdes, W. M. Solomon, E. J. Strait, M. Takechi, N. Asakura, R. V. Budny, G. L. Jackson, J. M. Hanson, R. J. La Haye, M. J. Lanctot, J. Manickam, K. Shinohara, and Y. B. Zhu, 2011, Phys. Plasmas **18**, 056112.
- Okuda, H., and J. M. Dawson, 1973, Phys. Fluids **16**, 408.
- O'Neil, T. M., 1965, Phys. Fluids **8**, 2255.
- O'Neil, T. M., and J. H. Malmberg, 1968, Phys. Fluids **11**, 1754.
- O'Neil, T. M., and J. H. Winfrey, 1972, Phys. Fluids **15**, 1514.
- O'Neil, T. M., J. H. Winfrey, and J. H. Malmberg, 1971, Phys. Fluids **14**, 1204.
- Onishchenko, I. N., A. R. Linetskii, N. G. Matsiborko, V. D. Shapiro, and V. I. Shevchenko, 1970a, Zh. Eksp. Teor. Fiz. Pis'ma Red. **12**, 407.
- Onishchenko, I. N., A. R. Linetskii, N. G. Matsiborko, V. D. Shapiro, and V. I. Shevchenko, 1970b, JETP Lett. **12**, 281.
- Onishchenko, O. G., O. A. Pokhotelov, R. Z. Sagdeev, L. Stenflo, R. A. Treumann, and M. A. Balikhin, 2004, J. Geophys. Res. **109**, A03306.
- Oono, M., S. M. Kaye, Y. M. Peng, G. Barnes, W. Blanchard, M. D. Cartera, J. Chrzanowski, L. Dudek, R. Ewig, D. Gates, R. E. Hatcher, T. Jarboe, S. C. Jardin, D. Johnson, R. Kaita, M. Kalish, C. E. Kessel, H. W. Kugel, R. Maingia, R. Majeski, J. Manickam, B. McCormack, J. Menard, D. Mueller, B. A. Nelson, B. E. Nelson, C. Neumeyer, G. Oliaro, F. Paoletti, R. Parsells, E. Perry, N. Pomphrey, S. Ramakrishnan, R. Raman, G. Rewoldt, J. Robinson, A. L. Roquemore, P. Ryana, S. Sabbagh, D. Swaina, E. J. Synakowski, M. Viola, M. Williams, J. R. Wilson, and NSTX Team, 2000, Nucl. Fusion **40**, 557.
- Oyama, N., and the JT-60 Team, 2009, Nucl. Fusion **49**, 104007.
- Pace, D. C., R. K. Fisher, M. García-Muñoz, W. W. Heidbrink, and M. A. Van Zeeland, 2011, Plasma Phys. Control. Fusion **53**, 062001.
- Park, W., E. V. Belova, G. Y. Fu, X. Z. Tang, H. R. Strauss, and L. E. Sugiyama, 1999, Phys. Plasmas **6**, 1796.
- Park, W., S. Parker, H. Biglari, M. Chance, L. Chen, C. Z. Cheng, T. S. Hahm, W. W. Lee, R. Kulsrud, D. Monticello, L. Sugiyama, and R. B. White, 1992, Phys. Fluids B **4**, 2033.
- Parker, J. B., and R. B. White, 2010, Bull. Am. Phys. Soc. **55**, BP9.117.
- Pegoraro, F., F. Porcelli, and T. J. Schep, 1989, Phys. Fluids B **1**, 364.
- Pegoraro, F., F. Porcelli, and T. J. Schep, 1991, Phys. Fluids B **3**, 1319.
- Pegoraro, F., and T. J. Schep, 1978, in *Plasma Physics and Controlled Nuclear Fusion Research*, Vol. 1 (IAEA, Vienna) p. 507.
- Pegoraro, F., and T. J. Schep, 1986, Plasma Phys. Control. Fusion **28**, 647.
- Pfirsch, D., and H. Tasso, 1971, Nucl. Fusion **11**, 259.
- Pikovskiy, A. S., and D. L. Shepelyansky, 2008, Phys. Rev. Lett. **100**, 094101.
- Pinches, S. D., L. C. Appel, J. Candy, S. E. Sharapov, H. L. Berk, D. Borba, B. N. Breizman, T. Hender, K. I. Hopcraft, G.T.A. Huysmans, and W. Kerner, 1998, Comput. Phys. Commun. **111**, 131.
- Pinches, S. D., H. L. Berk, D. N. Borba, B. N. Breizman, S. Briguglio, A. Fasoli, G. Fogaccia, M. P. Gryaznevich, V. Kiptily, M. J. Mantinen, S. E. Sharapov, D. Testa, R. G. L. Vann, G. Vlad, F. Zonca, and JET-EFDA Contributors, 2004a, Plasma Phys. Control. Fusion **46**, B187.
- Pinches, S. D., H. L. Berk, M. P. Gryaznevich, and S. E. Sharapov and JET-EFDA Contributors, 2004b, Plasma Phys. Control. Fusion **46**, S47.
- Pinches, S. D., V. G. Kiptily, S. E. Sharapov, D. S. Darrow, L. G. Eriksson, H. U. Fahrback, M. García-Muñoz, M. Reich, E. Strumberger, A. Werner, ASDEX Upgrade Team, and JET-EFDA Contributors, 2006, Nucl. Fusion **46**, S904.
- Pitaevskiy, L. P., 1961, Sov. Phys. JETP **13**, 451.
- Pizzuto, A., F. Gnesotto, M. Lontano, R. Albanese, G. Ambrosino, M. L. Apicella, M. Baruzzo, A. Bruschi, G. Calabrò, A. Cardinali, R. Cesario, F. Crisanti, V. Cocilovo, A. Coletti, R. Coletti, P. Costa, S. Briguglio, P. Frosi, F. Crescenzi,

- V. Coccoresse, A. Cucchiario, C. Di Troia, B. Esposito, G. Fogaccia, E. Giovannozzi, G. Granucci, G. Maddaluno, R. Maggiore, M. Marinucci, D. Marocco, P. Martin, G. Mazzitelli, F. Mirizzi, S. Nowak, R. Paccagnella, L. Panaccione, G. L. Ravera, F. Orsitto, V. Pericoli Ridolfini, G. Ramogida, C. Rita, M. Santinelli, M. Schneider, A. A. Tuccillo, R. Zagórski, M. Valisa, R. Villari, G. Vlad, and F. Zonca, 2010, *Nucl. Fusion* **50**, 095005.
- Podestà, M., 2012, *Private Communication*.
- Podestà, M., R. E. Bell, A. Bortolon, N. A. Crocker, D. S. Darrow, A. Diallo, E. D. Fredrickson, G.-Y. Fu, N. N. Gorelenkov, W. W. Heidbrink, G. J. Kramer, S. Kubota, B. P. LeBlanc, S. S. Medley, and H. Yuh, 2012, *Nucl. Fusion* **52**, 094001.
- Podestà, M., R. E. Bell, N. A. Crocker, E. D. Fredrickson, N. N. Gorelenkov, W. W. Heidbrink, S. Kubota, B. P. LeBlanc, and H. Yuh, 2011, *Nucl. Fusion* **51**, 063035.
- Podestà, M., W. W. Heidbrink, D. Liu, E. Ruskov, R. E. Bell, D. S. Darrow, E. D. Fredrickson, N. N. Gorelenkov, G. J. Kramer, B. P. LeBlanc, S. S. Medley, A. L. Roquemore, N. A. Crocker, S. Kubota, and H. Yuh, 2009, *Phys. Plasmas* **16**, 056104.
- Poedts, S., W. Kerner, J. P. Goedbloed, B. Keegan, G. T. A. Huysmans, and E. Schwarz, 1992, *Plasma Phys. Control. Fusion* **34**, 1397.
- Pogutse, O. P., and E. I. Yurchenko, 1978, *Nucl. Fusion* **18**, 1629.
- Pokhotelov, O. A., O. G. Onishchenko, R. Z. Sagdeev, M. A. Balikhin, and L. Stenflo, 2004, *J. Geophys. Res.* **109**, A03305.
- Porcelli, F., 1987, *Phys. Fluids* **30**, 1734.
- Porcelli, F., 1991a, *Plasma Phys. Control. Fusion* **33**, 1601.
- Porcelli, F., 1991b, *Phys. Rev. Lett* **66**, 425.
- Porcelli, F., D. Boucher, and M. N. Rosenbluth, 1996, *Plasma Phys. Control. Fusion* **38**, 2163.
- Porcelli, F., and M. N. Rosenbluth, 1998, *Plasma Phys. Control. Fusion* **40**, 481.
- Prigogine, I., 1962, *Nonequilibrium Statistical Mechanics* (Interscience, New York).
- Qin, H., and W. M. Tang, 2004, *Phys. Plasmas* **11**, 1052.
- Qin, H., W. M. Tang, and W. W. Lee, 2000, *Phys. Plasmas* **7**, 4433.
- Qin, H., W. M. Tang, W. W. Lee, and G. Rewoldt, 1999a, *Phys. Plasmas* **6**, 1575.
- Qin, H., W. M. Tang, and G. Rewoldt, 1998, *Phys. Plasmas* **5**, 1035.
- Qin, H., W. M. Tang, and G. Rewoldt, 1999b, *Phys. Plasmas* **6**, 2544.
- Qiu, Z., F. Zonca, and L. Chen, 2010, *Plasma Phys. Control. Fusion* **52**, 095003.
- Qiu, Z., F. Zonca, and L. Chen, 2011, *Plasma Sci. Technol.* **13**, 257.
- Qiu, Z., F. Zonca, and L. Chen, 2012, *Phys. Plasmas* **19**, 082507.
- Rebut, P. H., R. J. Bickerton, and B. E. Kenn, 1985, *Nucl. Fusion* **25**, 1011.
- Rebut, P. H., and B. E. Kenn, 1987, *Fusion Technol.* **11**, 13.
- Rewoldt, G., 1988, *Phys. Fluids* **31**, 3727.
- Rewoldt, G., and W. M. Tang, 1984, *Nucl. Fusion* **24**, 1573.
- Roberts, K. V., and J. B. Taylor, 1965, *Phys. Fluids* **8**, 315.
- Romanelli, F., B. Angelini, M. L. Apicella, G. Apruzzese, E. Barbato, A. Bertochi, G. Bracco, A. Bruschi, G. Buceti, P. Buratti, A. Cardinali, L. Carraro, C. Castaldo, C. Centioli, R. Cesario, S. Cirant, V. Cocilovo, F. Crisanti, R. De Angelis, M. De Benedetti, G. Giruzzi, F. De Marco, B. Esposito, M. Finkenthal, D. Frigione, L. Gabellieri, F. Gandini, L. Garzotti, G. Gatti, E. Giovannozzi, G. Gormezano, F. Gravanti, G. Granucci, M. Grolli, F. Iannone, H. Kroegler, E. Lazzaro, M. Leigheb, G. Maddaluno, C. Maffia, M. Marinucci, M. Mattioli, G. Mazzitelli, F. Mirizzi, S. Nowak, D. Pacella, L. Panaccione, M. Panella, P. Papitto, V. Pericoli-Ridolfini, A. A. Petrov, L. Pieroni, S. Podda, F. Poli, M. E. Puiatti, G. Ravera, G. B. Righetti, M. Romanelli, F. Santini, M. Sassi, A. Saviliev, P. Scarin, S. E. Segre, A. Simonetto, P. Smeulders, E. Sternini, C. Sozzi, N. Tartoni, B. Tilia, A. A. Tuccillo, O. Tudisco, M. Valisa, V. Vershkov, V. Vitale, G. Vlad, V. Zanza, M. Zerbini, and F. Zonca, 2002, in *Proceedings of the 19th International Conference on Fusion Energy 2002* (International Atomic Energy Agency, Vienna) pp. CD-ROM file OV/4-5 and <http://www.iaea.org/programmes/ripc/physics/fec2002/html/fec2002.htm>.
- Romanelli, F., and L. Chen, 1991, *Phys. Fluids B* **3**, 329.
- Rosenbluth, M. N., H. L. Berk, J. W. Van Dam, and D. M. Lindberg, 1992, *Phys. Rev. Lett.* **68**, 596.
- Rosenbluth, M. N., and F. L. Hinton, 1998, *Phys. Rev. Lett.* **80**, 724.
- Rosenbluth, M. N., and N. Rostoker, 1959, *Phys. Fluids* **2**, 23.
- Rosenbluth, M. N., and P. H. Rutherford, 1975, *Phys. Rev. Lett.* **34**, 1428.
- Ross, W., G. L. Chen, and S. M. Mahajan, 1982, *Phys. Fluids* **25**, 652.
- Rossby, C. G., 1940, *Q. J. Meteorol. Soc. Suppl.* **66**, 68.
- Rutherford, P. H., L. Chen, and M. N. Rosenbluth, 1978, in *Internal Report PPPL-1418* (PPL, Princeton, NJ).
- Rutherford, P. H., and E. A. Frieman, 1968, *Phys. Fluids* **11**, 569.
- Sabot, R., F. Clairet, G. D. Conway, L. Cupido, X. Garbet, G. Falchetto, T. Gerbaud, S. Hacquin, P. Hennequin, S. Heuraux, C. Honoré, G. Leclert, L. Meneses, A. Sirinelli, L. Vermare, and A. Truc, 2006, *Plasma Phys. Control. Fusion* **48**, B421.
- Sabot, R., A. Macor, C. Nguyen, J. Decker, D. Elbeze, L.-G. Eriksson, X. Garbet, M. Goniche, G. Huysmans, Y. Lacroix, P. Maget, and J. L. Segui, 2009, *Nucl. Fusion* **49**, 085033.
- Sagdeev, R. Z., and A. A. Galeev, 1969, *Nonlinear Plasma Theory* (W. A. Benjamin Inc.).
- Sagdeev, R. Z., V. D. Shapiro, and V. I. Shevchenko, 1978a, *Zh. Eksp. Teor. Fiz. Pis'ma Red.* **27**, 361.
- Sagdeev, R. Z., V. D. Shapiro, and V. I. Shevchenko, 1978b, *Sov. Phys. JETP* **27**, 340.
- Saigusa, M., H. Kimura, S. Moriyama, Y. Neyatani, T. Fujii, Y. Koide, T. Kondoh, M. Sato, M. Nemoto, and Y. Kamada, 1995, *Plasma Phys. Control. Fusion* **37**, 295.
- Sandquist, P., S. E. Sharapov, M. Lisak, T. Johnson, and JET-EFDA contributors, 2007, *Phys. Plasmas* **14**, 122506.

- Santoro, R. A., and L. Chen, 1996, *Phys. Plasmas* **3**, 2349.
- Sasaki, M., K. Itoh, and S. Itoh, 2011, *Plasma Phys. Control. Fusion* **53**, 085017.
- Savin, S., L. Zelenyi, E. Amata, V. Budaev, J. Buechner, J. Blecki, M. Balikhin, S. Klimov, V. E. Korepanov, L. Kozak, V. Kudryashov, V. Kunitsyn, L. Lezhen, A. V. Milovanov, Z. Nemecek, I. Nesterov, D. Novikov, E. Panov, J. L. Rauch, H. Rothkaehl, S. Romanov, J. Safrankova, A. Skalsky, and M. Veselov, 2011, *Planet. Space Sci.* **59**, 606.
- Scott, B., 1998, *Phys. Plasmas* **5**, 2334.
- Scott, B. D., 1997, *Plasma Phys. Control. Fusion* **39**, 1635.
- Scott, B. D., 2010, arXiv:0710.4899v3 [physics.plasm-ph].
- Sedláček, Z., 1971, *J. Plasma Physics* **5**, 239.
- Shapiro, V. D., 1963a, *Zh. Eksp. Teor. Fiz.* **44**, 613.
- Shapiro, V. D., 1963b, *Sov. Phys. JETP* **17**, 416.
- Shapiro, V. D., and V. I. Shevchenko, 1971a, *Zh. Eksp. Teor. Fiz.* **60**, 1023.
- Shapiro, V. D., and V. I. Shevchenko, 1971b, *Sov. Phys. JETP* **33**, 555.
- Sharapov, S. E., B. Alper, H. L. Berk, D. N. Borba, B. N. Breizman, C. D. Challis, A. Fasoli, N. C. Hawkes, T. C. Hender, J. Mailloux, S. D. Pinches, and D. Testa, 2002, *Phys. Plasmas* **9**, 2027.
- Sharapov, S. E., B. Alper, J. Fessey, N. C. Hawkes, N. P. Young, R. Nazikian, G. J. Kramer, D. N. Borba, S. Hacquin, E. De La Luna, S. D. Pinches, J. Rapp, D. Testa, and JET-EFDA contributors, 2004, *Phys. Rev. Lett.* **93**, 165001.
- Sharapov, S. E., D. Borba, A. Fasoli, W. Kerner, L.-G. Eriksson, R. F. Heeter, G.T.A. Huysmans, and M. J. Mantsinen, 1999, *Nucl. Fusion* **39**, 373.
- Sharapov, S. E., D. Testa, B. Alper, D. N. Borba, A. Fasoli, N. C. Hawkes, R. F. Heeter, M. Mantsinen, M. G. Von Hellermann, and contributors to the EFDA-JET work-programme, 2001, *Phys. Lett. A* **289**, 127.
- Shepelyansky, D. L., 1993, *Phys. Rev. Lett.* **70**, 1787.
- Shi, B., and G. Sui, 1997, *Phys. Plasmas* **4**, 2785.
- Shinohara, K., Y. Kusama, M. Takechi, A. Morioka, M. Ishikawa, N. Oyama, K. Tobita, T. Ozeki, S. Takeji, S. Moriyama, T. Fujita, T. Oikawa, T. Suzuki, T. Nishitani, T. Kondoh, S. Lee, M. Kuriyama, JT-60 Team, G. J. Kramer, N. N. Gorelenkov, R. Nazikian, C. Z. Cheng, G. Y. Fu, and A. Fukuyama, 2001, *Nucl. Fusion* **41**, 603.
- Shinohara, K., M. Takechi, and M. Ishikawa et al., 2004, *Plasma Phys. Control. Fusion* **46**, S31.
- Shukla, P. K., M. Y. Yu, H. U. Rahman, and K. H. Spatschek, 1984, *Phys. Rep.* **105**, 227.
- Sigmar, D. J., C. T. Hsu, R. B. White, and C. Z. Cheng, 1992, *Phys. Fluids B* **4**, 1506.
- Singhaus, H. E., 1964, *Phys. Fluids* **7**, 1534.
- Smeulders, P., P. Buratti, M. De Benedetti, G. Monari, and the FTU Team, 2002, *Eur. Conf. Abs.* **26B**, D.
- Smolyakov, A. I., X. Garbet, and M. Ottaviani, 2007, *Phys. Rev. Lett.* **99**, 055002.
- Smolyakov, A. I., X. Garbet, and M. Ottaviani, 2008, *Phys. Lett. A* **372**, 6750.
- Snipes, J. A., N. Basse, C. Boswell, E. Edlund, A. Fasoli, N. N. Gorelenkov, R. S. Granetz, L. Lin, Y. Lin, R. Parker, M. Porkolab, J. Sears, S. Sharapov, V. Tang, and S. Wukitch, 2005, *Phys. Plasmas* **12**, 056102.
- Snipes, J. A., A. Fasoli, P. Bonoli, S. Migliuolo, M. Porkolab, J. E. Rice, Y. Takase, and S. M. Wolfe, 2000, *Plasma Phys. Control. Fusion* **42**, 381.
- Snipes, J. A., R. R. Parker, P. E. Phillips, A. Schmidt, and G. Wallace, 2008, *Nucl. Fusion* **48**, 072001.
- Snipes, J. A., D. Schmittiel, A. Fasoli, R. S. Granetz, and R. R. Parker, 2004, *Plasma Phys. Control. Fusion* **46**, 611.
- Snyder, P. B., and G. W. Hammett, 2001, *Phys. Plasmas* **8**, 744.
- Sornette, D., 1992, *J. Phys. I France* **2**, 2065.
- Spong, D. A., E. M. Bass, W. Deng, W. W. Heidbrink, Z. Lin, B. Tobias, M. A. Van Zeeland, M. E. Austin, C. W. Domier, and N. C. Luhmann, Jr., 2012, *Phys. Plasmas* **19**, 082511.
- Spong, D. A., B. A. Carreras, and C. L. Hedrick, 1992, *Phys. Fluids B* **4**, 3316.
- Spong, D. A., B. A. Carreras, and C. L. Hedrick, 1994, *Phys. Plasmas* **1**, 1503.
- Spong, D. A., D. J. Sigmar, W. A. Cooper, D. E. Hastings, and K. T. Tsang, 1985, *Phys. Fluids* **28**, 2494.
- Spong, D. A., D. J. Sigmar, and J. J. Ramos, 1988, *Fus. Technol.* **13**, 428.
- Stix, T. H., 1972, *Plasma Phys.* **14**, 367.
- Stix, T. H., 1992, *Waves in Plasmas* (AIP, New York).
- Strait, E. J., W. W. Heidbrink, A. D. Turnbull, M. S. Chu, and H. H. Duong, 1993, *Nucl. Fusion* **33**, 1849.
- Stutman, D., L. Delgado-Aparicio, N. Gorelenkov, M. Finkenthal, E. Fredrickson, S. Kaye, E. Mazzucato, and K. Tritz, 2009, *Phys. Rev. Lett.* **102**, 115002.
- Sugama, H., 2000, *Phys. Plasmas* **7**, 466.
- Suzuki, T., S. Ide, T. Oikawa, T. Fujita, M. Ishikawa, M. Seki, G. Matsunaga, T. Hatae, O. Naito, K. Hamamatsu, M. Sueoka, H. Hosoyama, M. Nakazato, and JT-60 Team, 2008, *Nucl. Fusion* **48**, 045002.
- Swift, D. W., 1972, *Phys. Fluids* **15**, 1675.
- Takechi, M., A. Fukuyama, K. Shinohara, M. Ishikawa, Y. Kusama, S. Takeji, T. Fujita, T. Oikawa, T. Suzuki, N. Oyama, T. Ozeki, A. Morioka, C. Z. Cheng, N. N. Gorelenkov, G. J. Kramer, R. Nazikian, and JT-60 Team, 2002, in *Proceedings of the 19th International Conference on Fusion Energy 2002* (International Atomic Energy Agency, Vienna) pp. CD-ROM file EX/W-6 and <http://www.iaea.org/programmes/ripc/physics/fec2002/html/fec2002.htm>.
- Takechi, M., K. Toi, S. Takagi, G. Matsunaga, K. Ohkuni, S. Ohdachi, R. Akiyama, D. S. Darrow, A. Fujisawa, M. Gotoh, H. Idei, H. Iguchi, M. Isobe, T. Kondo, M. Kojima, S. Kubo, S. Lee, T. Minami, S. Morita, K. Matsuoka, S. Nishimura, S. Okamura, M. Osakabe, M. Sasao, M. Shimizu, C. Takahashi, K. Tanaka, and Y. Yoshimura, 1999, *Phys. Rev. Lett.* **83**, 312.

- Tamabechi, K., J. R. Gilleland, Y. A. Sokolov, R. Toschi, and ITER Team, 1991, *Nucl. Fusion* **31**, 1135.
- Tang, J. T., and N. C. Luhmann Jr., 1976, *Phys. Fluids* **19**, 1935.
- Tang, W. M., J. W. Connor, and R. J. Hastie, 1980, *Nucl. Fusion* **20**, 1439.
- Tataronis, J., 1975, *J. Plasma Phys.* **13**, 87.
- Taylor, J. B., 1967, *Phys. Fluids* **10**, 1357.
- Taylor, J. B., and R. J. Hastie, 1965, *Phys. Fluids* **8**, 323.
- Taylor, J. B., and R. J. Hastie, 1968, *Plasma Phys.* **10**, 479.
- Taylor, J. B., and B. McNamara, 1971, *Phys. Fluids* **14**, 1492.
- Tennyson, J. L., J. D. Meiss, and P. J. Morrison, 1994, *Physica D* **71**, 1.
- Testa, D., G. Y. Fu, A. Jaun, A. Fasoli, O. Sauter, and JET-EFDA contributors, 2003, *Nucl. Fusion* **43**, 479.
- Testa, D., N. Mellet, T. Panis, P. Blanchard, H. Carfantan, A. Fasoli, and JET-EFDA contributors, 2010, *Nucl. Fusion* **50**, 084010.
- Tetreault, D. J., 1983, *Phys. Fluids* **26**, 3247.
- Tobias, B. J., I. G. J. Classen, C. W. Domier, W. W. Heidbrink, N. C. Luhmann Jr., R. Nazikian, H. K. Park, D. A. Spong, and M. A. Van Zeeland, 2011, *Phys. Rev. Lett.* **106**, 075003.
- Todo, Y., 2006, *Phys. Plasmas* **13**, 082503.
- Todo, Y., H. L. Berk, and B. N. Breizman, 2003, *Phys. Plasmas* **10**, 2888.
- Todo, Y., H. L. Berk, and B. N. Breizman, 2010, *Nucl. Fusion* **50**, 084016.
- Todo, Y., H. L. Berk, and B. N. Breizman, 2012a, *Nucl. Fusion* **52**, 033003.
- Todo, Y., H. L. Berk, and B. N. Breizman, 2012b, *Nucl. Fusion* **52**, 094018.
- Todo, Y., and T. Sato, 1998, *Phys. Plasmas* **5**, 1321.
- Todo, Y., T. Sato, K. Watanabe, T. H. Watanabe, and R. Horiuchi, 1995, *Phys. Plasmas* **2**, 2711.
- Todo, Y., K. Shinohara, M. Takechi, and M. Ishikawa, 2005, *Phys. Plasmas* **12**, 012503.
- Todo, Y., T.-H. Watanabe, H.-B. Park, and T. Sato, 2001, *Nucl. Fusion* **41**, 1153.
- Toi, K., K. Ogawa, M. Isobe, M. Osakabe, D. A. Spong, and Y. Todo, 2011, *Plasma Phys. Control. Fusion* **53**, 024008.
- Toi, K., M. Takechia, M. Isobe, N. Nakajima, M. Osakabe, S. Takagia, T. Kondob, G. Matsunaga, K. Ohkuni, M. Sasao, S. Yamamoto, S. Ohdachi, S. Sakakibara, H. Yamada, K. Y. Watanabe, D. S. Darrow, A. Fujisawa, M. Goto, K. Ida, H. Idei, H. Iguchi, S. Lee, S. Kado, S. Kubo, O. Kaneko, K. Kawahata, K. Matsuoka, T. Minami, S. Morita, O. Motojima, K. Narihara, S. Nishimura, N. Ohyabu, Y. Oka, S. Okamura, T. Ozaki, K. Sato, M. Sato, A. Shimizu, T. Shimojima, Y. Takeiri, K. Tanaka, T. Tokuzawa, K. Tsumori, I. Yamada, Y. Yoshimura, and CHS and LHD Experimental Groups, 2000, *Nucl. Fusion* **40**, 1349.
- Toi, K., S. Yamamoto, N. Nakajima, S. Ohdachi, S. Sakakibara, M. Osakabe, S. Murakami, K. Y. Watanabe, M. Goto, K. Kawahata, Ya. I. Kolesnichenko, S. Masuzaki, S. Morita, K. Narihara, Y. Narushima, Y. Takeiri, K. Tanaka, T. Tokuzawa, H. Yamada, I. Yamada, K. Yamazaki, and LHD Experimental Group, 2004, *Plasma Phys. Control. Fusion* **46**, S1.
- Tsai, S., and L. Chen, 1993, *Phys. Fluids B* **5**, 3284.
- Tsai, S. T., J. W. Van Dam, and L. Chen, 1984, *Plasma Phys. Control. Fusion* **26**, 907.
- Tsang, K. T., D. J. Sigmar, and J. C. Whitson, 1981, *Phys. Fluids* **24**, 1508.
- Tuccillo, A. A., L. Amicucci, B. Angelini, M. L. Apicella, G. Apruzzese, E. Barbato, F. Belli, A. Bertocchi, A. Biancalani, A. Bierwage, W. Bin, L. Boncagni, A. Botrugno, G. Bracco, G. Breyannis, S. Briguglio, A. Bruschi, P. Buratti, G. Calabrò, A. Cardinali, C. Castaldo, S. Ceccuzzi, C. Centioli, R. Cesario, I. Chavdarovski, L. Chen, C. Cianfarani, S. Cirant, R. Coletti, F. Crisanti, O. D'Arcangelo, M. De Angeli, R. De Angelis, F. De Luca, L. Di Matteo, C. Di Troia, B. Esposito, G. Fogaccia, D. Frigione, V. Fusco, L. Gabellieri, A. Garavaglia, L. Garzotti, E. Giovannozzi, G. Granucci, G. Grossetti, G. Grosso, Z. O. Guimarães-Filho, F. Iannone, A. Jacchia, H. Kroegler, E. Lazzaro, M. Lontano, G. Maddaluno, M. Marinucci, D. Marocco, G. Mazzitelli, C. Mazzotta, A. Milovanov, F. C. Mirizzi, G. Monari, A. Moro, S. Nowak, F. Orsitto, D. Pacella, L. Panaccione, M. Panella, F. Pegoraro, V. Pericoli-Ridolfini, S. Podda, A. Pizzuto, G. Pucella, G. Ramogida, G. Ravera, M. Romanelli, A. Romano, G. Ramponi, C. Sozzi, G. Szepesi, E. Sternini, O. Tudisco, E. Vitale, G. Vlad, V. Zanza, M. Zerbini, F. Zonca, X. Wang, M. Aquilini, P. Cefali, E. Di Ferdinando, S. Di Giovenale, G. Giacomini, F. Gravanti, A. Grosso, V. Mellera, M. Mezzacappa, V. Muzzini, A. Pensa, P. Petrolini, V. Piergotti, B. Raspante, G. Rocchi, A. Sibio, B. Tilia, C. Torelli, R. Tulli, M. Vellucci, and D. Zannetti, 2011, *Nucl. Fusion* **51**, 094015.
- Turnbull, A. D., E. J. Strait, W. W. Heidbrink, M. S. Chu, J. M. Greene, L. L. Lao, T. S. Taylor, and S. J. Thompson, 1993, *Phys. Fluids* **B5**, 2546.
- Udintsev, V. S., M. Goniche, G. Giruzzi, G. T. A. Huysmans, F. Imbeaux, P. Maget, X. Garbet, R. Sabot, J. L. Ségui, F. Turco, T. P. Goodman, D. Molina, H. Weisen, and the Tore Supra team, 2006, *Plasma Phys. Control. Fusion* **48**, L33.
- Valovič, M., B. Lloyd, K. G. McClements, C. D. Warrick, S. J. Fielding, A. W. Morris, T. Pinfold, H. R. Wilson, COMPASS-D Team, and ECRH Team, 2000, *Nucl. Fusion* **40**, 1569.
- Van Dam, J. W., and M. N. Rosenbluth, 1998, *Bull. Am. Phys. Soc.* **43**, 1753.
- Van Dam, J. W., M. N. Rosenbluth, and Y. C. Lee, 1982, *Phys. Fluids* **25**, 1349.
- Van Hove, L., 1955, *Physica* **21**, 517.
- Vann, R. G. L., H. L. Berk, and A. R. Soto-Chavez, 2007, *Phys. Rev. Lett.* **99**, 025003.
- Vann, R. G. L., R. O. Dendy, and M. P. Gryaznevich, 2005, *Phys. Plasmas* **12**, 032501.
- Vann, R. G. L., R. O. Dendy, G. Rowlands, T. D. Arber, and N. d'Ambrumenil, 2003, *Phys. Plasmas* **10**, 623.
- Van Zeeland, M. A., M. E. Austin, T. N. Carlstrom, T. Deterly, D. K. Finkenthal, C. T. Holcomb, R. J. Jayakumar, G. J. Kramer, M. A. Makowski, G. R. McKee, R. Nazikian, W. A. Peebles, T. L. Rhodes, W. M. Solomon, and E. Strait, 2006a, *Nucl. Fusion* **46**, S880.

- Van Zeeland, M. A., G. J. Kramer, M. E. Austin, R. L. Boivin, W. W. Heidbrink, M. A. Makowski, G. R. McKee, R. Nazikian, W. M. Solomon, and G. Wang, 2006b, *Phys. Rev. Lett.* **97**, 135001.
- Vedenov, A. A., E. P. Velikhov, and R. Z. Sagdeev, 1961a, *Nucl. Fusion* **1**, 82.
- Vedenov, A. A., E. P. Velikhov, and R. Z. Sagdeev, 1961b, *Usp. Fiz. Nauk* **73**, 701.
- Vedenov, A. A., E. P. Velikhov, and R. Z. Sagdeev, 1961c, *Sov. Phys. Usp.* **4**, 332.
- Vernon Wong, H., and H. L. Berk, 1998, *Phys. Plasmas* **5**, 2781.
- Vlad, G., S. Briguglio, G. Fogaccia, and F. Zonca, 2004, *Plasma Phys. Control. Fusion* **46**, S81.
- Vlad, G., S. Briguglio, G. Fogaccia, and F. Zonca, 2011, in *12th IAEA Technical Meeting on Energetic Particles in Magnetic Confinement Systems* (IFS, Austin, TX) pp. P2–13 and <http://w3fusion.ph.utexas.edu/ifs/iaeaep/papers/>.
- Vlad, G., S. Briguglio, G. Fogaccia, F. Zonca, C. Di Troia, V. Fusco, and X. Wang, 2012, in *Proceedings of the 24th International Conference on Fusion Energy* (International Atomic Energy Agency, Vienna) pp. [http://www-naweb.iaea.org/napc/physics/FEC/FEC2012/papers/77\\_THP603.pdf](http://www-naweb.iaea.org/napc/physics/FEC/FEC2012/papers/77_THP603.pdf).
- Vlad, G., S. Briguglio, G. Fogaccia, F. Zonca, C. Di Troia, W. W. Heidbrink, M. A. Van Zeeland, A. Bierwage, and X. Wang, 2009, *Nucl. Fusion* **49**, 075024.
- Vlad, G., S. Briguglio, G. Fogaccia, F. Zonca, V. Fusco, and X. Wang, 2013, *Nucl. Fusion* **53**, 083008.
- Vlad, G., S. Briguglio, G. Fogaccia, F. Zonca, and M. Schneider, 2006, *Nucl. Fusion* **46**, 1.
- Vlad, G., S. Briguglio, C. Kar, F. Zonca, and F. Romanelli, 1992, in *Theory of Fusion Plasmas*, edited by E. Sindoni and J. Vaclavik (Editrice Compositori Società Italiana di Fisica, Bologna) p. 361.
- Vlad, G., C. Kar, F. Zonca, and F. Romanelli, 1995a, *Phys. Plasmas* **2**, 418.
- Vlad, G., F. Zonca, and S. Briguglio, 1999, *Riv. Nuovo Cimento* **22**, 1.
- Vlad, G., F. Zonca, and F. Romanelli, 1995b, *Nucl. Fusion* **35**, 1651.
- Vlad, M., and F. Spineanu, 2005, *Plasma Phys. Control. Fusion* **47**, 281.
- Walén, C., 1944, *Ark. Mat. Astron. Fys.* **30A** (15), 1.
- Wang, W.-M., and Z. Zhang, 2009, *J. Stat. Phys.* **134**, 953.
- Wang, X., S. Briguglio, L. Chen, C. Di Troia, G. Fogaccia, G. Vlad, and F. Zonca, 2011, *Phys. Plasmas* **18**, 052504.
- Wang, X., S. Briguglio, L. Chen, C. Di Troia, G. Fogaccia, G. Vlad, and F. Zonca, 2012, *Phys. Rev. E* **86**, 045401(R).
- Wang, X., S. Briguglio, G. Fogaccia, G. Vlad, C. Di Troia, F. Zonca, L. Chen, A. Bierwage, and H. Zhang, 2010a, in *Proceedings of the 23rd International Conference on Fusion Energy 2010* (International Atomic Energy Agency, Vienna) pp. CD-ROM file THW/2–4Ra.
- Wang, X., F. Zonca, and L. Chen, 2010b, *Plasma Phys. Control. Fusion* **52**, 115005.
- Wang, Z. T., Y. X. Long, A. K. Wang, J. Q. Dong, Long Wang, and F. Zonca, 2007, *Nucl. Fusion* **47**, 1307.
- Watanabe, T., X. J. Wang, J. B. Murphy, J. Rose, Y. Shen, T. Tsang, L. Giannessi, P. Musumeci, and S. Reiche, 2007, *Phys. Rev. Lett.* **98**, 034802.
- Weiland, J., and L. Chen, 1985, *Phys. Fluids* **28**, 1359.
- Weiland, J., M. Lisak, and H. Wilhelmsson, 1987, *Phys. Scr.* **T16**, 53.
- Weitzner, H., and G. M. Zaslavsky, 2003, *Commun. Nonlinear Sci. Numer. Simulation* **8**, 273.
- Wesson, J., 1990, *Nucl. Fusion* **30**, 245.
- Weyl, H., 1931, *The Theory of Groups and Quantum Mechanics* (Dover, New York).
- White, R., L. Chen, and F. Zonca, 2005, *Phys. Plasmas* **12**, 057304.
- White, R., and H. Mynick, 1989, *Phys. Fluids B* **1**, 980.
- White, R. B., 1989, *Theory of Tokamak Plasmas* (North Holland, Amsterdam).
- White, R. B., 2000, *Private Communication*.
- White, R. B., 2010, *Private Communication*.
- White, R. B., 2012, *Commun. Nonlinear Sci. Numer. Simul.* **17**, 2200.
- White, R. B., M. N. Bussac, and F. Romanelli, 1989, *Phys. Rev. Lett.* **62**, 539.
- White, R. B., L. Chen, F. Romanelli, and R. Hay, 1985, *Phys. Fluids* **28**, 278.
- White, R. B., R. J. Goldston, K. McGuire, A. H. Boozer, D. A. Monticello, and W. Park, 1983, *Phys. Fluids* **26**, 2958.
- White, R. B., N. Gorelenkov, W. W. Heidbrink, and M. A. Van Zeeland, 2010a, *Phys. Plasmas* **17**, 056107.
- White, R. B., N. Gorelenkov, W. W. Heidbrink, and M. A. Van Zeeland, 2010b, *Plasma Phys. Control. Fusion* **52**, 045012.
- White, R. B., F. Romanelli, and M. N. Bussac, 1990, *Phys. Fluids B* **2**, 745.
- White, R. B., P. H. Rutherford, P. Colestock, and M. N. Bussac, 1988, *Phys. Rev. Lett.* **60**, 2038.
- White, R. B., Y. Wu, Y. Chen, E. D. Fredrickson, D. S. Darrow, M. C. Zarnstorff, J. R. Wilson, S. J. Zweben, K. W. Hill, G. Y. Fu, and M. N. Rosenbluth, 1995, *Nucl. Fusion* **35**, 1707.
- Winsor, N., J. L. Johnson, and J. M. Dawson, 1968, *Phys. Fluids* **11**, 2448.
- Wong, K. L., R. J. Fonck, S. F. S. Paul, D. R. Roberts, E. D. Fredrickson, R. Nazikian, H. K. Park, M. Bell, L. Bretz, R. Budny, S. Cohen, G. W. Hammett, F. C. Jobs, D. M. Meade, S. S. Medley, D. Mueller, Y. Nagayama, D. K. Owens, and E. J. Synakowski, 1991, *Phys. Rev. Lett.* **66**, 1874.
- Wong, K. L., W. W. Heidbrink, E. Ruskov, C. C. Petty, C. M. Greenfield, R. Nazikian, and R. Budny, 2005, *Nucl. Fusion* **45**, 30.
- Wong, K.-L., 1999, *Plasma Phys. Control. Fusion* **41**, R1.
- Wong, K.-L., M. S. Chu, T. C. Luce, C. C. Petty, P. A. Politzer, R. Prater, L. Chen, R. Harvey, M. E. Austin, L. C. Johnson, R. J. La Haye, and R. T. Snider, 2000, *Phys. Rev. Lett.* **85**, 996.
- Wu, D., 2012, *Kinetic Alfvén Wave: Theory, Experiment and Application* (Scientific Press, Beijing).
- Wu, Y., C. Z. Cheng, and R. B. White, 1994, *Phys. Plasmas* **1**, 3369.

- Wu, Y., R. B. White, Y. Chen, and M. N. Rosenbluth, 1995, *Phys. Plasmas* **2**, 4555.
- Xiao, Y., and Z. Lin, 2011, *Phys. Plasmas* **18**, 110703.
- Zakharov, L., and B. Rogers, 1992, *Phys. Fluids B* **4**, 3285.
- Zakharov, V. E., 1968, *J. Appl. Mech. Tech. Phys.* **9**, 190.
- Zakharov, V. E., and V. I. Karpman, 1962, *Zh. Eksp. Teor. Fiz.* **43**, 490.
- Zakharov, V. E., and V. I. Karpman, 1963, *Sov. Phys. JETP* **16**, 351.
- Zelenyi, L. M., and A. V. Milovanov, 2004, *Phys. Usp.* **47**, 749.
- Zhang, H. S., Z. Lin, and I. Holod, 2012, *Phys. Rev. Lett.* **109**, 025001.
- Zhang, H. S., Z. Lin, I. Holod, X. Wang, Y. Xiao, and W. Zhang, 2010a, *Phys. Plasmas* **17**, 112505.
- Zhang, W., V. Decyk, I. Holod, Y. Xiao, Z. Lin, and L. Chen, 2010b, *Phys. Plasmas* **17**, 055902.
- Zhang, W., Z. Lin, and L. Chen, 2008a, *Phys. Rev. Lett.* **101**, 095001.
- Zhang, Y., W. W. Heidbrink, H. Boehmer, R. McWilliams, G. Chen, B. N. Breizman, S. Vincena, T. Carter, D. Leneman, W. Gekelman, P. Pribyl, and B. Brugman, 2008b, *Phys. Plasmas* **15**, 012103.
- Zhao, G., and L. Chen, 2002, *Phys. Plasmas* **9**, 861.
- Zhao, J. S., D. J. Wu, J. Y. Lu, L. Yang, and M. Y. Yu, 2011, *New J. Phys.* **13**, 063043.
- Zheng, L. J., M. T. Kotschenreuther, and J. W. Van Dam, 2010, *J. Comput. Phys.* **229**, 3605.
- Zheng, L.-J., and L. Chen, 1998a, *Phys. Plasmas* **5**, 444.
- Zheng, L.-J., and L. Chen, 1998b, *Phys. Plasmas* **5**, 1056.
- Zheng, L.-J., M. Kotschenreuther, and M. S. Chu, 2005, *Phys. Rev. Lett.* **95**, 255003.
- Zimmermann, O., H. R. Koslowski, A. Krämer-Flecken, Y. Liang, R. Wolf, and TEC-team, 2005, in *Proceedings of the 32nd EPS Conference on Plasma Physics, Tarragona, Spain, 27 June - 1 July, (2005), ECA*, Vol. 29C (EPS) pp. CD-ROM file P4.059.
- Zonca, F., 1993a, *Plasma Phys. Control. Fusion* **35**, B307.
- Zonca, F., 1993b, *Ph. D. Thesis* (Princeton University, Princeton, NJ).
- Zonca, F., 2003, in *8th Easter Plasma Meeting on Reconnection and Turbulence in Magnetically Confined Plasmas* (Turin, Italy) p. [http://www.afs.enea.it/zonca/references/seminars/zonca\\_easter03.pdf](http://www.afs.enea.it/zonca/references/seminars/zonca_easter03.pdf).
- Zonca, F., 2008, *Int. J. Mod. Phys. A* **23**, 1165.
- Zonca, F., A. Biancalani, I. Chavdarovski, L. Chen, C. Di Troia, and X. Wang, 2010, *J. Phys.: Conf. Ser.* **260**, 012022.
- Zonca, F., S. Briguglio, L. Chen, S. Dettrick, G. Fogaccia, D. Testa, and G. Vlad, 2002, *Phys. Plasmas* **9**, 4939.
- Zonca, F., S. Briguglio, L. Chen, G. Fogaccia, T. S. Hahm, A. V. Milovanov, and G. Vlad, 2006, *Plasma Phys. Control. Fusion* **48**, B15.
- Zonca, F., S. Briguglio, L. Chen, G. Fogaccia, and G. Vlad, 2000, in *Theory of Fusion Plasmas*, edited by J. W. Connor, O. Sauter, and E. Sindoni (SIF, Bologna) p. 17.
- Zonca, F., S. Briguglio, L. Chen, G. Fogaccia, and G. Vlad, 2005, *Nucl. Fusion* **45**, 477.
- Zonca, F., S. Briguglio, L. Chen, G. Fogaccia, G. Vlad, and X. Wang, 2013a, in *Proceedings of the 6th IAEA Technical Meeting on "Theory of Plasmas Instabilities"* (IAEA, Vienna, Vienna, Austria, May 27 - 29).
- Zonca, F., P. Buratti, A. Cardinali, L. Chen, J. Dong, Y. Long, A. V. Milovanov, F. Romanelli, P. Smeulders, L. Wang, Z. Wang, C. Castaldo, R. Cesario, E. Giovannozzi, M. Marinucci, and V. Pericoli Ridolfini, 2007a, *Nucl. Fusion* **47**, 1588.
- Zonca, F., P. Buratti, A. Cardinali, L. Chen, J. Dong, Y. Long, A. V. Milovanov, F. Romanelli, P. Smeulders, L. Wang, Z. Wang, C. Castaldo, R. Cesario, E. Giovannozzi, M. Marinucci, and V. Pericoli Ridolfini, 2007b, arXiv:0707.2852v1 [physics.plasma-ph].
- Zonca, F., and L. Chen, 1992, *Phys. Rev. Lett.* **68**, 592.
- Zonca, F., and L. Chen, 1993, *Phys. Fluids B* **5**, 3668.
- Zonca, F., and L. Chen, 1996, *Phys. Plasmas* **3**, 323.
- Zonca, F., and L. Chen, 2000, *Phys. Plasmas* **7**, 4600.
- Zonca, F., and L. Chen, 2006, *Plasma Phys. Control. Fusion* **48**, 537.
- Zonca, F., and L. Chen, 2007, in *Proceedings of the 34th EPS Conference on Plasma Physics, Warsaw, Poland, 2 - 6 July, (2007), ECA*, Vol. 31F (EPS) pp. CD-ROM file P4.071.
- Zonca, F., and L. Chen, 2008a, in *Frontiers in Modern Plasma Physics*, Vol. CP1061, edited by P. K. Shukla, B. Eliasson, and L. Stenflo (AIP) p. 34.
- Zonca, F., and L. Chen, 2008b, *Europhys. Lett.* **83**, 35001.
- Zonca, F., and L. Chen, 2008c, in *Theory of Fusion Plasmas*, Vol. CP1069, edited by O. Sauter, X. Garbet, and E. Sindoni (AIP) p. 355.
- Zonca, F., and L. Chen, 2013, *Phys. Plasmas*, submitted.
- Zonca, F., L. Chen, A. Botrugno, P. Buratti, A. Cardinali, R. Cesario, V. P. Ridolfini, and JET-EFDA contributors, 2009, *Nucl. Fusion* **49**, 085009.
- Zonca, F., L. Chen, S. Briguglio, G. Fogaccia, G. Vlad, and X. Wang, 2013b, *New J. Phys.*, submitted.
- Zonca, F., L. Chen, J. Q. Dong, and R. A. Santoro, 1999, *Phys. Plasmas* **6**, 1917.
- Zonca, F., L. Chen, and R. A. Santoro, 1996, *Plasma Phys. Control. Fusion* **38**, 2011.
- Zonca, F., L. Chen, R. A. Santoro, and J. Q. Dong, 1998, *Plasma Phys. Control. Fusion* **40**, 2009.
- Zonca, F., L. Chen, and R. B. White, 2004a, in *Theory of Fusion Plasmas*, edited by J. W. Connor, O. Sauter, and E. Sindoni (Editrice Compositori, Società Italiana di Fisica, Bologna, Italy) p. 3.
- Zonca, F., F. Romanelli, G. Vlad, and C. Kar, 1995, *Phys. Rev. Lett.* **74**, 698.
- Zonca, F., R. B. White, and L. Chen, 2004b, *Phys. Plasmas* **11**, 2488.

Zweben, S. J., R. V. Budny, D. S. Darrow, S. S. Medley, R. Nazikian, B. C. Stratton, E. J. Synakowski, and G. Taylor for the TFTR Group, 2000, Nucl. Fusion **40**, 91.

Zweben, S. J., D. S. Darrow, E. D. Fredrickson, G. Taylor, S. von Goeler, and R. B. White, 1999, Nucl. Fusion **39**, 1097.